UNITED STATES DEPARTMENT OF THE INTERIOR

GEOLOGICAL SURVEY

Pacific Enewetak Atoll Crater Exploration (PEACE) Program Enewetak Atoll, Republic of the Marshall Islands

Part 3: Stratigraphic analysis and other geologic and geophysical studies in vicinity of OAK and KOA craters

edited by

Thomas W. Henry and Bruce R. Wardlaw

U.S. Geological Survey

Open File Report 86-555

Prepared in cooperation with the Defense Nuclear Agency

1987

CLAY -- A sedimentologic term for a rock or mineral fragment or a detrital particle of any composition smaller than a very fine silt grain, having a diameter less than 1/256 mm (4 microns, or 0.00026 in., or 8 phi units).

COBBLE -- A sedimentologic term for a rock fragment or detrital particle larger than a pebble and smaller than a boulder, having a diameter in the range of 64 to 256 mm (2.5 to 10 in., or -6 to -8 phi units).

CONSOLIDATION -- Gradual or slow reduction in volume and increase in density of a material mass in response to increased loads or compressive stress; e.g., the adjustment of a saturated material involving the squeezing of water from pore spaces.

COMPACTION -- Any process by which a material mass loses pore space and achieves a higher density, thereby increasing the bearing capacity, reducing the tendency to settle or deform under load, and increasing the general stability of the material mass (soil).

CRATER -- A typically bowl-shaped or saucer-shaped pit or depression, generally of considerable size and with steep inner slopes, formed on a terrestrial or planetary surface or in the ground by the explosive release of chemical or kinetic energy; e.g., an impact crater or an explosion crater.

CRATER DIAMETER -- Distance measured from the crater rim, through ground zero, to the opposite crater rim.

CRATER RADIAL -- A transect at any given azimuth extending from ground zero outward; in this volume, the radials extend beyond the current edge of the crater (i.e., beyond the crater rim crest).

CRATER RIM CREST -- Current highest point on the crater rim (sensu Roddy, 1977, fig. 1).

CRATER WALL -- Escarpment at the current edge of the crater, extending from the (true) crater floor upward to the rim crest (sensu Roddy, 1977, fig. 1).

DEBRIS -- Used in this volume for sedimentary material that has been moved from its original position and deposited elsewhere by the effects (direct or indirect) of a nuclear explosion (Folger, and others, 1986, p. iv).

DIKE -- (See sedimentary dike.)

DISSOLUTION SURFACE -- See solution unconformity.

DISCONFORMITY -- A special type of unconformity in which the bedding planes above and below the break are essentially parallel, indicating a significant interuption in the orderly sequence of sedimentary rocks, generally by a considerable interval of erosion (or sometimes of nondeposition) and generally marked by a visible and irregular or uneven erosion surface of appreciable relief.

DISCONTINUITY or **DISCONTINUITY SURFACE** -- A bedding surface that represents some sort of interruption in the normal sedimentation process, whatever its cause or length; it is generally (but not always) a manifestation of nondeposition and accompanying erosion (see disconformity, unconformity, which are more specific terms).

DISTAL -- (Comparative term, equals farther) Said of a sedimentary deposit consisting of finer grained clastics formed farther from the source area of the sediment (see proximal.)

EJECTA -- In this volume, debris that was at some stage of its history blown out of the crater as a result of the energy of the explosion itself (i.e., became ballistic or airborne).

EXCAVATIONAL CRATER -- As used in this volume, the crater that was formed by the direct kinetic (ballistic and/or nonballistic) effects of the explosion itself.

EXPOSURE SURFACE -- In this volume, a stratigraphic horizon marking the top of a former surface subjected to subaerial conditions resulting from a sea-level lowstand. The strata just below such surfaces commonly exhibit paleosol fabrics and structures. (See disconformity.)

FIX POINT -- A position or point established from terrestrial, electronic, or astronomical data.

FLOATSTONE -- Term used by Embry and Klovan (1972) in their modification of Dunham's (1962) classification for carbonate rocks and sediments which contain more than 10 percent larger (granule-sized and greater) grains and in which these coarser grains do not support each other (see rudstone). In this volume and in Henry, Wardlaw, and others (1986), the term is expanded to include both allochthonous and autochthonous grain components.

FRAMESTONE -- Term used by Embry and Klovan (1972) in their modification of Dunham's (1962) classification of carbonate rocks for a carbonate sedimentary rock or sediment in which organisms themselves acted as framebuilders (e.g., intergrown reef corals, coralline algae) (see bafflestone, bindstone, boundstone).

GEOLOGIC CRATER -- The crater that is defined by the zone of sonic degradation.

GRADED BEDDING or **GRADED BED** -- A type of bedding or a bed in which each layer displays a gradual and progressive change in particle size, generally from coarse at the base of the bed to fine at the top. It may form under conditions in which the velocity of the prevailing current declined in a gradual manner, as by deposition from a single short-lived turbidity current.

GRAINSTONE -- A term used by Dunham (1962) for a mud-free (less than 1 percent of materials with diameters less than 20 microns), grain-supported, sedimentary carbonate rock. The term has been expanded to include unlithified carbonate sediments as well.

GRANULE -- A sedimentologic term for a rock fragment or detrital particle larger than a very coarse sand grain and smaller than a pebble, having a diameter in the range of 2 to 4 mm (1/12 to 1/6 in., or -1 to -2 phi units).

GROUND ZERO -- (Abbreviated GZ) The point on the ground directly underneath the explosive device.

KARST -- A geomorphic term for a type of topography formed on limestone and other easily soluble rocks by dissolution and that is characterized by sinkholes, caves, and underground drainage. (Adjective karstic; see microkarst.)

LIQUEFACTION. -- The sudden large decrease of the shearing resistance of a cohesionless material, caused by a collapse of the structure by shock or strain, and associated with a sudden but temporary increase of the pore fluid pressure (ASCE, 1958, Term 205). It involves a temporary transformation of the material into a fluid mass.

MASS WASTING -- A general term for the dislodgement and downslope transport of soil and rock material under the direct application of gravitational body stresses. It includes slow displacement such as creep and rapid movements such as earthflows, avalanches, and falls.

MICROKARST -- The small-scale dissolution features (e.g., solution-enlarged vugs, solution-enlarged fissures or cracks, etc.) associated with karst, generally on a hand-sample (i.e., core-sized) scale. (See karst; adjective microkarstic.)

MUD -- An unconsolidated sediment consisting of clay- and/or silt-sized particles; a mixture of silt and clay; the silt-plus-clay portion of a sedimentary rock.

MUDSTONE -- A term used by Dunham (1962) for a mud-supported sedimentary carbonate rock containing less than 10 percent grains (particles with dimensions greater than 20 microns). The term has been expanded to include uncemented carbonate sediments. (See grainstone, wackestone, packstone.)

PACKSTONE -- A term used by Dunham (1962) for a sedimentary carbonate rock whose granule-and-coarser sized material is arranged in a self-supporting framework, yet also containing some matrix of calcareous mud. The term has been explanded to include uncemented carbonate sediments. (See mudstone, grainstone, wackestone.)

PALEOSOL -- A buried, ancient soil profile, part of a soil profile, or a soil horizon.

PEBBLE -- A sedimentologic term for a small rock fragment or detrital particle larger than a granule and smaller than a cobble, having a diameter in the range of 5 to 64 mm (1/6 to 2.5 in., or -2 to -6 phi units).

PENECONTEMPORANEOUS -- Formed or existing at almost the same time as something else.

PIPE -- Used in this volume, equals sedimentary dike.

PIPING -- For this volume, movement of fluidized sedimentary materials and/or water predominantly vertically through cracks, fissures, or joints to form sedimentary dikes or pipes.

PROXIMAL -- (Comparative term, closer) Said of a sedimentary deposit, consisting of coarser-grained materials formed nearer the source area. (See distal).

REEF PLATE -- Rock formed from cemented reef rubble that occurs in a band several hundred meters wide lagoonward of the living reef (Folger, 1986, p. v).

RHIZOLITH -- In this volume, a commonly downward-branching, generally slender, concretion-like mass interpreted to have formed around the root or rootlet of a living plant. Equals rhizoconcretion, rootlet sheath (if hollow), and root cast (if completely filled) of Bates and Jackson (1980) usage. These structures commonly are (at least partially) filled with "tea-brown" micrite.

RUDSTONE -- Term used by Embry and Klovan (1972) in their modification of Dunham's (1962) classification of carbonate rocks for those that contain more than 10 percent larger (granule-sized and greater) grains and in which these coarser grains do support each other (see floatstone). The term also is used for uncemented carbonate sediments. In this volume and in Henry, Wardlaw, and others (1986), the term is expanded to include both allochthonous and autochthonous grain components.

RUBBLE -- In this volume, a deposit or mass of angular rock fragments, or the angular rock fragments themselves.

SAND -- A sedimentologic term for a rock fragment or detrital particle smaller than a granule and larger than a coarse-silt grain, having a diameter in the range of 1/16 to 2 mm (62 to 2,000 microns, or 0.0025 to 0.08 in., or 4 to -1 phi units).

SAND VOLCANO -- An accumulation of sand (and coarser material) resembling a miniature volcano or low volcanic mound, produced by expulsion of liquefied sand (and coarser sediment) to the surface (either the sediment-air or -water interface). These are the surface expressions of the sedimentary dikes or pipes.

SATURATION -- That state of a soil or rock where the pore space is occupied by a liquid (such as water) with no air (or other gaseous material) present except as dissolved material.

SEDIMENTARY DIKE -- A sheetlike or tubular mass of sedimentary material that cuts across the structure or bedding of preexisting strata in the manner of an igneous dike. It may contain a variety of clastic materials derived from various stratigraphic layers and is formed by the filling of a crack or fissure from below, above, or laterally by forcible injection or intrusion of fluidized sediments under abnormal pressure. For this volume equals pipe.

SEDIMENTARY INTERVAL -- (Introduced in Chapter 2) A term used for a major division of the stratigraphic sequence on Enewetak. A sedimentary interval consists of a set of two or more sedimentary packages, and each set is a major physical stratigraphic unit that apparently reflects a major event in the geologic history of the atoll.

SEDIMENTARY PACKAGE -- (Introduced in Chapter 2; abbreviated SP) The basic physical stratigraphic subdivision used for subsurface mapping purposes and construction of the physical stratigraphic framework on Enewetak.

SILT -- A sedimentologic term for a rock fragment or detrital particle smaller than a very fine sand grain and larger than coarse clay, having a diameter in the range of 1/256 to 1/16 mm (4 to 62 microns, or 0.00016 to 0.0025 in., or 8 to 4 phi units).

SLUMP -- A landslide, either subaqueous or subaerial, characterized by a shearing and rotary movement of a generally independent mass of rock or earth along a curved slip surface (concave upward) and about an axis parallel to the slope from which it descends, and by backward tilting of the mass with respect to that slope so that the slump surface often exhibits a reverse slope facing uphill.

SLUMPING -- The gravitationally induced process that forms slumps.

SOLUTION UNCONFORMITY -- A break in the sedimentary record caused by dissolution of a carbonate strata during subaerial exposure and/or by erosion (Schlanger, 1963). The strata immediately underlying a solution unconformity are commonly karstic (see karst).

SUBSIDENCE -- A local mass movement that involves principally the gradual downward settling or sinking of the ground surface with little or no horizontal motion. It may be due to one or more of a variety of causes. Densification-derived subsidence is that portion of the subsidence that can be explained fully by density increases of the sediments below the subsided surface.

"TEA-BROWN" MICRITE -- In this volume, a descriptive term for moderate- to dark-brown or rust-colored ("tea-brown"), fine-grained (i.e., silt-sized or finer) carbonate material. Although used without genetic implication, "tea-brown" micrite is commonly associated with paleosols, subaerial exposure surfaces, and rhizoliths.

TRANSIENT CRATER -- In the broader sense, the crater defined at any point in time; as used in this volume, the crater that existed post-dynamic rebound but pre-wall collapse. (B.L. Ristvet and E.L. Tremba, personal communications.)

TURBIDITE -- A sediment or rock deposited from, or inferred to have been deposited from, a turbidity current. It is characterized by graded bedding, moderate sorting, etc.

TURBIDITY CURRENT -- A density current in water, air, or some other fluid, caused by different amounts of matter in suspension. Specificially, it is a bottom-flowing current laden with suspended sediment, moving swiftly (under the influence of gravity) down a subaqueous slope and spreading horizontally on the floor of the body of water, having been set and/or maintained in motion by locally churned- or stirred-up sediment that gives the water a density greater than that of the surrounding or overying clear water.

UNCONFORMITY -- A general term for a break or gap in the sedimentary record where a rock unit is overlain by another that it not next in stratigraphic succession--that is, some strata are missing either due to nondeposition or erosion. (See disconformity).

WACKESTONE -- A term used by Dunham (1962) for a mud-supported sedimentary carbonate rock containing more than 10 percent grains (particles with diameters greatert than 20 microns). The term has been expanded to include uncemented carbonate sediments. (See mudstone, packstone, and grainstone.

ZONE OF SONIC DEGRADATION -- (Abbreviated **ZSD**; term introduced in Chapter 14.) That zone in which sonic velocity values are depressed below what would be expected from the same strata prior to the nuclear explosion. The ZSD represents units of rock and sediment that are fractured or shattered, mixed, and otherwise disturbed significantly enough to retard the sonic velocities (determined from the downhole, multichannel sonic logs) from their inferred pre-shot values. (See geologic crater.)

GLOSSARY REFERENCES CITED

Dunham, R.J., 1962, Classification of carbonate rocks according to depositional texture: p. 1-8-121, 7 pls., 1 tbl., in Ham, W.E., ed., Classificatin of Carbonate Rocks, A Symposium; American Association of Petroleum Geologists Memoir 1.

Embry, A.F., and Klovan, E.J., 1972, Absolute water depth limits of Late Devonian paleoecological zones; Geologisches Rundschau, v. 61, no. 23, p. 672-686, 10 figs.

Folger, D.W., ed., 1986, Sea-floor observations and subbottom seismic characteristics of OAK and KOA craters, Enewetak Atoll, Marshall Islands: U.S. Geological Survey Bulletin 1678, 301 p., 112 figs., glossary, 2 appendices.

Henry, T.W., Wardlaw, B.R., Skipp, B., Major, R.P., and Tracey, J.I., Jr., 1986, Pacific Enewetak Atoll Crater Exploration (PEACE) Program, Enewetak Atoll, Republic of the Marshall Islands; Part 1: Drilling operations and descriptions of boreholes in vicinity of KOA and OAK craters: U.S. Geological Survey Open-File Report 86-419, 497 p., 32 figs., 29 pls., 13 tbls., 3 appendices.

Roddy, D.J., 1977, Large-scale impact and explosion craters: Comparisons of morphological and structural analogs: p. 185-246, 10 figs., 2 tbls.; in Roddy, D.J., Pepin, R.O., and Merrill, R.B., eds., Impact and Explosion Cratering; Pergamon Press (New York).

Schlanger, S.O., 1963, Subsurface geology of Enewetok Atoll: U.S. Geological Survey Professional Paper 260-BB, p. 991-1066, pls. 281-288, figs. 306-318, 20 tbls. [with sections by other authors].

TABLE OF CONTENTS

TABLE OF CONTENTS (Continued)

TABLE OF CONTENTS (Continued)

FIGURE INDEX

FIGURE INDEX (Continued)

FIGURE INDEX (Continued)

TABLE INDEX

TABLE INDEX (Continued)

PACIFIC ENEWETAK ATOLL CRATER EXPLORATION (PEACE) PROGRAM
ENEWETAK ATOLL, REPUBLIC OF THE MARSHALL ISLANDS

Part 3: Stratigraphic analysis and other geologic and geophysical studies in vicinity of KOA and OAK craters

CHAPTER 1:

INTRODUCTION TO PART 3 OPEN-FILE REPORT

by

Thomas W. Henry[1] and Bruce R. Wardlaw[2]

U.S. Geological Survey

GENERAL REMARKS

This volume is the third in a series of U.S. Geological Survey (USGS) Open-File Reports presenting sets of geologic data, analyses, and interpretations for Phase II of the Pacific Enewetak Atoll Crater Exploration (PEACE) Program, conducted in cooperation with the Defense Nuclear Agency (DNA). Field work for Phase II (also called the Drilling Phase) was conducted jointly by the USGS, DNA, and the Department of Energy (DOE) on Enewetak Atoll, Marshall Islands (fig. 1-1) during the late winter through mid-summer of 1985. Phase I (Marine Phase) field work was executed the latter part of the previous summer by the USGS and supported by the DOE.

The purpose of the PEACE Program was to provide highly credible, multi-disciplinary set of geologic, geophysical, and material-properties data in order to identify crater dimensions and features for two high-yield nuclear craters (KOA and OAK, see figs. 1-1 and 1-2, respectively) and to better understand the dynamic processes that initially formed these craters and that subsequently modified them. These data are essential to the Department of Defense (DOD) to better understand the survivability of strategic defense systems in the event of a nuclear attack. The reader is referred to Henry, Wardlaw, and others (1986) and to Folger (1986b) for a more detailed discussion of the role of the USGS in the PEACE Program, of the participants and their responsibilities, of the setting of Enewetak and the Marshall Islands, of the history of previous geologic investigations, and of the events leading up to the program.

---

[1] Office of Regional Geology, Reston, VA.
[2] Branch of Paleontology & Stratigraphy, Washington, DC.

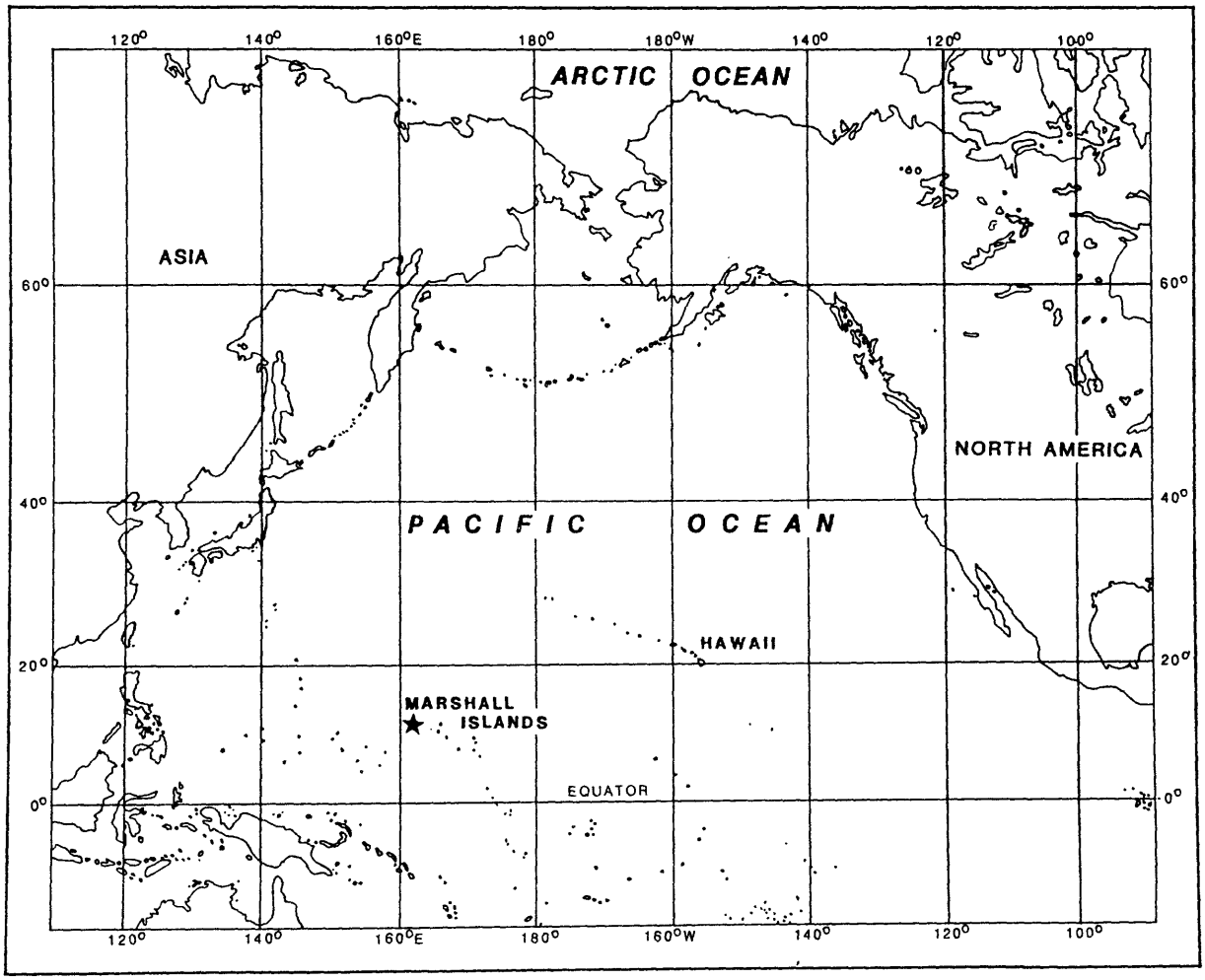

FIGURE 1-1. Location map of the Marshall Islands. Enewetak Atoll shown by small star.

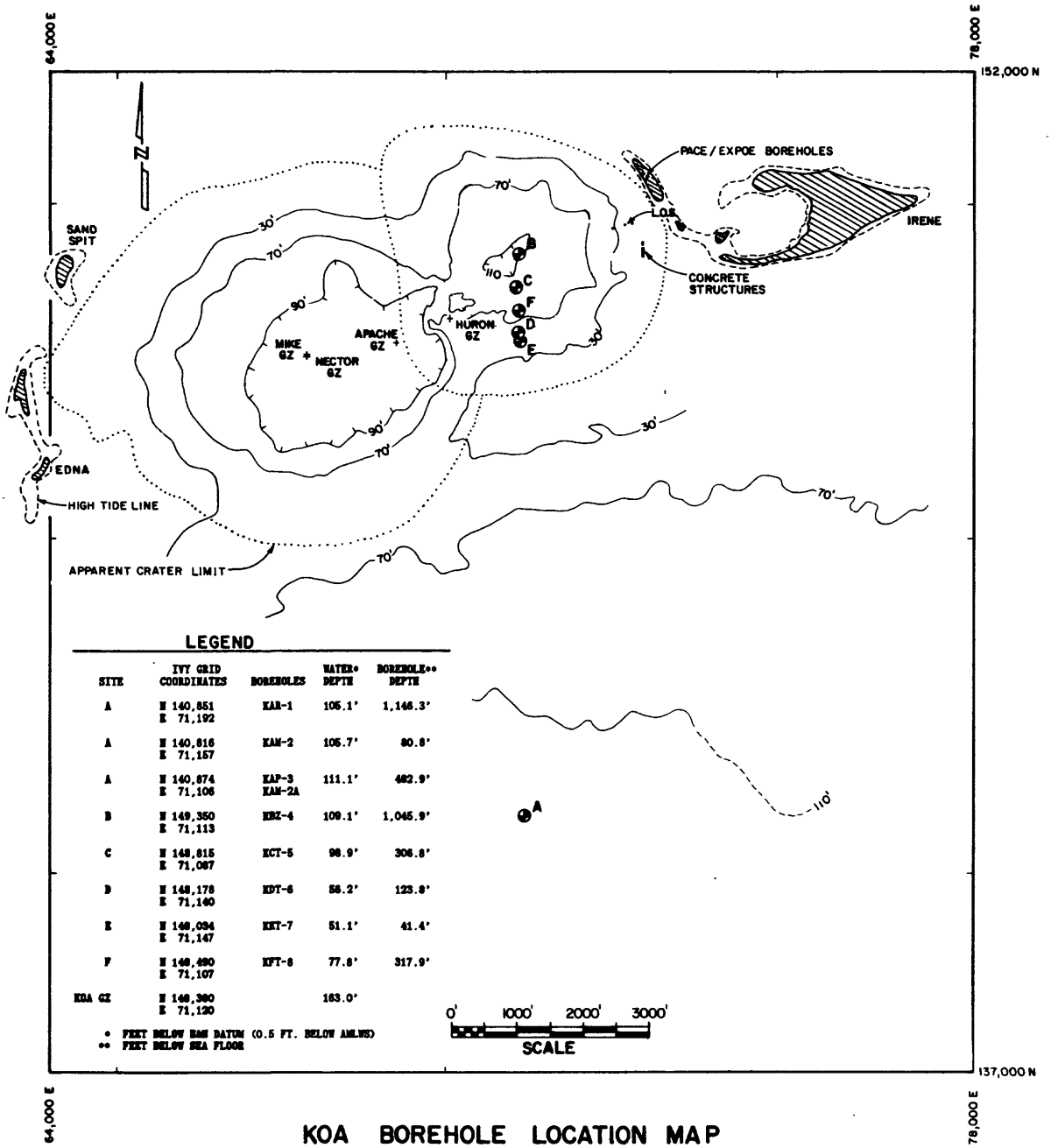

KOA BOREHOLE LOCATION MAP

FIGURE 1-2. -- Map of KOA crater showing borehole sites (depicted by letters) and general bathymetric contours (contours in ft, irregular intervals).

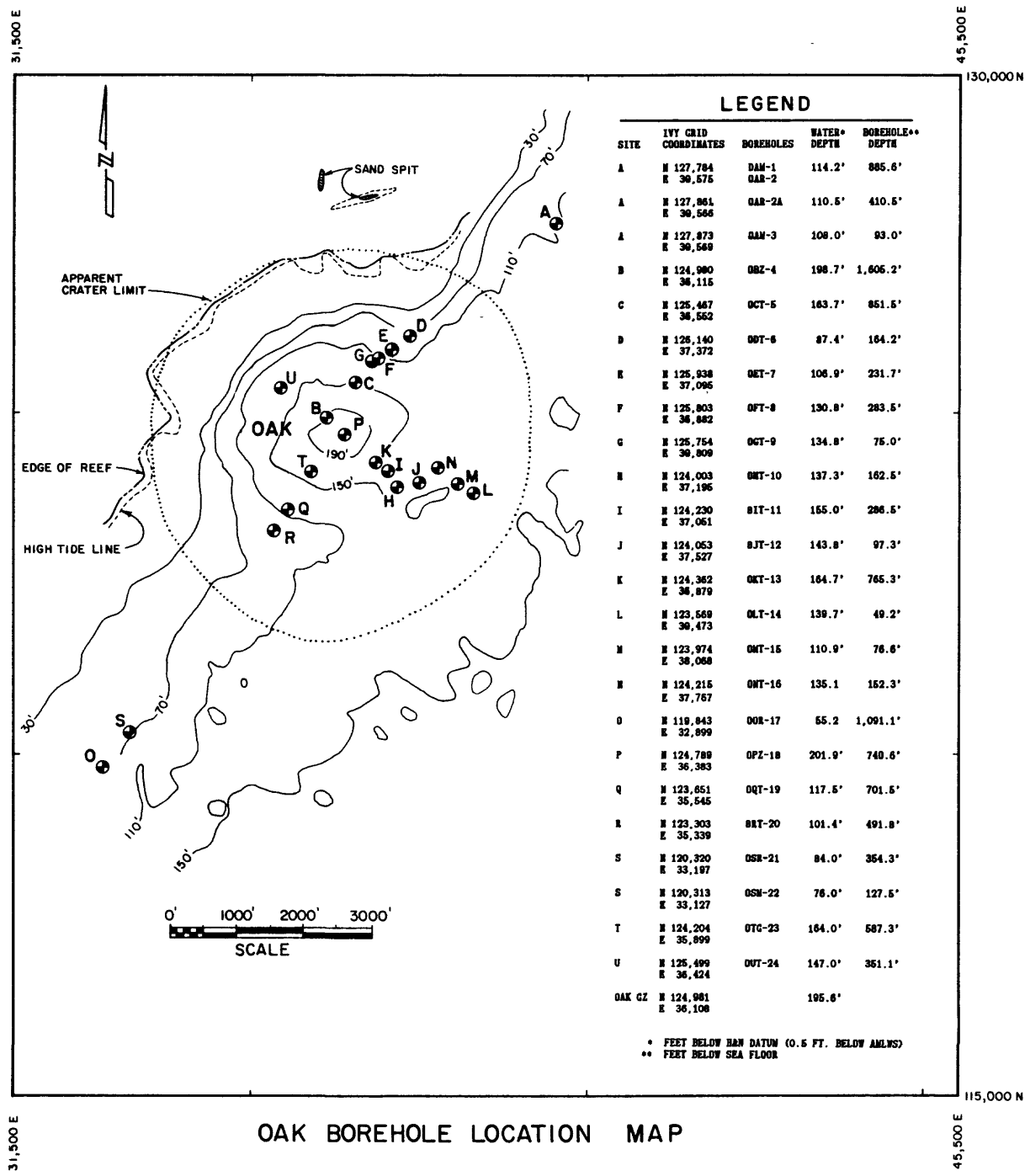

OAK BOREHOLE LOCATION MAP

FIGURE 1-3. -- Map of OAK crater showing borehole sites (depicted by letters) and general bathymetric contours (contour interval equals 40 ft).

USGS REPORTS

The PEACE Program originally was planned so that all field work was to be conducted concurrently. The geologic and geophysical investigations executed during the Marine Phase were to be done at the same time as the drilling and downhole geophysical logging (Drilling Phase of current terminology). For a number of reasons (see Henry, Wardlaw, and others, 1986, p. 26-27), it was not possible to field the drilling part of the program until the middle of January of 1985. This was approximately three months after the completion of the Marine Phase. Information from the Drilling Phase provides the subsurface geologic framework for the program and hence the ground-truth for the overwater geophysical investigation (single- and multichannel seismic and refraction studies) conducted during the Marine Phase. The conclusions drawn at the end the field work for the Marine Phase of the program are the best statements that could be made at that time. However, as in any scientific investigation, these conclusions are subject to revision. Thus, the editors emphasize the caveat that each of the USGS reports on the PEACE Program is a progress report on the data accumulated and analyzed prior to that specific publication. This statement also applies to the current report.

Most of the data sets and results of the Phase I (Marine Phase) are presented in USGS Bulletin 1678, released in March of 1986 and cited in the current Open-File Report as Folger (1986a).

> Folger, D.W., ed., 1986, Sea-floor observations and subbottom seismic characteristics of OAK and KOA craters, Enewetak Atoll, Marshall Islands: U.S. Geological Survey Bulletin 1678, 301 p., 112 figs., glossary, 2 appendices.

Bulletin 1678 is comprised of a series of multiauthored chapters on the bathymetry, the side-scan sonar survey, the single-channel seismic-reflection survey, the multichannel seismic-reflection survey, the seismic-refraction survey, observations from a two-man submersible, preliminary analyses of OAK debris samples, and scuba observations of the OAK and KOA craters and environs[1].

At the end of the Phase II field work for the PEACE Program, three USGS Open-File Reports were anticipated that would present the data and results of the Drilling Phase of the PEACE Program. However, because some of the Phase II data are still being analyzed by the USGS, a fourth Open-File Report will follow the current volume.

---

[1] Several investigations conducted during the Marine Phase were not reported in Bulletin 1678. These are included, at least in a preliminary fashion, in various Chapters of the current Open-File Report. These are: (1) the results of the pilot borehole gravity study conducted in the deep, island-based borehole (E-1) drilled by the USGS and the Atomic Energy Commission (AEC) in 1952 on Medren (ELMER) Island; (2) some of the sea-floor observations made from the submersible during the Marine Phase; and (3) the bottom (benthic) samples taken from the Enewetak lagoon in September of 1984.

The **first** of the four Open-File Reports--referred to in this volume as Henry, Wardlaw, and others (1986)--was released in August of 1986. Its complete bibliographic citation is:

> Henry, T.W., Wardlaw, B.R., Skipp, B., Major, R.P., and Tracey, J.I., Jr., 1986, Pacific Enewetak Atoll Crater Exploration (PEACE) Program, Enewetak Atoll, Republic of the Marshall Islands; Part 1: Drilling operations and descriptions of boreholes in vicinity of KOA and OAK craters: U.S. Geological Survey Open-File Report 86-419, 497 p., 32 figs., 29 pls., 13 tbls., 3 appendices.

In the report cited above, the procedures and drilling operations conducted from the drill ship M/V Knut Constructor in the vicinity of KOA and OAK craters (see figs. 1-2 and 1-3, respectively) in Enewetak lagoon are discussed, the lithic (geologic) descriptions of core/sample from the boreholes presented, and the drilling statistics and related data are appended. This report also includes a section (Appendix 2) in which is given the lithic (engineering) descriptions of the core/samples, compiled by the drilling subcontractor, McClelland Engineers, Inc., of Houston, TX.

The **second** Open-File Report (Cronin, Brouwers, and others, 1986) was released by the USGS in February and is a presentation of most of the paleontologic and biostratigraphic data and analyses of the core/sample for the PEACE Program. The complete citation for this report is:

> Cronin, T.M., Brouwers, E.M., Bybell, L.M., Edwards, E.E., Gibson, T.G., Margerum, R., and Poore, R.Z., 1986, Pacific Enewetak Crater Exploration (PEACE) Program, Enewetak Atoll, Republic of the Marshall Islands; Part 2: Paleontology and biostratigraphy application to OAK and KOA craters: U.S. Geological Survey Open-File Report 86-159, 39 p., 20 figs., 12 tbls., 3 appendices.

This paper also includes discussions of the details of the biostratigraphic framework for the upper 1,500 ft of section on Enewetak Atoll, the purpose of the paleontologic investigations, the sample and laboratory methodology, the data management, and the application of the biostratigraphy to crater-mixing studies.

The **third** report in this companion series of USGS Open-File Reports is the current volume. It consists of fourteen interrelated chapters entitled and authored as follows:

Chapter 1: Introduction to Part 3 Open-File Report (Henry and Wardlaw).

Chapter 2: Stratigraphic Framework (Wardlaw and Henry).

Chapter 3: Strontium-Isotope Stratigraphy of Undisturbed and Disturbed Carbonates (Ludwig, Halley, Simmons, and Peterman).

Chapter 4: X-ray Diffraction Mineralogy of Samples from Selected Boreholes (Tremba and Ristvet).

Chapter 5: Organic Geochemistry Studies of Selected Boreholes (Ristvet and Tremba).

Chapter 6: Insoluble Residues from Selected Boreholes (Ristvet and Tremba).

Chapter 7: Downhole Geophysical Logs (Melzer).

Chapter 8: Preliminary Density and Porosity Data and Field Techniques of Borehole Gravity Survey, OAK Crater (Beyer, Ristvet, and Oberste-Lehn).

Chapter 9: Seismic-Reference Surveys (Tremba and Ristvet).

Chapter 10: Benthic Samples from Enewetak Lagoon and Craters (Wardlaw, Henry, and Martin).

Chapter 11: Additional Paleontologic Studies of OAK and KOA Craters (Brouwers, Cronin, and Gibson).

Chapter 12: Radiation Chemistry of OAK and KOA Craters (Ristvet and Tremba).

Chapter 13: Additional Sea-Floor and Subbottom Characteristics of OAK and KOA Craters (Slater, Halley, Folger, Shinn, and Roddy).

Chapter 14: Geologic Interpretation of OAK and KOA Craters (Wardlaw and Henry).

The **fourth** USGS Open-File Report, anticipated early in calendar year 1987, will contain the results of the borehole gravity modeling and miscellaneous other geologic and geophysical analyses that were ongoing at the time that the current report was written. Results of the analyses of the downhole geophysical logs and the material properties studies will be published by one of the DNA contractors.

PROGRAM FIRSTS

The PEACE Program has produced a number of major technologic and scientific breakthroughs or "firsts":

* The first boreholes successfully drilled overwater within a high-yield nuclear crater (and in a carbonate terrain with a high recovery of sample and core).

* The first side-scan sonar photomosaics of a water-filled nuclear crater.

* The deepest "continuous" core/sample borehole drilled in the Marshall Islands (borehole OBZ-4, drilled to 1,805.2 ft below sea level in 200 ft of water). The boreholes drilled in the early 1950's on Enewetak Atoll (Emery, Tracey, and Ladd, 1956) were the deepest drilled; however, recovery from those boreholes was poor and not continuous. Much of the lithic descriptions were from cuttings.

* The first successful borehole gravity measurements made on a coral atoll and the first successful use of a slimline borehole gravity tool overwater from a drill ship.

* The first detailed biostratigraphic analyses of near-reef facies of an atoll, and the first widespread application of ostracodes in biostratigraphic analyses of a coral atoll.

SUMMARY OF PRINCIPAL CONCLUSIONS

The PEACE Program was a multidisciplinary geologic, geophysical, and material-properties study. With this wide array of disciplines brought to focus on program objectives, a much stronger set of conclusions can be made about: (1) the initial development of excavational craters in generally uncemented, water-saturated, carbonate terrains, (2) the subsequent, longer-term (hours to months) modification of these craters by gravity-induced forces set in operation by the detonations themselves, and (3) modification of these craters--particularly KOA--by even longer term processes. Current work by the USGS verifies many of the tentative major conclusions reached by Projects PACE/EXPOE (1970-74) (Couch and others, 1975; Ristvet and others, 1978) and EASI (1979-81) (Tremba, Couch, and Ristvet, 1982; Tremba, 1984), sponsored by the Air Force Weapons Laboratory (AFWL) and conducted on Enewetak Atoll. However, most of these conclusions are modified by the current investigations.

The principal conclusions (i.e., those of greatest interest to strategic planners within the DNA and the Department of Defense (DOD) from the USGS investigations of the high-yield nuclear craters OAK and KOA are given below and are amplified in subsequent Chapters of the current report, particularly Chapter 14.

- A number of the physiographic features observed in the submarine KOA and OAK craters are similar to those in land-based, high-explosive, low-yield nuclear, and terrestrial impact craters created in generally air-saturated, silicate terrains.

- KOA and OAK are very similar to each other in size and shape. Both had excavational craters significantly smaller than the apparent craters.

- Long-term phenomena dominate the formation of the present crater configuration. Major factors that modified the excavational crater are:

  - Major failure of the sidewalls of the excavational crater and consequent enlargement of the crater laterally.

  - Shock-induced liquefaction, consolidation, and subsidence in the sub-crater region.

  - Consequent subsidence of the region below and adjacent to the excavation.

  - Piping of liquefied materials, including pebble- and small cobble-sized particles, toward and to the surface.

- The current level of the base of the excavational crater (it was lowered by consolidation and subsidence) beneath the present-day crater is identified by:
  - Maximum depth of mixing of rock and fossil material from different stratigraphic layers.
  - Depth to the layer of highly shocked/pulverized sand (known as the "transition sand"[1]) that produces a strong kick in the natural-gamma logs partly resulting from presence of bomb-produced ("refractory") radioactive isotopes.
  - The multichannel-seismic-reflection profiles across the crater. These cross sections provide a more continuous three-dimensional picture of atoll sedimentary facies and generalized crater features, but they can be misleading in the absence of geologic data from the drill holes.
- Apparently large (but difficult to estimate) volumes of material were brought to the surface or "piped" from stratigraphic levels far below the base of the excavational craters in both OAK and KOA. Some of this material was piped along conduits from as deep as 900 ft below sea level.
  - More material probably was brought to shallow subsurface or surface levels in OAK crater than in KOA, which is characterized apparently by a narrower vertical zone in which piping occurred.
  - Piped material comes from as low as biostratigraphic zone LL in both craters (see Cronin, Brouwers, and others, 1986, and Chapters 11 and 14 of current report.)
- Base of zone of recognizable fracturing beneath each crater is delimited by base of zone of sonic degradation (i.e., depth at which downhole sonic-velocity logs return to normal from depressed values). The base of the zone of sonic degradation corresponds closely to the level at which strata are at pre-shot elevations as estimated from stratigraphic analysis. The refraction and multichannel-reflection data show a similar although slightly greater depth to the base of the zone of recognizable fracturing.

---

[1] The transition sands are preserved only under the central part of the crater (see Chapter 14 for discussion).

- Determination of depth of origin of debris within crater-fill and ejecta outside crater can be done with both strontium-isotope and paleontologic analyses (see Chapters 3 and 11, respectively). These techniques are complementary, each working best on different types and classes of materials.

  - Most of the larger clasts of ejecta and debris are more easily depth-zoned by strontium-isotope analyses.

  - Micropaleontologic analyses, on the other hand, can more quickly and inexpensively depth-zone large numbers of samples of sand- and finer-sized material than can isotopic analysis.

  - Most ejecta/debris lithoclasts are altered diagenetically and composed of calcite. Sr-isotope analyses can depth-zone this material successfully; paleontologic analyses cannot readily date such materials.

- Depth-of-origin studies can be combined with "shock-metamorphic" studies of the same samples[1] and may yield a more detailed picture of the pressure-regime distribution in the early-stage development of the excavational crater than thought possible.

MISCELLANEOUS

Table 1-1 presents the distances and bearings between key boreholes along various transects and radials for both OAK and KOA craters and general related information. This table has been corrected for the best estimate of the location of borehole OLT-14. It is emphasized that borehole OLT-14 was not located by Meridian Oceans Systems (MOS) navigators using the Motorola Miniranger System while this borehole was being drilled (see Henry, Wardlaw, and others, p. 390-391). The best estimate of the location of this borehole (IVY-Grid 123,569 ft N and 038,473 ft E) is based on a combination of knowledge of water depth at the site (139.7 ft below H&N datum), the position of the drill ship relative to several nearby prominent submarine features, and the distance and direction that the ship was moved from the previous borehole. The IVY-Grid location presented above is not the same as reported in USDOE (1985) and in communications from the drill ship to various interested parties stateside.

The key nomenclature presented for disconformities and discontinuities in Chapter 2 and used in Chapter 14 of the current report is not the same as the nomenclature labeled "major disconformity numbers" in the figures of the multichannel-seismic profiles or cross sections across KOA and OAK craters by Grow, Lee, and others (1986, for KOA, p. 14-19 and especially figs. 12B and 13B; and for OAK, p. 29-41 and figs. 22B through 30B and 31B through 34B). The terminology for the stratigraphic horizons was being developed at the time that the geophysical profiles were being analyzed. For clarification, the reader is referred to Chapter 14 and specifically to Table 14-6.

---

[1] These studies are being conducted at the California Institute of Technology.

TABLE 1-1. -- Distances and bearings between key boreholes for PEACE-Program crater transects (B.L. Ristvet, written communication, June 13, 1986; amended oral communication, September 3, 1986).

DISTANCES/BEARINGS BETWEEN KEY BOREHOLES

BOREHOLE (FROM/TO)	DISTANCE (FT)	BEARING (DEGREES)
General:		
OAR-2 TO KAR-1	34,211	067.5
OOR-17 TO KAR-1	43,677	061.2
OOR-17 TO OAR-2	10,374	040.0
OBZ-4 TO KBZ-4	42,664	055.1
KOA Radial:		
KBZ-4 TO KAR-1	8,499	179.5
KBZ-4 TO KCT-5	536	182.8
KCT-5 TO KFT-8	407	177.4
KFT-8 TO KDT-6	314	172.0
KDT-6 TO KET-7	141	177.2
OAK CRATER, Northeastern Radial:		
OBZ-4 TO OAR-2	4,454	51.0
OBZ-4 TO OCT-5	654	041.9
OCT-5 TO OGT-9	385	041.8
OGT-9 TO OFT-8	88	056.1
OFT-8 TO OET-7	252	057.6
OET-7 TO ODT-6	343	053.8
ODT-6 TO OAR-2	2,727	053.8
OAR-2 TO OAR-2A	76	353.3
OAK Crater, Northwestern-Southeastern Transect:		
OUT-24 TO OBZ-4	864	143.1
OBZ-4 TO OPZ-18	329	125.4
OPZ-18 TO OKT-13	655	130.7
OKT-13 TO OIT-11	217	127.5
OIT-11 TO OHT-10	269	147.6
OHT-10 TO OJT-12	336	081.5
OJT-12 TO ONT-16	290	056.0
ONT-16 TO OMT-15	386	128.6
OMT-15 TO OLT-14	309	121.8
OAK Crater, Southwestern (Borehole-Gravimetry) Transect:		
OPZ-18 TO OTG-23	759	219.6
OTG-23 TO OQT-19	657	212.6
OQT-19 TO ORT-20	404	210.6
ORT-20 TO OSR-21	3,674	215.7
OSR-21 TO OOR-17	562	212.0

REFERENCES CITED

Couch, R.F., Jr., Fetzer, J.A., Goter, E.R., Ristvet, B.L., Tremba, E.L., Walter, D.R., and Wnedland, V.P., 1975, Drilling operations on Eniwetok Atoll during Project EXPOE: Air Force Weapons Laboratory Technical Report AFWL-TR-75-216, Kirtland Air Force Base, New Mexico, 270 p., 17 figs., 4 tbls. (unclassified).

Cronin, T.M., Brouwers, E.M., Bybell, L.M., Edwards, E.E., Gibson, T.G., Margerum, R., and Poore, R.Z., 1986, Pacific Enewetak Crater Exploration (PEACE) Program, Enewetak Atoll, Republic of the Marshall Islands; Part 2: Paleontology and biostratigraphy application to OAK and KOA craters: U.S. Geological Survey Open-File Report 86-159, 39 p., 20 figs., 12 tbls., 3 appendices.

Folger, D.W., ed., 1986a, Sea-floor observations and subbottom seismic characteristics of OAK and KOA craters, Enewetak Atoll, Marshall Islands: U.S. Geological Survey Bulletin 1678, 301 p., 112 figs., glossary, 2 appendices.

Folger, D.W., 1986b,.Introduction to the volume; 7 p., 2 figs., 2 tbls.; in Folger, D.W., ed., Sea-floor observations and subbottom seismic characteristics of OAK and KOA craters, Enewetak Atoll, Marshall Islands: U.S. Geological Survey Bulletin 1678.

Grow, J.A., Lee, M.W., Miller, J.J., Agena, W.F., Hampson, J.C., Foster, D.S., and Woellner, R.A., 1986, Multichannel seismic-reflection survey of KOA and OAK craters; 46 p., 39 figs., in Folger, D.W., ed., Sea-floor observations and subbottom seismic characteristics of OAK and KOA craters, Enewetak Atoll, Marshall Islands: U.S. Geological Survey Bulletin 1678.

Henry, T.W., Wardlaw, B.R., Skipp, B., Major, R.P., and Tracey, J.I., Jr., 1986, Pacific Enewetak Atoll Crater Exploration (PEACE) Program, Enewetak Atoll, Republic of the Marshall Islands; Part 1: Drilling operations and descriptions of boreholes in vicinity of KOA and OAK craters: U.S. Geological Survey Open-File report 86-419, 497 p., 32 figs., 29 pls., 13 tbls., 3 appendices.

Ristvet, B.L., Tremba, E.L., Couch, R.F., Jr., Fetzer, J.A., Goter, E.R., Walter, D.R., and Wendland, V.P., 1978, Geologic and geophysical investigations of the Enewetak nuclear craters; Final reports: Air Force Weapons Laboratory Technical Report AFWL-TR-77-242, Kirtland Air Force Base, New Mexico, 298 p. (unclassified).

Tremba, E.L., 1984, Enewetak Atoll Seismic Invesitgation (EASI); PHASE III: Air Force Weapons Laboratory Technical Report AFWL-TR-84-105, Air Force Systems Command, Kirtland Air Force Base, New Mexico, 152 p., 36 figs., 11 tbls. (unclassified).

Tremba, E.L., Couch, R.F., Jr., and Ristvet, B.L., 1982, Enewetak Atoll Seismic Investigation (EASI); Phases I and II: Air Force Weapons Laboratory Technical Report AFWL=TR-82-20, Kirtland Air Force Base, New Mexico, 124 p., 38 figs., 3 tbls., 3 appendices (unclassified).

USDOE, 1985, Pacific Enewetak Atoll Cratering Exploration; Completion report; U.S. Department of Energy, Nevada Operations Office Report NVO-294, prepared by Holmes and Narver, Inc., Energy Support Division, Las Vegas, Nevada; 15 p., 2 figs., 1 tbl., 3 appendices.

CHAPTER 2:

PHYSICAL STRATIGRAPHIC FRAMEWORK

by

Bruce R. Wardlaw[1] and Thomas W. Henry[2]

U.S. Geological Survey

INTRODUCTION

The history of previous geologic investigations on Enewetak Atoll is discussed in detail in Henry, Wardlaw, and others (1986, p. 15-28). Nevertheless, it is appropriate to summarize briefly here the results of the earlier geologic studies that led to the development of the stratigraphic framework that had evolved for Enewetak and Bikini prior to the PEACE Program.

Previous Stratigraphic Studies. -- Drilling of three deep boreholes on Enewetak Atoll in the early 1950's by the U.S. Geological Survey (USGS) and the Atomic Energy Commission (AEC) revealed that about 4,500 ft of sedimentary, carbonate cap overlies an olivine-basalt volcanic basement. Those boreholes and two other deep holes drilled on Bikini a few years earlier provided the primary data base for the first stratigraphic framework for atolls in the central part of the Pacific Basin (Emery, Tracey, and Ladd, 1954). That the two sets of boreholes correlate closely demonstrated that Bikini and Enewetak had similar geologic histories (fig. 2-1).

The stratigraphic sequence overlying the volcanic basement of Enewetak and Bikini is characterized by thick units of leached, altered, cemented, calcite-rich carbonate rock (predominantly limestone) alternating with thick intervals of unleached, unaltered, uncemented, aragonite-rich carbonate sediments (fig. 2-1). Emery, Tracey, and Ladd (1954) and Schlanger (1963) noted that each of the cemented rock units grade downward into unaltered, uncemented zones of sediment. Commonly, the tops of the lithified units are sharp and exhibit dissolution and microkarstic features. Called "solution unconformities" by Schlanger (1963, p. 994), their formation was attributed to diagenetic changes that occurred at times when sea level was much lower than at the present and the atolls were emergent. It was noted that these major solution surfaces generally coincided with breaks in the faunal succession, indicating that periods of nondeposition and probably even erosion had punctuated the sedimentary history of the atolls.

---

[1] Branch of Paleontology and Stratigraphy, Washington, DC.
[2] Office of Regional Geology, Reston, VA.

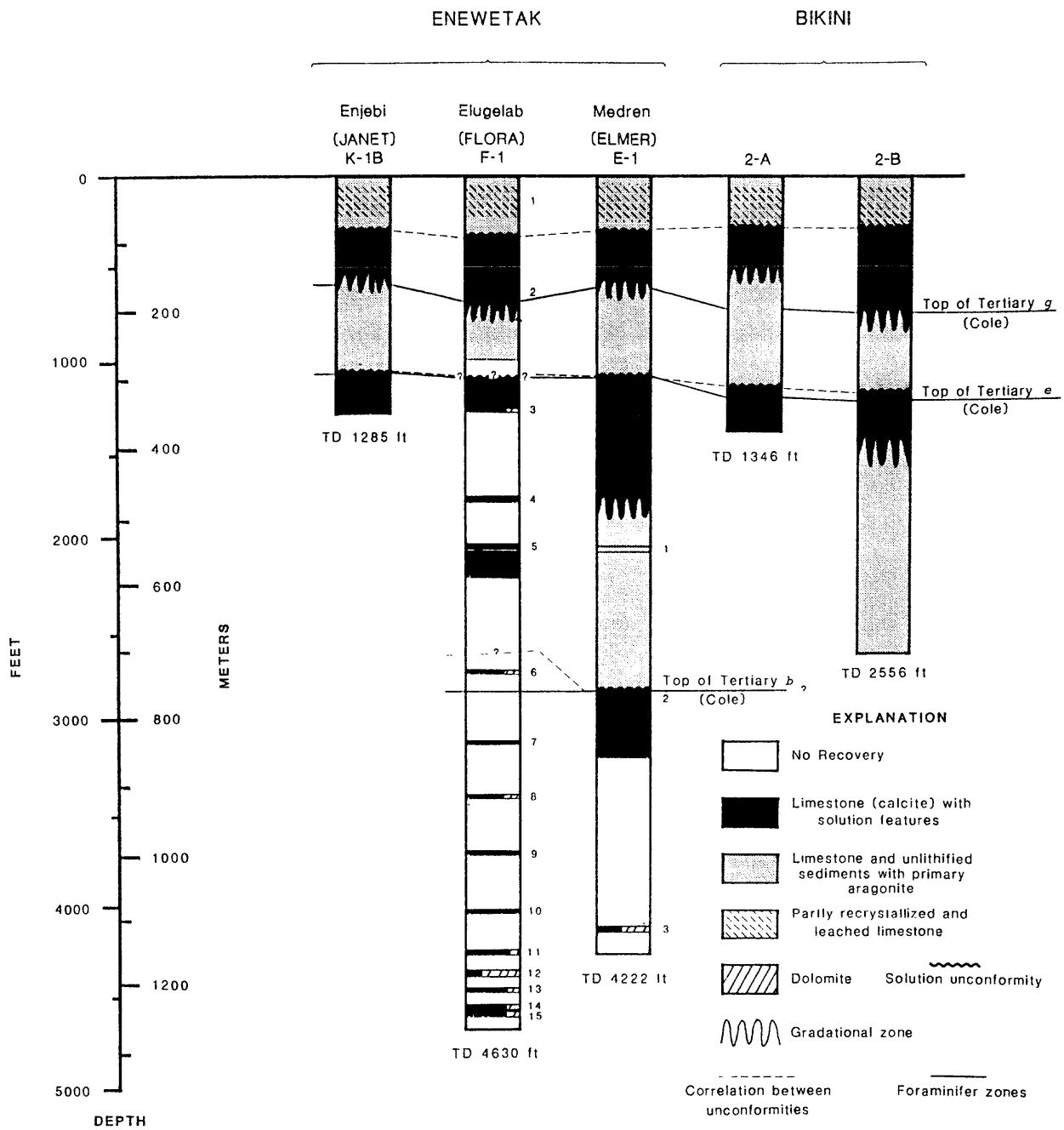

FIGURE 2-1. -- Correlation of USGS/AEC deep boreholes drilled on Enewetak and Bikini Atolls, showing zones of unaltered material and recrystallized and partly dolomitized intervals (from Schlanger, 1963, fig. 308).

Additional shallow boreholes (i.e., less than 300 ft deep) were drilled on the islands of Enewetak between 1970 and 1974 by the Air Force Weapons Laboratory (AFWL). The two programs, PACE and EXPOE, under which the boreholes were drilled, were designed to evaluate the generalized lithofacies differences between the leeward, windward, and transitional islands of the atoll and to evaluate the smaller scale geologic variation in borehole transects taken parallel and orthogonal to the reef front in the areas of interest to the cratering studies. The results of the PACE and EXPOE Programs are presented in Tremba, Couch, and Ristvet (1982) and Couch and others (1975), respectively. The general lack of lithofacies variation in transects parallel to the reef front and the marked lateral facies changes between boreholes in transects orthogonal to the reef front suggested that the atoll subsurface could be modeled successfully by comparing reefward to lagoonward facies (Couch and others, 1975, p. 23).

The PACE/EXPOE Programs did not include biostratigraphic analyses. Nevertheless, the new data base permitted far greater lithostratigraphic resolution in the upper 300 ft of section on Enewetak than the previous work, and six solution unconformities ultimately were recognized (Ristvet, Couch, and Tremba, 1980; see fig. 2-2 of current Chapter). These unconformities sloped gently lagoonward from the islands and were also interpreted as old subaerial-exposure surfaces correlatable with major glacially induced lowstands of sea level. They are commonly characterized by paleosols (laminated crusts, iron-staining, etc.), black manganese pore and cavity coatings, and dissolution features (karst). The borehole transects documented in the subsurface the general decrease in cementation from the oceanward edge of the reef through the islands and toward the lagoon (fig. 2-2).

General Comments. -- Other investigations, not related to Enewetak, have demonstrated that cementation occurs in two basic modes in a carbonate sequence on a coral atoll: (1) as various types of carbonate cements related to the exposure surfaces and the dissolution and reprecipitation of carbonate by meteoric waters and the complex of subsurface air/water and fresh-water/seawater interfaces and (2) as marine cements emplaced generally along the reef front effectively armoring the exterior of the atoll. Exposure surfaces can be atoll-wide or local, depending on a variety of factors, and a complex array of cementation histories or overprints and depths of effects can be produced by them.

Ongoing studies of the petrography, stable carbon and oxygen isotopes[1], and mineralogy of the PEACE Program core/samples are permitting differentiation of many of these factors and providing information on the global sea-level events related to them. Combined with the biostratigraphic and strontium-isotope correlations with the global geologic time scale, a more comprehensive geologic history of atoll formation and evolution will follow. However, the authors stress that these studies are ongoing, the data bases are being refined, and the stratigraphic framework presented in this Chapter is subject to revision.

---

[1] By R.K. Matthews and T.G. Quinn, at Brown University.

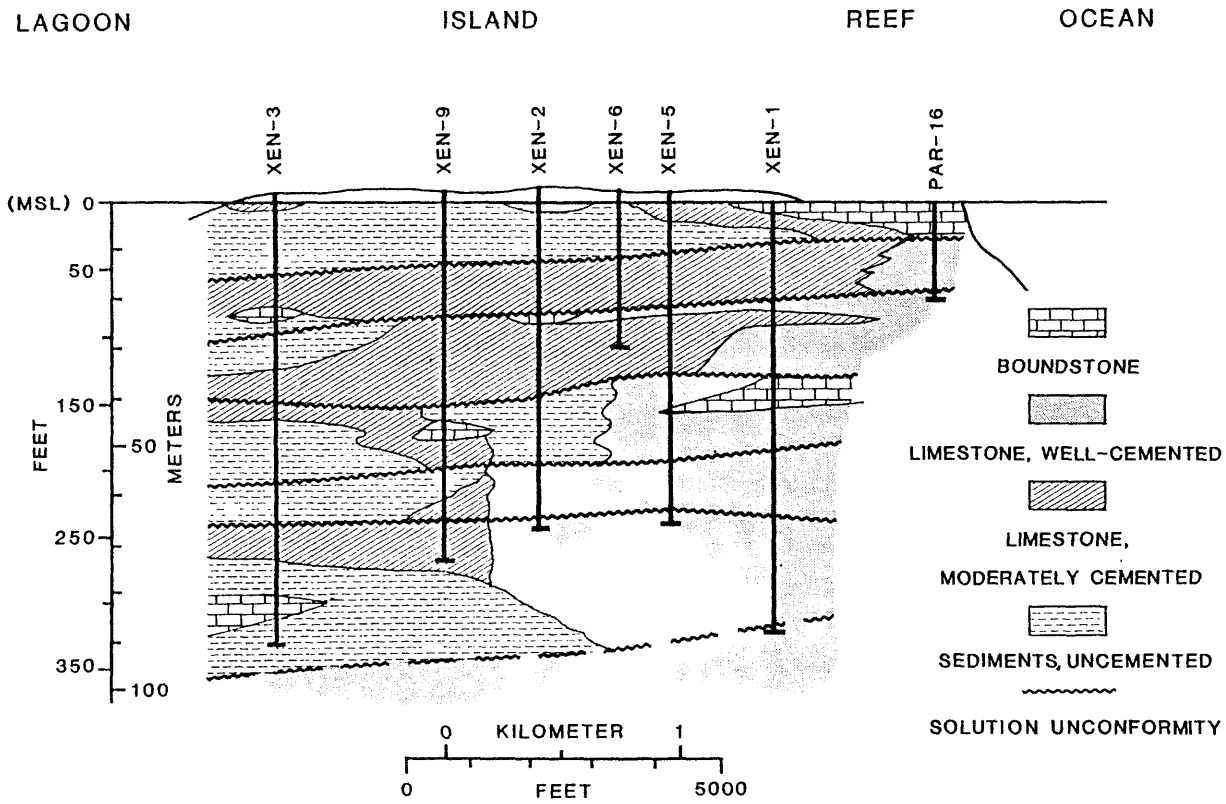

FIGURE 2-2. Geologic cross section from boreholes drilled perpendicular to reef front mainly on Enjebi (JANET) Island during EXPOE Project; section viewed looking northwestward (modified from Couch and others, 1975, fig. 15; reproduced from Henry, Wardlaw, and others, 1986, fig. 9). Note general increase in cementation toward ocean side of cross section.

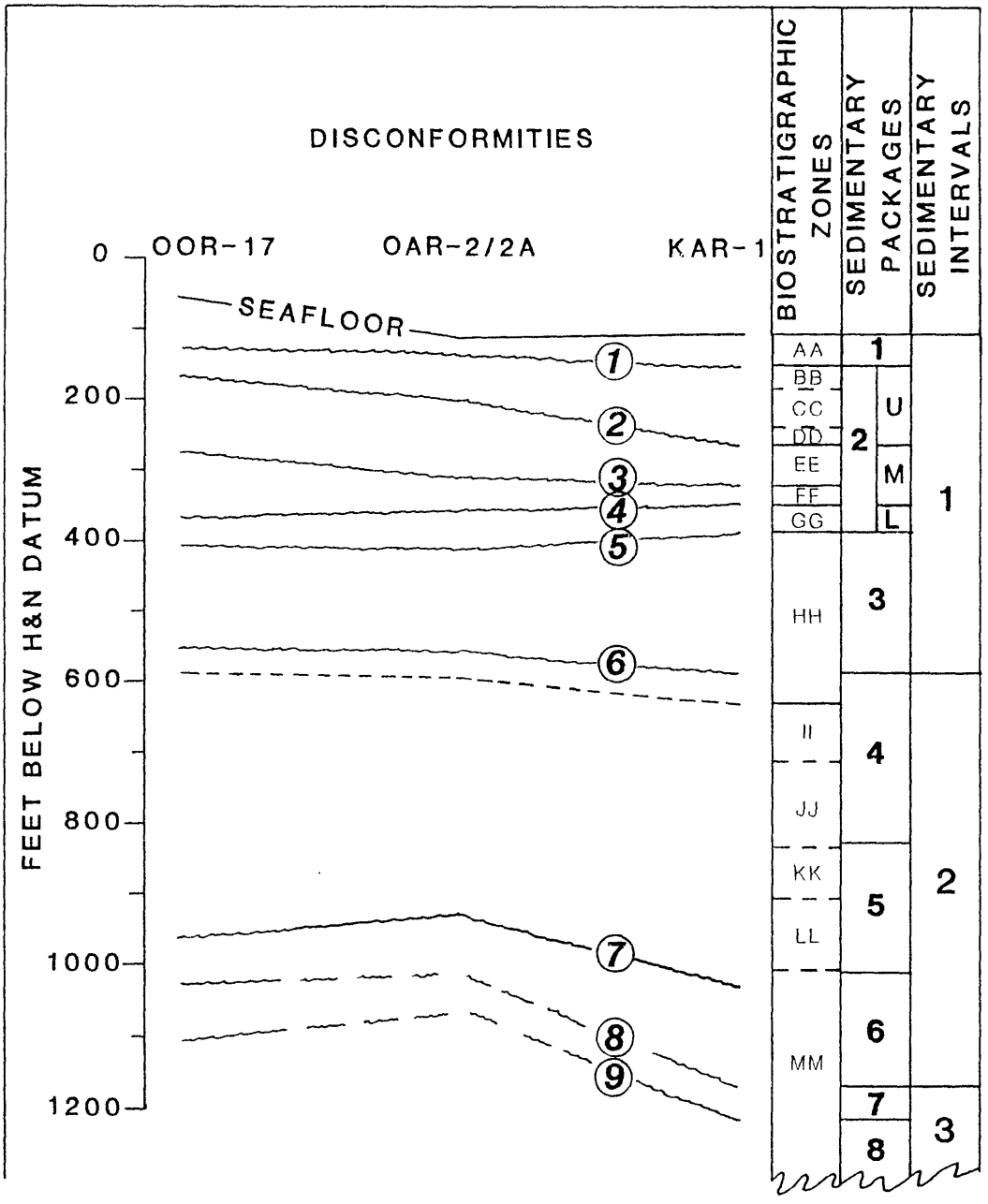

FIGURE 2-3. -- Generalized relationship of disconformities (circled), biostratigraphic zones, sedimentary packages, and sedimentary intervals for PEACE Program reference boreholes KAR-1, OAR-2/2A, and OOR-17. Interpretation of geologic age based on biostratigraphic data is preliminary. Borehole locations given in Figures 1-2 and 1-3.

STRATIGRAPHIC FRAMEWORK

The stratigraphic framework presented in this Chapter results from analyses of the lithic descriptions of the borehole core/samples from the PEACE Program (Henry, Wardlaw, and others, 1986), an assessment of previous stratigraphic investigations (i.e., Emery, Tracey, and Ladd, 1956; Schlanger, 1963; Couch, Fetzer, and others, 1965), including redescriptions of selected EXPOE/PACE core and samples. Combined with this is the vital, complementary information derived from the biostratigraphic analyses presented in Cronin, Brouwers, and others (1986) and in Chapter 11 of the current report. This biostratigraphic zonation is based on the studies of the evolutionary and ecologic changes in the faunas, primarily ostracodes and foraminifers, from the PEACE Program boreholes and selected EXPOE boreholes.

The authors point out that both the lithostratigraphic and biostratigraphic frameworks were developed primarily from the PEACE Program reference boreholes KAR-1, OAR-2/2A, and OOR-17. However, a series of secondary "reference" holes were used to supplement the stratigraphic framework, particularly in terms of the extent of the disconformities and other discontinuities, the lateral variability of the facies, and the changes in thickness of the various packages along various transects. These "secondary reference" boreholes are those in which the stratigraphic integrity of the sequence has not been affected by the nuclear explosions. In other words, the stratigraphic interval considered in these "secondary reference" boreholes is not mixed, although the horizons or surfaces themselves may not be at pre-shot elevations.

The upper approximately 1,250 ft of section on Enewetak can be subdivided conveniently into a series of eight sedimentary packages (SPs) or "formations" that form the basic physical stratigraphic framework, as shown in Figure 2-3. Figure 2-4 is a geologic cross section showing the correlation of the reference boreholes from EXPOE borehole XEN-3, located on Enjebi (JANET) Island in the northeastern corner of the atoll, west-southwestward through PEACE Program boreholes KAR-1, OAR-2/2A, and OOR-17. Note on Figure 2-4 that both the sedimentary packages (delimited by solid lines) and biostratigraphic zones (dashed lines), as would be expected, thicken and thin somewhat from borehole to borehole. Nevertheless, the sedimentary packages can be correlated easily from borehole to borehole (fig. 2-4), and these correlations are verified by the biostratigraphic data.

Preliminary geologic ages of the major stratigraphic units are also depicted in Figure 2-3. These ages represent preliminary interpretation of the paleontologic data.

The sedimentary packages (numbered 1 through 8 in fig. 2-3) are grouped into three major divisions (sedimentary intervals I, II, and III) that appear to reflect major events in the evolution of the atoll. The sedimentary packages are generally bounded by what are apparently widespread, major dissolution surfaces or disconformities, identified by circled arabic numerals

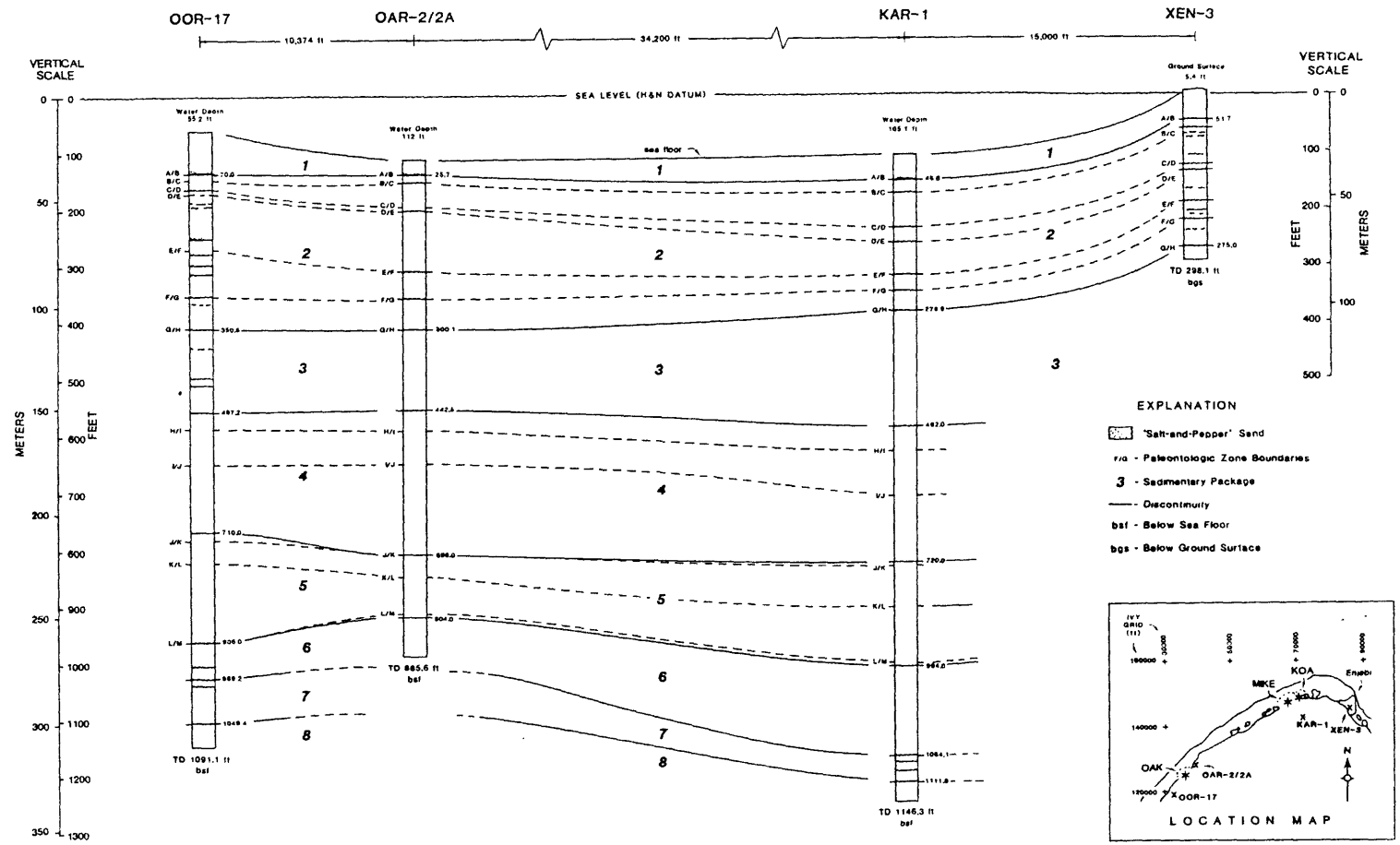

ENEWETAK REFERENCE HOLES

FIGURE 2-4. --Correlation of PEACE Program reference holes; sedimentary packages identified by italicized numbers, major disconformities and discontinuities by wavy lines (in boreholes) and solid lines, and biostratigraphic zones by dashed lines. Depths in holes given in ft below sea floor (bsf).

1 through 9 on Figure 2-3 and emplaced in parentheses in the text. Since the disconformities likely represent major hiatuses in the geologic history of the atoll, it is not surprising that they generally correspond to boundaries between some of the biostratigraphic zones. The exception to the statement that the sedimentary packages are bounded by disconformities are the three sedimentary packages (SPs 4, 5 and 6) that form sedimentary interval II (the organic interval), as discussed in a succeeding section.

In succeeding paragraphs, a generalized outline of the physical stratigraphic framework is presented. Additional discussions of the characteristics of each of the numbered disconformities, other sedimentary-package discontinuities, and generalized facies changes within these SPs are given later in the text.

Sedimentary Interval I. -- Sedimentary interval I ranges in age from the Recent to the Pliocene and is subdivided into three sedimentary packages (SPs 1, 2, and 3, from youngest to oldest). The top of sedimentary interval I is the contemporary land or sea-floor surface on the atoll, and disconformity (6) marks the base of this interval.

The types of sedimentary facies and their distribution of the modern sediments on Enewetak Atoll are discussed in Chapter 10 of this report. The strata of SP 1 generally mirror these modern, surficial sedimentary facies. In the reference boreholes that were drilled in the lagoon (KAR-1, OAR-2/2A, and OOR-17), these strata consists of uncemented Holocene sediments that are generally light-greenish-gray or yellowish-gray Halimeda, mollusc packstone and wackestone. In the island-based boreholes nearest the lagoon, SP 1 generally consists of skeletal carbonate sands (grainstone) in the beach areas, skeletal packstones to grainstones on the islands themselves, and coarse-grained gravels and rudstones to floatstones on the oceanward margin. In addition, the reef plate, which is marine-cemented reef facies, is part of the armor that envelopes the atoll. The variation in the degree of cementation in SP 1 (i.e., above the first disconformity in the section) is clearly shown in Figure 2-2.

As seen in Chapter 4, SP 1 strata are characterized by a high proportion of aragonite and high-magnesium calcite, attesting that these strata have not undergone extensive fresh-water diagenesis.

The uppermost (youngest) disconformity, labeled disconformity (1) in Figure 2-3, marks the base of SP 1 and divides the uncemented Holocene from the underlying sequence of generally uncemented sediments that contain thin cemented and leached zones of the upper part of the Pleistocene (SP 2). Disconformity (1) is equivalent to the AA/BB biostratigraphic zone boundary. Thus, the lithostratigraphic unit SP 1 and biostratigraphic zone AA are coincident.

Sedimentary package 2 is divided into upper, middle, and lower parts by disconformities (2), (3), and (4). Disconformity (2) corresponds to the DD/EE biostratigraphic zone boundary, and disconformity (4) to the FF/GG boundary (see fig. 2-3). Disconformity (3) is not as widespread (i.e., is not as easily recognized and/or may not be developed in all of the boreholes) as the

other disconformities. Where identifiable as a discrete surface, it is at or near the EE/FF boundary.

In the PEACE Program reference boreholes, SP 2 is generally very pale orange although it approaches white especially just beneath the disconformities where the strata have been leached. The marked decrease in metastable aragonite and high-magnesium calcite and corresponding increase in low-magnesium calcite in SP 2 compared with SP 1 is a striking feature of the stratigraphic section and is documented in Chapter 4.

Disconformity (5), coincident with the GG/HH biostratigraphic zone boundary, marks the boundary between SP 2 and SP 3. This disconformity separates the partly cemented sediments of the overlying Pleistocene section from the well-cemented, generally well-lithified, strongly diagenetically altered (leached) and karsted strata of the upper Pliocene. Sedimentary package 3 is the most structurally competent stratigraphic unit in the upper part of the section on Enewetak and greatly influenced the development of the craters (see Chapter 14). Whenever SP 3 has been encountered in drilling (in the early 1950's USGS/AEC boreholes and in the PACE/EXPOE and PEACE Programs), it has posed formidible challanges to continued drilling and sampling because of the large numbers of vugs, fissures, small caverns (many of them undoubtedly sediment-filled), and other dissolution or karst features contained in its upper part.

Sedimentary package 3 constitutes the bulk of biostratigraphic zone HH, which extends downsection into underlying strata. The extensive diagenetic alteration in this SP posed some problems in extracting identifiable microfossils to evaluate the faunas (see Cronin, Brouwers, and others, 1986).

Sedimentary Interval II. -- Sedimentary interval II extends from disconformity (6), marking the top of SP 4, and through SP 5 and SP 6 (figs. 2-3 and 2-4) in the Enewetak reference boreholes. Sedimentary interval II is also referred to as "the organic interval". Strata in this sequence are generally in marked color contrast to strata from either sedimentary intervals I or III.

The sedimentary packages comprising sedimentary interval 2 are divided arbitrarily on organic content. Unlike most of the rest of the section, the subdivisions are not coincident with disconformities. In fact, there are few disconformities and discontinuities in this interval.

Sedimentary package 5 contains the highest organic content, not necessarily in volatiles, but in lignitic material, is darker in color, and exhibits elevated gamma activity on the downhole logs (see Chapter 7). The SP 5 boundaries are defined by the top and bottom of the elevated gamma plateau in the gamma logs. A thin lignite bed occurs at the top of the SP 5 in one of the boreholes (KBZ-4), and fragments of lignitic wood occur commonly scattered in this sedimentary package. This SP was easily discerned in the old deep boreholes drilled on Enewetak and Bikini in the late 1940's and early 1950's (Emery, Tracey, and Ladd, 1954) in spite of the fact that the sample recovery throughout most of this interval was limited exclusively to cuttings. The

"charcoal" fragments that occur in the finer grained crater zone alpha and beta-1 (see Chapter 14) probably originated from within SP 5.

Disconformity (6), as mentioned above, separates the well-cemented rocks of the upper Pliocene (SP 3) and "middle" Pliocene (SP 4). This disconformity is one of the few "widespread" horizons in the Enewetak section that is not coincident with a major faunal change. Strata immediately under disconformity (6) are well cemented, leached, and otherwise strongly altered diagenetically; they grade downward into uncemented, unaltered sediments, containing a surprisingly high percentage of metastable aragonite (Chapter 4). The cemented interval at the top results in part from the diagnesis associated with disconformity (6), which was a subaerial-exposure surface. These strata may have been overprinted by later diagenetic effects, and in some instances, disconformity (6) is difficult to recognize. Disconformity (7) generally occurs a few tens of feet below the organically defined SP 5/6 boundary and the coincident LL/MM biostratigraphic zone boundary. No marked differences in the composition of the faunas accompany disconformity (7), suggesting that it represents little time or ecologic change, although it is a widespread surface.

The lower part of biostratigraphic zone HH corresponds to recrystallized, altered zone in the upper part of SP 4. As mentioned above, these faunas are generally poorly preserved. The HH/II biostratigraphic zone boundary corresponds closely to the bottom of the altered zone and the return of high aragonite content. The faunas in the remaining part of sedimentary interval II are highly diverse, generally very well preserved, and reflect major evolutionary events (Cronin, Brouwers, and others, 1986). They, like the other grain components of the organic interval, are colored with a brown organic stain and therefore can be recognized readily in samples from the upper parts of the craters (see Chapter 14).

Sedimentary Interval III. -- The lowest of the sedimentary intervals in the PEACE Program boreholes consists of sedimentary packages 7 and 8 (figs. 2-3 and 2-4). The deepest borehole drilled during this program on Enewetak (OBZ-4) extended slightly below 1,800 ft below the H&N datum. However, for purposes of the current report, the base of SP 8 is open-ended, because strata below about 1,250 ft have not been studied extensively and material is available only from one borehole.

Disconformity (8) separates the generally uncemented sediments of SP 6 (upper Miocene) from the partly cemented upper Miocene and possible lowest middle Miocene strata of SP 7. Disconformity (9) separates the partly cemented lower Miocene from well cemented and extensively recrystallized and sparsely dolomitic lower Miocene sediments of SP 8. Disconformities (8) and (9) are within biostratigraphic zone MM, characterized by abundant Lepidocyclina and other large foraminifers. Zone MM is the least-studied biostratigraphic zone in the PEACE Program. Changes in the larger foraminifers may be significant at disconformities (8) and (9) but data are sparse.

DISCONFORMITIES AND DISCONTINUITIES-- ADDITIONAL CRITERIA FOR RECOGNITION

The following section consists of a more detailed discussion of the characteristics of the numbered disconformities developed in the preceeding section, of the physical discontinuities that occur in the stratigraphic section between the numbered disconformities, of the criteria for their recognition in the PEACE Program boreholes, and preliminary conjecture on their significance. Also discussed is the relationship between these disconformities/discontinuities and the major seismic reflectors recognized during the Marine Phase of the PEACE Program (refer to Grow, Lee, and others, 1986, for the multichannel-seismic analysis, and to Robb and others, 1986, for the single-channel-seismic analysis). The correlation between the borehole lithology and the seismic reflectors is shown in Figures 2-8, 2-9, and 2-10, located at the end of this Chapter.

As mentioned previously, those surfaces that are widespread (i.e., can be recognized in most of the Enewetak boreholes), and that seem to represent major changes in the sedimentary history of the atoll are referred to in this report as disconformities. Other discontinuities in these boreholes do not appear to be as widespread. Some of these discontinuities in reality may be minor (local) subaerial exposure surfaces; others may reflect the physical changes induced by the interaction between fresh-water/seawater interfaces; others may be the tops of zones in which marine cementation occurred.

Figure 2-5a illustrates the disconformities and discontinuities for sedimentary packages 1 and 2, based on PEACE Program reference holes OOR-17, OAR-2A, and KAR-1; EXPOE borehole XEN-3; OAK "secondary reference" boreholes OSR-21, ORT-20, OQT-19, OLT-14, OIT-11, OET-7, and ODT-6; and KOA "secondary reference" hole KDT-6. In general, this is a west-southwest to east-northeast transect. Note that the boreholes are depicted as equidistant and that the elevations to the disconformities (numbered in parentheses) and discontinuities are in ft below the H&N datum. Thus, for the boreholes near the crater, these surfaces are lower than they were pre-blast. The authors re-emphasize that, in all of these boreholes, strata of SPs 1 and 2 have stratigraphic integrity (i.e., were not mixed by the dynamic effects of the nuclear events).

The disconformities/discontinuities of SP 3 and the upper part of SP 4 are shown in Figure 2-6, based on reference holes OOR-17, OAR-2, and KAR-1 and OAK holes ORT-20, OQT-19, OKT-13, AND OCT-5. Figure 2-7 shows comparable surfaces for SPs 5, 6, 7, and 8, based only on OOR-17, OBZ-4, OAR-2A, KAR-1, and KBZ-4. These two figures are located several pages farther in the text.

Disconformity (1). -- (AA/BB boundary, SP 1/2 boundary, R10 single-channel seismic reflector). This disconformity is represented by an increase in alteration of skeletal components below it (see Chapter 4) It can be commonly defined visually by the bleaching of the moderate-red or crimson, colonial foraminifer Homotrema in the overlying Holocene strata to pale red or white below this surface and by the change in Halimeda grains from "crisp" to "chalky". Very sparse microrhizoliths are noted in a few of the lagoon boreholes. Strata immediately below this disconformity in most of the lagoon boreholes are characterized by medium-gray to medium-bluish-gray stain and pore filling (phosphatic? or manganese? coatings); strata just above the surface commonly contains reworked microfossils (commonly partial internal

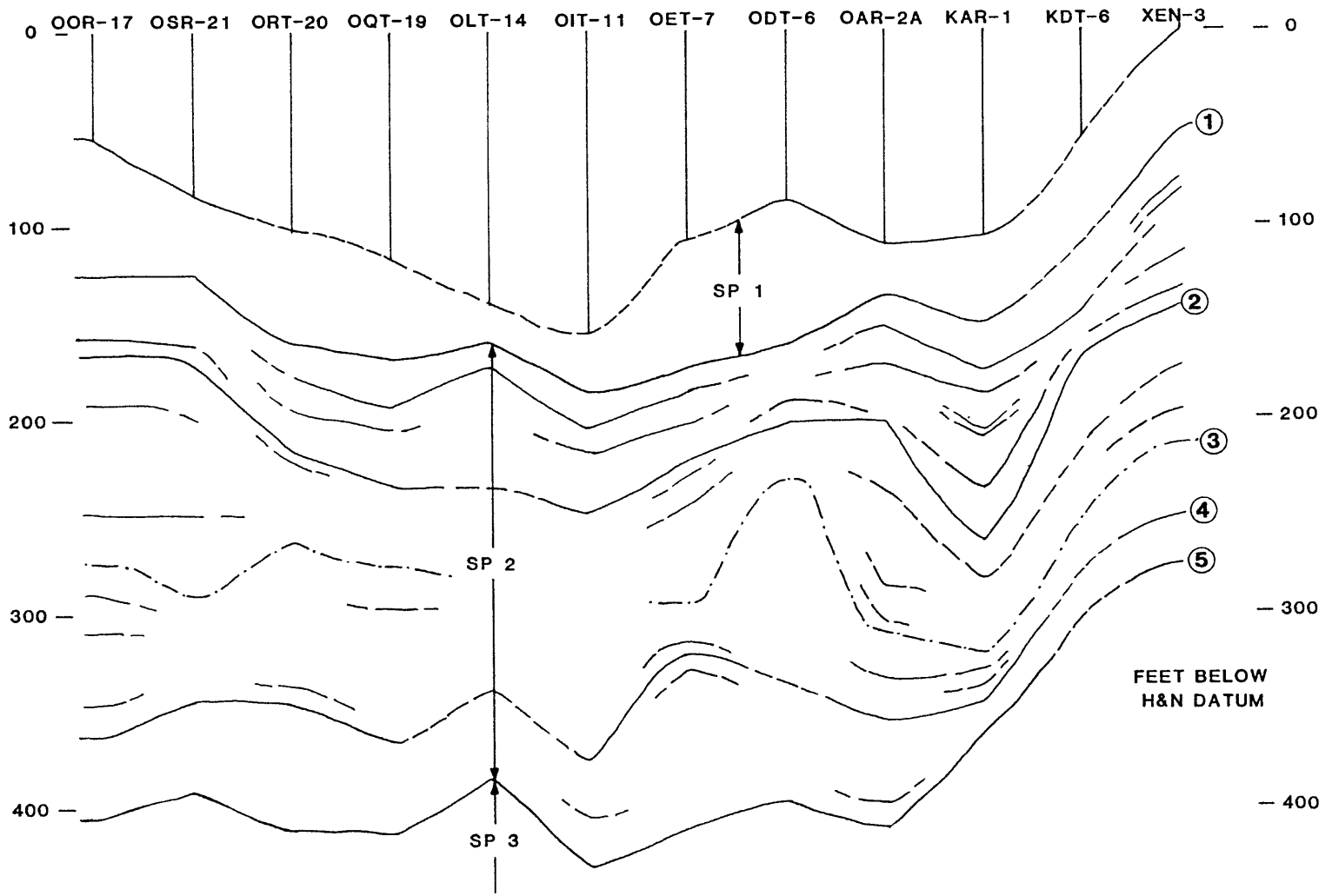

FIGURE 2-5a. -- Generalized relationship of discontinuities and disconformities (numbered) in sedimentary packages 1 and 2 for selected boreholes. Location of boreholes in Henry, Wardlaw, and others (1986) and in Figures 1-2 and 1-3. Major disconformities/discontinuities identified by circled numbers correspond to those identified in text by numbers in parentheses.

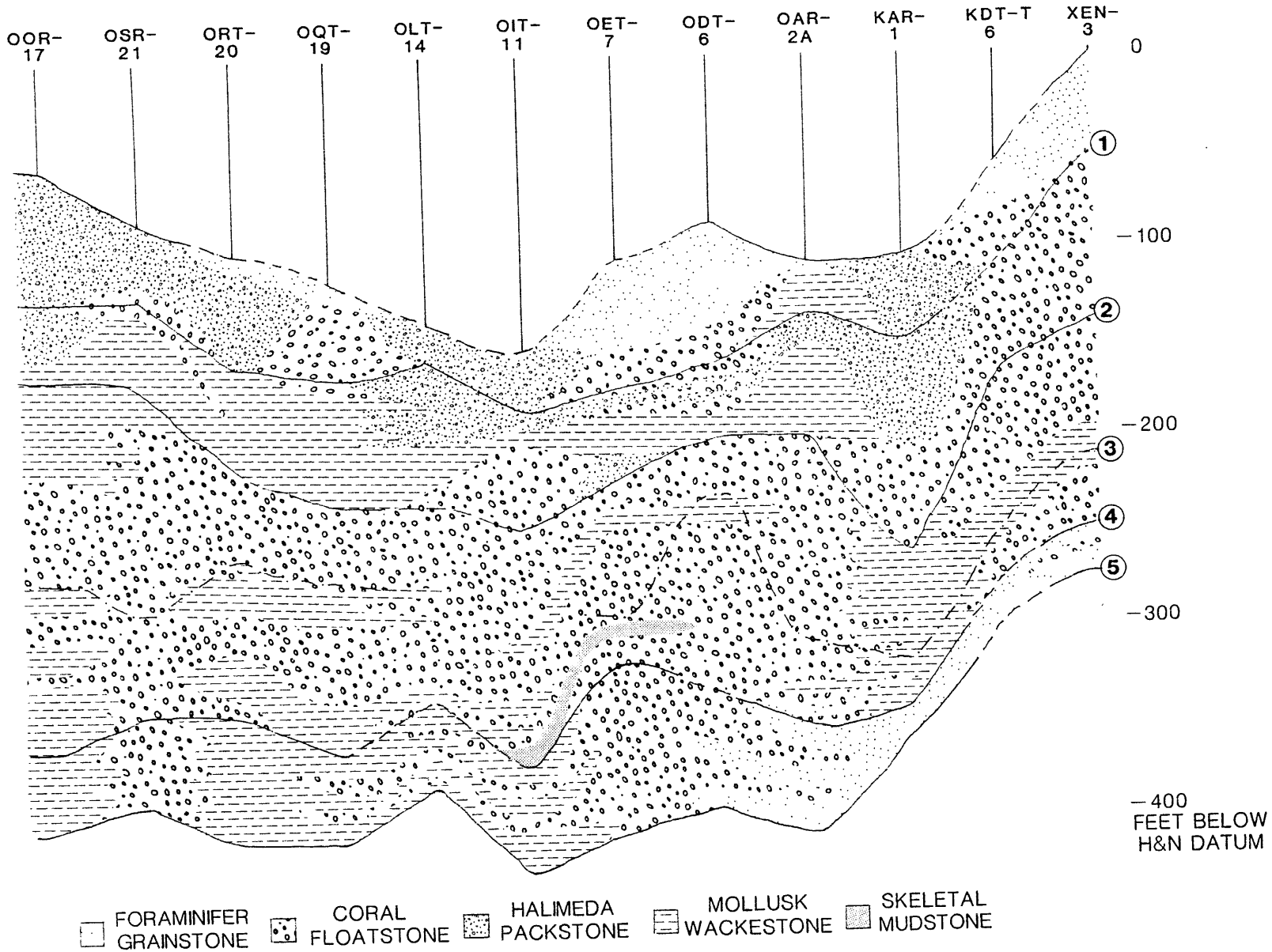

FIGURE 2-5b. -- Generalized sedimentary facies in sedimentary packages 1 and 2 for selected Enewetak boreholes (as in fig. 2-5a). See Table 2-1 for summary data for SP 1 and 2 and text for discussion. Major discontinuities that are numbered and circled correspond to those identified by numbers in parentheses in text.

casts or steinkerns) and skeletal fragments that are similarly stained. Commonly referred to as "salt and pepper" sands, these occur just above disconformity (1) in all of the primary and secondary reference boreholes except KDT-6 and XEN-3. Normally, only a slight increase in cementation accompanies this surface, but strata for a few inches or a few feet just below this surface are bleached, and the skeletal grains leached and partially dissolved.

BB/CC Discontinuity.--(R20 single-channel seismic reflector). This discontinuity within SP 2 is recognized by an increase in alteration and cementation in strata just below it. Generally, the strata are slightly better cemented than those below disconformity (1), and the first occurrence of "tea-brown" micrite, sparse dog-tooth spar, minor "vadose silt" partially infilling fossil molds (e.g., borehole OET-7), and rhizoliths (e.g., ODT-6, OQT-19) accompany this surface.

CC Discontinuities. -- Several local surfaces are represented by thin zones of increased cementation with the presence of "tea-brown" micrite and spar. Commonly these surfaces are accompanied by a change in lithofacies.

CC/DD Discontinuity. -- This poorly developed surface is similar to those within CC. It is typically accompanied by a slight increase in alteration.

Disconformity (2). -- (upper Pleistocene, DD/EE boundary). This disconformity is represented by an increase in cementation and alteration, presence of rhizoliths, "tea-brown" micrite, spar cement, and a common change in lithofacies. This surface is not much different from those within zone CC but is widespread and is marked by a significant change in the microfaunas.

EE Discontinuities. -- In the middle part of SP 2 are several local surfaces represented by thin zones of increased cementation and alteration, the occurrence of "tea brown" micrite and spar, and sparse drusy calcite lining fossil molds. Two paleosols indicating exposure surfaces are developed at 229.5 ft bsl in borehole OET-7 and at 237.1 ft bsl in OAR-2A. These two paleosols probably reflect a local exposure surface on the flanks of an apparent high caused by a large, natural carbonate build-up within zone FF (see figs. 2-5a and 2-5b).

Disconformity (3). -- (middle Pleistocene, EE/FF boundary). This disconformity is present in most of the boreholes studied and shows a great variation in depth (see fig. 2-5a). It corresponds roughly to the first major seismic reflector below R-20. The surface is represented by and increase in cementation, slight increase in alteration, and presence of spar and "tea brown" cement. Partially preserved paleosols, most commonly represented by rhizoliths, are present (OOR-17, OET-7, OQT-19) and a microkarstic surface with voids filled with overlying material is present at OAR-2A.

FF Discontinuities. -- Several local surfaces are represented by thin zones of increased cementation and "tea-brown" micrite. Marked increase in alteration is not common except at 291.5 ft bsl in OOR-17. A crust-like hardground is developed at 233.4 ft bsl in borehole OAR-2A and several large rhizoliths are present at 179.4 ft bsl in OQT-19. At 231.8 ft bls in borehole KAR-1, a thin, dusky-blue to medium-dark gray rind is developed on a surface and reworked into the unit immediately above.

Disconformity (4). -- (lower Pleistocene, FF/GG boundary). This surface generally is characterized by a marked increase in cementation and alteration. In the KOA area, this cemented zone just below this disconformity is thick. Preservation of parts of paleosol profiles at this level occur in KAR-1, OET-7, and OSR-21. Dark-gray and dusky-bluish-gray staining of the surface and reworked "salt-and-pepper" grains just above this surface occur in ORT-20 and OQT-19.

GG Discontinuities. -- A few local discontinuities within the lower part of SP 2 are indicated by an increase in cementation and porosity due to dissolution of fossils and skeletal grains. These commonly are lined with spar or are filled with spar.

Disconformity (5). -- (Pleistocene/Pliocene, GG/HH boundary, SP 2/3 boundary). This important surface is represented by a major increase in cementation and alteration of the stratigraphic sequence. Shortly below this surface, most corals and many molluscs have been completely dissolved and are preserved only as molds. Many of these molds have been enlarged by dissolution to small vugs, and many of the natural cracks that occur in the lithified rock have also been enlarged to form solution channels. Larger voids and small caverns also are common in the karsted strata. The strata throughout SP 3 are pervasively recrystallized to low-magnesium calcite (see Chapter 4), and the depth of pervasive alteration and recrystallization below disconformity (5) generally exceeds 100 ft. Commonly the upper 25 to 30 ft of SP 3 is so strongly altered that its original fabric (rock type) cannot be determined. This disconformity represents a major karst surface.

HH Discontinuities.--Most discontinuities noted within SP 3 are alteration zones and may not represent exposure surfaces. KAR-1 and OOR-17 contain local surfaces represented by an increase in cementation and the presence of "tea-brown" micrite.

Disconformity (6). -- (upper Pliocene, SP 3/4 boundary). The lower part of SP 3 commonly becomes progressively slightly less altered downward. Disconformity (6) is identified in the boreholes (fig. 2-6) by an increase in cementation and alteration including the reappearance downsection of moldic and vuggy porosity and by spar infilling molds and vugs.

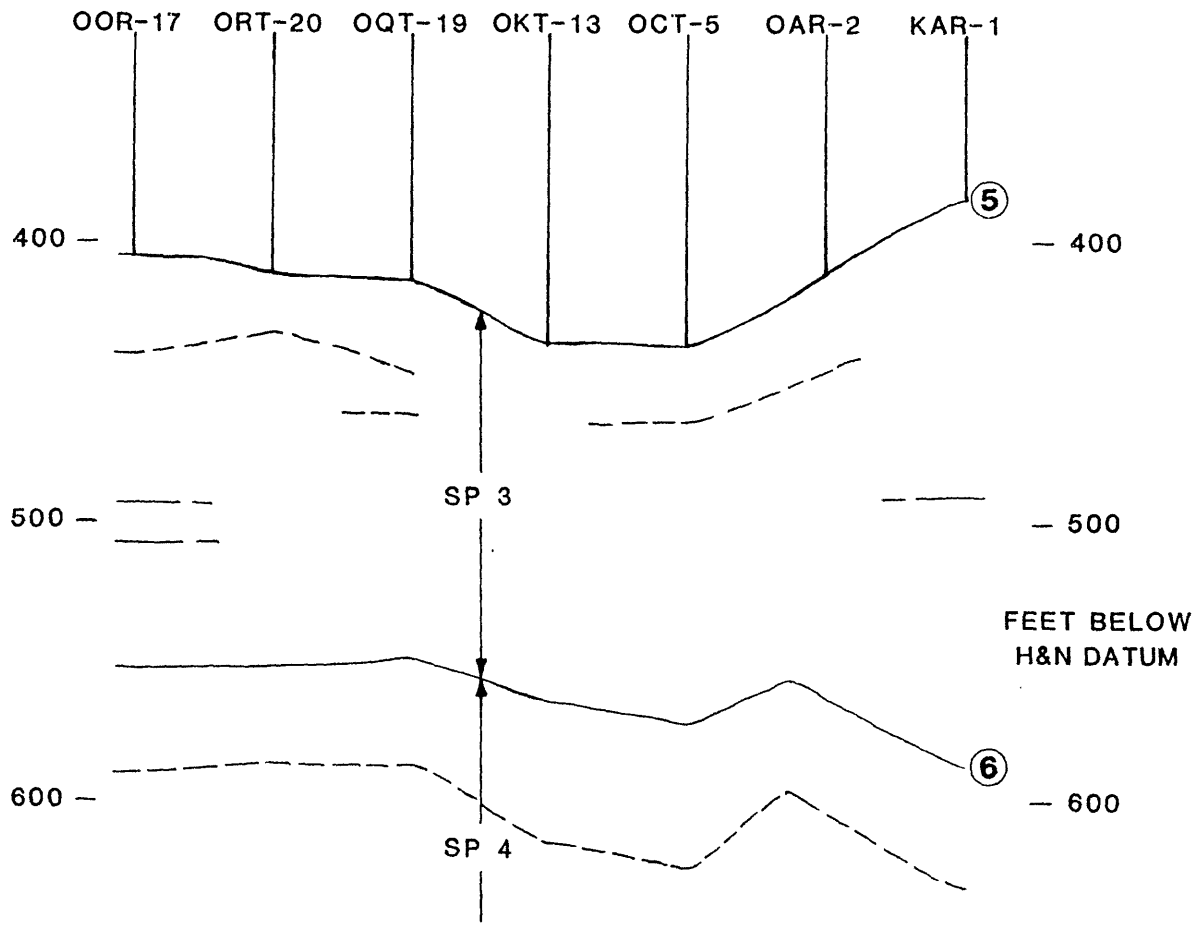

FIGURE 2-6. -- Generalized relationships of discontinuities and disconformities (numbered) in sedimentary package 3 and the alteration zone at the top of sedimentary package 4 for selected Enewetak boreholes. Major disconformities/ discontinuities identified by circled numbers correspond to those identified in text by numbers in parentheses.

LL/MM Discontinuities.--Discontinuities are sparse in SPs 4 and 5 (sedimentary interval II) above disconformity (7). Local ones exist in the KOA area (fig. 2-7). They generally are represented by the reoccurrence of cement downsection (particularly striking since almost all of the overlying strata are completely uncemented) and alteration of corals (there is generally little or no alteration in the overlying corals and other skeletal grains). The upper surface (at 794.5 ft bsl in KBZ-4) and middle surface (855.6 ft bsl in KAR-1) are overlain by a few inches of sediment containing cemented, reworked lithoclasts. Rhizoliths within one of the lithoclasts in KBZ-4 may indicate a nearby, local exposure surface. The reworked lithoclasts in KAR-1 are not accompanied by much cementation or alteration and may indicate subsurface erosion and/or soft-sediment deformation.

Disconformity (7). -- This surface is represented by a general marked increase in cementation and alteration with partially spar-replaced corals and common moldic porosity; some molds contain spar-infillings. A probable slump block occurs at the disconformity in OOR-17. A laminated crust and paleosol with rhizoliths and "tea-brown" micrite cement represents a preserved exposure surface in KAR-1.

Upper MM Discontinuities. -- Several discontinuites in SP 6 generally are represented by an increase in cementation, some with "tea-brown" micrite, and some with an increase in porosity. The discontinuities are common in the KOA area (fig. 2-7), less common in OAR-2 on the eastern side of OAK, and uncommon in the remaining OAK boreholes. At least one surface (at 952.4 ft bsl in KAR-1 and at 845.8 ft in OAR-2) has a paleosol profile or partial profile developed and represents local exposure.

Disconformity (8). -- This surface is represented by increased cementation and the presence of "tea-brown" cement in the OAK area and a preserved exposure surface in the KOA area. Borehole KAR-1 exhibits probable karsting just below this surface, and KBZ-4 contains rhizoliths and several laminated crusts below the disconformity (8), representing partially preserved soil profile(s).

Middle MM Discontinuities. -- Several surfaces within SP 7 in the KOA area (fig. 2-7) are represented by partially preserved paleosols commonly with rhizoliths and partially preserved laminated crusts, an increase in cementation, and the presence of "tea-brown" micrite. Some of these surfaces have vuggy and cavernous porosity developed just below them. They seem to represent local exposure surfaces.

Disconformity (9). -- This surface is represented by a marked increase in cementation and presence of "tea-brown" micrite in underlying strata. In KBZ-4, it marks a change in facies downsection to reefplate; in KAR-1, a karst surface occurs just below; and in OBZ-4, it is marked by a partially preserved paleosol.

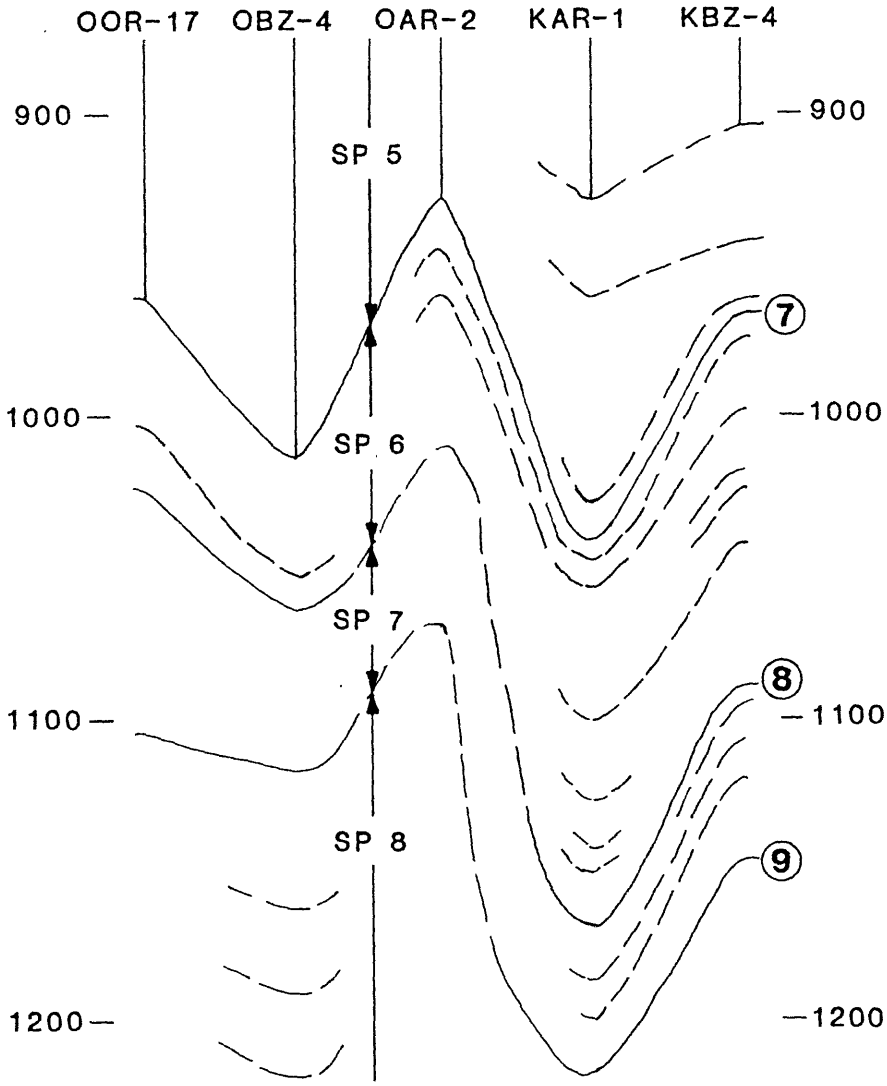

FIGURE 2-7. -- Generalized relationship of discontinuities and disconformities (numbered and circled) in sedimentary packages 5, 6, 7, and 8 for selected Enewetak boreholes. Major disconformities/discontinuities identified by circled numbers correspond to those identified in text by numbers in parentheses.

Lower MM Discontinuities. -- Many surfaces were recovered in core/sample from borehole OBZ-4 below disconformity (9). They are indicated by a myriad of features, from zones of increased cementation and alteration probably of fresh-water origin, paleosols, karsts, and reef-plate development.

LITHOFACIES

The multichannel-seismic profiles or cross sections presented by Grow, Lee, and others (1986) for both craters but particularly for KOA show what are probably major geologic facies changes occurring within the sedimentary cap of Enewetak Atoll. However, analysis of the lithofacies relationships inferrable from the PEACE Program boreholes is in a preliminary stage. The generalized facies relationships have been analyzed in the upper 400 ft of section, which is of primary interest to the crater-modeling community and is presented in this section.

The sediments and rocks in the upper 400 ft of section on Enewetak (i.e., SPs 1 and 2) can be classified into five general lithofacies, shown in Figure 2-5b and Table 2-1, as follows:

(1). Foraminifer grainstone (typically) and foraminifer packstone;
(2). Coral floatstone and packstone, typically with packstone matrix;
(3). Halimeda packstone and wackestone;
(4). Mollusc, skeletal wackestone and packstone; and
(5). Skeletal mudstone and wackestone.

Sedimentary package 3 (not shown in fig. 2-5b) represents the same general set of facies but is more difficult to differentiate because of the pervasive diagenesis that has destroyed much of the original rock fabric, particularly in its upper part. In SP 3, the coral floatstone facies appears to be characterized by wackestone and packstone matrix.

Sedimentary interval II (SPs 4, 5, and 6) commonly is represented by coral-mollusc floatstone and tight packstone with some wackestone.

Sedimentary packages 7 and 8 (interval III) commonly consists of foraminifer grainstone and packstone and coral floatstone and bafflestone.

PRELIMINARY GEOLOGIC HISTORY

A summary of the preliminary geologic ages of the strata in the upper 1,250 ft on Enewetak is given below (see also fig. 2-3).

SEDIMENTARY INTERVAL I:
Sedimentary Package 1. -- Holocene.
Sedimentary Package 2. -- Pleistocene.
Sedimentary Package 3. -- late Pliocene.

SEDIMENTARY INTERVAL II:
Sedimentary Package 4. -- "middle" Pliocene.
Sedimentary Package 5. -- late Miocene to early Pliocene.
Sedimentary Package 6. -- late Miocene.

(major hiatus)

SEDIMENTARY INTERVAL III:
Sedimentary Package 7. -- early Miocene, (?) earliest middle Miocene.
Sedimentary Package 8. -- early Miocene.

The three sedimentary intervals represent three major stages in the later evolution of Enewetak as an atoll. The configuration of the atoll appears to have changed to produce the general depositional setting of each sedimentary interval.

Sedimentary interval III (early Miocene to possibly earliest middle Miocene) is characterized by broad, shallow-water, back-reef facies of larger foraminifer sands and muds and of coral floatstones and bafflestones and framestones. The interval experienced several exposures which heavily recrystallized, cemented, and, in scattered cases, started to dolomitize the rock. A major hiatus (middle Miocene-early late Miocene) is represented by the boundary between sedimentary interval III and sedimentary interval II. The lack of deep or intermediate lagoon sediments suggests that a central island cluster existed and no deep lagoon existed. The presence of fresh olivine crystals and fresh euhedral quartz in insoluble residues (Chapter 6) from this interval further suggest that the hypothesized central island cluster included active volcanism (contributing olivine) and dike formation (contributing quartz).

Sedimentary interval II (late Miocene to "middle" Pliocene, the organic interval) is characterized by broad, shallow-water facies of coral-mollusc-rich sands and muds. The interval experienced only a few exposures near its base and is generally uncemented and unaltered. This interval was deposited after the major hiatus that represents long-term nondeposition and probable exposure and erosion. Schlanger and Premoli Silva (1986) report turbidite deposits of middle Miocene age with reworked fossil assemblages of late Oligocene and late(?) Eocene ages in the DSDP site 462 core from the Nauru basin, southwest of the Marshall Islands, that probably correspond to erosion and redeposition during this hiatus.

The sediments of interval II contain abundant palynomorphs that generally represent mangrove and related swamp pollens (Leopold, 1969). Sparse Gardenia pollen suggests high-island vegetation (Leopold, 1969). The insoluble

residues from sedimentary interval II consist solely of organic matter (see Chapter 6). The sediments and pollen assemblages suggest a central island cluster of probably eroding volcanic islands with extensive fringing swamps and a shallow lagoon.

Sedimentary interval I (late Pliocene to Holocene) is characterized by shallow to deep lagoon deposition of coral floatstones, Halimeda and foraminifer sands and mollusc muds. The interval experienced several exposures. A major exposure surface is indicated at the probable Pliocene/Pleistocene boundary (top of SP 3). The insoluble residues consist solely of organic matter. It appears that most of sedimentary interval I was deposited in conditions similar to today of an atoll with small peripheral islands and a deep central lagoon.

REFERENCES

Bates, R.L., and Jackson, J.A., eds., 1980, Glossary of Geology; Second Edition, American Geological Institute, Falls Church, Virginia, 751 p.

Couch, R.F., Jr., Fetzer, J.A., Goter, E.R., Ristvet, B.L., Tremba, E.L., Walter, D.R., and Wendland, V.P., 1975, Drilling operations of Eniwetok Atoll during Project EXPOE: Air Force Weapons Laboratory Technical Report AFWL-TR-75-216, Kirtland Air Force Base, New Mexico, 278 p., 17 figs., 4 tbls. (unclassified).

Cronin, T.M., Brouwers, E.M., Bybell, L.M., Edwards, E.E., Gibson, T.G., Margerum, R., and Poore, R.Z., 1986, Pacific Enewetak Atoll Crater Exploration (PEACE) Program, Enewetak Atoll, Republic of the Marshall Islands; Part 2: Paleontology and biostratigraphy, application to OAK and KOA craters: U.S. Geological Survey Open-File Report 86-159, 39 p., 20 figs., 12 tbls., 3 appendices.

Emery, K.O., Tracey, J.I., Jr., and Ladd, H.S., 1954, Geology of Bikini and nearby atolls: U.S. Geological Survey Professional Paper 260-A, 265 p., 73 pls., 84 figs., 11 charts, 27 tbls.

Grow, J.A., Lee, M.W., Miller, J.J. Agena, W.F., Hampson, J.C., Foster, D.S., and Woellner, R.A., 1986, Multichannel seismic-reflection survey of KOA and OAK craters; 46 p., 39 figs.; in Folger, D.W., ed., Sea-floor observations and subbottom seismic characteristics of OAK and KOA craters, Enewetak Atoll, Marshall Islands: U.S. Geological Survey Bulletin 1678.

Henry, T.W., Wardlaw, B.R., Skipp, B.A., Major, R.P., and Tracey, J.I., Jr., 1986, Pacific Enewetak Atoll Crater Exploration (PEACE) Program, Enewetak Atoll, Republic of the Marshall Islands; Part 1: Drilling operations and descriptions of boreholes in vicinity of KOA and OAK craters: U.S. Geological Survey Open-File Report 86-419, 497 p., 32 figs., 29 pls., 13 tbls., 3 appendices.

Leopold, E.B., 1969, Miocene pollen and spore flora of Eniwetok Atoll, Marshall Islands: U.S. Geological Survey Professional Paper 260-II, p. 1133-1184, pls. 304-311, figs. 322-342, 6 tbls.

Ristvet, B.L., Couch, R.F., Jr., and Tremba, E.L., 1980 Late Cenozoic solution unconformities at Enewetak Atoll: Geological Society of America Abstracts with Programs, v. 12, p. 510.

Ristvet, B.L., Couch, R.F., Jr., Fetzer, J.D., Goter, E.R., Tremba, E.L., Walter, D.R., and Wendland, V.P., 1974, A Quaternary diagenetic history of Eniwetok Atoll: Geological Society of Amnerica Abstracts with Programs, v. 6, p. 928-929.

Ristvet, B.L., Tremba, E.L., Couch, R.F., Jr., Fetzer, J.A., Goter, E.R., Walter, D.R., and Wendland, V.P., 1978, Geologic and geophysical investigations of the Enewetak nuclear craters; Final reports: Air Force Weapons Laboratory Technical Report AFWL-TR-77-242, Kirtland Air Force Base, New Mexico, 298 p. (unclassified).

Robb, J.M., Foster, D.S., Folger, D.W., Hampson, J.C., and Woellner, R.A., 1986, Single-channel seismic survey of OAK and KOA craters; 51 p., 24 figs.; in Folger, D.W., ed., Sea-floor observations and subbottom seismic characteristics of OAK and KOA craters, Enewetak Atoll, Marshall Islands: U.S. Geological Survey Bulletin 1678.

Schlanger, S.O., 1963, Subsurface geology of Eniwetok Atoll: U.S. Geological Survey Professional Paper 260-BB, p. 991-1066, pls. 281-288, figs. 306-318, 20 tbls. (with sections by other authors).

Schlanger, S.O., and Premoli Silva, I., 1986, Oligocene sea-level falls recorded in mid-Pacific atoll and archipelagic apron settings: Geology, v. 14, p. 392-395.

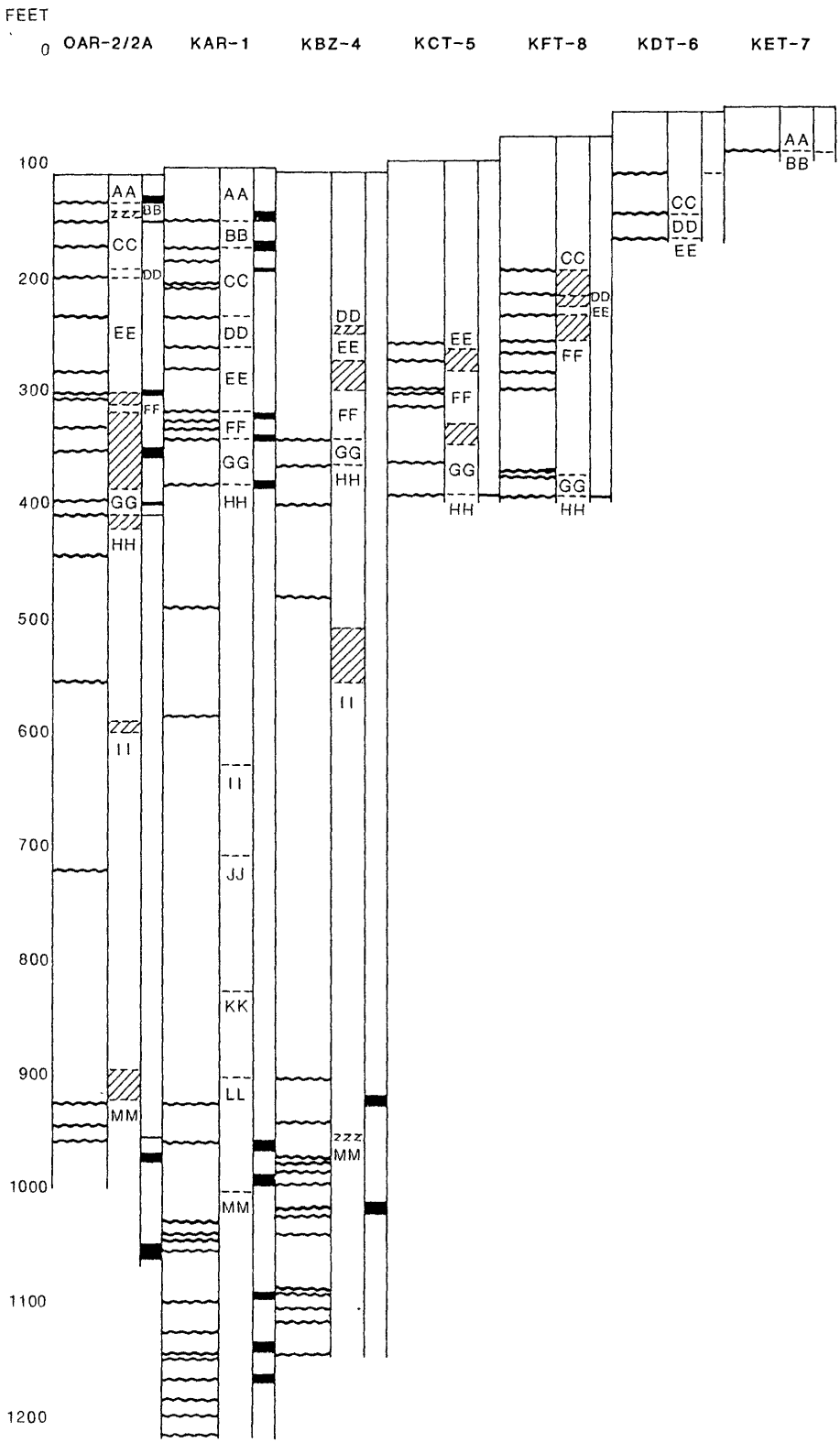

FIGURE 2-8. -- Position in borehole (in ft below H&N datum) of discontinuities, disconformities, actual biostratigraphic-zone determinations, and important seismic reflectors (black bars) in boreholes OAR-2/2A, KAR-1, KBZ-4, KCT-5, KFT-8, KDT-6, and KET-7. Borehole locations shown in Figures 1-2 and 1-3.

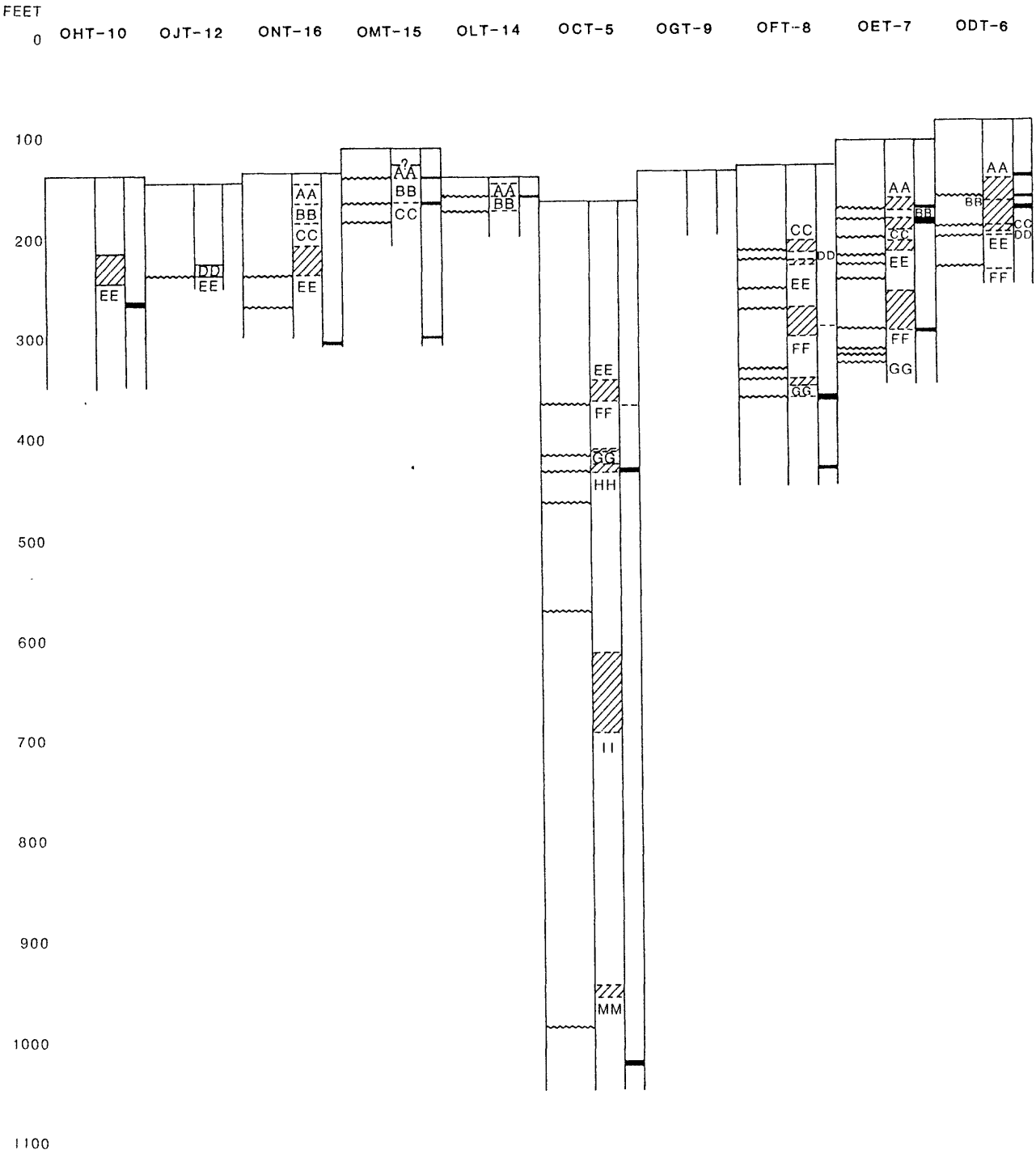

FIGURE 2-9. -- Position in borehole (in ft below H&N datum) of discontinuities, disconformities, actual biostratigraphic-zone determinations, and important seismic reflectors (black bars) in boreholes OHT-10, OJT-12, ONT-16, OMT-15, OLT-14, OCT-5, OFT-8, OET-7, and ODT-6. Borehole locations shown in Figure 1-3.

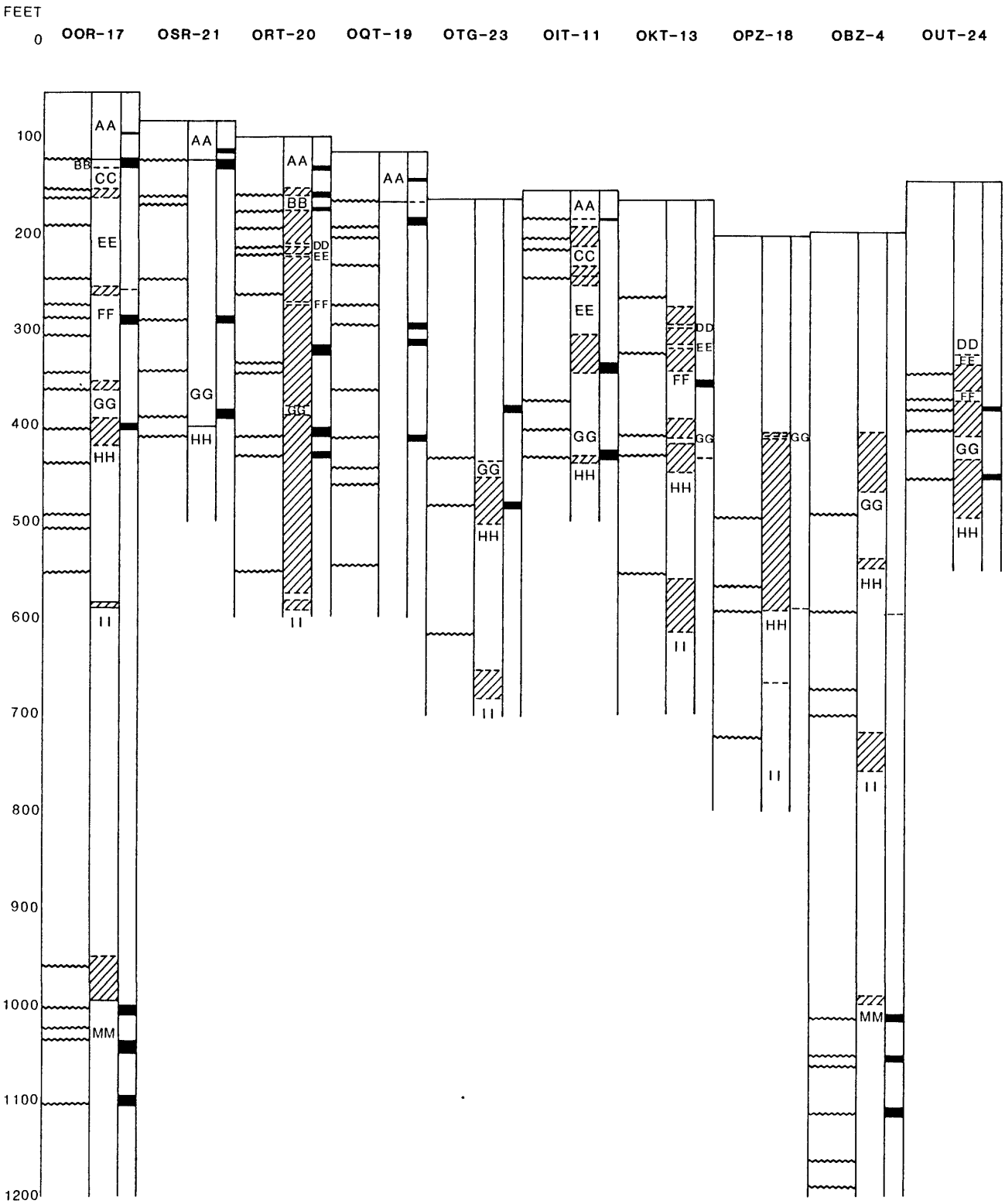

FIGURE 2-10. -- Position in boreholes (in ft below H&N datum) of discontinuities, disconformities, actual biostratigraphic-zone determinations, and important seismic reflectors (black bars) in boreholes OOR-17, OSR-21, ORT-20, OQT-19, OTG-23, OIT-11, OKT-13, OPZ-18, OBZ-4, and OUT-24. Borehole locations shown in Figure 1-3.

TABLE 2-1. -- Lithic characterization of Sedimentary Packages 1 and 2 in PEACE Program boreholes on Enewetak. Biostratigraphic zones shown as double capital letters in parentheses. (Page 1 of 5 pages.)

--SEDIMENTARY PACKAGE 1--

KAR-1. -- Skeletal, Halimeda wackestone with thin skeletal packstone with reworked grains at base.

KDT-6. -- Skeletal grainstone in upper part and coral floatstone with skeletal packstone in lower part.

OAR-2A.-- Mollusc, skeletal packstone and wackestone with thin Halimeda grainstone near top.

ODT-6. -- Foraminifer, skeletal grainstone with thin intervals of floatstone, rubble(?), with skeletal packstone, and Halimeda, skeletal packstone and wackestone with coral floatstone/bafflestone at base. Porites lutea on disconformable surface.

OET-7. -- Foraminifer, skeletal, Halimeda grainstone, and coral, Halimeda, skeletal packstone and wackestone at base. Astreopora on disconformable surface.

OIT-11.-- Halimeda, skeletal, mollusc wackestone beneath moderate debris blanket.

OLT-14.-- Skeletal, coral, Halimeda wackestone beneath debris blanket.

OOR-17.-- Halimeda, skeletal packstone to wackestone.

OQT-19.-- Skeletal, Halimeda grainstone and packstone near top and coral, Halimeda, skeletal packstone with intervals of coral floatstone for majority of unit.

ORT-20.-- Thin, foraminifer, skeletal, Halimeda grainstone near top and Halimeda, skeletal packstone with wackestone for majority of unit.

OSM-22.-- Halimeda, coral, skeletal packstone with wackestone approaching coral floatstone downward.

--UPPER PART OF SEDIMENTARY PACKAGE 2--

KAR-1. -- (BB). Halimeda, mollusc, skeletal packstone and wackestone with corals at top.

(CC). Skeletal, Halimeda packstone with minor wackestone in upper part, coral floatstone with mollusc, skeletal packstone in lower part.

Continued on next page.

TABLE 2-1 (continued, page 2 of 2 pages.)

--UPPER PART OF SEDIMENTARY PACKAGE 2 (cont.)--

KAR-1 (cont.) (DD). Skeletal, mollusc packstone to wackestone with coral floatstone, wackestone to mudstone matrix, and floatstone dominating lower part.

KDT-6. -- (BB/CC/DD). Coral, Halimeda, skeletal packstone with coral floatstone.

OAR-2A.-- (BB). Skeletal, Halimeda, coral packstone in upper part and skeletal, mollusc grainstone in lower part.

(CC/DD). Skeletal, mollusc wackestone with coral floatstone and skeletal, gastropod wackestone in the lowest part.

ODT-6. -- (BB/CC). Sparse coral floatstone with skeletal Halimeda packstone, thin skeletal foraminfer packstone at top and mollusc packstone at base.

(DD). Mollusc, Halimeda(?), skeletal packstone to wackestone.

OET-7. -- (BB). Coral floatstone with Halimeda, skeletal packstone to wackestone (laminated crust at top).

(CC/DD). Mollusc, skeletal packstone with coral floatstone and minor wackestone with Halimeda, foraminifer, skeletal, mollusc packstone in lowest part.

OIT-11.-- (BB). Halimeda packstone to wackestone grading downward to mollusc, skeletal; thin mollusc, skeletal wackestone at base.

(CC/DD). Coral floatstone, with skeletal wackestone and packstone matrix, with Halimeda, foraminifer, skeletal packstone with skeletal, foraminifer packstone in lowest part.

OLT-14.-- (BB). Halimeda, skeletal, coral packstone with thin mollusc, Halimeda wackestone at base.

(CC/DD). Mollusc-skeletal wackestone and packstone (only upper part sampled).

OOR-17.-- (BB/CC). Halimeda, skeletal, coral packstone.

(DD). Skeletal, mollusc packstone.

OQT-19.-- (BB). Coral, skeletal, Halimeda, mollusc packstone with coral floatstone.

Continued on next page.

TABLE 2-1 (continued, page 3 of 5 pages.)

--UPPER PART OF SEDIMENTARY PACKAGE 2 (cont.)--

OQT-19 (cont.) (CC/DD). Mollusc, Halimeda packstone to wackestone in upper part and skeletal, foraminifer packstone to wackestone in lower part.

ORT-20.-- (BB). Mollusc, skeletal, coral packstone.

(CC/DD). Mollusc, skeletal packstone with coral floatstone and minor wackestone with skeletal, mollusc packstone in lowest part.

OSR-21.-- (BB/CC). Skeletal, mollusc packstone with thin coral floatstone at top.

(DD). Muddy, mollusc, skeletal packstone.

OSM-22.-- (BB/CC). Skeletal packstone to floatstone.

(DD). Skeletal packstone.

--MIDDLE PART OF SEDIMENTARY PACKAGE 2--

KAR-1. -- (EE). Mollusc, skeletal packstone in upper part and mollusc, coral packstone, with coral framestone, bafflestone, and floatstone in lower part.

(FF). Mollusc, coral packstone and coral floatstone and bafflestone.

KDT-6. -- (EE). Coral bafflestone, floatstone, and packstone (only uppermost part).

OAR-2A.-- (EE). Coral floatstone, with skeletal, mollusc wackestone and packstone matrix, with minor bafflestone and framestone.

(FF). Coral floatstone, with foraminifer wackestone and mollusc packstone matrix, with mollusc, skeletal packstone in upper part and foraminifer, mollusc grainstone and packstone in lower part.

ODT-6. -- (EE). Coral floatstone, with skeletal packstone matrix, and coral, skeletal packstone and minor framestone.

(FF). Skeletal, foraminifer packstone with skeletal wackestone (only upper part).

OET-7. -- (EE). Coral floatstone, with skeletal packstone to mudstone matrix, with foraminifer packstone and wackestone.

Continued on next page.

TABLE 2-1 (continued, page 4 of 5 pages.)

--MIDDLE PART OF SEDIMENTARY PACKAGE 2 (cont.)--

OET-7 (cont.) (FF). Skeletal mudstone and wackestone in upper part and coral floatstone and bafflestone, with skeletal packstone matrix, and skeletal packstone in lower part.

OIT-11.-- (EE/FF). Coral floatstone, generally with skeletal wackestone matrix, with minor foraminifer packstone and coral bafflestone in upper part and mollusc, coral packstone and wackestone with minor coral floatstone and foraminifer wackestone at base.

OOR-17.-- (EE). Mollusc, coral packstone in upper part and coral, skeletal packstone and coral floatstone with skeletal wackestone in lower part.

(FF). Mollusc, coral packstone with some coral floatstone.

OQT-19.-- (EE). Coral floatstone, with mollusc skeletal packstone to wackestone matrix.

(FF). Coral floatstone and bafflestone with skeletal, mollusc packstone matrix and mollusc, skeletal packstone.

ORT-20.-- (EE). Coral floatstone, generally with wackestone matrix, and minor bafflestone and skeletal, mollusc packstone.

(FF). Coral mollusc packstone with minor coral floatstone and bafflestone.

OSR-21.-- (EE). Skeletal wackestone, coral floatstone, generally with wackestone matrix, and mollusc, skeletal packstone.

(FF). Coral floatstone and bafflestone, with skeletal packstone matrix with minor coral, mollusc packstone and skeletal wackestone.

OSM-22.-- (EE). Muddy, skeletal packstone and wackestone.

--LOWER PART OF SEDIMENTARY PACKAGE 2--

KAR-1. -- (GG). Foraminifer-skeletal packstone.

OAR-2A.-- (GG). Skeletal, foraminifer packstone and coral floatstone, with skeletal packstone and minor wackestone matrix, with minor skeletal, coral wackestone and coral bafflestone.

OET-7. -- (GG). Coral, skeletal packstone with minor coral, skeletal mudstone only upper part).

Continued on next page.

TABLE 2-1 (continued, page 5 of 5 pages.)

--LOWER PART OF SEDIMENTARY PACKAGE 2 (cont.)--

OIT-11.-- (GG). Mollusc, coral wackestone with some coral floatstone and minor skeletal, mollusc packstone.

OOR-17.-- (GG). Skeletal, mollusc packstone with foraminifer packstone to grainstone at base.

OQT-19. --(GG). Mollusc, coral packstone with coral floatstone and minor skeletal wackestone.

ORT-20.-- (GG). Mollusc, skeletal packstone with mollusc, skeletal grainstone and minor mollusc, skeletal wackestone.

OSR-21.-- (GG). Coral floatstone, with skeletal packstone matrix, and skeletal packstone and minor skeletal wackestone.

****

TABLE 2-2. -- Depths to various disconformities, discontinuities, and the HH/II biostratigraphic boundary in upper 1,200 ft of PEACE Program and selected EXPOE Program boreholes. Disconformity numbers at left and right side of table correspond to those in text; S = surface or sea floor. Depths in each column given outside of parentheses are in ft below the H&N datum; those in parentheses are in ft below the sea floor (bsf). (Page 1 of 6 pages.)

	BOREHOLE				
	XEN-3	KAR-1	KBZ-4	KCT-5	
S	0.0	105.1 (0.0)	109.1 (0.0)	98.9 (0.0)	S
1	51.7	150.7 (45.6)			1
	76.3	175.6 (70.0)			
	82.5	187.6 (82.5)			
	114.0	206.5 (101.4)			
		211.0 (105.9)			
	131.8	236.7 (131.6)			
2	141.2	262.8 (157.7)	(138.1)		2
				259.9 (161.0)	
3		320.9 (215.8)	(177.0)	274.3 (175.4)	3
		328.6 (223.5)		300.4 (201.5)	
		336.9 (231.8)		303.6 (204.7)	
				316.7 (217.8)	
4	249.8	345.7 (240.6)	344.0 (234.9)	365.4 (266.5)	4
5	275.0	384.0 (278.9)	368.6 (259.5)	392.9 (294.0)	5
		490.8 (385.7)	401.4 (292.3)		
6		587.1 (482.0)	480.7 (371.6)		6
HH/II					HH/II
		928.1 (823.0)	903.6 (794.5)		
		960.7 (855.6)	942.2 (833.1)		
		1030.0 (924.9)	973.6 (864.5)		
7		1040.8 (935.7)	979.0 (869.9)		7
		1047.9 (942.8)	986.5 (877.4)		
		1057.5 (952.4)	998.3 (889.2)		
		1100.4 (995.3)	1018.6 (909.5)		
		1127.7(1022.6)	1024.9 (915.8)		
		1145.5(1040.4)	1041.9 (932.8)		
		1150.5(1045.4)			
8		1169.2(1064.1)	1089.6 (980.5)		8
		1186.6(1081.5)	1094.4 (985.3)		
		1199.7(1094.6)	1107.0 (997.9)		
			1118.9(1009.8)		
9		1216.9(1111.8)	1147.3(1038.2)		9

Continued on next page.

TABLE 2-2 (continued, page 2 of 6 pages.)

	BOREHOLE			
	KDT-6	KET-7	KFT-8	OAR-2A/2	OBZ-4
s	56.2 (0.0)	51.1 (0.0)	77.8 (0.0)	110.5/114.2	198.7 (0.0)
1	110.1 (53.9)	89.8 (38.7)		136.2 (25.7)	1
				152.1 (41.6)	
				172.6 (62.1)	
			197.1 (119.3)		
	144.1 (87.6)		216.7 (138.9)		
2	166.8 (110.6)		233.1 (155.3)	201.2 (90.7)	2
				237.1 (126.6)	
				286.4 (175.9)	
				304.8 (194.3)	
3			257.4 (179.6)	310.0 (199.5)	3
			268.3 (190.5)	333.9 (223.4)	
			286.2 (208.4)		
			299.8 (222.0)		
4			372.0 (294.2)	355.6 (245.1)	
			377.7 (299.9)	398.6 (288.1)	493.0 (294.3)
5			395.6 (317.6)	410.6 (300.1)	593.0 (394.3)
				446.5 (336.0)	675.0 (476.3)
6				556.7 (442.5)	701.2 (502.5)
HH/II				596.2 (482.0)	738.7 (540.0)
				721.5 (607.3)	
7				927.2 (813.0)	1013.8 (815.1)
				944.2 (830.4)	1052.5 (853.8)
				960.0 (845.8)	
8					1065.1 (866.4)
9					1114.6 (915.9)
					1163.4 (964.7)
					1190.8 (992.1)
					1218.4(1019.7)

Continued on next page.

TABLE 2-2 (continued, page 3 of 6 pages.)

	BOREHOLE				
	OCT-5	ODT-6	OET-7	OFT-8	OGT-9
s	163.7 (0.0)	87.4 (0.0)	106.9 (0.0)	130.8 (0.0)	134.8 (0.0)
1		161.5 (74.1)	173.4 (66.5)		1
			185.7 (78.8)		
			202.2 (95.3)		
		190.6 (103.2)		214.0 (83.2)	
2		201.3 (113.9)	220.6 (113.7)	223.3 (92.5)	2
			229.5 (122.6)	251.9 (121.1)	
			243.7 (136.8)		
3	368.4 (204.7)	231.3 (144.2)	294.7 (187.8)	272.0 (141.2)	3
			314.6 (207.7)	332.8 (202.0)	
4	417.9 (254.2)		320.5 (213.6)	344.6 (213.8)	4
			329.6 (222.7)	361.2 (230.4)	
5	432.7 (269.0)				5
6	572.2 (408.5)				6
	623.7 (460.0)				HH/11
7					7
8					8
9					9

Continued on next page.

TABLE 2-2 (continued, page 4 of 6 pages.)

	BOREHOLE				
	OHT-10	OIT-11	OJT-12	OKT-13	OLT-14
s	137.1 (0.0)	155.0 (0.0)	143.8 (0.0)	164.7 (0.0)	139.7 (0.0)
1		185.4 (30.4)			159.4 (19.7)
		204.9 (49.9)			172.9 (33.2)
		217.8 (62.8)		267.6 (102.9)	
2		247.4 (92.4)	238.0 (94.2)		2
3				326.6 (161.8)	3
4		375.0 (220.0)		411.6 (247.6)	4
		406.0 (251.0)			
5		434.8 (279.8)		431.3 (266.6)	5
6				564.0 (399.3)	6
HH/11				614.7 (450.0)	HH/11
7					7
8					8
9					9

Continued on next page.

TABLE 2-2 (continued, page 5 of 6 pages.)

	BOREHOLE				
	OMT-15	ONT-16	OOR-17	OPZ-18	OQT-19
s	110.9 (0.0)	135.1 (0.0)	55.2 (0.0)	201.9 (0.0)	117.5 (0.0) s
1	140.8 (29.9)		125.9 (70.7)		168.0 (50.5) 1
	164.8 (53.9)				192.9 (75.4)
	183.5 (72.6)				206.0 (88.5)
			156.6 (101.4)		
2		238.6 (103.5)	166.2 (111.0)		233.9 (116.4) 2
		269.6 (134.5)	183.0 (127.8)		
			191.6 (136.4)		
			248.8 (193.6)		
3			273.8 (218.6)		274.7 (157.2) 3
			288.9 (233.7)	497.0 (295.1)	296.9 (179.4)
			308.5 (253.3)	507.5 (305.6)	
			346.7 (291.5)		
4			363.1 (307.9)	568.9 (367.0)	365.3 (247.8) 4
5			405.7 (350.5)	593.0 (391.1)	413.3 (295.8) 5
			440.9 (385.7)		447.2 (329.7)
			493.7 (438.5)		462.3 (344.8)
			507.8 (452.6)		
6			552.4 (497.2)	723.5 (521.6)	548.3 (430.8) 6
HH/II			587.2 (532.0)	761.9 (560.0)	587.5 (470.0)
7			961.0 (906.0)		7
			1003.4 (948.2)		
8			1024.4 (969.2)		8
			1037.7 (982.5)		
9			1104.6(1049.4)		9

Continued on next page.

TABLE 2-2 (continued, page 6 of 6 pages.)

	BOREHOLE				
	ORT-20	OSR-21	OTG-23	OUT-24	
S	101.4 (0.0)	84.0 (0.0)	164.0 (0.0)	147.0 (0.0)	S
1	160.6 (59.2) 177.9 (76.4) 194.9 (93.5)	125.0 (41.0)			1
2	216.2 (114.8) 222.2 (120.8)	161.5 (77.5) 170.8 (86.8) 248.9 (164.9)		346.9 (199.9)	2
3	262.7 (161.3) 336.4 (235.0)	290.1 (206.1)		373.0 (226.0) 386.0 (239.0)	3
4	346.7 (245.3)	344.2 (260.2)	434.0 (270.0)	407.0 (260.0)	4
5	411.7 (310.3) 432.0 (330.6)	391.7 (307.7) 411.6 (327.6)	484.0 (320.0)	457.1 (310.1)	5
6	552.0 (450.6)		619.0 (455.0)		6
HH/II	586.4 (485.0)		669.0 (505.0)		HH/II
7					7
8					8
9					9

****

CHAPTER 3:

Sr-ISOTOPE STRATIGRAPHY OF DISTURBED AND UNDISTURBED CARBONATES

by

K. R. Ludwig[1], R. B. Halley[2], K. R. Simmons[1], and Z. E. Peterman[1]

U.S. Geological Survey

INTRODUCTION

Because the application of Sr-isotope variations as a high-precision stratigraphic tool is a relatively recent development, a brief overview of the method and its application are presented here.

Basic Strontium-Isotope Geochemistry. -- Strontium has four stable isotopes: 84, 86, 87, and 88. Of these four, ^{87}Sr is produced as the result of the radioactive decay of naturally-occurring ^{87}Rb (half-life 49×10^9 years), and so varies in its abundance depending on the time-integrated history of its local Rb/Sr ratio. This variation as a function of age and geological/geochemical environments has been studied extensively, and is the basis for one of the most successfully and widely applied methods of absolute age determinations.

Strontium is a relatively abundant (about 8 ppm; Brass and Turekian, 1972), well-mixed, and long-lived (mean residence time about 5 m.y.[3]; (Taylor and McLennan, 1985) element in the oceans. However, because of the dependence of the $^{87}Sr/^{86}Sr$ ratio (by convention, the ^{87}Sr abundance is always reported relative to ^{86}Sr) on the geochemical history of the sources of strontium, the $^{87}Sr/^{86}Sr$ of the strontium input to the oceans has varied significantly over geologic time. These variations in marine $^{87}Sr/^{86}Sr$ can to some extent be correlated with major geologic processes and events, such as sea-level changes, glaciations, mountain-building events, and sea-floor spreading. For the purposes of this Chapter, however, the actual causes of the secular variation of seawater $^{87}Sr/^{86}Sr$ are not particularly important.

Because of the chemical similarity of strontium to calcium, marine carbonates incorporate relatively high concentrations of strontium ($\pm$200 to $\pm$8,000 ppm). Marine carbonates incorporate negligible concentrations of rubidium, however, so the $^{87}Sr/^{86}Sr$ ratio in marine carbonates has not increased measurably due to the decay of ^{87}Rb over geologic time. Also, because highly electropositive elements such as strontium do not isotopically fractionate to a significant degree in the natural environment, the isotopic composition of the strontium in unaltered marine carbonates must be very close to that of the strontium in the seawater from which it was derived.

---

[1] Denver, CO. [2] Woods Hole, MA. [3] m.y. = millions of years.

Perhaps the most powerful demonstration of this assertion is the data on natural isotopic fractionation of calcium isotopes (Russell and others, 1978) which, because of the much greater mass differences involved and the less-metallic nature of the element, should show an order of magnitude or greater effect than for strontium. The range of actual effects observed by Russell and others (1978) for calcium was about 0.5% per mass unit, equivalent to about 0.02% per mass unit in the mass range of strontium.

Regardless of the effect of any natural isotopic fractionation, however, it is important to recognize that such effects can be, and in normal practice are, essentially completely removed by using the measured ratio of two of the nonradiogenic isotopes to determine the amount of isotopic fractionation compared to some standard ratio. Because natural (and almost all types of artificial) isotopic fractionation is a near-linear function of the mass difference between any two isotopes, the analyst can then correct the observed $^{87}Sr/^{86}Sr$ for the significant amount of fractionation induced by the analytical process (about 0.3% per mass unit for the Enewetak data set), and at the same time for the much smaller amounts of fractionation that may have existed in the sample itself.

The procedure permits very precise measurements of the relative abundances of the radiogenic isotope, ^{87}Sr. Under the best conditions, analysts can detect differences between samples of as little as 20 ppm (0.002%) or so of the $^{87}Sr/^{86}Sr$ ratio.

Strontium-Isotope Record of Marine Carbonates. -- The systematic variation of the strontium isotopic composition of seawater over geologic time was first investigated by Peterman and others (1970). Since then, numerous studies have generated new data and discussions on this topic. The most useful of these for the purposes of this chapter is that of DePaolo (1986), because of the high precision of the data and the relatively large number of analyses for Tertiary and younger material. The most important features of DePaolo's data (fig. 3-1) are that:

(1). the $^{87}Sr/^{86}Sr$ of modern marine carbonates worldwide appears to be constant to a very high precision;

(2). for the last 35 m.y. or so, the $^{87}Sr/^{86}Sr$ of seawater has been increasing essentially monotonically; and

(3). the fine structure in the strontium-isotope record of marine carbonates for the last 35 m.y. indicates intervals of (a) relatively slow change in $^{87}Sr/^{86}Sr$, and (b) other, much shorter intervals of very rapid change.

For this Chapter, the data of DePaolo (1986) have been used for deep-water carbonates from cores of the Deep Sea Drilling Project (DSDP) to obtain "absolute" ages for the Enewetak carbonates. It is important to recognize, however, that in a truly absolute sense these "ages" are only as good as the paleontologic inferences and the time scale (that of Kennett and others, 1986) that DePaolo used to assign ages to the DSDP material that he analyzed. Certainly within a given interval, these age assignments are valid relative to

Figure 1

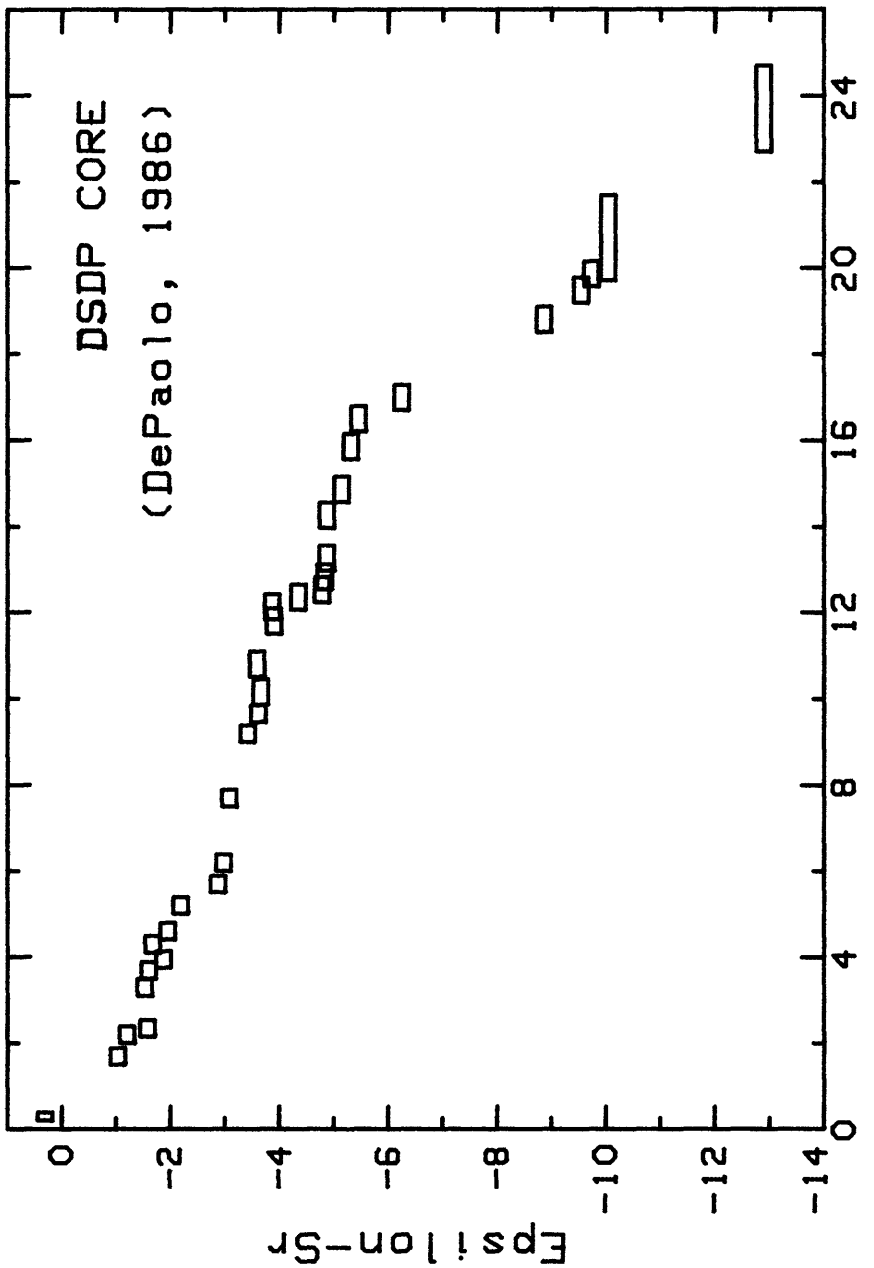

FIGURE 3-1. -- Epsilon-Sr versus age, in millions of years, for samples from DSDP site 590B. Data from DePaolo (1986), who used the time scale of Kennett and others (1986) to assign ages to the samples. Rectangles are error-boxes.

one another; however, any given point in the time scale for the late Tertiary may have uncertainties of over a million years.

Analytical Techniques and Notation. -- The Sr-isotope analyses presented in this chapter were performed using a fully-automated Micromass 54E thermal-ionization, single-collector, mass spectrometer operating under control of the ANALYST program (Ludwig, 1985), using a triple-filament method. Typically, these mass-spectrometer runs required about 30 minutes of filament pre-heating and instrument tune-up time, then 2.5 to 3.5 hours of data-taking to achieve a within-run precision of about 15 ppm of the $^{87}Sr/^{86}Sr$ ratio (all uncertainties in this chapter are at the 95%-confidence level). The sample-to-sample reproducibility of a single analysis is significantly greater, however, due to an "external" variation of 20 to 30 ppm of the ratio (0.708 to 0.709 for the Enewetak samples). Thus the overall precision of a single $^{87}Sr/^{86}Sr$ determination was about 30 ppm of the ratio.

In order to cancel out any effects of instrumental bias for these analyses, every third or fourth analysis was done on a standard carbonate sample derived from a very large pelecypod shell (Tridachna) collected alive from the lagoon floor at Enewetak. Because these analyses, like all of the sample analyses, were done entirely under computer control, they should have no bias compared to the sample analyses. All data are reported relative to the values obtained for this standard at the time of the analysis, and in effect represent the difference between the sample $^{87}Sr/^{86}Sr$ and that of modern seawater. The notation that is used:

$$\text{epsilon-Sr} = 10^4[(^{87}Sr/^{86}Sr)_{\text{sample}}/(^{87}Sr/^{86}Sr)_{\substack{\text{modern}\\\text{seawater}}} - 1)]$$

In other words, epsilon-Sr is the difference in the $^{87}Sr/^{86}Sr$ ratio (in parts per 10,000) between the sample and modern seawater. These epsilon-Sr values should be free of any instrumental or other laboratory bias, and so are directly comparable to epsilon-Sr values calculated from the data of other laboratories. The measured value that we obtained for our modern-seawater standard (the Tridachna shell) varied slightly over the course of the analyses due to various instrumental adjustments, but was always very close to 0.709250 (about 0.00007 lower than our value for the NBS-987 Sr-isotope standard).

Interferences of ^{87}Rb were corrected by monitoring the ^{85}Rb beam before and after each 13-minute block of data. These Rb beams were very small (generally about 0.002% and always less than 0.2% of the ^{87}Sr beam). Mass fractionation arising from the process of ionization (and, as discussed above, from any geologic processes as well) was corrected by normalizing the observed $^{86}Sr/^{88}Sr$ ratio (always in the range of 0.1198 to 0.1201) to 0.1194, using the exponential-fractionation law suggested by Russell and others (1978). Because the amount of fractionation was both small and tightly controlled, however, any linear or pseudolinear fractionation law would have yielded essentially the same results.

For the KAR-1 reference borehole, about half of the 54 analyzed samples were dominantly or entirely aragonite, with the remainder dominantly or entire calcite. Aragonite is preferred to calcite for this type of study because the

preservation of aragonite is a sensitive indicator of the lack of any alteration, recrystallization, or trace-element exchange by the carbonate.

To test the reliability of the calcitic samples, in six cases both calcitic and aragonitic material was sampled from the same depth (from between 95 and 518 ft bsf) in the core to compare their epsilon-Sr values. None of these pairs show resolvable differences in their epsilon-Sr values, and the mean difference between the pairs is indistinguishable from zero (table 3-1). It is concluded from these checks that alteration of the original strontium isotopic composition of the Enewetak carbonates due to diagenetic alteration is probably not a significant effect for samples in this depth range.

Sr-ISOTOPE STRATIGRAPHY OF REFERENCE-CORE KAR-1

Borehole KAR-1 (8,509 ft from ground zero) was used as a reference for the strontium-isotope stratigraphy for all samples of disturbed or possibly disturbed material. The trend of epsilon-Sr with depth for the KAR-1 samples (table 3-2, fig. 3-2) is a striking and powerful confirmation of the inferences from deep-sea samples (DePaolo, 1986) that epsilon-Sr has been increasing monotonically for the last 20 million years or more.

The two most important features of the KAR-1 data are that:

(1). from zero to about 1,000 ft bsf, epsilon-Sr decreases essentially monotonically with depth, with no convincing reversals and no statistically resolvable scatter from a monotonic trend;

(2). from zero to about 1,000 ft bsf, the epsilon-Sr trend with depth displays intervals of apparent continuous decrease, intervals where epsilon-Sr is essentially constant, and very narrow intervals with very abrupt changes in epsilon-Sr; and

(3). from about 1,000 ft bsf to the bottom of the hole at 1,145 ft bsf, there is a smooth and continuous decrease in epsilon-Sr broken by three apparent outliers. The epsilon-Sr values of these outliers lie just resolvably above this smooth trend.

At least some of the irregularities of the epsilon-Sr/depth trend must be due to similar irregularities in the global marine epsilon-Sr curve, which, for example, shows a rapid change in epsilon-Sr with age at epsilon-Sr values of about -1.7 (2.2 Ma[1]), -3.4 (4.7 Ma), and about -5.0 (12.2 Ma; DePaolo, 1986; fig. 3-1). To distinguish between these global secular changes in epsilon-Sr and changes due to processes unique to Enewetak atoll itself, the epsilon-depth curve for KAR-1 must be converted into a plot of apparent age versus depth, using the observed KAR-1 epsilon-Sr values and the deep-sea epsilon-Sr versus age trend defined by the data of DePaolo (1986). This plot (fig. 3-3) gives direct time-information on the evolution of Enewetak Atoll

---

[1] Ma = millions of years before today.

TABLE 3-1. -- Epsilon-Sr values for paired calcite and aragonite samples taken from within 1 ft of the same depth of reference core KAR-1. Uncertainty in the individual epsilon-Sr values is about 0.34, so the uncertainty in the difference between any two values is about 0.48. None of the six pairs shows an analytically resolvable difference in epsilon-Sr.

Sr-ISOTOPE DATA FOR COEXISTING CALCITE-ARAGONITE PAIRS

DEPTH (ft bsf)	%ARAGONITE[1]	$CALCITE_{epsilon-Sr}$-$ARAGONITE_{epsilon-Sr}$
95.0	90/40	+0.14
140.7	90/<1	+0.01
182.	80/20	-0.07
253.	80/20	-0.46
399.2	20/<1	+0.26
518.1	90/30	+0.22
AVERAGE	- - -	+0.01 $\pm$0.22

[1]First number refers to the "aragonite" sample, second number refers to "calcite" sample.

TABLE 2: DATA FOR REFERENCE BOREHOLE KAR-1

Depth (feet)	percent aragonite	sample-type	Epsilon Sr	Epsilon error	Apparent age (Ma)	Min. age (Ma)	Max. age (Ma)
9.2	90	C	-.37	.37	1.0	0.6	1.3
62.7	90	C	-.15	.37	0.7	0.6	1.1
72.3	70	MS	-.48	.35	1.0	0.8	1.3
95.0	60,90	WR,C	-.14	.27	.7	0.7	.87
103.5	90	C	-.51	.34	1.0	0.7	1.5
127.1	90	C	-.97	.34	1.6	1.2	2.1
140.7	0,90	WR,C	-.92	.26	1.6	1.3	2.0
152.9	90	C	-1.13	.34	1.8	1.3	2.4
165.5	90	C	-.66	.34	1.2	.9	1.7
181.1	20	WR	-.99	.36	1.6	1.2	2.2
182.0	80	C	-.98	.26	1.6	1.2	2.1
216.5	90	C	-1.36	.37	2.1	1.6	3.9
236.0	90	C	-1.65	.36	3.7	2.1	4.7
253.0	20,80	WR,BV	-1.58	.25	3.5	2.2	4.3
285.5	10	WR	-1.56	.35	3.3	2.1	4.6
309.3	10	WR	-1.50	.20	2.3	2.2	3.9
339.0	0	BV	-1.69	.34	3.8	2.2	4.8
367.5	0	WR	-1.52	.32	2.4	2.2	4.4
397.1	0	*WR	-1.95	.23	4.7	4.0	5.2
398.2	0	C	-1.64	.23	3.6	2.2	4.4
399.2	0,20	WR,C	-2.39	.22	5.3	5.2	5.4
403.5	0	WR	-2.00	.23	4.7	4.1	5.2
430.3	0	WR	-2.23	.34	5.2	4.5	5.3
452.3	0	WR	-2.34	.34	5.3	4.7	5.5
468.1	0	WR	-2.35	.36	5.3	4.7	5.5
518.1	90	C	-2.6	.27	5.4	5.3	5.9
537.4	90	C	-2.71	.34	5.5	5.1	7.6
593.9	100	C	-2.75	.34	5.5	5.4	7.8
606.8	100	C	-2.96	.23	6.7	5.5	8.2
627.3	100	C	-2.46	.35	5.3	5.0	5.6
705.0	100	C	-3.08	.35	7.9	5.5	9.3
736.8	100	C	-3.15	.36	8.0	5.6	9.5
801.0	90	C	-3.54	.37	9.7	8.2	12.0
867.2	100	C	-3.88	.37	11.9	9.4	12.5
896.7	90	C	-3.91	.23	12.0	10.9	12.3
924.8	90	C	-4.54	.25	12.4	12.3	12.5
926.0	0	WR	-7.64	.34	17.8	17.6	18.1
937.6	0	WR	-7.92	.34	18.1	17.8	18.3
943.5	0	WR	-7.98	.34	18.1	17.9	18.4
962.5	0	WR	-8.09	.34	18.3	18.2	18.5
969.9	n.d.	WR	-8.42	.23	18.4	18.2	18.8
972.1	n.d.	WR	-8.04	.31	18.1	17.9	18.4
982.0	0	WR	-8.35	.36	18.3	18.1	18.8
996.7	0	C	-8.60	.26	18.6	18.3	18.8
1023.0	0	C	-8.75	.35	18.8	18.4	19.1
1025.6	0	WR	-8.23	.39	18.3	18.2	18.6
1063.6	0	WR	-9.12	.27	19.1	19.1	19.4
1075	n.d.	n.d.	-8.70	.36	18.7	18.4	19.0
1076.3	0,0	WR,C	-9.12	.27	19.1	19.1	19.4
1084.8	0	C	-9.42	.35	19.5	19.1	19.9
1086.6	0	C	-9.47	.35	19.5	19.0	20.0
1107.5	0	WR	-8.76	.31	18.6	18.4	19.1
1132.2	0	WR	-9.99	.31	20.3	20.0	20.5
1145.0	0	WR	-9.84	.31	20.1	19.7	20.4

WR - whole-rock C - coral BV - bivalve MS - muddy sand
n.d. - not determined *clast

TABLE 3-2. -- Data for reference-core KAR-1. Apparent ages (in millions of years) are derived from the observed KAR-1 epsilon-Sr values and the trend of epsilon-Sr with age documented by DePaolo, using the time scale of Kennett and others (1986). The "apparent age" column contains the best-estimate ages, and the "min. age" and "max. age" columns contain the lower and upper limits on the ages, respectively. The latter values were obtained by propagating only the uncertainty in epsilon-Sr, and so assume no uncertainty in the time scale used by DePaolo. Data for replicate analyses and for calcite-aragonite pairs from the same depth (see table 3-1) are pooled.

Figure 2

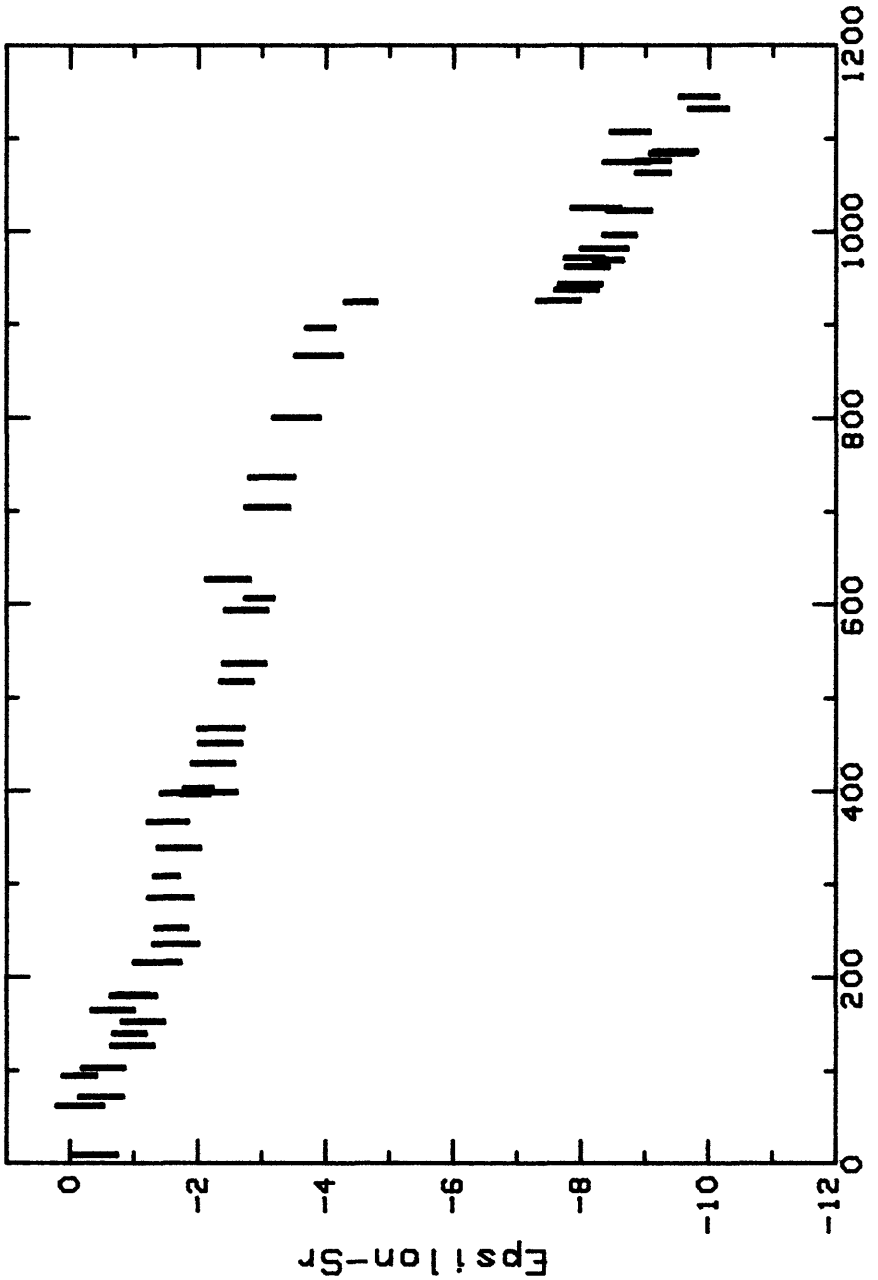

FIGURE 3-2. -- Epsilon-Sr versus depth for reference-core KAR-1. Rectangles are error-boxes.

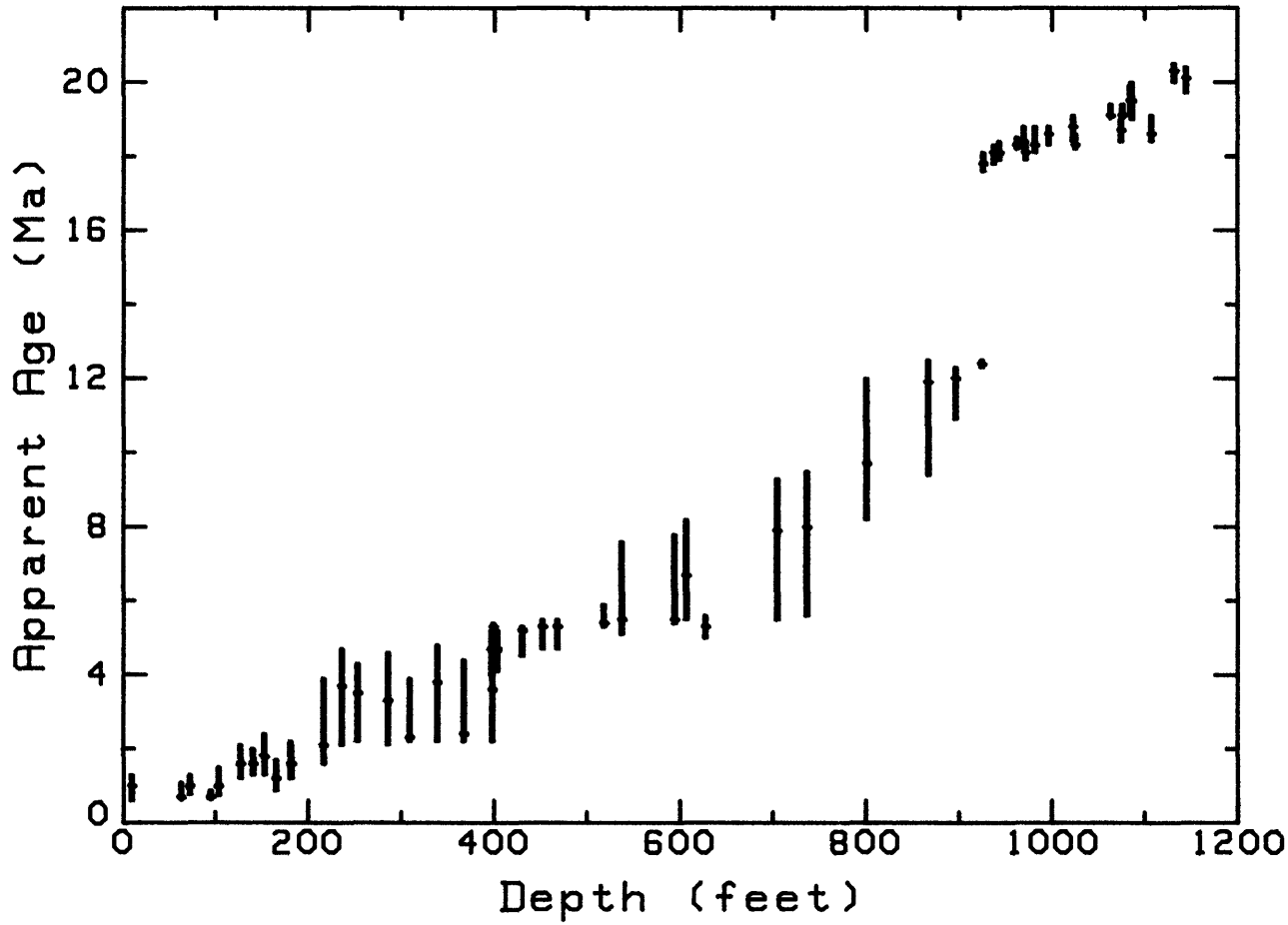

Figure 3

FIGURE 3-3. -- Apparent age (in millions of years) versus depth for reference-core KAR-1. Apparent ages were derived from the trend of epsilon-Sr with age for DSDP samples (see fig. 3-1). Rectangles are error-boxes, obtained by propagating only the analytical errors for epsilon-Sr; that is, no uncertainty in the (hand-fit) trend through the data of Figure 3-1 was assumed. Nicks in the error-boxes indicate the best-estimate ages for each sample.

(although, again, the "ages" are only as valid as the time-scale of Kennett and others, 1986).

The apparent-age variation of the KAR-1 carbonates with depth can be summarized as follows:

(1). From about 50 ft to 100 ft there is no resolvable increase in the apparent age of about 1.0 Ma. A slight but aparently abrupt increase in apparent age to about 1.6 Ma occurs between about 103.5 and 127.1 ft bsf. No resolvable increase in apparent age occurs between 127.1 and 182.0 ft bsf, but at roughly 200 ft another abrupt increase in apparent age occurs, to about 3.0 Ma. Between 200 and almost 400 ft bsf, there is no resolvable change in apparent age; however, in this interval the global epsilon-Sr curve also shows very little change with age, so steps as large as 1 m.y. could exist.

(2). At almost precisely 398 ft bsf, an abrupt increase in apparent age to 5.2 Ma occurs (fig. 3-4). Between 339 and 627 ft bsf, apparent ages increase by at most a few hundred thousand years. Somewhere between 627 and 705 ft bsf, apparent ages start to increase distinctly, and between 627 and 924.8 ft bsf increase from about 5.4 Ma to 12.4 Ma. Most of this time interval is poorly resolved by the global epsilon-Sr curve, so that any fine-structure in the KAR-1 curve is obscured.

(3). At almost precisely 925 ft bsf, apparent ages increase abruptly from 12.4 $\pm$0.1 Ma to 17.8+0.3/-0.2 Ma (fig. 3-5). This is the most pronounced and well-resolved break in apparent age for the KAR-1 samples. Between 926 ft and the deepest sample at 1,145.0 ft, apparent ages increase smoothly from 17.8 Ma to about 20 Ma, except for three samples that scatter slightly above this smooth trend. Because of the high time-resolution of this part of the core, any unresolved unconformities can be no greater than 0.1-0.2 m.y. in duration.

The three outliers from between 1,000 ft and 1,145 ft, though barely resolvable as such, appear to be real and may be very important in assessing the reliability of the Sr-isotope record in such deep samples. The simplest explanation for these outliers is that at least some samples at this depth have experienced significant diagenetic alteration of their Sr isotopes, such that their original Sr has exchanged with Sr derived from either modern seawater or from samples higher in the section. Though data on deeper samples would be necessary to confirm this explanation, the data may indeed indicate that the very high precision of the Sr-isotope stratigraphy may be lost at depths much deeper than about 1,000 ft.

Regardless of any complications in the Sr-isotope behavior for very deep samples, the record for the first thousand feet of KAR-1 (and XEN-3) borehole indicates that least for depths of less than 1,000 ft, Sr isotopes can be used as a reliable and unbiased method for determining both depth and (though requiring another layer of assumptions) absolute age of both aragonitic and calcitic samples. The Sr-isotope method can thus be used both as a complementary technique to paleontologic and lithologic studies, and as

Figure 4

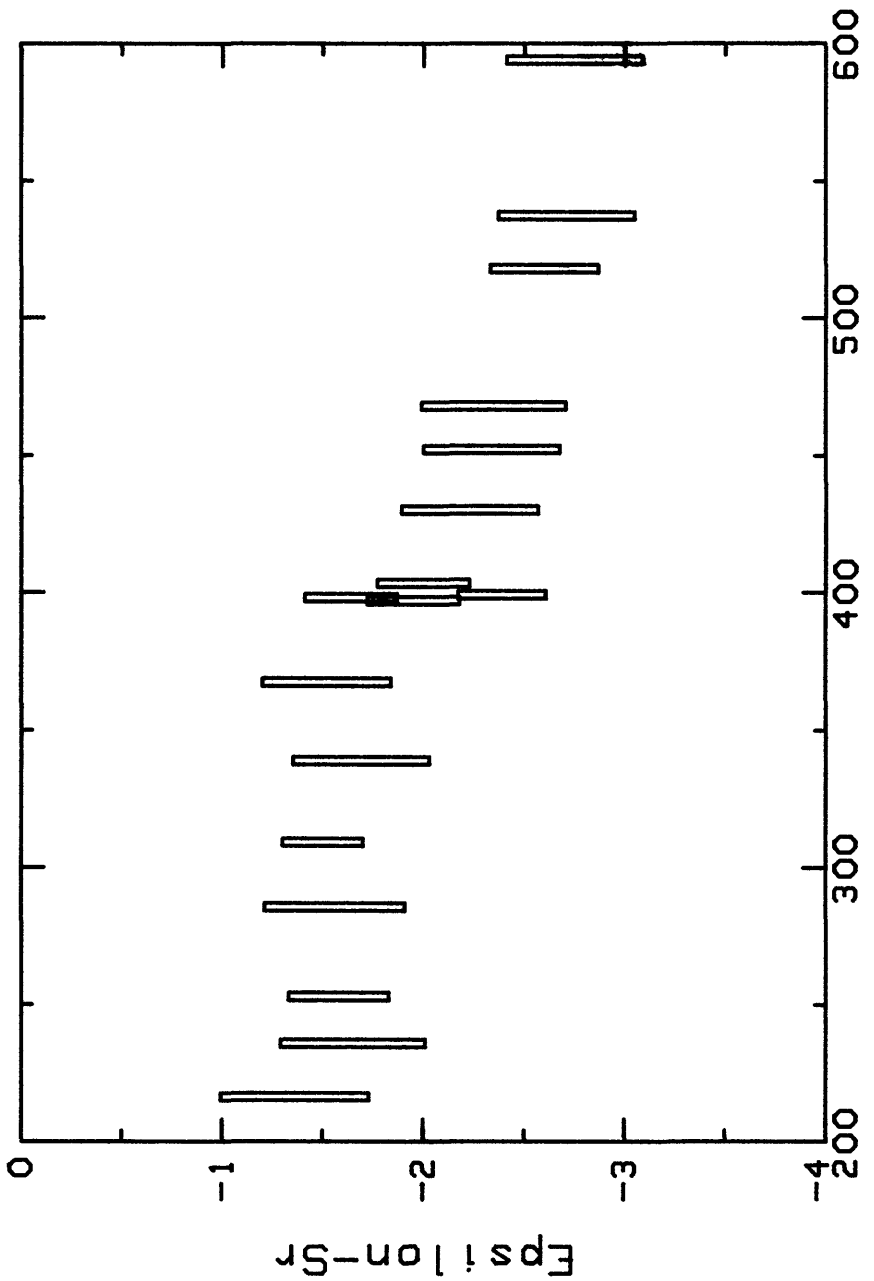

FIGURE 3-4. -- Detail of the abrupt change in the epsilon-Sr with depth at about 399 ft (bsf) for KAR-1 samples.

Figure 5

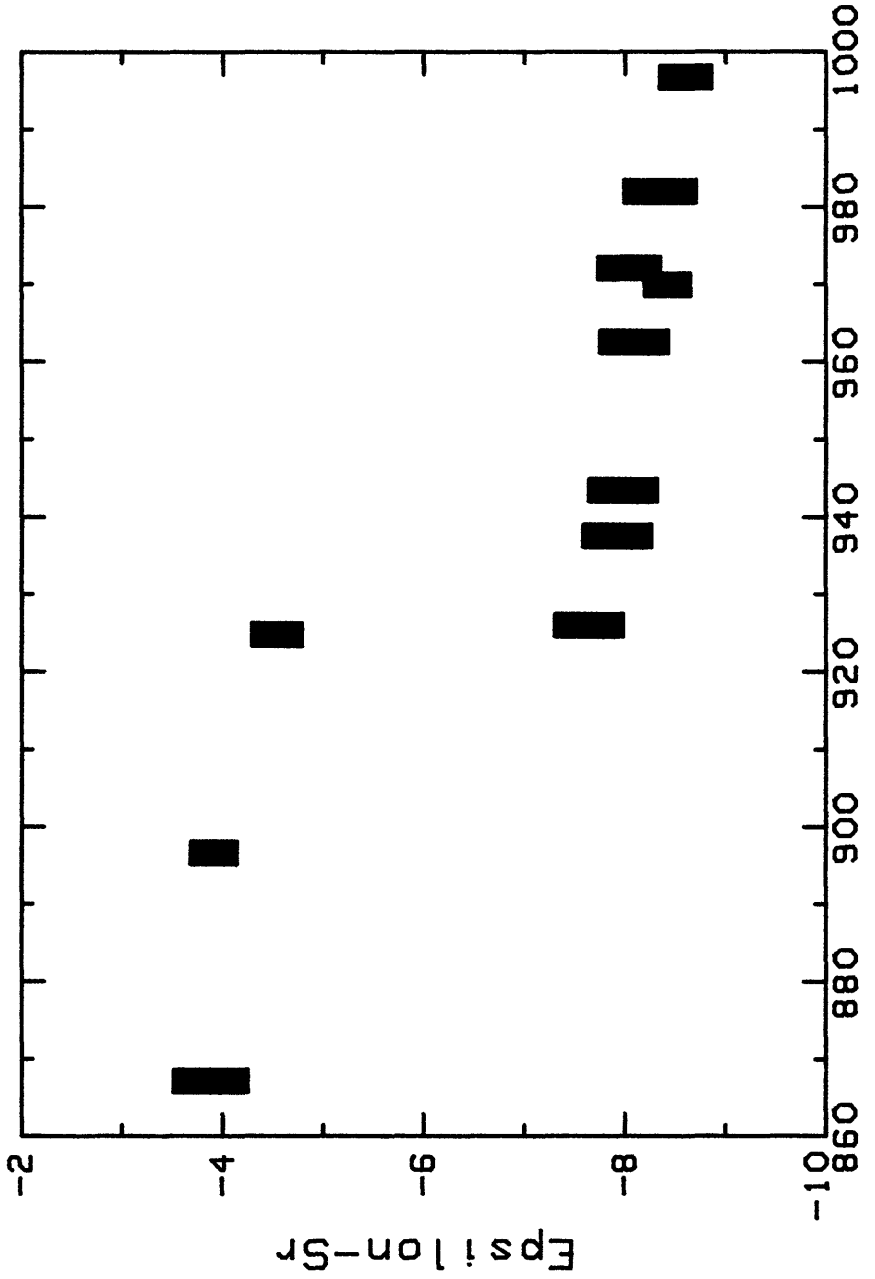

FIGURE 3-5. -- Detail of the abrupt change in epsilon-Sr with depth at about 925 ft (bsf) for KAR-1 samples.

completely independent technique for those intervals of core where either the paleontologic resolution is poor or the Sr-isotope resolution is very high.

Correlation between Sr-Isotope Stratigraphy and Lithostratigraphy of Borehole KAR-1. -- In most cases, the discontinuities in trend of apparent age versus depth for KAR-1 appear to correspond well to recognized lithologic discontinuities (unconformities, disconformities, karst surfaces, etc.). The correspondence between the two records is summarized in Table 3-3.

The strontium-isotope data resolves only those breaks which represent relatively large (at least 0.5 - 1 m.y.) time intervals. The actual age-resolution of individual data-points varies by an order of magnitude -- from about 0.2 m.y. to 2.0 m.y,. -- depending on the age of the samples. Nonetheless, because of the number of samples analyzed in any given interval, it appears that all significant time-breaks which could be present in the core are probably resolved by the data, with the possible exception of poorly resolved breaks in the 700 ft - 900 ft interval.

Reference Borehole XEN-3. -- Six samples from Project EXPOE borehole XEN-3 (in undisturbed ground, about 1.6 nautical miles from SEMINOLE crater, 2.4 miles from KOA, and 2.8 miles from MIKE) were analyzed on a manually operated mass-spectrometer of completely different design by different analysts than for the KAR-1 samples. These data (fig. 3-6, table 3-4), though somewhat less precise, are indistinguishable from the data for KAR-1 samples from similar depths.

SOURCE DEPTHS OF SAMPLES OF DISTURBED MATERIAL AS INFERRED FROM STRONTIUM ISOTOPES

Independent of the utility of strontium isotopes in the Enewetak carbonates as a geochronometer, it is apparent that the KAR-1 trend of epsilon-Sr with depth can be used to infer source-depths for samples of disturbed material, provided that:

(1). the stratigraphy represented in KAR-1 is reasonably consistent over the area of sampling, and;

(2). the samples have not experienced significant exchange of strontium.

The first point is assured by the nature of the geologic environment of Enewetak Atoll -- no major lateral changes in the stratigraphic succession are expected -- and is weakly confirmed by the limited data for XEN-3. The second point is supported for normal (undisturbed) carbonate samples from depths shallower than ±1,000 ft by the data set for KAR-1, and by the data for calcite-aragonite pairs from KAR-1. However, samples exposed to hot seawater for a significant length of time (perhaps tens of hours or days?) might well have experienced strontium exchange. In any case, no evidence for such alteration was observed in any of the Sr-isotope samples.

The nature of the KAR-1 calibration curve for epsilon-Sr -- with its flat intervals and abrupt changes -- is such that the depth resolution from the

TABLE 3-3. -- (Page 1 of 2 pages.) Correspondence between lithostratigraphy and Sr-isotope stratigraphy for reference core KAR-1. Lithostratigraphy modified from Henry, Wardlaw, and others (1986); only breaks or possible breaks in the stratigraphy are abstracted.

CORRESPONDENCE BETWEEN LITHOSTRATIGRAPHY AND Sr-ISOTOPE STRATIGRAPHY

DEPTH (ft bsf)	LITHOSTRATIGRAPHY	APPARENT-AGE TREND
70.0	Disconformity.	No change.
83.0	Disconformity.	No change.
105.9	Disconformity.	Abrupt increase of about 0.6 Ma.
131.6	Possible disconformity.	No change.
157.7	Disconformity.	No change.
177.0	Possible disconformity.	No change.
215.8	Disconformity.	Increase of about 1.4 Ma, possibly abrupt.
223.5	Disconformity.	No change, but apparent-age resolution is very poor.
231.8	Disconformity.	As above.
240.6	Disconformity.	As above.
278.9	Major disconformity.	As above.
319.8	Possible disconformity.	As above.
385.7	Disconformity.	As above.
399.0	Disconformity; break in caliper log, density log, and sonic log.	Abrupt increase of about 2 Ma.
482.0	Major disconformity.	No change.
555.7	Possible minor disconformity.	No change.
561.4	Possible minor disconformity.	No change.

(Table 3-3 continued on next page)

TABLE 3-3. -- (Continued from preceeding page).

CORRESPONDENCE BETWEEN LITHOSTRATIGRAPHY AND Sr-ISOTOPE STRATIGRAPHY

DEPTH (ft bsf)	LITHOSTRATIGRAPHY	APPARENT-AGE TREND
	(Continued from preceeding page)	
689.4	Major seismic reflecting horizon, abrupt downward-increase in organic material.	Possible abrupt increase in about 1 Ma, but in any case the start of an interval of rapid increase in apparent-age with depth. Apparent-age resolution is poor.
840.0	Minor disconformity.	As above.
857.2	Possible disconformity.	As above.
881.2	Disconformity.	As above.
903.9	Disconformity.	As above.
924.9	Disconformity.	Very abrupt, very well-resolved increase in apparent age from 12.4 Ma to 17.8 Ma.
935.7	Disconformity - "classic subaerial-exposure surface".	Apparently continuous increase (well-resolved) in apparent age from 17.8 Ma to 19.5 Ma for the next 160 ft.
942.8	Possible disconformity.	See above.
952.4	Disconformity.	See above.
995.3	Disconformity.	See above.
1,022.6	Disconformity.	See above.
1,025.4	Disconformity.	See above.
1,040.4	Disconformity.	See above.
1,045.4	Minor disconformity.	See above.
1,064.1	Major disconformity.	See above.

Figure 6

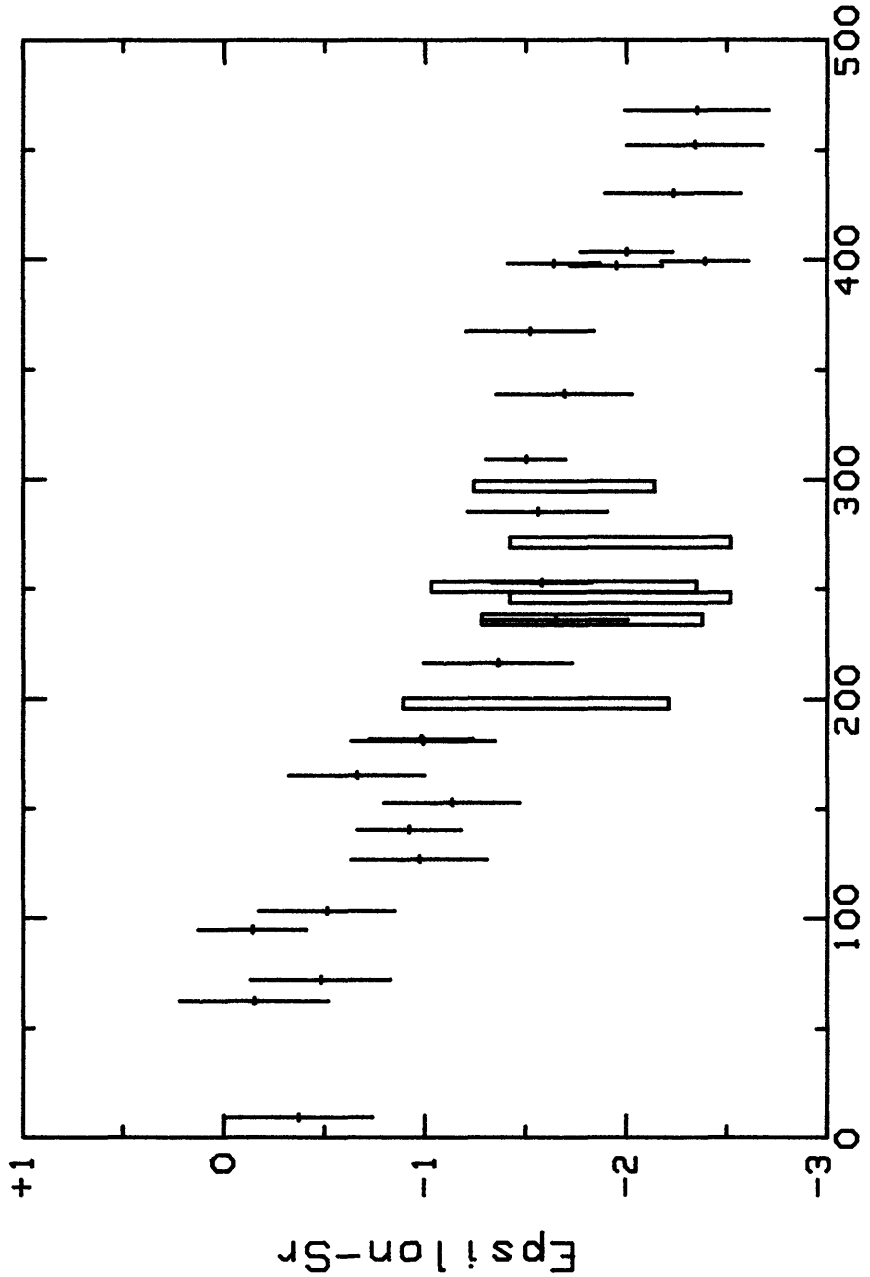

Figure 3-6. -- Epsilon-Sr versus depth for undisturbed core XEN-3 (error boxes) with KAR-1 data (error-crosses) shown for reference.

TABLE 3-4. -- Data for undisturbed EXPOE Project borehole XEN-3.

EPSILON-Sr VERSUS DEPTH, BOREHOLE XEN-3

CORE DEPTH (ft bgs[1])	Epsilon-Sr	error
198	-1.55	0.66
236	-1.83	0.55
246	-1.97	0.55
251	-1.69	0.66
271.5	-1.97	0.55
297	-1.69	0.45

[1] bgs = below ground surface

strontium-isotope analysis for a given sample can vary greatly. In the least-favorable intervals, the depth uncertainty can be as large as ±200 ft, whereas in the most-favorable intervals is uncertainty can be less than 50 ft. Moreover, the uncertainty in an inferred source-depth generally does not have a normal distribution; rather all possible depths within the range of the uncertainties may be equally probable, reflecting an interval in the KAR-1 calibration-curve that is flat and bounded by discrete steps.

Samples from the Surface of OAK Crater. -- Samples collected from the surface of OAK crater show an apparently smooth decrease in abundance with source-depth (fig. 3-7; table 3-5), within the resolution of the strontium isotopes. Most samples were derived from less than 200 ft depths bsf, and only one sample (166B) was clearly derived from a depth of 400 ft or more.

Borehole Samples from Disturbed Intervals. -- Core samples from disturbed intervals in boreholes (table 3-6, fig. 3-8) crudely suggest the following:

Borehole KCT-5: Disturbed stratigraphy to a depth of about 160 ft bsf. By 190 ft bsf, core depth is similar to inferred source depth.

Borehole KCT-8: Disturbed stratigraphy to a depth of at lest 60 ft bsf.

Borehole KBZ-4 (ground zero): From 60 ft to 200 ft bsf, all but 2 of the samples were apparently derived from depths in the 100-200 ft bsf range. The two exceptions (from about 65 and 125 ft bsf) are both derived from shallower than 100 ft bsf.

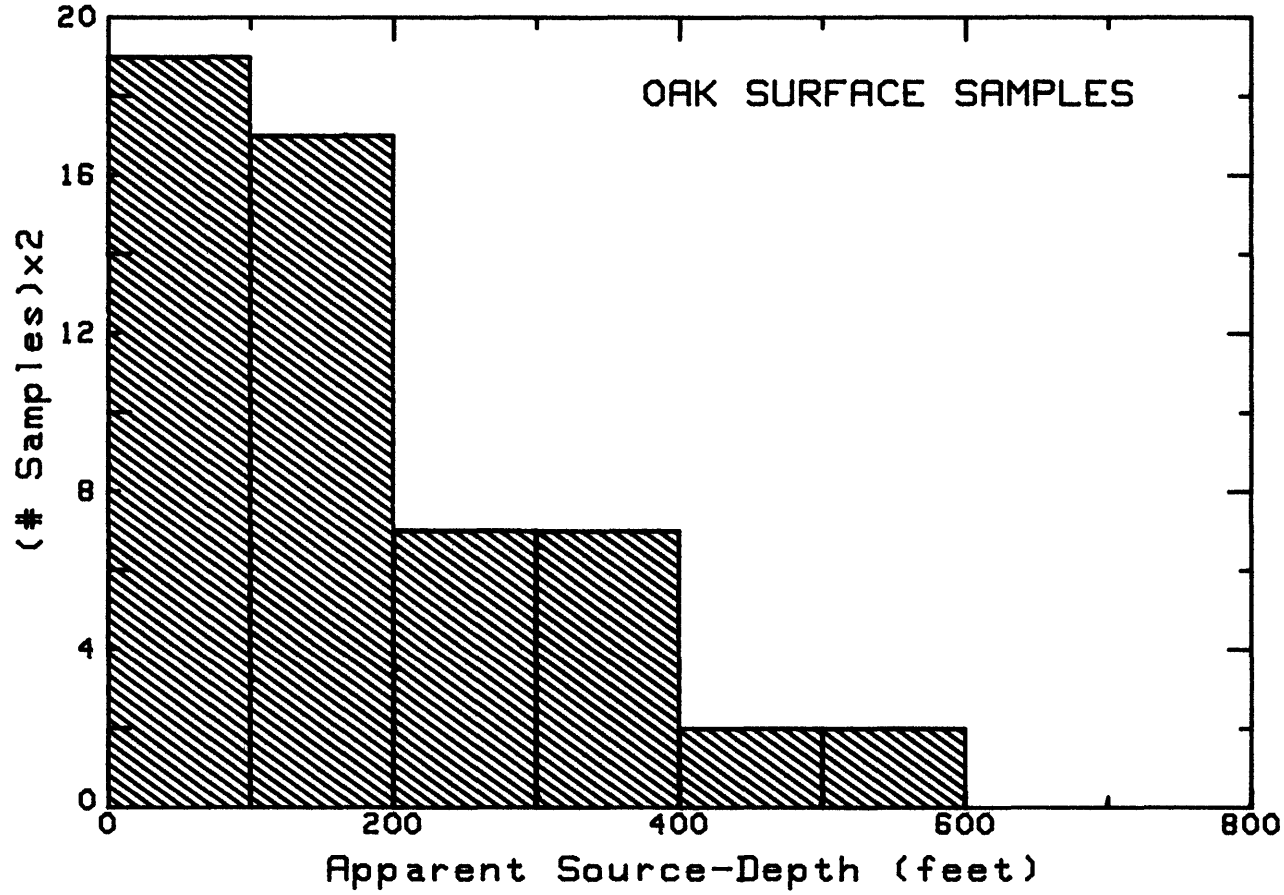

Figure 7

FIGURE 3-7. -- Histogram of source depths for samples collected on the surface of OAK crater. Source depths were calculated using the epsilon-Sr versus depth trend of KAR-1 samples. The cells in the histogram are normalized for uncertaintites in the estimated source-depths, and so should be unbiased compared to a histogram of precisely-known source-depths.

TABLE 5

DATA FOR SURFACE SAMPLES FROM OAK

SAMPLE	NAME	Epsilon Sr	Epsilon error	Source-depth (feet)
OAK	188	-0.23	.34	0-110
OAK	166C	-0.82	.34	100-200
OAK	171BD	-1.03	.34	100-400
OAK	168C	-1.81	.34	200-400
OAK	167A	-1.28	.34	110-400
OAK	171A	-1.14	.34	100-400
OAK	150	-0.39	.34	0-200
OAK	158	-1.32	.34	100-400
OAK	171(5)	-0.88	.34	50-200
OAK	173B	-0.76	.34	50-200
OAK	174	-1.18	.34	100-400
OAK	174(1)	-1.36	.34	100-400
OAK	179	+0.16	.34	0-50
OAK	166B	-2.47	.40	400-600
OAK	178	+0.15	.34	0-50
OAK	180D	-0.22	.34	0-100
OAK	189	+0.00	.34	0-100
OAK	191	-0.21	.34	0-100
OAK	125A1915A	-1.18	.34	100-400
OAK	125C1915C	-0.40	.34	0-200

TABLE 3-5. -- Epsilon-Sr and estimated source depths for samples from the surface of OAK crater. Source depths were estimated using the epsilon-Sr versus depth trend of reference core KAR-1 (fig. 3-2). Due to the nature of the KAR-1 trend, source depths are given as a possible range, not as a best estimate with uncertainties. Replicate analyses are pooled.

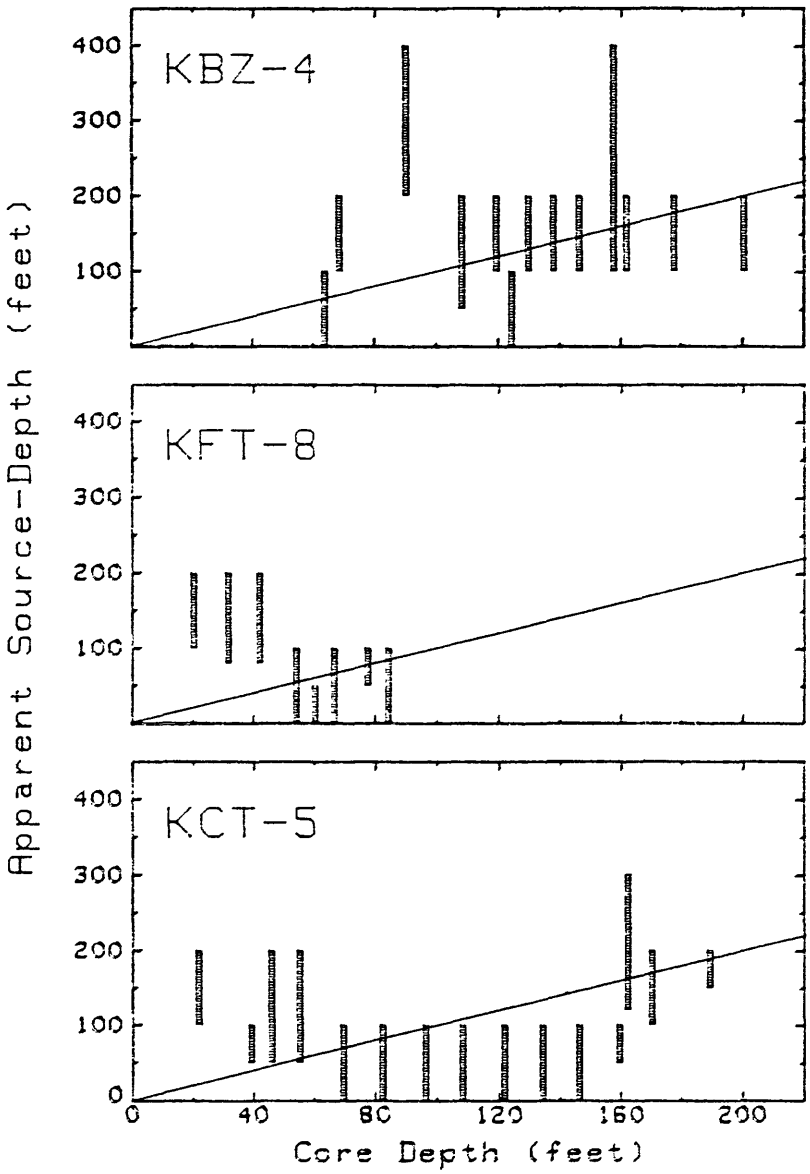

FIGURE 3-8. -- Source depths versus sample depths for samples from cores in disturbed ground. Source depths were calculated using the epsilon-Sr versus depth trend of KAR-1 samples; height of boxes indicates uncertainty in this estimate, obtained by propagating the epsilon-Sr uncertainty onto the hand-fit KAR-1 epsilon-Sr trend. Diagonal line is locus of perfect correspondence between source depth and sample depth.

TABLE 6

DATA FOR CORE-SAMPLES IN DISTURBED GROUND

Core#	Depth (feet)	Epsilon-Sr	Epsilon error	Source-Depth (feet)
KCT-5	21.5	-.96	.34	100-200
"	38.9	-.30	.21	50-100
"	45.7	-.70	.38	50-200
"	55.0	-.76	.18	50-200
"	69.3	-.16	.19	0-100
"	82.0	-.29	.34	0-100
"	96.0	+.01	.20	0-100
"	108.0	-.27	.19	0-100
"	121.5	-.18	.32	0-100
"	134.0	-.15	.34	0-100
"	146.0	-.25	.2	0-100
"	159.2	-.41	.34	50-100
"	162.0	-1.18	.34	120-300
"	170.0	-.78	.34	100-200
"	189.0	-.98	.34	150-200
KDT-6	24.0	-.12	.34	0-100
"	32.2	-.84	.34	100-200
"	43.9	-.08	.34	0-100
KET-7	17.6	-.23	.34	0-100
KFT-8	20.0	-.94	.34	100-200
"	31.4	-.67	.34	80-200
"	41.8	-.70	.34	80-200
"	54.0	-.13	.34	0-100
"	60.2	+.15	.34	0-50
"	66.4	-.10	.34	0-100
"	77.3	-.30	.34	50-100
"	84.0	-.05	.34	0-100
KBZ-4	63.3	+.02	.19	0-100
"	68.1	-.87	.22	100-200
"	89.8	-1.38	.19	200-400
"	107.9	-.75	.23	50-200
"	119.0	-.85	.19	100-200
"	124.0	-.16	.23	0-100
"	129.4	-.86	.23	100-200
"	137.5	-.86	.19	100-200
"	146.0	-.90	.26	100-200
"	157.2	-1.21	.25	100-400
"	161.5	-.93	.23	100-200
"	177.2	-1.04	.23	100-200
"	200.0	-1.02	.23	100-200

TABLE 3-6. -- Epsilon-Sr and estimated source depths for samples from cores in disturbed ground. Number after core name indicates the depth in the core from which the sample was obtained. Source depths were estimated using the epsilon-Sr versus depth trend of reference core KAR-1 (fig. 3-2). Due to the nature of the KAR-1 trend, source depths are given as a possible range, not as a best estimate with uncertainties. Replicate analyses are pooled.

REFERENCES

Brass, G. W., and Turekian, K. K., 1972, Strontium distributions in seawater profiles from the Geosecs I (Pacific) and Geosecs II (Atlantic) test stations: Earth Planetary Science Letters, v. 16, p. 117.

Burke, W. H., Dennison, R. E., Hetherington, E. A., Koepnick, R. B., Nelson, H. F., and Otto, J. B., 1982, Variation of seawater $^{87}Sr/^{86}Sr$ throughout Phanerozoic time: Geology, v. 10, p. 515-519.

DePaolo, D. J., 1986, Detailed record of the Neogene Sr isotopic evolution of seawater from DSDP site 590B: Geology, v. 14, p. 103-106.

Henry, T. W., Wardlaw, B. R., and others, 1986, Pacific Enewetak Crater Exploration (PEACE) Program, Enewetak Atoll, Republic of the Marshall Islands; Part 1: Drilling operations and description of boreholes in vicinity of KOA and OAK craters: U.S. Geological Survey Open-File Report 86-419, 502 p., 3 appendices.

Kennett, J. P., von der Borch, C., and others, 1986, Initial reports of the Deep Sea Drilling Project, volume XC, Part I, p. 14: Washington D.C., U.S. Government Printing Office.

Ludwig, K. R., 1985, User's manual for ANALYST, a computer program for control of an Isomass 54E thermal-ionization, single-collector mass-spectrometer: U.S. Geological Survey Open-File Report 85-141 (revision D), 96 p.

Peterman, Z. E., Hedge, C. E., and Tourtelot, H. A., 1970, Isotopic composition of strontium in seawater throughout Phanerozoic time: Geochimica Cosmochimica Acta, v. 34, p. 109-120.

Russell, W. A., Papanastassiou, D. A.,and Tombrello, T. A., 1978, Ca isotope fractionation on the earth and other solar system materials: Geochimica Cosmochimica Acta, v. 42, p. 1075-1090.

Taylor, S. R., and McLennan, S. M.,1985, The Continental Crust: its Composition and Evolution: Blackwell Scientific Publications, Boston, p. 14.

CHAPTER 4:

X-RAY DIFFRACTION MINERALOGY

by

E.L. Tremba and B.L. Ristvet

S-CUBED, A Division of Maxwell Laboratories[1]

INTRODUCTION

X-ray diffraction (XRD) studies were conducted on whole-rock samples to determine their bulk carbonate mineralogic compositions by weight percent. These results are applicable to three objectives of the PEACE Program: (1) estimate of the specific gravity (grain density) of the whole-rock samples to allow conversion of bulk density to porosity, particularly useful in the modeling of the borehole gravimetry, (2) to aid studies of petrogenesis-diagenesis and the construction of the stratigraphic framework, and (3) to provide a log for correlative purposes. The specific gravity estimates are discussed in Chapter 8. Details of the latter two objectives are discussed in Chapter 2. Previous XRD studies were conducted on Enewetak core material collected during the EXPOE and PACE Programs (Couch and others, 1975).

METHODS OF STUDY

The XRD technique used was similar to that reported by Neumann (1965). XRD samples were obtained either from the core boxes in the USGS Core Library (Denver, CO) or from the samples utilized for petrographic thin sections. The former samples, herein called stratigraphic samples, were chosen to be representative of the intervals of recovered sections of core. The sampling interval was generally between 15 and 30 ft unless a noticeable change in rock type occurred. XRD samples obtained from the remains of the thin-section samples provided specific bulk carbonate mineralogic data to aid thin-section studies.

XRD stratigraphic samples weighed approximately 100 grams (g). Thin-section samples weighed approximately 50 g. All samples were powdered and wet sieved with water to pass a 200-mesh screen [= 74 micron or 3.75 phi (Ø)].

All XRD powdered samples were mounted on glass slides by smearing a slurry of sample and powdered fluorite (CaF_2) in several drops of a dilute solution of Duco cement in acetone to act as a bonding agent. Fluorite was

---

[1] Albuquerque, NM.

added as an internal standard for calibrating the angle of diffraction on the sample runs. This was necessary to determine the mole percent $MgCO_3$ for any samples that have a magnesium-calcite phase.

Samples mounted on glass slides were run on a Picker x-ray unit owned and operated by the Air Force Weapons Laboratory (AFWL), Kirtland Air Force Base, NM. The x-ray unit is equipped with a Servo driven goniometer controlled by a California Scientific Systems computer. A Cu K-alpha x-ray tube was operated at 40 kV and 30 mA. The computer directed the goniometer to scan each sample nominally from 25.0 to 32.0 degrees 2 theta (deg 2θ) in steps of 0.05 deg 2θ. Each step was counted for 3 sec and the data recorded. To accommodate for peak shifts in the XRD analysis, the amount of the shift was determined by comparing the location of the fluorite peak (as determined by a self-contained program in the California Scientific Systems computer that uses a polynomial fit of the digitized data) to its nominal location of 28.3 deg 2θ. In some cases, the fluorite peak was not large enough to reliably determine a peak location. In these cases, the aragonite peak nominally at 26.24 deg 2θ was considered next, followed by the calcite peak at 29.4 deg 2θ.

The primary peaks of aragonite (26.24 deg 2θ) and calcite (29.4 deg 2θ) were integrated by summing the appropriate individual 0.05 deg 2θ count values and subtracting estimates of their respective background counts. These integrated peak values were used to calculate an aragonite to calcite XRD intensity ratio. It was necessary to determine a calibration curve to convert the aragonite to calcite XRD intensity ratios to weight ratios.

To determine a calibration curve, a sequence of nine laboratory standards consisting of mixtures of weighed "pure" aragonite and "pure" calcite powders were prepared. The aragonite was from a modern coral (Pocillopora elegans, collected at Enewetak) crushed to pass a 200-mesh screen. The calcite was a single crystal that was crushed to pass a 200-mesh screen. The "pure" aragonite and calcite powders as well as the synthetic fluorite powder were scanned on the XRD unit through the diffraction angles of interest (25 to 32 deg 2θ). None had any visible extraneous peaks (impurities).

The nine standard mixtures had weight percentages of aragonite and calcite that varied from approximately 10 to 90 in increments of about 10 percent. Five aliquants of each of the standard mixtures were mounted on glass slides and run twice on the XRD unit as described above, except fluorite was not added. The intensity ratios of aragonite to calcite for each of the ten runs per standard mixture were averaged. The average intensity ratios of aragonite to calcite for each of the nine standards were plotted against their respective aragonite weight percents. A curve consisting of two connected hyperbolic fits (one for values less than about 40 weight percent and one for values greater than 40 weight percent) was fit visually to the nine points by a reiterative, computer assisted approach (fig. 4-1).

The calibration curve was digitized and utilized in a computer program to calculate the weight percents of the carbonate minerals. Prior to any data reduction, all the digitized data for a given run was corrected for any goniometer shift. The computer program was designed to compute the intensity ratio of aragonite to calcite (including magnesium calcite, where present) for each sample run and then to convert that value to a weight percent using the

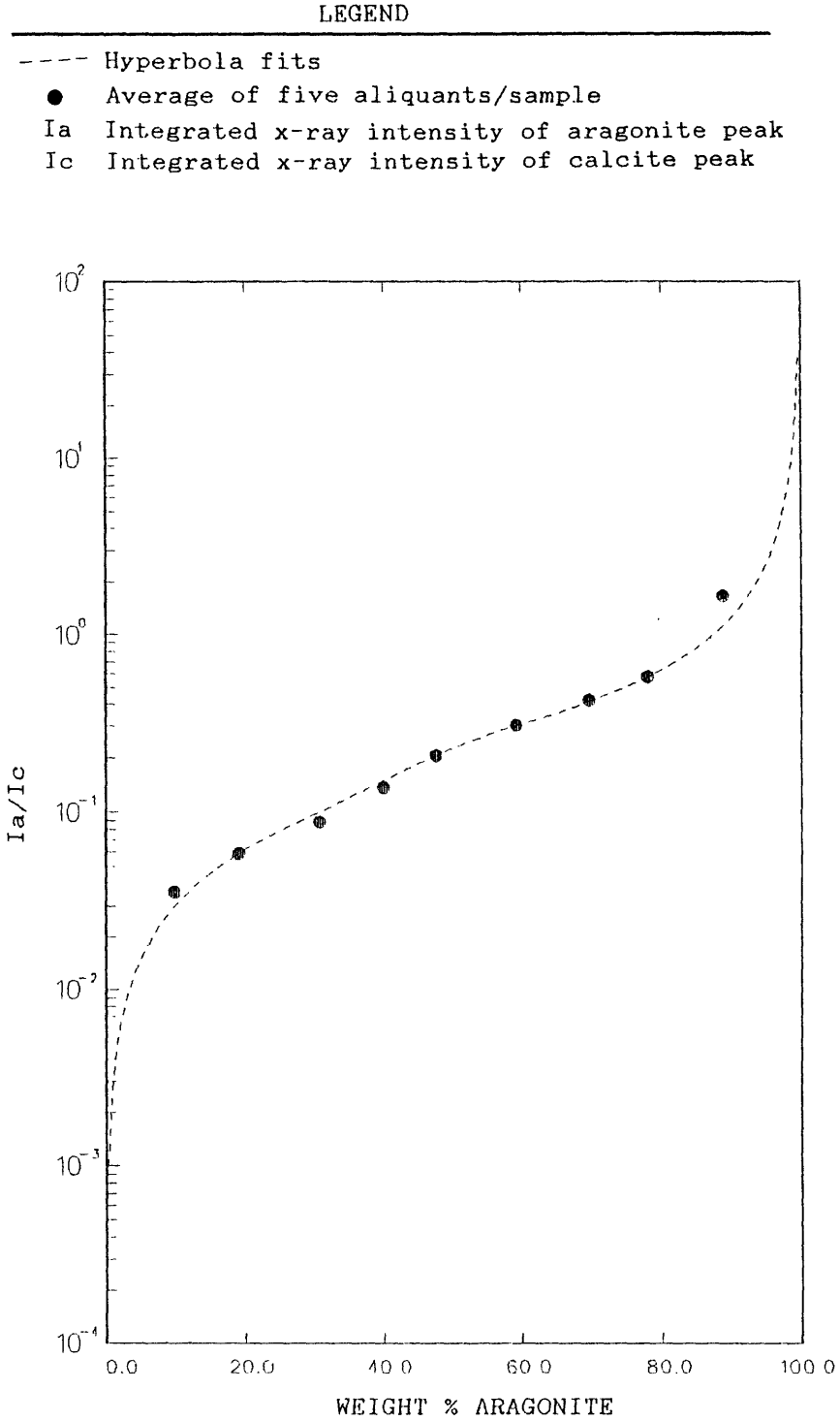

FIGURE 4-1. -- Calibration curve for converting aragonite/calcite x-ray intensity ratios (Ia/Ic) to weight percents of aragonite in a calcite matrix.

data from the calibration curve, assuming that aragonite and calcite equal 100 percent of the sample.

The weight percent magnesium calcite and dolomite were determined using similar techniques (see Neumann, 1965, and Goldsmith and Graf, 1958, respectively). Only three XRD samples had measurable quantities of dolomite on their diffraction patterns (KBZ-4: 917.5 and 1023.2 ft bsf; OOR-17: 1079.3 ft bsf). The weight percents of aragonite, calcite, and dolomite for the three dolomitic samples were determined manually using the digitized data.

Obviously, the calculated weight percents are for the carbonate phases. Total organic content analyses of selected PEACE samples had organic weight percents that ranged from approximately 0.3 to 4 (see Chapter 5). Acid insoluble-residue analyses of selected PEACE Program samples suggest non-carbonate, non-organic contents of less than 0.01 weight percent (see Chapter 6). The weight percent values calculated for the carbonate minerals using the XRD technique have estimated precision errors of 5 percent. Therefore, it is reasonable to assume that the computed weight percents of the carbonate minerals are representative of sample weight percents.

Estimates of the mole percent $MgCO_3$ in the magnesium-calcite phase of the PEACE Program samples were made by measuring the location (deg 2θ) of the magnesium-calcite peak, adjusting for any goniometer shift that may have occurred, and then computing the mole percent $MgCO_3$ by interpolating the location of the magnesium-calcite peak between the peak locations of "pure" calcite and dolomite.

RESULTS

Table 4-1 is a summary of the borehole distribution and types of PEACE Program XRD samples run by personnel from the AFWL and S-Cubed. A total of 657 samples from 15 boreholes was run, plus 22 grab samples (benthic samples) from the Enewetak lagoon floor (see Chapter 10). Stratigraphic XRD samples, mentioned earlier, were taken from the following sets of boreholes: (1) KAR-1 and the lower section of KBZ-4, the reference or control holes for the KOA area; (2) OAR-2-2A, the lower section of OBZ-4, and OOR-17, the reference holes for the OAK area; and (3) OOR-17, OPZ-18, OQT-19, ORT-20, OSR-21, and OTG-23, in each of which downhole gravimetry surveys were run (see Chapter 8).

Tables 4-2 through 4-23* list the weight percent carbonate minerals (calcite, magnesium calcite, dolomite, and aragonite) and the mole percent $MgCO^3$ in the magnesium-calcite phase for each sample x-rayed. Table 4-2 contains the results for the grab samples from the Enewetak lagoon. Tables 4-3 through 4-12 present results for the stratigraphic samples from each borehole. Tables 4-13 through 4-23 list results for the thin-section samples from each borehole. In these tables, the term "trace" indicates those samples that have XRD patterns that suggest the presence of a non-measurable amount of dolomite. The term "na" indicates that a measurement was not applicable.

---

* Tables 4-2 through 4-35 are at the back of this Chapter.

TABLE 4-1. -- Total number of x-ray diffraction samples run by the Air Force Weapons Laboratory and S-Cubed for the PEACE Program.

BOREHOLE	NUMBER OF SAMPLES	
	STRATIGRAPHIC	THIN-SECTION
KAR- 1	92	81
KBZ- 4	5	20
OAR- 2	49	31
OAR-2A	62	22
OBZ- 4	22	36
OCT- 5	0	1
ODT- 6	0	2
OET -7	0	1
OOR-17	82	29
OPZ-18	39	0
OQT-19	39	0
ORT-20	31	1
OSR-21	21	1
OTG-23	8	0
OUT-24	0	2
SUBTOTAL	450	227
BENTHIC*	22	0
TOTAL	477	227

* Recent benthic (grab) samples from floor of Enewetak lagoon (see Chapter 10).

Figures 4-2 through 4-11* show the depth profile of aragonite weight percent for each borehole with XRD stratigraphic samples. Included on the figures are the geologic (or sedimentary) packages and crater zones as presented in Chapters 2 and 14 of the current report, respectively. It is apparent on the figures for the reference holes (fig. 4-2, KAR-1; fig. 4-4, OAR-2/2A; fig. 4-5, OBZ-4; and fig. 4-6, OOR-17) that the weight percent aragonite varies systematically with depth nearly in phase with the geologic packages. The most noticeable discrepancy is the difference in depths between the boundary between Packages 6 and 7 and the shallower (within Package 6), sharp decrease in weight percent aragonite in borehole KAR-1 (fig. 4-2).

In general, XRD samples in Packages 1 and combined Packages 4,5, and 6 have relatively high values of weight percent aragonite. Packages 3, 7, and 8, in contrast, have low values of weight percent aragonite. Package 2 has variable values of weight percent aragonite that generally decrease with depth. These variations of the weight percent aragonite with depth are highly consistent from borehole to borehole and can be used as an important correlative tool.

Tables 4-24 through 4-33 present the average weight percent of carbonate minerals and the average mole percents of $MgCO_3$ (magnesium-calcite phase) for the geologic packages/crater zones (stratigraphic samples) from the boreholes represented by Figures 4-2 through 4-11. Table 4-34 lists the average weight percent of carbonate minerals and the mole percent $MgCO_3$ (magnesium carbonate) for the grab samples from the Enewetak lagoon. The average carbonate mineralogic content of the grab samples probably is representative of Recent Enewetak lagoon sediments. However, samples with relatively high amounts of silt-size particles --e.g. sample numbers 38 and 39-- may have significant amounts of debris related directly to the nuclear event itself (see Chapter 10). Samples 38 and 39 have the highest weight percent calcite (23 and 27, respectively) of the 22 grab samples (table 4-2). Compared with the average of 9 percent calcite for all the grab samples, the 23 and 27 percent calcite values for samples 38 and 39 suggest the original lagoonal sediments at these locations may have been mixed with a calcite-rich material probably from depth. The most likely sources of calcite-rich material are Packages 2 and 3.

Table 4-35 is a listing of the average weight percents of carbonate minerals and average mole percents of $MgCO_3$ (magnesium-calcite phase) for the geologic packages from all the OAK boreholes with stratigraphic samples. As expected, the averages for Package 1 are similar to those for the bottom grab samples from the Enewetak lagoon (cf. tables 4-34 and -35). The slightly lower percentage of aragonite and slightly higher percentages of calcite and magnesium calcite in Package 1 are based on averages of only 21 samples from five OAK boreholes and 22 grab samples.

Tables 4-23 through 4-35 quantify the mineralogic trends observed on Figures 4-2 through 4-11. Table 4-35 clearly shows the decreasing percentage

---

* Figures 4-2 through 4-11 are located at the end of this Chapter.

of aragonite with depth except for the sharp increase in aragonitic weight percents for Packages 4, 5, and 6. The decrease in aragonite and the complementary increase in calcite with depth suggest an increasing stabilization of the carbonate mineralogic assemblage has occurred with depth probably as a result of diagenesis. Supporting this statement is the virtual disappearance of magnesium calcite below Package 1, again except in Packages 4, 5, and 6. Both aragonite and magnesium calcite are relatively unstable compared to calcite in the presence of fresh water. Thus, Package 1 and most of Packages 4, 5, and 6 appear to be unaltered with respect to their original carbonate mineral composition -- i.e. their carbonate mineral percentages are similar to those of Recent benthic samples. The qualifier, "most of", was applied to Packages 4, 5, and 6 because (as was noted in the discussion of figs. 4-2 through 4-11) the geologic package boundaries do not strictly follow the mineralogic boundaries. The most alteration of carbonate minerals apparently occurred in Packages 3, 7, and 8, as indicated by the low aragonite percentages, high calcite percentages, and absence of magnesium calcite in all three packages. At least traces of dolomite were detected in some Package-6, -7, and -8 samples.

Two samples from the crater zones of borehole OPZ-18 had measurable quantities of magnesium calcite: 192.0 ft bsf in crater-zone Beta 2 and 231.6 ft bsf in crater-zone Beta 3 (table 4-8). These samples were taken from an interval dominated by greenish-gray wackestone and containing sparse moderate-red ("unaltered") Homotrema grains, typical Package 1 (see Henry, Wardlaw, and others, 1986, p. 440, for description). The presence of the magnesium calcite, the greenish-gray color, and the unaltered Homotrema grains suggest that this zone is buried Package 1 material that has not been mixed significantly with material from other biostratigraphic zones.

ACKNOWLEDGEMENTS

Special thanks are extended to Messers. Wayne E. Martin and Stephen M. Wessels, U.S. Geological Survey, for crushing and sieving the mineralogic samples. Appreciation is also extended to Dr. Robert Henny, Mr. Charles Miglianco, and SSgt. Robert Robinson, Air Force Weapons Laboratory, for making their facilities available and for operating the AFWL diffraction unit during most of the sample runs.

REFERENCES

Couch, R.F., Jr., Fetzer, J.A., Goter, E.R., Ristvet, B.L., Tremba, E.L., Walter, D.R., and Wendland, W.P., 1975, Drilling operations on Eniwetok Atoll during Project EXPOE: Air Force Weapons Laboratory Technical Report AFWL-TR-75-216, Kirtland Air Force Base, New Mexico, 270 p., 17 figs., 4 tbls. (unclassified).

Goldsmith, J.R., and Graf, D.L., 1958, Structural and compositional variations in some natural dolomites: Journal of Geology, v. 66, p. 678-693.

Henry, T.W., Wardlaw, B.R., Skipp, B., Major, R.P., and Tracey, J.I., Jr., 1986, Pacific Enewetak Atoll Crater Exploration (PEACE) Program, Enewetak Atoll, Republic of the Marshall Islands; Part 1: Drilling operations and descriptions of boreholes in vicinity of KOA and OAK craters: U.S. Geological Survey Open-File Report 86-419, 497 p., 32 figs., 29 pls., 13 tbls., 3 appendices.

Neumann, A.C., 1965, Processes of recent carbonate sedimentation in Harrington Sound, Bermuda: Bulletin of Marine Science, v. 15, p. 987-1035.

TABLE 4-2. -- Weight percents of carbonate minerals and mole percents of $MgCO_3$ (magnesium-calcite phase) determined by XRD for sediment (benthic) samples from the Enewetak lagoon. (See Chapter 10 for further discussion.)

SAMPLE # USGS	CALCITE Wt %	MgCALCITE Wt %	$MgCO_3$ Mol%	DOLOMITE Wt %	ARAGONITE Wt %
9	15	15	17	0	70
16	8	17	16	0	75
17	2	5	16	0	93
26	6	12	17	0	82
29	8	24	17	0	68
30	8	12	15	0	80
32	16	21	16	0	63
37	10	13	16	0	77
38	23	19	16	0	58
39	27	18	16	0	55
43	8	15	16	0	77
58	7	15	16	0	78
63	8	20	16	0	72
65	9	16	16	0	75
74	7	11	16	0	82
78	2	6	18	0	92
83	10	10	17	0	80
89	7	8	16	0	85
91	3	4	18	0	93
104	3	22	18	0	75
118	3	7	17	0	90
123	7	25	16	0	68

TABLE 4-3 (1/3 pages). -- Weight percents of carbonate minerals and mole percents of $MgCO_3$ (magnesium-calcite phase) determined by XRD for stratigraphic samples from borehole KAR-1.

DEPTH Ft bsf	CALCITE Wt %	MgCALCITE Wt %	$MgCO_3$ Mol%	DOLOMITE Wt %	ARAGONITE Wt %
22.9	7	13	16	0	80
35.2	5	14	16	0	81
47.5	23	5	16	0	72
56.2	26	0	na	0	74
65.1	11	0	na	0	89
73.6	56	0	na	0	44
95.5	13	0	na	0	87
106.3	43	0	na	0	57
126.2	29	0	na	0	71
131.9	9	13	16	0	78
142.6	91	0	na	0	9
143.0	23	0	na	0	77
152.1	27	0	na	0	73
163.2	59	0	na	0	41
172.7	48	0	na	0	52
182.9	48	0	na	0	52
193.7	38	0	na	0	62
207.2	46	0	na	0	54
216.2	33	0	na	0	67
225.2	48	0	na	0	52
231.1	25	0	na	0	75
232.1	95	0	na	0	5
233.4	94	0	na	0	6
245.6	43	0	na	0	57
255.0	79	0	na	0	21
267.8	78	0	na	0	22
278.7	86	0	na	0	14
282.3	95	0	na	0	5
292.6	31	0	na	0	69
302.7	91	0	na	0	9
312.6	93	0	na	0	7
316.2	36	0	na	0	64
325.6	96	0	na	0	4
335.8	92	0	na	0	8
346.5	98	0	na	0	2
352.8	94	0	na	0	6
362.9	97	0	na	0	3
372.5	99	0	na	0	1
385.7	99	0	na	0	1
399.1	94	0	na	0	6
414.0	5	0	na	0	95
435.1	100	0	na	0	0

(continued on next page)

TABLE 4-3 (cont., p. 2/3). -- Weight percents of carbonate minerals and mole percents of $MgCO_3$ (magnesium-calcite phase) determined by XRD for stratigraphic samples from borehole KAR-1.

DEPTH Ft bsf	CALCITE Wt %	MgCALCITE Wt %	$MgCO_3$ Mol%	DOLOMITE Wt %	ARAGONITE Wt %
487.6	100	0	na	0	0
518.2	71	0	na	0	29
540.8	98	0	na	0	2
550.8	33	0	na	0	67
555.6	17	0	na	0	83
557.7	30	0	na	0	70
569.7	13	0	na	0	87
584.4	16	0	na	0	84
591.7	11	0	na	0	89
604.3	31	0	na	0	69
616.3	23	0	na	0	77
626.5	7	0	na	0	93
635.6	7	2	14	0	91
655.1	33	0	na	0	67
665.8	10	3	14	0	87
680.3	100	0	na	0	0
697.5	5	6	15	0	89
703.7	6	4	14	0	90
717.3	5	1	15	0	94
728.7	9	0	na	0	91
739.7	10	10	14	0	80
745.1	13	14	14	0	73
754.5	8	6	15	0	86
761.3	7	20	15	0	73
776.6	5	7	15	0	88
791.2	8	7	15	0	85
809.7	10	7	15	0	83
823.8	13	11	14	0	76
848.5	14	0	na	0	86
855.0	17	5	14	0	78
856.1	31	3	14	0	66
870.5	23	0	na	0	77
881.2	14	9	14	0	77
896.8	9	3	12	0	88
918.1	46	0	na	0	54
924.6	40	0	na	0	60
925.2	82	0	na	0	18
943.1	100	0	na	trace	0
969.5	100	0	na	0	0
995.3	100	0	na	0	0
1023.0	100	0	na	0	0
1025.6	94	0	na	0	6

(continued on next page)

TABLE 4-3 (cont. p. 3/3). -- Weight percents of carbonate minerals and mole percents of $MgCO_3$ (magnesium-calcite phase) determined by XRD for stratigraphic samples from borehole KAR-1.

DEPTH Ft bsf	CALCITE Wt %	MgCALCITE Wt %	$MgCO_3$ Mol%	DOLOMITE Wt %	ARAGONITE Wt %
1040.8	100	0	na	trace	0
1048.1	92	0	na	trace	8
1049.0	88	0	na	trace	12
1096.1	100	0	na	0	0
1112.2	100	0	na	0	0
1114.3	96	0	na	0	4
1130.2	100	0	na	0	0
1136.1	100	0	na	0	0

TABLE 4-4. -- Weight percents of carbonate minerals and mole percents of $MgCO_3$ (magnesium-calcite phase) determined by XRD for stratigraphic samples from borehole KBZ-4.

DEPTH Ft bsf	CALCITE Wt%	MgCALCITE Wt%	$MgCO_3$ Mol%	DOLOMITE Wt%	ARAGONITE Wt%
750.9	6	8	15	0	86
758.2	9	7	14	0	84
828.9	30	14	11	0	56
834.8	21	1	14	0	78
1023.2	89	0	na	11	0

TABLE 4-5 (1/3 p.). -- Weight percents of carbonate minerals and mole percents of $MgCO_3$ (magnesium-calcite phase) determined by XRD for stratigraphic samples from boreholes OAR-2/2A.

DEPTH Ft bsf	CALCITE Wt %	MgCALCITE Wt %	$MgCO_3$ Mol%	DOLOMITE Wt %	ARAGONITE Wt %
0.2	3	7	16	0	90
9.7	4	15	16	0	81
20.1	5	12	16	0	83
24.1	16	0	na	0	84
25.4	16	0	na	0	84
28.4	40	0	na	0	60
28.9	35	0	na	0	65
34.0	35	0	na	0	65
34.6	13	0	na	0	87
40.1	7	0	na	0	93
41.7	9	0	na	0	91
62.1	22	0	na	0	78
62.4	35	0	na	0	65
63.4	46	0	na	0	54
75.7	35	0	na	0	65
75.8	37	0	na	0	63
90.7	76	0	na	0	24
101.0	36	0	na	0	64
114.8	50	0	na	0	50
130.0	42	0	na	0	58
148.9	96	0	na	0	4
157.3	43	0	na	0	57
177.0	43	0	na	0	57
181.0	35	0	na	0	65
183.5	67	0	na	0	33
188.1	31	0	na	0	69
195.1	51	0	na	0	49
195.3	23	0	na	0	77
204.9	30	0	na	0	70
214.5	18	0	na	0	82
223.4	64	0	na	0	36
227.3	11	0	na	0	89
236.1	52	0	na	0	48
245.0	69	0	na	0	31
246.7	26	0	na	0	74
249.5	32	0	na	0	68
250.7	64	0	na	0	36
263.3	23	0	na	0	77
273.4	14	0	na	0	86
278.0	14	0	na	0	86
281.6	46	0	na	0	54
282.9	10	0	na	0	90

(continued on next page)

TABLE 4-5 (cont. p. 2/3). -- Weight percents of carbonate minerals and mole percents of $MgCO_3$ (magnesium-calcite phase) determined by XRD for stratigraphic samples from boreholes OAR-2/2A.

DEPTH Ft bsf	CALCITE Wt %	MgCALCITE Wt %	$MgCO_3$ Mol%	DOLOMITE Wt %	ARAGONITE Wt %
297.7	11	0	na	0	89
300.1	57	0	na	0	43
307.2	88	0	na	0	12
307.5	87	0	na	0	13
310.3	75	0	na	0	25
319.4	83	0	na	0	17
320.4	90	0	na	0	10
323.8	100	0	na	0	0
328.6	84	0	na	0	16
331.3	97	0	na	0	3
337.9	94	0	na	0	6
347.1	37	0	na	0	63
360.2	95	0	na	0	5
370.0	100	0	na	0	0
379.6	90	0	na	0	10
391.6	47	0	na	0	53
399.7	65	0	na	0	35
401.6	50	0	na	0	50
406.5	60	0	na	0	40
406.6	61	0	na	0	39
409.1	70	0	na	0	30
419.9	76	0	na	0	24
430.9	100	0	na	0	0
443.5	100	0	na	0	0
453.5	95	0	na	0	5
456.0	90	0	na	0	10
460.4	89	0	na	0	11
470.7	30	0	na	0	70
480.0	35	0	na	0	65
490.0	20	0	na	0	80
500.4	11	0	na	0	89
512.2	6	0	na	0	94
525.0	9	0	na	0	91
531.7	10	0	na	0	90
533.1	9	0	na	0	91
542.7	31	0	na	0	69
564.6	19	0	na	0	81
573.5	14	0	na	0	86
584.1	8	0	na	0	92
595.8	18	0	na	0	82
605.4	9	0	na	0	91
614.4	2	0	na	0	98

(continued on next page)

TABLE 4-5 (cont. p. 3/3). -- Weight percents of carbonate minerals and mole percents of $MgCO_3$ (magnesium-calcite phase) determined by XRD for stratigraphic samples from boreholes OAR-2/2A.

DEPTH Ft bsf	CALCITE Wt %	MgCALCITE Wt %	$MgCO_3$ Mol%	DOLOMITE Wt %	ARAGONITE Wt %
623.8	2	0	na	0	98
633.9	5	0	na	0	95
646.2	6	3	15	0	91
654.3	2	0	na	0	98
663.9	5	6	10	0	89
673.1	5	8	16	0	87
682.0	7	3	15	0	90
691.0	3	1	14	0	96
701.3	5	2	14	0	93
714.0	7	4	14	0	89
725.3	11	2	10	0	87
733.5	9	7	14	0	84
744.8	6	3	13	0	91
753.9	9	4	16	0	87
766.5	15	3	14	0	82
776.1	15	11	13	0	74
784.5	21	5	16	0	74
793.4	19	6	15	0	75
803.4	16	4	16	0	80
813.7	57	0	na	0	43
823.0	6	0	na	0	94
833.7	97	0	na	0	3
844.4	93	0	na	0	7
851.9	91	0	na	0	9
854.4	100	0	na	0	0
873.5	96	0	na	0	4
883.0	91	0	na	0	9

TABLE 4-6 . -- Weight percents of carbonate minerals and mole percents of $MgCO_3$ (magnesium-calcite phase) determined by XRD for stratigraphic samples from borehole OBZ-4.

DEPTH Ft bsf	CALCITE Wt %	MgCALCITE Wt %	$MgCO_3$ Mol%	DOLOMITE Wt %	ARAGONITE Wt %
922.9	100	0	na	0	0
990.7	94	0	na	0	6
1030.4	100	0	na	trace	0
1180.5	99	0	na	trace	1
1198.5	93	0	na	0	7
1289.7	91	0	na	0	9
1390.8	100	0	na	0	0
1412.0	85	0	na	0	15
1417.4	99	0	na	0	1
1427.4	100	0	na	0	0
1436.8	100	0	na	0	0
1452.2	95	0	na	0	5
1494.8	100	0	na	0	0
1496.1	100	0	na	0	0
1500.2	99	0	na	0	1
1535.6	95	0	na	0	5
1566.5	97	0	na	0	3
1575.2	95	0	na	0	5
1579.6	93	0	na	0	7
1584.6	96	0	na	0	4
1586.4	100	0	na	0	0
1597.1	94	0	na	0	6

TABLE 4-7 (1/2 pages). -- Weight percents of carbonate minerals and mole percents of $MgCO_3$ (magnesium-calcite phase) determined by XRD for stratigraphic samples from borehole OOR-17.

DEPTH Ft bsf	CALCITE Wt %	MgCALCITE Wt %	$MgCO_3$ Mol%	DOLOMITE Wt %	ARAGONITE Wt %
1.1	4	6	16	0	90
11.7	6	8	16	0	86
31.0	4	6	17	0	90
52.0	4	11	17	0	85
58.6	4	9	17	0	87
69.0	5	10	16	0	85
73.1	41	0	na	0	59
88.0	34	0	na	0	66
96.5	24	0	na	0	76
102.7	47	0	na	0	53
109.0	54	0	na	0	46
122.3	31	0	na	0	69
131.1	42	0	na	0	58
137.0	44	0	na	0	56
152.0	29	0	na	0	71
169.7	38	0	na	0	62
178.5	28	0	na	0	72
200.2	37	0	na	0	63
209.6	43	0	na	0	57
220.0	43	0	na	0	57
231.0	83	0	na	0	17
242.3	60	0	na	0	40
273.4	32	0	na	0	68
289.0	4	0	na	0	96
299.0	7	0	na	0	93
321.0	83	0	na	0	17
333.3	47	0	na	0	53
345.5	85	0	na	0	15
356.5	92	0	na	0	8
365.2	70	0	na	0	30
371.0	45	0	na	0	55
386.0	97	0	na	0	3
401.0	95	0	na	0	5
415.0	92	0	na	0	8
426.0	94	0	na	0	6
436.0	93	0	na	0	7
447.0	88	0	na	0	12
447.4	92	0	na	0	8
453.0	92	0	na	0	8
470.7	88	0	na	0	12
478.4	91	0	na	0	9
503.5	94	0	na	0	6

(continued on next page

TABLE 4-7 (cont. p. 2/2). -- Weight percents of carbonate minerals and mole percents of $MgCO_3$ (magnesium-calcite phase) determined by XRD for stratigraphic samples from borehole OOR-17.

DEPTH Ft bsf	CALCITE Wt %	MgCALCITE Wt %	$MgCO_3$ Mol%	DOLOMITE Wt %	ARAGONITE Wt %
523.3	92	0	na	0	8
531.0	33	0	na	0	67
547.7	13	0	na	0	87
563.4	30	0	na	0	70
573.1	31	0	na	0	69
597.5	23	0	na	0	77
611.6	16	0	na	0	84
645.0	16	0	na	0	84
668.5	20	0	na	0	80
682.6	5	0	na	0	95
696.3	6	4	16	0	90
707.1	4	0	na	0	96
730.0	10	2	12	0	88
739.0	9	10	11	0	81
757.1	5	5	16	0	90
771.0	3	3	13	0	94
785.0	5	9	14	0	86
797.4	4	0	na	0	96
815.0	6	0	na	0	94
834.0	5	0	na	0	95
857.0	16	0	na	0	84
866.0	8	5	16	0	87
884.0	17	8	16	0	75
907.7	63	0	na	0	37
920.0	26	0	na	0	74
935.7	29	0	na	0	71
938.0	90	0	na	0	10
947.5	94	0	na	0	6
958.2	100	0	na	0	0
968.7	96	0	na	0	4
980.0	87	0	na	0	13
987.6	91	0	na	0	9
994.5	94	0	na	0	6
1010.3	93	0	na	trace	7
1025.3	94	0	na	0	6
1037.4	96	0	na	0	4
1047.0	89	0	na	0	11
1055.1	91	0	na	0	9
1065.3	88	0	na	0	12
1079.3	98	0	na	2	0
1085.4	93	0	na	0	7

TABLE 4-8. -- Weight percents of carbonate minerals and mole percents of $MgCO_3$ (magnesium-calcite phase) determined by XRD for stratigraphic samples from borehole OPZ-18.

DEPTH Ft bsf	CALCITE Wt%	MgCALCITE Wt%	$MgCO_3$ Mol%	DOLOMITE Wt%	ARAGONITE Wt%
31.1	29	0	na	0	71
48.0	21	0	na	0	79
64.4	19	0	na	0	81
76.0	17	0	na	0	83
93.0	18	0	na	0	82
112.0	24	0	na	0	76
129.2	24	0	na	0	76
145.5	23	0	na	0	77
160.0	32	0	na	0	68
174.5	35	0	na	0	65
192.0	12	6	16	0	82
217.0	54	0	na	0	46
231.6	8	7	11	0	85
251.0	34	0	na	0	66
274.0	9	0	na	0	91
290.0	55	0	na	0	45
315.8	29	0	na	0	71
331.2	18	0	na	0	82
357.0	25	0	na	0	75
377.0	7	0	na	0	93
391.6	76	0	na	0	24
400.6	100	0	na	0	0
414.5	96	0	na	0	4
429.7	95	0	na	0	5
449.8	91	0	na	0	9
466.6	51	0	na	0	49
470.6	95	0	na	0	5
507.3	91	0	na	0	9
518.0	95	0	na	0	5
535.8	19	0	na	0	81
565.0	4	0	na	0	96
592.1	5	0	na	0	95
607.1	11	0	na	0	89
611.7	5	0	na	0	95
621.3	4	0	na	0	96
631.0	5	9	15	0	86
650.3	9	8	15	0	83
664.9	8	10	16	0	82
669.6	2	0	na	0	98

TABLE 4-9. -- Weight percents of carbonate minerals and mole percents of $MgCO_3$ (magnesium-calcite phase) determined by XRD for stratigraphic samples from borehole OQT-19.

DEPTH Ft bsf	CALCITE Wt%	MgCALCITE Wt%	$MgCO_3$ Mol%	DOLOMITE Wt%	ARAGONITE Wt%
0.5	8	11	16	0	81
5.4	10	9	16	0	81
5.8	6	12	16	0	82
31.2	6	7	16	0	87
45.9	14	21	16	0	65
50.5	6	0	na	0	94
53.7	40	0	na	0	60
72.3	14	0	na	0	86
79.4	55	0	na	0	45
98.8	34	0	na	0	66
109.4	26	0	na	0	74
134.4	23	0	na	0	77
179.0	47	0	na	0	53
193.6	59	0	na	0	41
221.2	41	0	na	0	59
238.0	12	0	na	0	88
263.0	12	0	na	0	88
282.0	17	0	na	0	83
291.7	58	0	na	0	42
330.5	96	0	na	0	4
350.5	18	0	na	0	82
366.0	97	0	na	0	3
398.0	100	0	na	0	0
421.4	99	0	na	0	1
431.5	95	0	na	0	5
461.0	42	0	na	0	58
481.1	54	0	na	0	46
511.9	94	0	na	0	6
542.0	15	0	na	0	85
552.5	10	0	na	0	90
582.6	14	0	na	0	86
612.0	6	0	na	0	94
631.6	8	0	na	0	92
641.6	9	5	13	0	86
651.1	4	4	11	0	92
666.0	6	5	13	0	89
680.6	14	9	13	0	77
691.0	8	5	12	0	87
701.0	12	10	15	0	78

TABLE 4-10. -- Weight percents of carbonate minerals and mole percents of $MgCO_3$ (magnesium-calcite phase) determined by XRD for stratigraphic samples from borehole ORT-20.

DEPTH Ft bsf	CALCITE Wt%	MgCALCITE Wt%	$MgCO_3$ Mol%	DOLOMITE Wt%	ARAGONITE Wt%
30.5	12	10	16	0	78
45.2	7	21	16	0	72
59.7	6	5	16	0	89
64.5	44	0	na	0	56
76.7	9	0	na	0	91
89.0	66	0	na	0	34
99.5	20	0	na	0	80
110.0	19	0	na	0	81
120.8	15	0	na	0	85
132.2	29	0	na	0	71
153.0	43	0	na	0	57
171.0	32	0	na	0	68
182.4	45	0	na	0	55
201.9	47	0	na	0	53
211.9	66	0	na	0	34
231.0	18	0	na	0	82
250.0	9	0	na	0	91
266.0	43	0	na	0	57
286.3	14	0	na	0	86
300.5	51	0	na	0	49
315.5	89	0	na	0	11
330.7	99	0	na	0	1
341.4	97	0	na	0	3
363.4	96	0	na	0	4
380.2	94	0	na	0	6
410.2	98	0	na	0	2
426.0	95	0	na	0	5
436.0	92	0	na	0	8
450.5	94	0	na	0	6
471.0	78	0	na	0	22
490.0	27	0	na	0	73

TABLE 4-11. -- Weight percents of carbonate minerals and mole percents of $MgCO_3$ (magnesium-calcite phase) determined by XRD for stratigraphic samples from borehole OSR-21.

DEPTH Ft bsf	CALCITE Wt%	MgCALCITE Wt%	$MgCO_3$ Mol%	DOLOMITE Wt%	ARAGONITE Wt%
0.2	4	11	16	0	85
31.0	4	12	16	0	84
47.0	11	3	16	0	86
62.0	39	0	na	0	61
92.0	50	0	na	0	50
106.0	43	0	na	0	57
124.7	29	0	na	0	71
134.9	34	0	na	0	66
165.9	31	0	na	0	69
176.5	29	0	na	0	71
186.7	52	0	na	0	48
207.0	71	0	na	0	29
220.2	36	0	na	0	64
236.9	41	0	na	0	59
252.0	31	0	na	0	69
262.8	33	0	na	0	67
279.0	40	0	na	0	60
317.6	69	0	na	0	31
327.4	52	0	na	0	48
337.5	92	0	na	0	8
348.7	38	0	na	0	62

TABLE 4-12. -- Weight percents of carbonate minerals and mole percents of $MgCO_3$ (magnesium-calcite phase) determined by XRD for stratigraphic samples from borehole OTG-23.

DEPTH Ft bsf	CALCITE Wt%	MgCALCITE Wt%	$MgCO_3$ Mol%	DOLOMITE Wt%	ARAGONITE Wt%
276.3	17	0	na	0	83
308.4	7	0	na	0	93
339.5	59	0	na	0	41
371.4	84	0	na	0	16
402.5	87	0	na	0	13
495.6	19	0	na	0	81
525.3	22	0	na	0	78
556.0	2	0	na	0	98

TABLE 4-13 (1/2 pages). -- Weight percents of carbonate minerals and mole percents of $MgCO_3$ (magnesium-calcite phase) determined by XRD for thin-section samples from borehole KAR-1.

DEPTH Ft bsf	CALCITE Wt%	MgCALCITE Wt%	$MgCO_3$ Mol%	DOLOMITE Wt%	ARAGONITE Wt%
35.5	6	17	16	0	77
36.1	6	14	16	0	80
45.6	6	12	16	0	82
58.3	49	0	na	0	51
69.8	14	0	na	0	86
95.9	10	0	na	0	90
141.0	2	0	na	0	98
143.2	66	0	na	0	34
157.8	49	0	na	0	51
221.4	38	0	na	0	62
223.7	60	0	na	0	40
240.6	17	0	na	0	83
256.1	80	0	na	0	20
262.9	74	0	na	0	26
268.4	96	0	na	0	4
279.0	95	0	na	0	5
279.6	98	0	na	0	2
292.3	82	0	na	0	18
305.1	100	0	na	0	0
316.3	91	0	na	0	9
319.2	100	0	na	0	0
330.1	92	0	na	0	8
335.4	100	0	na	0	0
350.1	96	0	na	0	4
353.2	88	0	na	0	12
385.7	100	0	na	0	0
397.6	100	0	na	0	0
399.1	98	0	na	0	2
435.2	97	0	na	0	3
444.6	100	0	na	0	0
464.9	88	0	na	0	12
521.7	62	0	na	0	38
540.8	20	0	na	0	80
541.6	16	0	na	0	84
543.2	14	0	na	0	86
548.5	39	0	na	0	61
554.8	24	0	na	0	76
555.7	52	0	na	0	48
560.9	3	7	12	0	90
561.6	48	0	na	0	52
604.3	29	0	na	0	71
670.5	46	0	na	0	54
689.3	8	0	na	0	92

(continued on next page)

TABLE 4-13 (cont. p. 2/2). -- Weight percents of carbonate minerals and mole percents of $MgCO_3$ (magnesium-calcite phase) determined by XRD for thin-section samples from borehole KAR-1.

DEPTH Ft bsf	CALCITE Wt%	MgCALCITE Wt%	$MgCO_3$ Mol%	DOLOMITE Wt%	ARAGONITE Wt%
697.0	6	10	14	0	84
744.0	6	9	15	0	85
760.8	10	8	12	0	82
790.8	26	0	na	0	74
823.9	12	5	12	0	83
855.0	9	3	15	0	88
855.5	29	5	15	0	66
881.2	18	8	13	0	74
896.9	9	3	14	0	88
903.9	74	0	na	0	26
918.2	16	0	na	0	84
924.8	100	0	na	0	0
943.4	97	0	na	0	3
956.1	100	0	na	0	0
968.7	100	0	na	0	0
969.0	91	0	na	0	9
969.6	97	0	na	0	3
995.4	100	0	na	trace	0
997.9	99	0	na	0	1
1000.7	100	0	na	0	0
1007.0	93	0	na	trace	7
1014.2	100	0	na	0	0
1045.4	100	0	na	trace	0
1053.9	100	0	na	0	0
1064.8	100	0	na	0	0
1068.6	97	0	na	0	3
1081.9	98	0	na	0	2
1082.6	97	0	na	0	3
1083.5	100	0	na	0	0
1084.1	100	0	na	0	0
1095.2	100	0	na	0	0
1096.1	96	0	na	0	4
1098.9	94	0	na	trace	6
1111.7	100	0	na	0	0
1117.7	100	0	na	0	0
1118.1	99	0	na	0	1
1121.8	100	0	na	0	0
1130.2	97	0	na	0	3

TABLE 4-14. -- Weight percents of carbonate minerals and mole percents of $MgCO_3$ (magnesium-calcite phase) determined by XRD for thin-section samples from borehole KBZ-4.

DEPTH Ft bsf	CALCITE Wt%	MgCALCITE Wt%	$MgCO_3$ Mol%	DOLOMITE Wt%	ARAGONITE Wt%
315.7	100	0	na	0	0
870.9	98	0	na	0	2
889.7	100	0	na	0	0
894.0	84	0	na	0	16
917.5	78	0	na	22	0
961.3	100	0	na	0	0
967.0	99	0	na	trace	1
968.4	100	0	na	0	0
980.5	91	0	na	trace	9
982.8	94	0	na	trace	6
985.3	96	0	na	0	4
991.2	100	0	na	0	0
999.2	100	0	na	trace	0
1003.0	93	0	na	trace	7
1011.0	98	0	na	0	2
1017.4	99	0	na	0	1
1022.4	100	0	na	0	0
1022.8	88	0	na	0	12
1039.1	87	0	na	trace	13
1040.2	100	0	na	0	0

TABLE 4-15 (1/2 pages). -- Weight percents of carbonate minerals and mole percents of $MgCO_3$ (magnesium-calcite phase) determined by XRD for thin-section samples from boreholes OAR-2/2A.

DEPTH Ft bsf	CALCITE Wt%	MgCALCITE Wt%	$MgCO_3$ Mol%	DOLOMITE Wt%	ARAGONITE Wt%
41.7	10	0	na	0	90
62.1	12	0	na	0	88
75.8	55	0	na	0	45
126.6	59	0	na	0	41
176.7	54	0	na	0	46
185.3	62	0	na	0	38
195.1	54	0	na	0	46
199.2	59	0	na	0	41
199.5	88	0	na	0	12
206.6	34	0	na	0	66
212.8	28	0	na	0	72
223.4	81	0	na	0	19
286.5	58	0	na	0	42
300.1	58	0	na	0	42
307.2	81	0	na	0	19
320.4	89	0	na	0	11
331.3	85	0	na	0	15
336.7	94	0	na	0	6
350.2	91	0	na	0	9
361.7	98	0	na	0	2
366.9	96	0	na	0	4
372.0	96	0	na	0	4
416.1	81	0	na	0	19
432.2	78	0	na	0	22
443.8	93	0	na	0	7
454.0	82	0	na	0	18
456.0	53	0	na	0	47
463.9	94	0	na	0	6
488.6	37	0	na	0	63
586.9	53	0	na	0	47
605.2	13	0	na	0	87
606.9	7	0	na	0	93
639.7	2	0	na	0	98
664.4	5	4	16	0	91
669.1	7	5	14	0	88
689.0	4	2	14	0	94
738.8	7	9	14	0	84
760.9	11	0	na	0	89
771.9	22	12	14	0	66
812.3	24	3	13	0	73
816.8	42	4	16	0	54
835.5	98	0	na	0	2
837.5	98	0	na	0	2

(continued on next page)

TABLE 4-15 (cont. p. 2/2). -- Weight percents of carbonate minerals and mole percents of $MgCO_3$ (magnesium-calcite phase) determined by XRD for thin-section samples from boreholes OAR-2/2A.

DEPTH Ft bsf	CALCITE Wt%	MgCALCITE Wt%	$MgCO_3$ Mol%	DOLOMITE Wt%	ARAGONITE Wt%
845.3	98	0	na	0	2
845.9	100	0	na	0	0
851.1	94	0	na	0	6
872.0	100	0	na	0	0
876.0	100	0	na	0	0
876.9	96	0	na	0	4
878.0	3	0	na	0	97
878.8	95	0	na	0	5
879.8	88	0	na	0	12
882.1	95	0	na	0	5

TABLE 4-16. -- Weight percents of carbonate minerals and mole percents of $MgCO_3$ (magnesium-calcite phase) determined by XRD for thin-section samples from borehole OBZ-4.

DEPTH Ft bsf	CALCITE Wt%	MgCALCITE Wt%	$MgCO_3$ Mol%	DOLOMITE Wt%	ARAGONITE Wt%
437.1	96	0	na	0	4
503.5	94	0	na	0	6
505.0	91	0	na	0	9
916.1	91	0	na	0	9
983.1	100	0	na	trace	0
990.0	100	0	na	0	0
992.4	100	0	na	0	0
1029.9	92	0	na	trace	8
1080.7	100	0	na	0	0
1130.4	100	0	na	0	0
1180.1	100	0	na	0	0
1252.2	100	0	na	0	0
1267.3	100	0	na	0	0
1298.3	93	0	na	0	7
1465.8	100	0	na	0	0
1469.4	96	0	na	0	4
1470.1	100	0	na	0	0
1499.5	95	0	na	0	5
1511.2	100	0	na	0	0
1516.6	98	0	na	0	2
1517.6	91	0	na	0	9
1519.8	94	0	na	0	6
1523.5	98	0	na	0	2
1535.2	98	0	na	0	2
1562.4	100	0	na	0	0
1565.5	100	0	na	0	0
1565.9	100	0	na	0	0
1570.9	100	0	na	0	0
1574.6	88	0	na	0	12
1578.7	97	0	na	0	3
1579.2	95	0	na	0	5
1584.0	100	0	na	0	0
1585.9	100	0	na	0	0
1597.1	92	0	na	0	8
1601.3	95	0	na	0	5
1602.1	100	0	na	0	0

TABLE 4-17. -- Weight percents of carbonate minerals and mole percents of $MgCO_3$ (magnesium-calcite phase) determined by XRD for thin-section samples from borehole OCT-5.

DEPTH Ft bsf	CALCITE Wt%	MgCALCITE Wt%	$MgCO_3$ Mol%	DOLOMITE Wt%	ARAGONITE Wt%
383.7	96	0	na	0	4

TABLE 4-18. -- Weight percents of carbonate minerals and mole percents of $MgCO_3$ (magnesium-calcite phase) determined by XRD for thin-section samples from borehole ODT-6.

DEPTH Ft bsf	CALCITE Wt%	MgCALCITE Wt%	$MgCO_3$ Mol%	DOLOMITE Wt%	ARAGONITE Wt%
24.8	91	0	na	0	9
74.8	8	11	16	0	81

TABLE 4-19. -- Weight percents of carbonate minerals and mole percents of $MgCO_3$ (magnesium-calcite phase) determined by XRD for thin-section samples from borehole OET-7.

DEPTH Ft bsf	CALCITE Wt%	MgCALCITE Wt%	$MgCO_3$ Mol%	DOLOMITE Wt%	ARAGONITE Wt%
78.8	89	0	na	0	11

TABLE 4-20. -- Weight percents of carbonate minerals and mole percents of $MgCO_3$ (magnesium-calcite phase) determined by XRD for thin-section samples from borehole OOR-17.

DEPTH Ft bsf	CALCITE Wt%	MgCALCITE Wt%	$MgCO_3$ Mol%	DOLOMITE Wt%	ARAGONITE Wt%
80.4	64	0	na	0	36
106.6	67	0	na	0	33
317.0	100	0	na	0	0
346.0	94	0	na	0	6
362.6	91	0	na	0	9
379.6	100	0	na	0	0
474.9	94	0	na	0	6
500.2	93	0	na	0	7
550.8	65	0	na	0	35
593.8	50	0	na	0	50
608.6	46	0	na	0	54
665.2	46	0	na	0	54
676.4	88	0	na	0	12
680.2	28	0	na	0	72
682.0	43	0	na	0	57
748.4	2	0	na	0	98
839.6	32	0	na	0	68
864.1	46	0	na	0	54
908.4	59	0	na	0	41
910.7	9	0	na	0	91
920.4	40	0	na	0	60
937.0	100	0	na	0	0
1015.1	100	0	na	0	0
1030.8	96	0	na	0	4
1049.4	81	0	na	0	19
1083.0	83	0	na	trace	17
1089.0	100	0	na	0	0
1090.8	96	0	na	trace	4

TABLE 4-21. -- Weight percents of carbonate minerals and mole percents of $MgCO_3$ (magnesium-calcite phase) determined by XRD for thin-section samples from borehole ORT-20.

DEPTH Ft bsf	CALCITE Wt%	MgCALCITE Wt%	$MgCO_3$ Mol%	DOLOMITE Wt%	ARAGONITE Wt%
59.6	8	5	15	0	87

TABLE 4-22. -- Weight percents of carbonate minerals and mole percents of $MgCO_3$ (magnesium-calcite phase) determined by XRD for thin-section samples from borehole OSR-21.

DEPTH Ft bsf	CALCITE Wt%	MgCALCITE Wt%	$MgCO_3$ Mol%	DOLOMITE Wt%	ARAGONITE Wt%
77.5	49	0	na	0	51

TABLE 4-23. -- Weight percents of carbonate minerals and mole percents of $MgCO_3$ (magnesium-calcite phase) determined by XRD for thin-section samples from borehole OUT-24.

DEPTH Ft bsf	CALCITE Wt%	MgCALCITE Wt%	$MgCO_3$ Mol%	DOLOMITE Wt%	ARAGONITE Wt%
320.6	97	0	na	0	3
344.9	91	0	na	0	9

TABLE 4-24. -- Average weight percents of carbonate minerals and average mole percents of $MgCO_3$ (magnesium-calcite phase) for the geologic packages/ crater zones (stratigraphic samples) from borehole KAR-1.

Package/ Zone	Number Samples	Calcite Wt%	MgCalcite Wt%	$MgCO_3$ Mol%	Dolomite Wt%	Aragonite Wt%
1	2	6	14	16	0	80
2	25	47	1	16	0	52
3	15	81	0	na	0	19
4,5,6	45	39	3	14	trace	58
7	1	100	0	na	0	0
8	4	99	0	na	0	1

TABLE 4-25. -- Average weight percents of carbonate minerals and average mole percents of $MgCO_3$ (magnesium-calcite phase) for the geologic packages/crater zones (stratigraphic samples) from borehole KBZ-4.

Package/ Zone	Number Samples	Calcite Wt%	MgCalcite Wt%	$MgCO_3$ Mol%	Dolomite Wt%	Aragonite Wt%
1	0	-	-	-	-	-
2	0	-	-	-	-	-
3	0	-	-	-	-	-
4,5,6	4	16	8	14	0	76
7	1	89	0	na	11	0
8	0	-	-	-	-	-

TABLE 4-26. -- Average weight percents of carbonate minerals and average mole percents of $MgCO_3$ (magnesium-calcite phase) for the geologic packages/crater zones (stratigraphic samples) from boreholes OAR-2/2A.

Package/ Zone	Number Samples	Calcite Wt%	MgCalcite Wt%	$MgCO_3$ Mol%	Dolomite Wt%	Aragonite Wt%
1	5	9	7	16	0	84
2	38	37	0	na	0	63
3	22	78	0	na	0	22
4,5,6	46	31	1	14	0	68
7	0	-	-	-	-	-
8	0	-	-	-	-	-

TABLE 4-27. -- Average weight percents of carbonate minerals and average mole percents of $MgCO_3$ (magnesium-calcite phase) for the geologic packages/crater zones (stratigraphic samples) from borehole OBZ-4.

Package/ Zone	Number Samples	Calcite Wt%	MgCalcite Wt%	$MgCO_3$ Mol%	Dolomite Wt%	Aragonite Wt%
1	0	-	-	-	-	-
2	0	-	-	-	-	-
3	0	-	-	-	-	-
4,5,6	0	-	-	-	-	-
7	0	-	-	-	-	-
8	22	97	0	na	trace	3

TABLE 4-28. -- Average weight percents of carbonate minerals and average mole percents of $MgCO_3$ (magnesium-calcite phase) for the geologic packages/crater zones (stratigraphic samples) from borehole OOR-17.

Package/ Zone	Number Samples	Calcite Wt%	MgCalcite Wt%	$MgCO_3$ Mol%	Dolomite Wt%	Aragonite Wt%
1	6	5	8	16	0	87
2	22	43	0	na	0	57
3	13	87	0	na	0	13
4,5,6	31	31	2	14	0	67
7	7	92	0	na	trace	8
8	4	92	0	na	1	7

TABLE 4-29. -- Average weight percents of carbonate minerals and average mole percents of $MgCO_3$ (magnesium-calcite phase) for the geologic packages/crater zones (stratigraphic samples) from borehole OPZ-18.

Package/ Zone	Number Samples	Calcite Wt%	MgCalcite Wt%	$MgCO_3$ Mol%	Dolomite Wt%	Aragonite Wt%
Alpha	1	29	0	na	0	71
Beta1	9	24	0	na	0	76
Beta2	1	12	6	16	0	82
Beta3	8	29	1	11	0	70
1	0	-	-	-	-	-
2	1	7	0	na	0	93
3	9	88	0	na	0	12
4,5,6	10	7	3	15	0	90
7	0	-	-	-	-	-
8	0	-	-	-	-	-

TABLE 4-30. -- Average weight percents of carbonate minerals and average mole percents of $MgCO_3$ (magnesium-calcite phase) for the geologic packages/crater zones (stratigraphic samples) from borehole OQT-19.

Package/ Zone	Number Samples	Calcite Wt%	MgCalcite Wt%	$MgCO_3$ Mol%	Dolomite Wt%	Aragonite Wt%
1	6	8	10	16	0	82
2	13	34	0	na	0	66
3	5	82	0	na	0	18
4,5,6	15	26	3	13	0	71
7	0	-	-	-	-	-
8	0	-	-	-	-	-

TABLE 4-31. -- Average weight percents of carbonate minerals and average mole percents of $MgCO_3$ (magnesium-calcite phase) for the geologic packages/crater zones (stratigraphic samples) from borehole ORT-20.

Package/ Zone	Number Samples	Calcite Wt%	MgCalcite Wt%	$MgCO_3$ Mol%	Dolomite Wt%	Aragonite Wt%
1	2	10	15	16	0	75
2	18	32	0	16	0	68
3	9	95	0	na	0	5
4,5,6	2	52	0	na	0	48
7	0	-	-	-	-	-
8	0	-	-	-	-	-

TABLE 4-32. -- Average weight percents of carbonate minerals and average mole percents of $MgCO_3$ (magnesium-calcite phase) for the geologic packages/crater zones (stratigraphic samples) from borehole OSR-21.

Package/ Zone	Number Samples	Calcite Wt%	MgCalcite Wt%	$MgCO_3$ Mol%	Dolomite Wt%	Aragonite Wt%
1	2	4	12	16	0	84
2	15	38	0	16	0	62
3	4	63	0	na	0	37
4,5,6	0	-	-	-	-	-
7	0	-	-	-	-	-
8	0	-	-	-	-	-

TABLE 4-33. -- Average weight percents of carbonate minerals and average mole percents of $MgCO_3$ (magnesium-calcite phase) for the geologic packages/crater zones (stratigraphic samples) from borehole OTG-23.

Package/ Zone	Number Samples	Calcite Wt%	MgCalcite Wt%	$MgCO_3$ Mol%	Dolomite Wt%	Aragonite Wt%
1	0	-	-	-	-	-
2	2	12	0	na	0	88
3	3	77	0	na	0	23
4,5,6	3	14	0	na	0	86
7	0	-	-	-	-	-
8	0	-	-	-	-	-

TABLE 4-34. -- Average weight percents of carbonate minerals and average mole percents of $MgCO_3$ (magnesium-calcite phase) for the bottom grab samples (benthic samples) from the Enewetak lagoon.

Package/ Zone	Number Samples	Calcite Wt%	MgCalcite Wt%	$MgCO_3$ Mol%	Dolomite Wt%	Aragonite Wt%
1	22	9	14	16	0	77

TABLE 4-35. -- Average weight percents of carbonate minerals and average mole percents of $MgCO_3$ (magnesium calcite phase) for the sedimentary packages (stratigraphic samples) from the OAK boreholes.

SEDIMENTARY PACKAGE	NUMBER HOLES	NUMBER SAMPLES	CALCITE Wt%	MgCALCITE Wt%	$MgCO_3$ Wt%	DOLOMITE Wt%	ARAGONITE Wt%
1	5	21	7	9	16	0	84
2	6	109	36	0	16*	0	64
3	7	65	83	0	na	0	17
4,5,6	6	107	28	2	14	0	70
7	1	7	92	0	na	trace	8
9	2	26	96	0	na	trace	4

* Magnesium calcite phase detected in two samples; one from ORT-20, the other from OSR-21.

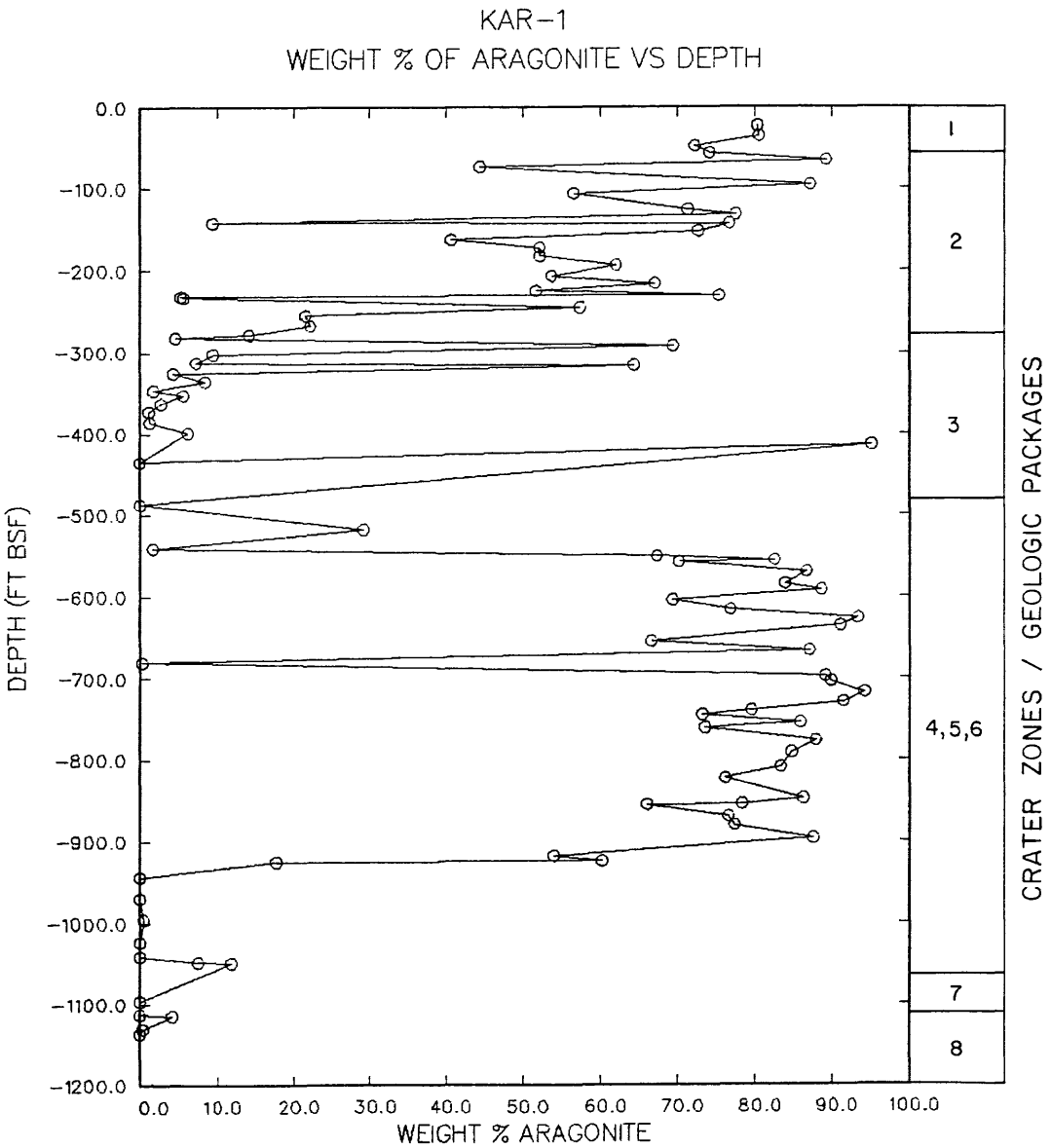

FIGURE 4-2. -- Depth profile of weight percent aragonite for stratigraphic samples from borehole KAR-1.

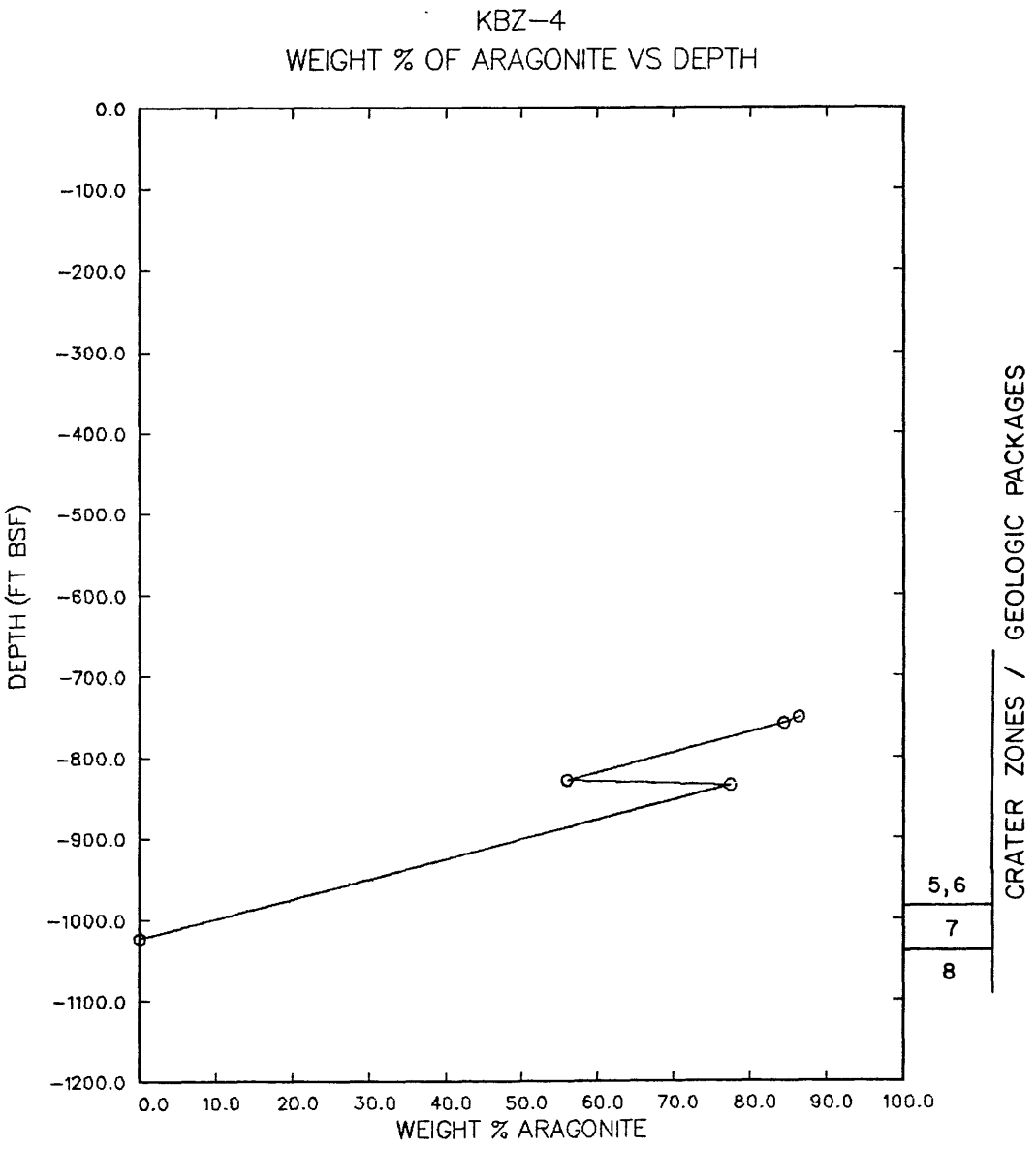

FIGURE 4-3. -- Depth profile of weight percent aragonite for stratigraphic samples from borehole KBZ-4.

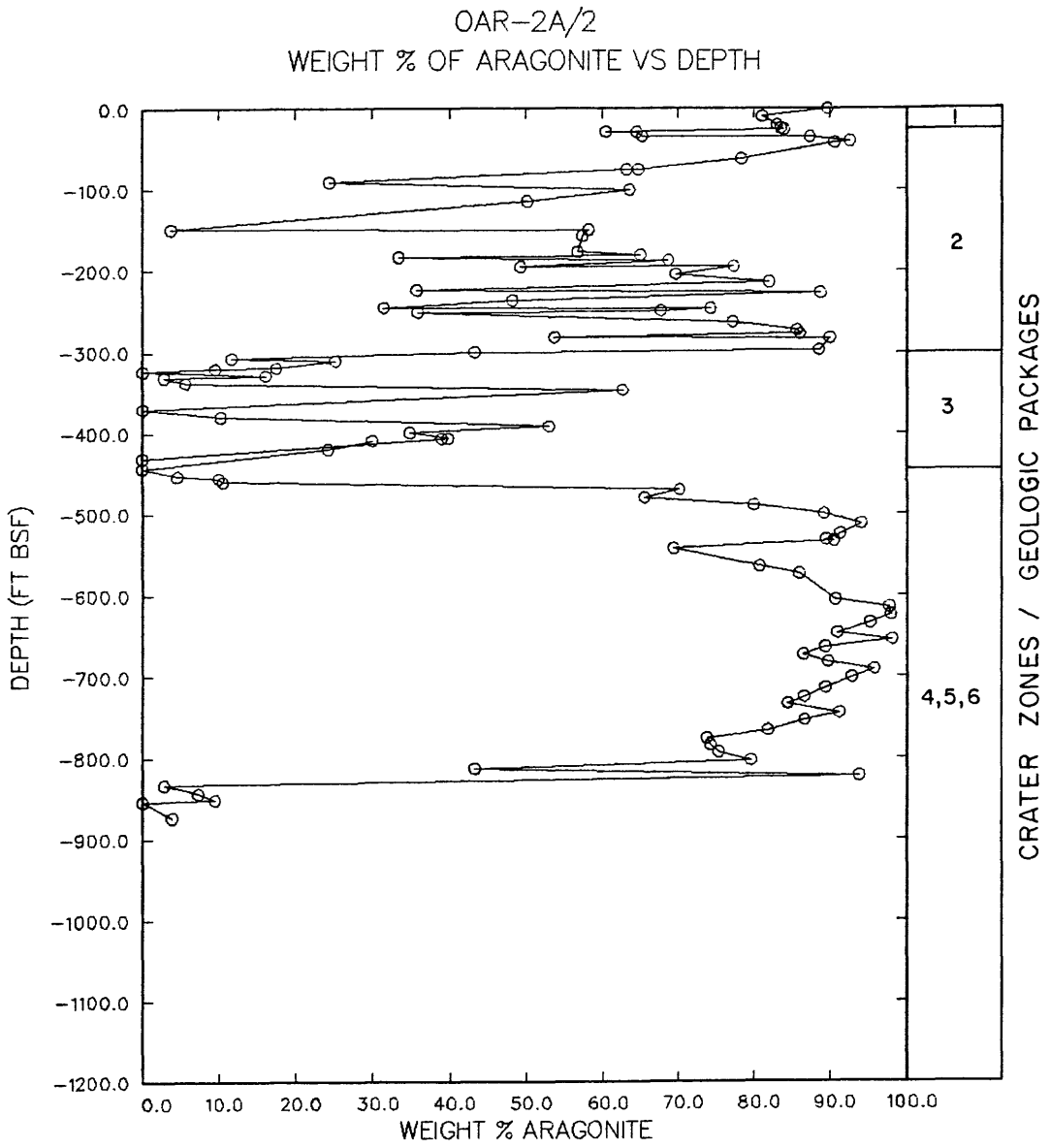

FIGURE 4-4. -- Depth profile of weight percent aragonite for stratigraphic samples from boreholes OAR-2/2A.

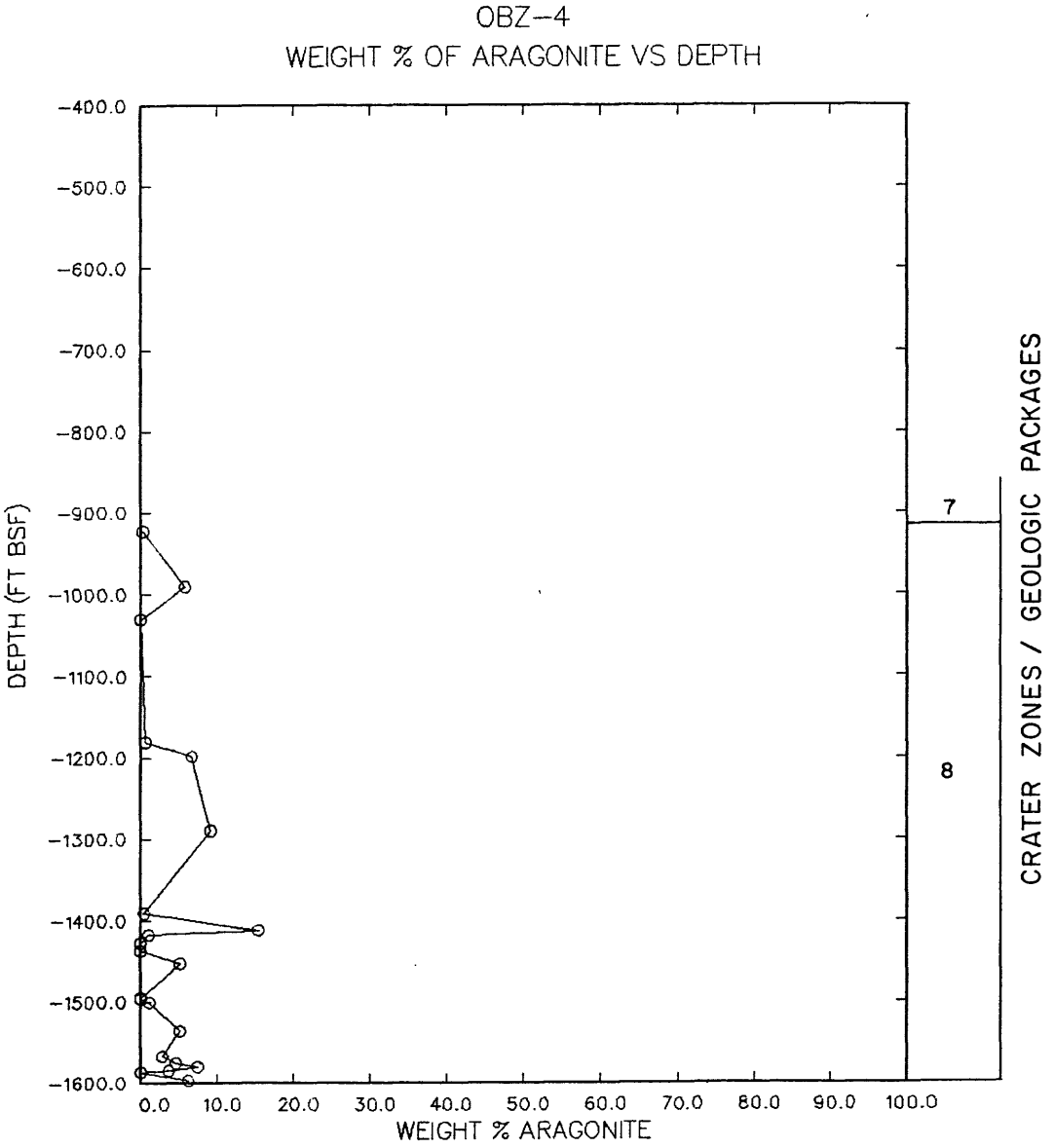

FIGURE 4-5. -- Depth profile of weight percent aragonite for stratigraphic samples from borehole OBZ-4.

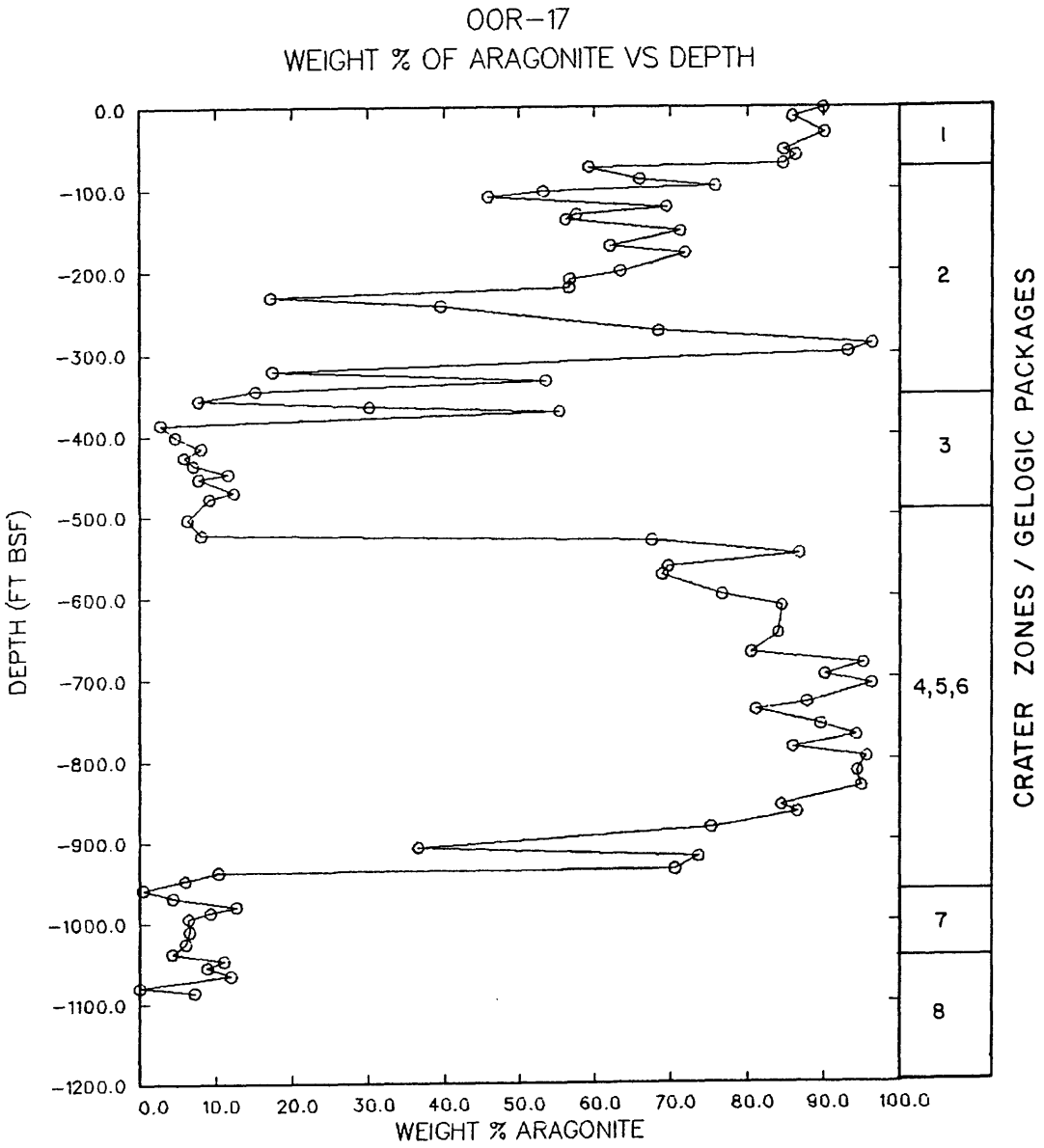

FIGURE 4-6. -- Depth profile of weight percent aragonite for stratigraphic samples from borehole OOR-17.

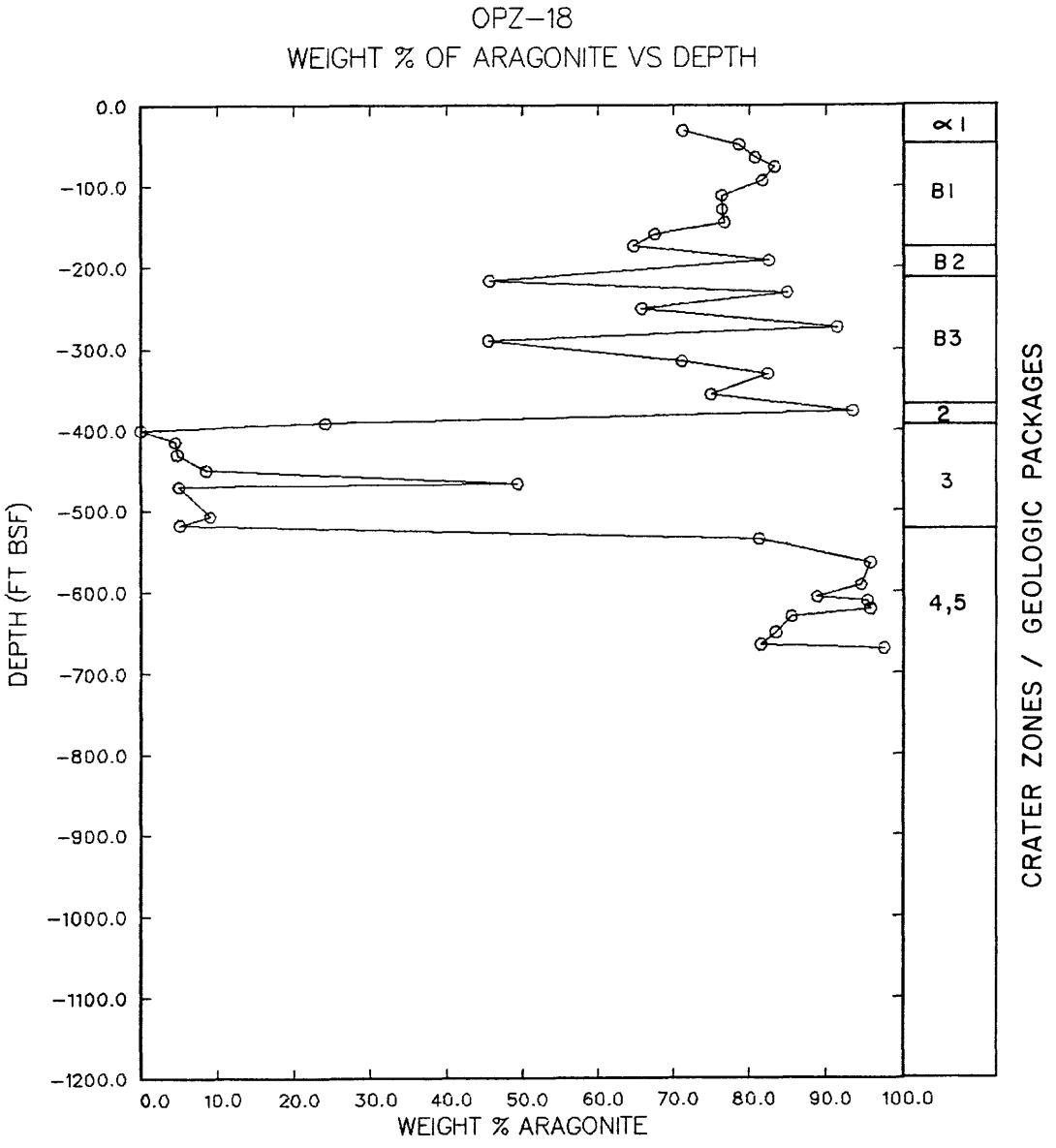

FIGURE 4-7. -- Depth profile of weight percent aragonite for stratigraphic samples from borehole OPZ-18.

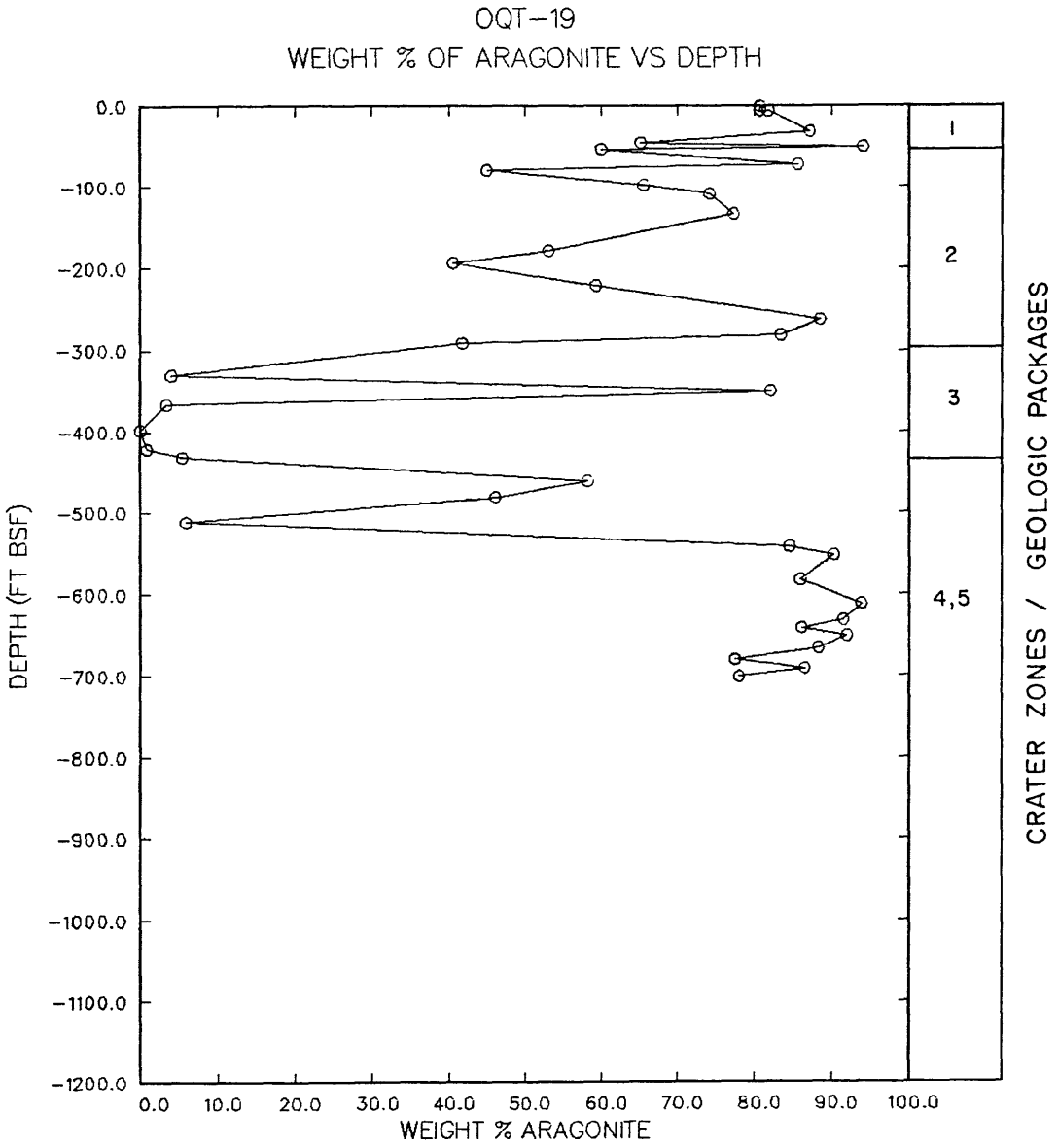

FIGURE 4-8. -- Depth profile of weight percent aragonite for stratigraphic samples from borehole OQT-19.

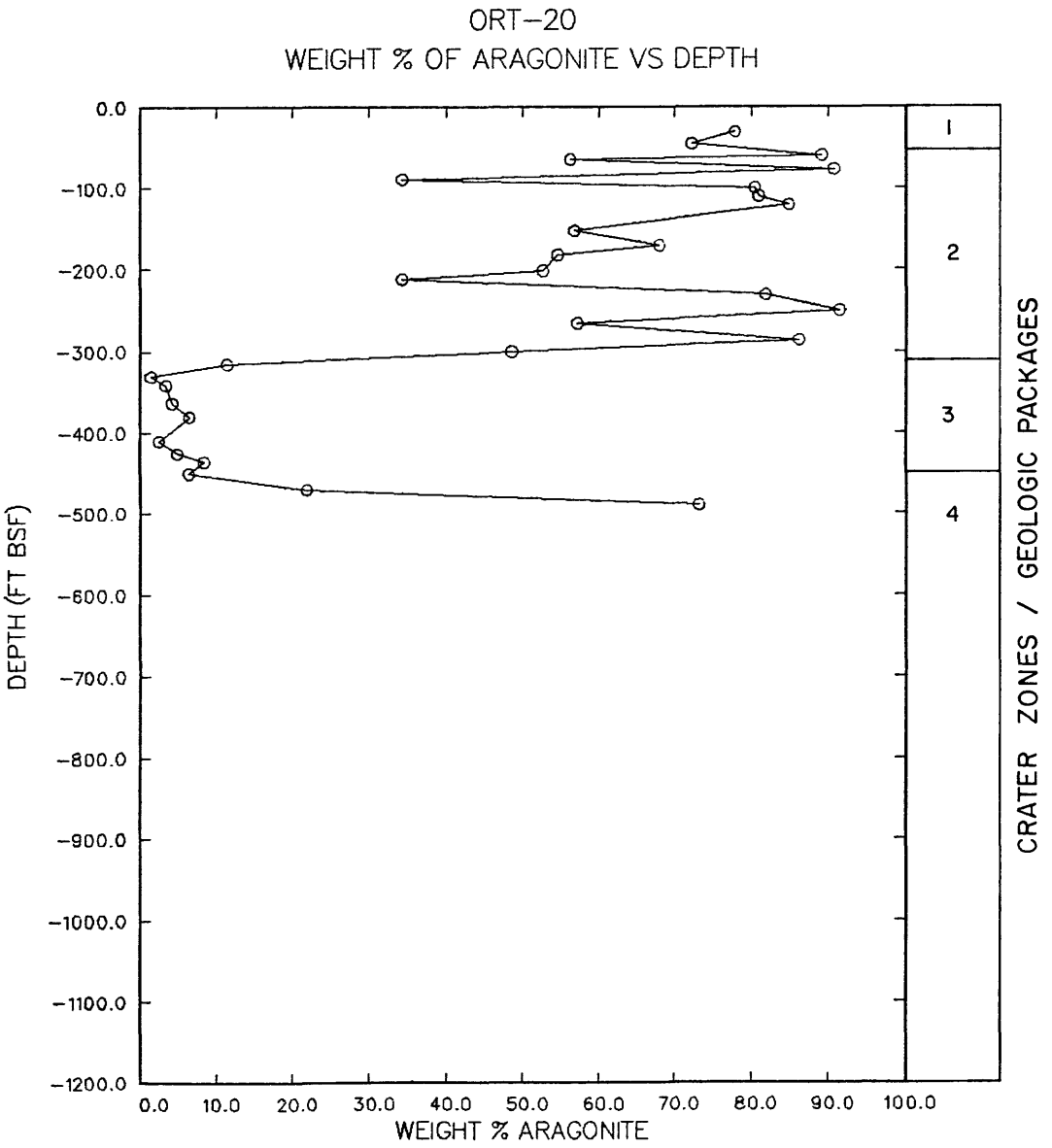

FIGURE 4-9. -- Depth profile of weight percent aragonite for stratigraphic samples from borehole ORT-20.

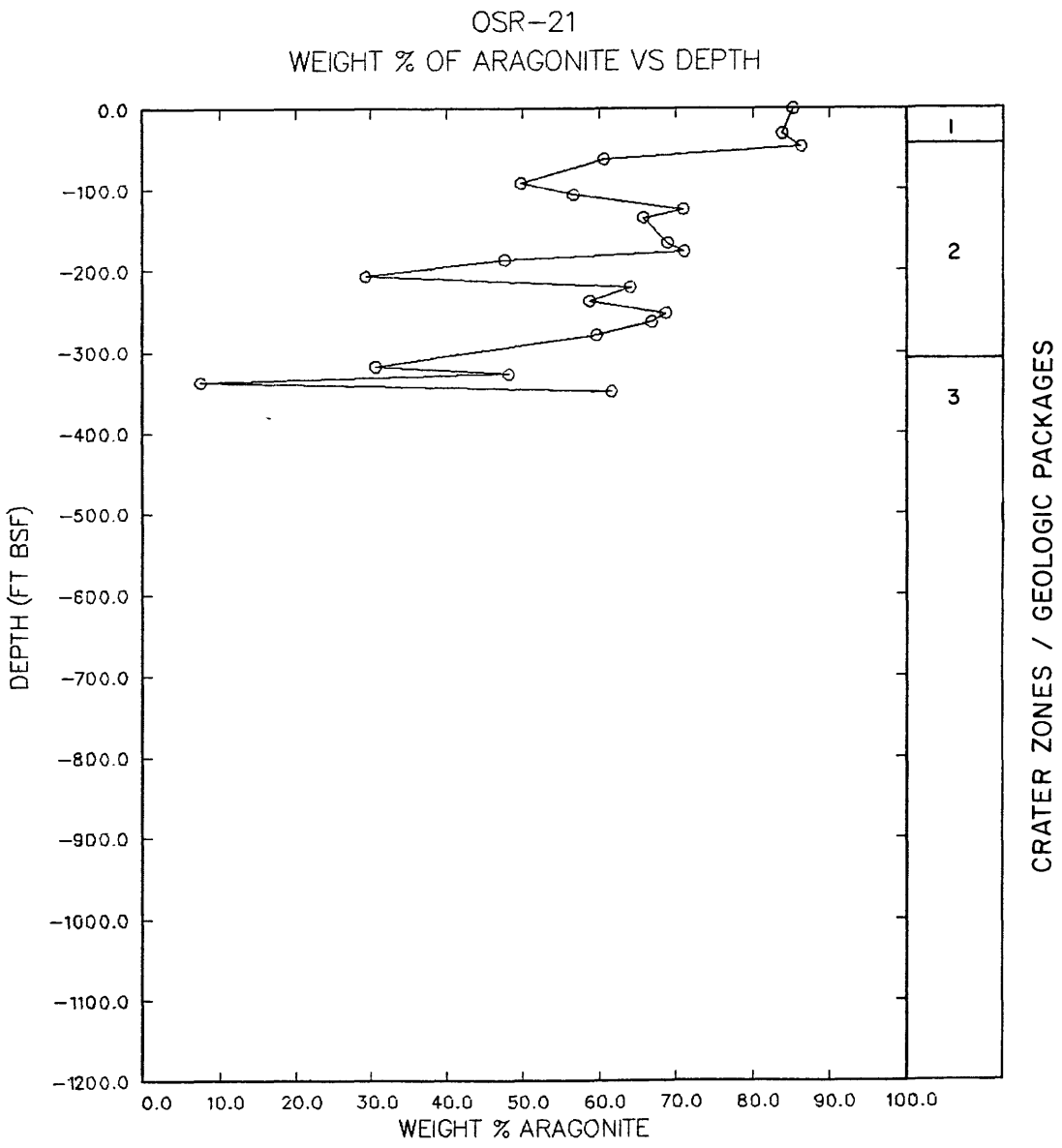

FIGURE 4-10. -- Depth profile of weight percent aragonite for stratigraphic samples from borehole OSR-21.

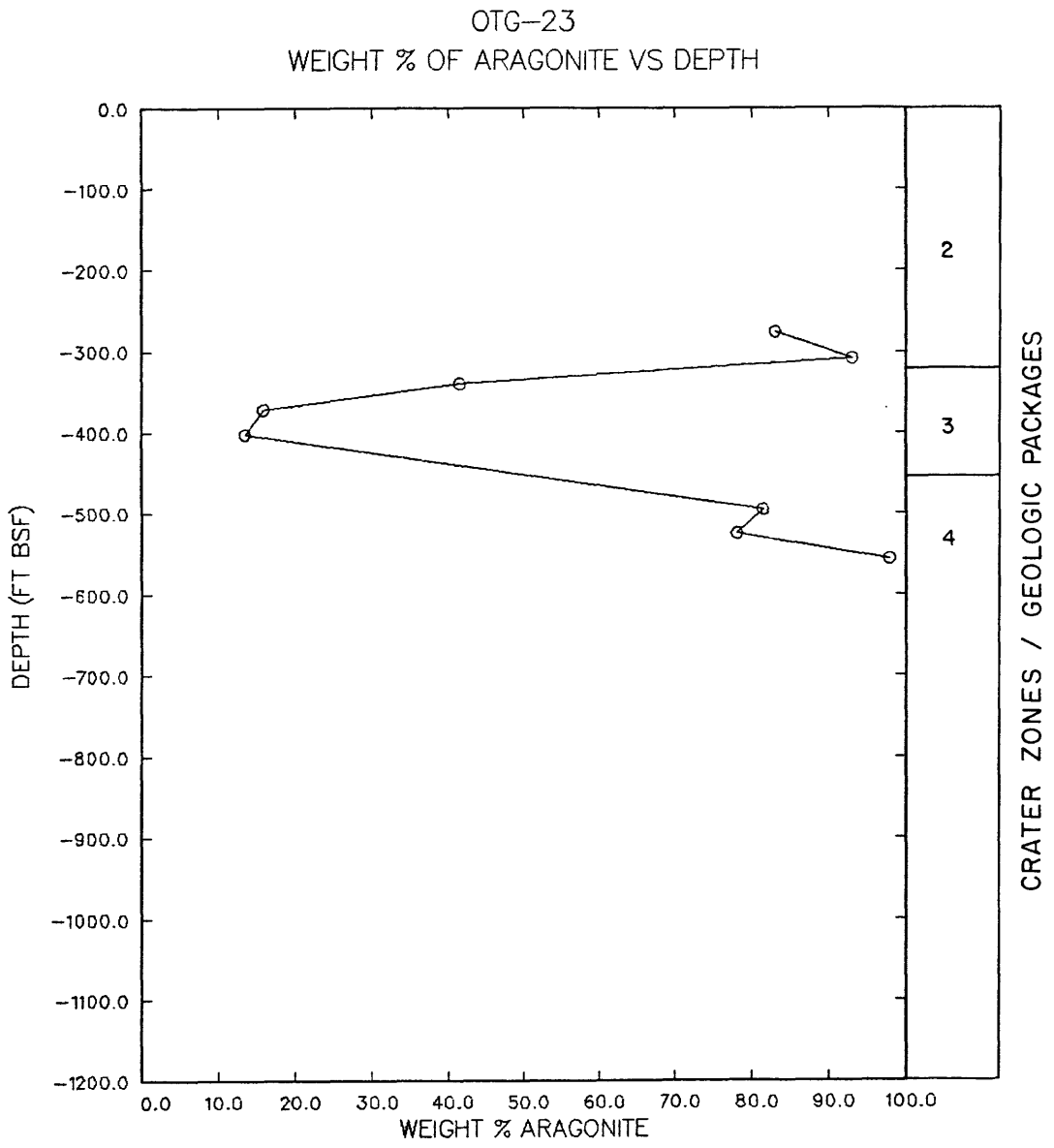

FIGURE 4-11. -- Depth profile of weight percent aragonite for stratigraphic samples from borehole OTG-23.

CHAPTER 5:

TOTAL ORGANIC CONTENT OF LAGOON BENTHIC SEDIMENTS AND OF SUBSURFACE SAMPLES FROM THE PEACE DRILLING PROGRAM

by

Byron L. Ristvet and Edward L. Tremba

S-CUBED, A Division of Maxwell Laboratories, Inc.[1]

INTRODUCTION

Total organic content was determined by loss-on-ignition for selected geologic samples obtained during the PEACE Program conducted at Enewetak Atoll, Marshall Islands, during 1984-85. Two types of samples were analyzed: Recent surface sediments collected from the lagoon floor (see Chapter 10 of this report) and subsurface samples obtained from boreholes in and adjacent to OAK crater. The purpose of the analyses was fourfold: (1) to aid in the estimation of grain density of the whole-rock samples to allow the conversion of bulk densities to total porosity, (2) to aid in petrogenesis and diagenesis studies, 3) to provide a log for correlative purposes, and (4) to provide a basis for estimating the volume of "piped" material within the mixed zone of OAK crater.

The locations of the Recent lagoon sediment samples (benthic samples) are presented in Chapter 10 of this report. The locations of the boreholes and their geologic logs are presented in Henry, Wardlaw, and others (1986).

METHODS OF STUDY

The determination of organic or carbonaceous matter by loss-on-ignition (LOI) is a standard technique that appears in texts on quantitative inorganic chemical analysis (cf. Kolthoff and Sandell, 1952; Fritz and Hammond, 1957; Vogel, 1961) and the American Society for Testing and Materials standards (ASTM, 1973). Dean (1974) presents an extensive review of the method for calcareous sediments and compares the LOI technique to other methods, e.g. selective chemical dissolution, gas evolution and gas chromatography. The technique utilized in this study is similar to that described by Dean (1974).

Table 5-1 lists all of the samples analyzed for total organic content in this study. All of samples from boreholes OBZ-4, OPZ-18, OQT-19, OSR-21 and and all of the lagoon sediments were analyzed by the authors utilizing the

---

[1] Albuquerque, NM.

TABLE 5-1. -- Summary of total organic content of PEACE Program samples, depth in ft below sea floor. Weight percent is dry weight percent of sample.

OOR-17		OOR-17 (cont.)		OSR-21		OQT-19	
DEPTH	WT %	DEPTH	WT %	DEPTH	WT %	DEPTH	WT %
1.0	3.0	531.0	1.6	0.2	3.4	5.4	3.2
11.7	3.7	547.7	2.1	47.0	3.1	31.2	2.8
31.0	2.9	563.4	2.0	92.0	2.4	50.5	3.1
52.0	3.5	573.1	1.9	124.7	2.1	72.3	2.0
58.6	2.6	597.5	1.8	165.9	3.4	98.9	1.5
69.0	3.5	611.6	2.1	186.7	1.5	134.4	2.3
73.1	1.3	645.0	2.0	220.2	1.6	193.6	1.1
88.0	1.8	668.5	1.6	252.0	2.3	238.0	2.2
96.5	1.0	682.0	2.0	279.0	2.4	282.0	2.6
102.8	1.6	696.3	2.3	327.4	1.7	330.5	1.1
109.0	1.2	707.1	2.1	348.7	1.0	366.0	1.1
122.4	1.9	730.0	2.9	**********		421.4	1.5
131.1	1.6	739.0	3.5			461.0	1.2
137.1	2.6	739.0	3.8			511.9	0.7
152.0	2.5	757.0	2.5			552.5	2.7
169.8	2.3	771.0	2.8			612.0	2.8
178.5	2.0	785.0	3.0			641.6	2.9
200.3	1.8	797.4	2.1			666.0	3.4
209.6	1.6	797.4	2.4			691.0	2.6
220.1	1.4	815.0	3.1			**********	
242.4	1.1	834.0	2.1				
273.4	2.5	857.0	2.0				
289.1	2.4	866.0	3.6				
299.0	2.3	884.0	2.1				
299.1	2.5	907.7	2.6				
321.1	0.8	920.0	2.6				
333.3	1.0	935.7	1.8				
345.6	0.5	938.0	1.3				
356.5	1.0	947.5	1.2				
365.2	2.1	958.2	0.7				
371.0	1.4	968.7	1.1				
386.1	1.2	980.0	1.1				
401.0	0.3	987.6	0.7				
415.0	1.0	994.5	0.6				
426.0	0.7	1010.3	1.0				
436.0	1.3	1025.6	0.7				
447.0	0.9	1037.4	1.0				
453.0	0.7	1047.0	1.3				
470.7	0.8	1055.1	0.6				
478.4	0.7	1065.3	1.3				
503.5	0.6	1079.3	0.5				
523.3	0.7	1085.4	1.2				
(cont. above)		**********					

(Table 5-1 continued on next page.)

TABLE 5-1 (continued).

OBZ- 4		OPZ-18		SEDIMENTS	
DEPTH	WT %	DEPTH	WT %	SMPL.	WT %
990.6	0.4	31.8	3.4	S- 9	3.7
1031.5	0.7	48.0	2.8	S- 17	3.0
1100.1	0.5	64.4	2.5	S- 37	3.5
1180.1	0.6	76.0	2.4	S- 30	2.8
1252.0	1.7	93.0	1.8	S- 56	3.4
1289.3	0.7	112.0	1.9	S- 65	3.3
1390.1	1.0	129.2	3.1	S- 78	3.5
1417.2	0.8	145.5	2.6	S- 89	3.1
1452.3	0.6	160.0	2.3	S-118	3.0
1500.9	1.7	174.5	2.3	S-123	3.9
1566.8	0.9	192.0	3.2	**********	
1581.6	1.7	217.0	1.5		
1597.6	0.8	231.6	3.6		
**********		251.0	1.9		
		290.0	1.4		
		357.0	2.3		
		391.6	0.9		
		414.5	0.3		
		449.8	0.7		
		470.6	0.6		
		518.0	0.8		
		565.0	2.7		
		607.1	2.2		
		621.3	2.2		
		650.3	3.7		
		669.6	2.8		
		**********			

facilities of the Material Sciences Laboratory located within the Air Force Weapons Laboratory (AFWL). One half of the samples from borehole OOR-17 were analyzed at AFWL and one half at the Soils Laboratory located within the U.S. Army Corps of Engineers Waterways Experiment Station (WES), Vicksburg, Mississippi. Nearly identical methodologies were utilized at the two laboratories with each laboratory analyzing alternate samples downhole. Replicates were conducted on two samples as a check on the precision variance between the two laboratories.

Each of the carbonate samples were washed in deionized water to remove soluble salts and drilling fluids. The samples were then crushed to pass through either a 74 or 100 micron seive and oven dried at 105 deg C for two hours. Approximately two grams of sample was then weighed on a microbalance in a preweighed ceramic crucible, which had been acid rinsed and dried for two hours at 105 deg C. The crucible and sample were then placed in an analytical muffle furnace at 550 deg C for two hours. A temperature this high will cause the complete combustion of all organic carbon compounds based on the temperatures of combustion for carbonaceous organic matter presented by Grimshaw and Roberts (1957). The samples were then removed from the furnace, were allowed to cool to room temperature in a dessicator, and were reweighed. The difference between this weight and the dry weight is the dry weight percent of ignited organic carbon compounds. Precision of the method is estimated to be $\pm$ 0.15 dry weight percent based on replicate analyses. Interlaboratory precision is estimated to be within the range of the precision of the analytical method.

RESULTS

Table 5-1 presents a summary of the total organic contents expressed as dry weight percent of the samples analyzed. Figures 5-1 and 5-2 display the total organic content versus borehole depth in ft below the seafloor for the OAK area boreholes. Table 5-2 presents a summary of the data versus the stratigraphic framework developed in Chapter 2 of this report or versus crater zones as defined in Chapter 14 of this report.

The Recent lagoon surface sediments show a very uniform total organic content regardless of location within the Enewetak lagoon. This mean organic content is 3.3 weight percent, standard deviation 0.33 (Table 5-2).

Each sedimentary package presented in Table 5-2 appears to have a total organic content "signature," that is a reflection of either its petrogenetic or diagenetic history or both. The following generalizations can be made.

- Package 1, the Holocene sediments, has a mean of 3.0 weight percent and reflect the total organic content of Recent lagoonal surface sediments, suggesting that burial was so rapid during most of the Holocene that there was little oxidation of organic matter.

- Package 2, the Pleistocene, has a mean of 2.0 weight percent and displays a significant reduction in total organic content from that of Package 1, reflecting its repeated exposure to diagenesis by meteoric waters (Ristvet, Tremba, and others, 1978).

TABLE 5-2. -- Summary of total organic contents of PEACE samples analyzed in this study versus sedimentary package or crater zone. All values reported as dry weight percent.

PACKAGE OR ZONE	NO. OF SAMPLES	MEAN	STND. DEV.
Lagoon sediments	10	3.32	0.33
Package 1	11	3.00	0.62
Package 2	35	1.96	0.64
Package 3	25	1.12	0.50
Package 4	20	1.90	0.66
Package 5	18	2.81	0.59
Package 6	7	1.61	0.69
Package 7	7	0.91	0.23
Package 8	17	0.92	0.42
Crater Zone Alpha	1	3.40	--
Crater Zone Beta-1	9	2.41	0.38
Crater Zone Beta-2	1	3.20	--

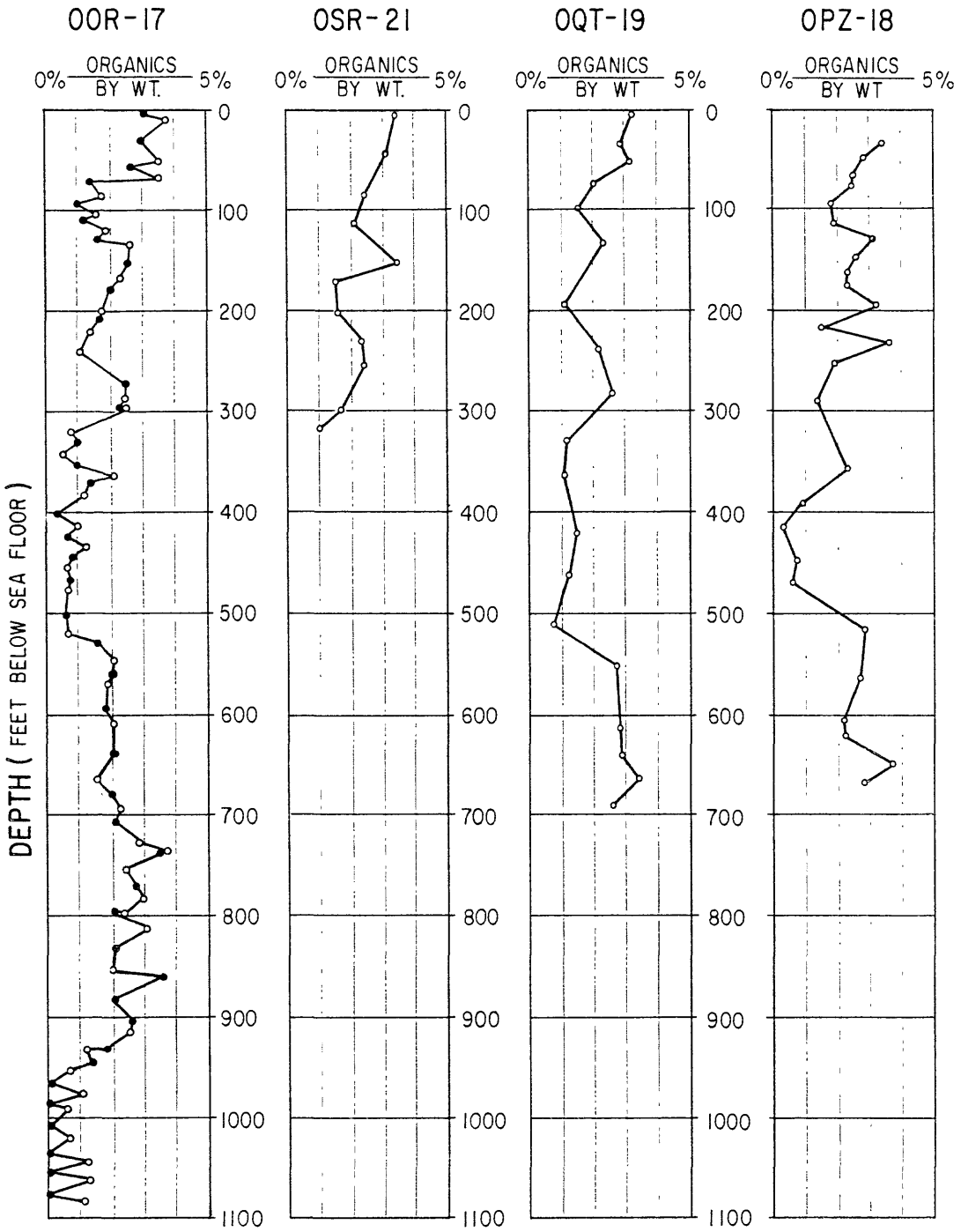

FIGURE 5-1. -- Total organic content versus depth for boreholes OOR-17, OSR-21, OQT-19, and OPZ-18. Open circles represent analyses at AFWL, solid circles at WES.

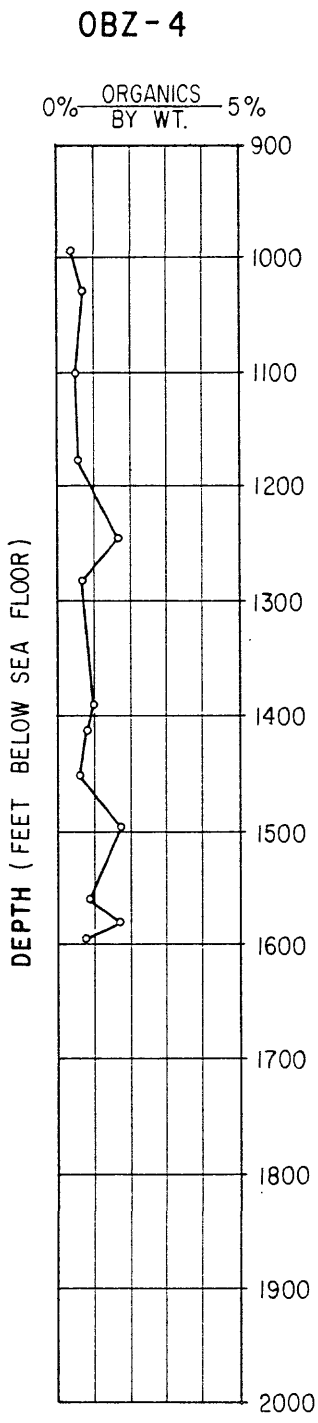

FIGURE 5-2. -- Total organic content versus depth for the deep portion of borehole OPZ-4.

- Package 3 has a mean of 1.1 weight percent organic material and shows significant loss of total organic matter, mirroring its intense diagenetic history, as shown in the stablization of its mineralogy from calcite/aragonite to nearly all calcite (Chapter 4 of this report).

- Package 4, with a mean of 1.9 weight percent, reflects only moderate alteration of the sediments following burial.

- Package 5, with a mean of 2.8 weight percent, depicts an organic-rich interval during its deposition that has not been subjected to the alteration of meteoric waters. Studies of the insoluble residues of this interval show that the organic material in this sedimentary package has undrergone alteration in terms of maturation from elementary organic compounds to lignite (Chapter 6 of this report).

- Package 6, with a mean of 1.6 weight percent, again reflects only moderate alteration of the sediments by meteoric waters.

- Packages 7 and 8, with average total organic contents of less than 1 percent, reflect the intense diagensis of the sediments as indicated by the stabilization of mineralogy (Chapter 4 of this report) and the petrography of well-cemented rocks that have undergone repeated exposure to meteoric waters (Chapter 2 of this report).

Analyses of the crater zone samples tend to support the conclusions from petrographic and paleontologic studies (Chapter 14 of this report), that Crater Zone Alpha appears to consist of Recent sediments and piped sediments from sedimentary packages 4, 5, and 6. In contrast, Crater Zone Beta-1 shows the apparent mixing of sedimentary packages 1 and 2.

One sample, from 231.6 ft bsf in OPZ-18, was omitted from the analyses presented in Table 5-2. This is because it was petrographically identified as being a mass of sedimentary package 1 interpreted to have been "injected" into the highly fractured sedimentary package 3 beneath the transition sands of OAK crater (see Chapter 4, p. 6, for discussion; and Henry, Wardlaw, and others, 1986, p. 440 for description of this unit). The total organic content of this sample supports the interpretation that it is an intact unit of Holocene (package 1) material (Chapter 14 of this report).

ACKNOWLEDGEMENTS

The authors would like to thank Drs. Bruce R. Wardlaw and T.W. "Woody" Henry, USGS, and Lt. Col. Robert Couch, Jr., DNA for discussions and support throughout this study. Special thanks is extended to Wayne E. Martin, Robert G. Stamm, and Stephen M. Wessels, USGS, for the preparation of many of the samples. Appreciation is extended to Dr. Robert Henny, Mr. Charles Miglianco, and SSgt. Robert Robertson, AFWL, for making their facilities available to perform much of the analyses reported. Special appreciation is extended to Joseph Zelasko, Steven Akers, and Paul Burke, WES, for the analyses of half of the OOR-17 samples.

REFERENCES

American Society for Testing and Materials, 1973, Moisture, ash, and organic matter of peat materials: ASTM Standard D-2974-71, in Annual Book of ASTM Standards, Part II.

Dean, W.E., Jr.,1974, Determination of carbonate and organic matter in calcareous sediments and sedimentary rocks by loss on ignition: comparison with other methods, Journal of Sedimentary Petrology, v. 44, p. 242-248.

Fritz, J.S., and Hammond, G.S., 1957, Quantitative Organic Analysis; John Wiley and Sons, Inc., New York.

Grimshaw, R.W. and Roberts, A.L., 1957, Carbonaceous materials; 404-417, in MacKenzie, R.C., ed., The differential thermal investigations of clays: Mineralogical Society of London.

Kolthoff, I.M., and Sandell, E.B., 1952, Quantitative Inorganic Analysis; MacMillan Co., New York.

Ristvet, B.L., Tremba, E.L., Couch, R.F., Jr., Fetzer, J.A., Goter, E.R., Walter, D.E., and Wendland, V.P., 1978, Geologic and geophysical investigations of the Eniwetok nuclear craters: Air Force Weapons Laboratory Technical Report AFWL TR 77-242, Kirtland Air Force Base, NM.

Vogel, A.I., 1961, Quantitative Inorganic Analysis; 3rd ed., John Wiley and Sons, New York.

CHAPTER 6:

INSOLUBLE RESIDUE ANALYSES OF CARBONATE SEDIMENTS FROM THE SUBSURFACE OF ENEWETAK ATOLL

by

Byron L. Ristvet and Edward L. Tremba

S-CUBED, A Division of Maxwell Laboratories, Inc.[1]

INTRODUCTION

The characteristics of the acid insoluble residues of selected subsurface samples from PEACE boreholes OOR-17 and OBZ-4 were determined by this study. The purpose of the insoluble residue analyses was twofold: (1) to aid in understanding the geologic history of Enewetak Atoll, and (2) to aid in grain-density determinations. The locations of the drill holes and their geologic logs are presented in Henry, Wardlaw, and others (1986).

METHODS OF STUDY

The method utilized for this study was that described by Krumbein and Pettijohn (1938). Samples were disaggregated initially by hand or, for the well-cemented samples, broken with a hammer to increase the surface area. The samples were then washed with deionized water to remove soluble salts and drilling fluids and dried in an oven at 105 deg C. Approximately 100 g of the washed and dried sample were weighed on a microbalance and placed into a 2000 ml Erlenmeyer flask with 50 to 100 ml of deionized water. 1500 ml of 10 percent (V/V) reagent hydrochloric acid was added slowly to the flask at room temperature and occasionally stirred until complete dissolution of the calcite and aragonite had occurred as evidenced by the cessation of the release of carbon dioxide gas bubbles within the fluid. Dissolution took between 6 to 24 hrs depending on the surface area of the samples.

Following dissolution, the contents of the flask were then filtered through preweighed Whatman #2 filter paper (approximate pore size of 0.2 microns, μ), rinsed with deionized water, dried in an oven at 105 deg C, and reweighed on a microbalance to obtain the mass of the insoluble residues. The filter papers were then examined with a binocular microscope to identify any insoluble residues on the filter paper. Several individual mineral grains subsequently were hand picked from the filter paper after examination with the binocular microscope for examination with a Scanning Electron Microscope (SEM) and for Energy Dispersive Analysis of X-rays (EDAX) for elemental analysis to aid in positive identification of the mineralogy. The grains were coated with approximately 100 Angstroms of carbon to prevent charging in the SEM.

---

[1] Albuquerque, NM.

RESULTS

Table 6-1 presents a summary of the dry weight percent of the total and the inorganic insoluble residues and their descriptions. Most of the insoluble residue of the samples analyzed was composed of organic matter. The total quantity of organic residue generally mirrors the trend of total organic content of the sediments as presented in Chapter 5 of this report. Inorganic residues were present only in those samples taken from beneath the sedimentary package 6/7 boundary and only in trace amounts, i.e. a few mineral grains. Minor amounts of contaminants from the drilling operations were discovered in four of the samples analyzed. The contaminates were minute pieces of steel from the drill bits or pipes and/or isolated flakes of 50- to 100-μ diameter muscovite. The muscovite was utilized as a lost circulation recovery material during drilling.

A distinct change in the morphology of the organic insoluble residues occurs at the sedimentary package 3/4 boundary. Below this boundary, the residues are solitary grains that are 5 to 50 μ in diameter, dark brown to black, vitreous in appearance, and lignitic and/or possibly bituminous. Above the sedimentary packages 3/4 boundary, the organic matter appears primarily as a yellow-brown stain of the filter paper with a few "clumps" of ochre-colored, 30- to 100-μ diameter, "fluffy" masses. In addition to the organic matter retained on the filter paper, a significant quantity apparently was dissolved in the supernate as evidenced by its color. Similar to the residue, the color of the supernate was yellow for the samples from above the sedimentary package 3/4 boundary and dark yellowish brown from below. The sedimentary package 3/4 boundary appears to reflect a major change in the maturation index of the organic matter, from apparently humic matter above, to primarily lignitic and possibly bituminous material below.

The inorganic portion of the insoluble residues is restricted to a few samples from below the sedimentary package 6/7 boundary, which marks a major hiatus between Lower and Upper Miocene (Chapter 2 of this report). The prime constituents of the inorganic insoluble residues are grains of subrounded, 30- to 50-μ diameter, light-yellowish-green olivine. SEM/EDAX analyses on three olivine grains from the sample from borehole OOR-17 at 1,022.0 feet bsf show only Fe, Mg, and Si elemental peaks with the Fe/Mg ratio approximently 2.5 and the Fe/Si ratio approximately 5.0 in atomic proportions. These ratios are consistent with the olivine reported by Macdonald (1963) for the basalts recovered from drill hole E-1 on Medren Island in the southeast portion of Enewetak Atoll. The subrounded shape and the freshness of the olivine grains does <u>not</u> suggest sediment transport over great distances.

Four, 10-μ diameter, well-rounded, frosted, quartz grains were present in the insoluble residues from 1,022.0 ft bsf in borehole OOR-17. Their grain size and surface textures are similar to the eolian quartz grains described by Rex, and others (1969) and Jackson, and others (1971) for other areas of the northern Pacific Basin. However, the quartz grain from the insoluble residues from 1,417.2 feet bsf in OBZ-4 appears to have a different origin. This grain consists of a single, clear, euhederal crystal

TABLE 6-1. -- (Page 1 of 2 pages) Dilute hydrochloric-acid insoluble residues from samples from boreholes OOR-17 and OBZ-4.

DEPTH (ft bsf)	TOTAL IR[1] (dry wt %)	INORGANIC IR[1] (dry wt %)	DESCRIPTION
		Borehole OOR-17	
357.0	0.005	0.000	Yellow-brown organic stain
470.1	0.022	0.000	Yellow-brown organic stain
610.0	0.561	0.000	Vitreous, dark-brown, lignitic material
711.7	0.648	0.000	Vitreous, dark-brown, lignitic material
799.1	0.701	0.000	Vitreous, dark-brown, lignitic material
951.6	0.342	0.000	Vitreous, dark-brown, lignitic material
1022.0	0.081	0.017	15 grains, 30 - 50-μ[2] dia., light-green, subrounded olivine; 1 grain, obsedian (?); 4 grains,10-μ dia., well-rounded, frosted quartz; 1 grain, dolomitized, 70 μ-long, coral septa; vitreous, dark-brown, lignitic material
		Borehole OBZ-4	
990.6	0.010	0.000	Vitreous, dark-brown, lignitic material
1031.5	0.051	0.000	Vitreous, dark-brown, lignitic material
1100.1	0.137	Tr	4 grains, 30-40 micron dia., light-green subrounded olivine; vitreous, dark-brown, lignitic material
1180.1	0.105	0.000	Vitreous, dark-brown, lignitic material
1252.0	0.031	0.000	Vitreous, dark-brown, lignitic material
1289.3	0.063	Tr	1 grain, 50 x 100 μ, oblate, well-rounded, quartz (?); vitreous, dark-brown, lignitic material
1390.1	0.079	0.000	Vitreous, dark-brown, lignitic material

Continued on next page

[1] IR = insoluble residue; [2] μ = micron.

TABLE 6-1 (continued, p. 2/2).

DEPTH (ft bsf)	TOTAL IR[1] (dry wt %)	INORGANIC IR[1] (dry wt %)	DESCRIPTION
		Borehole OBZ-4 (cont.)	
1417.2	0.077	Tr	1 grain, 20-μ[2] dia., light-gray feldspar (??); 1 grain, 10 x 40-μ, euhedral, clear, glassy quartz crystal; vitreous, dark-brown, lignitic material
1452.3	0.030	Tr	1 grain, 40-μ dia., light-green, subrounded olivine; vitreous, dark-brown, lignitic material
1550.9	0.083	0.000	Vitreous, dark-brown, lignitic material
1566.8	0.110	Tr	2 grains, 40-μ dia., light-green, subrounded, olivine; vitreous, dark-brown, lignitic material
1581.0	0.081	Tr	1 grain, 20 x 60-μ oblate, black, obsedian shard (?); vitreous, dark-brown, lignitic material
1597.6	0.177	0.000	Vitreous, dark-brown, lignitic material

[1] IR = insoluble residue; [2] μ = micron.

approximately 10 by 40 μ in dimension. Its origin is probably from late-time hydrothermal alteration of a nearby dike. The well-preserved nature of the crystalline faces does not suggest significant transport. Like the olivine grains, the size of the quartz crystal and its fresh surface appearance, eliminate the possibility of an eolian origin. Similar quartz crystals exist within the dikes of the Koolau Basalts on Oahu, Hawaii (Wentworth and Winchell, 1947), and are present within the sediments of the windward streams (Ristvet, 1977).

One grain consisting of a dolomitized coral septum was present in the insoluble residues from 1,022.0 ft bsf in OOR-17. This is consistent with the report of a trace of X-ray detectable dolomite in a sample at 1,010.3 feet bsf from the OOR-17 borehole (Chapter 4 of this report).

The analyses of the insoluble residues of Enewetak subsurface carbonate sediments strongly suggest the presence of a subaerially exposed volcanic rock feature within the Enewetak lagoon at least through the middle Miocene, i.e. the sedimentary package 6/7 boundary (Chapter 2 of this report).

ACKNOWLEDGEMENTS

The authors would like to thank Drs. Bruce R. Wardlaw and T.W. "Woody" Henry, USGS, and Lt. Col. Robert Couch, Jr., DNA, for discussions and support throughout this study. The efforts of Dr. Robert Henny and Mr. Charles Miglianco, AFWL, are greatly appreciated for making available the facilities to perform the analyses reported.

REFERENCES

Jackson, M.L., Levelt, T.W.M., Syers, J.K., Rex, R.W., Clayton, R.D., Sherman, G.D., and Uhera, G., 1971, Geomorphological relationships of tropospherically-derived quartz in soils of the Hawaiian Islands: Proceedings of the Soil Science Society of America, v. 35, p 515-525.

Krumbein, W.K. and Pettijohn, F.P., 1938, Manual of Sedimentary Petrography; Appleton-Century Crofts, New York.

Macdonald, G.A., 1963, Petrography of the basalts beneath the limestones; p. 1038-1048; in Schlanger, S.O., Subsurface Geology of Eniwetok Atoll, U.S. Geological Survey Professional Paper 260-BB.

Rex, R.W., Syers, J.K., Jackson, M.L., and Clayton, R.D.,1969, Eolian origin of quartz in soils of Hawaiian Islands and in Pacific pelagic sediments. Science, v. 163, p. 277-279.

Ristvet, B.L., 1977, Reverse weathering reactions within Recent nearshore marine sediments, Kaneohe Bay, Oahu: unpublished Ph.D. dissertation, Northwestern University, Evanston, Illinois.

Wentworth, C.K., and Winchell, H., 1947, Koolau basalt series, Oahu, Hawaii: Geological Society of America Bulletin, v. 58, p. 49-78.

CHAPTER 7:

DOWNHOLE GEOPHYSICAL LOGS

by

L. Stephen Melzer

Science Applications International, Corp.
Midland, TX

INTRODUCTION

Most boreholes drilled during the PEACE Program at Enewetak Atoll were logged with several different types of downhole geophysical tools to support the basic objectives of the program (see Chapter 1 of this report and Henry, Wardlaw, and others, 1986, p. 51-53, for discussion). A complete inventory of logs made during this program is given in Table 7-1. Selected borehole logs for the KOA crater area are presented in Figures 7-1 through 7-5, at the end of this Chapter, and those for OAK in Figures 7-6 through 7-16, also at the end of the Chapter.

A discussion is presented on the theory of operation and principles of measurement for each of the following tools: (1) the gamma ray, also commonly referred to as the natural gamma, (2) the sonic (also called multichannel sonic or acoustic), (3) the compensated density, occasionally called the gamma-gamma, and (4) the compensated neutron. Cautionary notes about the application of data from these logs to specific kinds of analyses are included in the discussion. Borehole gravimetry logs are discussed in Chapter 8. The seismic reference survey logs and the depth integrated sonic logs are discussed in detail in Chapter 9. A complete general reference for logging principles can be found in Hilchie (1982).

For the gamma ray, sonic, compensated density, and compensated neutron logs, each tool makes continuous measurements of specific borehole parameters as the tool is pulled by wireline up the hole. Specifications for these tools are available upon request from the PEACE Program logging subcontractor and operator, BPB Instruments, Inc.

GAMMA RAY

The gamma ray log measures natural gamma radiation. The source material for this radiation normally comes from elements of three groups: The uranium-radium series, the thorium series, and potassium 40. (see Chapter 12 for additional discussion). Different lithologies, for various reasons, exhibit different radioactive levels. For example, quartz is a mineral with a well-ordered crystal with strong bonding planes in all directions. During crystallization, most impurities are excluded from the crystal lattice, making the inclusion of any radioactive elements highly unlikely. Sandstone, most commonly composed of quartz grains, is therefore very low in radioactivity. Also, carbonate sediments and limestones, composed of calcite and aragonite

TABLE 7-1. -- Types of downhole geophysical logs used in PEACE Program boreholes (from Henry, Wardlaw, and others, 1986, p. 53, table 7).

BOREHOLE	LOG TYPE						
	MCS	GR/NU**	GR/DN/CP	TAC	SRS	CR/CP	BHG
KAR- 1	X	X	X	-	X	-	-
KAM- 2	-	-	-	-	-	-	-
KAM-2A/KAP-3	-	X	-	-	-	-	-
KBZ- 4	X	X	X	-	X	-	-
KCT- 5	X	X	X	-	X	-	-
KDT- 6	-	X	X	-	X	-	-
KET- 7	-	-	-	-	-	-	-
KFT- 8	-	X	X	-	X	-	-
OAM-1/OAR-2	-	X	X	X	X	-	-
OAR- 2A	X	X	X	-	-	-	-
OAM- 3	-	X	X	-	-	-	-
OBZ- 4	X	X*	X	-	X	-	-
OCT- 5	X	X*	X	-	X	-	-
ODT- 6	-	-	-	-	-	-	-
OET- 7	X	X*	X	-	-	-	-
OFT- 8	X**	X	-	-	-	-	-
OGT- 9	-	X	-	-	-	-	-
OHT-10	-	X	-	-	-	-	-
OIT-11	X	X	X	-	-	-	-
OJT-12	-	X	-	-	-	-	-
OKT-13	X	X*	X	-	-	-	-
OLT-14	-	-	-	-	-	-	-
OMT-15	-	X	-	-	-	-	-
ONT-16	-	X	-	-	-	-	-
OOR-17	X	X	X	-	X	-	X+
OPZ-18	-	X*	X	-	-	-	X+
OQT-19	X	X*	X	-	-	-	X+
ORT-20	-	-	X	-	-	-	X+
OSR-21	-	-	X	-	-	-	X+
OSM-22	-	-	-	-	-	-	-
OTG-23	-	-	-	-	-	X+	X+
OUT-24	-	X	-	-	-	-	-

* Run in open hole. + Run in casing. **Run in drill pipe only
Symbol "X" denotes presence of log, "-" absence.

MSC, multichannel sonic (sonic or accoustic log)
GR/NU, gamma-ray / neutron-neutron
GR/DN/CP, gamma-ray / density / caliper
TAC, three-arm caliper
SRS, seismic reference survey
GR/CP, gamma-ray / caliper
BHG, borehole gravimetry

fragments, tests, and shells of once-living creatures, generally have little or no radioactivity because of the low levels of radioactive isotopes incorporated in the calcite and aragonite lattices when they formed. Aragonite contains approximately 4 ppm uranium, 0.5 ppm thorium, and 2 ppm potassium-40; calcite contains only slightly higher levels of these isotopes. Organic- and thorium-rich sediments such as some shales and clays contain much higher levels of radioactivity. Igneous rocks and arkosic sandstones, containing appreciable concentrations of radioactive potassium, also produce high levels of natural radioactivity.

The BPB gamma-ray tool was run in conjunction with either the compensated neutron or the compensated density tool. The tool uses an uncollimated sodium iodide crystal coupled to a photo multiplier tube to detect incoming gamma rays. The photo multiplier serves to amplify the flashes of light caused by gamma rays scintillating within the sodium iodide crystal. The light flashes are converted to counts and the log is presented as radiation intensity in API units[1].

The depth of investigation of the gamma ray tool normally is considered to be approximately 6 inches for high-density solids, that is, ninety percent of the total received signal normally originates from within this distance. Any material interposed between the sediment and the detector will attenuate the amount of incoming radiation. Logging through casing and/or drill pipe, heavy muds, or in large or washed-out holes serves to attenuate the flux of gamma radiation detected by the tool. The natural gamma attenuation produced by logging through the drill pipe and casing with the gamma ray/compensated density log is illustrated in Figure 7-2 in the interval from 360 to 365 ft below the seafloor (bsf). The borehole above and below this interval was logged open hole.

As mentioned above, natural radioactivity is commonly a clue to the amount of clay or shale in a given sequence of strata. However, the Enewetak sedimentary sequence is exclusively carbonate, containing no shales or clays. Zones of relatively higher natural radioactivity are commonly zones of higher organic content. In the subsurface of Enewetak, in areas outside of the influence of the craters themselves, the most highly radioactive materials generally contain only about 2 to 4 percent organic material by weight (see Chapter 5). However, there are zones that are characterized by significantly higher concentrations of organic material, including some lignitic packstones and a thin lignite (see Chapter 2). These zones are generally light brown to dark brown, due to the concentration of organic materials, and generally have higher levels of natural radioactivity. The plateau of relatively higher gamma activity within the organic interval in the Enewetak section was used to define sedimentary package 5 (see Chapter 2). It generally starts with a sharp upper peak, maintains a high background downhole, and is characterized

---

[1] One (1) API unit is defined as 1/200th of the difference in log deflection between two specific zones of different radiation intensity in the API test pit, located in Houston, Texas; 1 API unit equals the gamma rays produced from 0.084 prcocuries (pCi) of radium-226 per equivalent gram).

by a broad, gradual decline at its base. The return to low background levels of radioactivity at the base of sedimentary package 5 is a reliable correlative horizon both within the OAK and KOA areas and between the two sites.

Higher organic content in the strata does not explain all of the increases in natural radioactivity as recorded by the gamma logs in the Enewetak boreholes. A few, localized intervals of elevated gamma activity appear to be caused by various factors related to some of the disconformities within the section and diagenetically altered (recrystallized) zones just below these.

The gamma radiation that occurs in the crater zones, in part due to device-produced radionuclides, is discussed in Chapters 12 and 14.

SONIC

The sonic log is a geophysical tool used to determine the acoustic properties of the material adjacent to the borehole. The depth of investigation is generally considered to be 6 to 12 inches.

The BPB sonic tool is designed with one transmitter and four receivers. The first receiver is placed 60 cm below the transmitter and the remaining three receivers are placed in succeeding 20-cm increments. The tool is run in the center of the borehole and the transmitter fired every tenth of a second. The arrival of the compressional wave is recorded as it passes each receiver in succession. The BPB system has the capability of recording transit time over intervals of 20, 40, and 60 cm, depending on user need. Interval transit times for the 20-cm R1 - R2 receiver spacing and the 60-cm R1 - R4 spacing were the ones chosen for display in the field and are shown in the logs at the end of this Chapter. The longer of the spacings, the 60-cm travel path, was used primarily for the log analyses.

In unconsolidated, uncemented, and saturated sediment, the first wave arrival is controlled by the water within the sediment. Unfortunately, washout zones also register a water- (or drilling fluid-) controlled first-wave arrival. Preliminary field interpretation of sonic data for the PEACE Program suggested that the numerous washout zones were invalidating the sonic data in the washed-out intervals. However, subsequent analysis has shown that water-controlled velocities also are indicative of unconsolidated, uncemented (but saturated) materials and that the washed-out zones generally correlate with the softer zones in the profile. The apparently erroneous readings, in fact, may be indicative of unconsolidated and uncemented materials whose arrival velocities are essentially fluid velocities. The logs can be used as indicators of consolidation/cementation in boreholes KAR-1 and KBZ-4. However, precise sonic velocity values are unobtainable within the washed-out intervals.

Table 7-2 exhibits some typical materials and their respective matrix (or crystalline) compressional wave travel time.

In many materials, laboratory tests (Wyllie and others, 1956) have shown that there is a linear relationship between porosity and sonic velocity transit time (Δt). The relationship is commonly used for the determination of porosity from sonic log data, and such deviations of porosity can be approximated by Wyllie's "time average formula":

$$T = \text{Porosity} \times T_f + (1 - \text{Porosity}) \times T_{ma}$$

thus,

$$\text{Porosity} = \frac{T - T_{ma}}{T_f - T_{ma}}$$

where:

T = Travel time of the first-arriving compressional wave,
T_{ma} = Travel time of the compressional waves in the rock matrix,
T_f = Travel time of compressional wave in the interstitial fluids.

This relationship assumes that the porosity is homogeneous. Granular rock, such as quartzose sandstone, gives excellent results. Material with large-scale voids (vuggy porosity) commonly found in carbonates and, especially, in sedimentary package 3 in the Enewetak section (see Chapter 2), is not accurately detected by the sonic tool. The tool bases its measurements on the first arrival or fastest sonic travel path. For this reason the sonic indicates accurate readings only in intergranular porosity wherein the travel path would involve crossing many pores. Measurements of gross or total porosity in materials with vuggy or moldic should be considered more accurate by utilizing one of the other porosity tools such as the compensated neutron or compensated density sonde.

The sonic logs taken for the PEACE Program are invaluable mechanical property indicators. Material strength variations within materials from the Pacific Proving Grounds are controlled predominantly by the type and degree of cementation. Cementation in these materials does affect their sonic velocities but does not generally greatly affect their densities. The reason for this lies in changes in the materials accompanying the cementation process; simply stated, the cementation of matrix is accompanied by dissolution of many of the grain components (particularly those composed of aragonite). The total pore space for the materials, at least at depths less than 1000 ft below sea level, ranges between 40 and 55 percent, regardless of whether the material is an unconsolidated, uncemented sand or a well-cemented limestone. The sonic log will easily discriminate the degree of cementation when the compensity density, borehole gravimeter, and compensated neutron-log readings will not. For this reason, the sonic log (taken together with the core/sample descriptions) provide key data for mechanical property profile construction for cratering studies.

TABLE 7-2. -- Grain (matrix) compressional-wave travel time of selected materials.

MATERIAL	TRAVEL TIME (in μsec/ft)
Sandstone (consolidated)	52.6
Calcite	47.6
Dolomite	43.5
Aragonite	53.0
Water (pure)	218.0
Water (10% NaCl)	208.0
Water (15% NaCl)	200.0
Enewetak borehole fluid	196.0*
Water (20% NaCl)	189.0
Water (Enewetak)**	197.9

* estimated. ** measured by Grow, Lee, and others (1986).

COMPENSATED NEUTRON

The compensated neutron is a geophysical tool designed to measure the ability of the sediment to attenuate the energy of fast neutrons. Such attenuation is a function of the materials present in the matrix and the interstitial fluids, with hydrogen being the dominant attenuator. Table 7-3 shows the relative ability of different elements to absorb energy from fast neutrons.

Because hydrogen is so highly efficient in reducing neutron energy, the number of thermalized neutrons is approximately proportional to the hydrogen concentration of the material. Since most interstitial liquids contain about the same proportion of hydrogen, the neutron log is an indicator of fluid-filled porosity. The inclusion of gas or air in the material will lower the hydrogen concentration, causing the tool to give spuriously low values for total porosity.

The BPB compensated neutron tool generates "fast" neutrons in the 4.5 MeV range produced by a one curie Americium 241-Beryllium source. Alpha particles generated by the Americium 241 react with the Beryllium to produce the 4.5 MeV neutrons. Two uncollimated helium tubes are utilized as neutron detectors. One neutron detector is placed 45 cm from the source (long-spaced), the other detector is located 25 cm from the source (short-spaced). Material porosity is determined from the ratio of the long- and short-spaced count rates.

Compensated neutron logs are subject to several borehole-induced effects. Increases in fluid-filled borehole diameter increases the amount of hydrogen present in the near vicinity of the tool leading to false indications of higher porosity in washed-out holes. Also, since iron is a moderately efficient absorber, casing or drill pipe between the tool and the sediment will cause higher apparent porosities than the same interval logged open-hole. The effect of these conditions can be determined and readings corrected if the casing and/or drill-pipe size and weight and the hole size are known. The casing and/or drill-pipe effect is not a major factor and is an additive linear shift that easily can be subtracted from the log reading. The additional apparent porosity due to larger hole size may be computed from a hole size correction chart for that particular tool provided by the service company.

CALIPER LOG

The borehole size is determined by measuring the extension of a single protruding caliper arm on the compensated density tool as it passed along the borehole wall. Variations in borehole diameter cause the motorized, spring loaded arm to move. This movement is detected by a potentiometer located at the axis of the single arm which converts the deflection to an electric signal that is transmitted to the surface for display. Since the arm is located directly opposite the density pad, the tool normally will align itself along the major axis of the borehole (i.e., the greatest diameter) if the hole is not circular in cross section.

TABLE 7-3. -- Energy absorption from fast neutrons of selected elements.

ELEMENT	AVERAGE NUMBER OF COLLISIONS REQUIRED TO THERMALIZE NEUTRON	MAXIMUM ENERGY LOSS/COLLISION
Calcium	371	08%
Chlorine	316	10%
Silicon	261	12%
Oxygen	150	21%
Carbon	115	28%
Hydrogen	18	100%

Note: Thermalization is defined as lowering the state of energy below 0.025 ev.

Borehole-size data were used in many ways. Determination of proper environmental corrections for other logging tools was its most common usage at Enewetak, but caliper logs also were valuable in other ways as well. Uncemented and/or unconsolidated sediments were detected on the caliper log by their tendency to wash-out during the drilling process. In addition, the measurement of hole diameter was evaluated onsite for selection and running of optimal casing size after hole reaming. Also, the effectiveness of various mud systems was compared by the smoothness of the borehole walls and frequency of wash-outs as measured by the caliper log.

COMPENSATED DENSITY

The compensated density tool is a pad-type tool that determines the attenuation effect of the material on relatively low-energy gamma rays. Gamma rays generated by a radioactive source are either scattered by Compton scattering, or absorbed by photoelectric effect. Both processes involve interactions with the electrons in the material. If the source of gamma rays is held reasonably constant, then the number of returning gamma rays is a function of the electron density of the material. Electron density for most materials is directly proportional to bulk density because the ratio of the number of electrons, Z, to the atomic mass, A, for most materials is an approximate constant of 0.5 (see table 7-4). As a result, the number of returning gamma rays is inversely proportional to the atomic mass which, in turn, can be related directly to the bulk density of the sediment.

The BPB compensated density tool utilizes a 100-millicurie Cesium-137 source and two scintillation detectors at different spacings from the source. The long-spaced detector is spaced 48 cm above the source, and the short-spaced detector 15 cm above the source. Both detectors incorporate crystal shielding to reduce borehole effects. Optimum results are obtained in smooth boreholes with a diameter of less than 20 cm (30 cm with the optional long caliper arm attached). Loss of pad contact due to washouts or extreme borehole rugosity generates data heavily biased by the density of borehole fluids rather than the materials drilled.

Compensated density logs run at Enewetak indicated not only extremely low bulk density values in much of the shallow sediments, but also suggested predominantly uncemented zones. This lack of cementation or cohesion, as indicated as washouts on the caliper log, were represented as low-density readings on the density logs. Low bulk density and high density correction (delta rho) readings are indicative of these materials. These uncemented, uncohesive zones (as well as washed-out intervals, as discussed earlier) also are indicated by the sonic tool by sonic travel times representative of borehole fluids and/or pore water. (See Chapter 9 for discussion of the integrated sonic logs.)

TABLE 7-4. -- Ratio of number of electrons (Z) to atomic mass (A) for selected elements and minerals.

ELEMENT OR SUBSTANCE	Z/A RATIO
Oxygen	0.500
Carbon	0.499
Calcium	0.499
Silcon	0.498
Sulfur	0.499
Magnesium	0.495
Calcite	0.500
Dolomite	0.499
Water	0.555
Hydrogen*	0.992

* free

Bulk density may be related to the porosity of the sediment if the density of the matrix and pore fluids are known. This relationship is expressed by the following equation:

$$\text{Porosity} = \frac{\rho_m - \rho_b}{\rho_m - \rho_f}$$

where: ρ_m = Grain (matrix) density,
ρ_b = Bulk Density (log measurement),
ρ_f = Interstitial fluid density

Table 7-5 shows common materials and their respective grain densities.

SEISMIC REFERENCE SURVEY

Seismic wave velocities were also determined within some boreholes using a BPB seismic reference sonde. The results are presented in Chapter 9 of this report. This tool, also commonly called a "check shot" velocity or downhole velocity survey, was used to measure the amount of time required for a seismic compressional wave to travel from a source located on the surface to the receiver held against the wall of the borehole. The seismic wave velocity is a function of many parameters including mineralogy of the rock, grain packing, porosity, microfracturing, and cementation. Variations in the nature of the interstitial fluid and especially its gas content also can have significant effects upon the seismic wave velocities.

The seismic reference sonde used by BPB is approximately 7.5 ft in length and 2.5 in. in diameter. The instrument is held against the borehole wall by a motorized arm to achieve good acoustic coupling with the sediment. Seismic energy was generated by the firing of a 100-cubic-inch air gun approximately 10 ft below the ocean surface. The mean time difference was measured between energy arrival at a hydrophone located 3 ft from the gun, and the reference sonde located in the borehole. Data were recorded via oscillograph paper records and times picked manually. The data were then corrected for horizontal offset of the gun to derive two-way travel time, average velocity, interval velocity, and R.M.S. velocity for each station. Measurements generally were taken at intervals of approximately 10 m (some shallow holes were logged on 5-m spacings), unless rugose hole conditions prevented acoustic coupling of the downhole reference sonde. Measurements within the casing were attempted; however, shallower station readings were generally too noisy to obtain accurate readings due to wave-induced casing vibration.

Wave velocities computed from the seismic reference survey are representative of long travel paths and are generated in the same fashion as seismic reflection data, so that the technique is most commonly used to provide seismic velocity profiles to convert time-domain seismic-reflection data to depths. Sonic log data are also commonly used for the same purpose, especially in oil field applications, but can produce slightly misleading data in certain materials owing to the short source distance to receiver distance. This technique is very time consuming, forcing measurement intervals to be very thick. In addition, the tool requires coupling to the borehole wall, which may be impossible under poor borehole conditions.

TABLE 7-5. -- Grain (matrix) densities of common materials.

MINERAL	GRAIN DENSITY (g/cc)
Calcite	2.71
Dolomite	2.86
Quartz	2.71
Aragonite	2.92

RESULTS

Visual, "hands-on" examination of subsurface materials during the PEACE drilling project was vital to accomplishing Program objectives (Chapter 1 of this report and Henry, Wardlaw, and others, 1986, p. 51-53). Lithic, paleontologic, and mechanical property classifications were dependent upon sample acquisition, examination, and testing. However, one important limitation to the visual examination process was always on the minds of those individuals performing sample examinations--that is, what to assume for those materials not recovered in the sampling/coring process. The only real data to assist in filling gaps and answering the question of the interval relevance of the examined sample were provided by the downhole logs.

The geophysical logs generally were utilized by comparing log response of an interval to the actual sample examination results of the same interval. In this manner, the logs were "calibrated" to the investigator's parameters of interest and then could be utilized to extrapolate to intervals of little or no sample recovery. The continuous readings available on the logs could thus help in mitigating the effect of the inevitable "missing" samples.

Downhole geophysical logs are being used in many applications within the PEACE Program. Some of these uses contrast with the more widely accepted general use of the logs. Table 7-6 summarizes the principal use of each major logging type for the normal non-cratering application and how it was used in the PEACE Program. The uses of logs during the PEACE Program can be generally classified into three categories: (1) onboard drilling assistance, (2) mechanical property determinations and profile idealization, and (3) crater process analysis. Discussion of each type of use within each of the three general uses proves to be lengthy and, as a result, will be the subject of a future separate report. Some of the specific applications of the individual log types have already been discussed within this and other Chapters of the current report. Other uses are still in the analysis stage at the time of writing. The log analysis for mechanical property purposes will be included in a future report of the PEACE material property committee.

Finally, Table 7-7 provides a summary of the major areas of geophysical log contributions to the PEACE Program. The "drilling time" log reported in Henry, Wardlaw, and others, 1986 also is included for completeness, although it is not a geophysical log. At the time of the preparation of this report, additional uses of the logs are being investigated so it is possible that other applications will be added to the list prior to completion of the PEACE Program.

TABLE 7-6. -- Principal uses of downhole geophysical logs and specific PEACE PROGRAM applications.

LOG TYPE	GENERAL APPLICATION	PEACE PROGRAM USE
Caliper	Hole rugosity, hole volume	Density log correlation, Loose sand ID (washouts)
Natural Gamma Ray	'Shaleyness', clay content	Stratigraphic correlation, subcrater zonations
Formation Density	Index prop. (density/porosity) determination	In-situ porosity values
Neutron Porosity	Index prop. (porosity/density) determination; 'gas effect'*; tool can be effectively used in cased hole	In-situ porosity/density values - valuable due to lack of clays at PPG
Sonic	Prop. velocity for seismic "truth", porosity	Propagation velocity control, best lithologic log, ID of crater 'degradation' zone
Downhole Velocity	Seldom used	Interval prop. velocities for seismic "truth"
Borehole Gravity	Seldom used	Large volume interval density determinations, crater densification effects
Cone Penetrometer	Foundation strength investigations, sands versus clays	Shear strength determination, operational problems (generally unsuccessful)
Resistivity	Pore fluid characterization, permeability	Not used
Temperature	Hole temperature profiles for reservoir fluid volume calculation	Not used

* Used with density log to establish presence of gas in sands (neutron reads low due to low density gas in pores).

TABLE 7-7. -- Summary of geophysical log contributions and applications in PEACE Program. H = heavily utilized, M = moderately utilized, L = of relatively little value.

	NATURAL GAMMA	SONIC	SRS	FORMATION DENSITY	POROSITY	CALIPER	BHG	DRILLING TIME
CRATER ANALYSIS								
Crater "Fill" Zonation	H							
Transition Sand Location	M							
Material Property Degredation		H	H					
Consolidation/Densification				H	H		H	
Bed Thinning	M	L						L
Lithologic Unit Correlation	M	L						L
Grain (Matrix) Density				H*	H*			
MECHANICAL PROPERTIES OF UNDISTURBED (PRETEST) MATERIALS								
Strength/Degree of Cementation		H	H			H		M
Density/Porosity				H	H		H	
Profile Idealization		H	M	L	M			L
DRILLING ASSISTANCE								
Mud System Effectiveness "Washout" Determination						H		

*Requires both formation density and neutron porosity for 'back' calculation of matrix density.

REFERENCES

Grow, J.A., Lee, M.W., Miller, J.J., Agena, W.F., Hampson, J.C., Foster, D.S., and Woellner, R.A., 1986, Multichannel seismic-reflection survey of OAK and KOA craters; 46 p., 39 figs.; in Folger, D.W., ed., Sea-floor observations and subbottom seismic characteristics of OAK and KOA craters, Enewetak Atoll, Marshall Islands: U.S. Geological Survey Bulletin 1678.

Henry, T.W., Wardlaw, B.R., Skipp, B.A., Major, R.P., and Tracey, J.I., Jr., 1986, Pacific Enewetak Atoll Crater Exploration (PEACE) Program, Enewetak Atoll, Republic of the Marshall Islands; Part 1: Drilling operations and descriptions of boreholes in vicinity of KOA and OAK craters: U.S. Geological Survey Open-File Report 86-419, 497 p., 32 figs., 29 pls., 13 tbls., 3 appendices.

Hilchie, D.W., 1982, Applied Open Hole Log Interpretation; Privately published by Douglas W. Hilchie, Inc., Golden, Colorado.

Willie, M.R.J., Gregory, A.R., and Gardner, G.H.F., 1956, Elastic Wave Velocities in heterogenous and porous media: Geophysics, v. 21, no. 1, (also in SPWLA reprint volume "Acoustic Logging", March 1978.).

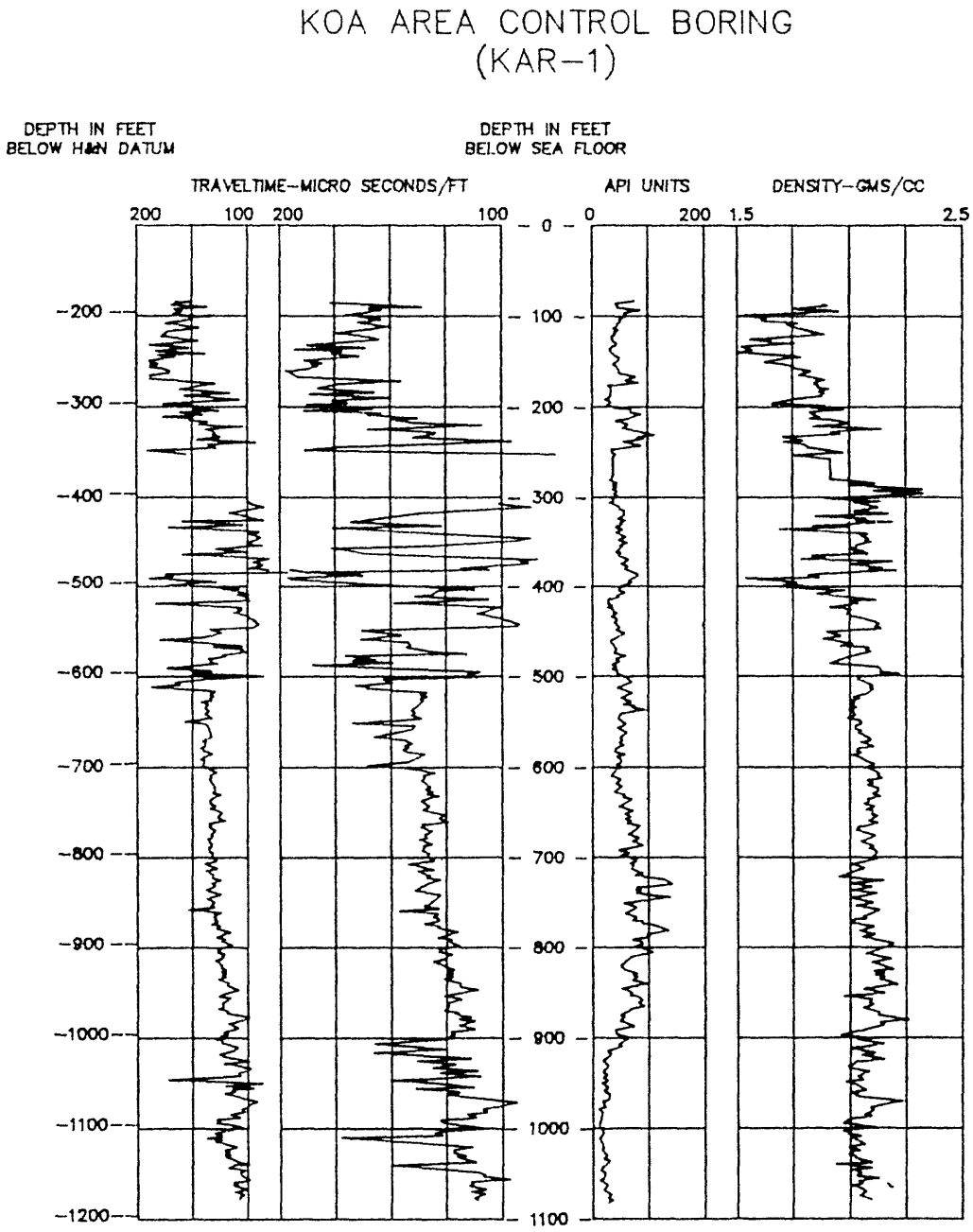

FIGURE 7-1. -- Multichannel sonic and gamma-ray/density logs for borehole KAR-1.

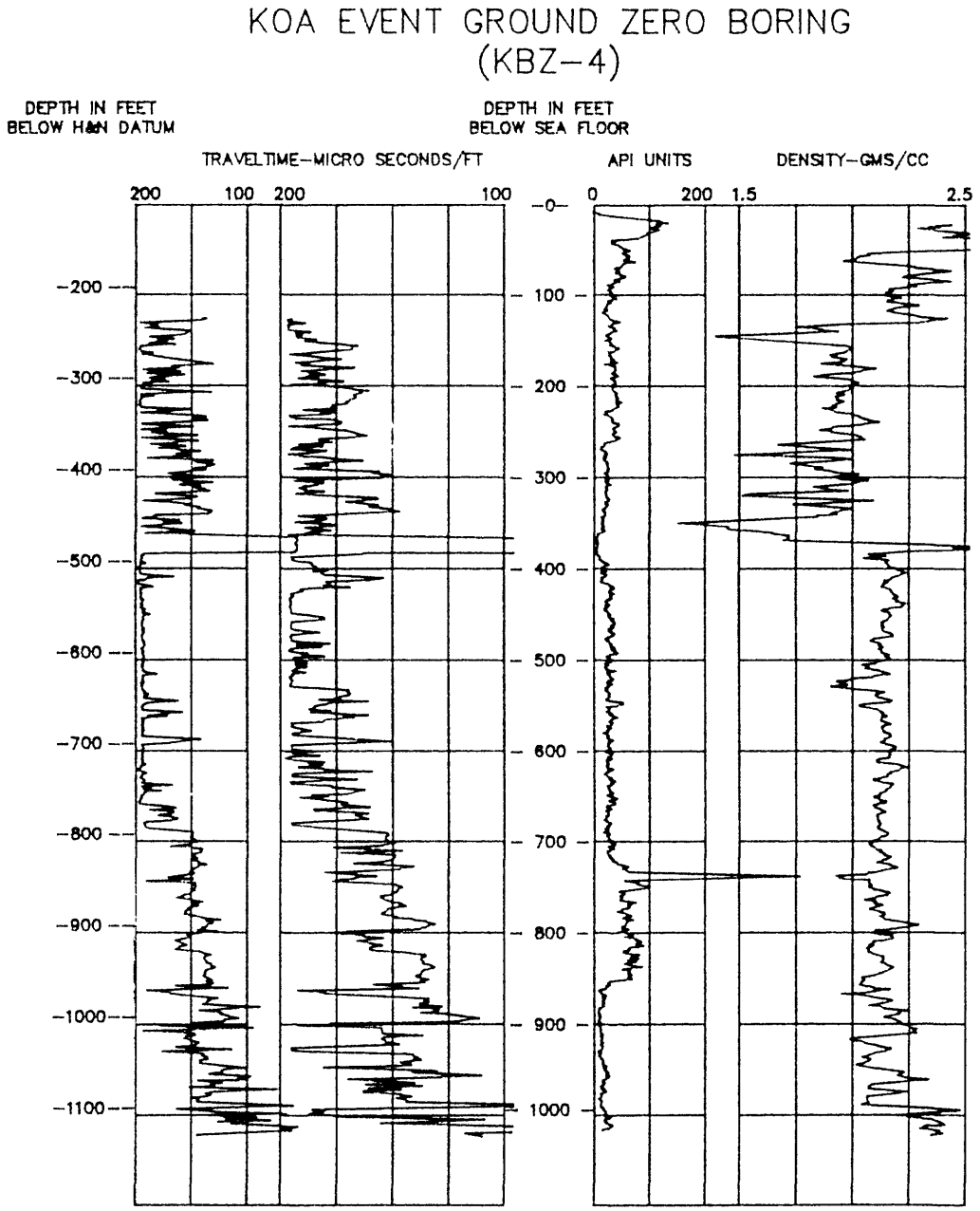

FIGURE 7-2. -- Multichannel sonic and gamma-ray/density logs for borehole KBZ-4.

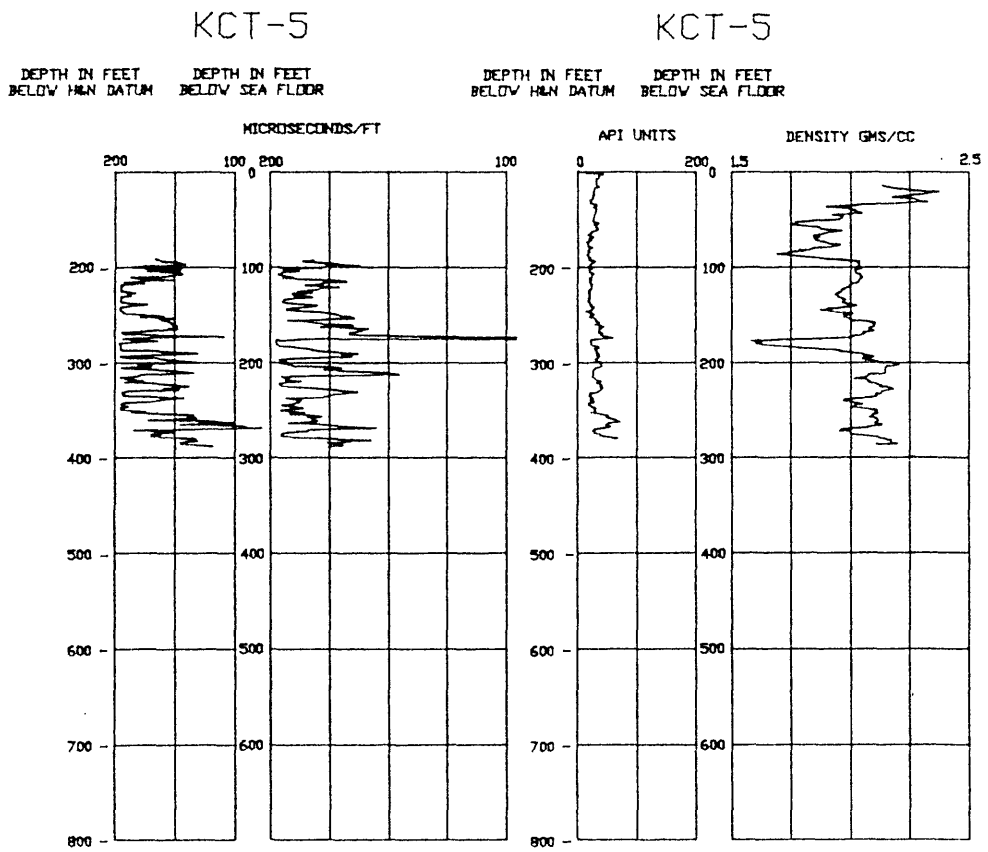

FIGURE 7-3. -- Multichannel sonic and gamma-ray/density logs for borehole KCT-5.

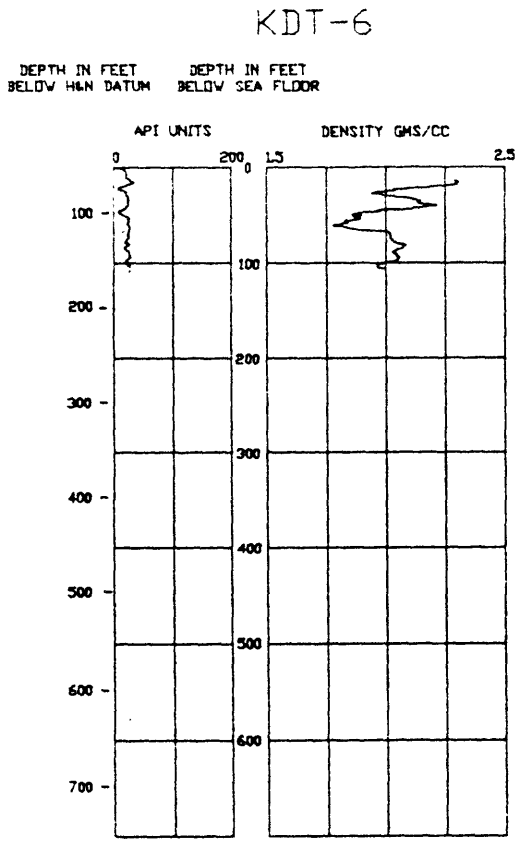

FIGURE 7-4. -- Gamma-ray/density log for borehole KDT-6.

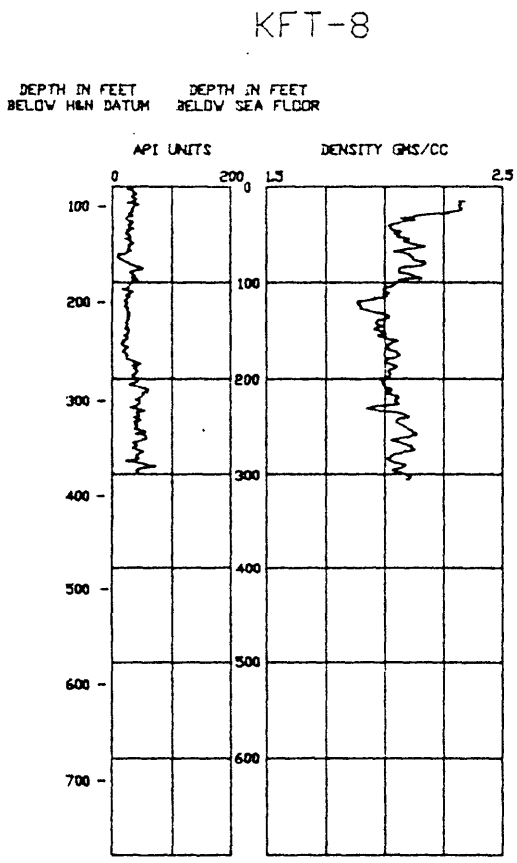

FIGURE 7-5. -- Gamma-ray/density log for borehole KFT-8.

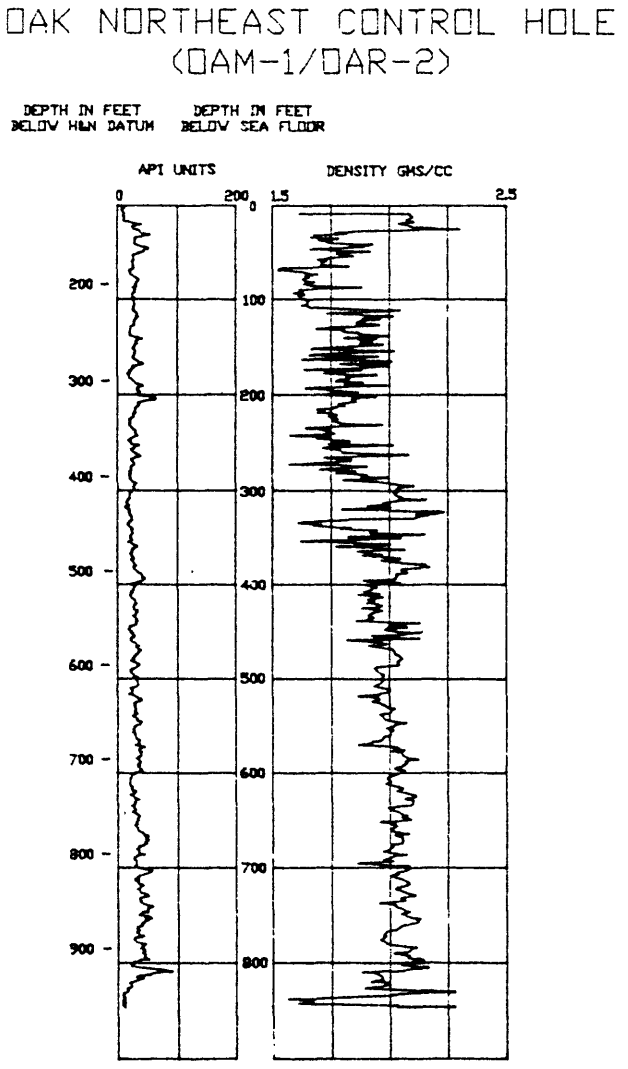

FIGURE 7-6. -- Gamma-ray/density log for borehole OAM-1/OAR-2.

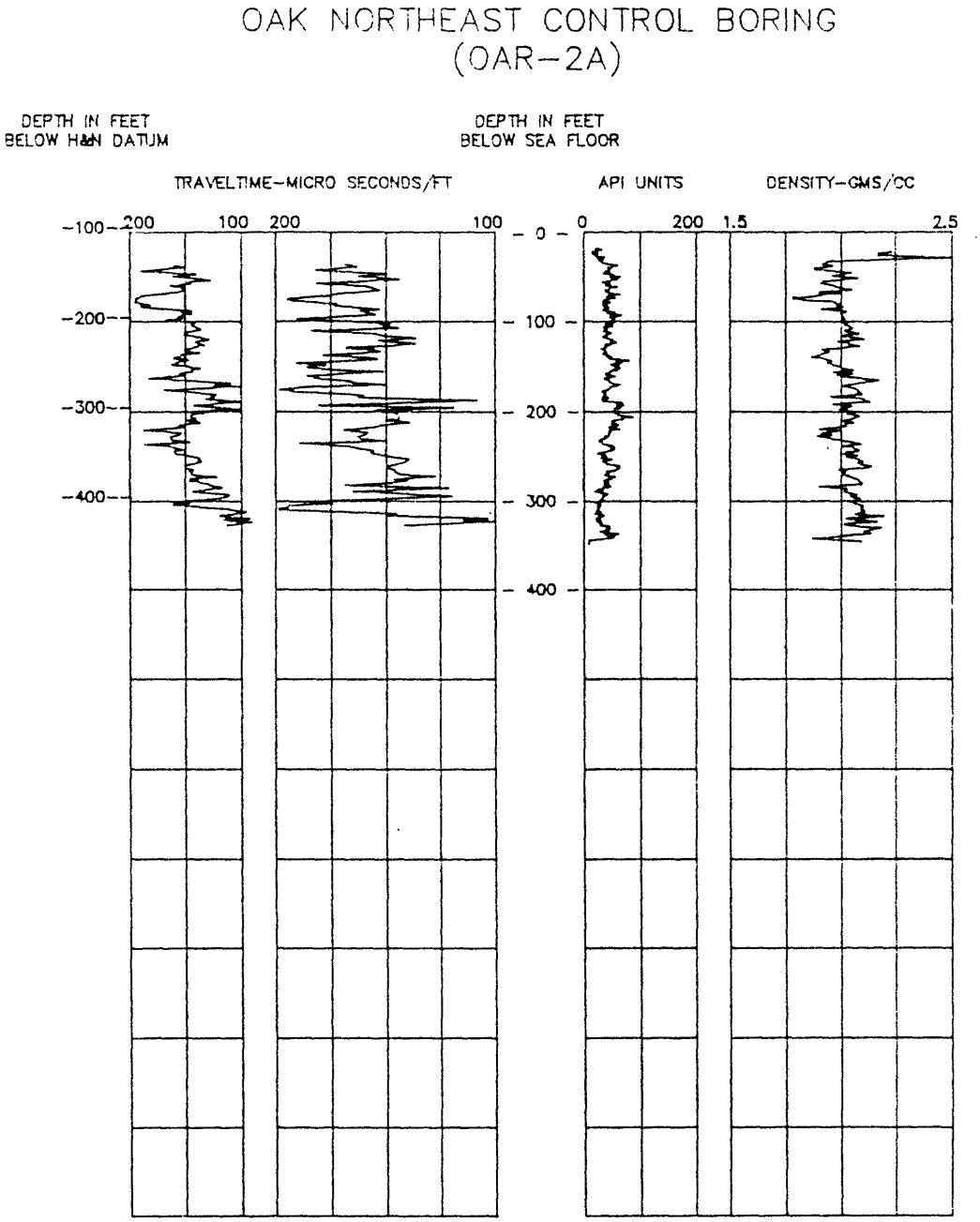

FIGURE 7-7. -- Multichannel sonic and gamma-ray/density logs for borehole OAR-2A.

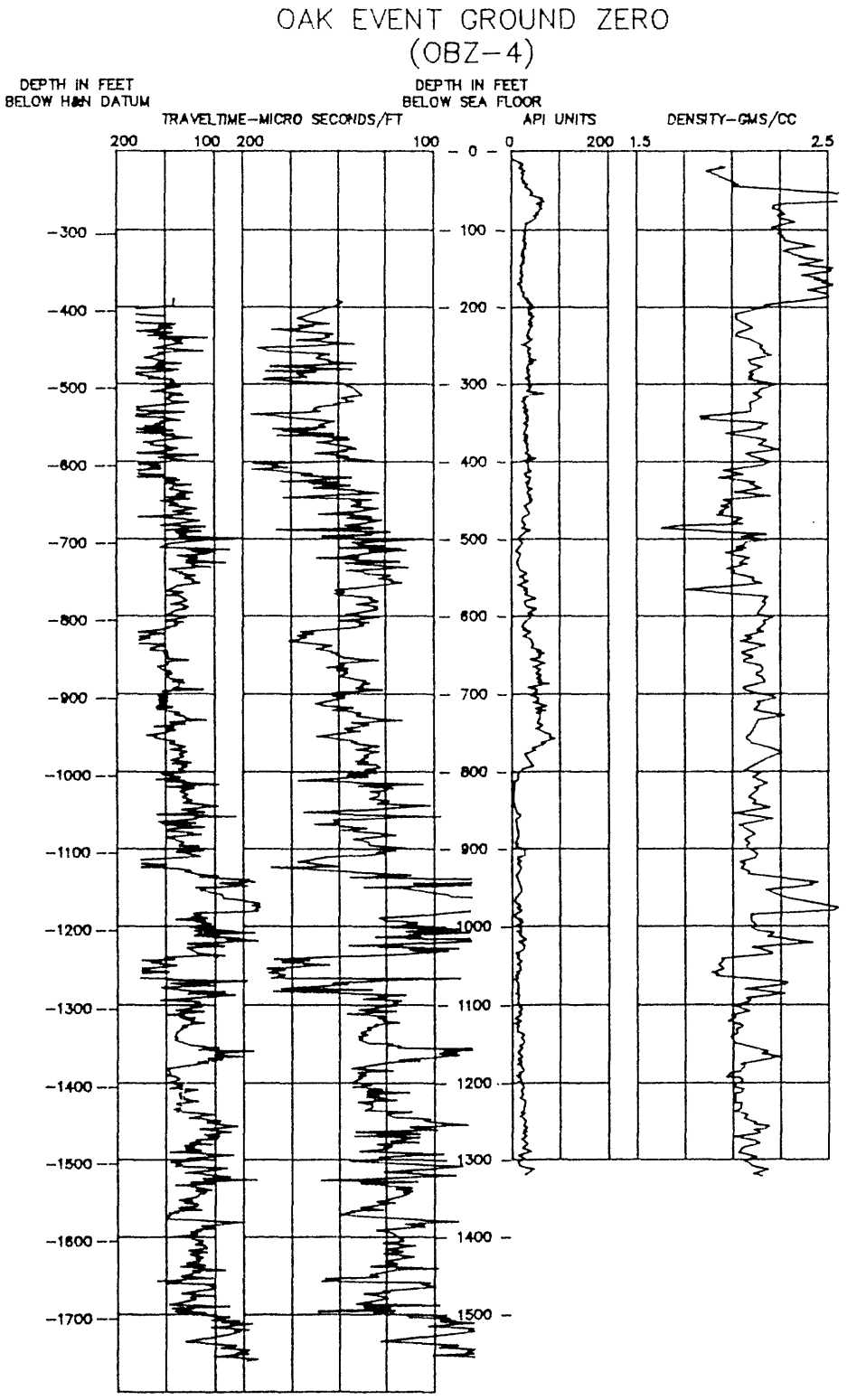

FIGURE 7-8. -- Multichannel sonic and gamma-ray/density logs for borehole OBZ-4.

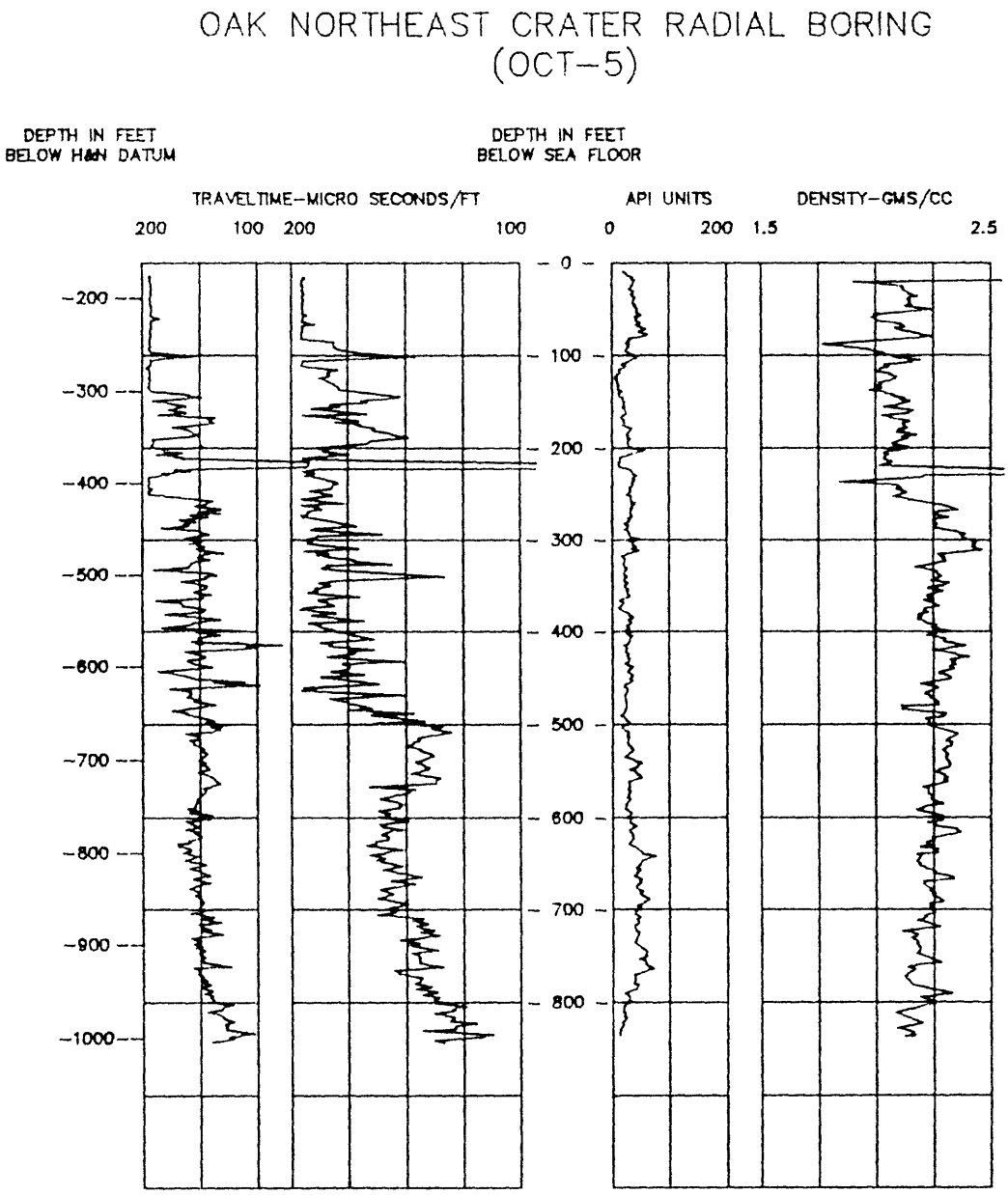

FIGURE 7-9. -- Multichannel sonic and gamma-ray/density logs for borehole OCT-5.

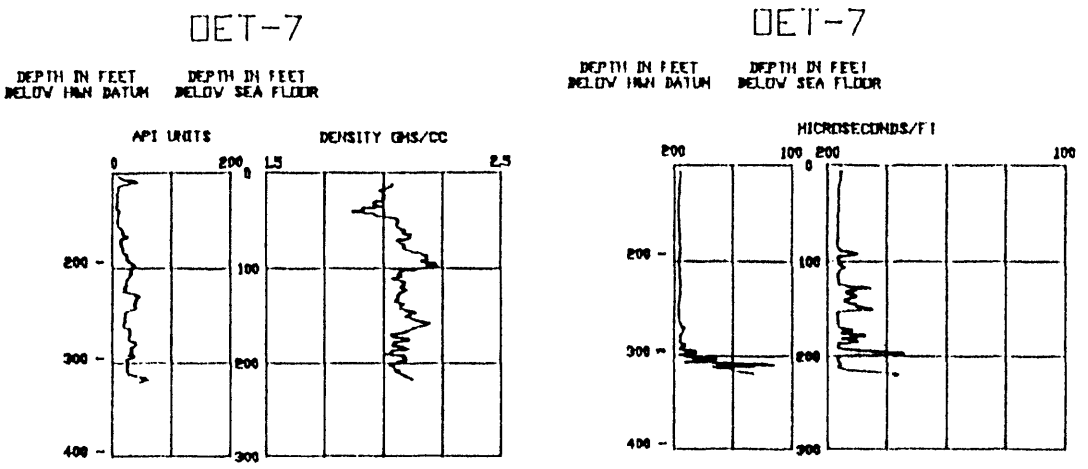

FIGURE 7-10. -- Gamma-ray/density and multichannel sonic logs for borehole OET-7.

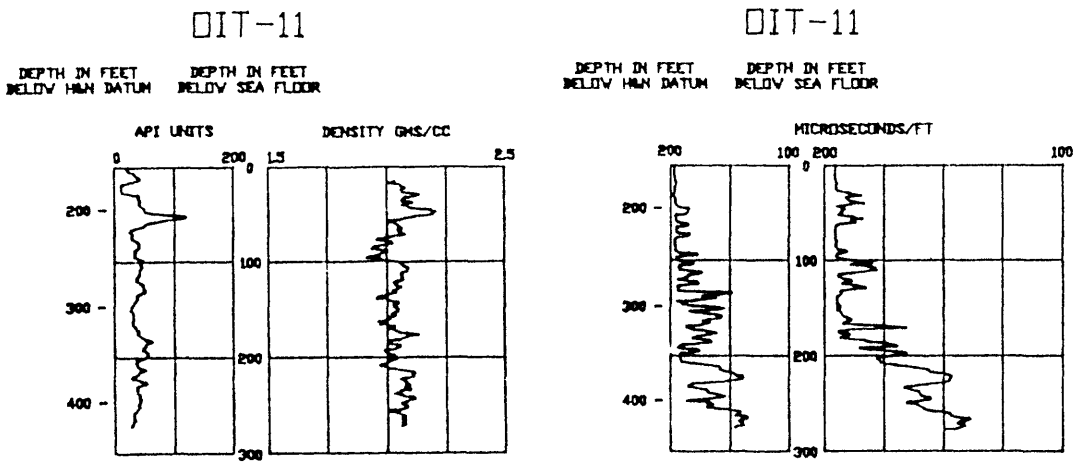

FIGURE 7-11. -- Gamma-ray/density and multichannel sonic logs for borehole OIT-11.

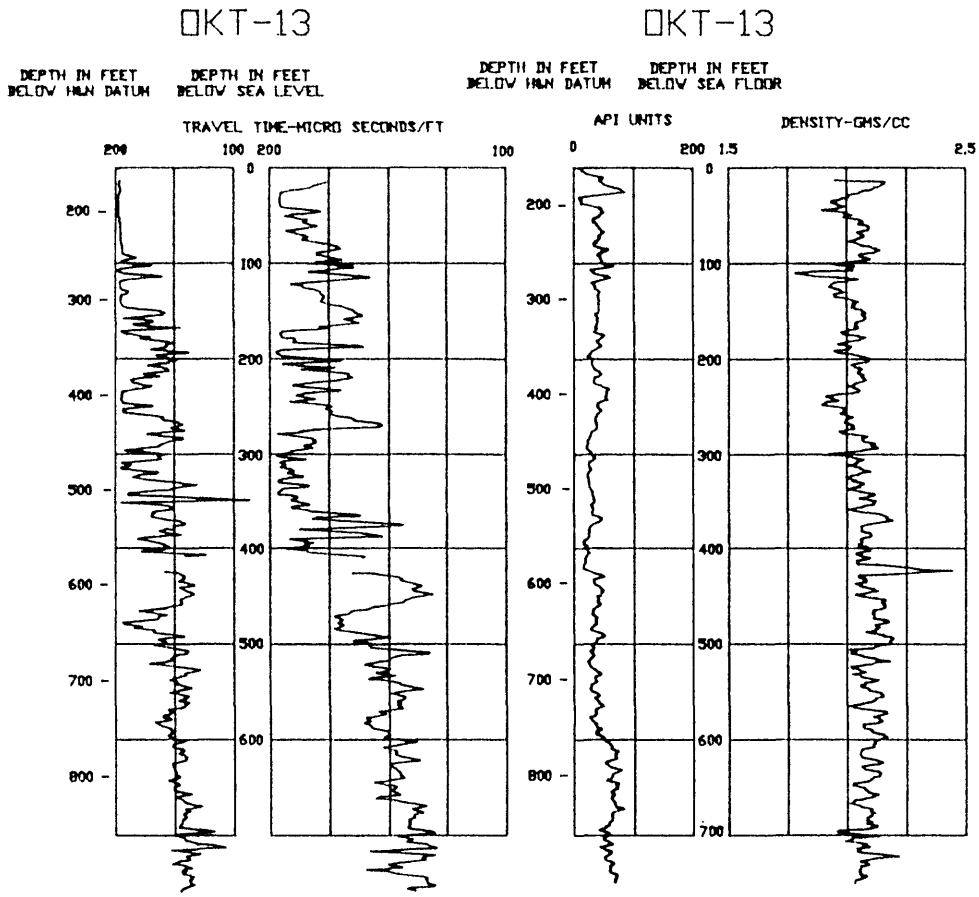

FIGURE 7-12. -- Multichannel sonic and gamma-ray/density logs for borehole OKT-13.

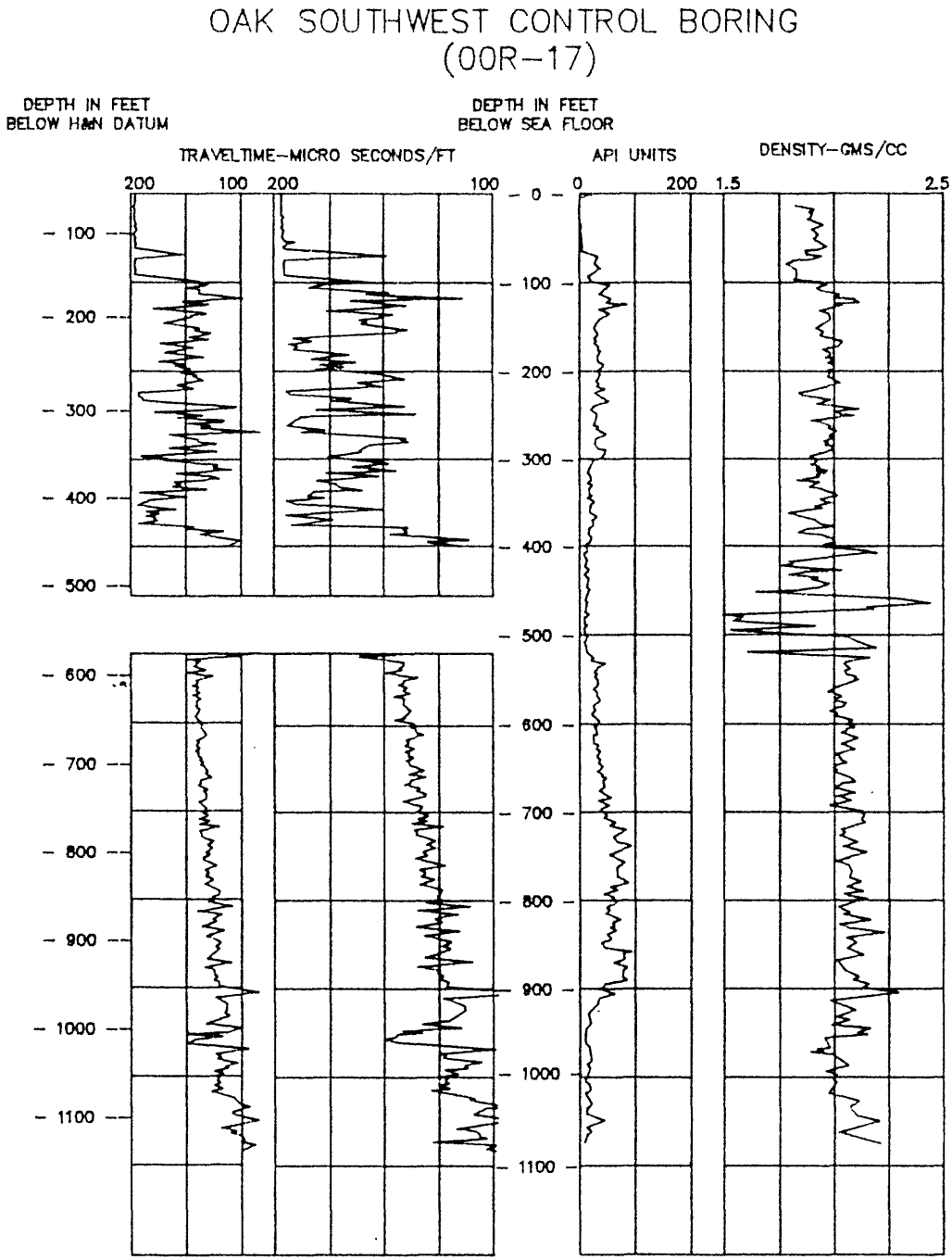

FIGURE 7-13. -- Multichannel sonic and gamma-ray/density logs for borehole OOR-17.

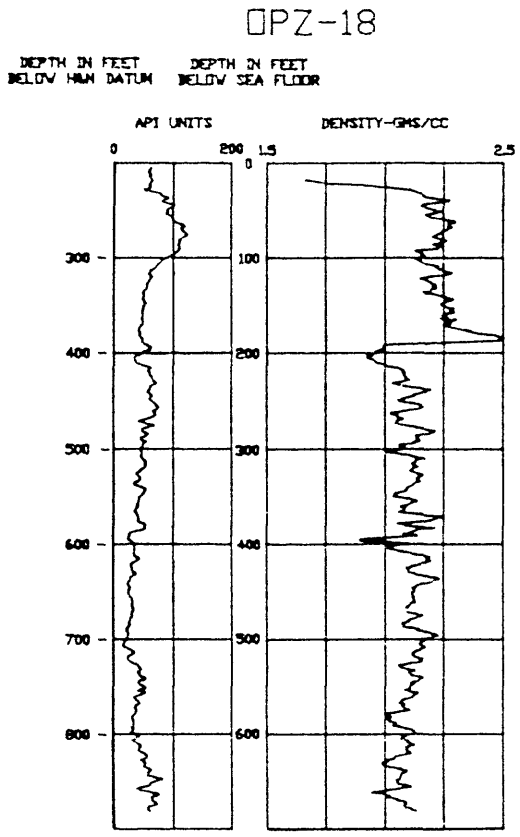

FIGURE 7-14. -- Gamma-ray/density log for borehole OPZ-18.

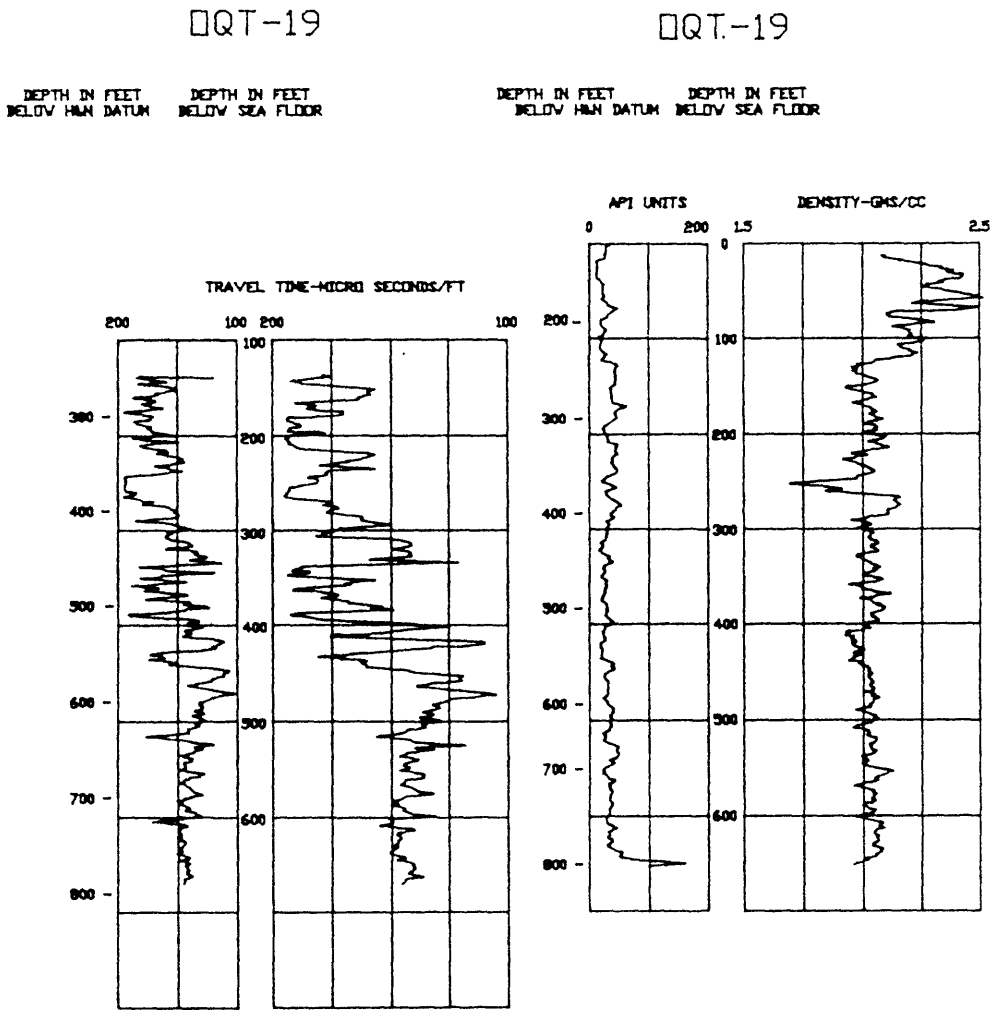

FIGURE 7-15. -- Multichannel sonic and gamma-ray/density logs for borehole OQT-19.

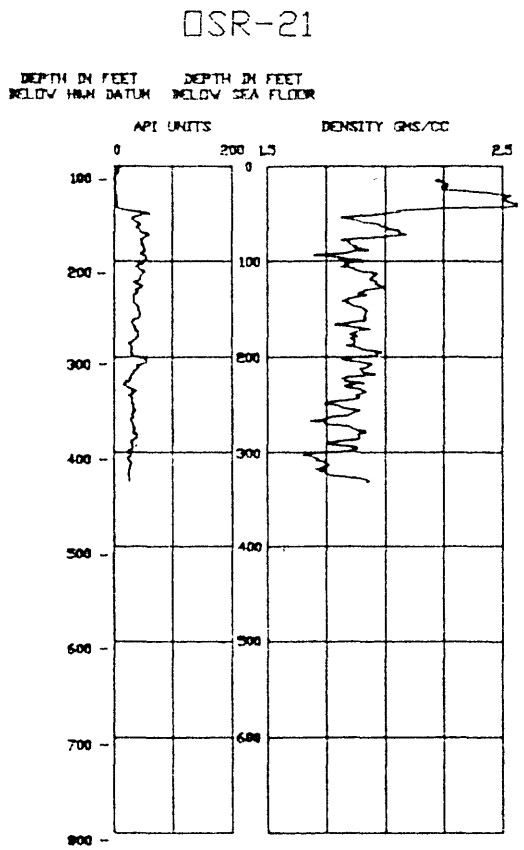

FIGURE 7-16. -- Gamma-ray/density log for borehole OSR-21.

CHAPTER 8:

PRELIMINARY DENSITY AND POROSITY DATA AND FIELD TECHNIQUES OF BOREHOLE GRAVITY SURVEYS, OAK CRATER

by

L. A. Beyer[1], B. L. Ristvet[2] and D. Oberste-Lehn[3]

PURPOSE

Borehole gravity (BHG) surveys were made in selected boreholes at OAK crater on Enewetak Atoll (fig. 8-1) because they provide the only means to directly and accurately measure in situ bulk density and total porosity of large volumes of rock and sediment that surround the boreholes[4]. The differences between the density and porosity of undisturbed atoll materials and the sediment and rock involved in the excavational and apparent craters are crucial to understanding various cratering phenomena. In addition, accurate and representative density and porosity of undisturbed atoll materials provide important geologic and material-properties information and improved initial conditions for nuclear-event calculations.

The apparent densities and porosities presented in this Chapter are interim values that have been corrected for topography but have not yet been corrected for lateral density changes due to cratering phenomena and large-scale natural facies. A three-dimensional model of lateral density variations due to cratering processes and a two-dimensional model of lateral density variations in facies across the atoll margin are being developed to estimate these corrections. The models will be tested and refined by USGS computer programs that calculate BHG values for simulated boreholes. The final adjusted density and porosity values based on the models and calculations will be presented in the subsequent (i.e., Part 4) USGS Open-File Report.

PREVIOUS AND PREPARATORY WORK

Prior to the 1985 borehole gravity surveys at OAK crater (fig. 8-2), no surface, seafloor, shipboard, or borehole gravity measurements had been made on or around the northwest part of Enewetak Atoll. The only other gravity survey that had been done in the area of the atoll was conducted by the USGS in 1984 on Medren (ELMER) Island (fig. 8-1) in one of the old USGS boreholes drilled in 1952 (Daniels and others, 1984; see Appendix 8-1). The feasibility of using sea-floor gravity measurements to interpret crater-induced density distributions was

---

[1]Branch of Sedimentary Processes, U.S. Geological Survey, Menlo Park, CA.
[2]S-Cubed, A Division of Maxwell Laboratories, Albuquerque, NM.
[3]R & D Associates, Marina del Rey, CA.

[4]Bulk density and total porosity are abbreviated as density and porosity in this Chapter.

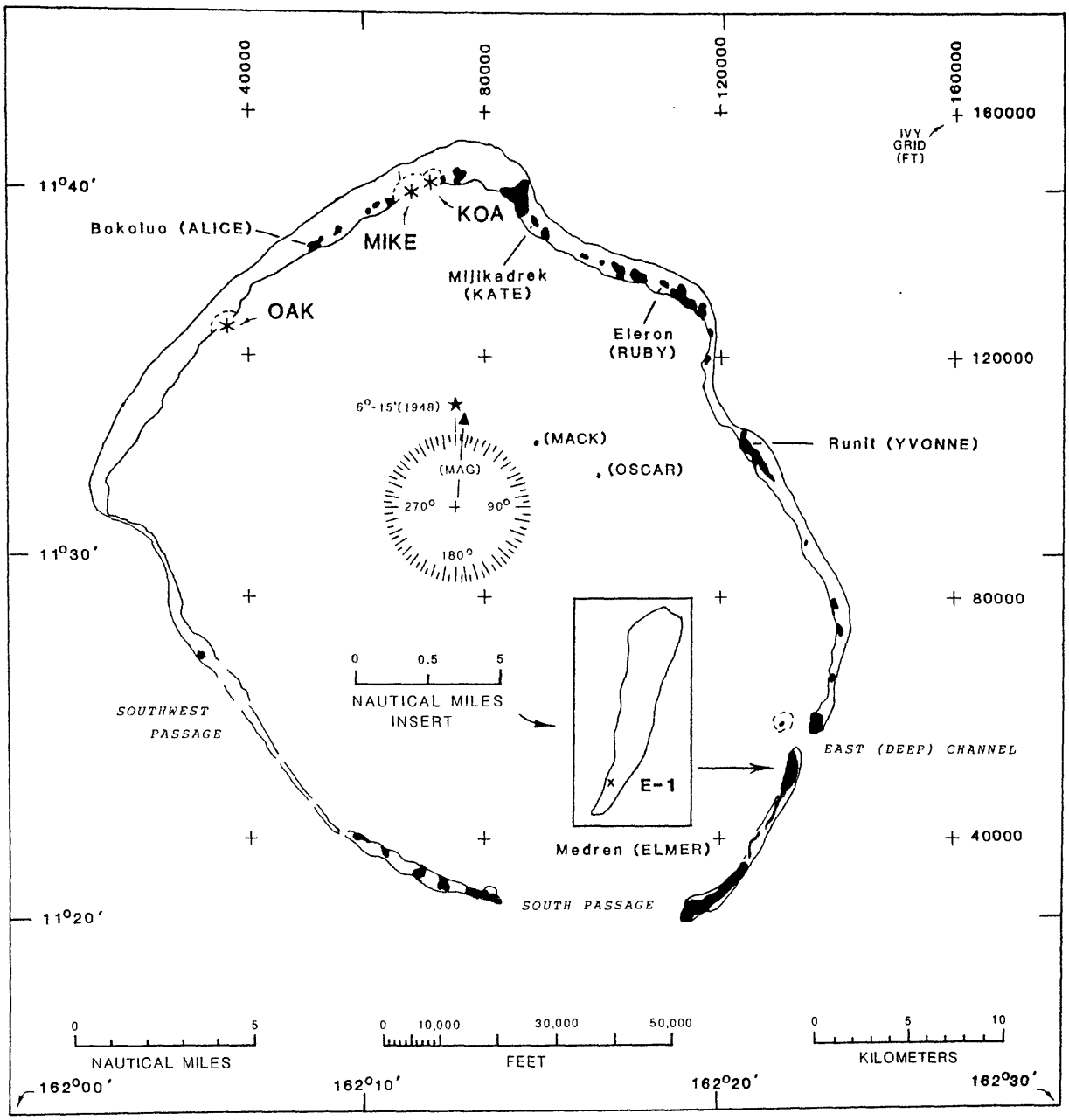

FIGURE 8-1. - Map of Enewetak Atoll, showing location of OAK, KOA, and MIKE craters and Medren (ELMER) Island. Borehole E-1 (shown by "x" on insert map) was site of 1984 USGS borehole gravity survey. Current study was conducted in vicinity of OAK crater.

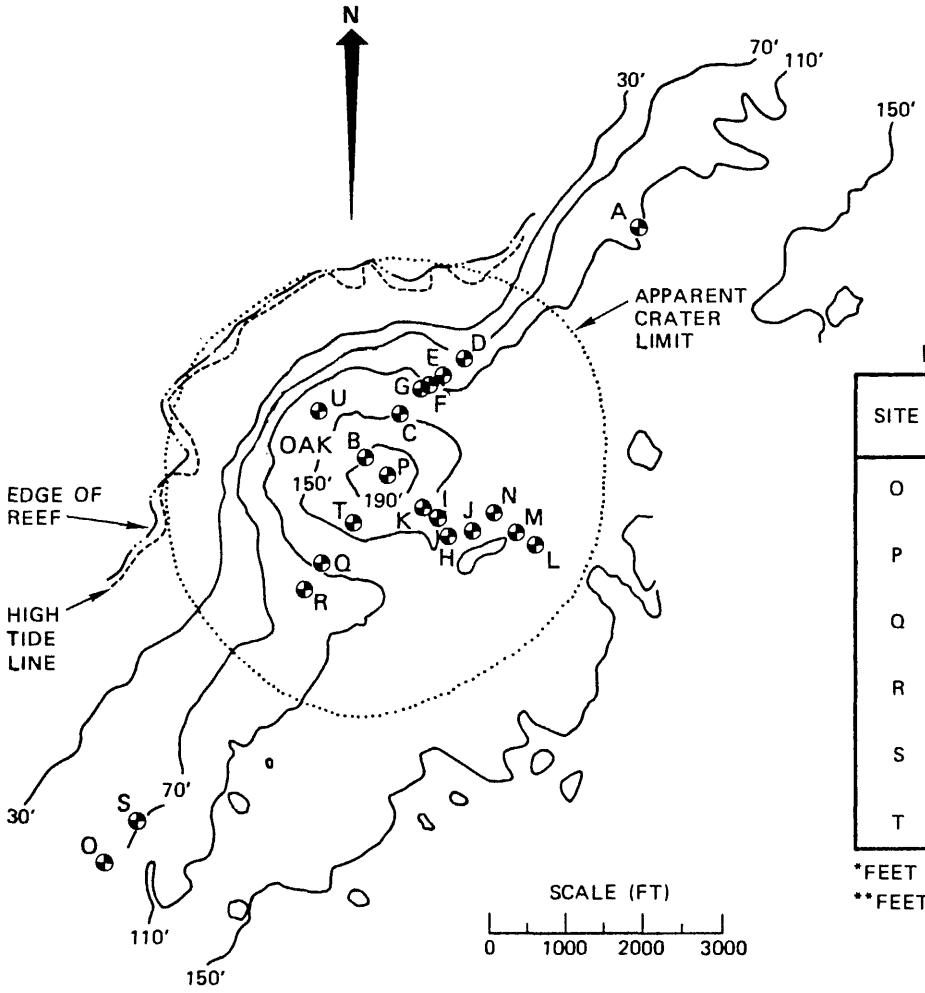

LEGEND – GRAVITY BOREHOLES

SITE	BOREHOLE	WATER* DEPTH	BOREHOLE** DEPTH
O	OOR-17	55.2	1091.1
P	OPZ-18	201.9	748.6
Q	OQT-19	117.5	701.5
R	ORT-20	101.4	491.8
S	OSR-21	84.0	354.3
T	OTG-23	164.0	587.3

*FEET BELOW SEA LEVEL (H AND N DATUM)
**FEET BELOW SEA FLOOR

FIGURE 8-2.- Index map showing location of boreholes of PEACE Program at OAK crater. Inset shows designation, water depth, and total subsea-floor depth of holes dedicated to borehole gravity surveys.

investigated for the EASI geophysical program (Oberste-Lehn, 1979). Areal gravity anomalies calculated from hypothetical density models of OAK and KOA craters, using data from EXPOE and earlier drilling programs, were deemed to be detectable by high-precision sea-floor gravity measurements. However, meaningful interpretation of these gravity anomalies was not possible at the time due to no borehole information at this site, and sea-bottom gravity measurements were not recommended.

In 1983, it was proposed that borehole gravity surveys be included in the drilling phase of the PEACE Program to provide the most accurate and representative measure of in situ density and porosity. The prospect of making borehole gravity surveys at the OAK or KOA craters raised a number of questions, many of which were satisfactorily answered between early 1984 and June 1985 when the surveys commenced:

1. Could borehole gravity surveys reliably determine crater-related density changes? An early 1984 cooperative effort by Beyer and Oberste-Lehn used a two-dimensional density model based on data from KOA and OAK craters to address this question. Gravity calculations in a number of hypothetical boreholes through this model showed that (1) crater-related density changes were detectable by borehole-gravity surveys at distances less than about 3,000 ft from crater center; (2) measured densities probably were accurate to about 3 percent even without corrections for crater-related structure; and (3) interpretations in crater flank locations would benefit most from independent geophysical and borehole data.

2. Could reliable borehole gravity measurements be made in the microseismic environment of an atoll reef? How large was the background of natural density variations of reef-forming materials against which the crater-related density changes would have to be dectected? These questions were partly answered by a borehole-gravity survey conducted by members of the U.S. Geological Survey and Ristvet in the existing E-1 borehole on Medren (ELMER) Island in the southeast part of Enewetak Atoll (fig. 8-1) in April 1984 (see Appendix 8-1). This survey was made from 60 to 1,800 ft below the island surface at station spacings of 10 to 60 ft. Short period vibrations caused by sea wave action had minimal influence on borehole gravity measurements in this well, and measurement repeatabilities were comparable to the excellent results characteristic of surveys in continental areas (J.J. Daniels, personal communication, 1984). Natural density variations of reef-forming rocks surrounding the E-1 drillhole range within a 0.2 g/cm^3 envelope for station spacings of 10 and 30 ft at depths between 60 and 700 ft.

3. Could reliable borehole gravity measurements be made in shallow drillholes from a floating vessel anchored in shallow water? Although considerable preparation and planning was done by the commercial contractor and Beyer to insure that measurements would be possible, this question remained unanswered until the first measurements were made at OAK crater (see section on Field Techniques, this Chapter).

4. If the expensive and time-consuming borehole gravity surveys became part of the PEACE Program, what number, locations, and depths of surveys would effectively satisfy program needs while remaining within budget,

time, and operational constraints? This question gradually was answered with a series of meetings and memoranda that involved E.L. Tremba, J.G. Trulio, and the authors between late 1984 and the June 1985, after which a planning meeting for borehole-gravity field operations was held with the borehole gravity contractor (EDCON, Inc.).

SURVEY SITES AND OBJECTIVES

OAK crater was selected for the borehole gravity surveys because, unlike KOA crater, it is a larger, solitary crater with less post-event deposition of new sediments. Secondly, the shape of OAK crater suggested that suspected subsidence on crater flanks might be large enough to be seen as density changes in properly located boreholes. Lastly, the most favorable weather was predicted for the drilling period at OAK, and borehole gravity mobilization could be accomplished better for the time period at OAK crater.

After all operational and budgetary constraints were determined in May 1985, final recommendations for the borehole-gravity surveys were made. A series of boreholes, dedicated to borehole gravity, was recommended from the bathymetric center of OAK crater (borehole OPZ-18) along a south-southwest trending line nearly parallel to the outer reef margin. Gravitational effects caused by atoll facies changes and topography were reasoned to be the most constant along a line parallel to the outer reef margin thereby simplifying interpretations of the gravity measurements. This set of borehole sites is referred to as the southwest transect by Henry, Wardlaw, and others (1986, p. 78-81), who describe the rationale for borehole location, depth, well logging, and sampling. Map and section views of the drillholes along the southwest transect are shown in Figures 8-2 and 8-3. Recommended and actual locations and depth intervals of borehole-gravity surveys at OAK crater are summarized in Table 8-1.

Changes in the density and porosity of atoll rocks and sediments caused by cratering phenomena can only be seen as departures from the normal ranges of density and porosity of undisturbed reef materials. Consequently, baseline or reference borehole-gravity surveys of undisturbed material outside the zone of cratering effects were recommended and obtained (boreholes OOR-17 and OSR-21). Borehole gravity surveys in at least two different reference boreholes, ideally spaced about 500 to 1,000 ft apart, were needed to provide minimum statistics on the range of values of density and porosity of atoll-forming material and the likely variation of density and porosity over distances equivalent to the OAK crater radius. Recommended distances for the reference boreholes were selected to be outside the region of measurable density changes in reef-forming materials caused by cratering processes yet close to the crater to maximize the likelihood of similar facies relationships with crater borehole sites on the southwestern transect. Actual drilled locations were 1,000 to 1,500 ft farther away from OAK crater than recommended (due to other PEACE Program objectives and ship anchoring needs). This introduces a somewhat larger uncertainty in the comparisons between the density and porosity of undisturbed and disturbed materials along the southwestern transect. Also, the lack of successful gravity measurements above 157 ft below the sea floor in OOR-17 and above 50 ft in OSR-21 prevents comparisons with some of the shallowest intervals in crater-flank boreholes.

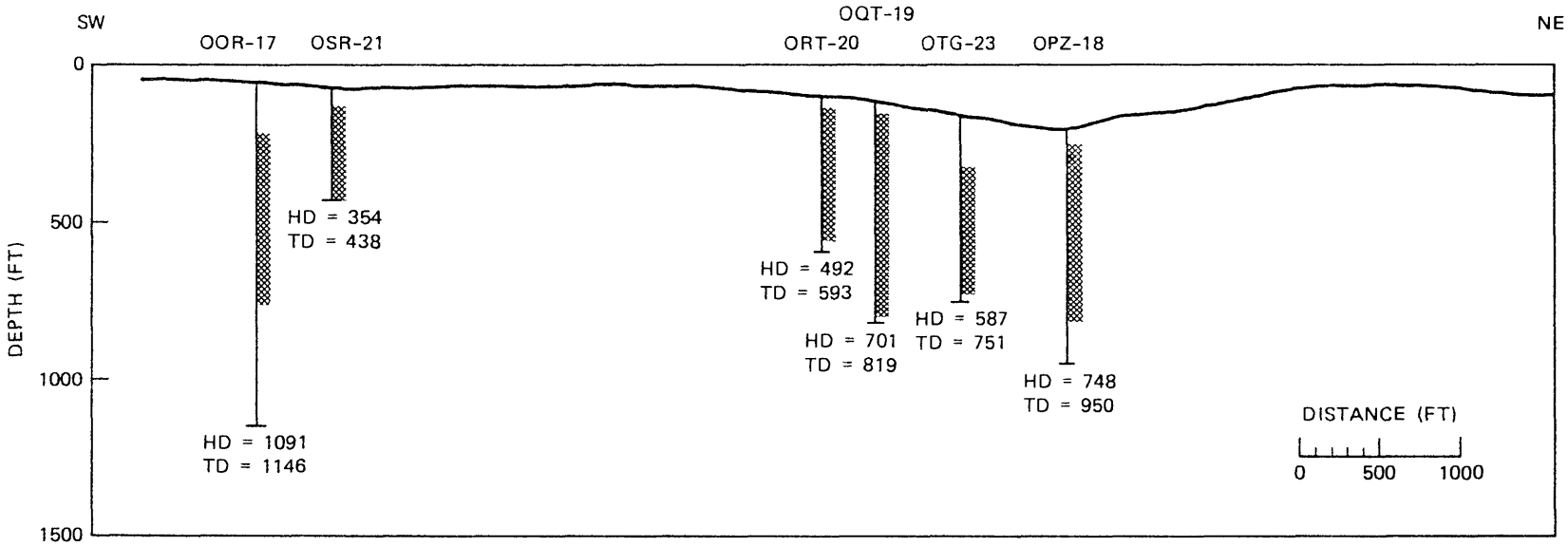

BHG SURVEY SW "RADIAL" 335-FT LAGOONWARD OF GZ PARALLEL TO REEF

HD = DEPTH BELOW SEA FLOOR

TD = DEPTH BELOW SEA LEVEL

FIGURE 8-3 Vertical section showing borehole gravity boreholes along southwest transect. ▒▒▒ indicate portions of boreholes logged with borehole gravity meter.

TABLE 8-1.--Recommended and actual locations and depth intervals of borehole gravity surveys at OAK crater.

Borehole Number	Recommended Priority (Order of Surveys)	Recommended (Actual) Distances from Bathymetric Center of OAK Crater (ft)		Recommended (Actual) Survey Depth (ft below sea floor)	Interval[1]
OOR-17	1 (1)	4,500-5,000	(6,055)[2]	0-700	(157-692)[3]
OPZ-18	1 (2)	0	(0)	0-700	(30-590)
OQT-19	1 (3)	1,600	(1,416)	0-700	(20-680)
ORT-20	2 (4)	2,000	(1,820)	0-350	(20-450)
OSR-21	2 (5)	3,500-4,000	(5,493)[2]	0-350	(50-340)
OTG-23	3 (6)	800	(759)	0-500	(150-570)[4]

[1]Even with optimum conditions, gravity measurements could not be made above 20 to 30 ft below the sea floor.

[2]OSR-21 and OOR-17 were placed at greater than recommended distances from OAK crater because of other PEACE program objectives and ship anchoring needs.

[3]Gravity measurements at shallower depths were not possible because the borehole lock-in device on logging tool could not be operated in mistakenly run 10 3/4-in. surface casing.

[4]Unfavorable weather prevented measurements at shallower depths.

Borehole gravity surveys also were recommended in two boreholes spaced about 400 ft apart, more or less along a crater radial line, short distances outside of the excavational crater. Several mechanisms for subsidence in this crater-flank area have been proposed that might be seen as densification of the atoll materials. The placement of boreholes OQT-19 and ORT-20 in the crater flank and the subsequent borehole-gravity surveys in them fully satisfied these recommendations. Subtle changes in density and porosity caused by event and cratering processes are more likely to be observed against the background of natural variations of density and porosity by two different borehole-gravity surveys in the crater-flank region.

Gravity measurements were recommended in the bathymetric center (or most likely mass symmetric center) of OAK crater to better understand the overall crater-induced density changes in atoll-forming materials. A borehole gravity survey at this location examines densification beneath the excavational crater, the less dense excavational crater fill, and, when compared with reference boreholes, may help to estimate mass removed from the central crater region. Gravity measurements in borehole OPZ-18 at the bathymetric center of OAK crater and in supplemental borehole OTG-23, located 759 ft along the southwest transect from OPZ-18, satisfied survey requirements in this part of the crater.

The zone of greatest departure of density and porosity from undisturbed atoll values presumably is beneath the central region of OAK crater where maximum excavation and stresses in deeper materials occurred. This disturbed volume of sediment and rock constitutes a mass or density anomaly in the atoll whose gravitational effects are judged to be measurable with gravity meters at distances of at least several thousand feet from the crater center. Consequently, borehole gravity measurements on the crater flank are affected slightly by this crater-related, anomalous density distribution. In order to calculate accurate values for the density and porosity of sediments beneath the crater flank where subsidence is suspected, gravity measurements in OQT-19 and ORT-20 need to be corrected for the approximate anomalous gravitational effect of the excavational crater and underlying densified zone--another important reason for surveys in the central crater region.

FIELD TECHNIQUES

The borehole gravity surveys at OAK crater constituted an important technological experiment because downhole gravity measurements had not been previously attempted in shallow boreholes in shallow water from a floating vessel. The success of these surveys required a very quiet inertial environment because the gravity meter, unable to distinguish between gravitational and inertial forces, has a reading resolution of 1×10^{-9} the acceleration due to gravity at the earth's surface. Borehole gravity measurements in the E-1 borehole on Medren Island (fig. 8-1) showed that measurements, comparable in quality to continental measurements, could be obtained in the atoll environment. Nevertheless, the step from land-based to marine borehole gravity measurements was a large one, and successful measurements in boreholes in the OAK crater area required special conditions, some of which were controllable and others of which were unknown in advance or beyond control:

1. A very stablely anchored and relatively vibration-free floating vessel. The drill ship M/V Knut Constructor, a 237-ft long converted freighter with a 4- to 6-point mooring system and bow thruster, proved entirely satisfactory when it was placed in a quiet operation mode and weather was favorable.

2. Adequate uncoupling of the surface casing from the floating vessel. The spacious 13 x 13-ft moonpool, stabilization of the Knut Constructor, and installed cushioning between the surface casing and essentially free-standing riser all contributed to acceptable uncoupling of the ship from the casing except during unfavorable weather conditions.

3. A reliable borehole clamping device that locked the borehole gravity meter against the casing to uncouple it from the logging cable. The borehole clamping device provided by the borehole-gravity contractor (Black and Herring, 1983) worked very well except when it became clogged with sediment in some drillhole intervals.

4. Firm placement of the casings in reef sediments, lagoon currents against the riser that had acceptably small magnitudes and fluctuations, and favorable weather conditions. The combination of these factors prevented gravity measurements in the uppermost 20 to 30 ft below the sea floor in three boreholes and above 50 and 150 ft in two others. Inclement weather temporarily stopped gravity measurements at any depth several times and made measurements more difficult at other times. Operations during the period of most favorable annual weather were crucial to the successful surveys. (Gravity measurements probably could be made up to the sea floor if the riser were removed and the casing terminated just above the sea floor. However, other operational problems arise from such a completion configuration.)

5. An experienced, ingenious, and hardworking field crew, capable of overcoming inevitable, unexpected problems. Borehole-gravity surveys are never routine, and the surveys from the drill ship were uniquely challenging. The highly professional and experienced people who conducted the surveys were crucial to their success (see Acknowledgements).

Borehole gravity surveys are conducted by stopping and reading the gravity meter at predetermined downhole stations to obtain a series of relative gravity values. Downhole stations are generally selected from examination of well logs to bracket rock units in a manner that meets the survey objectives. Because borehole gravity surveys require positioning and repositioning of the gravity meter at downhole locations within a fraction of a foot, a fixed vertical reference onboard the Knut Constructor was devised by the survey team. This fixed vertical reference was immune to the up and down motion of the ship caused by waves and tides and worked effectively for the gravity surveys at OAK crater (fig. 8-4).

The scheme for occupying borehole gravity stations was to initially loop back and forth between the deepest two stations until satisfactory repeatability was obtained. Then, measurements proceeded up the drillhole from the deepest station by repeatedly occupying and reading two stations up, one station down, until the uppermost station had been read several times. This resulted in at least two and frequently three repeated measurements at each station.

The gravity meter used for the OAK crater surveys was LaCoste and Romberg BHG #4. The LaCoste gravity meter is an astatized, long-period horizontal pendulum whose torque is countered by a zero-length tension spring. The original gravity meter design is explained by LaCoste (1934) and the present-day version is especially well described by Krieg (1981). Borehole gravity meters are operated and read remotely by electrical control through conductors in the well logging cable (McCulloh and others, 1967).

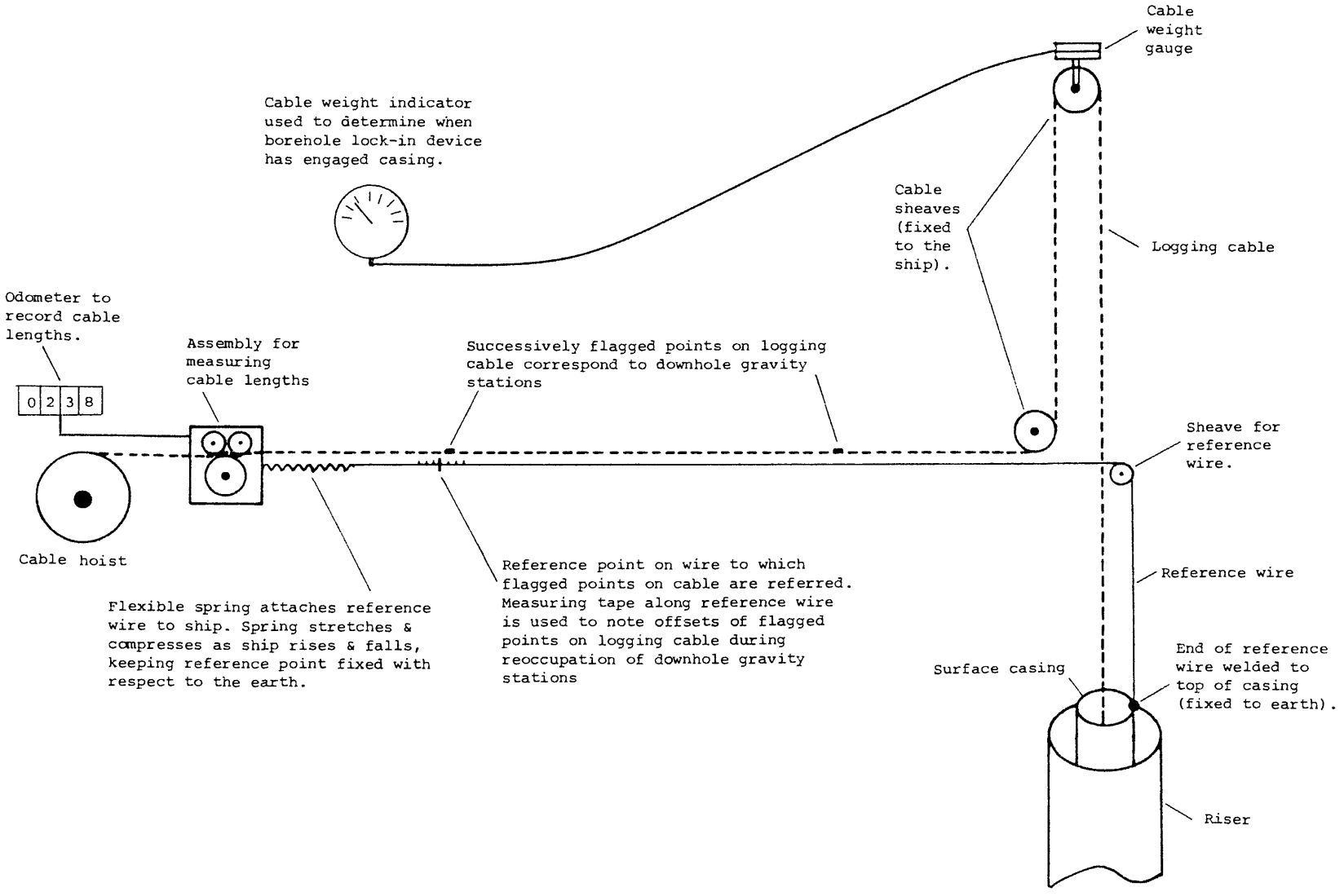

FIGURE 8-4. - Schematic diagram showing method used to establish a fixed vertical reference on the M/V Knut Constructor and make depth measurements for the borehole gravity surveys.

CHARACTERISTICS OF AND FACTORS AFFECTING BOREHOLE GRAVITY MEASUREMENTS

Density and porosity data derived from borehole gravity surveys are particularly important in geologic settings like OAK crater because of the large volume of sediments investigated and the high relative or absolute accuracy that is inherent and unique to the gravity method. The large volume of rock examined by the gravity method makes it immune to formation damage caused by drilling and coring. Conventional geophysical well-logging methods (gamma-gamma, neutron, acoustical) depend on indirect, less precise means to derive density and porosity. Together with core analysis, these other methods also examine many orders of magnitude less volume of formation surrounding the borehole, a distinct disadvantage when working with the soft, unconsolidated and easily disturbed sediments found a OAK crater (Table 8-2). Core analysis and conventional geophysical logs often give low precision, faulty or ambiguous density and porosity data in unconsolidated, soft sediments like those found in OAK boreholes because the limited volume of material they examine generally has been altered during drilling, coring, or core handling and processing.

Borehole gravity surveys provide a set of gravity difference (Δg) and depth difference (Δz) measurements that constitute the interval vertical gradient of gravity ($\Delta g/\Delta z$) between successive stations. Smith (1950) recognized that, from a practical viewpoint, $\Delta g/\Delta z$ is responsive to (1) the vertical density variations of the rocks traversed by the survey, (2) possible lateral rock-density variations (anomalous density distributions) of detectable magnitudes that may occur in the region surrounding the borehole, and (3) possible significant influences of topography. In practice, density (or mass) effects on $\Delta g/\Delta z$, unlike gravity, attentuate as a function of the inverse cube of the distance rather than as the inverse square of the distance. Thus, calculated densities and porosities are less sensitive than gravity itself to remote anamalous density distributions by a factor of the inverse of the distance.

Topographic effects caused by the nearby outer reef slope and the bowl-shaped sea floor of OAK crater are significant but adequately corrected for with available bathymetric data. Topography was taken from the bathymetric map of OAK crater by Folger and others (1986), supplemental data of the 1984 PEACE bathymetric surveys in the vicinity of boreholes OOR-17 and OSR-21 provided by J.C. Hampson (personal communication, 1985), multichannel seismic line 411 of the 1984 PEACE Program survey provided by J.A. Grow (personal communication, 1985), distances from OAK boreholes to the ocean reef edge provided by one of us (Ristvet; see Table 8-3), and various published large-scale bathymetric charts. Corrections for topography out to a distance of 103 statute miles were calculated using modified Hayford-Bowie zones B2 and O and the technique of Beyer and Corbato (1972).

To a first approximation, an overall atoll density of 1.90 g/cm^3 was used. This is a value weighted in favor of reef-forming materials in the upper thousand feet where nearby topography causes large gravitational effects. Corrections to densities calculated from borehole gravity measurements for topography ranged from -.077 to +.156 g/cm^3, depending on the drillhole location and depth. Further modeling of density variations in reef-forming materials can refine or supplant these corrections.

TABLE 8-2.--Radial distances investigated (to encompass 90% of the effects) by gamma-gamma, neutron, and acoustical type logs, and borehole gravity survey with corresponding formation volumes over a 10-ft (3.05 m) vertical interval. Borehole radius is assumed to be 6 in (16.2 cm) and gamma-gamma, neutron, and acoustical logs are assumed to investigate one-half of the circular annulus around the borehole. Conventional 5.25-in. core is included for comparison. Investigative radii of gamma-gamma, neutron, and acoustical logs are chosen very liberally from petroleum industry sources (Beyer, 1986).

Logging Method Distance for 90% Effect in. (cm)	Radial Investigated Investigated ft^3 (m^3)		Formation Volume	
Conventional 5.25 in. (13 cm) core	2.6	(6.6)	1.5	(.04)
Gamma-gamma log	8	(20)	17	(0.5)
Neutron log	14	(36)	40	(1.1)
Sonic log	18	(46)	59	(1.7)
Borehole gravity survey	600	(1,500)	78,532	(2,224)

TABLE 8-3. -- Distances of gravity survey boreholes from ocean edge of outer reef, determined from H&N and USGS bathymetric maps and aerial photographs. The values have an estimated precision of ± 20 ft.

BOREHOLE NUMBER	DISTANCE TO OCEAN-REEF EDGE (ft)
OOR-17	4,995
OPZ-18	4,405
OQT-19	4,410
ORT-20	4,465
OSR-21	4,915
OTG-23	4,380

Significant lateral density changes in atoll-forming material at the OAK site are caused by crater-related phenomena and large-scale changes of facies and diagenesis along lines perpendicular to the reef (e.g., density differences between forereef slope, reef core, backreef, and lagoon facies). The effect of these lateral density changes on $\Delta g/\Delta z$ values is not the subject of this preliminary report. When generalized models of the lateral density variations beneath OAK crater and the large-scale reef facies have been developed, further adjustments to the density and porosity data of this report can be made. The terms apparent BHG density and apparent BHG porosity are used here.

PRELIMINARY DENSITY AND POROSITY DATA

Tables 8-4 through 8-9 (located at the end of the Chapter preceeding Appendix 8-1) list apparent BHG density and apparent BHG porosity by depth interval for each surveyed well. The methods used to calculate the data given in these tables are discussed in Appendix 8-2. Plots of density and porosity versus depth can be prepared from Tables 8-4 through 8-9 but are most meaningful after corrections have been applied for lateral density changes.

SUMMARY

Borehole gravity surveys were conducted at OAK crater to obtain accurate, large-volume estimates of in situ bulk-density and total porosity of reef-forming materials found beneath and outside the crater. Other geophysical well-logging and core analysis methods have inherent limitations that make them less able to accurately measure differences in density and porosity of soft, unconsolidated sediments like those found at OAK crater. Differences between the density and porosity of reef-forming material involved in the excavational and apparent craters and undisturbed atoll sediment and rock are needed to more fully understand cratering processes.

The successful borehole gravity surveys at OAK crater are particularly noteworthy because the highly sensitive gravity meter had not been previously operated in shallow boreholes in an atoll environment or from a ship anchored in shallow water. The excellent survey measurements and accomplishment of practically all objectives were the result of careful planning, a test borehole gravity survey in the E-1 drillhole on Medren Island, proper equipment, a well-configured ship, a particularly skillful survey and support team, and the selection of a favorable weather period during which the seas were mostly calm.

Six boreholes were drilled and successfully logged with a borehole gravity meter along a 6,000 ft southwest transect from the bathymetric center of OAK crater. Gravity measurements were made in these cased boreholes from 20 to 157 ft below the sea floor down to 340 to 692 ft below the sea floor, generally at spacings of 20 to 35 ft.

To obtain reference values of the density and porosity of undisturbed reef-forming material for comparison with material disturbed by cratering processes, gravity surveys were conducted in boreholes OSR-21 and OOR-17, separated by 562 ft and located approximately 5,500 and 6,050 ft south-

southwest of the bathymetric center of OAK crater. In combination these surveys extended from 50 to 692 ft below the sea floor with 210 ft of depth overlap. Apparent BHG density ranges from 1.78 to 2.02 g/cm^3 over the surveyed intervals of these drillholes. Apparent BHG porosity in OOR-17 ranges from 42 to 55 percent.

Possible densification caused by suspected subsidence on the crater flank just outside the excavational crater was investigated by gravity surveys made in boreholes OQT-19 and ORT-20. These holes were separated by 404 ft and located approximately 1,400 and 1,800 ft south-southwest of the bathymetric center of OAK crater. In combination these surveys extended from 20 to 680 ft below the sea floor with 414 ft of depth overlap. Apparent BHG density ranges from 1.72 to 2.02 g/cm^3 over the surveyed intervals of these drillholes. Apparent BHG porosity in OQT-19 ranges from 41 to 62 percent.

Gravity surveys were made in borehole OOR-17 at the bathymetric center of OAK crater and in OTG-23 located 759 ft south-southwest of OOR-17 to measure densification beneath the excavational crater and the density of fill within the excavational crater. The data from these surveys will help to correct gravity measurements made in crater flank drillholes for the anomalous mass of the excavational crater and the densified zone beneath it. In combination these surveys extended from 30 to 590 ft below the sea floor with 420 ft of depth overlap. Apparent BHG density ranges from 1.65 to 2.09 g/cm^3 over the surveyed intervals of these drillholes. Apparent BHG porosity in OPZ-18 ranges from 40 to 65 percent.

The preliminary density data presented in this report have been corrected by amounts ranging from -.077 to .156 g/cm^3 for topography that extends out to a distance of 103 statute miles from OAK crater by using an average atoll density of 1.90 g/cm^3. Errors in apparent BHG density and porosity, estimated from repeated survey measurements, are less than 0.02 g/cm^3 and 1 porosity percent, respectively.

Corrections have not yet been determined for lateral density changes within reef-forming materials that are due to cratering phenomena and large-scale natural facies changes across the atoll margin, or for departure of the overall atoll density from 1.90 g/cm^3. A two-dimensional model of lateral density variations in the geologic facies across the atoll margin and a three-dimensional model of lateral density variations due to cratering processes, both by necessity of a generalized nature, are being developed to estimate these corrections. Consequently, the apparent BHG density and porosity data reported here should not be used to quantify density or porosity changes due to cratering processes until these corrections have been determined.

ACKNOWLEDGEMENTS

The authors wish to thank the many individuals without whose help the borehole gravity phase of the PEACE program would not have been possible. Lt. Col. R.F. Couch, Jr., of the Defense Nuclear Agency authorized the six maximum proposed boreholes for gravity surveys and joined the field operations for the survey of the last gravity borehole. J.G. Trulio of Applied Theory, Inc., addressed critical issues of survey objectives and strongly supported the borehole gravity phase from the time of its initial consideration. D.L.

Orphal of California Research & Technology, Inc., provided input for early crater density models used in feasibility studies and represented cratering calculation interests. E.A. Nixon, formerly of the USGS, helped perform early feasibility calculations from a hypothetical density model of OAK crater. J.J. Daniels, F.G. Clutsom, D. Glover, all of the USGS, and one of us (Ristvet) conducted the borehole gravity survey in the E-1 borehole on Medren Island.

T.A. Weaver of the Los Alamos National Laboratory (LANL) authorized use of their LaCoste and Romberg borehole gravity meter for the field measurements and A.H. Cogbill from LANL participated in the first borehole gravity survey. A.J. Black, T.W. Ashcraft, D.J. Joiner and L. Prado of EDCON, Inc., (the gravity contractor) provided crucial technical expertise for planning the operation phase, the latter two working tirelessly to operate the borehole gravity meter in the OAK boreholes. A. LeBreton of BPB, Inc., flawlessly operated the wireline hoist and helped to make depth measurements during the surveys. Others who assisted onboard the M/V Knut Constructor were R. Clark of the Department of Energy, and G.L. Holloway, G. Mooney and C. Pelletier of the drilling team from McClelland Engineers, Inc., E.L. Tremba of S-Cubed, Inc., coordinated and managed the exchange of information and recommendations between the field team and the steering committee during the surveys. H. Brown headed the Pacific Area Support Office of the Department of Energy in Honolulu through which logistics were managed and communications exchanged. The steering committee that defined objectives, set survey standards, developed field plans and interacted with the field team consisted of J.G. Trulio, E.L. Tremba, and the authors. One of us (Ristvet) directed the scientific work onboard the M/V Knut Constructor during the borehole gravity surveys.

REFERENCES

Beyer, L. A., 1986 (in press), Porosity of unconsolidated sand, diatomite and fractured shale reservoirs, South Belridge and West Cat Canyon oil fields, California; in R. F. Meyer, ed., Exploration for Heavy Oil and Bitumen, American Association of Petroleum Geologists, Studies in Geology, 39 p., 9 figs., 6 tbls.

Beyer, L. A., and Corbato, C. E., 1972, A Fortran IV computer program for calculating borehole gravity terrain corrections: U.S. Geological Survey Open-File Report, 30 p.

Black, A. J., and Herring, A. T., 1983, Borehole gravity: Expanded operating limits and performance: Expanded Abstracts with Bibliographies, 1983 Technical Program, 53rd Annual International Society of Economic Geologists Meeting, September 11-15, 1983, Las Vegas, Nevada, p. 21-23.

Daniels, J.J., Clutsom, F.G., Glover, D., and Ristvet, B.L., 1984, Borehole gravity survey of drillhole E-1, Enewetak Atoll, Marshall Islands: unpublished manuscript.

Folger, D. W., Hampson, J. C., Robb, J. M., Woellner, R. A., Foster, D. S., and Tavares, L. A., 1986, Bathymetry of OAK and KOA craters: U.S. Geological Survey Bulletin 1678-A, 35 p., 21 figs.

Henry, T. W., Wardlaw, B. R., Skipp, B. A., Major, R. P., and Tracey, J. I., 1986, Pacific Enewetak Atoll Crater Exploration (PEACE) Program, Enewetak Atoll, Republic of the Marshall Islands, Part 1: Drilling operations and descriptions of boreholes in vicinity of KOA and OAK craters: U.S. Geological Survey Open-File Report 86-419, 497 p., 32 figs., 29 pls., 13 tbls., 3 appendices.

Krieg, L. A., 1981, Mathematical modelling of the behavior of the LaCoste and Romberg "G" gravity meter for use in gravity network adjustments and data analyses: Reports of the Department of Geodetic Science and Surveying, Report No. 321, Ohio State University, Columbus, Ohio, 172 p.

LaCoste, L. J. B., 1934, A new type long period vertical seismograph: Physics, v. 5, no. 7, p. 178-180.

McCulloh, T. H., LaCoste, L. J. B., Schooellhamer, J. E., and Pampeyan, E. H., 1967, The U.S. Geological Survey - LaCoste and Romberg precise borehole gravimeter system--Instrumentation and support equipment; in Geological Survey Research 1967: U.S. Geological Survey Professional Paper 575-D, p. D92-D100.

Oberste-Lehn, D., 1979, Preliminary summary report on prospective gravity survey of nuclear craters at Eniwetok Atoll, RDA-TR-113204-002, R & D Associates, Marina del Rey, California, 17 p.

TABLE 8-4. -- Apparent BHG density and porosity expressed as means with estimated errors for depth intervals surveyed in borehole OOR-17. Estimated grain densities used to calculate porosities were determined from X-ray mineralogy and organic analyses (Chapters 4 and 5, this report). Depths are expressed to nearest foot. See the Appendix 8-2 for an explanation of the calculations used to obtain values.

Depth Interval		Apparent BHG Density			Apparent BHG Porosity		Mean Grain Density
(ft below sea level)	(ft below sea floor)	ρ_a (g/cm^3)	ρ_a error (g/cm^3)	Number of $\Delta g/\Delta z$ values	ϕ_a (%)	ϕ_a error (Porosity %)	ρ_g (g/cm^3)
212-237	157-182	1.928	.003	3	50.2	0.2	2.87
237-271	182-216	1.924	.008	3	49.3	0.4	2.83
271-289	216-234	1.863	.015	3	51.6	0.9	2.79
289-317	234-262	2.017	.006	2	41.5	0.3	2.75
317-345	262-290	1.882	.003	2	52.4	0.2	2.86
345-363	290-308	1.852	.013	3	54.0	0.7	2.86
363-388	308-333	1.931	.015	2	46.8	0.9	2.76[1]
388-417	333-362	1.924	.009	3	47.2	0.5	2.76[1]
417-446	362-391	1.947	.022	3	45.8	1.3	2.76[1]
446-477	391-422	1.956	.003	3	43.7	0.2	2.71
477-505	422-450	1.967	.001	2	43.0	0.1	2.71
505-528	450-473	2.007	.010	3	41.0	0.6	2.72
528-560	473-505	1.954	.008	3	44.5	0.5	2.73
560-603	505-548	1.955	.016	3	45.9	0.9	2.78
603-645	548-590	1.972	.004	2	44.8	0.2	2.84
645-683	590-628	2.015	.009	3	44.7	0.5	2.85
683-713	628-658	1.997	.004	2	46.0	0.2	2.86
713-747	658-692	1.992	.007	3	46.3	0.4	2.86

[1] Uncertainty in value assumed to be ±.04 g/cm^3

TABLE 8-5. -- Apparent BHG density and porosity expressed as means with estimated errors for depth intervals surveyed in borehole OPZ-18. Estimated grain densities used to calculate porosities were determined from X-ray mineralogy and organic analyses (Chapters 4 and 5, this report). Depths are expressed to nearest foot. See the Appendix 8-2 for an explanation of the calculations used to obtain values.

Depth Interval		Apparent BHG Density			Apparent BHG Porosity		Mean Grain Density
(ft below sea level)	(ft below sea floor)	ρ_a (g/cm^3)	ρ_a error (g/cm^3)	Number of $\Delta g/\Delta z$ values	ϕ_a (%)	ϕ_a error (Porosity %)	ρ_g (g/cm^3)
232-262	30-60	1.796	.009	3	56.1	0.5	2.81
262-292	60-90	1.792	.001	3	56.8	0.1	2.83
292-322	90-120	1.921	.001	2	49.9	0.1	2.84
322-352	120-150	1.941	.008	3	48.6	0.4	2.83
352-382	150-180	1.976	.010	2	46.0	0.6	2.82
382-457	180-255	1.961	-	1	46.6	-	2.81
457-492	255-290	2.092	.008	3	38.3	0.5	2.80
492-522	290-320	1.979	.010	2	44.8	0.6	2.81
522-552	320-350	2.058	.010	2	41.4	0.6	2.84
552-582	350-380	2.149	.007	2	36.0	0.4	2.84
582-610	380-408	2.096	.009	2	34.9	0.5	2.74
610-637	408-435	2.064	.009	3	36.1	0.5	2.72
637-672	435-470	2.077	.003	3	35.2	0.2	2.72
672-707	470-505	2.061	.005	2	36.1	0.3	2.72
707-742	505-540	2.066	.007	3	35.6	0.4	2.72
742-772	540-570	2.003	.011	3	44.2	0.6	2.86
772-807	570-605	2.007	.002	3	44.0	0.1	2.86
807-837	605-634	1.906	.017	3	49.8	0.9	2.87
837-867	634-665	1.986	.006	3	44.8	0.3	2.85

TABLE 8-6. -- Apparent BHG density and porosity expressed as means with estimated errors for depth intervals surveyed in borehole OQT-19. Estimated grain densities used to calculate porosities were determined from X-ray mineralogy and organic analyses (Chapters 4 and 5, this report). Depths are expressed to nearest foot. See the Appendix 8-2 for an explanation of the calculations used to obtain values.

Depth Interval		Apparent BHG Density			Apparent BHG Porosity		Mean Grain Density
(ft below sea level)	(ft below sea floor)	ρ_a (g/cm^3)	ρ_a error (g/cm^3)	Number of $\Delta g/\Delta z$ values	ϕ_a (%)	ϕ_a error (Porosity %)	ρ_g (g/cm^3)
138-148	20-30	1.791	.034	3	56.9	2.1	2.84
148-178	30-60	1.917	.010	3	50.2	0.5	2.85
178-208	60-90	1.921	.020	3	49.3	1.1	2.83
208-238	90-120	1.869	.017	5	52.2	0.9	2.83
238-273	120-155	1.884	.006	3	51.7	0.3	2.84
273-298	155-180	1.878	.008	3	51.7	0.4	2.83
298-328	180-210	1.922	.009	3	48.3	0.5	2.81
328-358	210-240	1.945	.011	3	47.0	0.6	2.81
358-380	240-262	1.896	.008	3	49.8	0.4	2.81
380-403	262-285	1.978	.009	3	45.3	0.5	2.82
403-433	285-315	1.981	.014	3	45.4	0.8	2.83
433-468	315-350	2.017	.007	3	40.9	0.4	2.75
468-498	350-380	2.030	.012	3	38.9	0.7	2.71
498-528	380-410	1.975	.007	3	42.4	0.4	2.71
528-558	410-440	1.925	.017	3	45.4	1.0	2.71
558-588	440-470	1.927	.008	3	46.2	0.5	2.74
588-618	470-500	2.016	.002	3	43.9	0.1	2.83
618-648	500-530	2.008	.015	3	44.7	0.8	2.84
648-678	530-560	1.992	.005	3	46.2	0.3	2.86
678-708	560-590	1.996	.009	3	45.9	0.5	2.86
708-738	590-620	1.989	.005	3	46.6	0.3	2.87
738-768	620-650	2.019	.022	3	44.6	1.2	2.86
768-798	650-680	1.934	.008	3	48.7	0.4	2.84

TABLE 8-7. -- Apparent BHG density and porosity expressed as means with estimated errors for depth intervals surveyed in borehole ORT-20. Estimated grain densities used to calculate porosities were determined from X-ray mineralogy and organic analyses (Chapters 4 and 5, this report). Depths are expressed to nearest foot. See the Appendix 8-2 for an explanation of the calculations used to obtain values.

Depth Interval		Apparent BHG Density			Apparent BHG Porosity		Mean Grain Density[1]
(ft below sea level)	(ft below sea floor)	ρ_a (g/cm^3)	ρ_a error (g/cm^3)	Number of $\Delta g/\Delta z$ values	ϕ_a (%)	ϕ_a error (Porosity %)	ρ_g (g/cm^3)
136-160	35-59	1.823	.013	3	55.1	0.7	2.84
160-186	59-85	1.990	.012	3	46.4	0.7	2.86
186-211	85-110	1.807	.007	3	55.9	0.4	2.84
211-226	110-125	1.953	-	1	48.4	-	2.86
226-256	125-155	1.908	-	1	50.6	-	2.85
256-271	155-170	1.790	-	1	56.4	-	2.82
271-301	170-200	1.925	.004	3	48.8	0.2	2.82
301-331	200-230	1.905	.002	3	48.8	0.1	2.78
331-361	230-260	1.931	.007	3	50.1	0.4	2.88
361-391	260-290	1.972	.010	3	46.4	0.6	2.83
391-421	290-320	1.986	.014	3	43.1	0.8	2.75
421-451	320-350	1.997	.012	3	40.8	0.7	2.70
451-471	350-370	2.031	.008	3	38.7	0.5	2.70
471-491	370-390	1.992	.017	3	41.1	1.0	2.70
491-521	390-420	1.932	.009	3	44.3	0.5	2.69
521-551	420-450	1.910	.010	4	45.9	0.6	2.70

[1] In absence of measurements of organic content of core samples from ORT-20, grain density values calculated from X-ray mineralogy have been decreased by .03 g/cm^3 to account for organic matter.

TABLE 8-8. -- Apparent BHG density and porosity expressed as means with estimated errors for depth intervals surveyed in borehole OSR-21. Estimated grain densities used to calculate porosities were determined from X-ray mineralogy and organic analyses (Chapters 4 and 5, this report). Depths are expressed to nearest foot. See the Appendix 8-2 for an explanation of the calculations used to obtain values.

Depth Interval		Apparent BHG Density			Apparent BHG Porosity		Mean Grain Density
(ft below sea level)	(ft below sea floor)	ρ_a (g/cm^3)	ρ_a error (g/cm^3)	Number of $\Delta g/\Delta z$ values	ϕ_a (%)	ϕ_a error (Porosity %)	ρ_g (g/cm^3)
134-159	50-75	1.971	.004	3	46.4	0.2	2.82
159-184	75-100	1.902	.018	3	49.7	1.0	2.80
184-209	100-125	1.826	.014	3	54.2	0.8	2.81
209-234	125-150	1.818	.009	3	54.9	0.5	2.82
234-264	150-180	1.894	.007	3	50.1	0.4	2.80
264-294	180-210	1.926	.009	3	48.3	0.5	2.80
294-324	210-240	1.869	.008	3	52.1	0.4	2.82
324-354	240-270	1.871	.009	3	52.0	0.5	2.82
354-384	270-300	1.870	.007	3	51.7	0.4	2.81
384-404	300-320	1.902	.016	6	49.3	0.9	2.79
404-424	320-340	1.966	.020	4	45.1	1.1	2.77

TABLE 8-9. -- Apparent BHG density and porosity expressed as means with estimated errors for depth intervals surveyed in borehole OTG-23. Estimated grain densities used to calculate porosities were determined from X-ray mineralogy and organic analyses (Chapters 4 and 5, this report). Depths are expressed to nearest foot. See the Appendix 8-2 for an explanation of the calculations used to obtain values.

Depth Interval		Apparent BHG Density			Apparent BHG Porosity		Mean Grain Density
(ft below sea level)	(ft below sea floor)	ρ_a (g/cm^3)	ρ_a error (g/cm^3)	Number of $\Delta g/\Delta z$ values	ϕ_a (%)	ϕ_a error (Porosity %)	ρ_g (g/cm^3)
314-344	150-180	1.977	.003	3	45.9	0.2	2.85[2]
344-374	180-210	1.997	.007	3	44.8	0.4	2.85[2]
374-404	210-240	1.971	.010	3	46.3	0.5	2.85[2]
404-434	240-270	1.960	.013	3	46.9	0.7	2.85[2]
434-464	270-300	1.977	.010	3	46.0	0.5	2.87
464-494	300-330	2.009	.012	3	44.0	0.7	2.84
494-539	330-375	1.971	.006	2	43.0	0.4	2.74
539-584	375-420	2.075	.005	2	35.6	0.3	2.72
584-629	420-465	1.986	.008	3	41.9	0.5	2.73
629-674	465-510	2.035	.018	2	41.3	1.0	2.81
674-734	510-570	2.113	.015	2	39.2	0.8	2.88

[1] In absence of measurements of organic content of core samples from OTG-23, grain density values calculated from X-ray mineralogy have been decreased by .03 g/cm^3 to account for organic matter.

[2] Uncertainty in value assumed to be $\pm.04$ g/cm^3.

APPENDIX 8-1

PRELIMINARY DENSITY DATA FROM BOREHOLE GRAVITY SURVEY IN BOREHOLE E-1, MEDREN (ELMER) ISLAND, ENEWETAK ATOLL

The gravity survey in borehole E-1 on Medren (ELMER) Island (see fig. 8-1) was conducted during the Marine Phase of the PEACE Program in April 1984 by the U.S. Geological Survey, using LaCoste and Romberg BHG #1 first to determine if reliable borehole gravity measurements could be made in the microseismic environment of an atoll island and second to evaluate the range of natural density variations of reef-forming materials. Although the senior author has not seen the raw data from this survey, J.J. Daniels (personal communication, 1984) stated that the effect of the near-surface vibrations caused by wave action was minimal and that the repeatability of measurements generally was excellent. The preliminary density data given in Table 8-10 was prepared by J.J. Daniels and includes corrections made by the senior author for topography out to a distance of 103 statute miles using an overall atoll density of 1.90 g/cm^3.

TABLE 8-10. -- Apparent BHG density for depth intervals surveyed in borehole E-1, Medren Island, Enewetak Atoll (J. J. Daniels, personal communication, 1984) (see fig. 8-1 for location). Top of surface casing is 14.4 feet above mean low water.

Depth Interval (ft below top of surface casing)	Apparent BHG Density (g/cm^3)	Depth Interval (ft below top of surface casing	Apparent BHG Density (g/cm^3)
60-120	1.934	960-1020	1.950
120-180	1.997	1020-1050	1.910
180-240	1.956	1050-1080	1.849
240-300	1.953	1080-1110	1.927
300-330	1.999	1110-1120	1.985
330-360	2.080	1120-1130	1.894
360-390	2.020	1130-1140	2.027
390-420	2.032	1140-1150	2.203
420-450	2.009	1150-1160	2.269
450-480	2.006	1160-1170	2.339
480-510	1.994	1170-1180	1.858
510-540	1.990	1180-1190	2.100
540-570	2.001	1190-1200	2.033
570-600	1.949	1200-1210	2.170
600-610	1.992	1210-1220	2.271
610-620	1.945	1220-1230	2.149
620-630	1.906	1230-1260	2.243
630-640	1.930	1260-1290	2.084
640-650	2.094	1290-1320	1.987
650-660	1.972	1320-1350	1.987
660-670	2.026	1350-1380	2.037
670-680	2.089	1380-1410	2.291
680-690	1.932	1410-1440	1.609
690-700	2.046	1440-1470	1.975
700-710	2.042	1470-1500	1.942
710-720	1.943	1500-1530	1.966
720-750	1.978	1530-1560	1.987
750-780	1.972	1560-1590	2.040
780-810	1.957	1590-1620	1.994
810-840	1.932	1620-1650	2.019
840-870	2.035	1650-1680	1.925
870-900	1.981	1680-1710	1.883
900-930	1.984	1710-1740	1.930
930-960	1.951	1740-1770	1.865
		1770-1800	1.981

APPENDIX 8-2

CALCULATION OF APPARENT BHG DENSITY AND POROSITY WITH ERROR ESTIMATES

Borehole gravity data are easily converted to vertical density profiles, after any significant topographic effects have been removed, with

$$\rho = 1/4\pi k \, (F - \Delta g/\Delta z) \qquad (1)$$

where ρ = in situ bulk density or BHG density

k = universal Newtonian gravitational constant

F = normal free-air vertical gradient of gravity

and $\Delta g/\Delta z$ = measured interval vertical gradient of gravity

If Δg is understood to still include effects due to lateral density variations and numerical values of constants are substituted, equation 1 becomes

$$\rho_a = 3.682 - 39.127 \, (\Delta g/\Delta z) \qquad (2)$$

where ρ_a = apparent BHG density (g/cm^3)

and $\Delta g/\Delta z$ = measured interval vertical gradient of gravity uncorrected for possibly significant lateral density changes (mgal/ft or 10^{-3} $cm/sec^2/ft$)

Measurement of relative gravity in boreholes is a function of vertical position of the gravity meter as well as rock density. Because exact vertical repositioning of the gravity meter for repeat measurements was difficult during the OAK surveys, the best measure of survey precision is the scatter of repeated values of $\Delta g/\Delta z$. Bad gravity values, particularly small instrument tares, were found by plotting repeated relative gravity readings as a function of time and of the slightly different vertical position of the gravity meter as evidenced from depth measurements made on the ship. This process was used to reject 22 of the 306 (or 7%) of the $\Delta g/\Delta z$ values obtained in the six drillholes.

Apparent BHG density, ρ_a, was calculated from the arithmetic mean of repeated $\Delta g/\Delta z$ values with Equation 1. Error in apparent BHG density, $\rho_{a\ error}$, was taken as the standard deviation of repeated $\Delta g/\Delta z$ values, expressed in g/cm^3 with

$$\rho_{a\ error} = 1/4\pi k\ (\sigma)$$

where σ = standard deviation of repeated $\Delta g/\Delta z$ values

Porosity is calculated from BHG density by use of the familiar equation for porosity:

$$\phi_a = 100\ (\rho_g - \rho_a)/(\rho_g - \rho_f) \qquad (3)$$

where ϕ_a = apparent BHG porosity (%)

ρ_g = mean grain density of solid constituents of the rocks contained in the interval (g/cm^3)

ρ_f = mean density of pore fluids contained in the interval (g/cm^3)

and ρ_a = apparent BHG density (g/cm^3)

Errors in BHG porosity require an understanding of the effects of error in the three variables on the right side of Equation 3. An error equation is

$$\phi_{a\ error} = \frac{100}{(\rho_g - \rho_f)} \left((1 - \phi) \left| \rho_{g\ error} \right| + \phi \left| \rho_{f\ error} \right| + \left| \rho_{a\ error} \right| \right) \qquad (4)$$

where $\rho_{g\ error}$, $\rho_{f\ error}$, and $\rho_{a\ error}$ represent the errors or uncertainties in the values of grain density, pore-fluid density and apparent BHG density, respectively, expressed in g/cm^3. ϕ is expressed fractionally and $\phi_{a\ error}$ is the resultant error in apparent BHG porosity given in porosity percent.

The magnitude of each error on the right side of Equation 3 depends on the inverse of $(\rho_g - \rho_f)$ which, at the OAK crater area, has a maximum value

of 0.60 $(g/cm^3)^{-1}$, based on ρ_f = 1.03 g/cm^3 and $\rho_g \leq$ 2.93 g/cm^3. Thus, assuming $\rho_{f\ error}$ is negligibly small because the density of sea water is well known, Equation 4 can be rewritten for the OAK surveys as

$$\phi_{a\ error} = 60((1 - \phi_a)\rho_{g\ error} + \rho_{a\ error})$$

Apparent BHG density (ρ_a), apparent BHG density error ($\rho_{a\ error}$), apparent BHG porosity (ϕ_a), apparent BHG porosity error ($\phi_{a\ error}$), and mean grain density (ρ_g) appear in Tables 8-4 to 8-9. At this time, mean grain density error ($\rho_{g\ error}$) is assumed to be .02 g/cm^3 for all intervals except when noted.

CHAPTER 9:

SEISMIC REFERENCE SURVEYS

by

E.L. Tremba and B.L. Ristvet

S-Cubed, A Division of Maxwell Laboratories[1]

INTRODUCTION

Seismic reference surveys (SRS), also called checkshot and downhole velocity surveys, were conducted in nine PEACE-Program boreholes to determine interval seismic (compressional wave) velocities. The results were applied to two primary objectives: (1) an independent source of velocity data to convert multichannel seismic reflection results from time to depth and (2) interval-velocity data relatively unimpaired by borehole rugosity effects to assess the wave speeds of various units of material. The former objective is discussed by Grow, Lee, and others (1986, USGS Bulletin 1678). The latter objective is discussed primarily in the current Chapter and secondarily in Chapter 7.

METHODS

SRS were conducted in nine PEACE-Program boreholes (KAR-1, KBZ-4, KCT-5, KDT-6, KFT-8, OAR-2/2A, OBZ-4, OCT-5, and OOR-17) by personnel of BPB Instruments, Inc. The technique used and preliminary results for those surveys are presented in Grow, Lee, and others (1986). The data generally were acquired at approximately 30-ft depth intervals, although some of the shallow boreholes were surveyed at 15-ft intervals. Grow presented SRS-derived velocity profiles with approximately 150-ft intervals for several boreholes. The 150-ft interval was thought to be sufficiently large to yield interval velocity values having reasonable errors of measurement.

In order to quantify the precision of the SRS technique, the difference in SRS arrival-time values determined by BPB for stations in borehole OOR-17 with multiple readings were computed (table 9-1). The average difference in 29 SRS arrival-time values is approximately 1 msec. Thus, the precision of each SRS arrival time is estimated to be 1 msec. Because each SRS interval velocity calculation requires two time-of-arrival values, the time for the velocity calculation has an estimated precision of 2 msec. Thus, the smaller the travel-time interval, the larger the estimated precision error of the calculated interval velocity.

---

[1] Albuquerque, NM.

TABLE 9-1. -- List of arrival-time values for 29 SRS stations in borehole OOR-17 that had multiple readings.

MEASURED ARRIVAL TIMES (msec)		DIFFERENCE ARRIVAL TIMES (msec)
33.0	32.0	1.0
36.0	34.0	2.0
40.0	39.0	1.0
40.0	42.0	2.0
43.0	42.0	1.0
52.0	51.0	1.0
58.0	59.0	1.0
63.0	63.0	0.0
66.0	65.0	1.0
74.0	75.0	1.0
77.5	77.5	0.0
80.0	81.0	1.0
96.3	96.3	0.0
103.0	103.7	0.7
106.2	105.0	1.2
110.0	110.0	0.0
115.0	115.0	0.0
120.0	121.3	1.3
122.5	122.5	0.0
128.0	130.0	2.0
137.5	136.3	0.8
140.0	140.0	0.0
142.5	143.7	1.2
147.5	150.0	2.5
150.0	151.3	1.3
157.5	157.5	0.0
160.0	161.0	1.0
167.0	165.0	2.0
170.0	168.0	2.0
		average = 0.97 msec

RESULTS

The average velocities of crater zones and sedimentary (geologic) packages were calculated from SRS measurements and integrated sonic logs (Chapter 7) for the nine PEACE-Program boreholes listed on Table 9-2 . Tables 9-3 through 9-11 (located at the end of this Chapter) present the calculated values of the crater-zones/sedimentary-packages (see Chapters 14 and 2, respectively, for discussion of these) for each borehole. In Tables 9-3 through 9-11, under column DEPTH INTERVAL, the abbreviation DISC. followed by a number refers to a disconformity number given in Chapter 2; under column ZONES/SEDIMENTARY PACKAGES, the numbers standing alone or preceeded by "PART" refer to sediment package numbers (or part of a sediment package) given in the same Chapter, "α" refers to crater zone alpha, "β_1" (etc.) to beta, etc. Sedimentary Packages 1 and 2 were combined because Package 1 is relatively thin. Packages 4, 5, and 6 were combined because they are geologically similar.

To compare the results of the SRS velocity measurements with those determined by integrated sonic logs, 21 pairs of values were plotted in Figure 9-1 . Sixteen points lie above the 1:1 correlation line, and five points lie below it. Although the relatively large precision error for the SRS technique limits definitive statements, the data suggest that some of the interval velocity values determined from the integrated sonic logs are spuriously low. In particular, all five Package 3 points lie above the 1:1 correlation line. Generally, Package 3 was the most difficult zone to drill and sample due to its variable degree of in situ cementation. This resulted in borehole walls with a high degree of rugosity as shown on the caliper logs (Chapter 7). The sonic tool measures velocities within one or two feet of the borehole wall (see Table 8-2), whereas most of the material measured using the SRS technique is considerably farther away from the borehole wall. Thus, sonic-log velocity measurements are likely to be more sensitive to borehole size and/or rugosity problems than are SRS measurements. Based on these considerations and on the comparison of the two sets of velocity measurements, it is likely that the velocity values for Package 3 determined from the integrated sonic logs are spuriously low.

As shown in Figure 9-1, eight of the nine hammer-sampled intervals plotted lie above the 1:1 correlation line. This suggests the possibility that the hammer-sampling process affected the integrity (hammer-8induced fractures) of the in-situ material near the borehole wall. The results also suggest the possibility that other PEACE logging techniques that rely on the integrity of the in situ material near the borehole wall [e.g, gamma-gamma (density) and neutron (porosity)] also may have been affected by the hammer-sampling process.

SRS package velocities for the three geologic reference boreholes are listed in Table 9-12 (also located at end of this Chapter). Interval velocities (see fig. 9-1) for the Package 1 and 2 combination are quite consistent and range from 5,900 to 6,400 ft/sec. Package 3 interval velocities range from 7,700 to 8,700 ft/sec and are significantly higher than those for Package 1 and 2. Interval velocities for the Package 4, 5, and 6 combination are lower than those for Package 3 in boreholes KAR-1 and OOR-17 (cf. 7,400 and 7,600 ft/sec contrasted with 8,400 and 8,700 ft/sec, respectively), but higher than that for Package 3 in borehole OAR-2 (cf.

TABLE 9-2. -- Summary of PEACE Program boreholes with SRS. Depths are given in ft below Holmes & Narver (H&N) datum. For additional downhole geophysical logs run in these boreholes, refer to Table 7-1.

BOREHOLE NUMBER	DEPTH WATER	DEPTH TOTAL	SRS	INTEGRATED SONIC (CH#3)[1]
KAR-1	105.1	1251.1	0 -1216.9	189.1 - 354.0 412.6 - 1185.1
KBZ-4	109.1	1155.0	0 -1080.0	233.1 - 1135.1
KCT-5	98.9	405.5	0 - 392.9	189.0 - 387.9
KDT-6	56.2	180.0	0 - 174.0	Not Run
KFT-8	77.8	395.7	0 - 386.0	Not Run
OAR-2/2A	114.2 (OAR-2)	999.8 (OAR-2)	0 - 972.0 (OAR-2)	143.5 - 438.5 (OAR-2A)
OBZ-4	198.7	1803.9	0 -1774.0	390.7 - 1784.7
OCT-5	163.7	1015.2	0 -1000.1	181.7 - 1016.7
OOR-17	55.2	1146.3	0 -1135.0	59.2 - 1140.2

[1] CH#3 refers to channel 3 receiver.

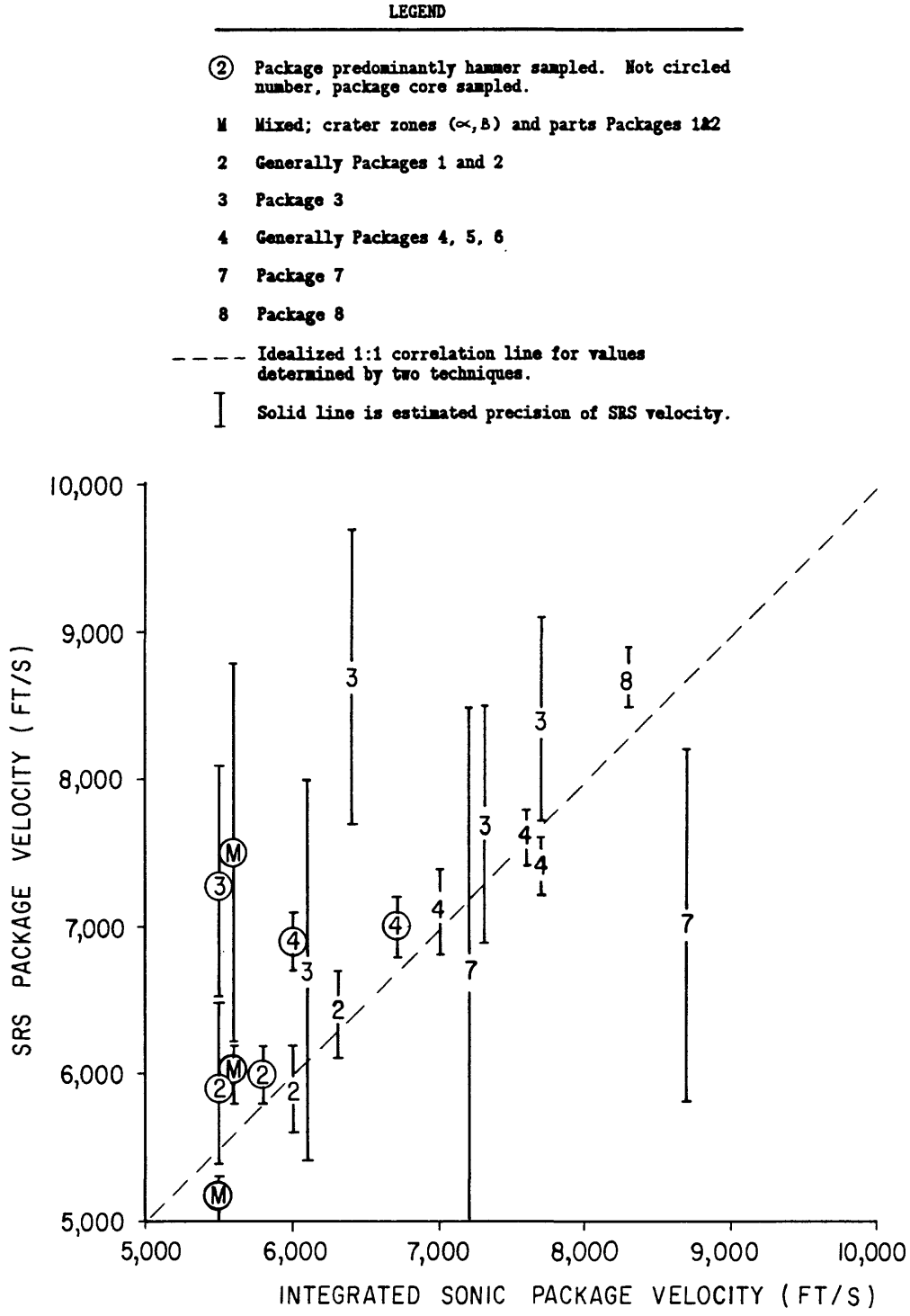

FIGURE 9-1. -- Comparison of geologic (sedimentary) package/crater zone average velocity values determined from SRS and integrated sonic logs.

8,300 to 7,700 ft/sec). The high velocity value (8,300 ft/sec) for Package 4, 5, and 6 in borehole OAR-2 may be due partially to the reef facies that was noted near the lower portion of Package 6 in borehole OAR-2. Reef facies tend to have relatively higher degrees of penecontemporaneous cemententation (and hence higher sonic velocities) than most other atoll carbonates. The interval velocities of Package 7 range from 6,300 to 7,000 ft/sec.

The package velocity data in Table 9-12 for the three geologic reference boreholes suggest that Package 3 is generally the most competent of Packages 1 through 7. The only exception to this is Package 4, 5, and 6, which is the most competent in borehole OAR-2/2A. The data in Table 9-12 show that the package velocities of borehole KAR-1 are very similar to those for borehole OOR-17.

Tables 9-4 and 9-9 show that the Package 3 velocities for the two ground-zero boreholes, KBZ-4 and OBZ-4, respectively, are less than 7,000 ft/sec. The lower Package 3 velocities of the ground-zero boreholes compared to those for the reference boreholes probably resulted from disruption of the inherent cementation by the blast effects of the respective explosions. Transition borehole OCT-5 (Table 9-10) has an intermediate Package 3 velocity of 7,300 ft/sec.

As expected, Tables 9-4 (KBZ-4), 9-5 (KCT-5), 9-7 (KFT-8), 9-9 (OBZ-4), and 9-10 (OCT-5) show that the crater zones all have interval velocities of less than 6,000 ft/sec. This suggests that the material in the crater zones has no competent layers that are significantly thick.

REFERENCE

Grow, J.A., Lee, M.W., Miller, J.J., Agena, W.F., Hampson, J.C., Foster, D.S., and Woellner, R.A., 1986, Multichannel seismic-reflection survey of KOA and OAK craters: U.S. Geological Survey Bulletin 1678-D, 46 p., 39 figs.

TABLE 9-3. -- Seismic reference survey (SRS) and integrated sonic velocities for crater zones/geologic packages in borehole KAR-1.

DEPTH INTERVAL (ft below H&N datum)		ZONES/ SEDIMENTARY PACKAGES	SRS VELOCITY (ft/sec)[2]	INTEGRATED SONIC (CH#3)[1] (ft/sec)[2]
0 H&N	105.1 Seafloor	Water	N.A.	N.A.
105.1 Seafloor	384.0 DISC.5	1 & 2	5900 ±300	6100 (189.1 - 354.0 ft)
384.0 DISC.5	587.1 DISC.6	3	8400 ±700	7700 (412.6 - 587.1 ft)
587.1 DISC.6	1169.2 DISC.8	4,5,&6	7400 ±200	7700
1169.2 DISC.8	1216.9 T.D.	7	6300 ±1700	8800 (1169.2 - 1185.1 ft)

[1] CH#3 refers to Channel 3 receiver.

[2] The estimated precision for SRS is based on the average time differences of 1 msec for 29 repeated measurements in borehole OOR-17. The estimated precision for integrated sonic is about an order of magnitude less than that for SRS based on a reading uncertainty of approximately 0.1 msec. However, the integrated sonic is more sensitive to changes in borehole rugosity than the SRS technique.

TABLE 9-4. -- Seismic reference survey (SRS) and integrated sonic velocities for crater zones/sedimentary packages in borehole KBZ-4.

DEPTH INTERVAL (ft below H&N datum)		ZONES/ SEDIMENTARY PACKAGES	SRS VELOCITY (ft/sec)*	INTEGRATED SONIC (CH#3) (ft/sec)*
0 H&N	109.1 Seafloor	Water	N.A.	N.A.
109.1 - Seafloor	233.1 Begin Sonic	α, PARTβ_1	No Log	No Log
233.1 - Begin Sonic	266.2 β_3	PARTβ_1 β_2	No Log	5300
266.2 - β_3	368.6 DISC.5	β_3, PART2	No Log	5600
109.1 - Seafloor	412.0 Begin SRS	α,β, PART2 PART3	6000 $\pm$200	5600 (233.1 - 412.0 ft)
412 - Begin SRS	480.7 DISC.6	PART3	6700 $\pm$1300	6100
480.7 - DISC.6	1080 T.D. SRS	4,5, PART6	6900 $\pm$200	6000 (480.7 - 1089.6 ft)
1089.6 - DISC.8	1135.1 T.D. Sonic	PART7	No Log	7800

*The estimated precision for SRS is based on the average time differences of 1 msec for 29 repeated measurements in borehole OOR-17. The estimated precision for integrated sonic is about an order of magnitude less than that for SRS based on a reading uncertainty of approximately 0.1 msec. However, the integrated sonic is more sensitive to changes in borehole rugosity than the SRS technique.

TABLE 9-5. -- Seismic reference survey (SRS) and integrated sonic velocities for crater zones/sedimentary packages in borehole KCT-5.

DEPTH INTERVAL (ft below H&N datum)	ZONES/ SEDIMENTARY PACKAGES	SRS VELOCITY (ft/sec)*	INTEGRATED SONIC (CH#3) (ft/sec)*
0 - 98.9 H&N Seafloor	Water	N.A.	N.A.
98.9 - 189.0 Seafloor Bottom Casing	α, β_1 PARTβ_2	4900 $\pm$500	No Logs
189.0 - 274.3 Bottom Casing DISC.3	PARTβ_2, β_3	7500 $\pm$1300	5600
274.3 - 392.9 DISC.3 DISC.5	PART2	5900 $\pm$600	5500 (274.3 - 387.9 ft)

*The estimated precision for SRS is based on the average time differences of 1 msec for 29 repeated measurements in borehole OOR-17. The estimated precision for integrated sonic is about an order of magnitude less than that for SRS based on a reading uncertainty of approximately 0.1 msec. However, the integrated sonic is more sensitive to changes in borehole rugosity than the SRS technique.

TABLE 9-6. -- Seismic reference survey (SRS) velocities for sedimentary packages in borehole KDT-6.

DEPTH INTERVAL (ft below H&N datum)	ZONES/ SEDIMENTARY PACKAGES	SRS VELOCITY (ft/sec)*	INTEGRATED SONIC (CH#3) (ft/sec)*
0 H&N - 56.2 Seafloor	Water	N.A.	Not Run
56.2 Seafloor - 174 Bottom SRS	PART2	6900 ±800	N.A.

*The estimated precision for SRS is based on the average time differences of 1 msec for 29 repeated measurements in borehole OOR-17. The estimated precision for integrated sonic is about an order of magnitude less than that for SRS based on a reading uncertainty of approximately 0.1 msec. However, the integrated sonic is more sensitive to changes in borehole rugosity than the SRS technique.

TABLE 9-7. -- Seismic reference survey (SRS) velocities for geologic packages in borehole KFT-8.

DEPTH INTERVAL (ft below H&N datum)	ZONES/ SEDIMENTARY PACKAGES	SRS VELOCITY (ft/sec)*	INTEGRATED SONIC (CH#3) (ft/sec)*
0 H&N - 77.8 Seafloor	Water	N.A.	Not Run
77.8 Seafloor - 145.0 Begin SRS	α, β_1 β_2	5400 $\pm$900	N.A.
145.0 Begin SRS - 386 TD SRS	β_2, β_3 PART2	6300 $\pm$300	N.A.

*The estimated precision for SRS is based on the average time differences of 1 msec for 29 repeated measurements in borehole OOR-17. The estimated precision for integrated sonic is about an order of magnitude less than that for SRS based on a reading uncertainty of approximately 0.1 msec. However, the integrated sonic is more sensitive to changes in borehole rugosity than the SRS technique.

TABLE 9-8. -- Seismic reference survey and integrated sonic velocities for crater zones/geologic packages in boreholes OAR-2/2A.

DEPTH INTERVAL (ft below H&N datum)	ZONES/ SEDIMENTARY PACKAGES	SRS VELOCITY (ft/sec)*	INTEGRATED SONIC (CH#3) (ft/sec)*
		OAR-2	OAR-2A
0 - 114.2 H&N Seafloor (OAR-2)	Water	N.A.	N.A.
114.2 - 414.3 Seafloor DISC.5	1 & 2	6400 ±300	6300 (143.5 - 414.3 ft)
414.3 - 556.7 DISC.5 DISC.6	3	7700 ±800	7300 (414.3 - 438.5 ft)
556.7 - 972 DISC.6 T.D. SRS	4,5 PART6	8300 ±300	No Logs

*The estimated precision for SRS is based on the average time differences of 1 msec for 29 repeated measurements in borehole OOR-17. The estimated precision for integrated sonic is about an order of magnitude less than that for SRS based on a reading uncertainty of approximately 0.1 msec. However, the integrated sonic is more sensitive to changes in borehole rugosity than the SRS technique.

TABLE 9-9. -- Seismic reference survey (SRS) and integrated sonic velocities for crater zones/sedimentary packages in borehole OBZ-4.

DEPTH INTERVAL (ft below H&N datum)	ZONES/ SEDIMENTARY PACKAGES	SRS VELOCITY (ft/sec)*	INTEGRATED SONIC (CH#3) (ft/sec)*
0 H&N - 198.7 Seafloor	Water	N.A.	N.A
198.7 - 390.7 Bottom Casing	α,PARTβ_1	N.A.	N.A.
390.7 Bottom Casing - 415.1 TOP.B3	PARTβ_1, β_2	N.A.	6000
415.1 TOP B3 - 593 DISC.5	β_1,PART2	N.A.	6300
593 DISC.5 - 701.2 DISC.6	3	N.A	6700
198.7 Seafloor - 701.2 DISC.6	$\alpha,\beta_{1/3}$, PART2,3	5900 $\pm$200	N.A.
701.2 DISC.6 - 1065.1 DISC.8	4,5,6	7100 $\pm$300	7000
1065.1 DISC.8 - 1114.6 DISC.9	7	6700 $\pm$1800	7200
1114.6 DISC.9 - 1774.0 T.D. SRS	PART8	8700 $\pm$200	8300 (1114.6 - 1784.7 ft)

*The estimated precision for SRS is based on the average time differences of 1 msec for 29 repeated measurements in borehole OOR-17. The estimated precision for integrated sonic is about an order of magnitude less than that for SRS based on a reading uncertainty of approximately 0.1 msec. However, the integrated sonic is more sensitive to changes in borehole rugosity than the SRS technique.

TABLE 9-10. -- Seismic reference survey(SRS) and integrated sonic velocities for crater zones/sedimentary packages in borehole OCT-5.

DEPTH INTERVAL (ft below H&N datum)	ZONES/ SEDIMENTARY PACKAGES	SRS VELOCITY (ft/sec)*	INTEGRATED SONIC (CH#3) (ft/sec)*
0 - 163.7 H&N Seafloor	Water	N.A.	N.A.
181.7 - 244.1 Begin Sonic B2	α & β_1	No Log	5100
163.7 - 432.7 Seafloor DISC.5	α,β_1 PART2	5200 $\pm$200	5500 (181.7 - 432.7 ft)
432.7 - 572.2 DISC.5 DISC.6	3	7300 $\pm$800	5500
572.2 - 1000.1 DISC.6 T.D. SRS	4,5, PART6	7000 $\pm$200	6700 (572.2 - 1016.7 ft)

*The estimated precision for SRS is based on the average time differences of 1 msec for 29 repeated measurements in borehole OOR-17. The estimated precision for integrated sonic is about an order of magnitude less than that for SRS based on a reading uncertainty of approximately 0.1 msec. However, the integrated sonic is more sensitive to changes in borehole rugosity than the SRS technique.

TABLE 9-11. -- Seismic reference survey (SRS) and integrated sonic velocities for crater zones/sedimentary packages in borehole OOR-17.

DEPTH INTERVAL (ft below H&N datum)		ZONES/ SEDIMENTARY PACKAGES	SRS VELOCITY (ft/sec)*	INTEGRATED SONIC (CH#3) (ft/sec)*
0 H&N	55.2 Seafloor	Water	N.A.	N.A.
55.2 - Seafloor	405.7 DISC.5	1 & 2	6000 ±200	5800 (59.2 - 405.7 ft)
405.7 - DISC.5	552.4 DISC.6	3	8700 ±1000	6400 (405.7 - 457.2 ft)
552.4 - DISC.6	1024.4 DISC.8	4,5,6	7600 ±200	7600 (579.2 - 1024.4 ft)
1024.4 - DISC.8	1104.6 DISC.9	7	7000 ±1200	8700
1104.6 - DISC.9	1140.2 T.D. Sonic	PART8	No log	9800

*The estimated precision for SRS is based on the average time differences of 1 msec for 29 repeated measurements in borehole OOR-17. The estimated precision for integrated sonic is about an order of magnitude less than that for SRS based on a reading uncertainty of approximately 0.1 msec. However, the integrated sonic is more sensitive to changes in borehole rugosity than the SRS technique.

TABLE 9-12. -- Comparison of SRS velocities for sedimentary packages in the PEACE-Program reference boreholes.

SEDIMENTARY PACKAGE(S)	KAR-1 (ft/sec)	OOR-17 (ft/sec)	OAR-2/2A (ft/sec)
1 & 2	5900 ±300	6000 ±200	6400 ±300
3	8400 ±700	8700 ±1000	7700 ±800
4, 5, & 6	7400 ±200	7600 ±200	8300 ±300
7	6300 ±1700	7000 ±1200	NA

CHAPTER 10:

BENTHIC SAMPLES FROM ENEWETAK ATOLL

by

Bruce R. Wardlaw[1], T. W. Henry[2], and Wayne E. Martin[1]

U.S. Geological Survey

INTRODUCTION

A suite of 117 bottom surface (benthic) samples was taken from Enewetak lagoon during Phase I (Marine Phase) of the PEACE Program, and a second set of 49 samples was taken from the drill ship M/V Knut Constructor in the vicinity of KOA and OAK craters during Phase II (Drilling Phase) (see fig. 10-1). These samples were taken (1) to familiarize project geologists with the distribution of sediment types and facies within the Enewetak lagoon, (2) to increase the understanding of the occurrence and distribution of modern microfaunas in the lagoon, and (3) to supplement the studies of the seafloor features both within and near OAK and KOA. These studies facilitated much greater understanding onsite of the rock and sediment penetrated during the drilling and in the construction of the litho- and biostratigraphic framework.

Previous Benthic Sampling. -- The first benthic samples were collected from Enewetak lagoon and surrounding areas in 1946 prior to nuclear testing (Emery, Tracey, and Ladd, 1954). This suite of 365 samples was taken primarily from the U.S.S. Blish, which was gathering data concurrently for a detailed bathymetric map of Enewetak Atoll. Most of these samples were taken with a small underway sampler ("scoopfish") along bathymetric-traverse lines. The main sedimentary components were the remains of Halimeda, corals, shells of molluscs, and other fine material, similar to benthic samples taken from other Pacific Atolls. The distribution and average abundance of the sedimentary components were described by Emery, Tracey, and Ladd (1954). A number of the 1946 samples were included in the study of the Recent foraminifer faunas of the Marshall Islands by Cushman, Todd, and Post (1954). Some of the same samples were reexamined by Cronin, Brouwers, and others (1986).

Numerous additional benthic samples were taken from Enewetak after the period of nuclear testing (1948-1958) almost solely to determine the distribution of radionuclides on Enewetak and to assess their impact on

---

[1] Branch of Paleontology and Stratigraphy, Washington, DC.
[2] Office of Regional Geology, Reston, VA.

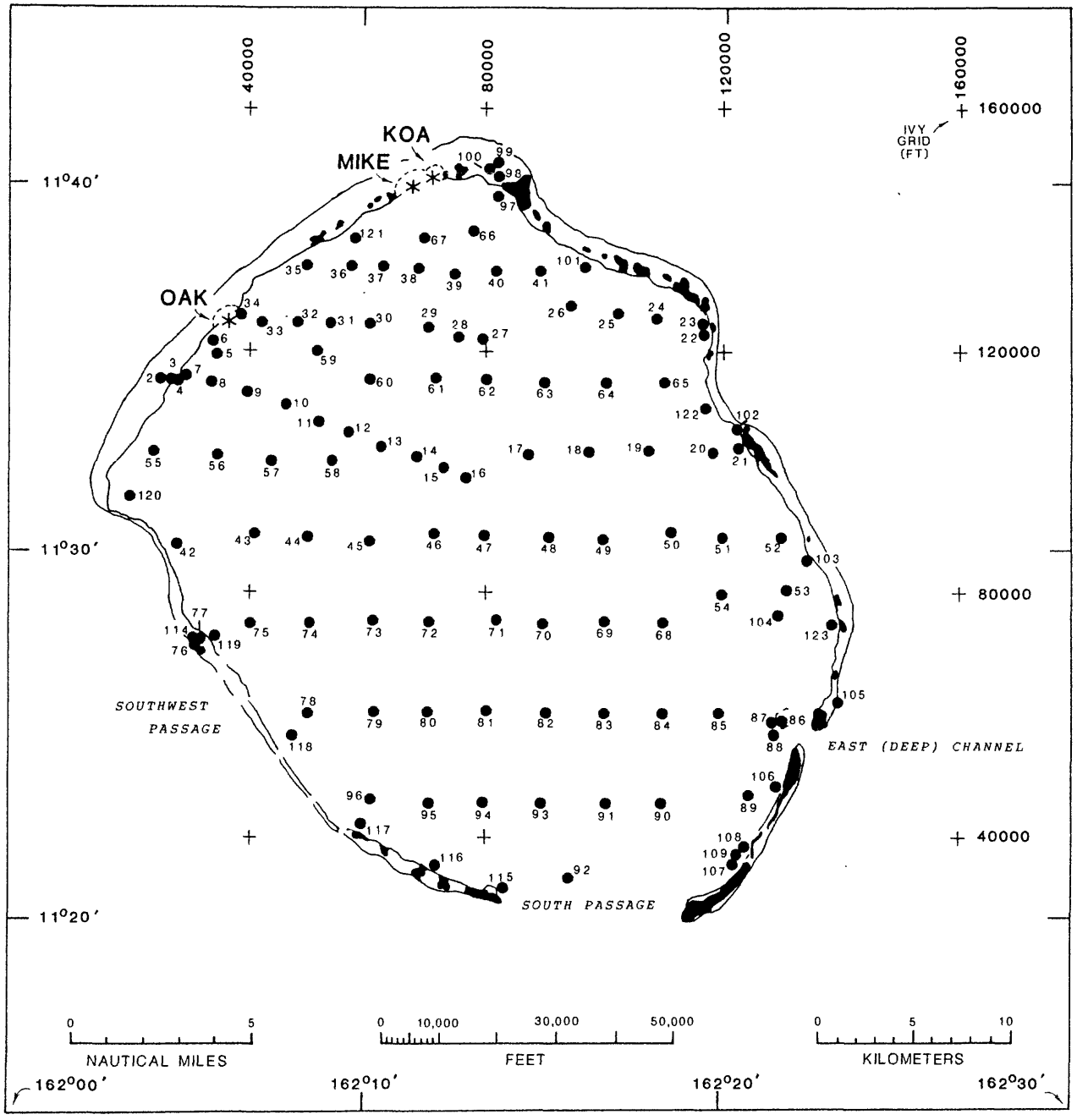

FIGURE 10-1. -- Map of Enewetak Atoll showing location of benthic samples taken during PEACE Program.

human populations. The most extensive of these programs was conducted during the Enewetak Radiological Survey of 1972 and involved both the sediments of the islands and surface sediments of the lagoon. Two areas of significant contamination were identified in the report of this survey (USAEC, 1973), a large area encompassing most of the northwestern part of the lagoon, and a smaller area lagoonward from the island of Runit (YVONNE). More recently, McMurtry, Schneider, and others (1985) studied the vertical distribution of fallout radionuclides in a series of shallow sediment cores (<200 cm in length) taken off Runit (YVONNE).

Field Procedures. -- The first 117 benthic samples taken during the PEACE Program were collected in September of 1984, during the Marine Phase (fig. 10-1 and table 10-1). Sampling was conducted on a modified grid (fig. 10-1) from a 21-ft Boston whaler equipped with a Motorola Falcon IV Miniranger navigational computer, effectively utilizing the navigational network of five transponder stations established around the atoll for the program. A Meridian Oceans Systems (MOS) navigational specialist was aboard the whaler when the samples were collected. Most of these samples were taken with a lead-weighted snap-jaw grab sampler. In many instances, multiple grabs were made at a given site in order to obtain an acceptable volume of material for analysis. In shallower water where the grab sampler was not effective, geologists collected them by diving from the surface and scooping the sediment into an approximately 2-liter metal can.

From February to July of 1985 during the Drilling Phase, an additional 48 benthic samples were taken from the starboard bow and starboard stern of the drill ship, M/V Knut Constructor, at most borehole sites using the same grab sampler (table 10-1). One additional sediment sample was scooped from the top of the reaction mass when it was retrieved from the lagoon bottom at the end of the program. Samples taken from aboard the drill ship were located trigonometrically from the borehole location, as determined by a Miniranger navigational computer (see Henry, Wardlaw, and others, 1986, p. 32-39), the heading of ship, and the distance from the moonpool to the bow or stern sampling station.

For both sample sets, the material was scooped and washed into a zip-lock plastic bag that was marked with the appropriate sample number. The samples taken by the grab-samplers generally weighed about 1 kg; those taken with the metal can were about twice that size.

The samples taken during the Marine Phase were transported back to the University of Hawaii/DOE Mid-Pacific Research Laboratory on Enewetak (FRED) Island. Excess sea water was decanted from the samples after the sediment was allowed to settle completely. About 50 to 75 ml of 5 percent methanol and a few drops of buffered formaldyhyde were added to each sample. The bags were resealed and inserted into larger zip-lock bags and sealed for shipment.

Samples collected during the Drilling Phase were sealed, labeled, and inserted into larger zip-lock bags for packing and shipment.

TABLE 10-1. -- Location of benthic samples taken during PEACE Program on Enewetak Atoll. IVY-grid coordinates in ft. Note that sample #1 was lost in transit. Asterisk (*) denotes a location estimated from a map of the atoll.

SAMPLE	IVY-GRID COORDINATES		SAMPLE	IVY-GRID COORDINATES	
2	116,563N	025,625E	55	104,893N	023,570E
3	116,250N	026,250E	56	103,787N	034,358E
4	116,255N	027,500E	57	102,496N	043,504E
5	120,169N	034,022E	58	102,488N	053,802E
6	120,349N	033,675E	59	120,760N	050,924E
7	116,864N	028,860E	60	116,225N	060,082E
8	115,594N	033,997E	61	116,539N	071,146E
9	113,923N	039,437E	62	116,104N	079,923E
10	111,869N	045,446E	63	115,837N	090,031E
11	109,779N	051,012E	64	116,078N	100,618E
12	107,672N	056,308E	65	115,972N	100,092E
13	105,389N	062,053E	66	143,198N	077,635E
14	103,059N	068,016E	67	142,035N	068,681E
15	100,911N	072,994E	68	075,024N	110,040E
16	099,550N	076,310E	69	075,108N	100,323E
17	104,000N	087,200E	70	074,938N	090,070E
18	105,600N	096,400E	71	075,486N	081,692E
19	105,000N	105,700E	72	075,273N	070,622E
20	105,400N	114,700E	73	075,377N	060,633E
21	105,600N	123,500E	74	075,000N	050,359E
22	124,700N	117,700E	75	075,000N	040,038E
23	125,800N	117,700E	76	071,333N *	031,200E
24	126,500N	108,400E	77	072,200N *	031,817E
25	127,400N	102,200E	78	059,907N	050,165E
26	128,400N	094,100E	79	060,263N	060,919E
27	123,700N	079,571E	80	059,850N	070,209E
28	123,433N	075,155E	81	060,084N	080,327E
29	125,083N	070,078E	82	059,976N	090,360E
30	125,929N	059,865E	83	059,899N	100,169E
31	125,423N	053,733E	84	060,122N	100,004E
32	125,436N	047,996E	85	060,078N	119,780E
33	125,649N	042,008E	86	058,730N	130,262E
34	126,928N	038,264E	87	059,790N	129,627E
35	135,333N	048,432E	88	056,721N	129,518E
36	135,164N	056,891E	89	046,609N	125,333E
37	135,119N	062,314E	90	044,985N	110,053E
38	135,052N	068,260E	91	045,356N	100,708E
39	134,957N	074,334E	92	032,115N	095,191E
40	134,474N	081,830E	93	045,006N	090,014E
41	134,750N	088,045E	94	045,034N	080,008E
42	089,900N	027,665E	95	045,159N	070,432E
43	090,339N	040,438E	96	045,553N	060,673E
44	090,143N	049,953E	97	147,500N	082,450E
45	090,125N	060,312E	98	151,300N	082,188E
46	090,278N	070,766E	99	153,125N	082,188E
47	090,111N	079,886E	100	151,563N	080,625E
48	090,256N	090,418E	101	135,625N	096,875E
49	089,847N	100,030E	102	106,250N	124,000E
50	090,269N	110,628E	103	086,563N	135,000E
51	090,114N	120,257E	104	076,563N	130,625E
52	090,051N	130,701E	105	062,188N	139,688E
53	081,528N	131,360E	106	048,120N	130,000E
54	080,083N	120,271E	107	035,156N	123,438E

Continued on next page.

TABLE 10-1. -- (Continued from previous page.) Location of benthic samples taken during PEACE Program on Enewetak Atoll. IVY-grid cooordinates in ft. Note that samples #110 - #114 were never taken.

S = stern sample, B = bow sample.
C = midship sample.
RXNMASS = reaction-mass sample.

SAMPLE	IVY-GRID COORDINATES		SAMPLE	IVY GRID-COORDINATES	
108	037,500N	124,531E	OGT-9S	125,723N	036,685E
109	037,344N	124,375E	OHT-10B	123,996N	037,295E
115	031,250N	082,500E	OIT-11S	124,214N	036,924E
116	034,688N	069,688E	OIT-11B	124,216N	037,150E
117	041,250N	059,063E	OJT-12S	124,031N	037,401E
118	056,250N	047,344E	OJT-12B	124,044N	037,627E
119	072,656N	034,219E	OKT-13S	124,327N	036,756E
120	096,875N	019,375E	OKT-13B	124,364N	036,979E
121	140,625N	057,188E	OLT-14S	123,561N	038,334E
122	112,188N	117,500E	OLT-14B	123,550N	038,573E
123	075,313N	139,375E	OMT-15S	123,956N	037,941E
KBZ-4S	149,290N	071,000E	OMT-15B	123,962N	038,167E
KBZ-4B	149,382N	071,208E	ONT-16S	124,204N	037,639E
KBZ-4C	149,350N	071,113E	ONT-16B	124,198N	037,865E
KCT-5S	148,758N	070,971E	OOR-17S	119,843N	032,771E
KCT-5B	148,828N	071,189E	OOR-17B	119,817N	032,996E
KDT-6S	148,129N	071,018E	OPZ-18S	124,787N	036,255E
KDT-6B	148,240N	071,240E	OPZ-18B	124,765N	036,480E
KET-7S	147,985N	071,023E	OQT-19S	123,631N	035,419E
KET-7B	148,049N	071,247E	OQT-19B	123,640N	035,644E
OAM-3	127,818N	039,450E	ORT-20S	123,281N	035,213E
OBZ-4B	124,983N	036,211E	ORT-20B	123,294N	035,439E
OCT-5S	125,434N	036,428E	OSR-21S	120,304N	033,297E
OCT-5B	125,467N	036,652E	OSR-21B	120,308N	033,297E
ODT-6S	126,109N	037,248E	OSM-22S	120,282N	033,003E
ODT-6B	126,138N	037,472E	OTG-23S	124,204N	035,771E
OET-7S	125,898N	036,973E	OTG-23B	124,180N	035,997E
OET-7B	125,943N	037,195E	OUT-24S	125,482N	035,552E
OFT-8S	125,768N	036,759E	OUT-24B	125,538N	035,331E
OFT-8B	125,805N	036,982E	RXNMASS	121,824N	033,363E

Laboratory Procedures. -- Laboratory processing of the sediment samples was conducted at the Natural History Museum (Smithsonian) in Washington, DC. The benthic samples were washed free of preservatives (if applicable) and then dried at low temperature (70 deg C). After equilibration to standard conditions (room temperature and humidity), samples were weighed on a Mettler P-1200, top-loading balance. The sample was then split with a standard sediment splitter into paleontologic (P) and sedimentologic (S) fractions. Fragments (generally coral) too large for the splitter were weighed separately and retained with excess sedimentologic fractions as archival material.

The paleontologic (P) split was transferred to the USGS laboratories in Reston, VA, where selected samples were processed and picked for microfaunal studies to augment knowledge of the modern Enewetak lagoonal faunas (see Cronin, Brouwers, and others, 1986, p. 36-37).

From the sedimentologic (S) fraction, 100- to 200-g samples were weighed and cleaned of organics with a 30-percent hydrogen-peroxide solution[1]. An approximately 50-g split was taken for grain-size analysis. Grain-size analysis began with wet sieving to separate the silt and clay fraction from the sand and small-granule fraction. This was done by flooding the sample with less than a liter of 0.03 percent "calgon" water and washing the sample through a 4-phi- (#230-) mesh brass screen. The sample retained on the sieve was dried, weighed, dumped into nested seives, and placed into a RO-TAP (sediment shaker) for 15 min. Sieve sizes were selected for the major sediment-size catergories, which include -1, 0, 1, 2, 3, and 4 phi (Ø) (see fig. 10-2). Material retained on each sieve screen then was weighed, and the size fractions were recombined and archived.

The material caught in the bottom pan after wet sieving was subjected to pipette analysis in 1-liter graduated cylinders using the method described by Folk (1974). Pipette samples were dried, allowed to equilabrate to standard room conditions, and weighed on a Mettler H51 analytic balance.

FACIES

The benthic-sample locations collected during the Marine Phase of the PEACE Program are shown in Figure 10-1. Histograms for each of the sediment samples are presented at the end of the Chapter as Plates 10-1 through 10-29. Craters OAK, KOA, and MIKE are shown as asterisks on that figure; sample locations taken from the crater areas during the Drilling Phase are too closely spaced to be shown at the scale of the figure. The IVY-grid locations for both sets of benthic samples are given in Table 10-1. The depth of each Marine Phase sample was estimated from the available bathymetric maps (U.S.

---

[1] Organic content of the Recent benthic samples from Enewetak lagoon averages slightly more than 3 percent by weight (see Chapter 5); however, organic content was not accounted in the sedimentologic analysis of the current set of benthic samples. Thus, the percent figures given in the sedimentologic tables are compared to the total weight of the carbonate material only. Non-organic insoluble residues are negligible (Chapter 6).

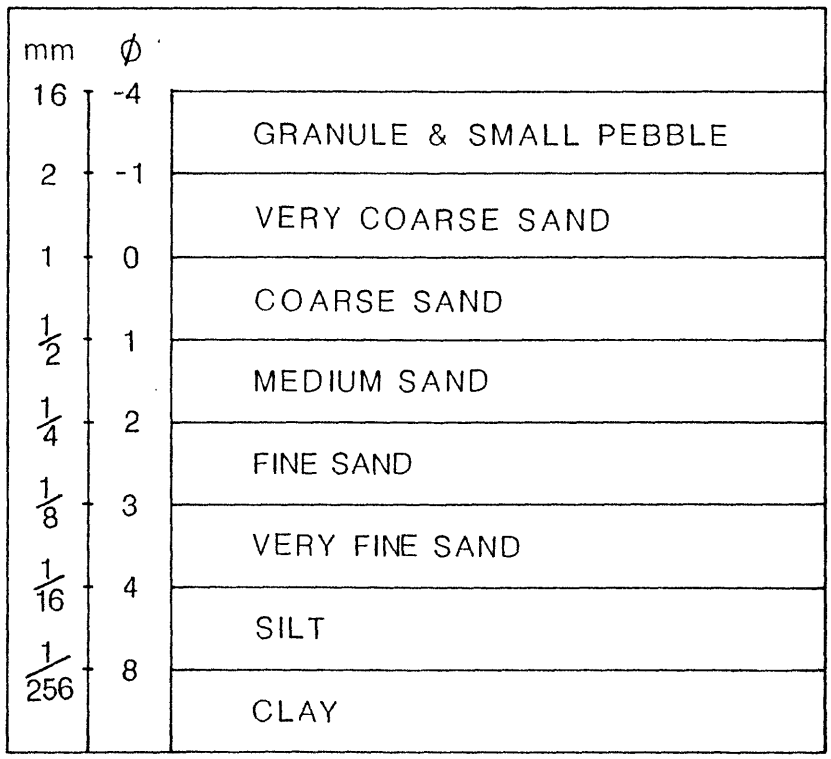

FIGURE 10-2. -- Grain-size chart used for benthic samples from PEACE Program.

Navy Hydrographic Maps) and that for each Drilling Phase sample from measurements made from the drill ship at the borehole sites. The general pretest bathymetry of the atoll is shown in Figure 10-3.

For each sample, the ratio of Granule:Sand:Mud was determined (table 10-2) (see Folk, 1974). For samples with 65 percent or greater sand, the sand size was differentiated into very coarse and coarse:medium:fine and very fine fractions. Histograms of the size fractions of each sample follow the text.

Plotted on a tertiary diagram of mud, sand, and granule, eight facies can be distinguished for the PEACE Program benthic samples from Enewetak lagoon (see fig. 10-4). (It should be noted that the term "granule", as used in this report, means granule-sized and coarser.) These facies are defined as follows:

(1). Granule -- greater than 47 percent granule,less than 15 percent mud.

(2). Granule-sand -- 30 to 47 percent granule, less than 5 percent mud.

(3). Sand-granule -- 10 to 30 percent granule, less than 10 percent mud.

(4). Granule-sand-mud -- 18 to 35 percent granule, 7 to 25 percent mud.

(5). Sand -- less than 13 percent granule, less than 9 percent mud.

(6). Muddy sand -- less than 13 percent granule, 9 to 19 percent mud.

(7). Sand-mud -- less than 15 percent granule, 19 to 39 percent mud.

(8). Mud -- greater than 39 percent mud.

Halimeda plates, mollusc shells and fragments, and corals and coral fragments constitute most of the very coarse sand fraction. Foraminifers and skeletal elements constitute most of the remaining sand fraction. Broken skeletal elements comprise the silt and clay (mud) fraction.

DISTRIBUTION OF SEDIMENT FACIES

Figure 10-5 is a map of Enewetak Atoll showing the distribution of sediment facies.

The Granule, Granule-sand, and Sand-granule facies (facies 1 - 3 above) intergrade over short distances on the floor of the lagoon and on the islands. Thus, for mapping purposes, these facies can be treated as one composite facies, termed the Granule-coarse sand facies. This facies represents relatively high energy environments of heterogeneous sediment distribution.

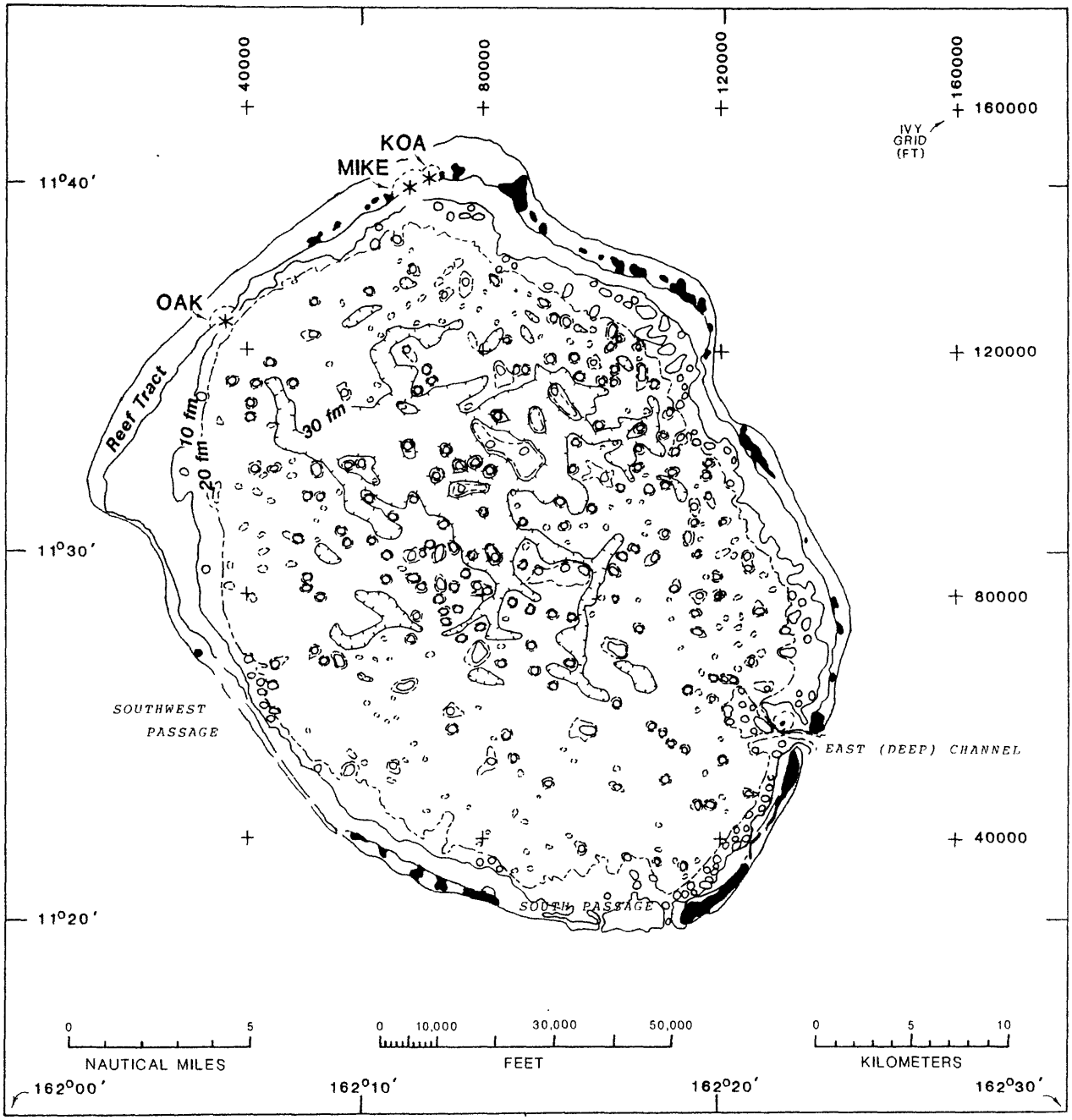

FIGURE 10-3. -- General pretest bathymetric map of Enewetak Atoll.

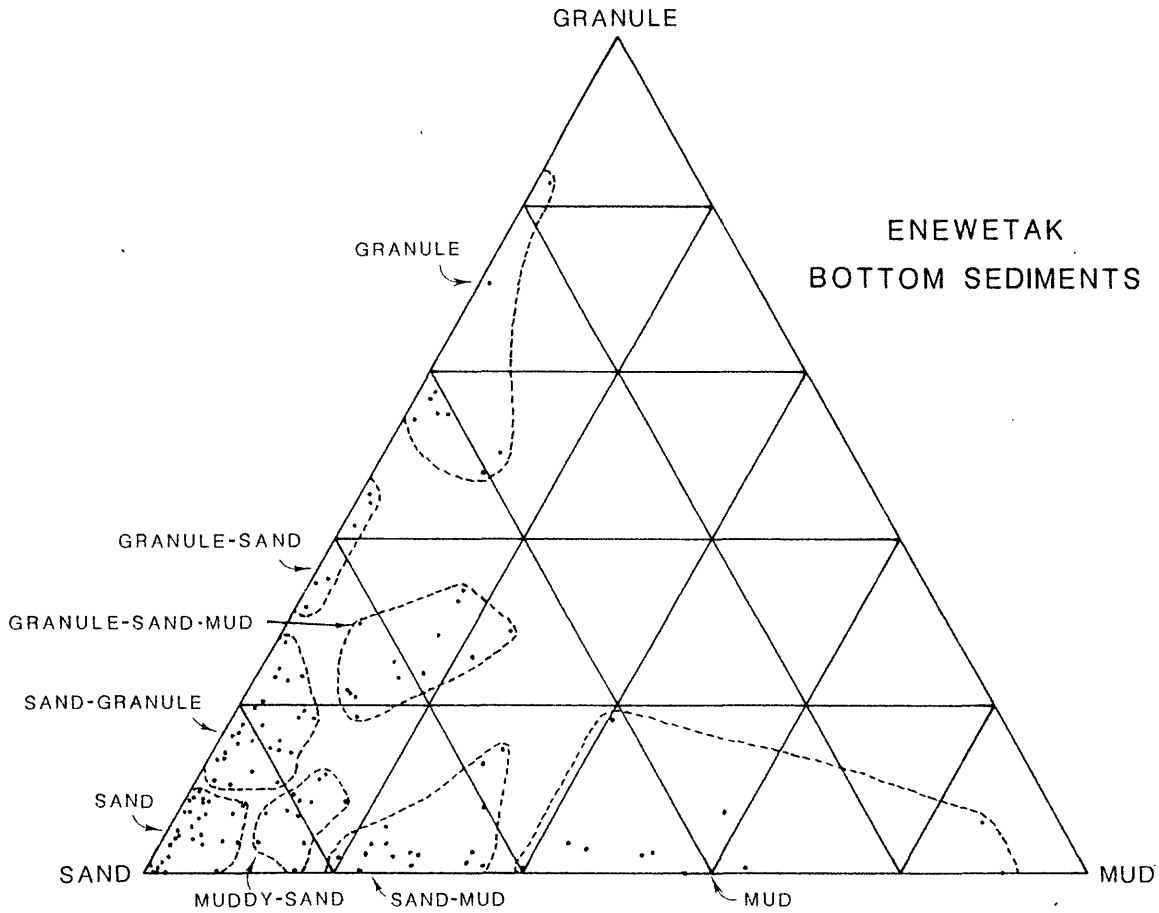

FIGURE 10-4. -- Plot of Enewetak benthic samples on tertiary diagram of weight-percent granule (and small pebble), sand, and mud (silt and clay). Sediment facies are enclosed by dashed line. See text for explanation.

TABLE 10-2. -- Analyses of Enewetak benthic samples. Depth given in ft below H&N datum for all samples except for samples marked with "+", which were taken above that datum.

SAMPLE	FACIES	RATIO	(SAND)	DEPTH
1	(Sample lost in transit.)			
2	GRANULE-SAND	44.3:54.0: 1.7		+2
3	GRANULE-SAND	35.1:63.1: 1.7		2
4	SAND	2.0:96.2: 1.8	(32.4:60.5:17.2)	3
5	SAND-GRANULE	15.3:82.3: 2.4	(52.4:34.9:12.7)	72
6	GRANULE-SAND-MUD	25.9:52.4:21.7		30
7	SAND-GRANULE	17.5:80.7: 1.8	(34.3:51.5:14.2)	15
8	GRANULE-SAND-MUD	23.3:61.6:15.1		108
9	MUD	2.5:45.0:52.5		162
10	MUD	7.2:35.0:57.8		186
11	SAND	4.1:92.7: 3.2	(42.7:28.3:29.0)	159
12	SAND	8.5:88.8: 2.7	(54.7:28.4:16.9)	192
13	SAND-MUD	1.0:63.7:35.3		186
14	SAND	8.7:89.3: 2.0	(43.3:30.7:26.0)	168
15	GRANULE	82.7:15.7: 1.6		120
16	SAND-GRANULE	18.4:74.5: 7.1	(71.0:15.4:13.6)	192
17	SAND-GRANULE	11.0:87.0: 2.0	(54.9:26.8:18.3)	96
18	MUDDY SAND	6.8:80.3:12.9	(45.1:20.9:34.0)	102
19	SAND-MUD	2.5:70.5:27.0	(39.8:22.4:37.7)	180
20	SAND	4.1:94.3: 1.6	(52.9:32.3:14.8)	60
21	SAND	0.1:98.8: 1.1	(31.2:56.8:12.0)	18
22	SAND	5.1:93.7: 1.2	(51.1:40.3: 8.6)	10.5
23	GRANULE	70.7:28.1: 1.2		6
24	SAND-MUD	1.0:71.2:27.8	(25.4:21.7:52.9)	58.5
25	GRANULE-SAND-MUD	25.2:61.0:13.8		72
26	MUDDY SAND	3.5:81.2:15.3	(23.8:32.3:43.9)	144
27	SAND-MUD	7.8:60.0:32.2		132
28	SAND-MUD	2.2:75.5:22.3	(46.6:21.2:32.2)	174
29	SAND-MUD	2.5:63.9:33.6		174
30	MUDDY SAND	8.4:78.3:13.3	(59.3:18.9:21.9)	174
31	MUDDY SAND	8.7:79.2:12.1	(50.4:22.2:27.4)	174
32	MUD	0.8:36.0:63.2		174
33	GRANULE-SAND-MUD	32.7:50.6:16.7		138
34	SAND	3.3:92.0: 4.7	(22.3:20.3:57.5)	50
35	SAND	3.3:95.3: 1.4	(24.3:23.8:52.0)	21
36	MUD	18.1:41.5:40.4		132
37	MUD	3.6:53.2:43.2		150
38	MUD	6.1: 8.2:85.7		120
39	MUD	0.1: 9.1:90.8		114
40	MUDDY SAND	9.2:79.6:11.2	(32.3:24.2:43.6)	126

Table 10-2 continued on next page.

TABLE 10-2 (continued, p. 2/5)

SAMPLE	FACIES	RATIO	(SAND)	DEPTH
41	GRANULE	50.3:37.1:12.6		96
42	SAND	7.3:91.4: 1.3	(69.1:23.0: 7.9)	12
43	MUD	2.3:46.5:51.2		132
44	SAND-MUD	5.6:71.5:22.9	(52.7:20.2:27.1)	60
45	MUDDY SAND	11.1:75.9:13.0	(52.6:21.1:26.4)	168
46	MUDDY SAND	8.6:74.5:16.9	(48.5:21.6:29.9)	144
47	SAND-MUD	3.4:72.7:23.9	(47.0:21.9:31.0)	180
48	GRANULE	54.8:40.6: 4.6		180
49	MUDDY SAND	3.7:86.1:10.2	(57.8:19.5:22.7)	126
50	GRANULE	47.9:40.1:12.0		60
51	SAND-GRANULE	10.8:80.4: 8.8	(48.8:25.2:26.1)	144
52	SAND	3.9:88.0: 8.1	(42.2:16.0:41.9)	43.5
53	MUDDY SAND	0.2:83.9:15.9	(22.5:29.1:48.4)	126
54	SAND-GRANULE	15.7:80.7: 3.6	(55.8:26.4:17.8)	28.5
55	SAND-MUD	3.4:74.3:22.3	(9.5: 7.9:82.7)	28.5
56	MUD	0.5:59.8:39.7		126
57	MUD	2.9:51.8:45.3		126
58	MUDDY SAND	7.1:83.6: 9.3	(62.3:19.2:18.5)	192
59	SAND-GRANULE	10.5:85.6: 3.9	(63.2:22.0:14.9)	138
60	SAND-MUD	1.5:65.2:33.3	(45.4:20.2:34.4)	150
61	SAND-GRANULE	22.9:73.4: 3.7	(67.6:21.2:11.2)	120
62	SAND	6.4:89.7: 3.9	(43.6:27.6:28.8)	180
63	SAND-GRANULE	12.1:82.6: 5.3	(65.5:18.1:16.4)	180
64	SAND-MUD	2.0:78.5:19.5	(43.9:22.9:33.2)	114
65	SAND-MUD	2.1:72.7:25.2	(18.4:21.0:60.6)	120
66	MUD	0.0:42.9:57.1		96
67	SAND-MUD	0.2:77.0:22.8	(14.4:13.5:72.1)	126
68	SAND	8.8:90.6: 0.6	(77.2:13.3: 9.5	144
69	SAND-GRANULE	17.5:78.7: 3.8	(53.1:20.5:26.4)	162
70	GRANULE	54.9:41.5: 3.6		144
71	MUDDY SAND	7.5:81.1:11.4	(71.1:14.5:14.4)	192
72	SAND-GRANULE	14.2:77.3: 8.5	(57.5:22.3:20.2)	168
73	SAND-GRANULE	14.9:79.2: 5.9	(51.8:24.1:24.1)	168
74	GRANULE-SAND-MUD	18.7:68.2:13.1	(43.3:24.6:32.0)	126
75	SAND-MUD	13.0:57.6:29.4		132
76	GRANULE-SAND	41.7:57.0: 1.3		+5
77	GRANULE-SAND	45.3:53.6: 1.1		+1
78	SAND	7.0:85.3: 7.7	(34.1:29.4:36.6)	120
79	GRANULE-SAND-MUD	21.6:67.6:10.8	(49.4:24.5:26.1)	132
80	SAND-GRANULE	19.3:73.5: 7.2	(45.9:25.5:28.6)	126
81	GRANULE-SAND-MUD	21.1:67.2:11.7	(39.1:21.1:39.8)	168
82	SAND	7.1:87.0: 5.9	(51.8:23.4:24.8)	144
83	SAND-GRANULE	15.8:77.8: 6.4	(53.3:21.7:25.0)	144

Table 10-2 continued on next page.

TABLE 10-2 (continued, p. 3/5)

SAMPLE	FACIES	RATIO	(SAND)	DEPTH
84	SAND-GRANULE	18.4:72.9: 8.8	(42.5:24.2:33.3)	168
85	SAND	8.5:89.4: 2.1	(38.1:31.0:30.9)	132
86	SAND-GRANULE	20.6:77.2: 2.2	(47.1:44.7: 8.2)	60
87	SAND	4.5:93.9: 1.6	(26.6:54.3:19.1)	120
88	SAND-GRANULE	14.5:84.3: 1.5	(53.2:39.2: 7.6)	108
89	SAND-MUD	2.2:69.9:27.9	(13.9:21.0:65.1)	138
90	SAND	6.6:90.8: 2.6	(49.3:27.6:23.1)	150
91	SAND	4.8:91.3: 3.9	(38.1:34.7:27.2)	138
92	SAND	1.3:97.2: 1.5	(24.2:36.0:39.8)	102
93	SAND-GRANULE	14.5:78.6: 6.9	(39.5:28.2:32.2)	126
94	SAND	7.0:89.9: 3.1	(40.6:33.0:26.4)	114
95	GRANULE-SAND-MUD	21.6:67.5:10.9	(43.1:23.7:33.2)	114
96	SAND-GRANULE	23.5:71.6: 4.9	(59.8:20.6:19.6)	96
97	SAND	0.9:98.6: 0.5	(8.6:20.2:71.2)	6
98	GRANULE	54.2:44.5: 1.3		4
99	GRANULE	56.9:41.4: 1.7		1
100	SAND-GRANULE	16.3:82.3: 1.4	(64.9:31.0: 4.1)	3
101	SAND	9.0:90.1: 0.9	(84.0:15.0: 1.0)	10
102	GRANULE-SAND	34.7:64.6: 0.7		10
103	SAND-GRANULE	24.5:73.5: 2.0	(83.9:10.8: 5.3)	16
104	SAND	0.2:92.1: 7.7	(6.3:16.7:77.0)	126
105	SAND-GRANULE	27.7:71.2: 1.1	(76.8:18.6: 4.6)	30
106	SAND	1.2:97.0: 1.8	(69.7:26.1: 4.3)	10
107	SAND	0.0:98.8: 1.2	(1.2:67.0:31.8)	10
108	GRANULE-SAND	31.9:67.0: 1.1	(83.4:14.8: 1.8)	10
109	SAND	7.2:91.9: 0.9	(65.6:32.6: 1.8)	14
	Note: Samples 110 - 114 were not collected.			
114	GRANULE	57.5:40.5: 2.0		4
115	SAND	0.7:98.1: 1.2	(7.5:81.7:10.8)	10
116	SAND-GRANULE	19.6:78.4: 2.0	(46.8:33.3:19.9)	12
117	SAND-GRANULE	16.7:81.6: 1.7	(50.9:42.6: 6.5)	14
118	SAND-GRANULE	13.6:85.3: 1.1	(67.7:29.9: 2.4)	108
119	SAND-GRANULE	23.3:74.6: 2.1	(35.4:27.5:37.1)	30
120	SAND	5.6:92.0: 2.4	(63.3:27.1: 9.6)	12
121	SAND	0.1:97.6: 2.3	(3.8:54.0:42.2)	12
122	SAND-GRANULE	13.8:84.5: 1.7	(83.6:12.4: 3.9)	15
123	SAND	9.8:89.1: 1.1	(57.4:40.9: 1.7)	14

Table 10-2 continued on next page.

TABLE 10-2 (continued, p. 4/5)

SAMPLE	FACIES	RATIO	(SAND)	DEPTH
		SEDIMENT SAMPLES FROM DRILL SHIP (BOW/STERN)		
KBZ-4S	MUD	0.0:34.7:65.3		109
KBZ-4B	MUD	0.0:25.1:74.9		109
KBZ-4C1	MUD	0.8:19.8:79.4		109
KBZ-4C2	MUD	0.1:16.5:83.5		109
KCT-5S	SAND	1.5:88.7: 9.9	(32.9:31.9:35.2)	99
KCT-5B	MUDDY SAND	0.0:87.3:12.7	(9.7:28.7:61.6)	99
KDT-6S	GRANULE	60.5:34.2: 5.3		56
KDT-6B	SAND-MUD	0.1:74.6:25.3	(13.3:17.9:68.8)	56
KET-7S	SAND	0.4:90.6: 9.0	(9.7:21.3:69.0)	51
KET-7B	SAND-MUD	0.3:73.0:26.8	(5.2:11.9:82.9)	51
OAM-3	MUDDY SAND	11.8:75.0:13.2	(17.8:11.8:70.4)	108
OBZ-4B	SAND-MUD	0.0:62.5:37.5		199
OCT-5S	SAND-MUD	0.2:66.8:33.0		164
OCT-5B	GRANULE-SAND	31.9:60.6: 7.5		164
ODT-6S	SAND	0.9:89.0:10.1	(27.0:31.1:41.9)	87
ODT-6B	SAND	0.6:94.2: 5.3	(37.4:44.0:18.5)	87
OET-7S	SAND	0.7:93.7: 5.6	(25.2:38.8:36.0)	107
OET-7B	SAND	0.1:91.8: 8.1	(8.3:33.3:58.5)	107
OFT-8S	MUDDY SAND	0.0:84.2:15.8	(14.5:39.0:46.5)	131
OFT-8B	SAND	0.3:94.1: 5.6	(19.6:35.2:45.1)	131
OGT-9S	MUDDY SAND	0.2:79.4:20.5	(7.6:28.0:64.4)	135
OHT-10B	SAND-MUD	0.1:68.8:31.2	(6.8:19.3:73.9)	137
OIT-11S	SAND-MUD	0.5:68.5:31.1	(12.6:20.2:67.1)	155
OIT-11B	SAND-MUD	0.0:64.5:35.4		155
OJT-12S	SAND-MUD	0.0:71.4:28.6	(10.3:20.6:69.1)	144
OJT-12B	GRANULE-SAND-MUD	34.0:54.4:11.6		144
OKT-13S	SAND-MUD	0.0:62.5:37.5		165
OKT-13B	SAND-MUD	0.4:80.1:19.5	(15.0:32.3:52.7)	165
OLT-14S	GRANULE-SAND	42.6:52.3: 5.1		140
OLT-14B	SAND	1.7:88.8: 9.4	(33.8:40.1:26.1)	140
OMT-15S	SAND-MUD	0.5:62.6:37.0		111
OMT-15B	GRANULE	65.6:31.0: 3.6		111
ONT-16S	SAND-MUD	8.3:53.4:38.2		135
ONT-16B	GRANULE	90.7: 6.2: 3.1		135
OOR-17S	GRANULE-SAND-MUD	29.9:62.3: 7.8		55
OOR-17B	GRANULE-SAND-MUD	28.5:54.7:16.8		55
OPZ-18S	SAND-MUD	0.1:63.9:36.0		202
OPZ-18B	MUD	0.1:43.5:56.4		202
OQT-19S	MUDDY SAND	3.9:82.0:14.1	(25.4:27.2:47.3)	118
OQT-19B	SAND-MUD	0.1:78.2:21.7	(15.8:22.8:61.4)	118
ORT-20S	SAND	0.2:90.0: 9.9	(25.9:33.1:40.9)	101
ORT-20B	MUDDY SAND	8.7:79.9:11.4	(28.6:29.2:42.3)	101

Table 10-2 continued on next page.

TABLE 10-2 (continued, p. 5/5)

SAMPLE	FACIES	RATIO	(SAND)	DEPTH
OSR-21S	GRANULE-SAND-MUD	33.9:49.3:16.8		84
OSR-21B	GRANULE-SAND-MUD	29.1:46.7:24.2		84
OSM-22S	SAND-MUD	14.8:54.7:30.5		76
OTG-23S	SAND-MUD	0.3:67.3:32.4	(8.3:19.8:71.9)	164
OTG-23B	MUD	0.0:54.6:45.4		164
OUT-24S	SAND	0.0:95.6: 4.4	(21.7:33.2:45.1)	147
OUT-24B	SAND	0.0:93.7: 6.3	(13.1:31.5:55.4)	147
RXNMASS	GRANULE-SAND-MUD	24.0:58.5:17.5		?

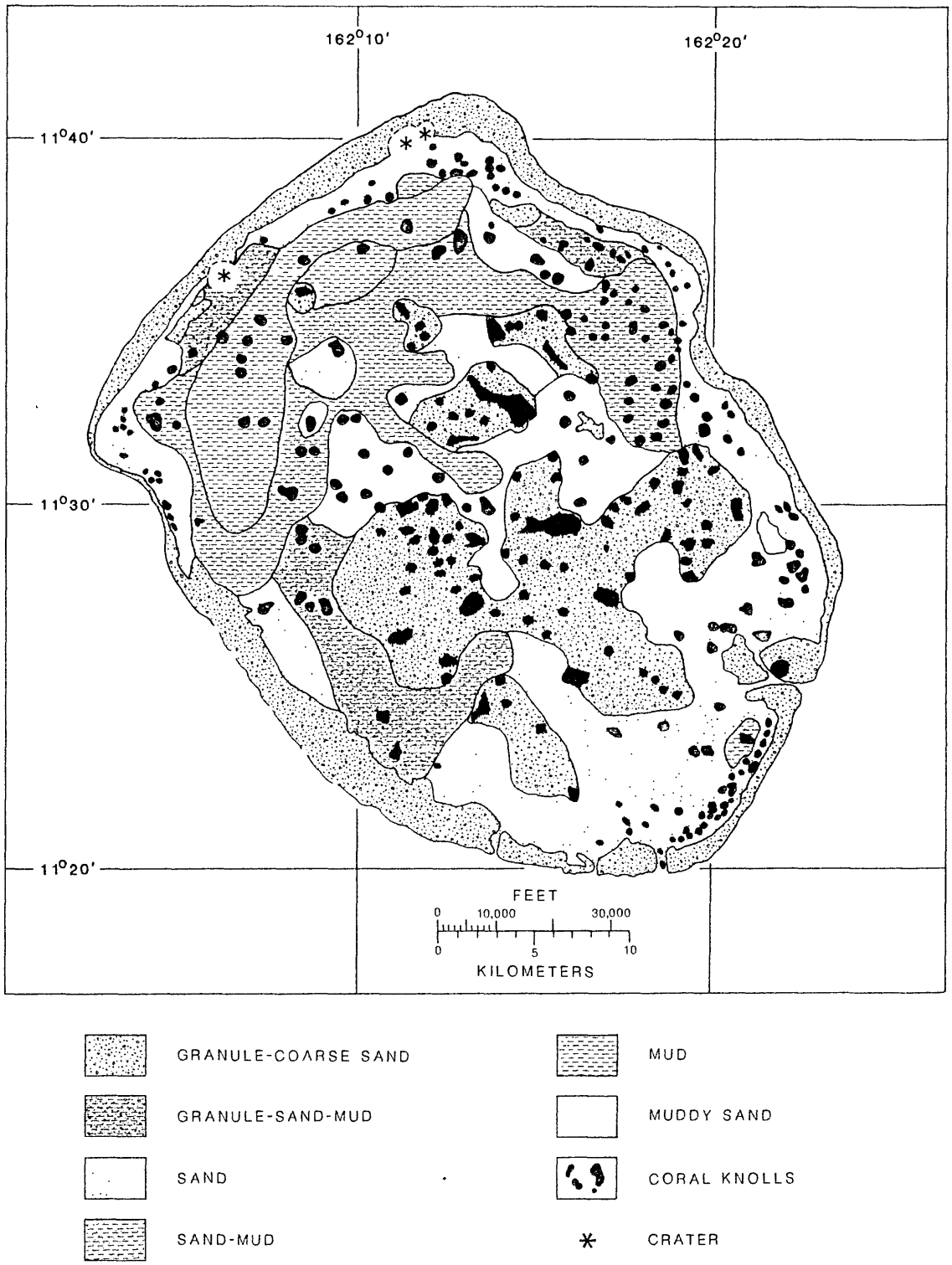

FIGURE 10-5. -- Distribution of sediment facies in Enewetak lagoon (see fig. 10-6).

The Granule-coarse sand (composite) facies forms a band around the edge of the lagoon around most of the reef tract (see fig. 10-5). Note that coarser-grained facies (i.e., facies containing substantial quantities of gravel, cobbles, and boulders) dominate the oceanward side of the islands, particularly on the windward side of the atoll (see Emery, Tracey, and Ladd, 1954, p. 91-95, and referenced plates). These commonly include large coral heads and blocks of cemented reef plate or beach rock ripped up during storms. However, these coarser-grained facies are not separated out from the Granule-coarse sand facies in the current report.

The Granule-coarse sand facies also dominates the sediments in the vicinity of the coral knolls or patch reefs, but these areas are generally too small to map at the scale of Figure 10-5. Dominated by this facies is a large area in the south-central part of the lagoon (fig. 10-5) that contains many large coral knolls that profusely shed sediment.

The Sand facies (facies 5 above, generally foraminifer-rich) forms a band around the lagoonward edge of much of the atoll (fig. 10-5). The small band just inside the lagoon from the reef tract on the northwest side of the atoll extending westward and southward from OAK crater is dominated by well-sorted medium sand characterized by large ripple marks. This particular subfacies occurs in water generally less than 25 ft deep on a broad terrace that rims this part of the lagoon. This area is referred to as the "sand slope" in Halley, Slater, and others (1986, p. 6-7, figs. 4A-B). The Sand facies also occurs peripherally to some large coral knolls and knoll clusters (fig. 10-5).

Mud-rich sediments (Muddy sand, Sand-mud, and Mud facies; facies 6, 7, and 8, respectively) dominate the bottom in the northern half of the lagoon (fig. 10-5). A true Mud facies occurs only in one area, in the northwest, extending from near Enjebi (JANET) toward Biken (LEROY).

CRATER SEDIMENTS

The reader is referred to Folger, Robb, and others (1986) for discussion of the side-scan sonar mosaics of OAK and KOA craters and to Halley, Slater, and others (1986) and Chapter 13 of the current report for generalized details of the bottom features of the craters as observed and mapped from the submersible. These descriptions are augmented from the bottom samples analyzed in the current Chapter.

Generally, sediments sampled within the apparent craters of KOA and OAK are markedly depleted in granule- and coarser-sized grains in comparison with the rest of the lagoon (compare fig. 10-6 with fig. 10-4). Although the northern part of the lagoon tends to be a natural trap for fine-grained sediments, the crater samples, not surprisingly, are apparently enriched in mud (silt plus clay) and fine sand. Most of the exceptions to this generalization are samples taken from the slopes of sand volcanoes or coarse-grained slump deposits, particularly common on the reefward side of OAK crater.

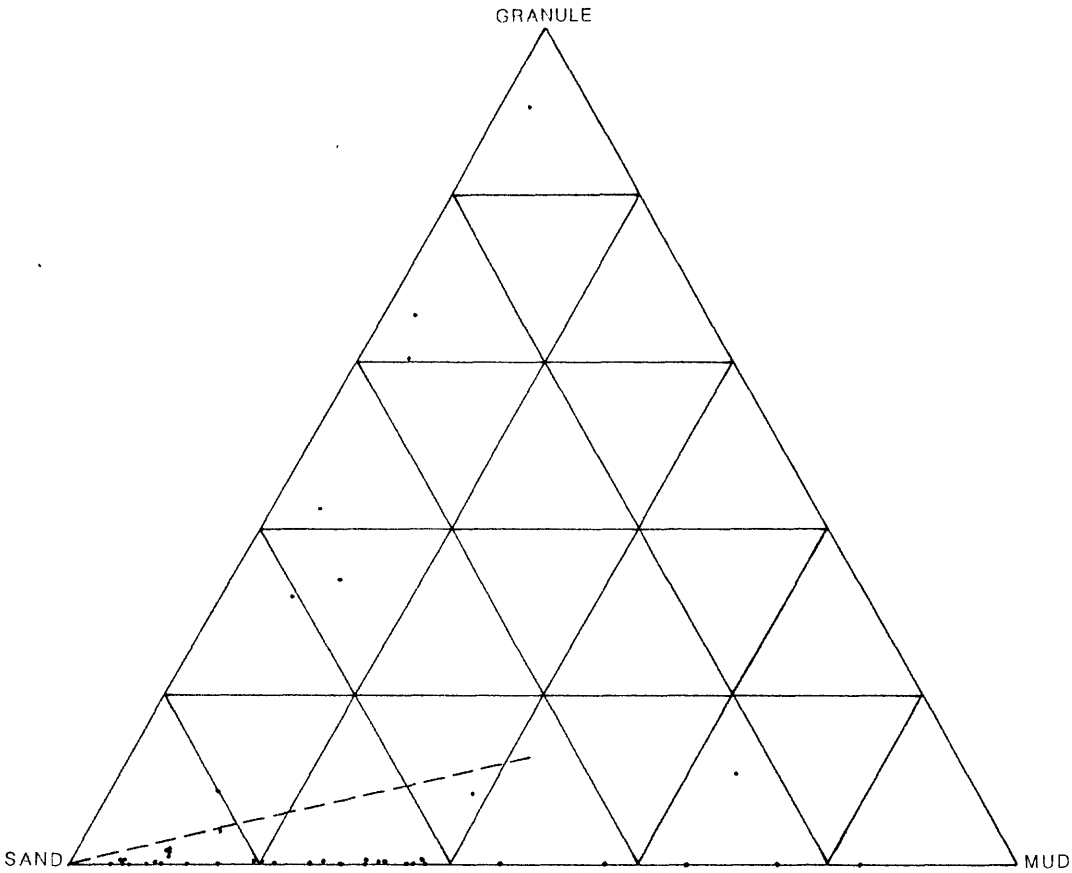

FIGURE 10-6. -- Crater sediments plotted on tertiary diagram of granule, sand, and mud.

The inner bowl of KOA appears to be characterized by a Mud facies whereas OAK appears to be characterized by a Sand-mud facies. KOA and OAK sediments appear to grade outward from the inner bowl to Sand facies. The debris blanket lagoonward of OAK appears to represent patchy sediment distribution of Sand-mud facies and various granule-dominated facies. The distribution of crater sediments was not mapped in detail from the benthic samples because the facies are variable and because of the dearth of data points compared to the size of the craters.

X-RAY MINERALOGY

Twenty-two benthic samples from the PEACE Program were analyzed by x-ray diffraction (Chapter 4). The facies breakdown is given in Table 10-3. Although the data base is not dense, preliminary x-ray analysis of the benthic samples in the northern part of the lagoon shows an anomolous enrichment of calcite (over aragonite and Mg-calcite) in the finer-grained facies in areas near the craters. It is reasonable to infer that much of this muddy material was brought to the surface by the the nuclear explosions from sedimentary layers below the crater that have been diagenetically altered and contain higher percentages of low-magnesium calcite than the modern lagoon sediments.

SUMMARY

Benthic samples from Enewetak Atoll can be subdivided by sediment size-analysis into eight facies: (1) Granule, (2) Granule-sand, (3) Sand-granule , (4) Granule-sand-mud , (5) Sand, (6) Muddy sand, (7) Sand-mud, and (8) Mud. The Granule, Granule-sand, and Sand-granule facies intergrade laterally over short distances and were combined into a composite Granule-coarse sand facies for mapping purposes. The Granule-coarse sand composite facies dominates the reef tract, small areas adjacent to the coral knolls, and much of the south-central portion of the lagoon. The Mud, Sand-mud, and Muddy sand facies dominate the northern part of the lagoon.

Samples from within the apparent craters of KOA and OAK are depleted in coarser-grained components in comparison to the rest of the lagoon floor. Furthermore, the samples are apparently enriched in mud and fine sand. Preliminary x-ray analyses of benthic samples show an anomolous enrichment of calcite (over aragonite and low-Mg calcite) in the finer-grained facies both within the craters and in areas adjacent to them. Some of this finer-grained material undoubtedly was brought to the surface by the numerous nuclear explosions, probably from calcite- depleted layers from beneath the surface that were exposed to diagenesis. And some of this finer-grained material certainly was brought to the surface by piping after the nuclear explosion (see Chapter 14). It should be noted that aerial photographs made a short time after the OAK event (8 hrs) show large plumes of fine-grained, muddy sediment being trailed to the west-southwest from OAK crater by tide-driven currents. Most of these finer-grained sediments were redistributed by normal sedimentary and biologic processes within the northern part of the lagoon, which tends to be a sink or trap for finer-grained material.

TABLE 10-3. -- Results of x-ray diffraction analyses of benthic samples from Enewetak lagoon (data combined from Tables 4-34 and 10-2).

Sample Number	Facies	Weight Percent Calcite	Mg Calcite	Aragonite
9	Mud	15	15	70
16	Sand-granule	8	17	75
17	Sand-granule	2	5	93
26	Muddy sand	6	12	82
29	Sand-mud	8	24	68
30	Muddy sand	8	12	80
32	Mud	16	21	63
37	Mud	10	13	77
38	Mud	23	19	58
39	Mud	27	18	55
43	Mud	8	15	77
58	Muddy sand	7	15	78
63	Sand-granule	8	20	72
65	Sand-mud	9	16	75
74	Granule-sand-mud	7	11	82
78	Sand	2	6	92
83	Sand-granule	10	10	80
89	Sand-mud	7	8	85
91	Sand	3	4	93
104	Sand	3	22	75
118	Sand-granule	3	7	90
123	Sand	7	25	68

REFERENCES

Cronin, T.M., Brouwers, E.M., Bybell, L.M., Edwards, E.E., Gibson, T.G.,Margerum, R., and Poore, R.Z., 1986, Pacific Enewetak Atoll Crater Exploration (PEACE) Program, Enewetak Atoll, Republic of the Marshall Islands; Part 2: Paleontology and biostratigraphy, application to OAK and KOA craters: U.S. Geological Survey Open-File Report 86-159, 39 p., 20 figs., 12 tbls., 3 appendices.

Cushman, J.A., Todd, Ruth, and Post, R.J., 1986, Recent Foraminifera of the Marshall Islands: U.S. Geological Survey Professional Paper 260-H, p. 319-333, pls. 82-93, figs. 116-118, 5 tbls.

Emery, K.O., Tracey, J.I., Jr., and Ladd, H.S., 1954, Geology of Bikini and nearby atolls: U.S. Geological Survey Professional Paper 260-A, 265 p., 73 pls., 84 figs., 11 charts, 27 tbls.

Folger, D.W., Robb, J.M., Hampson, J.C., Davis, P.A., Bridges, P.M., and Roddy, D.J., 1986, Sidescan-sonar survey of OAK and KOA craters; 18 p., 6 figs.; in Folger, D.W., ed., Sea-floor observations and subbottom seismic characteristics of OAK and KOA craters, Enewetak Atoll, Marshall Islands: U.S. Geological Survey Bulletin 1678.

Folk, R.L., 1974, Petrology of Sedimentary Rocks; Hemphill Publishing Company, Austin, Texas, 182 p., unnumbered figs. [Note: this laboratory guide was published in several versions beginning in 1968 and was copyrighted in 1974.]

Halley, R.B., Slater, R.A., Shinn, E.A., Folger, D.W., Hudson, J.H., Kindinger, J.L., and Roddy, D.J., 1986, Observations of OAK and KOA craters from the submersible; 32 p., 13 figs., 1 appendix; in Folger, D.W., ed., Sea-floor observations and subbottom seismic characteristics of OAK and KOA craters, Enewetak Atoll, Marshall Islands: U.S. Geological Survey Bulletin 1678.

Henry, T.W., Wardlaw, B.R., Skipp, B.A., Major, R.P., and Tracey, J.I., Jr., 1986, Pacific Enewetak Atoll Crater Exploration (PEACE) Program, Enewetak Atoll, Republic of the Marshall Islands; Part 1: Drilling operations and descriptions of boreholes in vicinity of KOA and OAK craters: U.S. Geological Survey Open-File Report 86-419, 497 p., 32 figs., 29 pls., 13 tbls., 3 appendices.

McMurtry, G.M., Schneider, R.C., Colin, P.K., Buddemeier, R.W., and Suchanek, R.H., 1985, Redistribution of fallout radionuclides in Enewetak Atoll lagoon sediments by calianassid bioturbation: Nature, v. 313, no. 6004, p. 674-677, 3 figs., 1 tbl.

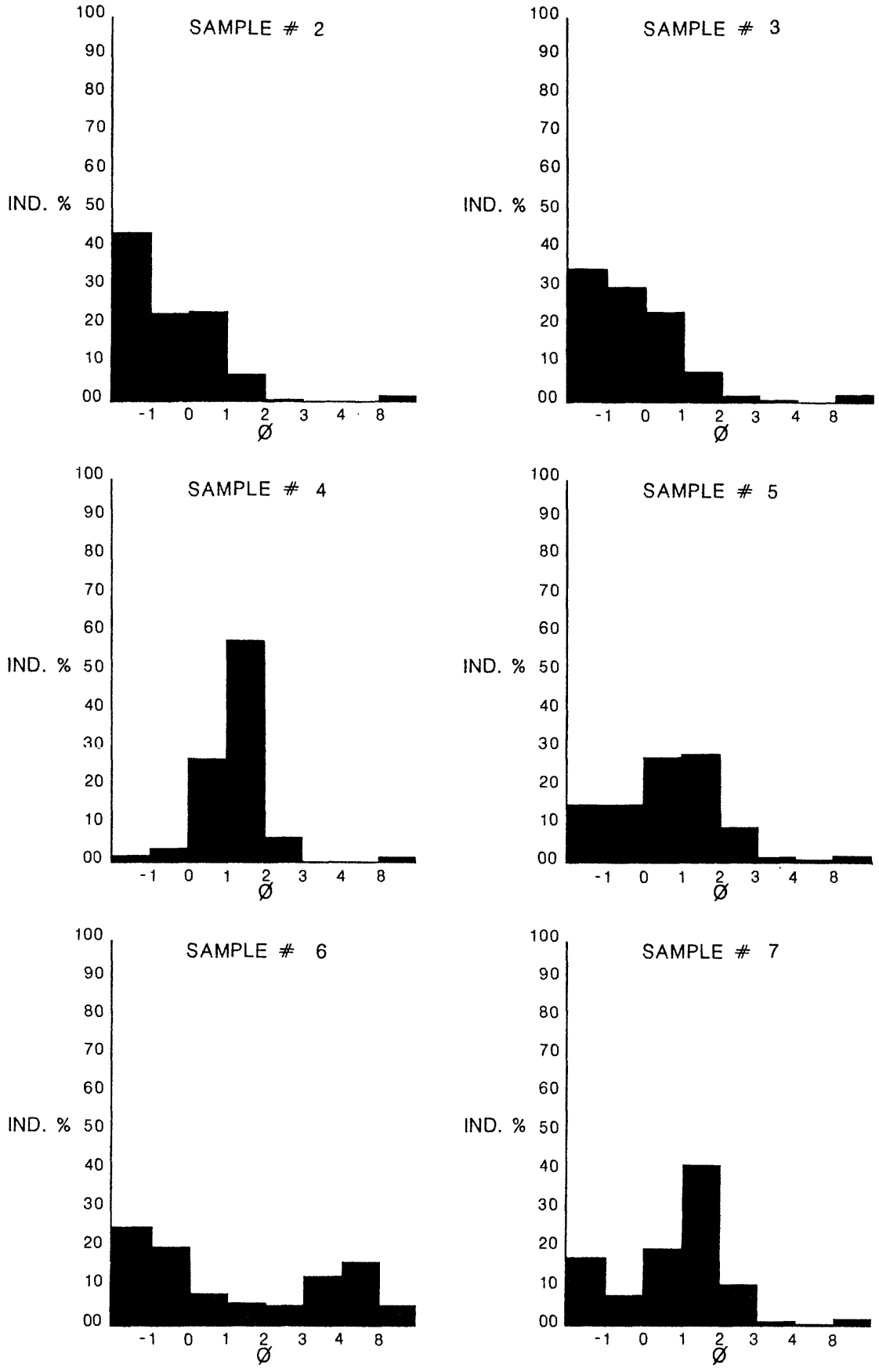
SAMPLE # 2
SAMPLE # 3
SAMPLE # 4
SAMPLE # 5
SAMPLE # 6
SAMPLE # 7
IND. %
100
90
80
70
60
50
40
30
20
10
00
-1 0 1 2 3 4 8
Ø

PLATE 10-1

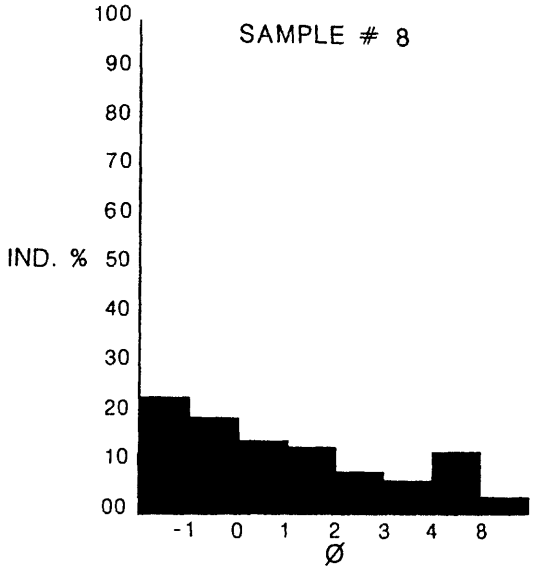
SAMPLE # 8
IND. %
100
90
80
70
60
50
40
30
20
10
00
-1 0 1 2 3 4 8
Ø

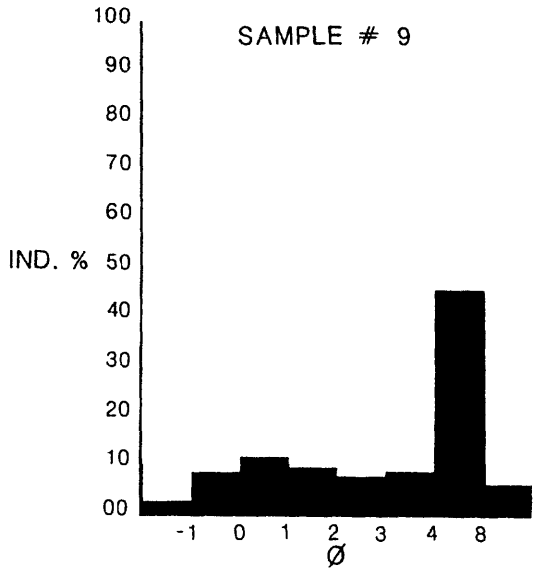
SAMPLE # 9
IND. %
100
90
80
70
60
50
40
30
20
10
00
-1 0 1 2 3 4 8
Ø

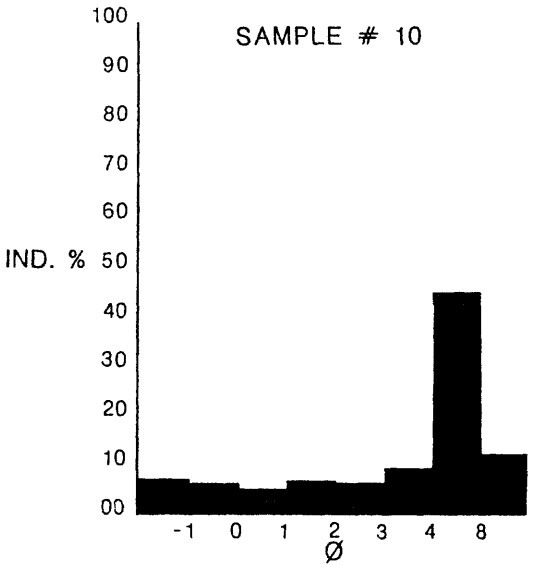
SAMPLE # 10
IND. %
100
90
80
70
60
50
40
30
20
10
00
-1 0 1 2 3 4 8
Ø

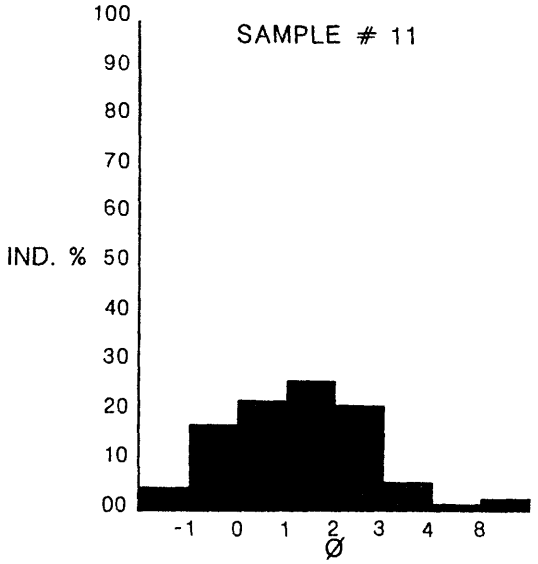
SAMPLE # 11
IND. %
100
90
80
70
60
50
40
30
20
10
00
-1 0 1 2 3 4 8
Ø

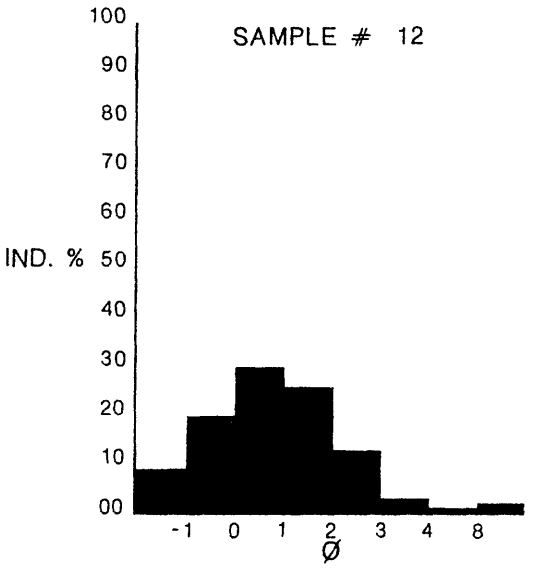
SAMPLE # 12
IND. %
100
90
80
70
60
50
40
30
20
10
00
-1 0 1 2 3 4 8
Ø

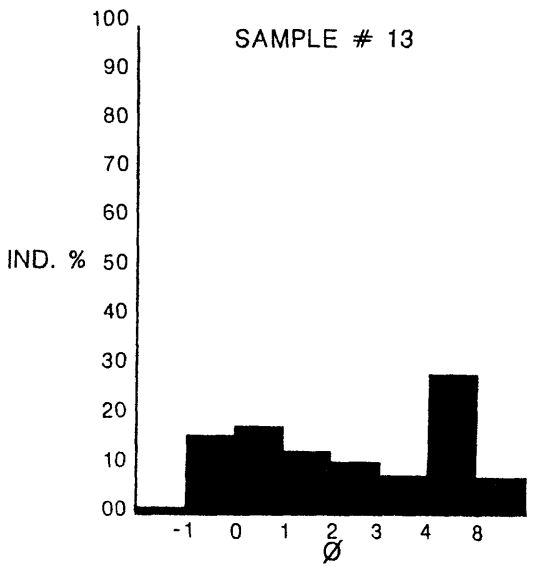
SAMPLE # 13
IND. %
100
90
80
70
60
50
40
30
20
10
00
-1 0 1 2 3 4 8
Ø

PLATE 10-2

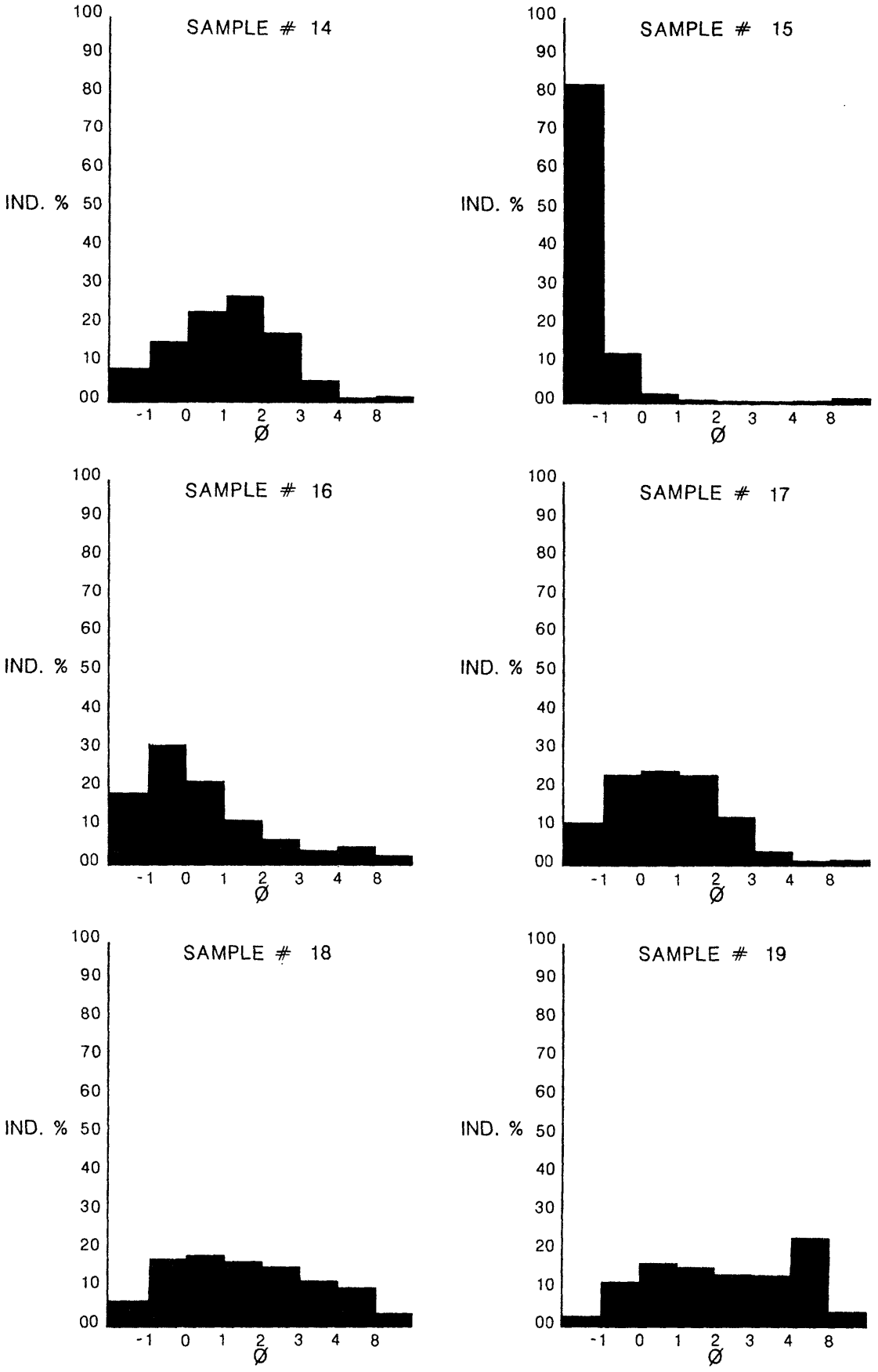
SAMPLE # 14
SAMPLE # 15
SAMPLE # 16
SAMPLE # 17
SAMPLE # 18
SAMPLE # 19
IND. %
100
90
80
70
60
50
40
30
20
10
00
-1 0 1 2 3 4 8
Ø

PLATE 10-3

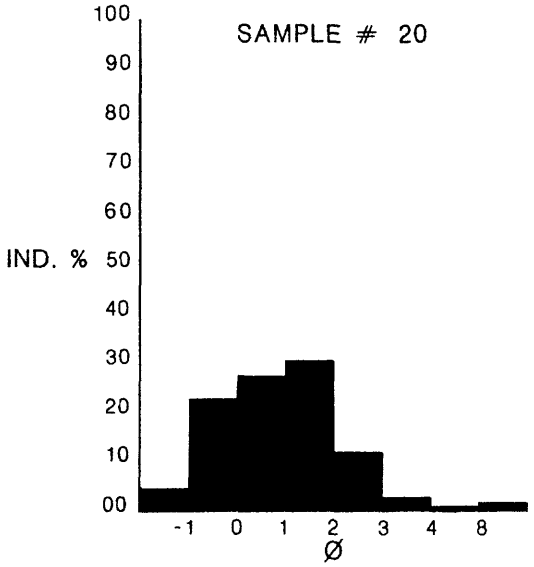
SAMPLE # 20
IND. %
100
90
80
70
60
50
40
30
20
10
00
-1 0 1 2 3 4 8
Ø

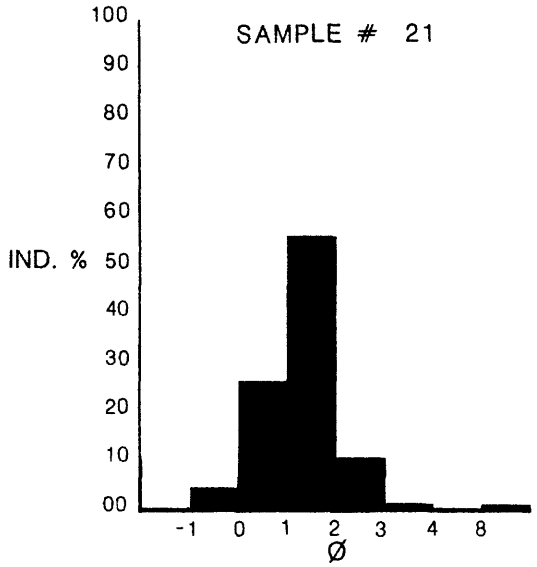
SAMPLE # 21
IND. %
100
90
80
70
60
50
40
30
20
10
00
-1 0 1 2 3 4 8
Ø

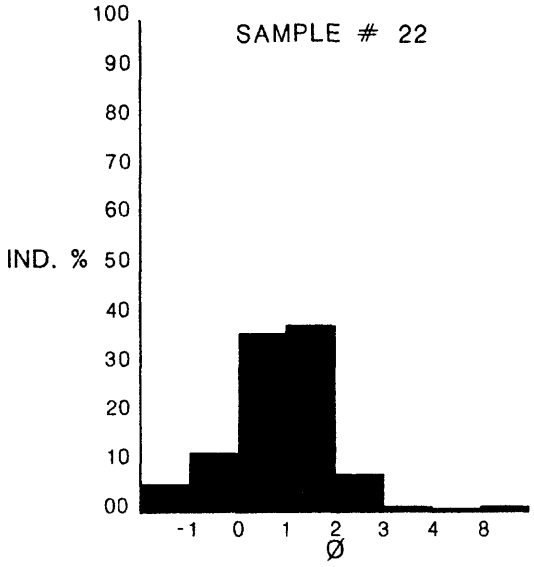
SAMPLE # 22
IND. %
100
90
80
70
60
50
40
30
20
10
00
-1 0 1 2 3 4 8
Ø

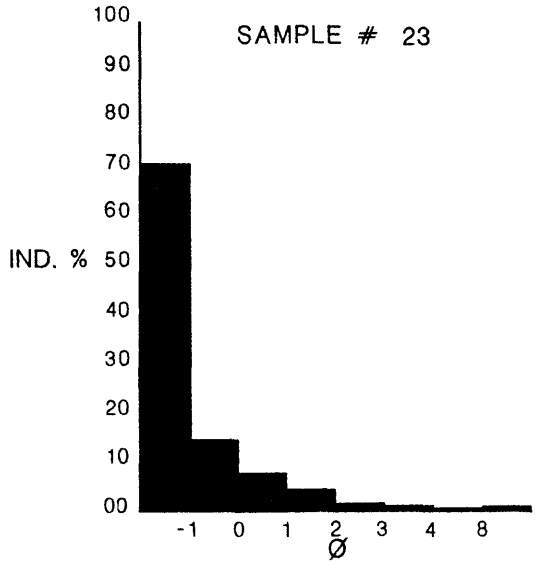
SAMPLE # 23
IND. %
100
90
80
70
60
50
40
30
20
10
00
-1 0 1 2 3 4 8
Ø

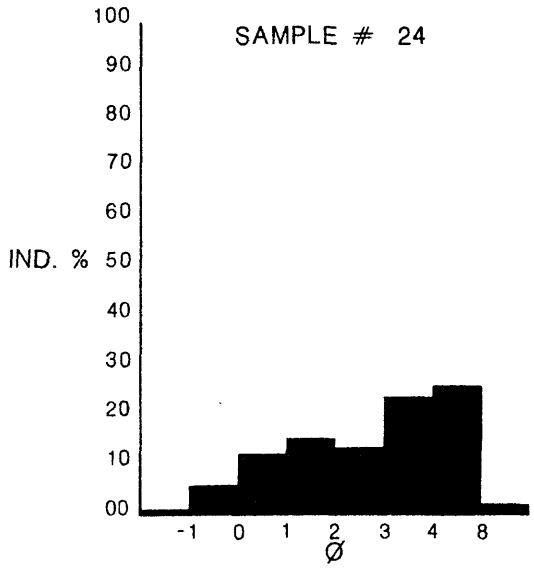
SAMPLE # 24
IND. %
100
90
80
70
60
50
40
30
20
10
00
-1 0 1 2 3 4 8
Ø

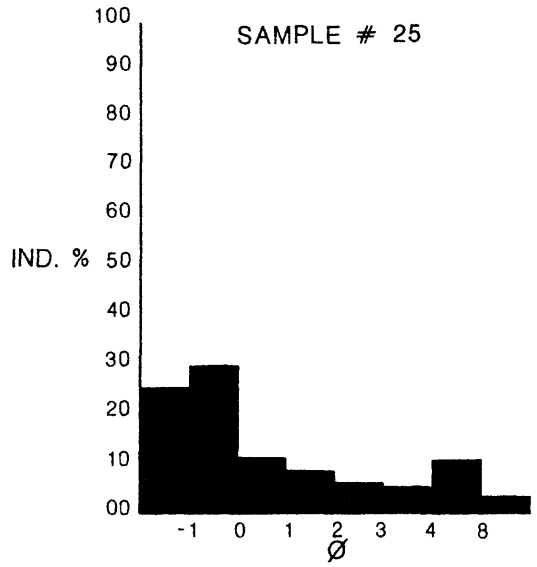
SAMPLE # 25
IND. %
100
90
80
70
60
50
40
30
20
10
00
-1 0 1 2 3 4 8
Ø

PLATE 10-4

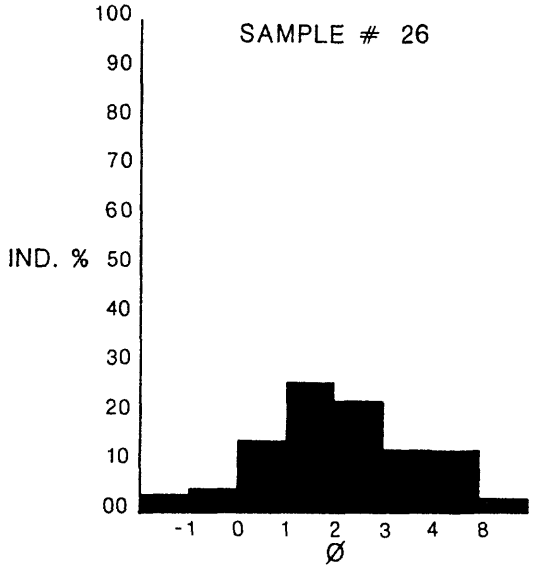
SAMPLE # 26
IND. %
100
90
80
70
60
50
40
30
20
10
00
-1 0 1 2 3 4 8
Ø

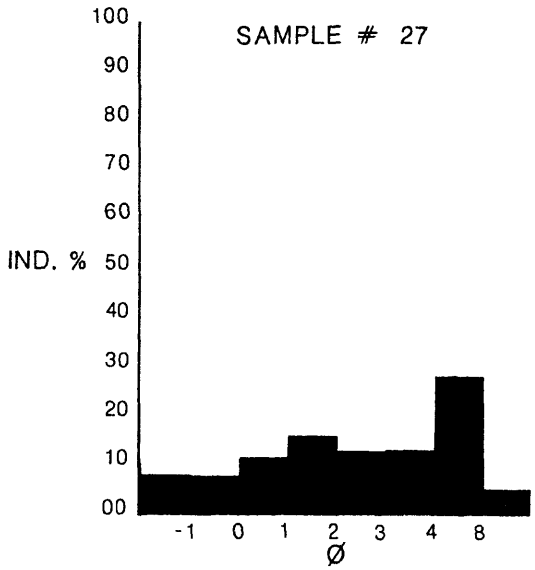
SAMPLE # 27
IND. %
100
90
80
70
60
50
40
30
20
10
00
-1 0 1 2 3 4 8
Ø

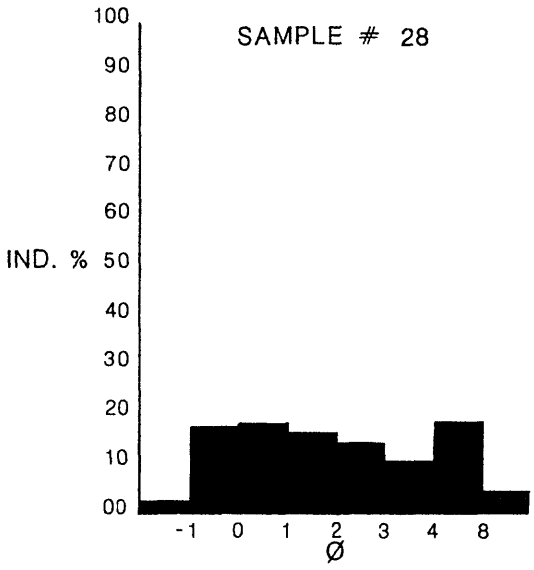
SAMPLE # 28
IND. %
100
90
80
70
60
50
40
30
20
10
00
-1 0 1 2 3 4 8
Ø

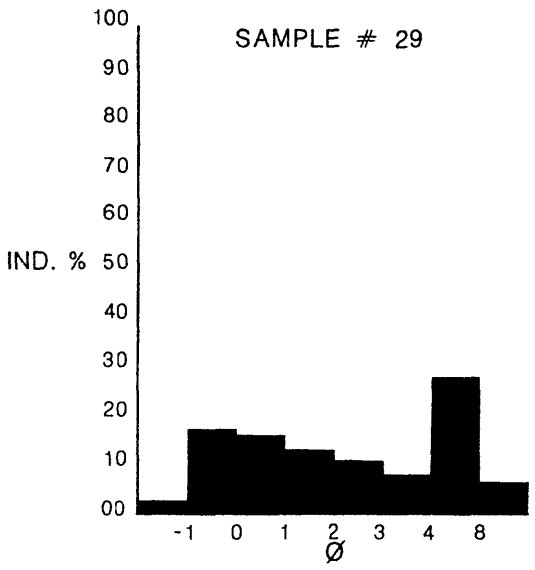
SAMPLE # 29
IND. %
100
90
80
70
60
50
40
30
20
10
00
-1 0 1 2 3 4 8
Ø

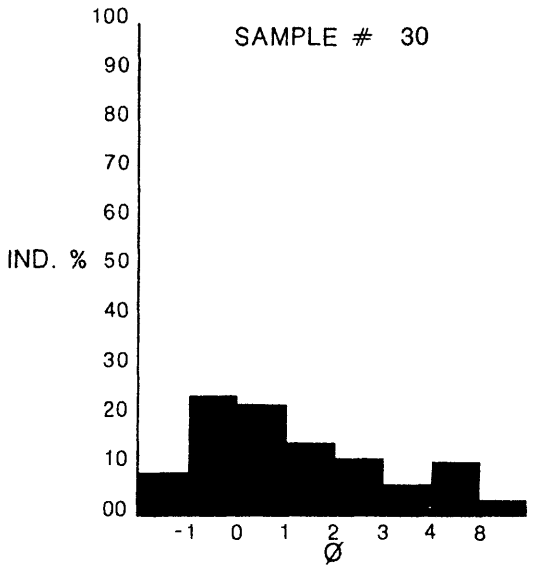
SAMPLE # 30
IND. %
100
90
80
70
60
50
40
30
20
10
00
-1 0 1 2 3 4 8
Ø

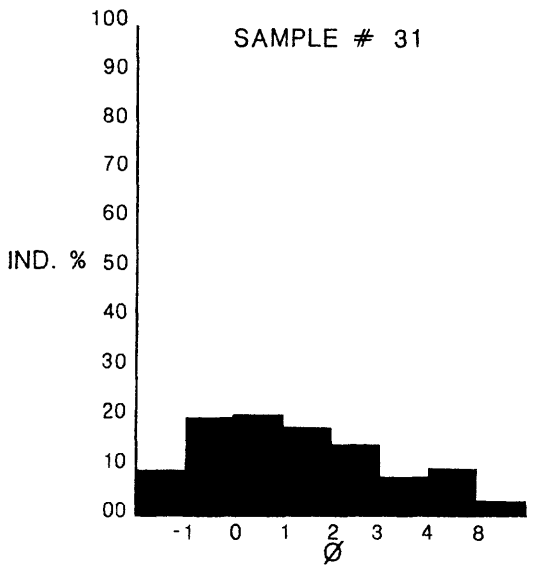
SAMPLE # 31
IND. %
100
90
80
70
60
50
40
30
20
10
00
-1 0 1 2 3 4 8
Ø

PLATE 10-5

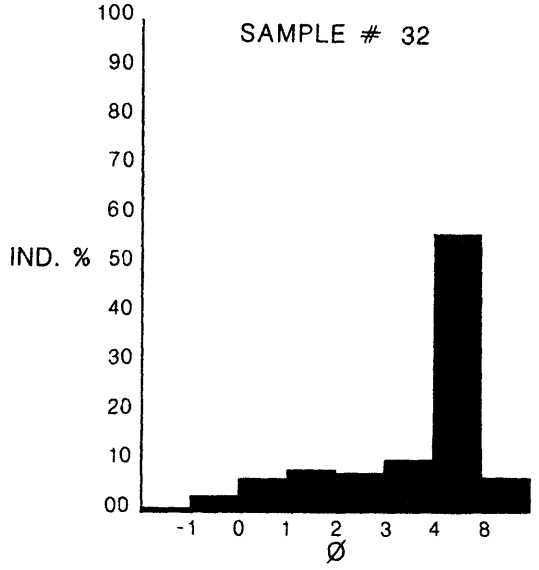
SAMPLE # 32
IND. %
100
90
80
70
60
50
40
30
20
10
00
-1 0 1 2 3 4 8
Ø

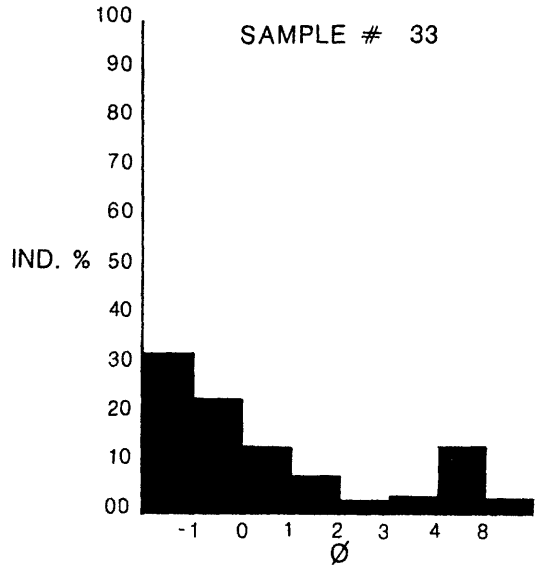
SAMPLE # 33
IND. %
100
90
80
70
60
50
40
30
20
10
00
-1 0 1 2 3 4 8
Ø

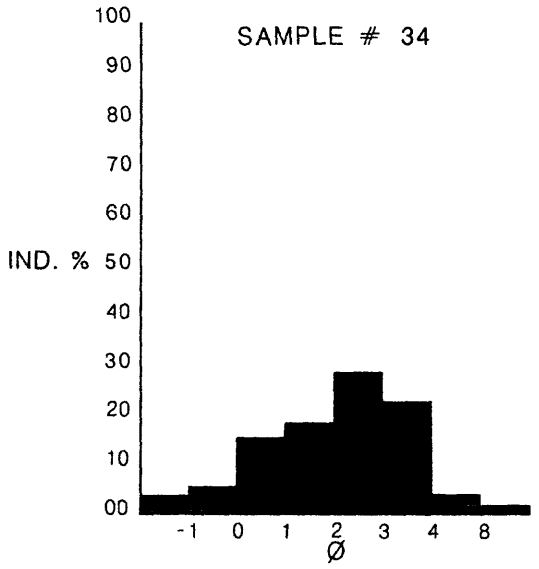
SAMPLE # 34
IND. %
100
90
80
70
60
50
40
30
20
10
00
-1 0 1 2 3 4 8
Ø

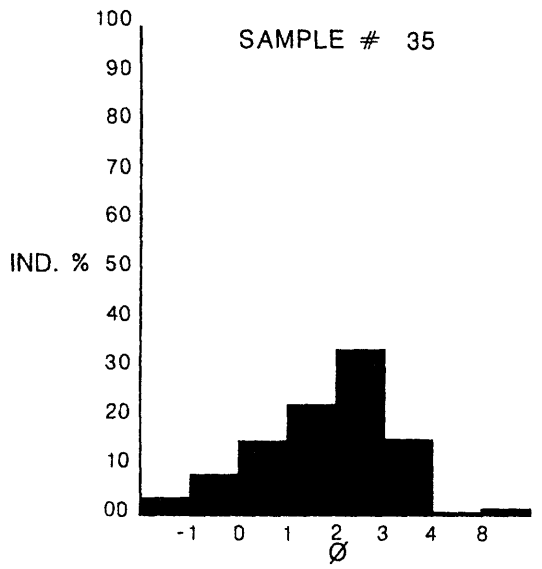
SAMPLE # 35
IND. %
100
90
80
70
60
50
40
30
20
10
00
-1 0 1 2 3 4 8
Ø

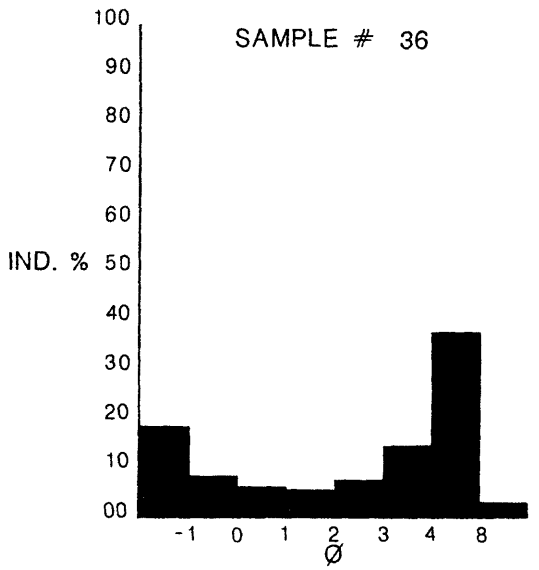
SAMPLE # 36
IND. %
100
90
80
70
60
50
40
30
20
10
00
-1 0 1 2 3 4 8
Ø

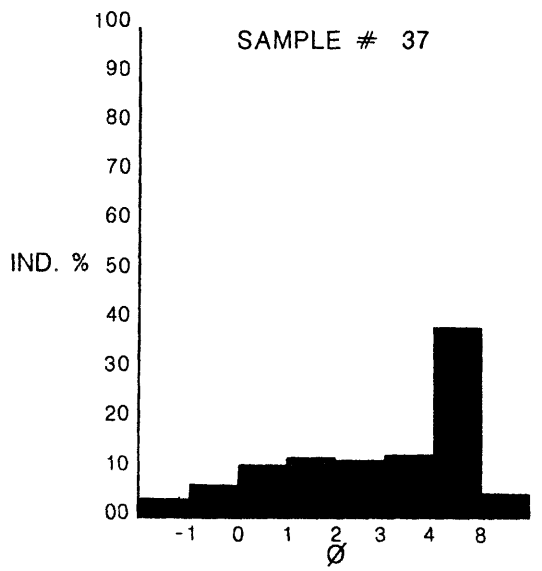
SAMPLE # 37
IND. %
100
90
80
70
60
50
40
30
20
10
00
-1 0 1 2 3 4 8
Ø

PLATE 10-6

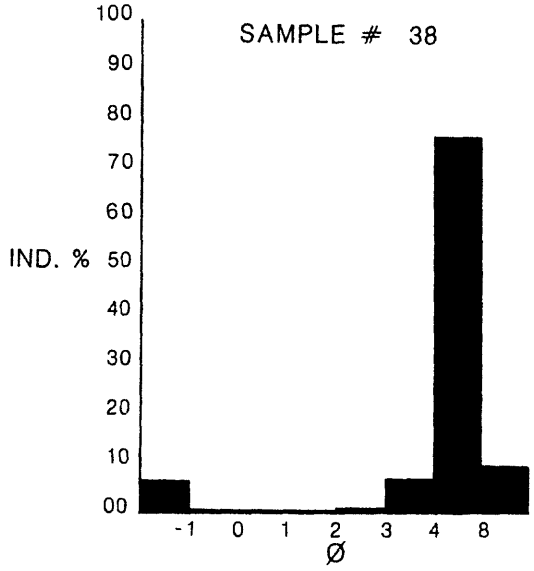
SAMPLE # 38
IND. %
100
90
80
70
60
50
40
30
20
10
00
-1 0 1 2 3 4 8
Ø

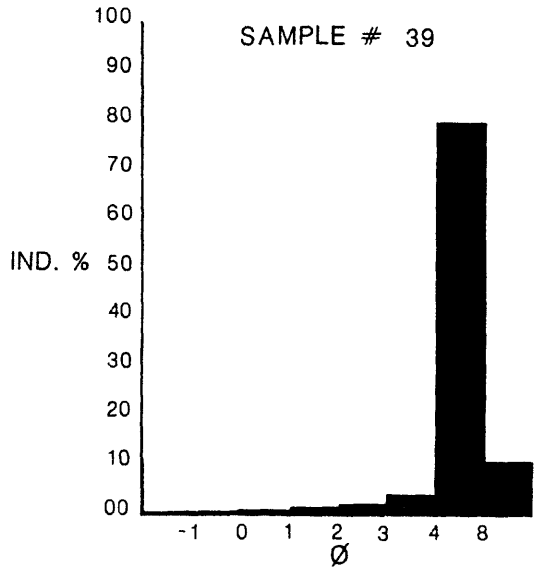
SAMPLE # 39
IND. %
100
90
80
70
60
50
40
30
20
10
00
-1 0 1 2 3 4 8
Ø

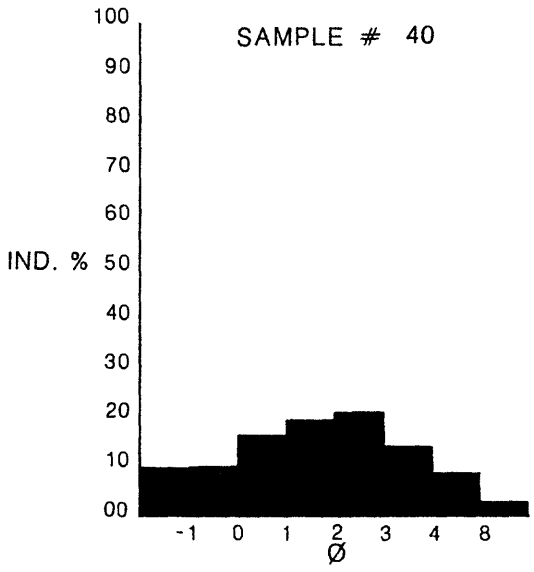
SAMPLE # 40
IND. %
100
90
80
70
60
50
40
30
20
10
00
-1 0 1 2 3 4 8
Ø

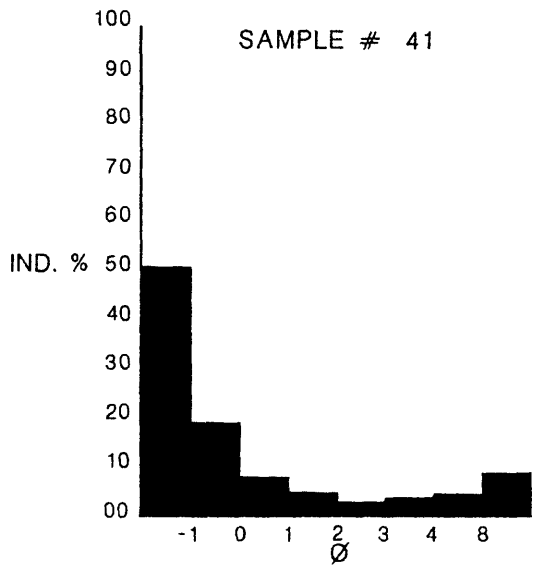
SAMPLE # 41
IND. %
100
90
80
70
60
50
40
30
20
10
00
-1 0 1 2 3 4 8
Ø

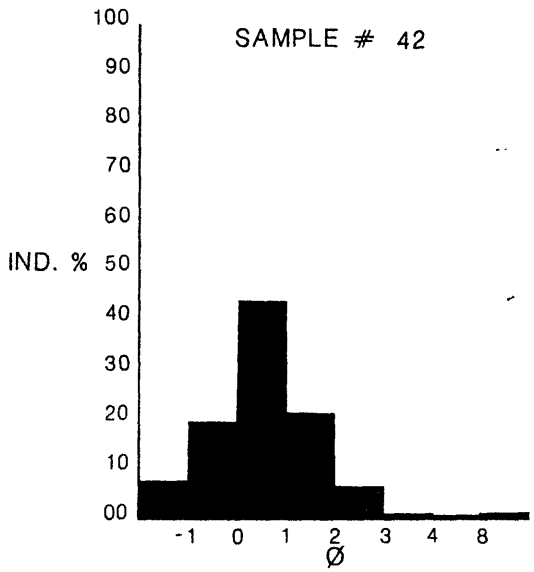
SAMPLE # 42
IND. %
100
90
80
70
60
50
40
30
20
10
00
-1 0 1 2 3 4 8
Ø

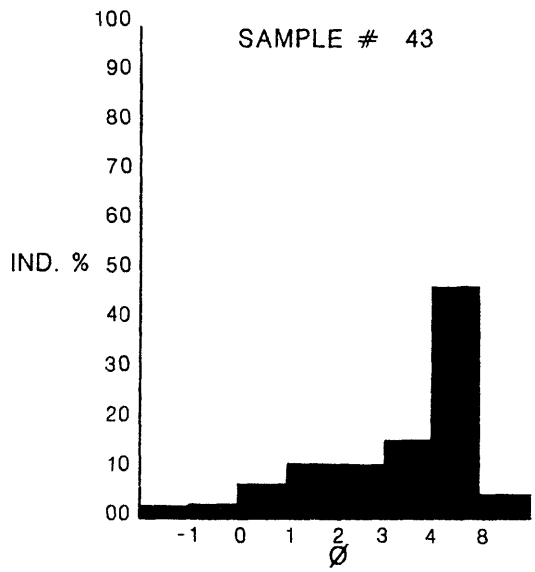
SAMPLE # 43
IND. %
100
90
80
70
60
50
40
30
20
10
00
-1 0 1 2 3 4 8
Ø

PLATE 10-7

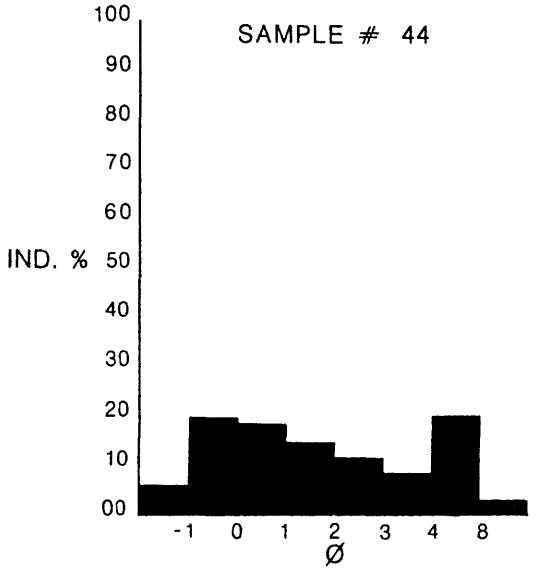
SAMPLE # 44
IND. %
100
90
80
70
60
50
40
30
20
10
00
-1 0 1 2 3 4 8
Ø

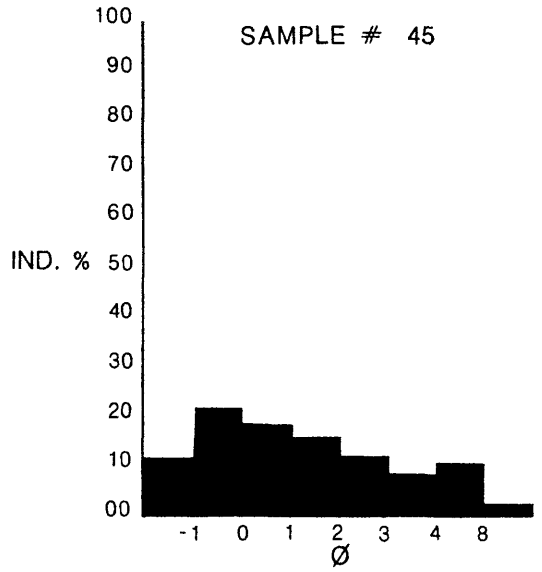
SAMPLE # 45
IND. %
100
90
80
70
60
50
40
30
20
10
00
-1 0 1 2 3 4 8
Ø

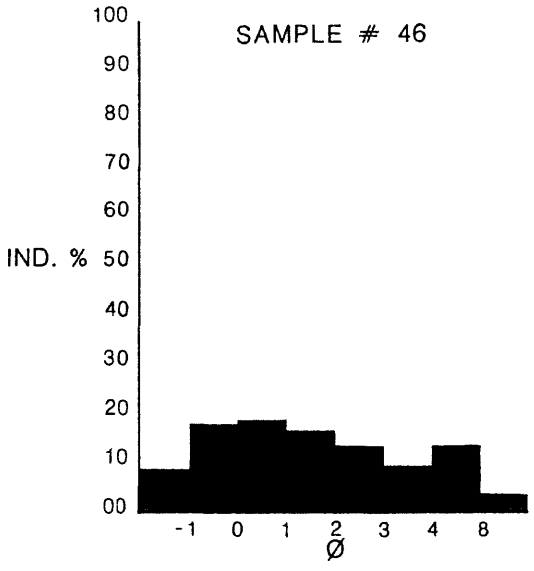
SAMPLE # 46
IND. %
100
90
80
70
60
50
40
30
20
10
00
-1 0 1 2 3 4 8
Ø

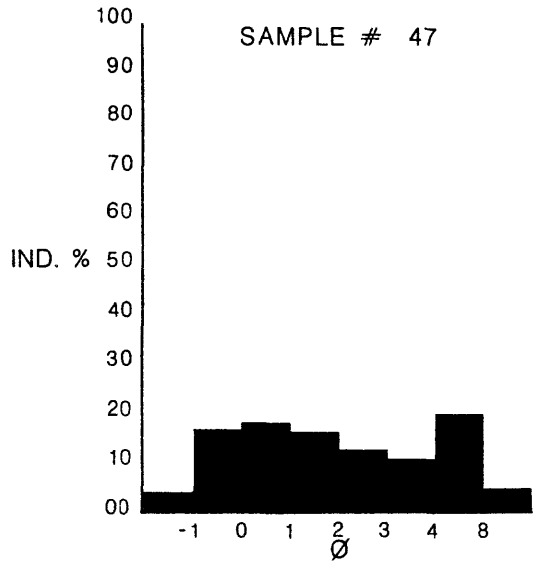
SAMPLE # 47
IND. %
100
90
80
70
60
50
40
30
20
10
00
-1 0 1 2 3 4 8
Ø

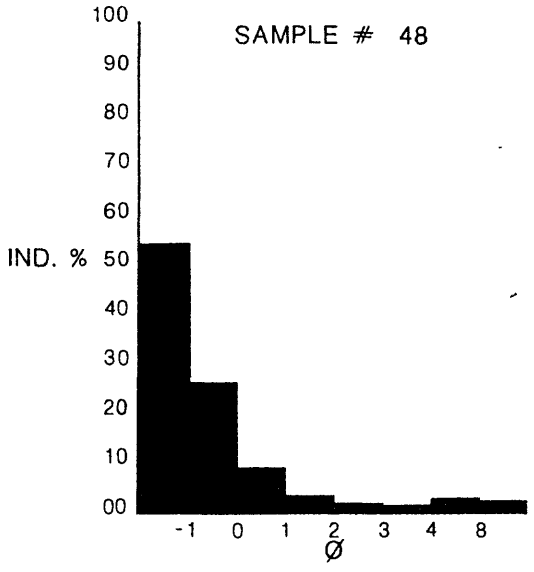
SAMPLE # 48
IND. %
100
90
80
70
60
50
40
30
20
10
00
-1 0 1 2 3 4 8
Ø

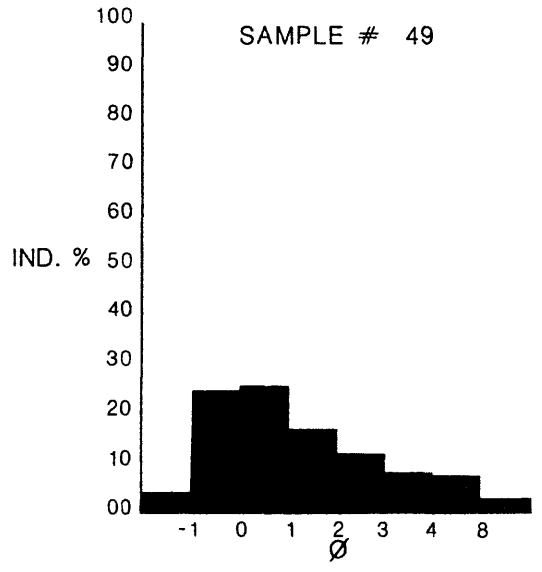
SAMPLE # 49
IND. %
100
90
80
70
60
50
40
30
20
10
00
-1 0 1 2 3 4 8
Ø

PLATE 10-8

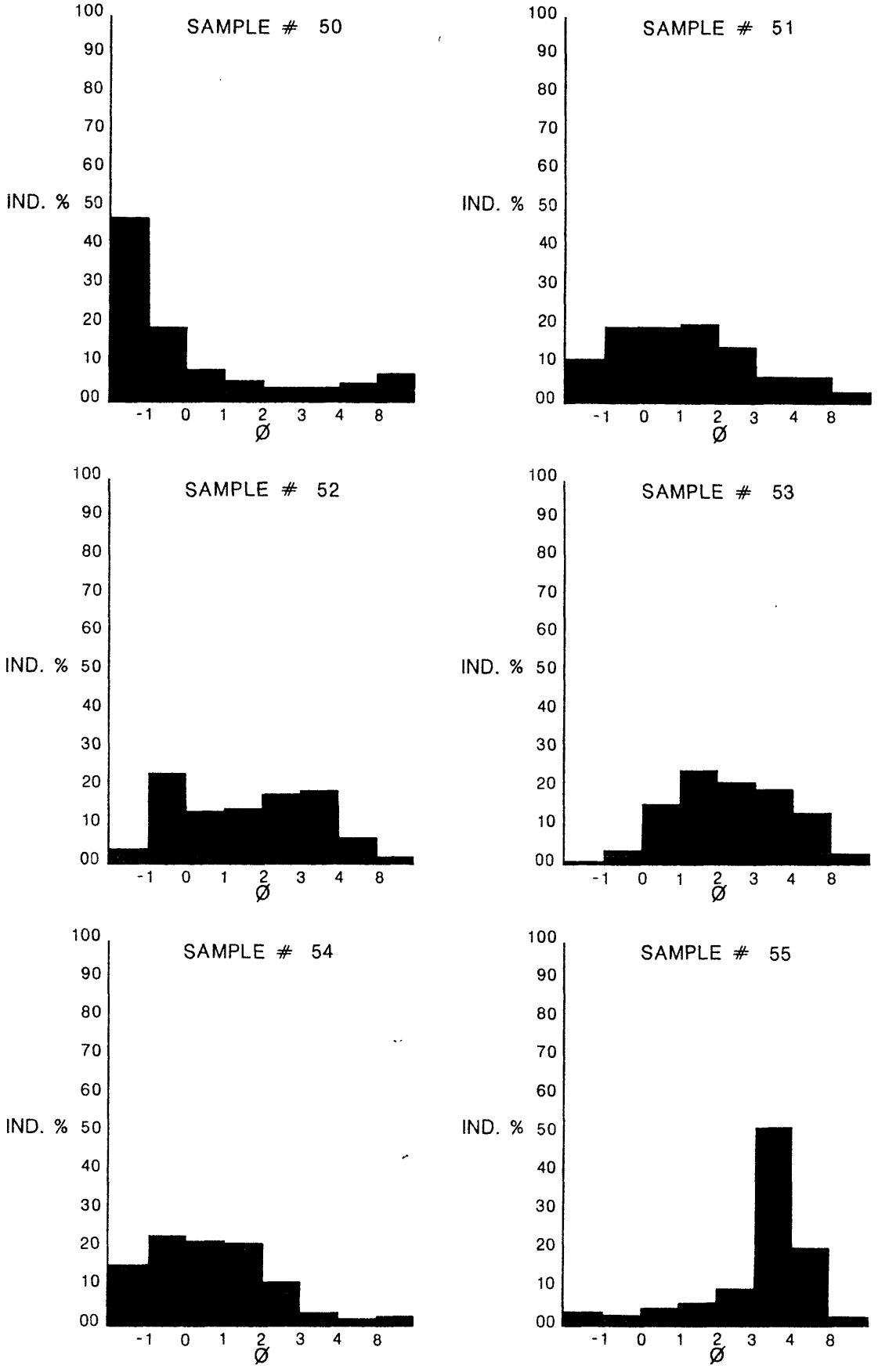
SAMPLE # 50
SAMPLE # 51
SAMPLE # 52
SAMPLE # 53
SAMPLE # 54
SAMPLE # 55
IND. %
100
90
80
70
60
50
40
30
20
10
00
-1 0 1 2 3 4 8
Ø

PLATE 10-9

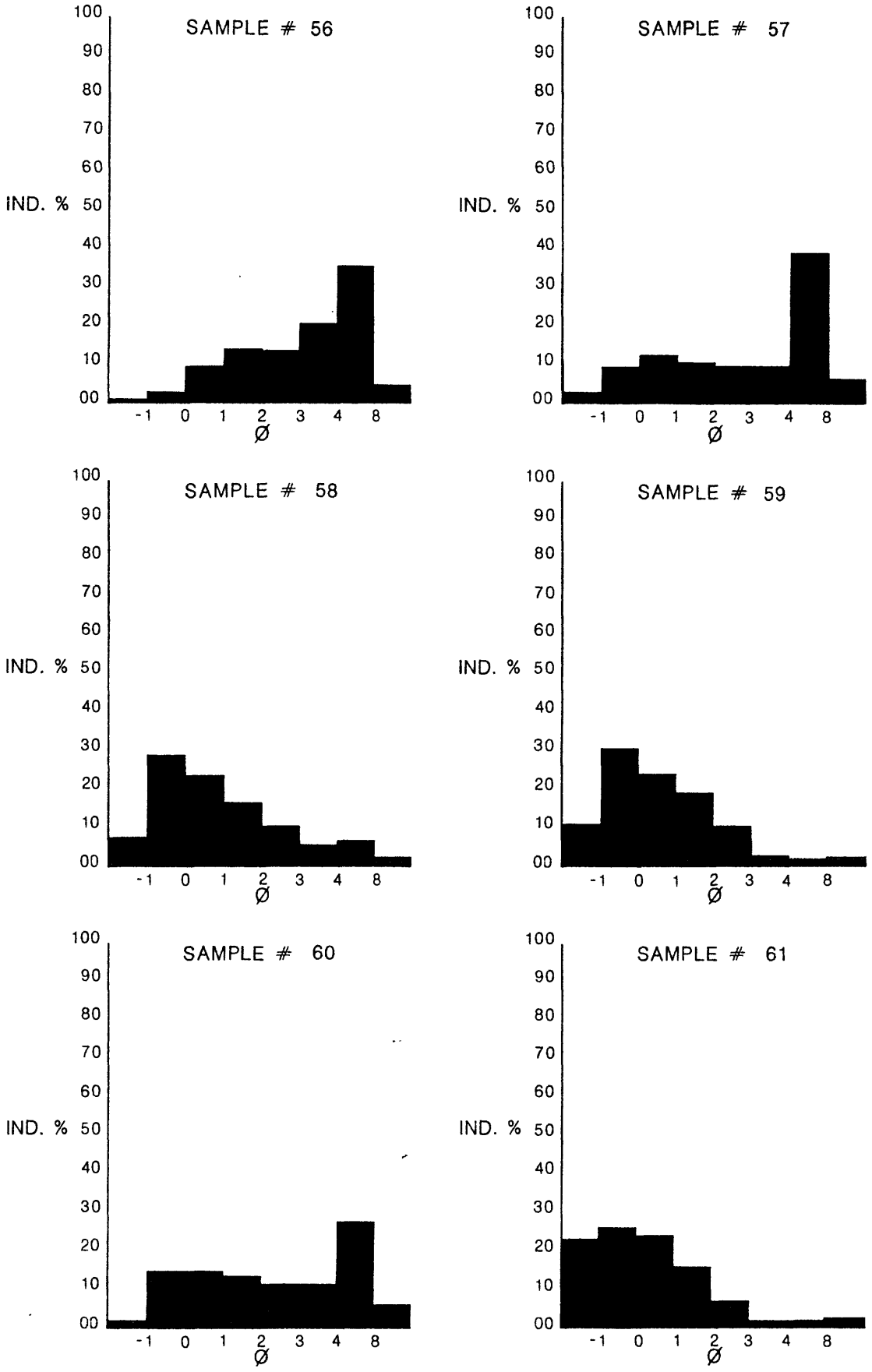
SAMPLE # 56
SAMPLE # 57
SAMPLE # 58
SAMPLE # 59
SAMPLE # 60
SAMPLE # 61
IND. %
100
90
80
70
60
50
40
30
20
10
00
-1 0 1 2 3 4 8
Ø

PLATE 10-10

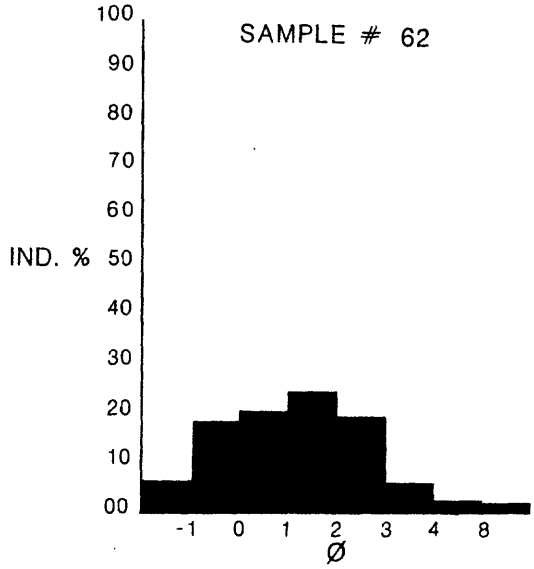
SAMPLE # 62
IND. %
100
90
80
70
60
50
40
30
20
10
00
-1 0 1 2 3 4 8
Ø

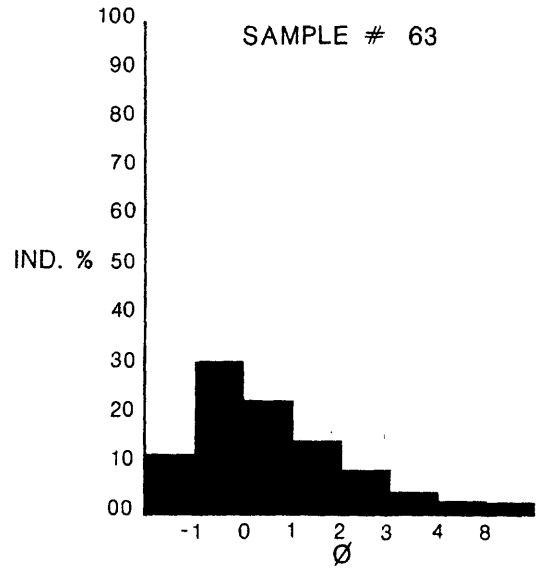
SAMPLE # 63
IND. %
100
90
80
70
60
50
40
30
20
10
00
-1 0 1 2 3 4 8
Ø

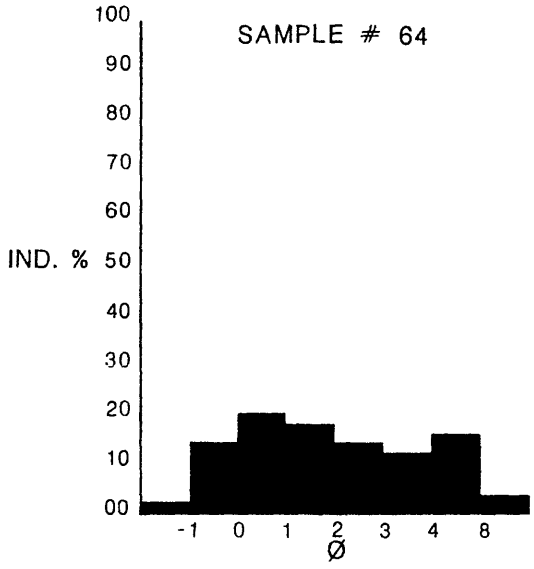
SAMPLE # 64
IND. %
100
90
80
70
60
50
40
30
20
10
00
-1 0 1 2 3 4 8
Ø

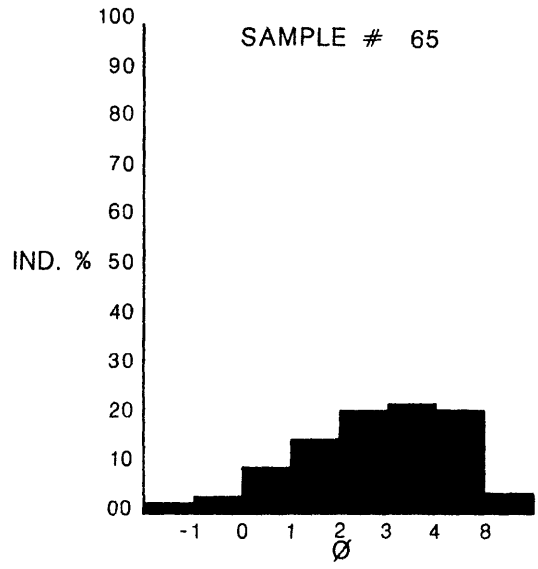
SAMPLE # 65
IND. %
100
90
80
70
60
50
40
30
20
10
00
-1 0 1 2 3 4 8
Ø

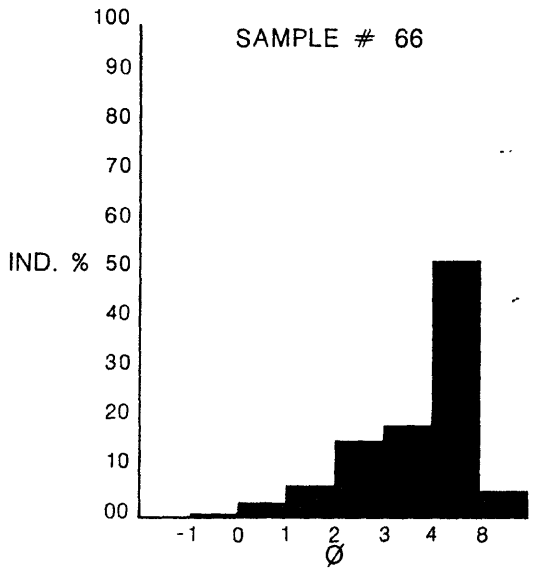
SAMPLE # 66
IND. %
100
90
80
70
60
50
40
30
20
10
00
-1 0 1 2 3 4 8
Ø

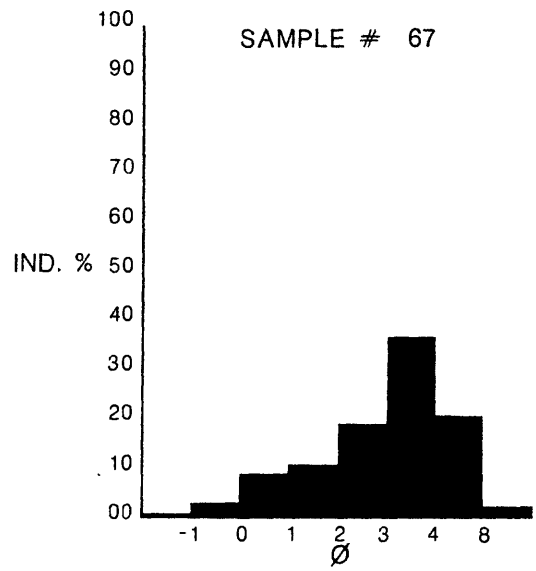
SAMPLE # 67
IND. %
100
90
80
70
60
50
40
30
20
10
00
-1 0 1 2 3 4 8
Ø

PLATE 10-11

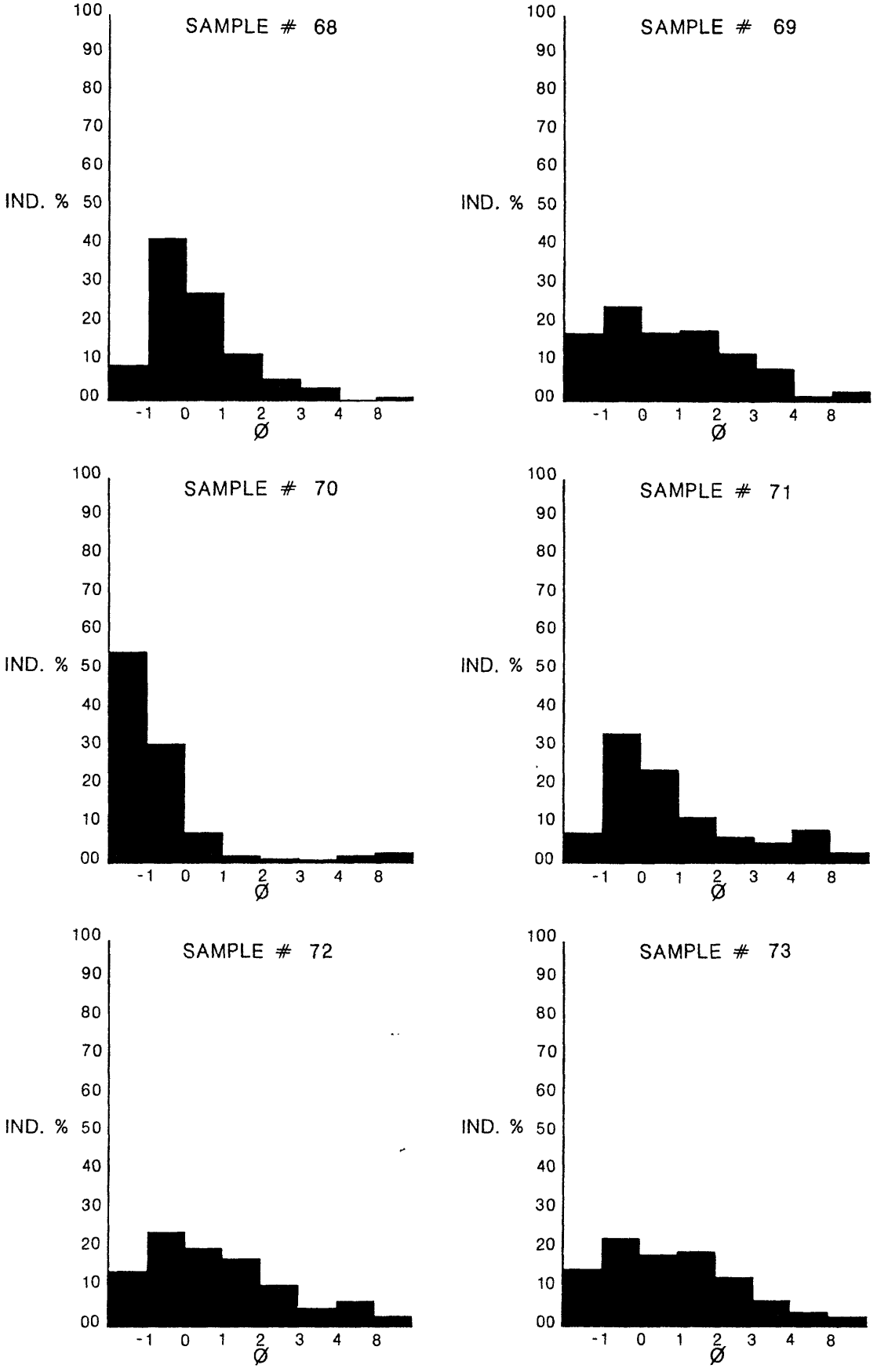
SAMPLE # 68
SAMPLE # 69
SAMPLE # 70
SAMPLE # 71
SAMPLE # 72
SAMPLE # 73
IND. %
100
90
80
70
60
50
40
30
20
10
00
-1 0 1 2 3 4 8
Ø

PLATE 10-12

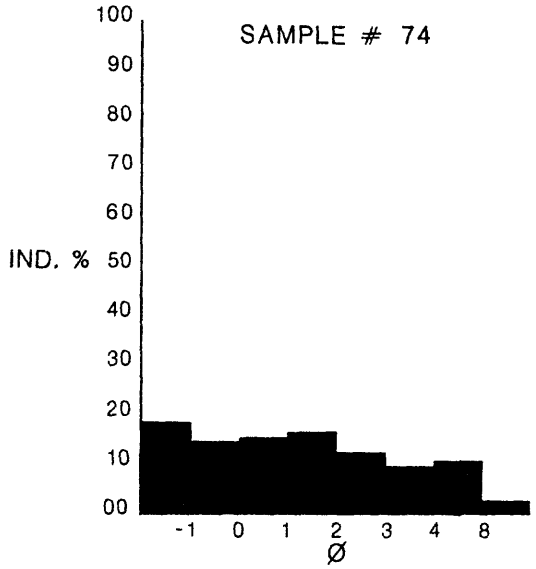
SAMPLE # 74
IND. %
100
90
80
70
60
50
40
30
20
10
00
-1 0 1 2 3 4 8
Ø

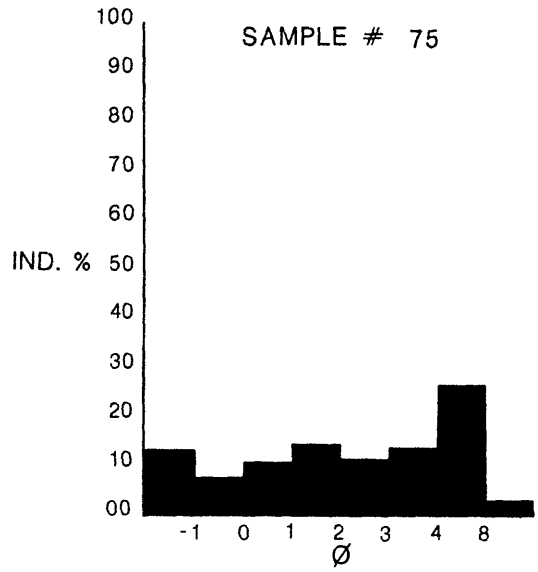
SAMPLE # 75
IND. %
100
90
80
70
60
50
40
30
20
10
00
-1 0 1 2 3 4 8
Ø

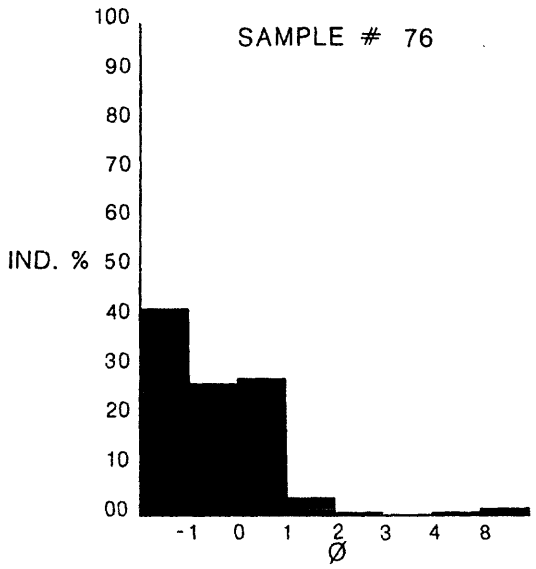
SAMPLE # 76
IND. %
100
90
80
70
60
50
40
30
20
10
00
-1 0 1 2 3 4 8
Ø

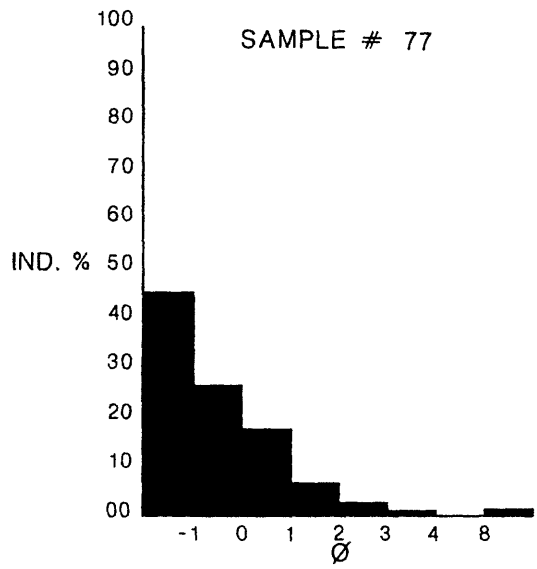
SAMPLE # 77
IND. %
100
90
80
70
60
50
40
30
20
10
00
-1 0 1 2 3 4 8
Ø

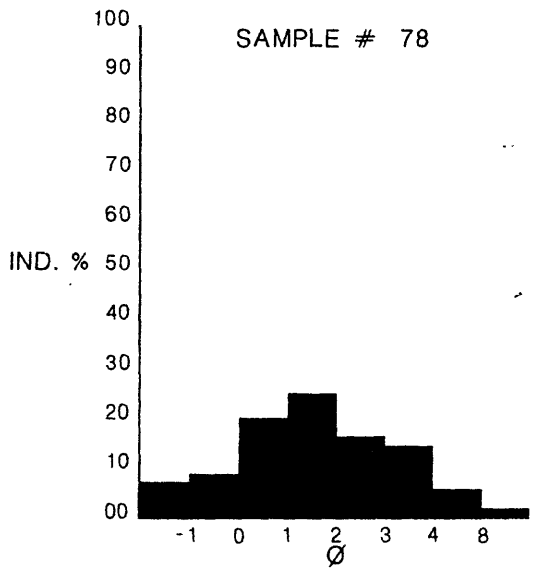
SAMPLE # 78
IND. %
100
90
80
70
60
50
40
30
20
10
00
-1 0 1 2 3 4 8
Ø

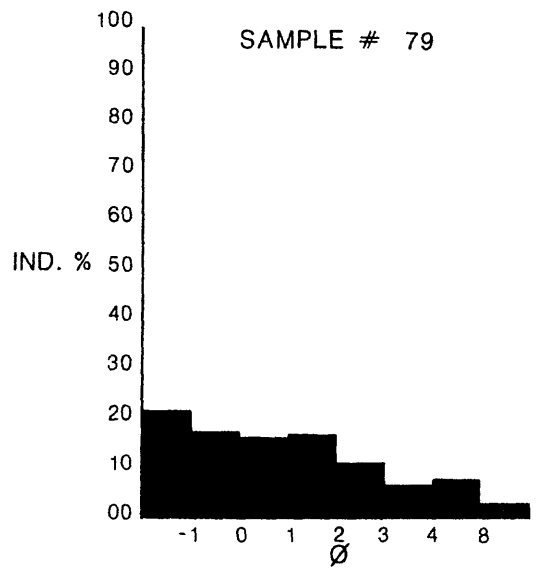
SAMPLE # 79
IND. %
100
90
80
70
60
50
40
30
20
10
00
-1 0 1 2 3 4 8
Ø

PLATE 10-13

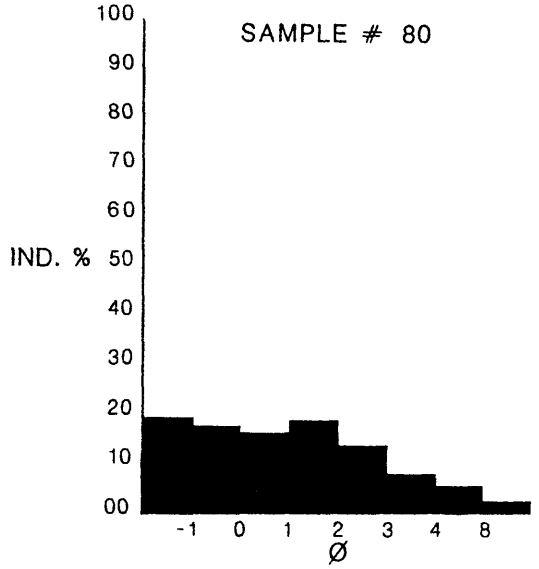
SAMPLE # 80
IND. %
100
90
80
70
60
50
40
30
20
10
00
-1 0 1 2 3 4 8
Ø

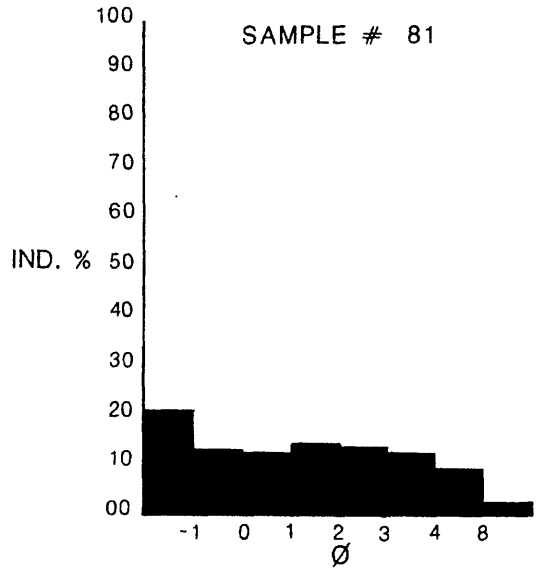
SAMPLE # 81
IND. %
100
90
80
70
60
50
40
30
20
10
00
-1 0 1 2 3 4 8
Ø

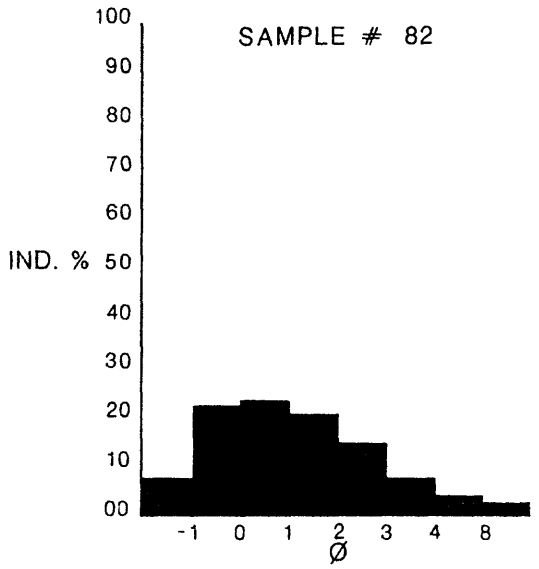
SAMPLE # 82
IND. %
100
90
80
70
60
50
40
30
20
10
00
-1 0 1 2 3 4 8
Ø

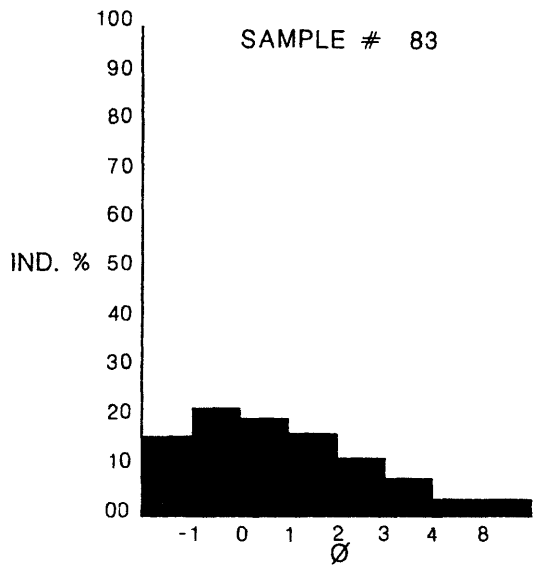
SAMPLE # 83
IND. %
100
90
80
70
60
50
40
30
20
10
00
-1 0 1 2 3 4 8
Ø

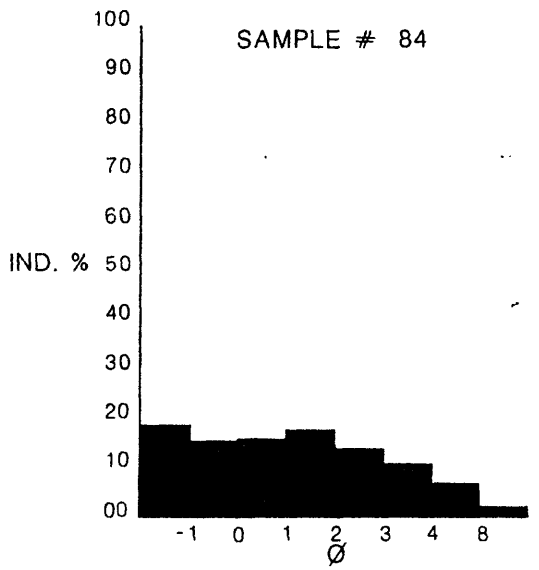
SAMPLE # 84
IND. %
100
90
80
70
60
50
40
30
20
10
00
-1 0 1 2 3 4 8
Ø

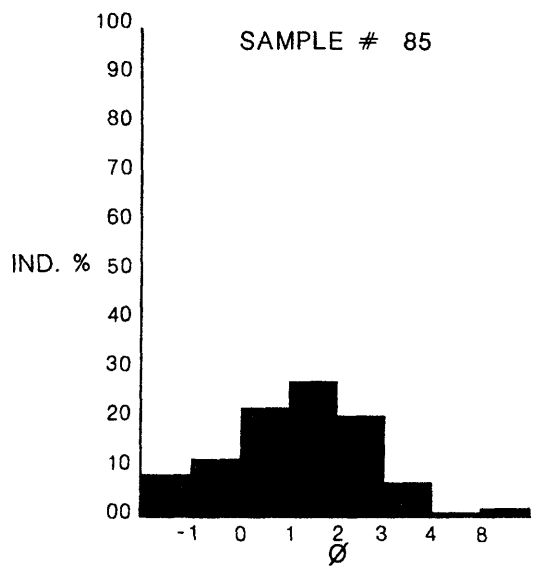
SAMPLE # 85
IND. %
100
90
80
70
60
50
40
30
20
10
00
-1 0 1 2 3 4 8
Ø

PLATE 10-14

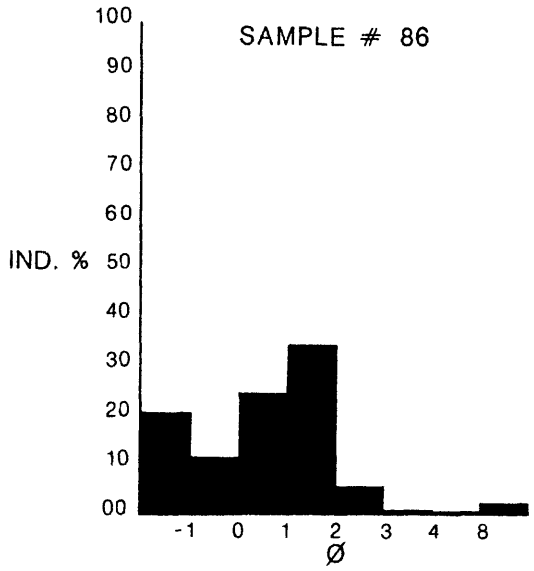
SAMPLE # 86
IND. %
100
90
80
70
60
50
40
30
20
10
00
-1 0 1 2 3 4 8
Ø

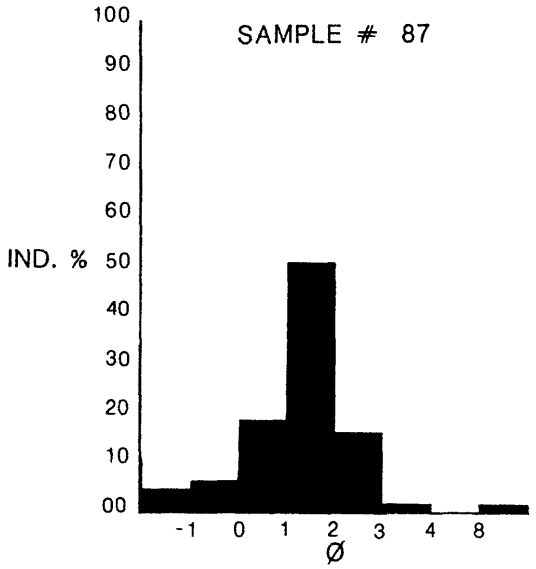
SAMPLE # 87
IND. %
100
90
80
70
60
50
40
30
20
10
00
-1 0 1 2 3 4 8
Ø

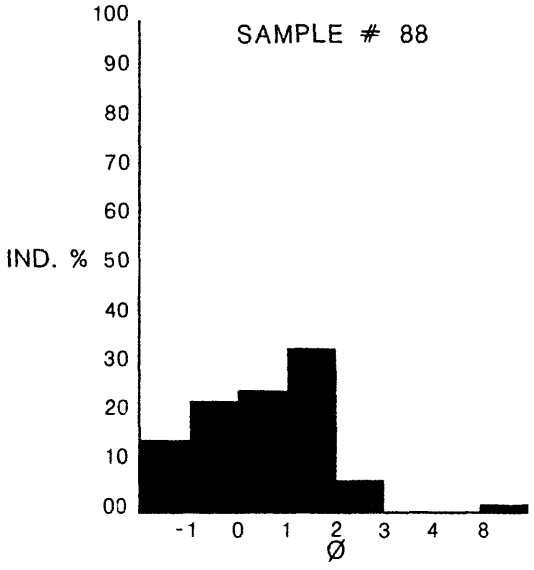
SAMPLE # 88
IND. %
100
90
80
70
60
50
40
30
20
10
00
-1 0 1 2 3 4 8
Ø

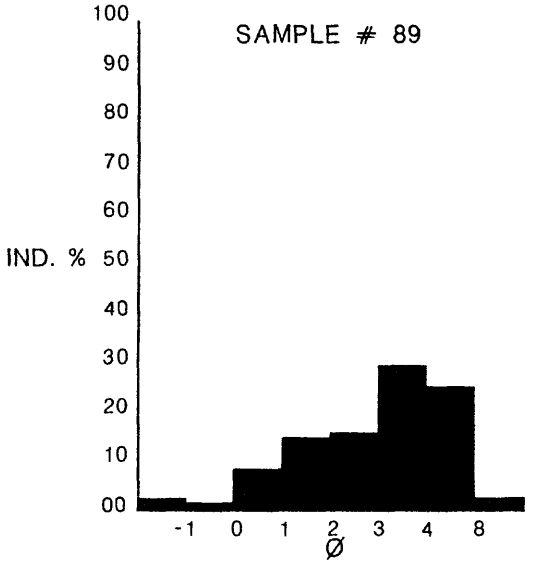
SAMPLE # 89
IND. %
100
90
80
70
60
50
40
30
20
10
00
-1 0 1 2 3 4 8
Ø

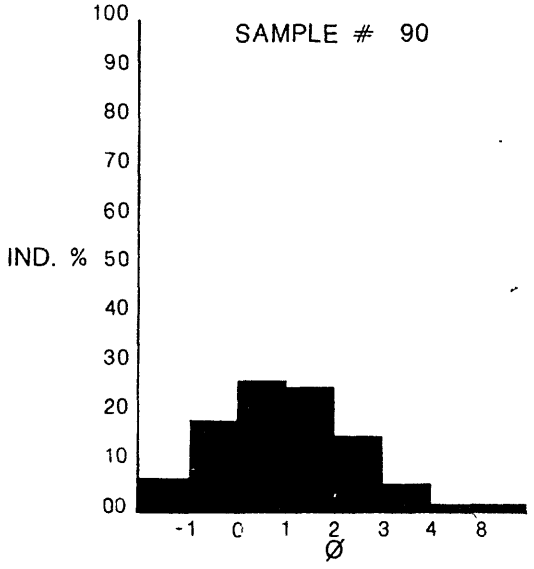
SAMPLE # 90
IND. %
100
90
80
70
60
50
40
30
20
10
00
-1 0 1 2 3 4 8
Ø

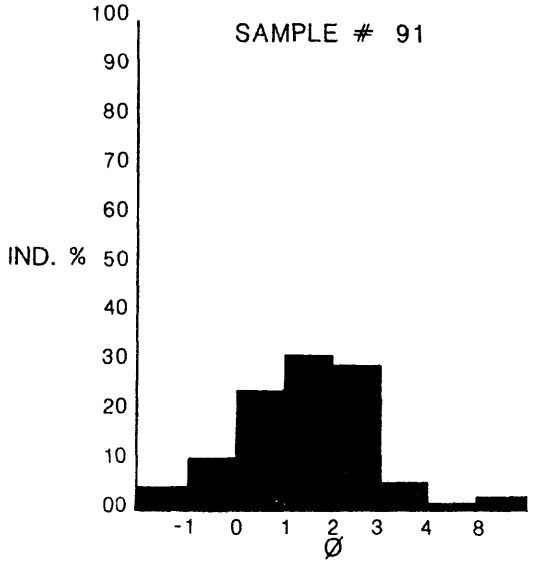
SAMPLE # 91
IND. %
100
90
80
70
60
50
40
30
20
10
00
-1 0 1 2 3 4 8
Ø

PLATE 10-15

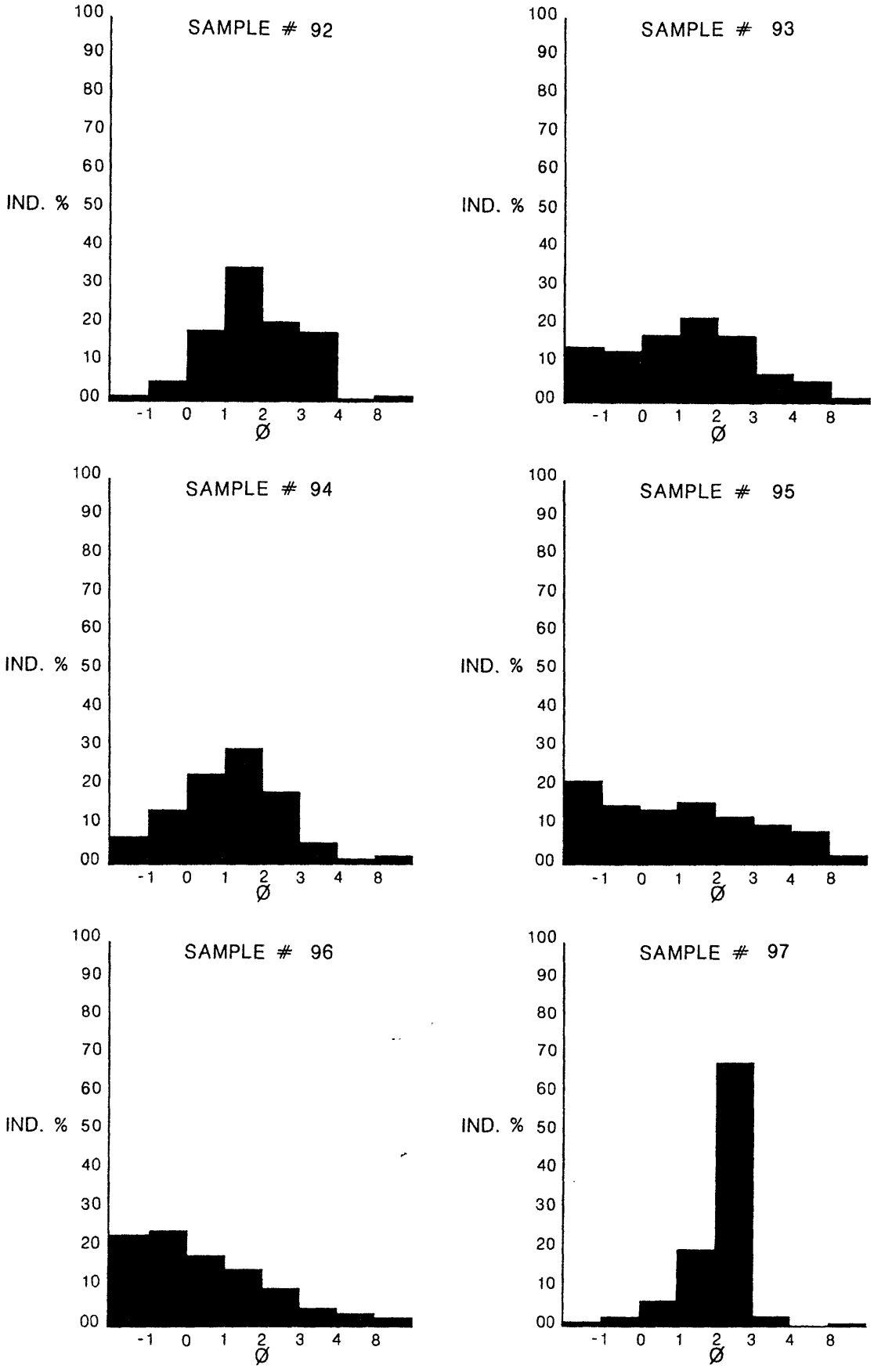
SAMPLE # 92
SAMPLE # 93
SAMPLE # 94
SAMPLE # 95
SAMPLE # 96
SAMPLE # 97
IND. %
100
90
80
70
60
50
40
30
20
10
00
-1 0 1 2 3 4 8
Ø

PLATE 10-16

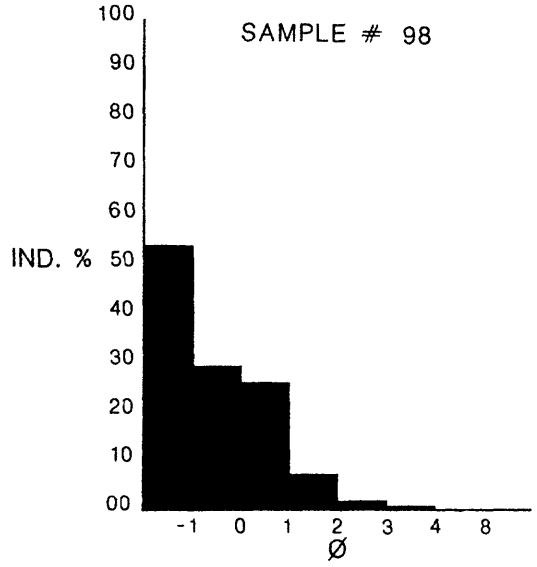
SAMPLE # 98
IND. %
100
90
80
70
60
50
40
30
20
10
00
-1 0 1 2 3 4 8
Ø

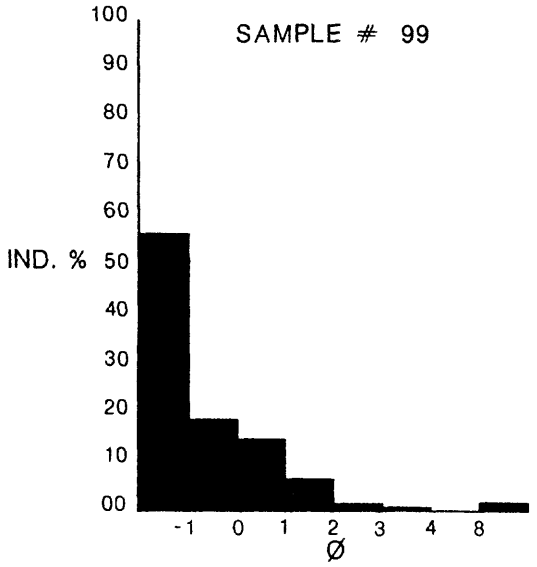
SAMPLE # 99
IND. %
100
90
80
70
60
50
40
30
20
10
00
-1 0 1 2 3 4 8
Ø

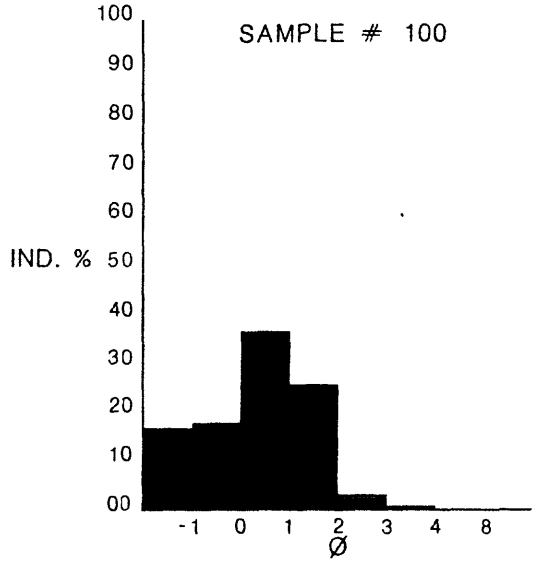
SAMPLE # 100
IND. %
100
90
80
70
60
50
40
30
20
10
00
-1 0 1 2 3 4 8
Ø

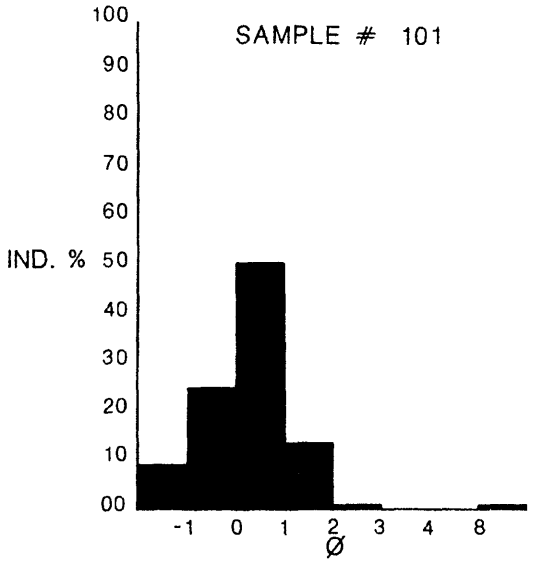
SAMPLE # 101
IND. %
100
90
80
70
60
50
40
30
20
10
00
-1 0 1 2 3 4 8
Ø

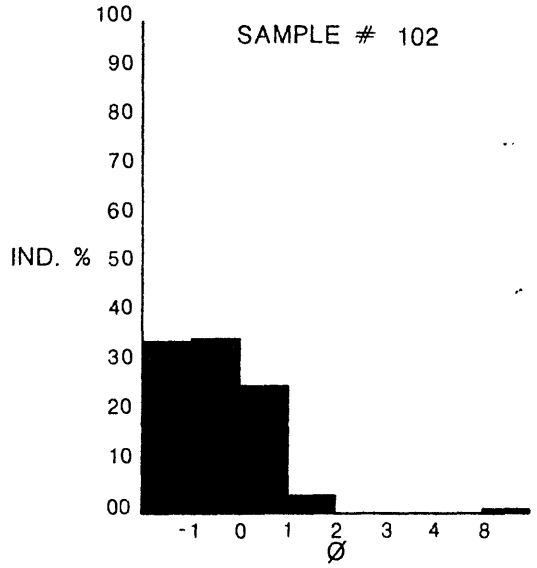
SAMPLE # 102
IND. %
100
90
80
70
60
50
40
30
20
10
00
-1 0 1 2 3 4 8
Ø

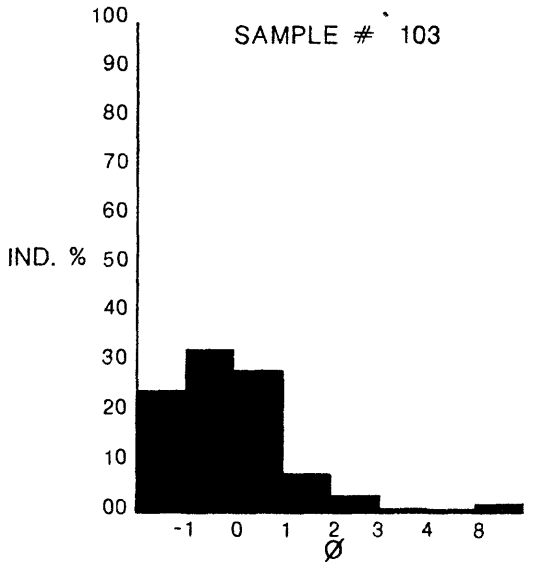
SAMPLE # 103
IND. %
100
90
80
70
60
50
40
30
20
10
00
-1 0 1 2 3 4 8
Ø

PLATE 10-17

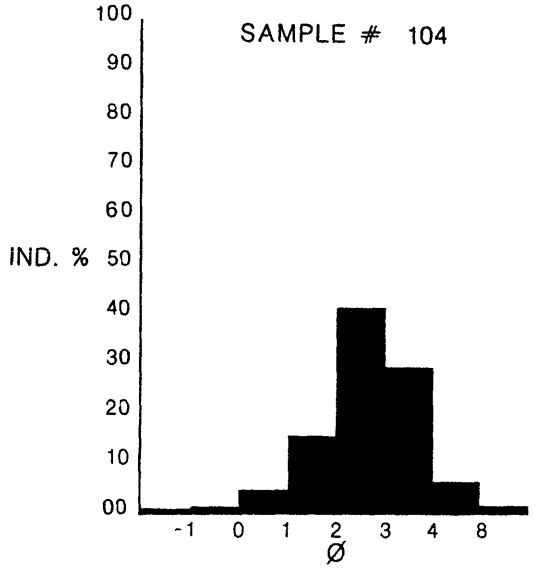
SAMPLE # 104
IND. %
100
90
80
70
60
50
40
30
20
10
00
-1 0 1 2 3 4 8
Ø

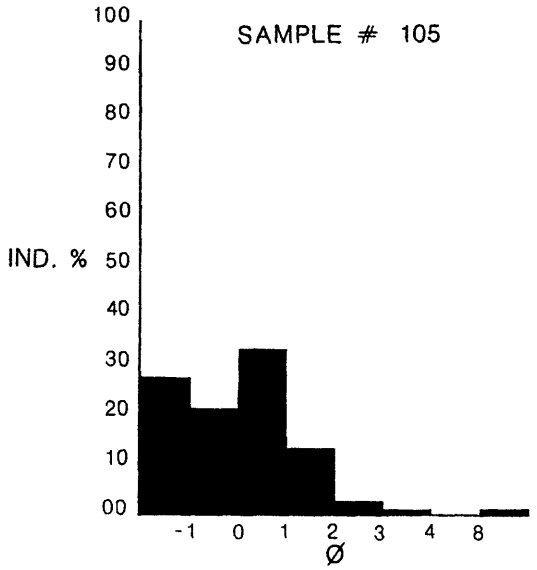
SAMPLE # 105
IND. %
100
90
80
70
60
50
40
30
20
10
00
-1 0 1 2 3 4 8
Ø

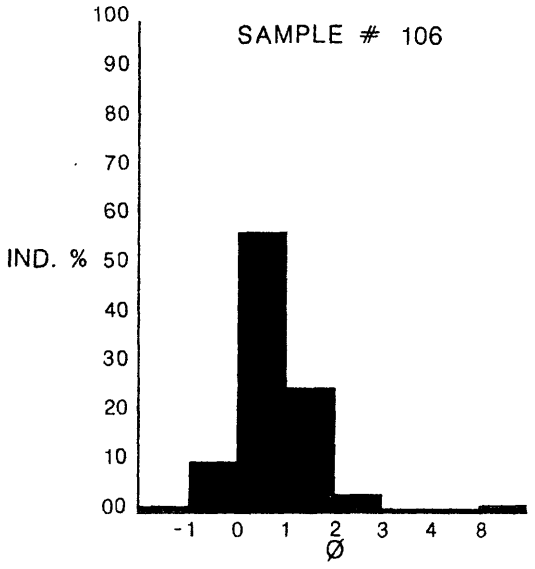
SAMPLE # 106
IND. %
100
90
80
70
60
50
40
30
20
10
00
-1 0 1 2 3 4 8
Ø

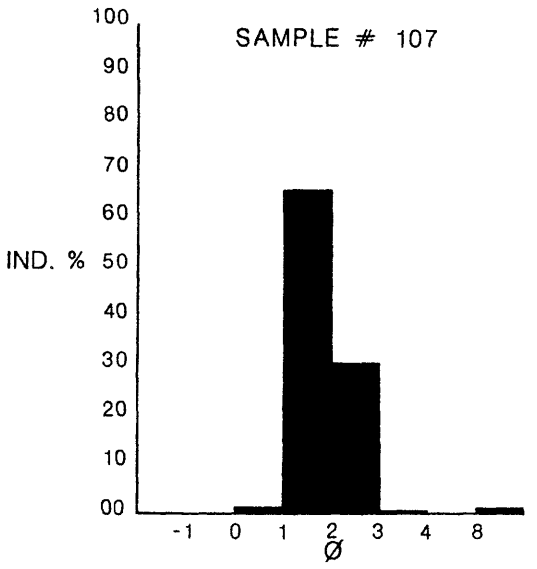
SAMPLE # 107
IND. %
100
90
80
70
60
50
40
30
20
10
00
-1 0 1 2 3 4 8
Ø

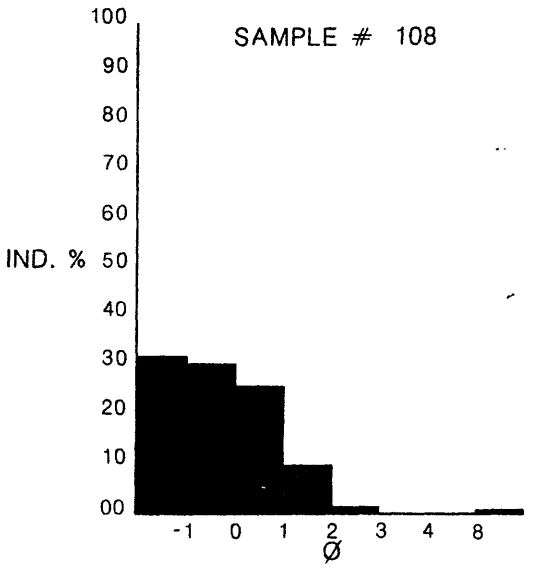
SAMPLE # 108
IND. %
100
90
80
70
60
50
40
30
20
10
00
-1 0 1 2 3 4 8
Ø

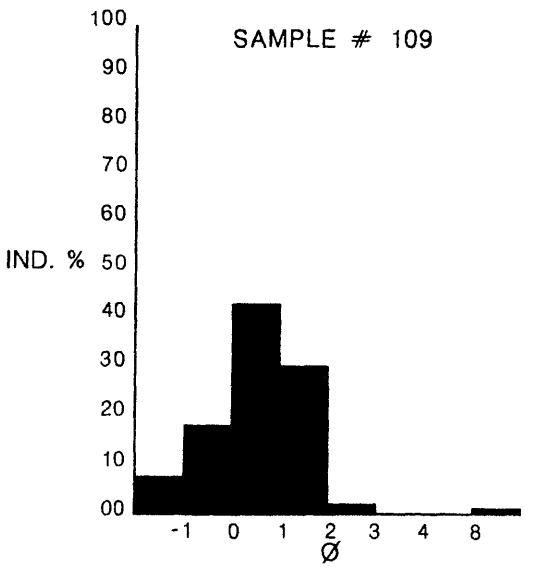
SAMPLE # 109
IND. %
100
90
80
70
60
50
40
30
20
10
00
-1 0 1 2 3 4 8
Ø

PLATE 10-18

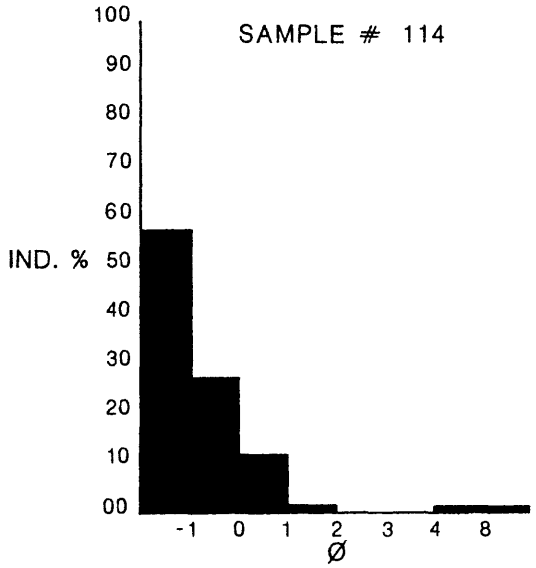
SAMPLE # 114
IND. %
100
90
80
70
60
50
40
30
20
10
00
-1 0 1 2 3 4 8
Ø

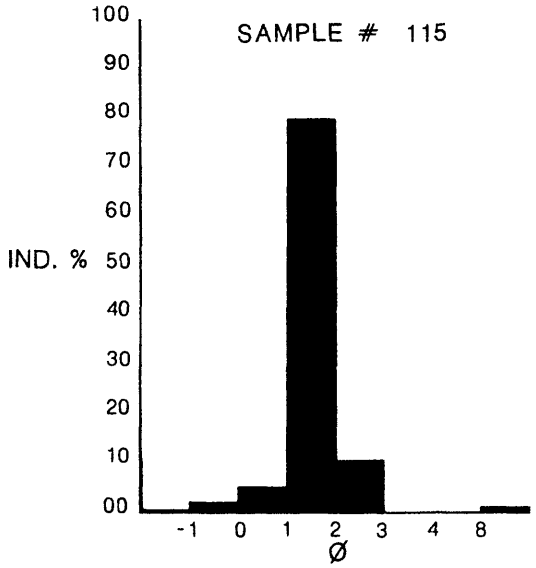
SAMPLE # 115
IND. %
100
90
80
70
60
50
40
30
20
10
00
-1 0 1 2 3 4 8
Ø

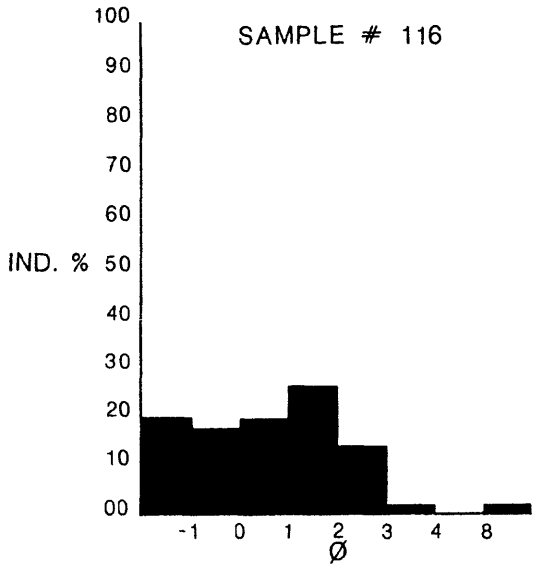
SAMPLE # 116
IND. %
100
90
80
70
60
50
40
30
20
10
00
-1 0 1 2 3 4 8
Ø

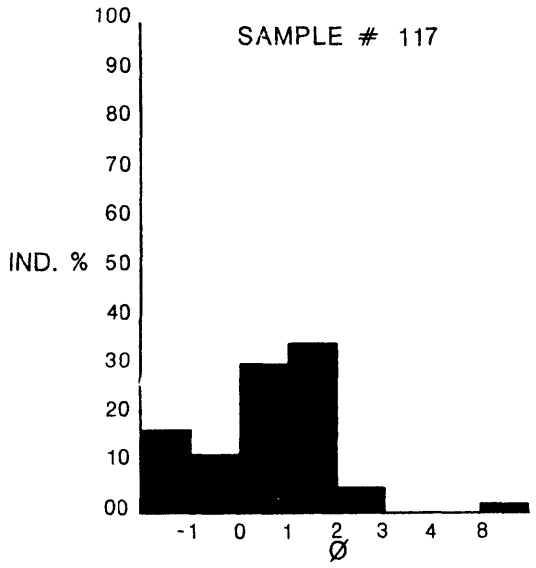
SAMPLE # 117
IND. %
100
90
80
70
60
50
40
30
20
10
00
-1 0 1 2 3 4 8
Ø

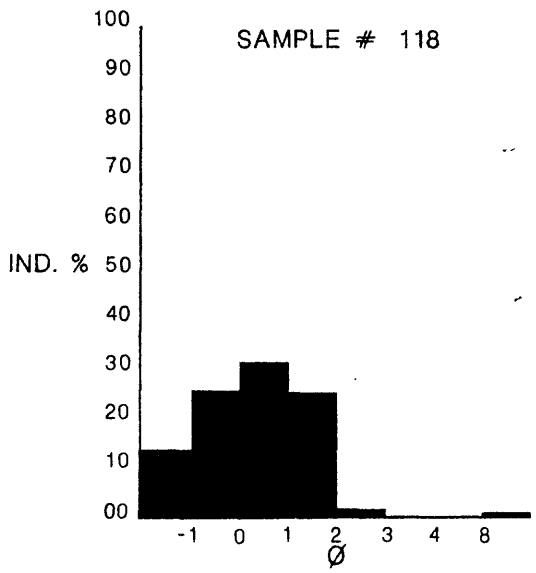
SAMPLE # 118
IND. %
100
90
80
70
60
50
40
30
20
10
00
-1 0 1 2 3 4 8
Ø

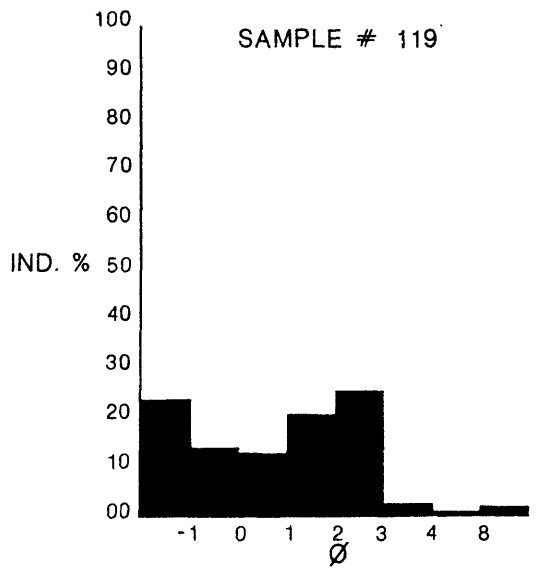
SAMPLE # 119
IND. %
100
90
80
70
60
50
40
30
20
10
00
-1 0 1 2 3 4 8
Ø

PLATE 10-19

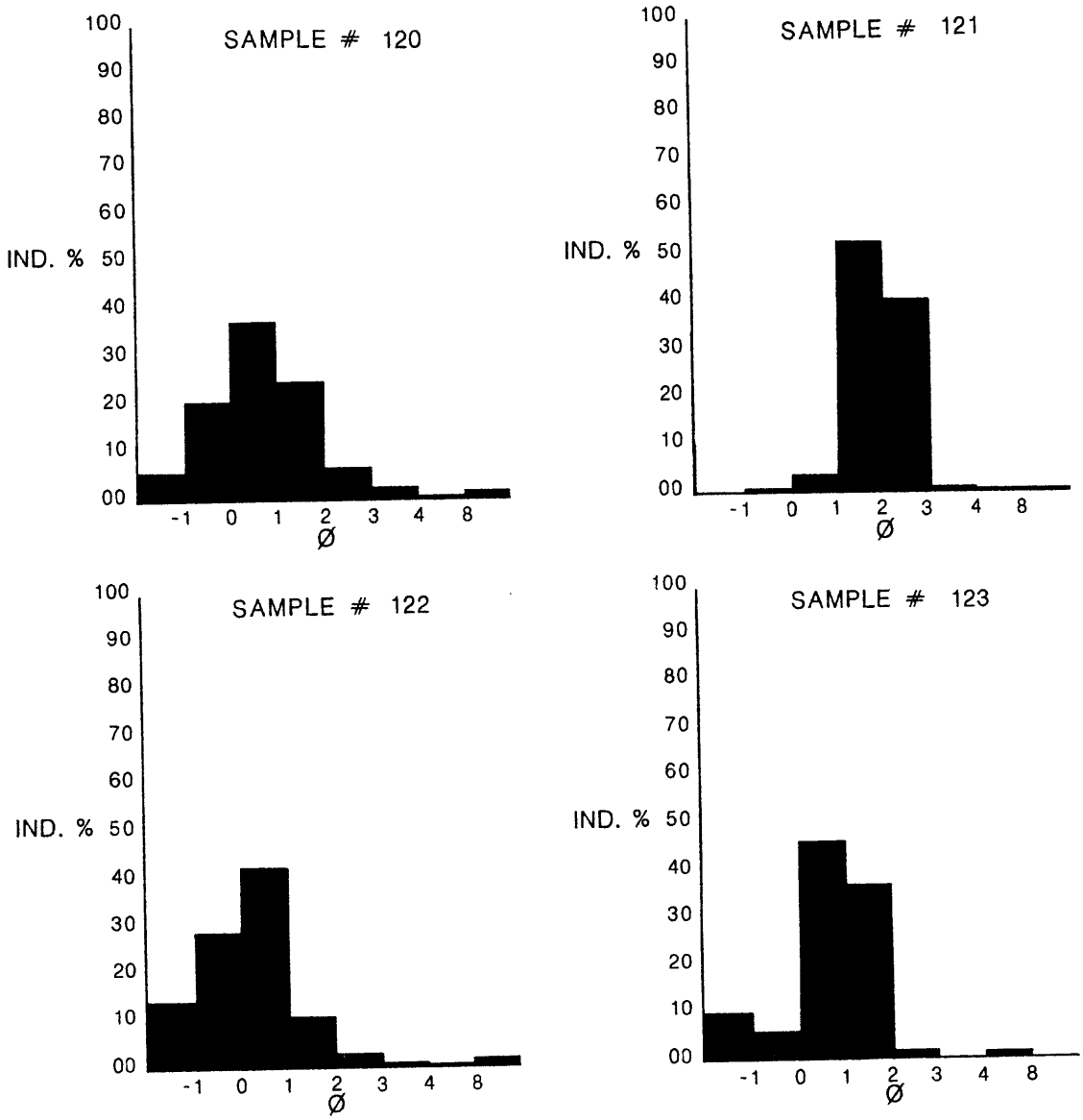
SAMPLE # 120
SAMPLE # 121
SAMPLE # 122
SAMPLE # 123
IND. %
100
90
80
70
60
50
40
30
20
10
00
-1 0 1 2 3 4 8
Ø

PLATE 10-20

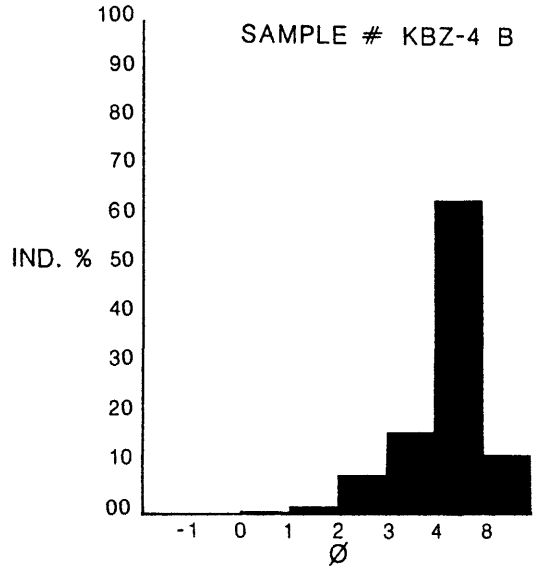
SAMPLE # KBZ-4 B
IND. %
100
90
80
70
60
50
40
30
20
10
00
-1 0 1 2 3 4 8
Ø

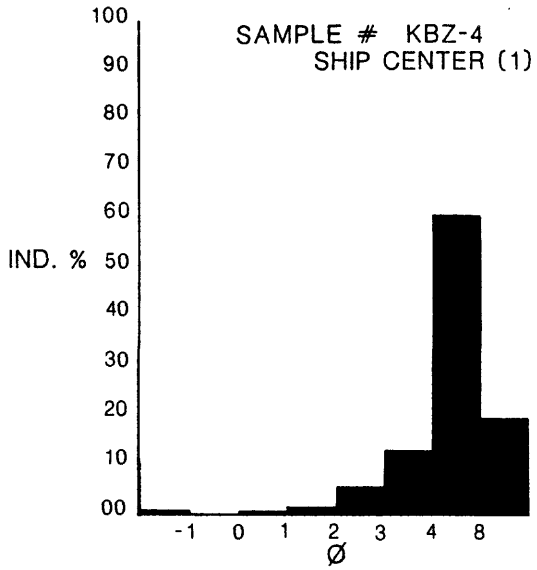
SAMPLE # KBZ-4
SHIP CENTER (1)
IND. %
100
90
80
70
60
50
40
30
20
10
00
-1 0 1 2 3 4 8
Ø

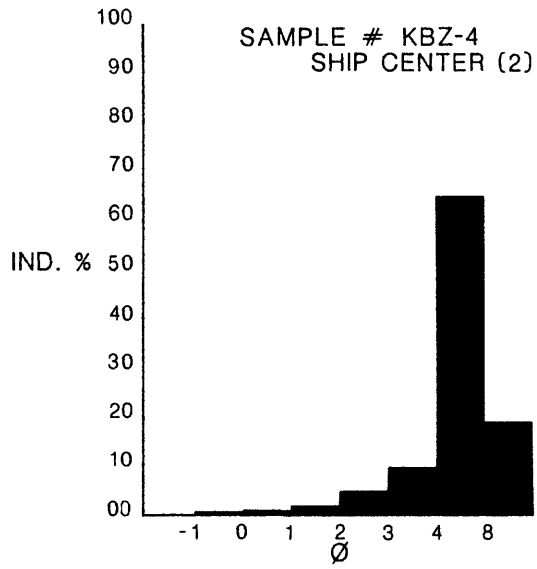
SAMPLE # KBZ-4
SHIP CENTER (2)
IND. %
100
90
80
70
60
50
40
30
20
10
00
-1 0 1 2 3 4 8
Ø

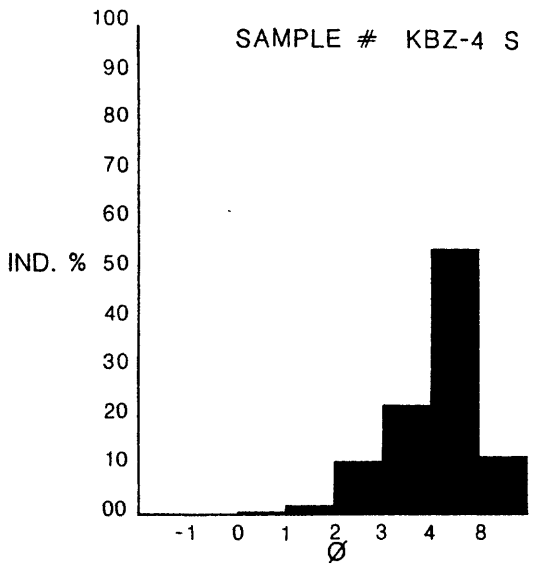
SAMPLE # KBZ-4 S
IND. %
100
90
80
70
60
50
40
30
20
10
00
-1 0 1 2 3 4 8
Ø

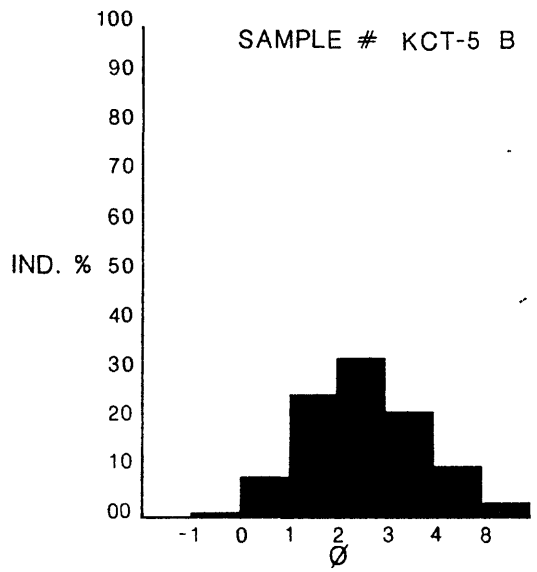
SAMPLE # KCT-5 B
IND. %
100
90
80
70
60
50
40
30
20
10
00
-1 0 1 2 3 4 8
Ø

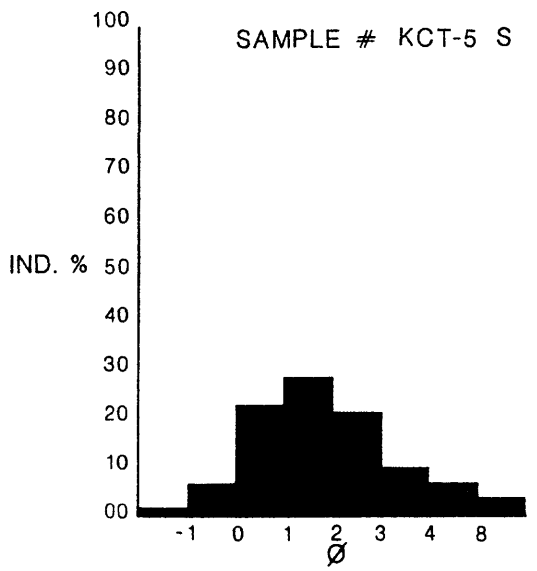
SAMPLE # KCT-5 S
IND. %
100
90
80
70
60
50
40
30
20
10
00
-1 0 1 2 3 4 8
Ø

PLATE 10-21

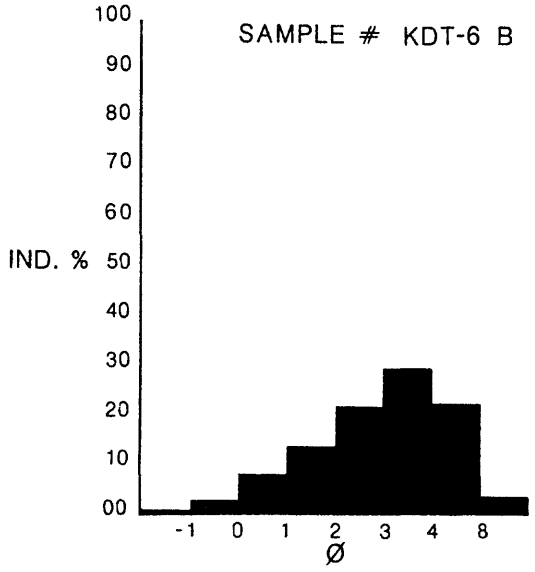
SAMPLE # KDT-6 B
IND. %
100
90
80
70
60
50
40
30
20
10
00
-1 0 1 2 3 4 8
Ø

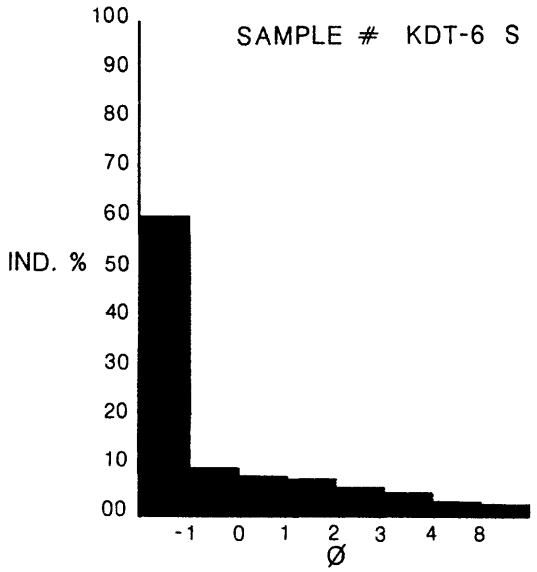
SAMPLE # KDT-6 S
IND. %
100
90
80
70
60
50
40
30
20
10
00
-1 0 1 2 3 4 8
Ø

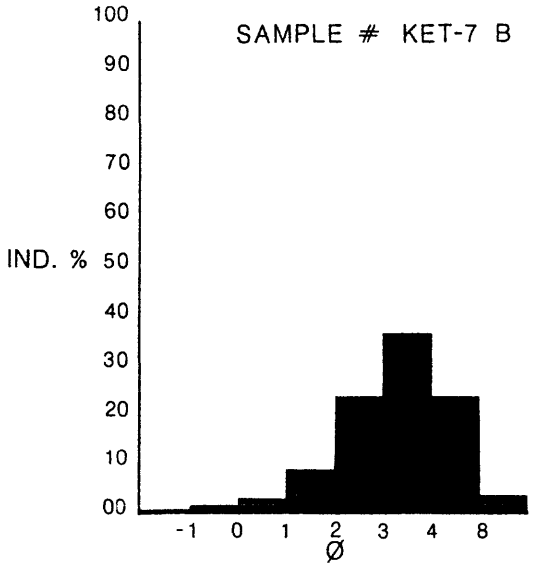
SAMPLE # KET-7 B
IND. %
100
90
80
70
60
50
40
30
20
10
00
-1 0 1 2 3 4 8
Ø

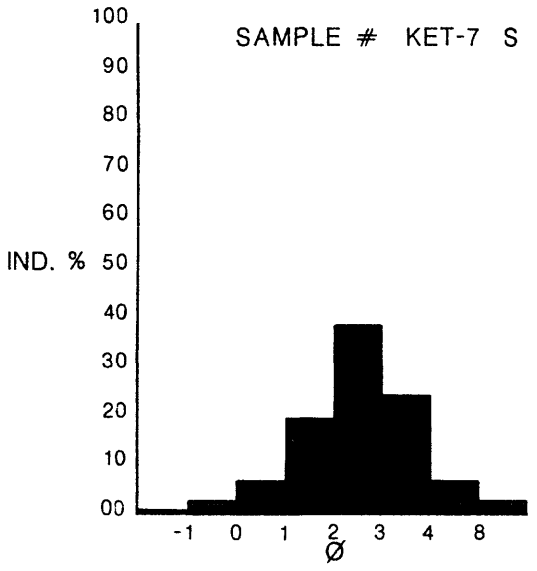
SAMPLE # KET-7 S
IND. %
100
90
80
70
60
50
40
30
20
10
00
-1 0 1 2 3 4 8
Ø

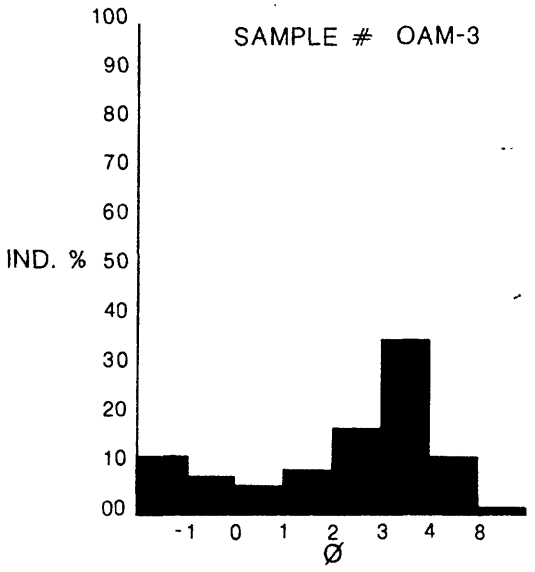
SAMPLE # OAM-3
IND. %
100
90
80
70
60
50
40
30
20
10
00
-1 0 1 2 3 4 8
Ø

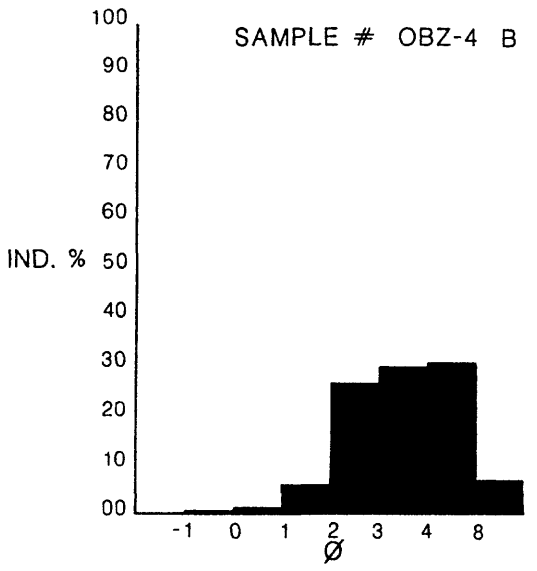
SAMPLE # OBZ-4 B
IND. %
100
90
80
70
60
50
40
30
20
10
00
-1 0 1 2 3 4 8
Ø

PLATE 10-22

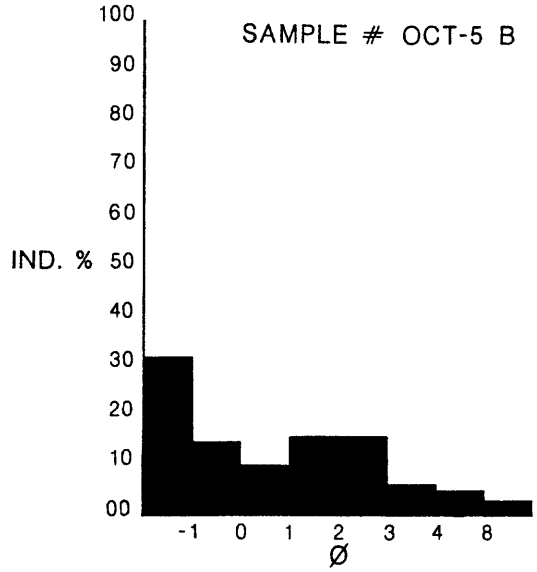
SAMPLE # OCT-5 B
IND. %
100
90
80
70
60
50
40
30
20
10
00
-1 0 1 2 3 4 8
Ø

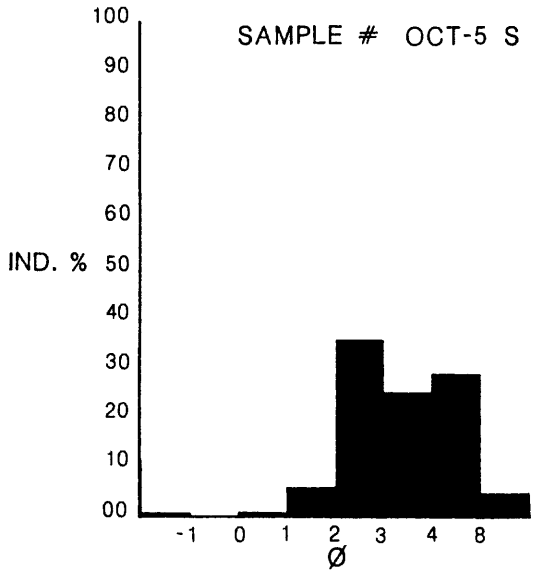
SAMPLE # OCT-5 S
IND. %
100
90
80
70
60
50
40
30
20
10
00
-1 0 1 2 3 4 8
Ø

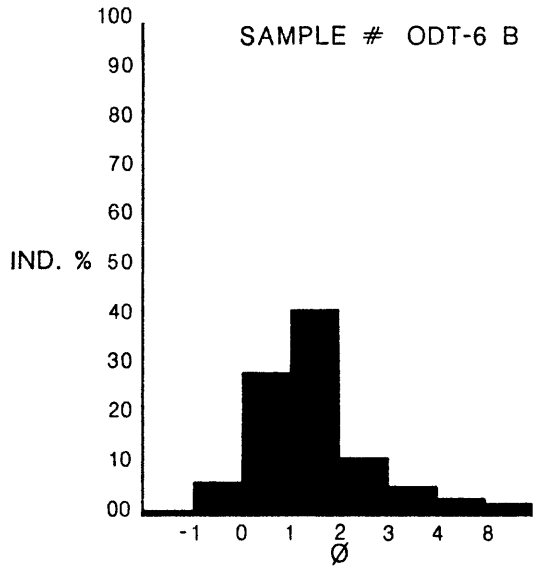
SAMPLE # ODT-6 B
IND. %
100
90
80
70
60
50
40
30
20
10
00
-1 0 1 2 3 4 8
Ø

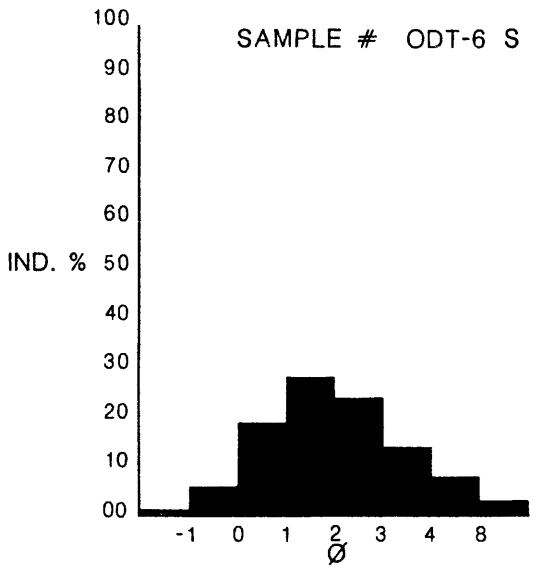
SAMPLE # ODT-6 S
IND. %
100
90
80
70
60
50
40
30
20
10
00
-1 0 1 2 3 4 8
Ø

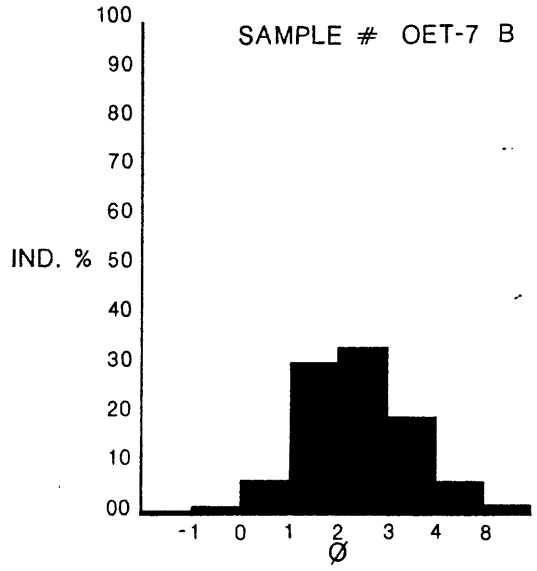
SAMPLE # OET-7 B
IND. %
100
90
80
70
60
50
40
30
20
10
00
-1 0 1 2 3 4 8
Ø

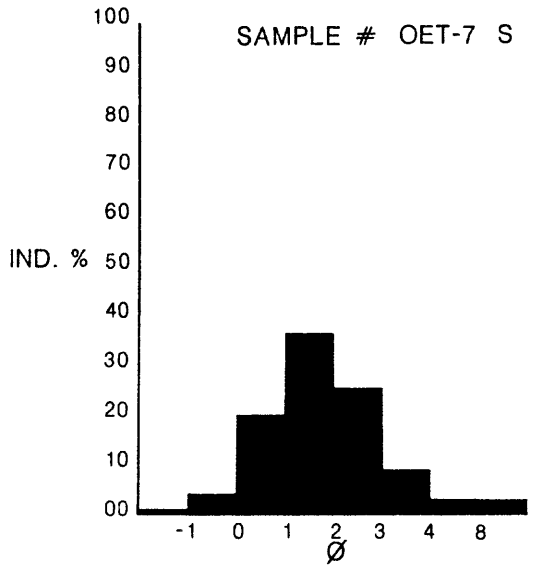
SAMPLE # OET-7 S
IND. %
100
90
80
70
60
50
40
30
20
10
00
-1 0 1 2 3 4 8
Ø

PLATE 10-23

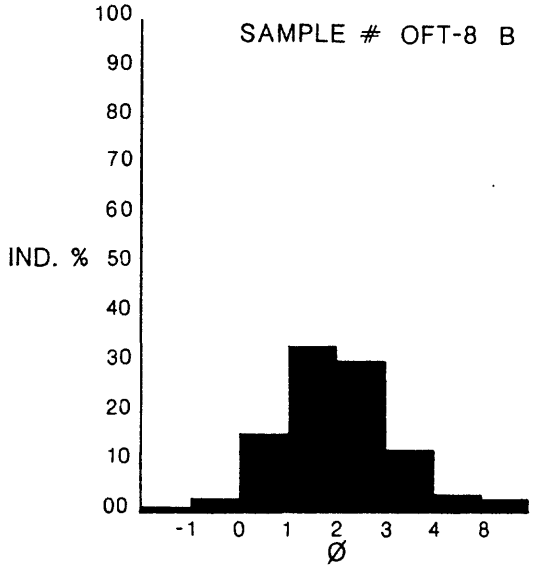
SAMPLE # OFT-8 B
IND. %
100
90
80
70
60
50
40
30
20
10
00
-1 0 1 2 3 4 8
Ø

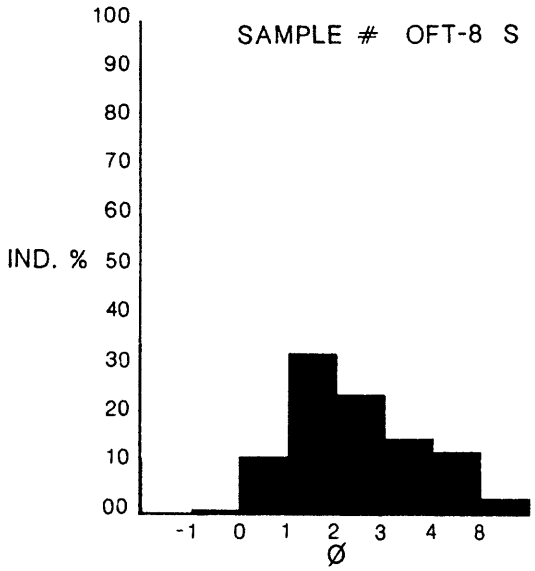
SAMPLE # OFT-8 S
IND. %
100
90
80
70
60
50
40
30
20
10
00
-1 0 1 2 3 4 8
Ø

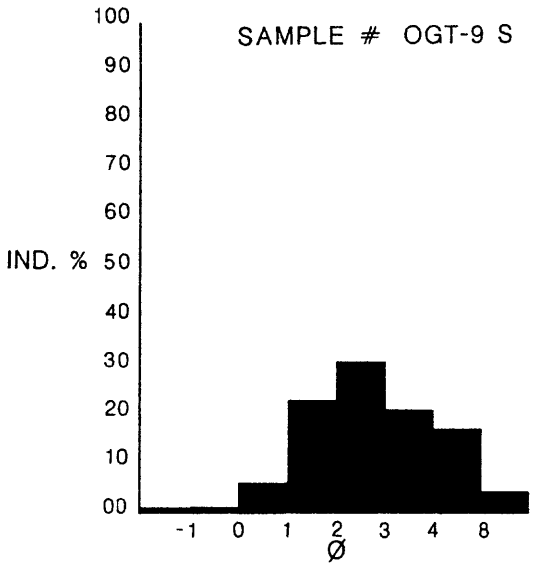
SAMPLE # OGT-9 S
IND. %
100
90
80
70
60
50
40
30
20
10
00
-1 0 1 2 3 4 8
Ø

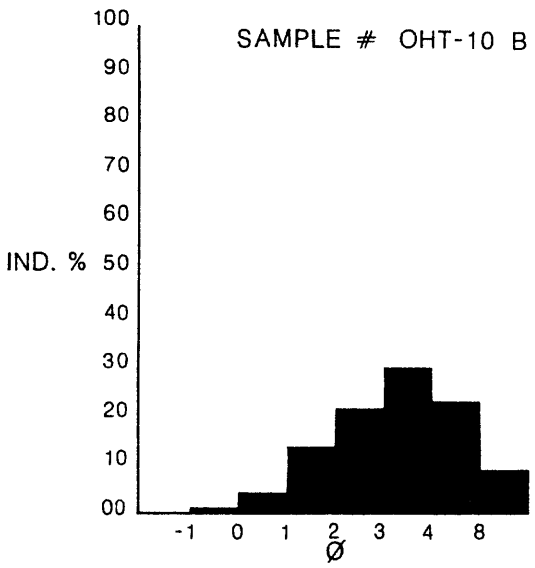
SAMPLE # OHT-10 B
IND. %
100
90
80
70
60
50
40
30
20
10
00
-1 0 1 2 3 4 8
Ø

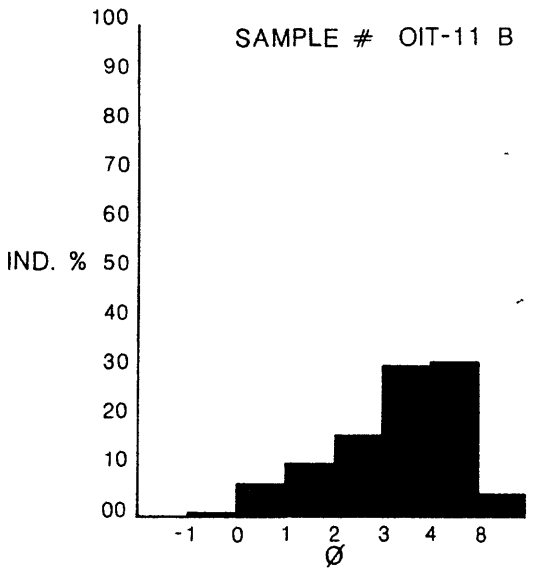
SAMPLE # OIT-11 B
IND. %
100
90
80
70
60
50
40
30
20
10
00
-1 0 1 2 3 4 8
Ø

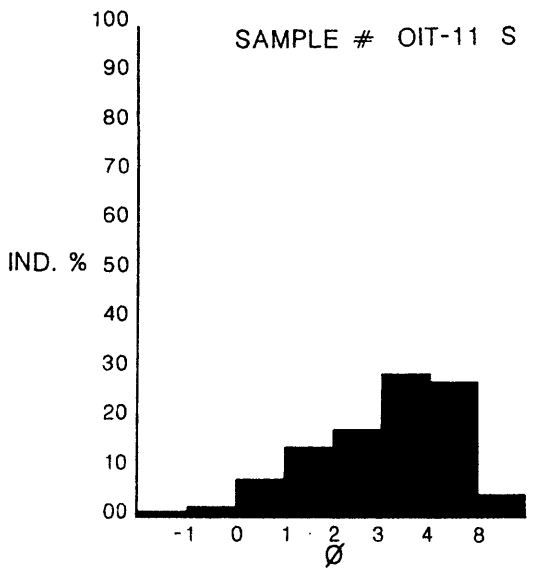
SAMPLE # OIT-11 S
IND. %
100
90
80
70
60
50
40
30
20
10
00
-1 0 1 2 3 4 8
Ø

PLATE 10-24

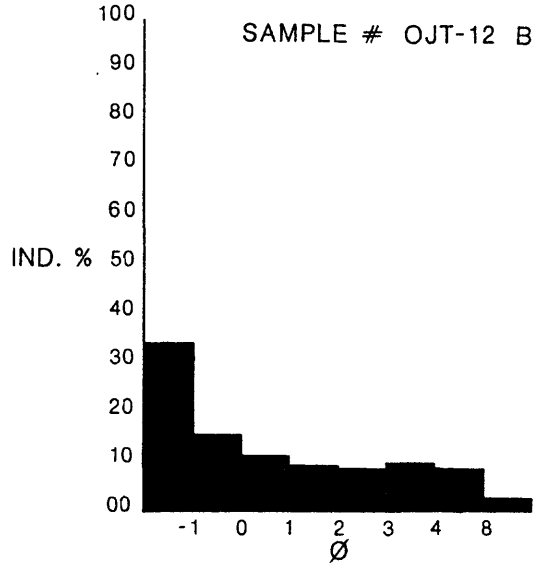
SAMPLE # OJT-12 B
IND. %
100
90
80
70
60
50
40
30
20
10
00
-1 0 1 2 3 4 8
Ø

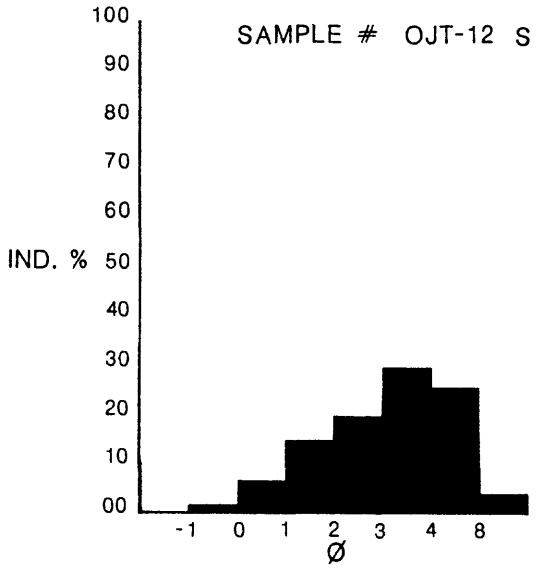
SAMPLE # OJT-12 S
IND. %
100
90
80
70
60
50
40
30
20
10
00
-1 0 1 2 3 4 8
Ø

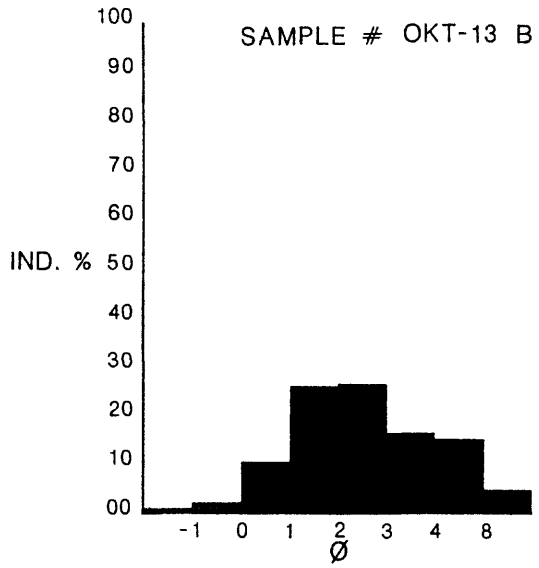
SAMPLE # OKT-13 B
IND. %
100
90
80
70
60
50
40
30
20
10
00
-1 0 1 2 3 4 8
Ø

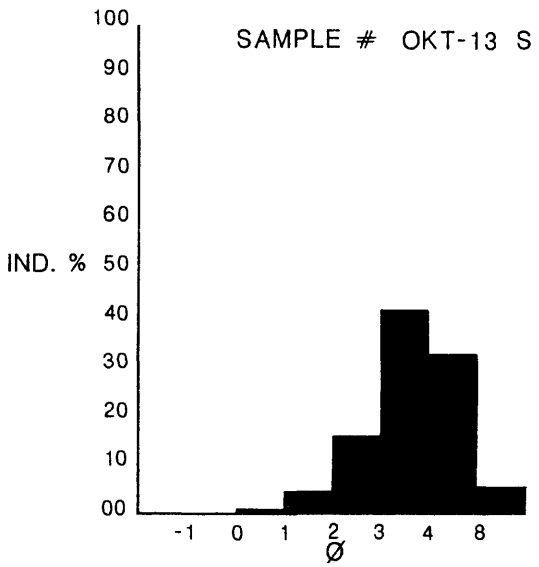
SAMPLE # OKT-13 S
IND. %
100
90
80
70
60
50
40
30
20
10
00
-1 0 1 2 3 4 8
Ø

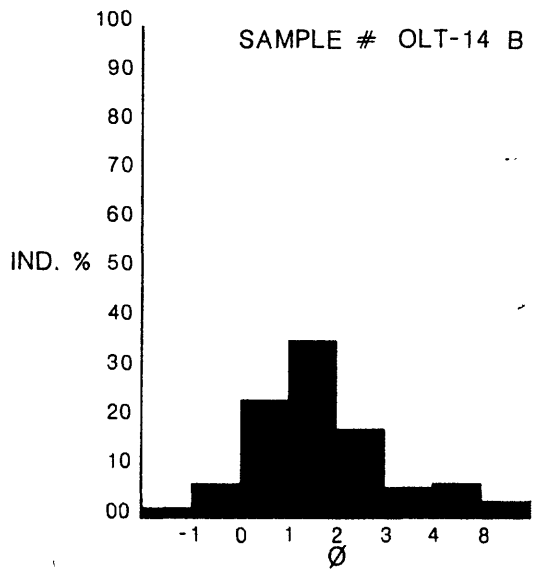
SAMPLE # OLT-14 B
IND. %
100
90
80
70
60
50
40
30
20
10
00
-1 0 1 2 3 4 8
Ø

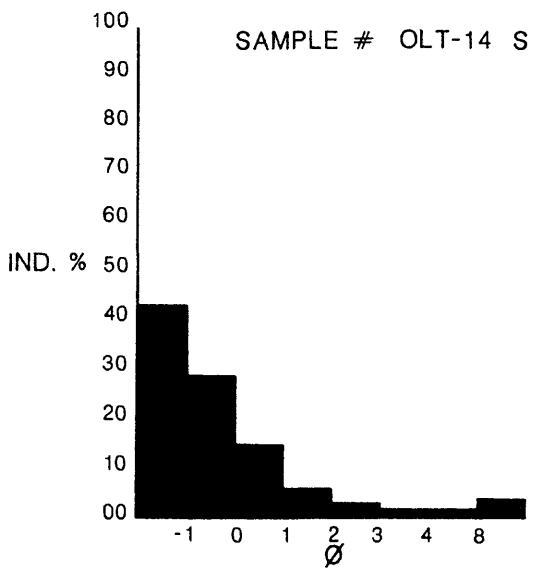
SAMPLE # OLT-14 S
IND. %
100
90
80
70
60
50
40
30
20
10
00
-1 0 1 2 3 4 8
Ø

PLATE 10-25

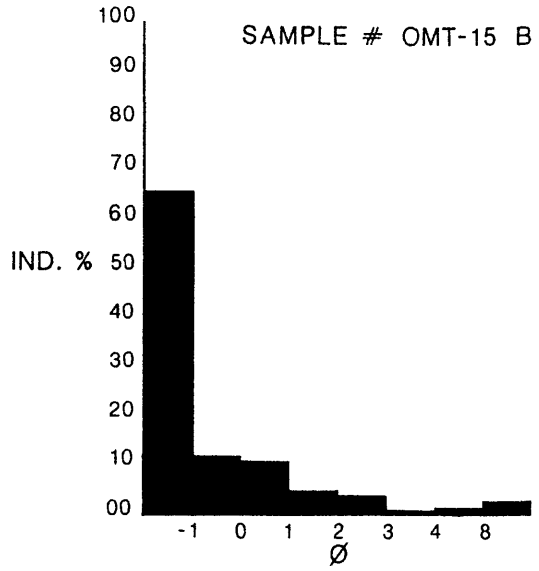
SAMPLE # OMT-15 B
IND. %
100
90
80
70
60
50
40
30
20
10
00
-1 0 1 2 3 4 8
Ø

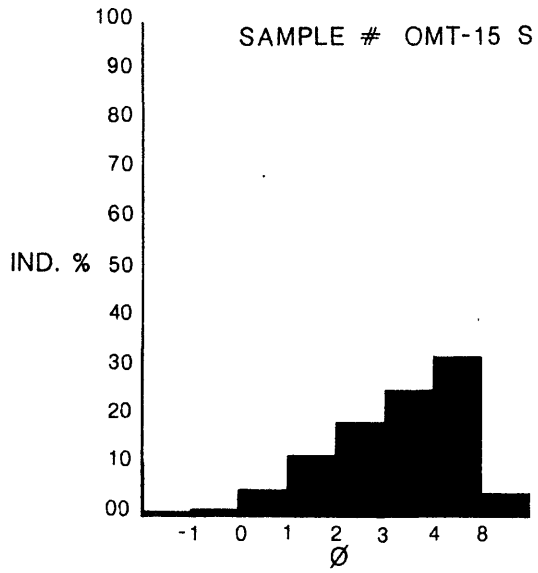
SAMPLE # OMT-15 S
IND. %
100
90
80
70
60
50
40
30
20
10
00
-1 0 1 2 3 4 8
Ø

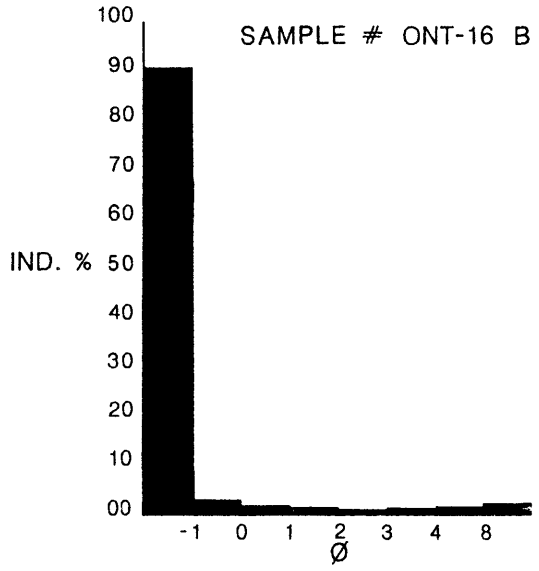
SAMPLE # ONT-16 B
IND. %
100
90
80
70
60
50
40
30
20
10
00
-1 0 1 2 3 4 8
Ø

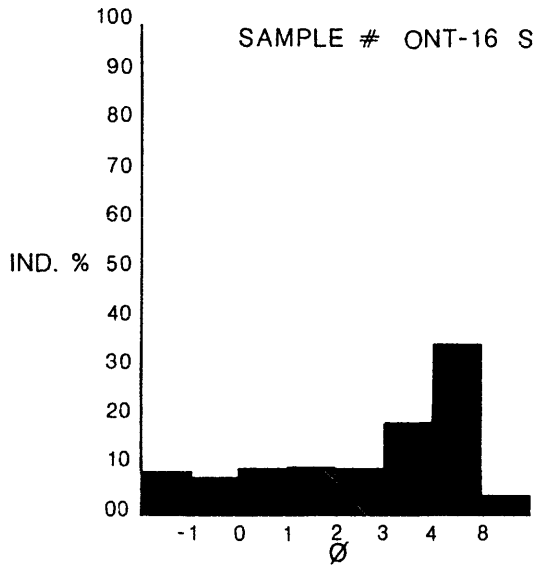
SAMPLE # ONT-16 S
IND. %
100
90
80
70
60
50
40
30
20
10
00
-1 0 1 2 3 4 8
Ø

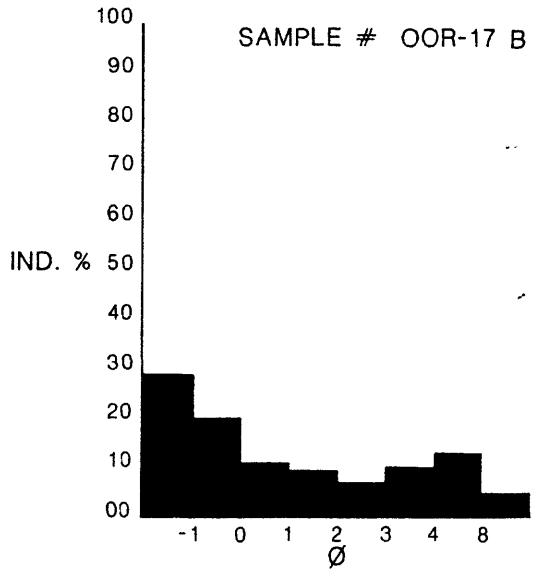
SAMPLE # OOR-17 B
IND. %
100
90
80
70
60
50
40
30
20
10
00
-1 0 1 2 3 4 8
Ø

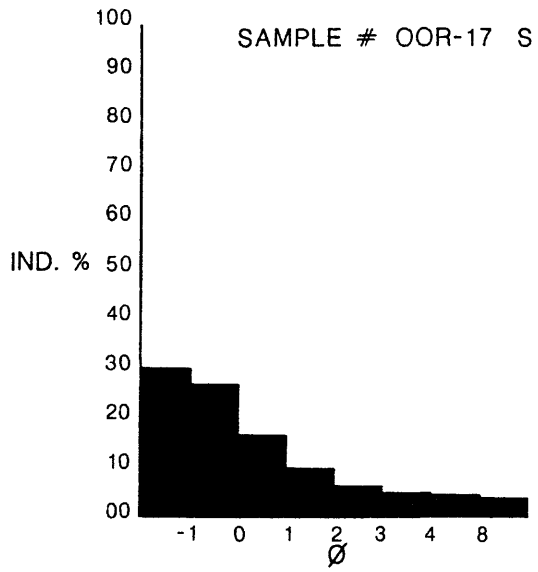
SAMPLE # OOR-17 S
IND. %
100
90
80
70
60
50
40
30
20
10
00
-1 0 1 2 3 4 8
Ø

PLATE 10-26

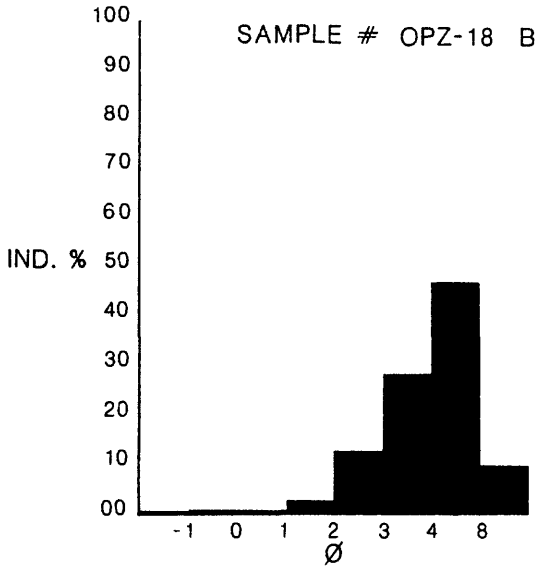
SAMPLE # OPZ-18 B
IND. %
100
90
80
70
60
50
40
30
20
10
00
-1 0 1 2 3 4 8
Ø

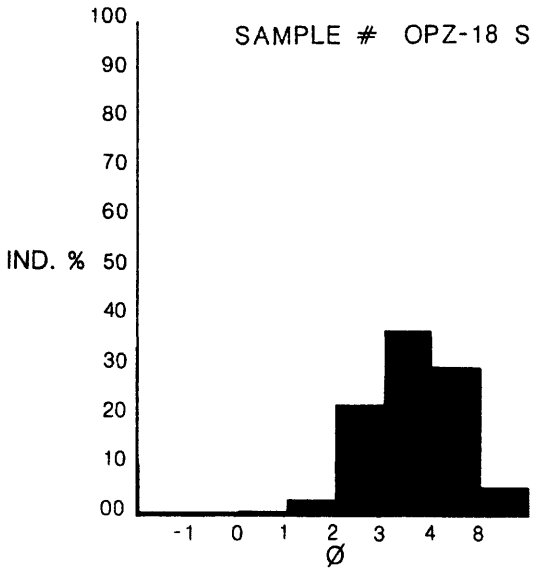
SAMPLE # OPZ-18 S
IND. %
100
90
80
70
60
50
40
30
20
10
00
-1 0 1 2 3 4 8
Ø

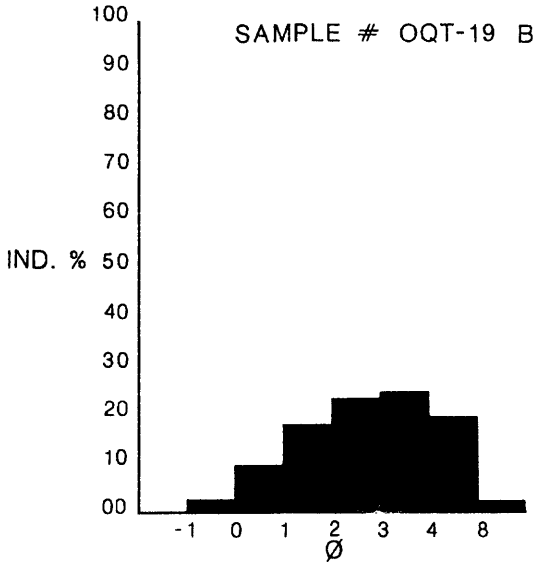
SAMPLE # OQT-19 B
IND. %
100
90
80
70
60
50
40
30
20
10
00
-1 0 1 2 3 4 8
Ø

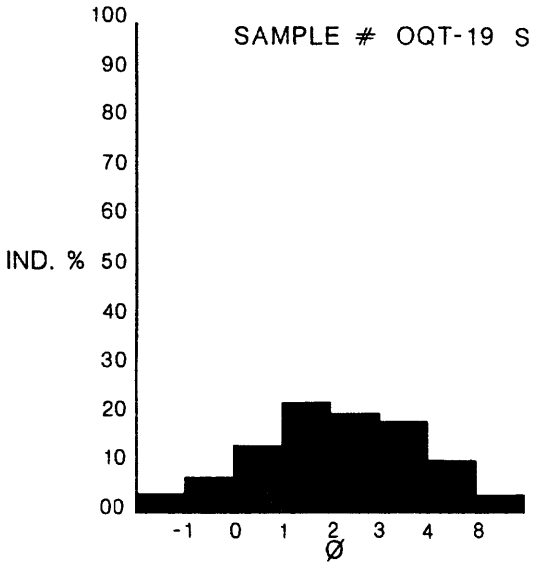
SAMPLE # OQT-19 S
IND. %
100
90
80
70
60
50
40
30
20
10
00
-1 0 1 2 3 4 8
Ø

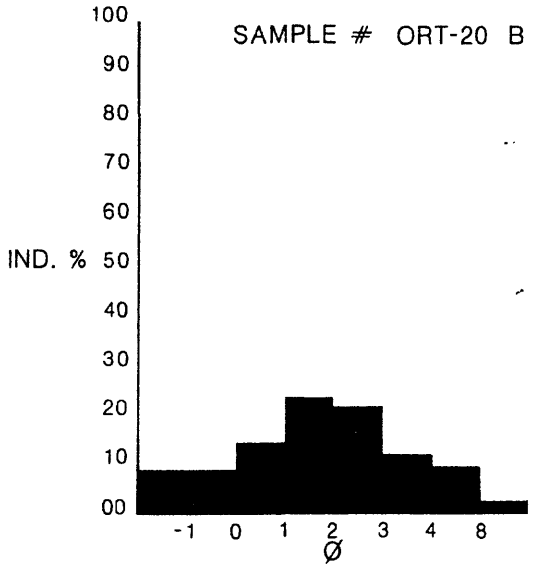
SAMPLE # ORT-20 B
IND. %
100
90
80
70
60
50
40
30
20
10
00
-1 0 1 2 3 4 8
Ø

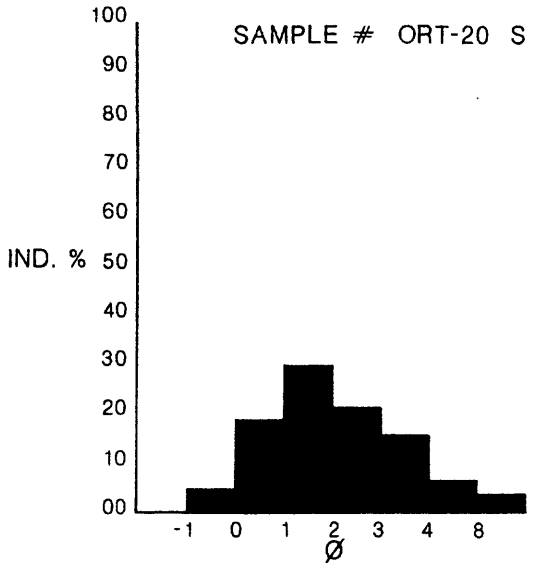
SAMPLE # ORT-20 S
IND. %
100
90
80
70
60
50
40
30
20
10
00
-1 0 1 2 3 4 8
Ø

PLATE 10-27

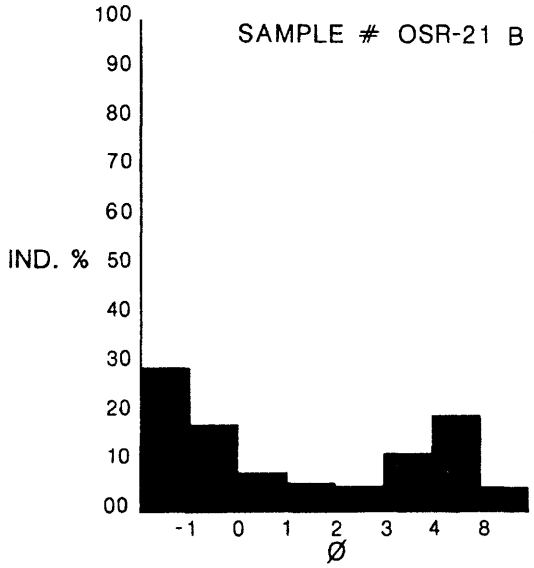
SAMPLE # OSR-21 B
IND. %
100
90
80
70
60
50
40
30
20
10
00
-1 0 1 2 3 4 8
Ø

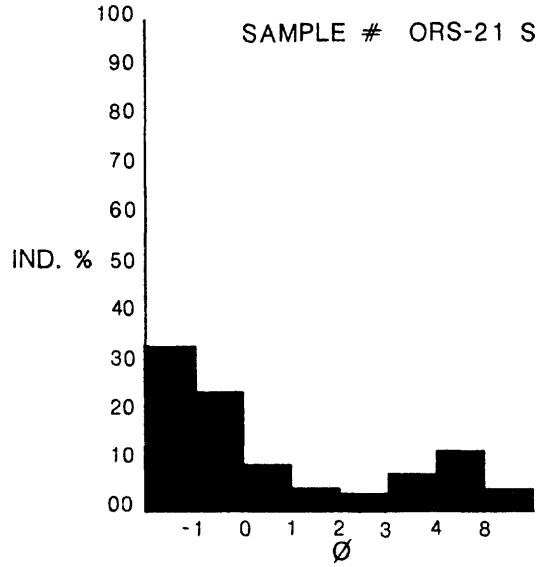
SAMPLE # ORS-21 S
IND. %
100
90
80
70
60
50
40
30
20
10
00
-1 0 1 2 3 4 8
Ø

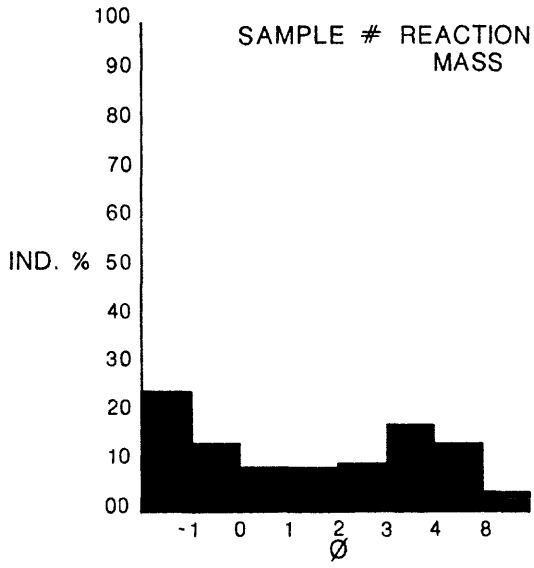
SAMPLE # REACTION MASS
IND. %
100
90
80
70
60
50
40
30
20
10
00
-1 0 1 2 3 4 8
Ø

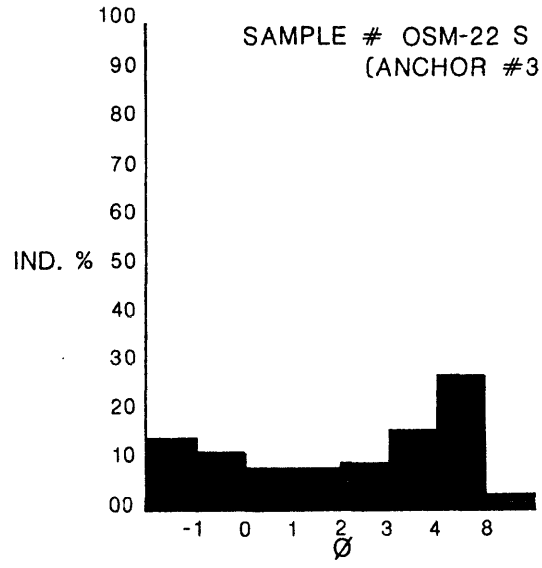
SAMPLE # OSM-22 S (ANCHOR #33)
IND. %
100
90
80
70
60
50
40
30
20
10
00
-1 0 1 2 3 4 8
Ø

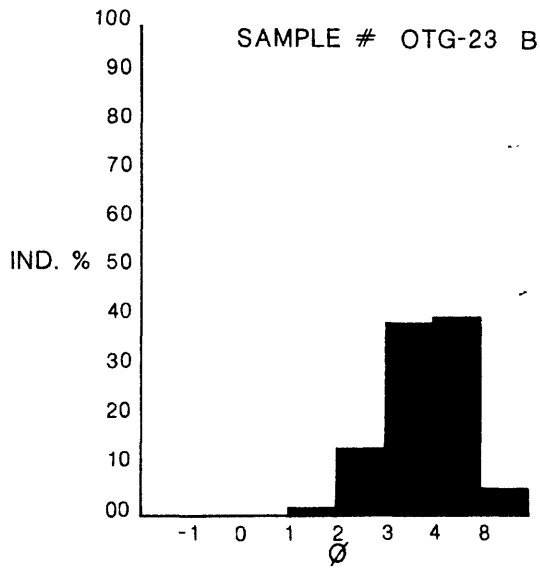
SAMPLE # OTG-23 B
IND. %
100
90
80
70
60
50
40
30
20
10
00
-1 0 1 2 3 4 8
Ø

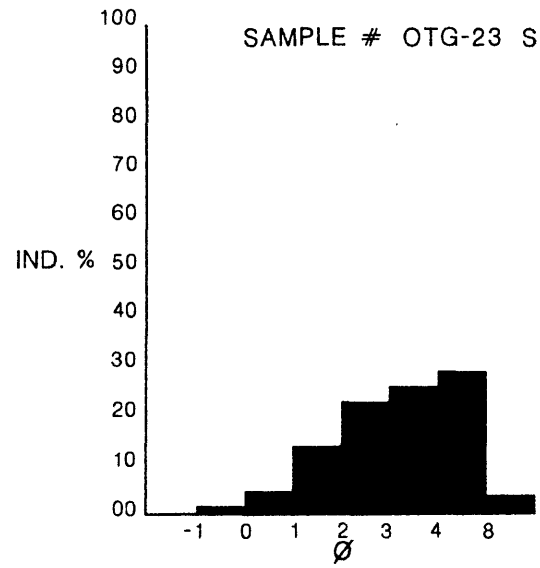
SAMPLE # OTG-23 S
IND. %
100
90
80
70
60
50
40
30
20
10
00
-1 0 1 2 3 4 8
Ø

PLATE 10-28

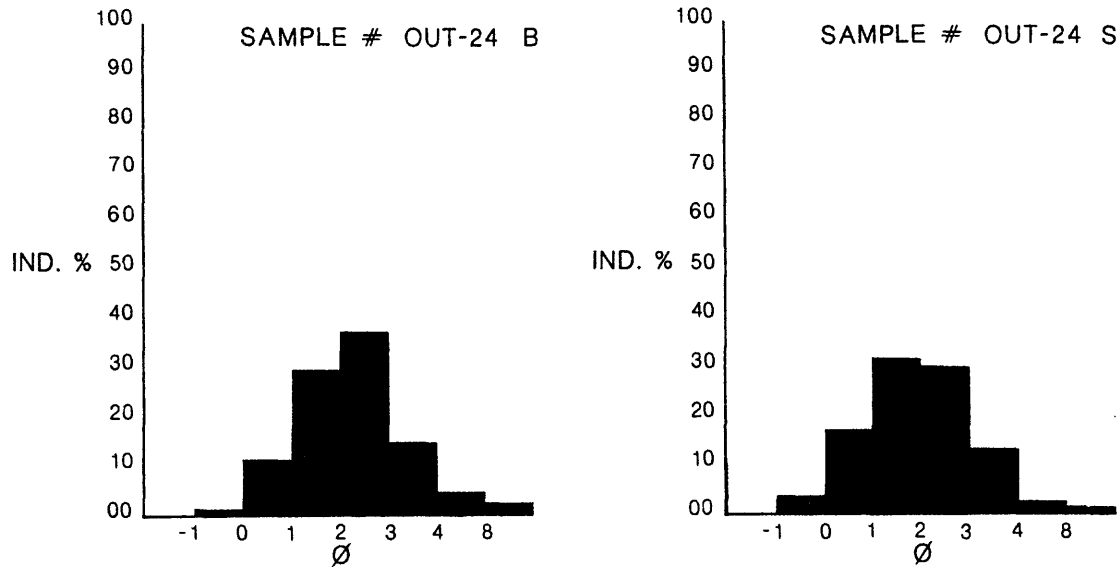
SAMPLE # OUT-24 B
SAMPLE # OUT-24 S
IND. %
100
90
80
70
60
50
40
30
20
10
00
-1 0 1 2 3 4 8
Ø

PLATE 10-29

CHAPTER 11:

ADDITIONAL PALEONTOLOGIC STUDIES, OAK AND KOA CRATERS

by

Elisabeth M. Brouwers[1], Thomas M. Cronin[2], and Thomas G. Gibson[2]

Branch of Paleontology and Stratigraphy

U.S. Geological Survey

INTRODUCTION

The biostratigraphic framework for the PEACE Program consists of thirteen discrete microfaunal zones (AA through MM) from the upper approximately 1,500 ft of section on Enewetak Atoll (figs. 11-1a - 1b, tables 11-1a - 1b). This framework was developed primarily from analyses of benthic ostracodes and foraminifers from core, split-spoon, and Shelby tube samples from geologic boreholes drilled during Phase II of the PEACE Program and is presented in Cronin, Brouwers, and others (1986; U.S. Geological Survey Open-File Report 86-159). The reader is referred to that report for discussions of the details of the biostratigraphic framework itself, the purpose of PEACE Program paleontologic studies, sample and laboratory methodology, data management, and application to crater-mixing analysis. The intent of that publication was to document all of the pre-drilling, onsite, and post-drilling paleontologic analyses for the PEACE Program and was presented as a complement of the report by Henry, Wardlaw, and others (1986, U.S. Geological Survey Open-File Report 86-417) in which are included the geologic descriptions of these boreholes.

As with most programs of this scope, additional questions arose from subsequent geologic analyses that required further paleontologic investigations. These questions involved: (1) the characterization of material from a potential debris flow located on the southeastern side of OAK crater and (2) the depth of origin (stratigraphic provenance) of micro- and macrofossils mixed in KOA crater and the extent of mixing of these components from strata of various depths beneath KOA. Thus, both questions involved an analysis of strata mixed by the direct and immediate effects of the nuclear explosions themselves or by subsequent longer-term (hours, days, weeks, etc.) dynamic responses of the geologic framework to these nuclear events. This chapter reports the results of the paleontologic analyses of 167 samples from 10 boreholes (see table 11-2).

---

[1] Denver, CO.; [2] Reston, VA.

Note: Authorship is presented in alphabetical order.

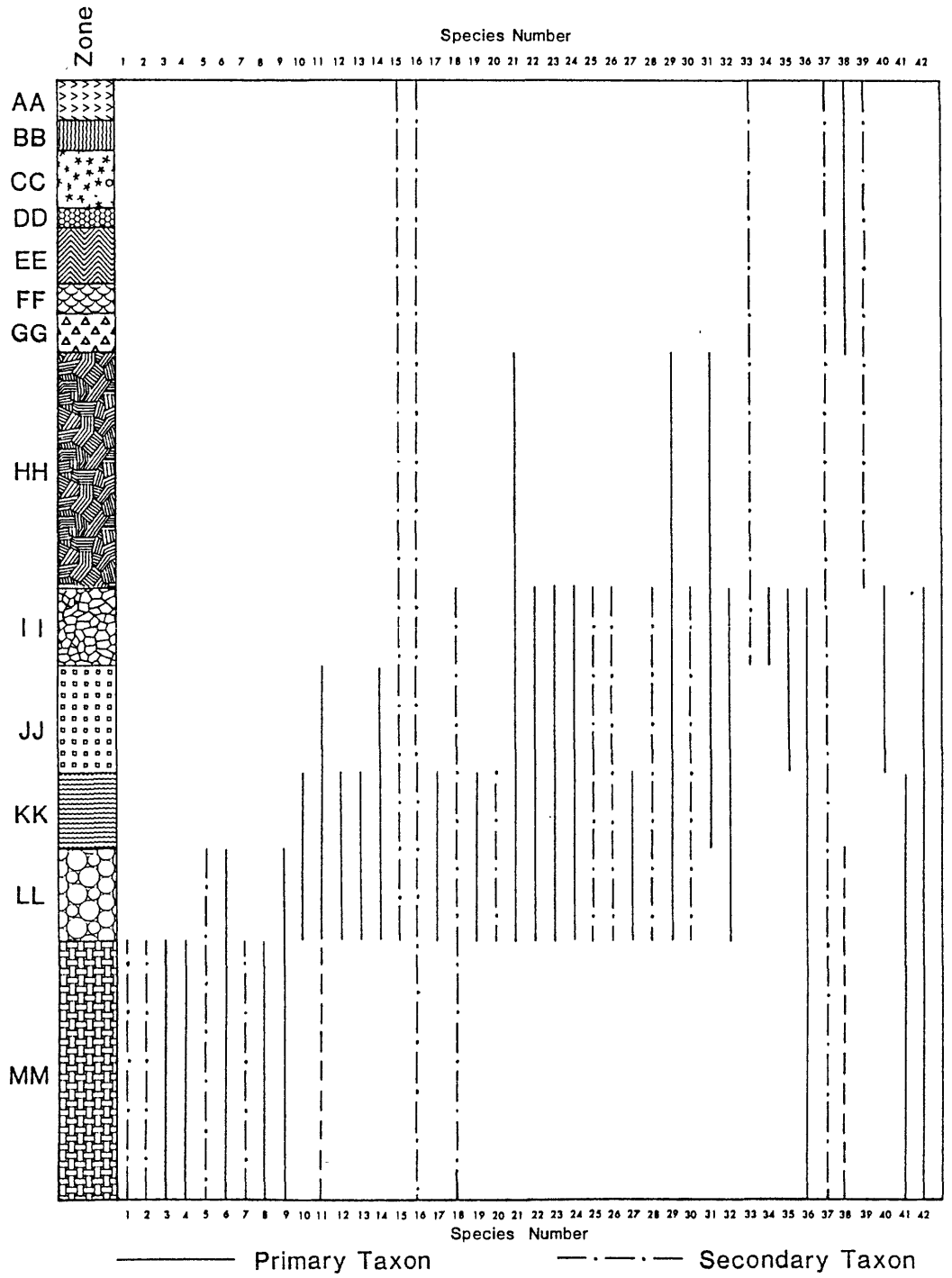

FIGURE 11-1a. -- Generalized composite biostratigraphic ranges of key species of ostracodes from PEACE Program reference boreholes. Composite microfaunal zones AA through MM form the biostratigraphic framework for the roughly upper 1,500 ft of section on Enewetak. Figure modified from Cronin, Brouwers, and others (1986, figs. 14 and 15); for explanation of "species number", refer to Table 11-1a.

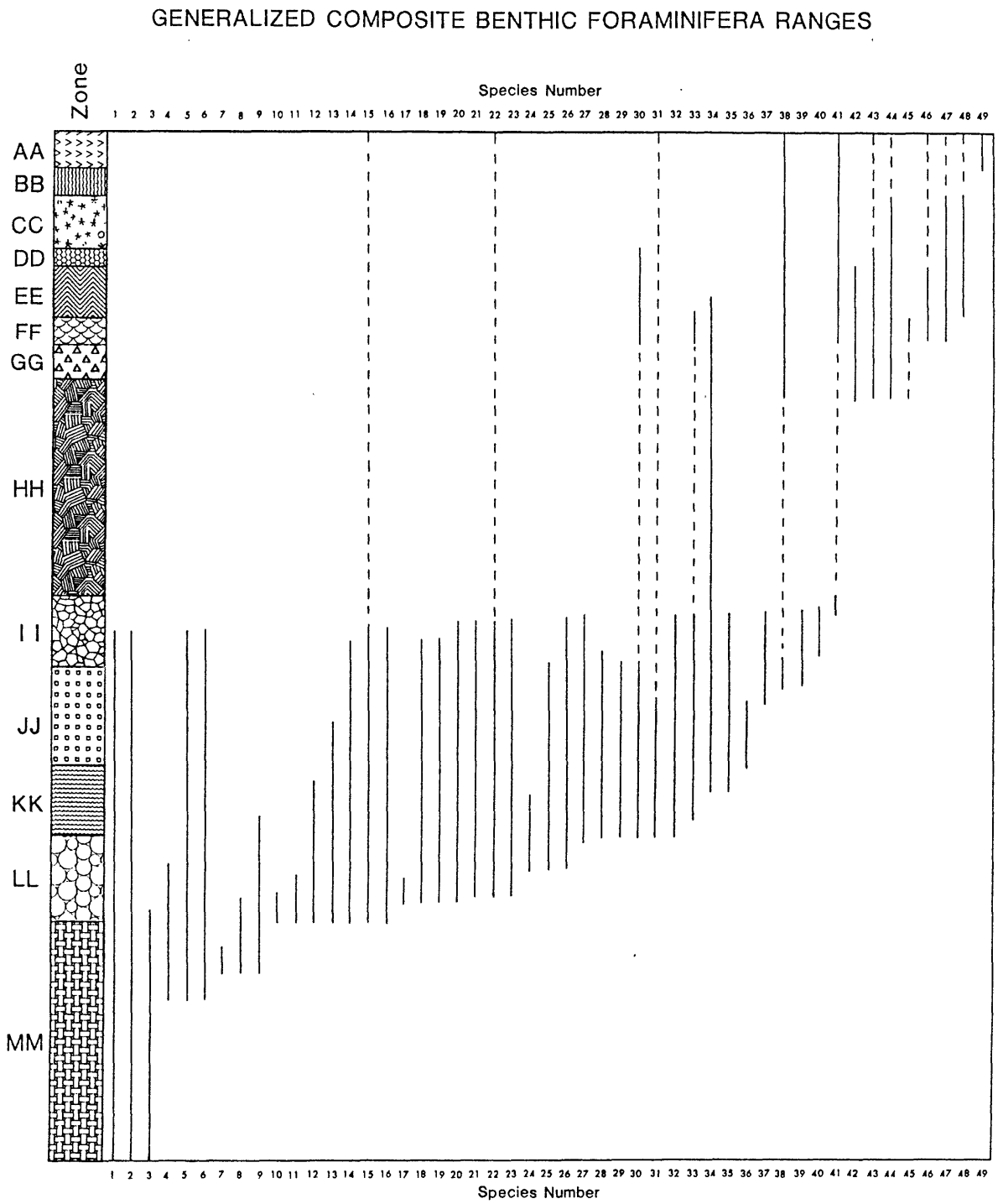

FIGURE 11-1b. -- Generalized composite biostratigraphic ranges of key species of benthic foraminifers from PEACE Program reference boreholes. Composite microfaunal zones AA through MM form the biostratigraphic framework for the roughly upper 1,500 ft of section on Enewetak. Figure modified from Cronin, Brouwers, and others (1986, figs. 14 and 15); for explanation of "species number:, refer to Table 11-1b.

TABLE 11-1a. -- List of key ostracode species used for biostratigraphic framework of Enewetak Atoll. Numbers correspond to "species number" on Figure 11-1a.

OD-1. Hermanites aff. H. transoceanica Teeter, 1975
OD-2. Capricornia sp. A
OD-3. Pokornyella sp. A. (ovate form)
OD-4. Tenedocythere setigera Holden, 1976
OD-5. Pokornyella aff. P. pseudojaponica Holden, 1976
OD-6. Jugosocythereis cf. J. pannosa (Brady, 1869)
OD-7. Hermanites aff. H. tschoppi (van den Bold, 1946)
OD-8. Australomoosella sp. B
OD-9. Radimella sp. A
OD-10. Pokornyella pseudojaponica Holden, 1976
OD-11. Procythereis northpacifica Holden, 1976 (crater morphology)
OD-12. Hermanites tschoppi (van den Bold, 1946)
OD-13. "Palauella" cf. P. spinosa Briggs, 1963
OD-14. Quadracythere trijugis Holden, 1976
*OD-15. Hermanites transoceanica Teeter, 1975 (O-6)
*OD-16. Jugosocythereis sp. A (O-7)
OD-17. Hemicythere gordoni Holden, 1976
OD-18. Paracytheridea sp. A
OD-19. Triebelina crumena (Stephenson, 1944)
OD-20. Radimella sp. B
OD-21. Cletocythereis canaliculata (Holden, 1976)
OD-22. Callistocythere crenata (Brady, 1880)
OD-23. Orionina aff. O. flabellacosta Holden, 1976
OD-24. Hermanites sp. A
OD-25. Morkhovenia sp. A
OD-26. Semicytherura sp. B
OD-27. Capricornia cristatella (Brady, 1868)
*OD-28. Bairdoppilata algicola (O-1)
OD-29. Miocyprideis punctata Briggs, 1963
OD-30. Cytherelloidea semipunctata Holden, 1976
OD-31. Australomoosella sp. A
OD-32. Caudites cf. C. shortlandensis Titterton, 1984
*OD-33. Paracytheridea dromedaria (O-16)
OD-34. Caudites sp. A
OD-35. Aurila sp. A
OD-36. Procythereis sp. A (few pits)
OD-37. Keijia sp. A
*OD-38. Cletocythereis sp. A (O-5)
*OD-39. Callstocythere parakeijia Titterton (O-3)
OD-40. Occultocythereis aff. O. angusta (van den Bold 1967)
OD-41. Hemicythere sp. A
OD-42. Aurila sp. B

TABLE 11-1b. -- List of key benthic foraminifer species used for biostratigraphic framework of Enewetak Atoll. Numbers correspond to "species number" on Figure 11-1b.

BD-1. Clavulina angularis d'Orbigny, 1826
BD-2. Tubulogenerina butonensis Keyzer, 1953
BD-3. Valvulina prominens Todd and Post, 1954
BD-4. Asterigerina tentoria Todd and Post, 1954
BD-5. Nonion grateloupi (d'Orbigny, 1826)
BD-6. Discorbis balcombensis Chapman, Parr and Collins, 1934
BD-7. Valvulammina marshallana Todd and Post, 1954
BD-8. Austrotrilla sp. A
BD-9. Valvulina martii Cushman and Bermudez, 1937
BD-10. Spirolina sp. A
BD-11. Buccella ? perforata Todd and Low, 1960
BD-12. Siphonina sp. A
BD-13. Spiroloculina corrugata Cushman and Todd, 1944
BD-14. Schlumbergina alveoliniformis (Brady, 1879)
BD-15. Hauerina involuta Cushman, 1946
BD-16. Lamarckina sp. A
BD-17. Cribrogoesella parvula Todd and Low, 1960
BD-18. Hauerina diversa Cushman, 1946
BD-19. Spirolina arietina (Batsch, 1791)
BD-20. Pararotalia byramensis (Cushman, 1922)
BD-21. Peneroplis honestus Todd and Post, 1954
*BD-22. Epistominella tubulifera (Heron-Allen and Earland, 1915) (B-8)
BD-23. Ammonia beccarii (Linne, 1839)
BD-24. "Slitoeponides" sp. A
BD-25. Hauerina aspergilla (Karrer, 1868)
BD-26. Elphidium striatopunctatum (Fichtel and Moll, 1803)
BD-27. Clavulina sp. A
BD-28. Svratkina sp. A
BD-29. Epistomaroides sp. A
*BD-30. Loxostomum limbatum (H.B. Brady, 1881) (B-9)
BD-31. Pyrgo denticulata (H.B. Brady, 1884)
BD-32. Quinqueloculina distorqueata Cushman, 1954
*BD-33. Bolivina rhomboidalis (Millett, 1899) (B-2)
BD-34. Cymbaloporetta bradyi (Cushman, 1924)
BD-35. Valvulammina globularis (d'Orbigny,
BD-36. Quinqueloculina byramensis Cushman, 1923
BD-37. Buccella sp. A
*BD-38. Anomalina sp. A (B-1)
BD-39. Asterigerina indistincta Todd and Post, 1954
BD-40. Gaudryina (Siphogaudryina) rugulosa Cushman, 1932
BD-41. Anomalinella rostrata (H.B. Brady, 1881)
BD-42. Calcarina delicata Todd and Post, 1954
*BD-43. Quinqueloculina sp. A (B-12)
*BD-44. Calcarina hispida H.B. Brady, 1876 (B-6)
*BD-45. Calcarina calcar (d'Orbigny, 1826) (B-4)
*BD-46. Neouvigerina porrecta (H.B. Brady, 1879) (B-10)
*BD-47. Quinqueloculina parkeri (H.B. Brady, 1881) (B-11)
*BD-48. Bolivinella folia (Parker and Jones, 1865) (B-3)
BD-49. Calcarina spengleri (Gmelin, 1788)

TABLE 11-2. -- Boreholes examined or reexamined for current study, intervals studied, and number of samples taken. Depths in feet below sea floor. See Figures 11-2 and 11-3 for location maps.

BOREHOLE NO.	TOTAL INTERVAL	NO. SAMPLES
KAR-1	171.9 - 741.25	38
KBZ-4	6.0 - 569.4	40
KCT-5	6.0 - 241.25	16
KDT-6	3.5 - 115.9	16
KET-7	6.8 - 41.4	6
KFT-8	15.75 - 263.45	32
OHT-10	7.45 - 135.05	8
OJT-12	12.5 - 66.95	5
OLT-14	6.90 - 7.15	1
ONT-16	10.45 - 72.75	5
	TOTAL NUMBER OF SAMPLES	167

The terminology used in this Chapter is the same as that developed and/or used in Open-File Report 86-159 with the exception that the term in situ (p. 23) is hereby discontinued for an interval either within or near the crater that contains fossils from only one discrete stratigraphic level. The term "unmixed" is used instead for an interval that contains fossils from only one biostratigraphic zone. The "paleontologic zones" for the material in and beneath the nuclear craters, in order of descending depth, are:

MIXED ZONE
TRANSITION ZONE
UNMIXED ZONE

All depths in the current Chapter are reported in feet (ft) below the sea floor (bsf).

SUPPLEMENTAL PALEONTOLOGIC STUDIES OF OAK CRATER

Microfossils were examined from four boreholes (OHT-10, OJT-12, OLT-14, and ONT-16; see fig. 11-2) that penetrated material believed to represent a debris flow on the southeastern side of OAK crater. Samples from these boreholes were studied only in a preliminary fashion before the release of the Open-File Report by Cronin, Brouwers, and others (1986). For the current study, additional microfossil sampling was conducted primarily in the upper 75 ft of the boreholes (tables 11-2 and 11-3) to determine the depth and extent of mixing of biostratigraphic components. A geologic cross section of the boreholes on the southeast transect of OAK crater, modified to incorporate the new paleontologic information is given on Plate 11-1 (in pocket). This cross section supersedes Figure 18 of Cronin, Brouwers, and others (1986).

All four boreholes showed a pattern of mixed microfaunas in the upper 20 ft, including species from zones AA through FF (see fig. 11-1). The mixing resembles that found in crater fill in the ground-zero boreholes, OBZ-4 and OPZ-18. Between depths of about 20 to 50 ft in both OHT-10 and OJT-12, a mixed assemblage was not obvious, but neither was a normal sequence found. This anomolous microfaunal pattern is interpreted to represent a unique taphonomic[1] situation not encountered in other boreholes and probably related to a unique process of disturbance involved in the formation of the debris blanket.

OHT-10. --The lowest sample from borehole OHT-10 containing a definitely mixed microfauna is at 7.45 ft. This sample contains species from zones AA through FF. Significant markers include: AA - red Homotrema, Calcarina spengleri; BB - CC - Loxoconcha heronislandensis, Cletocythereis sp. A; CC - Loxocorniculum insulaecapricornensis; and EE - GG - Cletocythereis rastromarginata, Orionina sp., Calcarina delicata. It is emphasized that preservation of all specimens is moderate to poor, which is not typical of preservation of microfossils in zone AA. At 24.2 and 33.2 ft, the microfauna

---

[1] Taphonomy, as defined by Bates and Jackson (1980, p. 638) is that branch of paleoecology concerned with the manner of burial and preservation of plant and animal remains.

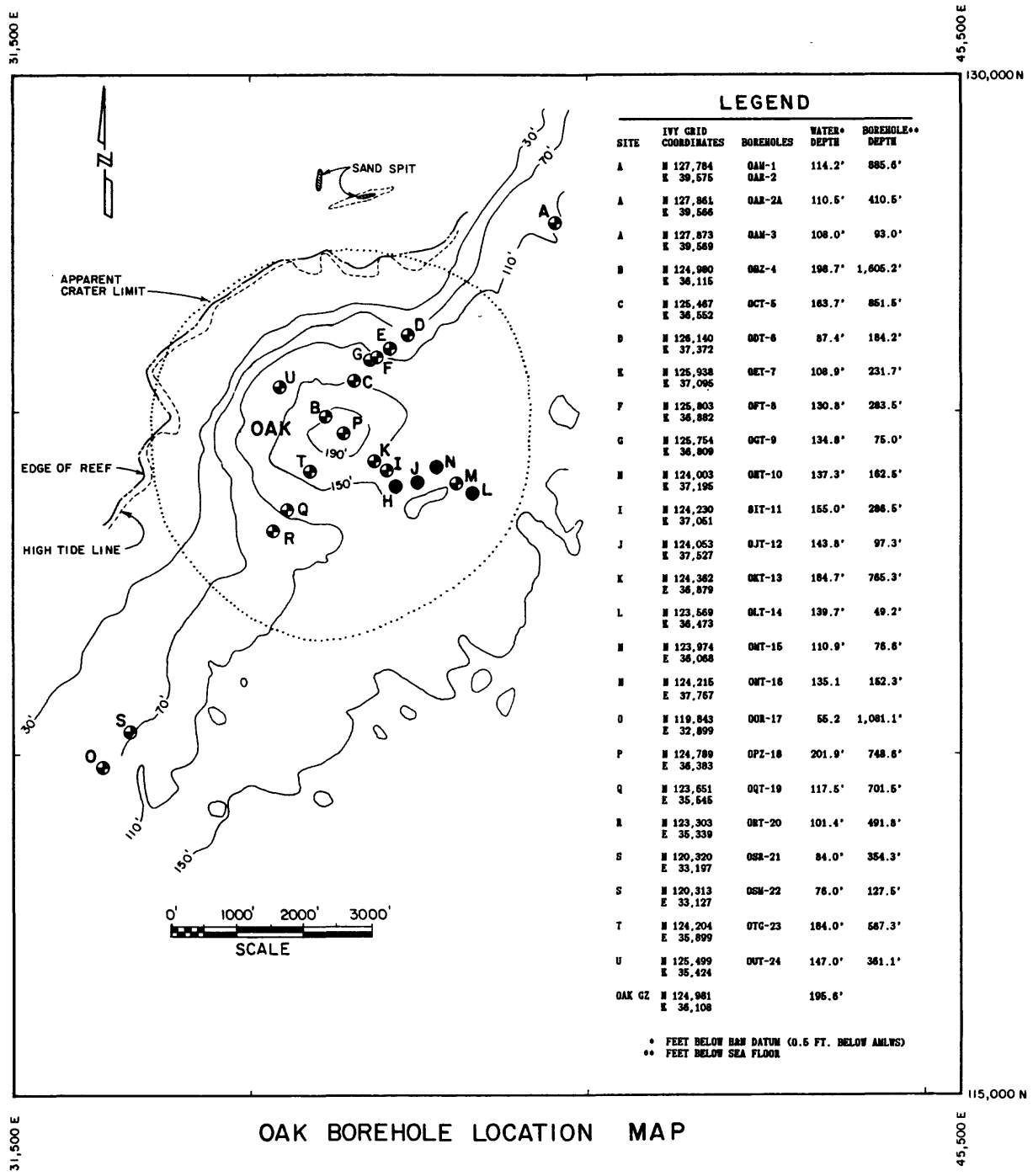

FIGURE 11-2. -- Map of OAK crater showing borehole sites (depicted by letters) and general bathymetric contours (contour interval equals 40 ft). Solid dots are boreholes referenced in this Chapter.

TABLE 11-3. -- Samples examined or reeexamined from OAK crater area for current study. See Plate 11-1 for revised biostratigraphic correlation of the southwest transect. Depths given in ft below sea floor.

OHT-10	Zone Assignment
7.45 - 7.70	AA-FF, ?GG mixed
24.1 - 24.45	?
33.2 - 33.45	?
53.5 - 53.75	EE mixed
75.85 - 76.1	CC-GG mixed
107.4 - 107.65	EE unmixed
116.05 - 116.3	EE unmixed
134.8 - 135.05	EE unmixed

OJT-12	Zone Assignment
12.5 - 12.8	AA-FF,?GG mixed
18.65 - 18.9	AA-CC mixed
29.4 - 29.65	AA ? mixed
41.0 - 41.25	AA-FF mixed
54.0 - 54.25	EE-FF mixed
66.75 - 66.95	EE-FF mixed

OLT-14	Zone Assignment
6.90 - 7.15	AA-BB mixed
14.4 - 14.65	AA unmixed
30.45 - 30.7	BB unmixed
50.15 - 50.4	CC unmixed
72.5 - 72.75	CC unmixed

ONT-16	Zone Assignment
10.45 - 10.7	AA-EE mixed

is anomalously sparse, containing only 2 specimens and 1 specimen, respectively, of ostracodes. This suggests that this interval is unlike any other examined in the upper 50 ft of section in other boreholes. For example, it does not show direct evidence for mixed faunas nor evidence of an unmixed assemblage. It was concluded that some type of disturbance has altered the original faunal sequence and that the process is not like that involved with typical mixing of the crater fill found in other boreholes in the central crater region.

The sample from 47.75 ft reported in Cronin, Brouwers, and others (1986, p. 31) also contained evidence of mixing with the anomolous occurrence of a zone CC assemblage. The sample from 53.5 ft contains abundant, diverse microfossils, some representing zone EE. Mixing of specimens from several zones is probable to at least this depth.

The sample at 75.85 ft has less convincing evidence for mixing in that a typical CC fauna occurs. However, two ostracode species generally found in zones FF or GG and some foraminifers ranging below zone CC suggest that a minor amount of mixing may have occurred. The interval between 54 and 76 ft is thus referred to as a basal mixed zone. Between 76 and 107 ft, unmixed zone CC is assumed to exist.

At 107.4 and 116.05 ft, microfossils are less common and show no evidence for mixing in either fossil group. At 134.8 ft, a typical zone EE fauna occurs. Because no typical zone DD faunas have been found in this borehole, the interval from 107 to 135 ft is assigned to zone EE.

In summary, definitely mixed faunas occur in borehole OHT-10 down to 54 ft and possibly mixed faunas down to 76 ft. Probable unmixed material occurs between 107 and 135 ft.

OJT-12. -- Extensive faunal mixing occurs in samples taken from 12.5 and 18.65 ft. Samples from 29.4, 41.0, 54.0, and 66.75 ft contain variously mixed microfaunal assemblages that are also characterized by the lack of a typical AA/BB/CC zonal sequence. Whereas the mixing of specimens from many zones is not as obvious in this interval as it is in ground-zero boreholes, there is nonetheless evidence that the normal sequence has been disturbed to a depth of about 67 ft.

At 82.65 and 92.0 ft, the ostracode Paracytheridea dromedaria occurs in an otherwise sparse assemblage. This zone DD marker taxon suggests that the interval from 82 to 93 ft is unmixed and represents zone DD. The sparse assemblage at 96.3 ft is typical of zone EE. These zone assignments are modifications of the original summary in Cronin, Brouwers, and others (1986).

In summary, material from OJT-12 probably is mixed to at least 67 ft; the interval between 67 and 82 ft was not sampled; unmixed zone DD occurs between 82 ft and the unconformity at 94.2 ft; and zone EE occurs below 94.2 ft.

OLT-14. -- A single sample was taken from this borehole at 6.9 ft. This sample contains a mixture of components from zones AA and BB. Specimens are well-preserved, including mostly clean, translucent individuals. Species diversity is moderate and abundance is fairly high.

ONT-16. -- The lowest sample in borehole ONT-16 containing definite evidence of mixed microfaunas is at 10.45 ft. This sample contains a mixture of material from zones AA - EE, including the following zonal markers: AA - red Homotrema; BB-CC - Cletocythereis sp. A., Loxoconcha heronislandensis; CC - Loxocorniculum insulaecapricornensis, Calcarina rustica; DD - Paracytheridea dromedaria; EE - FF - Australimoosella sp. A. Species diversity is low to moderate.

The microfauna in the lowest four samples indicates a normal (unmixed) stratigraphic sequence: 14.4 ft = zone AA; 30.45 ft = probable zone BB; 50.15 ft = zone CC; and 72.5 ft = zone CC. Preservation is moderate, with most specimens opaque and filled with matrix. At 50.15 ft, many of the specimens are partly dissolved and fragmented. Restudy of a sample at 101.7 ft reported in Cronin, Brouwers, and others (1986, p. 33) is reinterpreted as containing a zone EE assemblage.

KOA MIXING STUDY

During the drilling of boreholes in OAK crater, it was noticed by the geologists onsite that (1) abundant light-brown to moderate-yellowish-brown coral fragments, typical of both the taxa and staining of corals from deeper stratigraphic provenances, (2) charcoal suspected of coming from deeper stratigraphic horizons, and (3) microfaunal species from deep biostratigraphic zones (zones II through LL) all occurred in the mixed zone of crater fill. Subsequent lithic and paleontologic evidence from the OAK boreholes suggested that these materials were piped to the surface from strata below the crater. "Piped" specimens are those specimens most probably hydrodynamically admixed from horizons below the geologic crater, and are distinguished from mixed specimens that represent shallow zone material (zones AA - EE) that were directly involved with the formation of the geologic crater and became mixed during crater infilling. Within a reasonably defined crater radius, crater fill can be characterized as the material containing mixed faunas. Detailed analysis of the mixed zones and piped specimens can have considerable importance in defining the depth of the crater and may yield important clues to the crater dynamics that led to the mixing. In the KOA area, however, evidence for piped specimens from comparably deep levels was inconclusive from the initial studies reported in Cronin, Brouwers, and others (1986), and the lithic descriptions of the cores/samples made onboard the drill ship and afterward (see Henry, Wardlaw, and others, 1986) revealed far fewer fragments of brown-stained coral and almost no charcoal.

This section describes the results of a detailed paleontologic study of the KOA crater ground-zero borehole (KBZ-4) and radial boreholes (KCT-5, KDT-6, KET-7, and KFT-8; see fig. 11-3) to obtain information on suspected piping and extent of piping of deep materials up to surface or shallow (i.e., near-surface) levels in KOA crater.

The results show that, in KOA crater, material from biostratigraphic zones comprising a portion of the upper part of the normal stratigraphic sequence (from zones EE, FF, and GG) are common in boreholes KBZ-4 and KCT-5. However, a portion of the mixed faunas in KBZ-4 and KCT-5 is from considerably deeper stratigraphic horizons. This indicates piping from depth similar in style to that inferred for OAK crater. The most extensive piping in terms of the number of specimens and the number of samples in which they

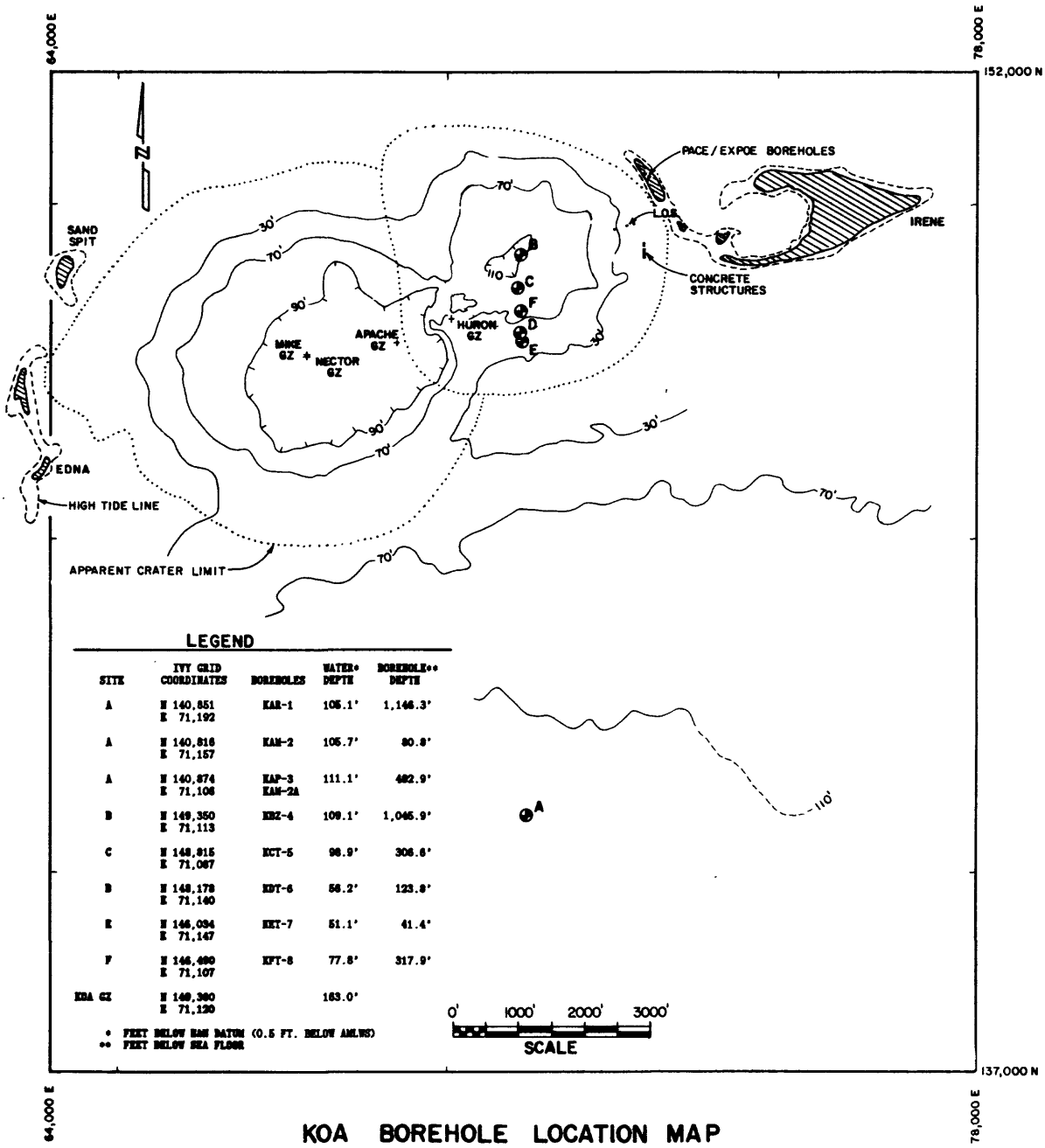

KOA BOREHOLE LOCATION MAP

FIGURE 11-3. -- Map of KOA-MIKE crater area showing borehole sites (depicted by letters) and general bathymetric contours (contour interval in ft, irregular interval).

occur was found in KBZ-4. This situation is similar to that in the ground-zero borehole OBZ-4 in OAK crater. Deep specimens were only found in one sample each from near the top of boreholes KCT-5 and KDT-6.

Figure 11-4 is a plot of the distribution of species in the upper 140 ft of KBZ-4. Figure 11-5 is a plot of species diversity in KBZ-4. Table 11-4 lists all samples examined for this study, and Table 11-5 summarizes occurrence of piped material by sample.

The following are detailed discussions of each borehole.

KBZ-4. -- Microfaunal evidence indicates that crater-fill material occurs from the surface to 142 ft, and an undisturbed faunal sequence occurs below about 143 ft. Most specimens piped from zones II through LL occur in the interval between 6.0 and 43.85 ft, although some occur as deep as 93.15 ft (table 11-5).

The interval between 6.0 to 28.8 ft (and probably extending to the surface) is dominated by ostracodes and foraminifers from zones AA, BB, and CC, with some contribution from zones DD and EE. Diagnostic zonal markers include: AA - red Homotrema, Anchistrocheles, Calcarina spengleri; BB - Loxoconcha heronislandensis, Cletocythereis sp. A; CC - Loxocorniculum insulaecapricornensis, Baculogypsina; and EE - FF - Calcarina delicata. The ostracode species diversity and abundance are anomalously high (see figure 11-5), containing between 20 and 40 species. Typical undisturbed modern atoll samples and samples from zones AA, BB and CC generally contain only 12-15 species.

The piped material between 6.0 and 28.8 ft consists of two groups of species. One group includes ostracodes from intermediate depths (zones FF - HH) and the second includes foraminifers from deep zones (II - KK). The ostracode assemblages from the highest samples (6.0, 10.95, and 15.45 ft) contain piped specimens from zones FF, GG, and the upper part of HH. Most piped specimens in the lowest samples (20.55, 21.2, and 25.8 ft) came from zones KK and LL.

The interval from 28.8 to 43.85 ft contains ostracodes and foraminifers from zones AA - EE. The ostracode species diversity and abundance are high and both decrease significantly toward the 44-ft level. The piped material consists of two groups: half of the ostracodes are from intermediate depths (zones FF, GG, HH), and the remaining ostracodes and all of the foraminifers are from deep zones (KK - MM). The number and diversity of ostracodes and foraminifers believed to be piped is greater in this interval than in the upper 28 ft, constituting up to 7 percent of the total assemblage.

Between 53.8 and 124.0 ft, ostracodes and foraminifers from zones AA - EE were found. Species diversity and abundance of ostracodes show a peak in the middle of this interval and both values drop markedly near 124 ft. The piped material consists of ostracodes from intermediate depths (zones FF - II) and foraminifers from deep zones (KK - LL).

The interval between 133.05 and 137.5 ft contains species representative of zones BB - EE. The dominant species come from zones CC to DD, with very sparse specimens from zones BB and EE. Species diversity and abundance are

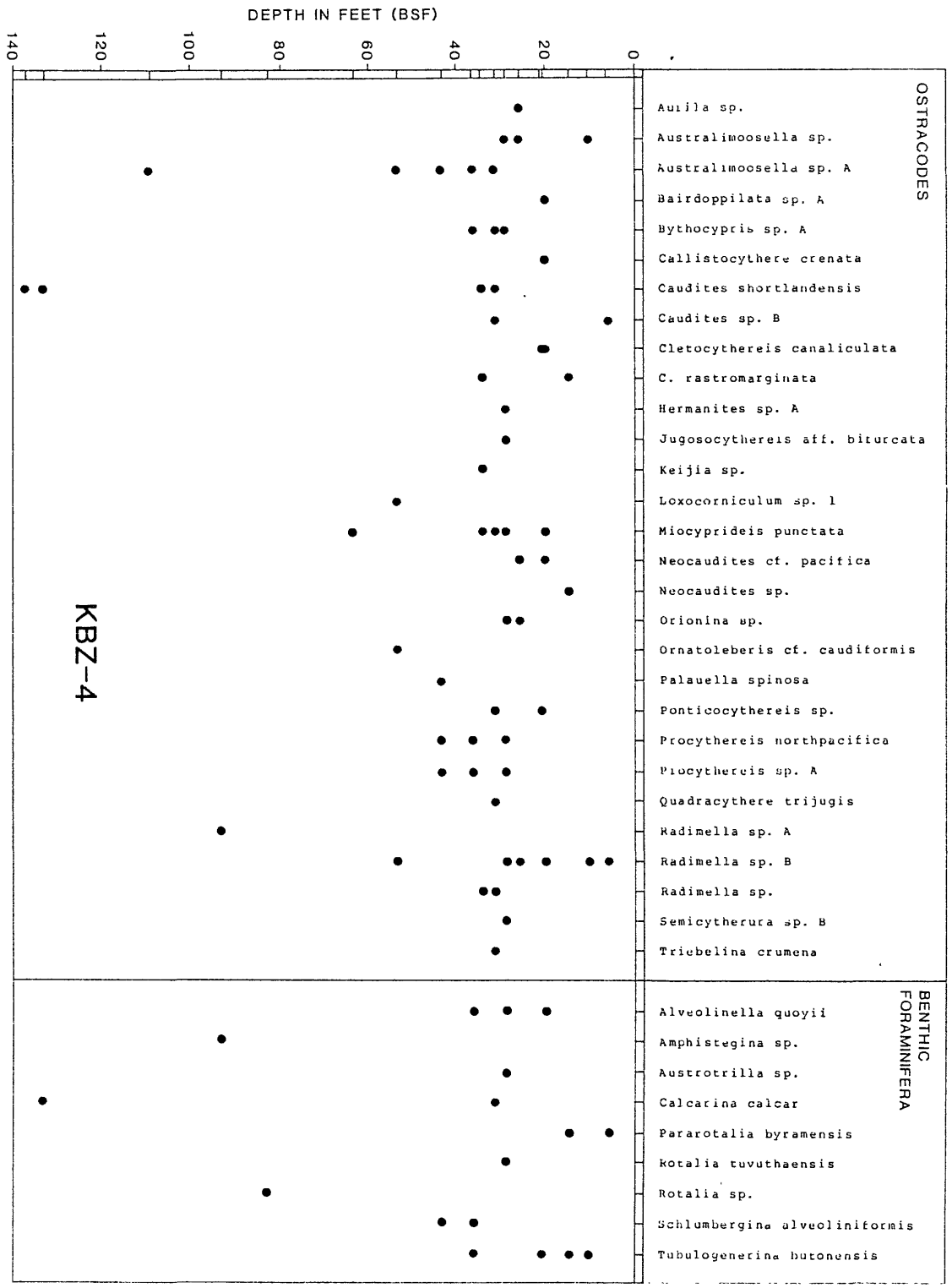

FIGURE 11-4. -- Occurrence chart of selected taxa of ostracodes and foraminifers in samples from upper 140 ft of borehole KBZ-4. The locations of samples (in ft bsf) are indicated at top of figure by tick marks. The species in this figure that do not occur in the upper 140 ft of the reference cores from Enewetak and their occurrences in KBZ-4 are interpreted to represent piping from greater depths. Note the greatest concentration of piped specimens is between 15 and 50 ft. See text for discussion.

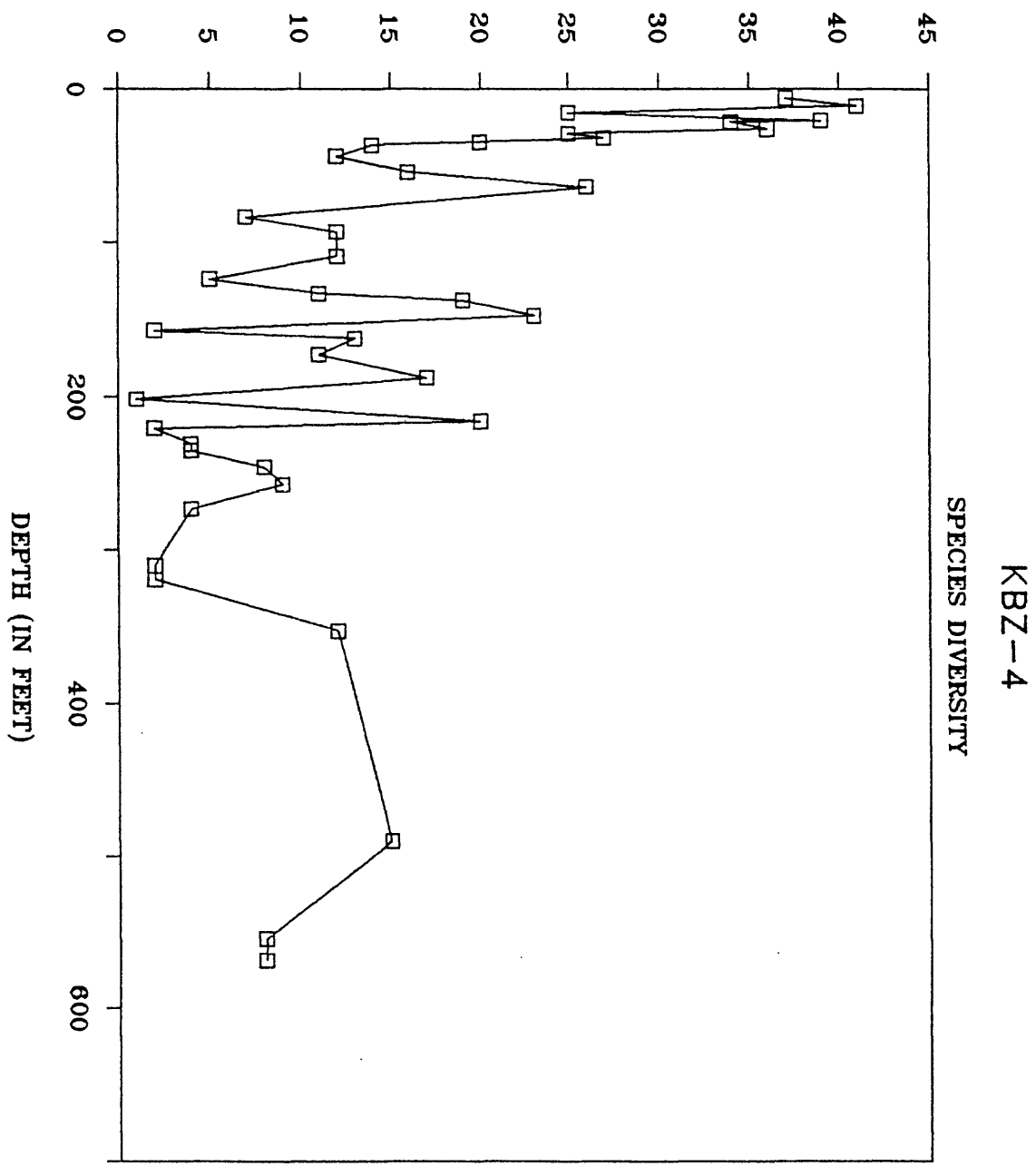

FIGURE 11-5. -- Diversity of ostracodes (number of species) in samples from upper part of borehole KBZ-4. Peaks in abundance in the upper 150 ft of the borehole probably are related to crater infilling.

TABLE 11-4. -- Samples examined or reexamined for KOA mixing study. Depth given in ft bsf. See Figure 11-3 for location map.

KAR-1	KBZ-4	KCT-5	KDT-6	KET-7	KFT-8
171.9	6.0 - 6.25	6.0 - 6.25	3.5 - 3.75	6.80-7.05	15.75- 16.00
177.4-177.85	10.95-11.2	15.0 -15.25	15.25- 15.5	12.55-12.8	20.00- 20.25
178.5	15.45-15.7	38.9 -39.15	24.5- 24.75	18.00-18.25	34.50- 34.75
192.6	20.55-20.8	52.3 -52.55	29.75-30.0	28.30-28.55	38.40- 38.65
203.0	21.2 -21.45	78.0 -78.25	43.55-43.8	36.25-36.5	60.20- 60.45
212.4	25.8 -26.05	89.75-90.0	54.55-54.8	41.15-41.4	63.75- 64.0
223.0	28.8 -29.05	101.75-102.0	67.75-68.0		79.95- 80.20
230.3-230.9	31.4 -31.65	124.15-124.4	76.0 -76.25		84.10- 84.35
239.65	34.5 -34.75	130.75-131.0	81.5 -81.75		95.65- 95.90
255.0	36.5 -36.75	144.75-145.0	85.35-85.60		106.25-106.50
262.0	43.6 -43.85	170.5 -170.75	90.10-90.35		110.00-110.25
273.85	53.8 -54.05	181.1 -181.35	95.5 -95.75		115.25-115.5
282.2	63.25-63.5	195.75-196.0	100.05-100.30		122.5-122.75
298.2	83.15-83.4	206.25-206.5	105.0 -105.25		128.25-128.5
339.1	93.0 -93.15	220.6 -220.85	110.3 -110.55		132.5- 132.75
348.5	109.1-109.35	241.0 -241.25	115.65-115.9		139.15- 139.4
366.4	123.75-124.0				145.75- 146.0
397.4	133.05-133.3				152.5 - 152.75
423.9	137.5-137.75				164.10- 164.35
442.4	147.25-147.5				175.35- 175.6
448.0-448.8	156.95-157.2				182.75- 183.0
460.5	161.85-162.1				187.75- 188.0
481.8-482.0	172.3-172.55				193.6 - 193.85
483.1-483.4	187.4-187.65				198.75- 199.0
495.8	201.7-201.95				202.0 - 202.5
539.2-540.3	216.0-216.25				215.65- 215.9
554.8-555.8	220.5-220.75				224.82- 225.05
568.9-569.15	230.8-231.05				231.3 - 231.55
584.3-584.55	235.15-235.4				241.2 - 241.45
591.0-591.25	246.1-246.35				251.5 - 251.75
591.9	257.10-257.35				257.8 - 258.05
626.4-626.9	273.5-273.75				263.2 - 263.45
644.5-645.6	309.95-310.2				
656.75-657.0	319.0-319.25				
670.0-670.25	352.5-352.75				
702.35-702.6	370.6-370.85				
732.2-732.8	400.2-400.45				
741.0-741.25	489.6-489.85				
	555.2-555.45				
	569.15-569.4				

TABLE 11-5. Intermediate- and deep-zone piped material in KOA crater. Biostratigraphic range for each taxon in parentheses. Depth in ft bsf.

DEPTH	OSTRACODES	FORAMINIFERS	BROWN MATERIAL
	BOREHOLE KBZ-4		
6.0 - 6.25	Radimella sp. B (upper form) (FF-GG) Caudites sp. B (lower EE-GG)	Pararotalia byramensis (variety from II-JJ)	brown foraminifera (?KK-LL)
10.95- 11.2	Australimoosella sp. (EE-GG) Radimella sp. B (upper form) (FF-GG)	Tubulogenarina butonensis (II-JJ, white preservation)	brown foraminifers (?KK-LL)
15.45- 15.70	Cletocythereis rastromarginata (?FF-GG) Neocaudites sp. (FF-GG)	Tubulogenerina butonensis (II-JJ) Pararotalia byramensis (II-JJ)	
20.55- 20.8	Radimella sp.B (upper form) (FF-GG) Neocaudites cf. pacifica (FF-GG) Cletocythereis canaliculata (HH-LL) Miocyprideis punctata (HH-LL) Bairdoppilata sp. A II-KK Callistocythera crenata (II-LL)	Alveolinalla quoyii (KK-LL, dark brown)	brown foraminifers
21.20- 21.45	Ponticocythereis sp. (GG) Cletocythereis canaliculata (HH-LL)	Tubulogenerina butonensis (II-JJ)	brown foraminifers (?KK-LL)
25.8 - 26.05	Neocaudites cf. pacifica (FF-GG) Radimella sp. B (FF-GG) Orionina sp. (upper form) (FF-GG) Australimoosella sp. (FF-HH) Aurila sp. (upper form) (FF-HH) Radimella sp. B (lower form) (KK-LL)		brown foraminifers (?KK-LL)
28.8 - 29.05	Radimella sp. B (upper form) (FF-GG) Orionina sp. (upper form) (FF-GG) Australimoosella sp. (FF-HH) Hermanites sp. A (intermediate form) (GG-II) Bythocypris sp. A (GG-KK) Miocyprideis punctata (HH-LL) Semicytherura sp. B (JJ-LL) Procythereis sp. A (JJ-MM) Jugosocythereis aff. bifurcata (old form) (?JJ-LL) Procythereis northpacifica (crater) (LL-MM)	Alveolinella quoyii (KK-LL) Austrotrilla sp. (LL-MM) Rotalia tuvuthaensis (LL-MM)	
31.4 - 31.65	Caudites sp. B (bottom EE-GG) Ponticocythereis sp. (FF-GG) Caudites shortlandensis (FF-GG) Radimella sp. (FF-GG) Bythocypris sp. A (GG-KK) Miocyprideis punctata (HH-LL) Australimoosella sp. A (HH-LL) Quadracythere trijugis (JJ-LL) Triebelina crumena (KK-LL)	Calcarina calcar (FF)	brown coral
34.50- 34.75	Cletocythereis rastromarginata (FF-GG) Radimella sp. (FF-GG) Caudites shortlandensis (FF-GG) Keijia sp. (FF-HH) Miocyprideis punctata (HH-LL)		brown foraminifers (?KK-LL) brown coral
36.50- 36.75	Bythocypris sp. A (GG-KK) Australimoosella sp. A (HH-LL) Procythereis sp. A (JJ-MM) Procythereis northpacifica (JJ-LL)	Tubulogenerina butonensis (JJ-LL) Alveolinella quoyii (KK-LL) Schlumbergina alveoliniformis (KK-LL)	brown coral
43.6 - 43.85	Australimoosella sp. A (HH-LL) Procythereis sp. A (JJ-MM) Palauella spinosa (KK-LL) Procythereis northpacifica (LL-MM)	Schlumbergina alveoliniformis (KK-LL)	brown coral
53.8 - 54.05	Radimella sp. B (upper form) (FF-GG) Loxocorniculum sp. I (HH-KK) Australimoosella sp. A (HH-LL) Ornatoleberis cf. caudiformis (II-KK)	None	
63.25- 63.5	Miocyprideis punctata (HH-LL)	None	
83.15- 83.4	None	Rotalia sp. (KK-LL)	brown foraminifers (?KK-LL)
93.0 - 93.15	Radimella sp. A (upper form) (FF-GG)	Amphistegina sp. (?KK-LL)	brown foraminifers (?KK-LL)
109.1 -109.35	Australimoosella sp. A (HH-LL)	None	
133.05-133.3	Caudites shortlandensis (EE-GG)	Calcarina calcar (FF)	
137.5 -137.75	Caudites shortlandensis (EE-GG)		
	BOREHOLE KCT-5		
6.0 - 6.25	None	None	
15.0 - 15.25	Miocyprideis punctata (HH-LL)	None	
	BOREHOLE KDT-6		
3.5 - 3.75	Miocyprideis punctata (HH-LL) Australimoosella sp. A (HH-LL) Cletocythereis canaliculata (HH-LL) Aurila sp. A (II-JJ) Procythereis sp. A (II-MM)	Pararotalia byramensis (JJ-KK variaty)	brown foraminifers

low. The overall assemblage indicates less mixing and homogenization than in the upper 133 ft. Only ostracodes from intermediate depths (zones FF and GG) are suspected as being piped.

The sample at 147.25 ft consists predominantly of taxa characteristic of zones DD and EE plus one specimen of Radimella sp. The Radimella sp. raises the possibility that the basal mixing zone previously identified at 142 ft in this core (Cronin, Brouwers, and others, 1986, p. 25) extends down to 147.5 ft, but this is doubtful at present.

KCT-5. --In borehole KCT-5, the sample from 15.0 - 15.25 ft contained three specimens of the ostracode Miocyprideis punctata (zones HH - LL) together with a mixed assemblage from zones AA - EE (table 11-5). These specimens from HH - LL may represent piping or simple reworking of piped material from other sites.

KDT-6. -- Sixteen samples were examined from borehole KDT-6 from depths between 3.5 and 115.9 ft. Crater-fill material occurs between the surface and about 85.6 ft, and a normal faunal sequence occurs between 90.1 and 115.9 ft (table 11-5). Seven percent of the assemblage in the sample from 3.5 ft consists of piped species from zones HH - LL. The remainder of the assemblage is dominated by zone AA - BB ostracodes and foraminifers. No other piped material was observed in KDT-6.

KET-7. -- Six samples from depths between 6.8 and 41.4 ft were examined. KET-7 was drilled outside of the proposed excavational crater and contains a normal unmixed biostratigraphic sequence. Zone AA occurs down to 36.5 ft, and the sample at 41.4 ft contains a zone BB fauna.

KFT-8.-- Crater-fill material extends from the surface to 132.5 ft in this borehole, and from depths between 139.15 and 263.45 ft an unmixed faunal sequence occurs. No piped material was observed in the crater fill.

REFERENCES

Bates, R.L., and Jackson, J.A., EDS.,1980, Glossary of Geology; Second Edition, American Geological Institute, Falls Church, Virginia, 751 p.

Cronin, T.M., Brouwers, E.M., Bybell, L.M., Edwards, E.E., Gibson, T.G., Margerum, R., and Poore, R.Z., 1986, Pacific Enewetak Atoll Crater Exploration (PEACE) Program, Enewetak Atoll, Republic of the Marshall Islands; Part 2: Paleontology and biostratigraphy, application to OAK and KOA craters: U.S. Geological Survey Open-File Report 86-159, 39 p., 20 figs., 12 tbls., 3 appendices.

Henry, T.W., Wardlaw, B.R., Skipp, B., Major, R.P., and Tracey, J.I., Jr., 1986, Pacific Enewetak Atoll Crater Exploration (PEACE) Program, Enewetak Atoll, Republic of the Marshall Islands; Part 1: Drilling operations and descriptions of boreholes: U.S. Geological Survey Open-File Report 86-419, 497 p., 32 figs., 29 pls., 13 tbls., 3 appendices.

CHAPTER 12:

RADIATION CHEMISTRY OF THE SUBSURFACE OF OAK AND KOA CRATERS

by

Byron L. Ristvet and Edward L. Tremba

S-CUBED, A Division of Maxwell Laboratories, Inc.[1]

INTRODUCTION

Analyses of the gamma-emitting radionuclides of 121 PEACE Program borehole samples from within and adjacent to OAK and KOA craters were completed for this study. The purpose of the study was to characterize the type and occurrence of radionuclides in the subsurface beneath OAK and KOA to aid in the interpretation of the mechanism(s) of crater formation. A secondary purpose was to help in the interpretation of the continuous downhole natural-gamma geophysical logs (Chapter 7 of this report). A similar study of radionuclide distributions was conducted during Project EXPOE in 1974 for the CACTUS crater on the northern end of Runit Island (Ristvet, Tremba, and others, 1978). Interpretation of the radionuclide distribution in CACTUS crater allowed for the definition of the "true crater" dimensions and provided insight into the mechanics of the crater formation.

The locations of the OAK and KOA drill holes sampled for this study are shown in Figure 12-1 and 12-2. Henry, Wardlaw, and others (1986) present the geologic logs for these boreholes.

The detonation of a thermonuclear device produces both fission products and neutron-activated isotopes of many elements. Fission products are formed when either uranium (generally U-235) or plutonium (generally Pu-239) nuclei capture neutrons and undergo fission. Because there are many different manners in which the nuclei can split, about 200 or so different isotopes of approximately 36 lower atomic-number elements can be formed. Approximately 57 grams of fission products are produced per kiloton of fission yield (Dolan, 1959a; Glasstone and Dolan,1977).

Reactions resulting from the fusion of isotopes of hydrogen into helium produce large quantities of high-energy neutrons. These "fast" neutrons can cause the fission of U-238 and other isotopes of uranium and plutonium (Dolan, 1959b). These fusion reaction-generated neutrons also can result in the "activation" of the nuclei of other elements within the "device debris" or within the surrounding environment by the addition of one or more neutrons (i.e., the production of a new isotope). Fission reactions also release excess neutrons but at lower energy levels and fluxes. Some of the "slow"

---

[1] Albuquerque, NM.

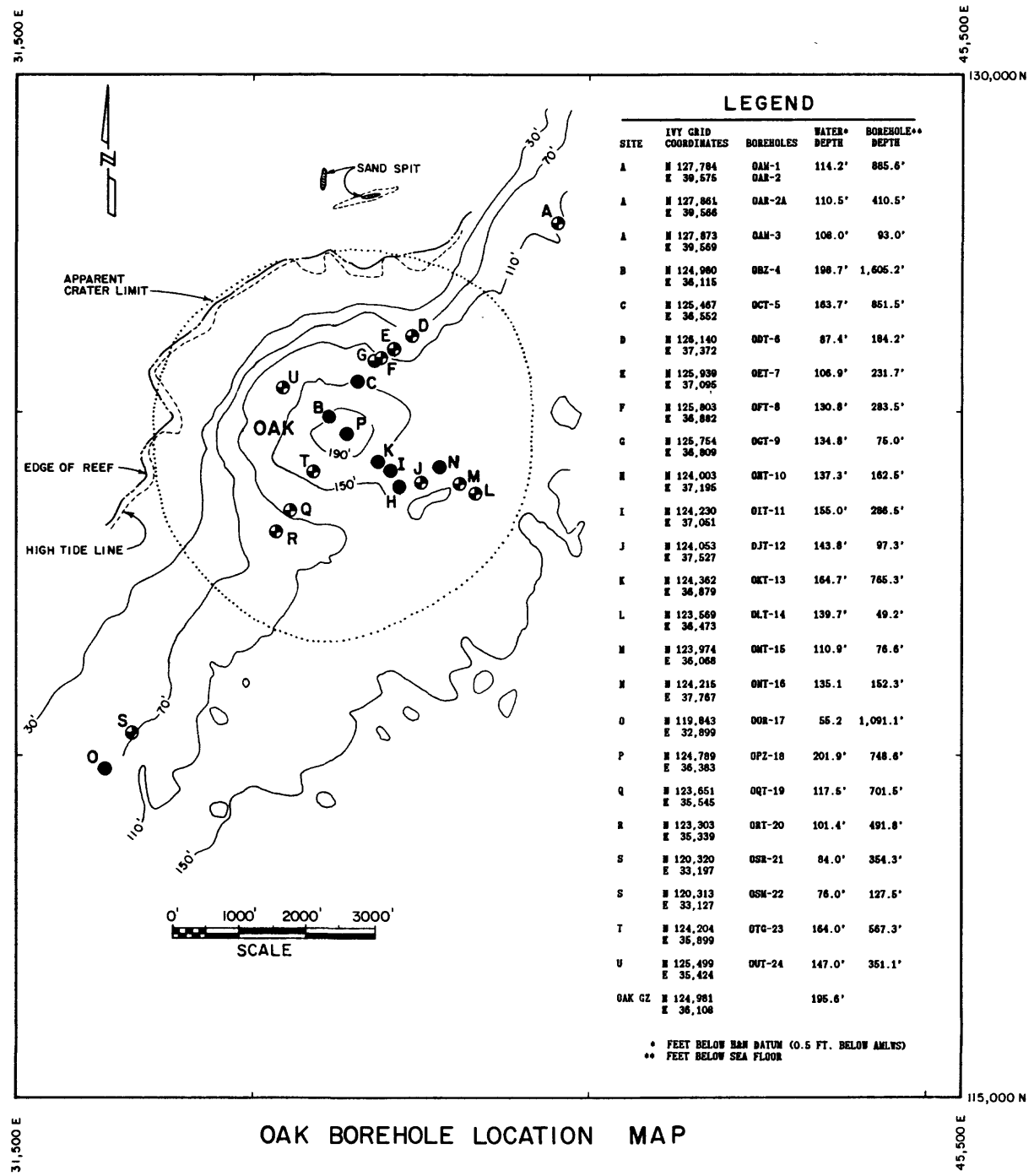

OAK BOREHOLE LOCATION MAP

FIGURE 12-1. -- Location of boreholes within OAK crater with radionuclide analyses (shown as solid circles). Contour interval equals 40 ft.

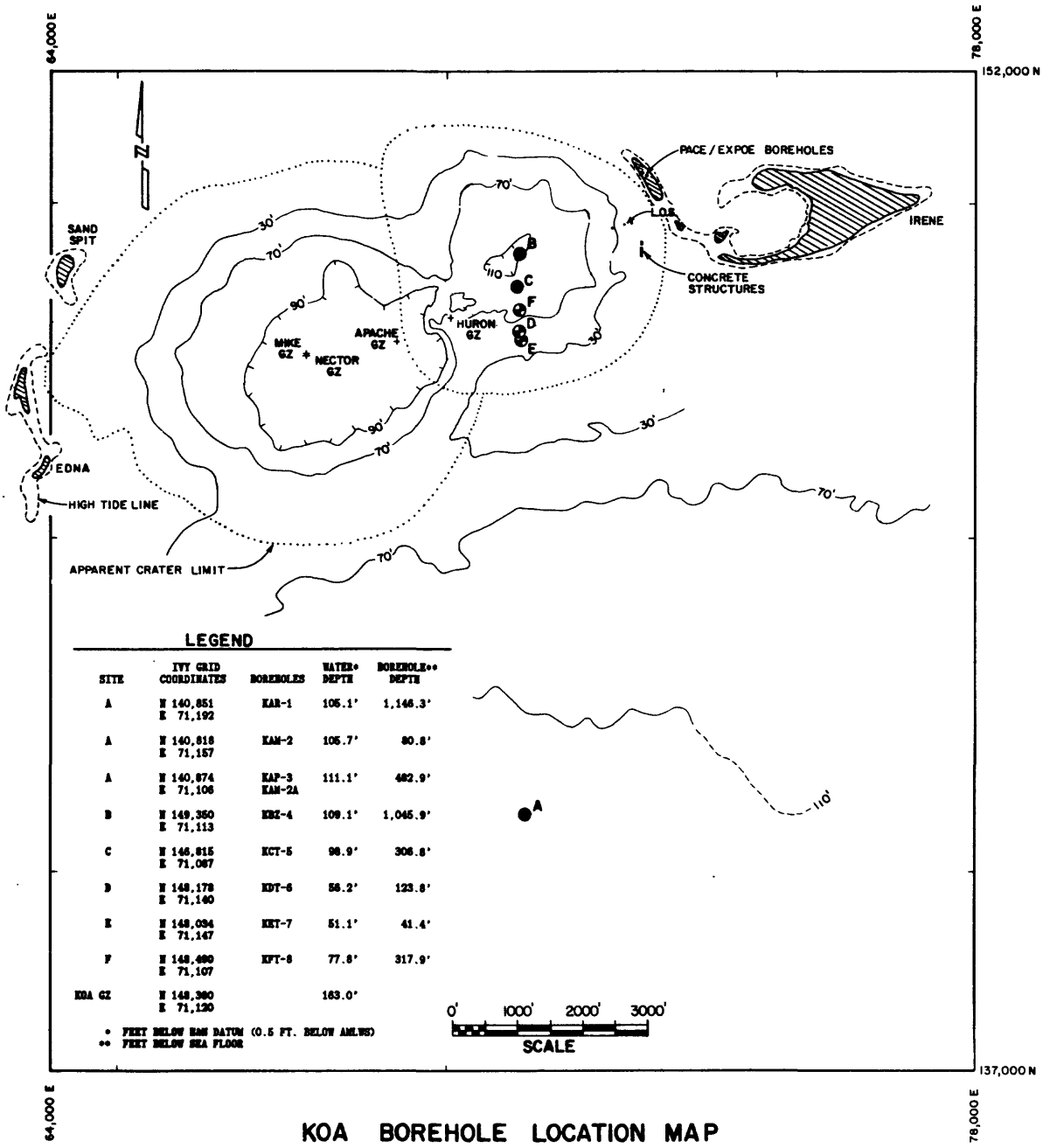

FIGURE 12-2. -- Location of boreholes within KOA crater with radionuclide analyses (shown as solid circles). Contour interval irregular, in feet.

fission-reaction-produced neutrons also result in the production of neutron-activated isotopes.

The nature of the distribution of the radionuclides produced from a nuclear explosion is complex and dependent on the specifics of the design, composition, and performance of the device, as may be deduced from the previous two paragraphs.

Most of the isotopes generated through the nuclear-fission or neutron-activation processes are unstable and undergo radioactive decay to a stable isotope. The resulting radioactivity generally is manifested by the emission of beta particles, which is commonly, but not always, accompanied by gamma radiation, which removes excess energy. In a few special cases, only gamma radiation is emitted as a result of radioactive decay. Most of the radionuclides produced from the detonation of a nuclear device have extremely short half-lives of a few microseconds to a few days. Ninety percent of the radionuclides produced from a nuclear explosion will have decayed to a stable form within 24 hours of the detonation, 99 percent within 48 hours, and 99.9 percent within 14 days. Only a very few radionuclides have half-lives that permit their existence for more than a few years.

The OAK and KOA devices both were detonated in the summer of 1958 during Operation Hardtack, 27 years prior to the analyses of the residual radionuclides within subsurface samples of the crater regions for the current study. By contrast, similar analyses of the CACTUS crater (Ristvet, Tremba, and others, 1978) were conducted within 16 years of the CACTUS detonation. Unfortunately, the long hiatus between the OAK and KOA detonations and the current analyses has resulted in not only low abundances of device-related radionuclides but also in a limited diversity of radionuclides still detectable from the detonations. Table 12-1 lists some of the long half-life radionuclides that might be detectable utilizing state-of-the-art gamma ray detectors 25 years following a nuclear explosion.

Naturally occurring radioactivity within the earth's environment primarily results from the radioactive decay of radioisotopes in the earth, dissolved in the oceans, and in the atmosphere, and from cosmic rays generated by the nuclear reactions of the sun. Of the naturally occurring radionuclides, potassium, thorium, and uranium-radium are the most important quantitatively. Table 12-1 also lists the most abundant naturally occurring radionuclides and their half-lives.

METHODS

Analyses of total and selected gamma-emitting radionuclides were performed using lithium-drifted germanium crystal [Ge(Li)] detector equipment by either the McClellan Central Laboratory (MCL), U.S. Air Force Technical Applications Center, or by the Environment Sciences Laboratory, Nevada Test Site (operated by the Reynolds Electrical Engineering Co. for the U.S. Department of Energy). Twelve of the 21 samples from the KBZ-4 borehole were analyzed at the NTS laboratory; all the remaining samples were analyzed by MCL. The Ge(Li) detector records the number of decays that occur per unit time and the specific energy level of each gamma ray. The data are recorded and the gamma-ray energy "signatures" identified giving values of number of

TABLE 12-1. -- Nuclear-device produced, gamma-emitting radionuclides that might be detectable in the earth's environment 25 years following production and commonly occurring natural radionuclides (U.S. Department of Health, Education, and Welfare, 1970).

RADIONUCLIDE	CHARACTERISTIC GAMMA ENERGY (MeV)	HALF LIFE (years)
DEVICE-PRODUCED RADIONUCLIDES		
Sm-151	0.022	87.0
I-129	0.040	1.70×10^{7}
Am-241	0.060	458.0
Ba-133	0.356	7.2
Eu-152	0.344	12.0
Eu-154	1.278	16.0
Ra-226	0.186	1602.0
Rh-101	0.198	10.0
Sb-125	0.599	2.7
Kr-85	0.514	10.8
Bi-207	0.570	30.0
Cs-137	0.662	30.0
Co-60	1.173	5.3
COMMONLY OCCURRING RADIONUCLIDES		
K-40	1.460	1.26×10^{7}
Ra-226	0.186	1.60×10^{3}
Th-228	0.084	2.0
Th-230	0.068	8.00×10^{4}
Th-232	---	1.41×10^{10}
U-235	0.185	7.10×10^{8}
U-238	---	4.51×10^{9}

disintegrations per unit time for each radionuclide. These values are then converted to values of specific activity per unit weight -- picoCuries per gram (pCi/g).

Approximately 20 grams of sample in plastic bags were provided for each Ge(Li) analysis. The samples were placed in a standard geometry directly against the Ge(Li) detector face and measured for up to 1000 minutes. Analyses were made for total gamma-emitting radionuclides and for specific gamma radionuclides. The following fission products were specifically analyzed for: Rh-101, Sb-125, Cs-137, Eu-152, Eu-154, and Eu-155. Co-60 and Am-241 were the only neutron-activation products specifically analyzed. Analyses for the naturally occurring K-40 and Th-230 also were performed. In addition, specific analyses were performed for Ra-226, U-235, and U-238, all of which can orginate either naturally or from the detonation of a nuclear device.

The level of detectability of specific radionuclides is a function of the energy level of the emitted gamma ray and its position within the gamma-ray spectrum relative to interferences from other radionuclides. In general, the higher the specific energy level, the lower the limit of detection. For each radionuclide detected, a percent standard error was calculated by the analyzing laboratory using standard Ge(Li)-count rates versus background statistics. A threshold limit of detection was established for each sample. For samples with a percent error greater than 50, it is highly unlikely that the radionuclide is present in the sample. For errors of 20 to 50 percent, it is highly questionable if the isotope is truly present in the sample. For errors between 3 and 20 percent, identification of the isotope is positive but only semiquantitatively measured with a precision of $\pm$ 10 to 50 percent of the value reported. Whereas, errors less than 3 percent are considered to be quantitatively reliable to $\pm$ 5 percent of the value reported.

RESULTS

Table 12-2 summarizes the results of the gamma-emitting radionuclide analyses. The values listed are in pCi/g and are referenced against known standards. Radionuclides not specifically analyzed for are shown by na (not analyzed) in Table 12-2. Radionuclide values with a percent error of between 20 and 50 are indicated with an asterisk (*); to reiterate, it is highly questionable whether or not such isotopes are indeed present in the sample. Radionuclide analyses with percent errors greater than 50 are shown as not being detectable in Table 12-2.

Figure 12-1 and 12-2 show the locations of the sampled borholes for OAK and KOA crater areas, respectively. Four reference borehole samples were analyzed as shown in Table 12-2 -- two from the organic-rich interval, sedimentary package 5, in borehole OOR-17 (748.0 and 824 ft bsf) and one each from within sedimentary package 1 from both OOR-17 (35.1 ft bsf) and KAR-1 (40.2 ft bsf). With the exception of a highly questionable Am-241 value for the KAR-1 sample, no device-produced radionuclides were detected. Meaningful values of U-235 and probable values of Th-230 and U-238 were present in the organic-rich samples from OOR-17. These are naturally occurring radionuclides and are the cause of the elevated gamma-ray log values within the organic-rich intervals (refer to Chapter 7).

TABLE 12-2. -- (Page 1 of 4 pages) Summary of radionuclide analyses of PEACE borehole samples. Analyses marked with an asterisk are questionable to as to their detection, na = not analyzed,-- = not detected.

BSF(ft) Depth	H&N(ft) Depth	Radionuclides (pCi/g) Cs-137	Eu-155	Am-241	Co-60	Th-230	U-235	U-238	K-40	Ra-226	Rh-101	Sb-125
Borehole OOR-17												
35.1	92.2	--	--	--	--	na	na	na	na	na	--	--
748.0	805.1	--	--	--	na	92.34*	0.31	450.4*	--	na	na	na
824.0	881.1	--	--	--	na	92.34*	0.31	--	--	na	na	na
Borehole OPZ-18												
35.2	257.1	8.37	2.50	2.77	--	na	na	na	na	na	--	--
60.8	262.7	31.70	--	--	--	na	na	na	na	na	--	--
74.3	276.2	44.79	1.27	--	--	na	na	na	na	na	--	--
76.8	278.7	30.88	--	--	--	na	na	na	na	na	--	--
91.8	293.7	25.22	--	0.61	--	na	na	na	na	na	--	--
99.9	301.8	16.36	--	--	0.30	na	na	na	na	na	--	--
112.2	314.1	11.97	0.45*	0.40*	--	na	na	na	na	na	--	--
125.2	327.1	6.16	--	--	--	na	na	na	na	na	--	--
136.8	338.7	5.16	0.70*	0.59*	--	na	na	na	na	na	--	--
148.4	350.3	4.01	0.62	--	0.26*	na	na	na	na	na	--	--
160.0	361.9	2.61	0.65	--	0.24*	na	na	na	na	na	--	--
172.6	374.5	2.61	0.22*	0.36*	--	na	na	na	na	na	--	--
186.0	387.9	4.15	0.41	--	--	na	na	na	na	na	--	--
191.8	393.7	6.99	--	0.23*	--	na	na	na	na	na	--	--
201.1	402.0	6.13	--	--	na	--	0.16*	--	--	na	na	na
210.4	412.3	1.38	--	--	na	--	0.11*	--	--	na	na	na
220.2	422.1	2.32	0.42*	0.34*	0.13*	na	na	na	na	na	--	--
230.2	432.1	1.80	0.14*	0.20*	na	--	0.16*	--	--	na	na	na
251.0	452.9	0.41	0.62*	0.43*		na	na	na	na	na	--	--
300.1	502.0	0.99	--	--	na	--	0.14*	--	--	na	na	na
351.5	553.4	0.39*	--	--	na	--	0.13*	--	--	na	na	na

Continued on next page

BSF(ft) Depth	H&N(ft) Depth	Radionuclides (pCi/g) Cs-137	Eu-155	Am-241	Co-60	Th-230	U-235	U-238	K-40	Ra-226	Rh-101	Sb-125
Borehole OBZ-4												
34.5	233.2	5.65	0.81	0.83	0.41	na	na	na	na	na	--	--
60.1	258.8	13.08	0.38*	--	--	na	na	na	na	na	--	--
72.0	270.7	8.55	--	--	--	na	na	na	na	na	--	--
74.9	273.6	7.31	0.41	0.32	0.14	na	na	na	na	na	--	--
84.4	283.1	3.60	0.54*	--	0.19*	na	na	na	na	na	--	--
93.1	291.8	1.57	--	--	0.11*	na	na	na	na	na	--	--
104.1	302.8	0.78	0.14*	--	0.06*	na	na	na	na	na	--	--
112.0	310.7	0.30	--	--	--	na	na	na	na	na	--	--
119.5	318.2	0.45	--	--	--	na	na	na	na	na	--	--
120.8	319.5	0.52	--	--	--	na	na	na	na	na	--	--
129.6	328.3	0.55	--	--	--	na	na	na	na	na	--	--
138.5	337.2	0.54	--	--	0.06*	na	na	na	na	na	--	--
147.3	346.0	0.43	0.09*	--	0.06*	na	na	na	na	na	--	--
156.9	355.6	0.29	0.09*	0.04*	0.05*	na	na	na	na	na	--	--
166.5	365.2	0.38	0.09*	0.09*	--	na	na	na	na	na	--	--
199.9	398.6	0.40	--	--	--	na	na	na	na	na	--	--
216.6	415.3	0.24	--	--	na	87.84*	0.29	270.2*	--	na	na	na
219.8	418.5	0.94	0.18	0.13*	0.10	na	na	na	na	na	--	--
231.3	430.0	0.51	0.23*	0.25*	na	--	0.13*	--	--	na	na	na
249.8	448.5	0.59	0.15	0.15*	0.07*	na	na	na	na	na	--	--
300.0	498.7	--	--	--	na	--	--	--	--	na	na	na
350.0	548.7	--	--	--	na	--	0.13*	--	--	na	na	na
Borehole: OCT-5												
20.1	183.8	0.55*	--	--	--	na	na	na	na	na	--	--
28.1	191.8	--	--	--	--	na	na	na	na	na	--	--
35.1	198.8	0.16*	--	--	--	na	na	na	na	na	--	--
42.6	206.3	0.84	0.21*	0.21*	--	na	na	na	na	na	--	--
51.5	215.2	2.36	--	--	0.34*	na	na	na	na	na	--	--
63.5	227.2	0.50*	--	--	--	na	na	na	na	na	--	--
70.6	234.3	2.88	1.15*	0.72*	0.39*	na	na	na	na	na	--	--
82.3	246.0	--	--	--	--	na	na	na	na	na	--	--
91.6	255.3	--	--	--	--	na	na	na	na	na	--	--
101.6	265.3	--	--	--	--	na	na	na	na	na	--	--
112.3	276.0	--	--	--	--	na	na	na	na	na	--	--
116.5	280.2	--	--	--	--	na	na	na	na	na	--	--
130.4	294.1	--	--	--	--	na	na	na	na	na	--	--
160.3	324.0	0.19*	--	--	--	na	na	na	na	na	--	--
179.6	343.3	--	--	--	na	--	0.07*	--	--	na	na	na
199.5	363.5	--	--	--	na	--	0.16	123.8*	--	na	na	na
Borehole: OKT-13												
10.2	174.9	1.50	0.42	--	0.18*	na	na	na	na	na	--	--
12.3	177.0	1.20	0.33	0.33*	0.14*	na	na	na	na	na	--	--
20.1	184.8	2.65	--	--	--	na	na	na	na	na	--	--
28.7	193.4	--	--	--	--	na	na	na	na	na	--	--
36.0	200.7	--	--	--	--	na	na	na	na	na	--	--
44.6	209.3	2.49	1.43*	1.53*	0.48	na	na	na	na	na	--	--
51.8	216.5	8.35	0.97	1.14	0.31*	na	na	na	na	na	--	--
60.0	224.7	0.19*	--	--	--	na	na	na	na	na	--	--
74.3	239.0	0.52*	--	--	na	78.83*	0.24*	--	--	na	na	na
97.1	261.8	0.36*	--	--	na	92.34*	0.23	--	--	na	na	na

Continued on next page

TABLE 12-2 -- (Page 3 of 4 pages).

BSF(ft) Depth	H&N(ft) Depth	Radionuclides (pCi/g) Cs-137	Eu-155	Am-241	Co-60	Th-230	U-235	U-238	K-40	Ra-226	Rh-101	Sb-125
Borehole: OIT-11												
45.0	200.0	0.83	--	--	na	--	0.22*	--	--	na	na	na
47.3	202.3	0.22	--	--	na	--	0.18*	--	--	na	na	na
49.5	204.5	0.29	--	--	na	--	0.45	--	--	na	na	na
52.5	207.5	0.31	--	--	na	159.90*	0.75	--	--	na	na	na
54.5	209.5	0.11*	--	--	na	--	0.54	473.0*	--	na	na	na
Borehole: OHT-10												
20.1	157.4	0.07*	--	--	na	63.06*	0.20*	--	--	na	na	na
25.8	163.1	--	--	--	na	--	0.36	--	--	na	na	na
31.8	169.1	--	--	--	na	--	0.25	360.4*	--	na	na	na
48.3	185.6	--	--	--	na	--	0.22*	--	--	na	na	na
Borehole: ONT-16												
20.0	155.1	--	--	0.27*	na	--	--	--	--	na	na	na
40.0	175.1	--	--	--	na	--	0.27*	--	--	na	na	na
Borehole: KAR-1												
40.2	145.3	--	--	0.18*	--	na	na	na	na	na	--	--
Borehole: KBZ-4												
21.5	130.6	7.06	2.56	4.10	4.52	na	na	na	na	--	--	--
74.3	183.4	1.15	0.40	0.52	0.55	na	na	na	na	--	--	--
112.9	222.0	--	--	--	--	na	na	na	na	--	--	--
118.0	227.1	--	--	--	--	na	na	na	na	--	--	--
123.5	232.6	--	--	--	--	na	na	na	na	--	--	--
127.6	236.7	--	--	--	--	na	na	na	na	--	--	--
132.2	241.3	--	--	--	--	na	na	na	na	1.11*	--	--
137.0	246.1	0.58*	--	--	--	na	na	na	na	--	--	--
138.2	247.3	--	--	--	na	--	0.11*	--	--	na	na	na
142.0	251.1	0.29	--	--	na	--	0.14*	--	--	na	na	na
142.0	251.1	--	--	--	--	na	na	na	na	0.72*	--	--
146.6	255.7	0.32*	--	--	--	na	na	na	na	0.94*	--	--
147.6	256.7	0.36	--	--	na	--	0.14*	--	--	na	na	na
151.8	260.9	--	--	--	--	na	na	na	na	0.32*	--	--
156.5	265.6	--	--	--	--	na	na	na	na	0.17	--	--
161.3	270.4	0.20	--	--	na	--	0.22*	--	--	na	na	na
161.3	270.4	0.24*	--	--	--	na	na	na	na	0.98	--	--
181.9	291.0	0.18	--	--	na	54.05*	--	247.7	--	na	na	na
201.2	310.3	0.11*	--	--	na	67.62*	--	--	--	na	na	na
201.2	310.3	0.13	--	--	--	na	na	na	na	--	--	--
220.0	229.1	0.29	--	--	na	--	0.18	--	--	na	na	na

Continued on next page

TABLE 12-2 -- (Page 4 of 4 pages).

BSF(ft) Depth	H&N(ft) Depth	Radionuclides (pCi/g) Cs-137	Eu-155	Am-241	Co-60	Th-230	U-235	U-238	K-40	Ra-226	Rh-101	Sb-125
Borehole: KCT-5												
21.4	120.3	--	--	--	--	na	na	na	na	--	--	--
40.4	139.3	--	--	--	--	na	na	na	na	--	--	--
56.0	154.9	0.13*	--	--	--	na	na	na	na	--	--	--
60.7	159.6	0.43	--	--	0.12	na	na	na	na	--	--	--
75.1	174.0	--	--	--	--	na	na	na	na	--	--	--
90.0	188.9	--	--	--	--	na	na	na	na	--	--	--
105.9	204.8	--	--	--	--	na	na	na	na	--	--	--
120.8	219.7	--	--	--	--	na	na	na	na	--	--	--
128.0	226.9	--	--	--	--	na	na	na	na	--	--	--
133.5	232.4	--	--	--	--	na	na	na	na	--	--	--
136.6	235.5	--	--	--	na	--	0.11*	--	--	na	na	na
143.6	242.5	0.05*	--	--	na	--	0.11	--	--	na	na	na
147.8	246.7	0.07*	--	--	na	--	0.09*	--	--	na	na	na
155.1	254.0	--	--	--	na	--	--	--	--	na	na	na
162.0	260.9	0.11*	--	--	na	--	0.09*	247.7*	--	na	na	na
170.7	269.6	0.07*	--	--	na	--	0.09	180.2*	--	na	na	na
199.4	298.3	--	--	--	na	--	0.16	--	--	na	na	na

Figure 12-3 presents the distribution of Cs-137, the most abundant device-produced fission product, as function of depth for the four boreholes, OBZ-4, OPZ-18, OCT-5, and OKT-13, all located within OAK crater. Also shown in Figure 12-3 are the downhole gamma logs for these four boreholes. As may been seen in Figure 12-3, the trends in the abundance of Cs-137 correspond closely to the gamma-log response for the crater zones. The relatively higher abundance of Cs-137 in the OPZ-18 samples versus the other three boreholes is probably a manifestation of the relative position of the sediments to the detonation fireball. All the crater features (Chapter 14 of this report) appear to be reflected in the radionuclide distributions. All four of the OAK crater holes show highly elevated levels of Cs-137 and other device-produced radionuclides within the alpha 2 and the top of the beta 1 crater zones (see table 14-1 of this report for definitions of the crater zones). This may represent distal, near-surface material not excavated but exposed to the fireball, which has been transported into the crater by both early and late-time slumping and possibly ejecta fallback. The high Cs-137 values for borehole OPZ-18 suggest that the materials found at the bathymetric center of OAK crater (OPZ-18) may have their origins very close to the OAK ground zero and have moved to their present position during slumping.

The lower part of the OAK crater zone beta-1 has abundances of Cs-137 and other device-produced radionuclides ranging from relatively low to non-detectable, suggesting that the materials that compose this unit had little exposure to the OAK fireball. Although sparse piped materials from the organic-rich stratigraphic packages 4 and 5 were recognized petrographically and paleontologically within this crater zone, the radionuclide analyses failed to detect any of the naturally occurring radionuclides as seen in the two OOR-17 reference-hole samples, confirming the sparsity of piped material (see Table 12-2).

The base of the OAK transition sands (crater zone beta-2) appears to be a demarcation between the occurrence and non-occurrence of device debris. Only minor amounts of Cs-137 are found below the OAK transition sands as sampled in the OBZ-4 and OPZ-18 boreholes and probably result from injected debris during crater growth. It should also be noted that cesium is chemically a highly mobile element; therefore, some of the Cs-137 within crater zones beta-3 and gamma may be due to postshot chemical migration. Within the samples from boreholes OCT-5 and OKT-13, the demarcation between occurrence and nonoccurrence of device-produced radionuclides is at the boundary between crater zones beta-1 and gamma. The transition sands are not present within the OCT-5 and OKT-13 boreholes.

Within crater zone beta-3 in borehole OBZ-4, there is some evidence from the radionuclide analyses for piped organic-rich debris as indicated by the presence of U-235 and probable quantities of Th-230 and U-238. Similarly, the top of crater zone gamma in borehole OKT-13 shows probable presence of these three naturally occurring radionuclides.

Figure 12-4 presents the levels of Cs-137 analyzed and the downhole gamma logs for boreholes located on the OAK debris blanket (OHT-10, OJT-12, OMT-15, ONT-16). The spikes in the gamma logs seem to be explainable by the presence of naturally occurring radionuclides and not device debris.

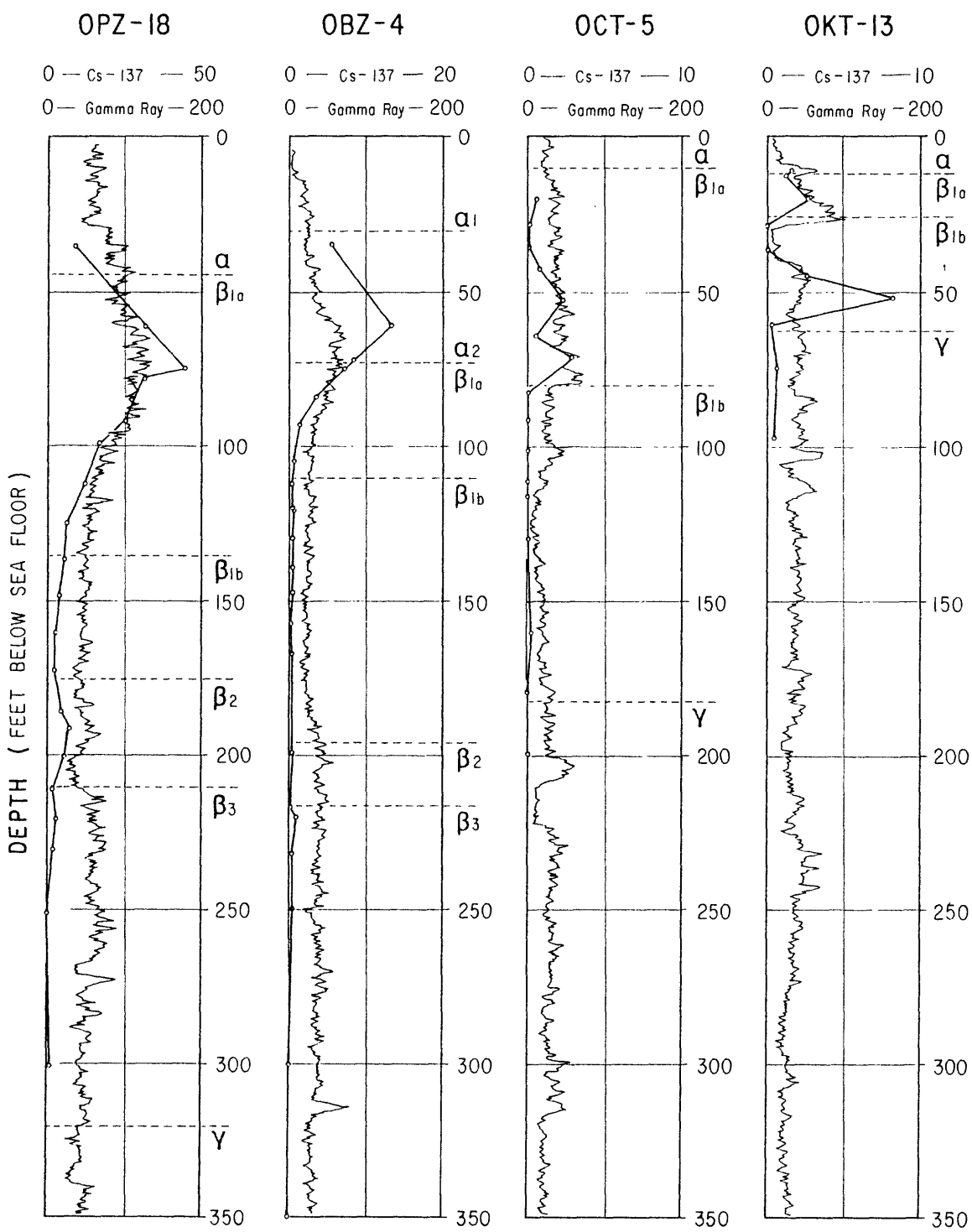

FIGURE 12-3. -- Cs-137 levels of samples and downhole gamma logs from the OAK crater boreholes versus depth below sea floor. Crater zone boundaries are indicated for each drill hole (see Chapter 14 for explanation of crater zones).

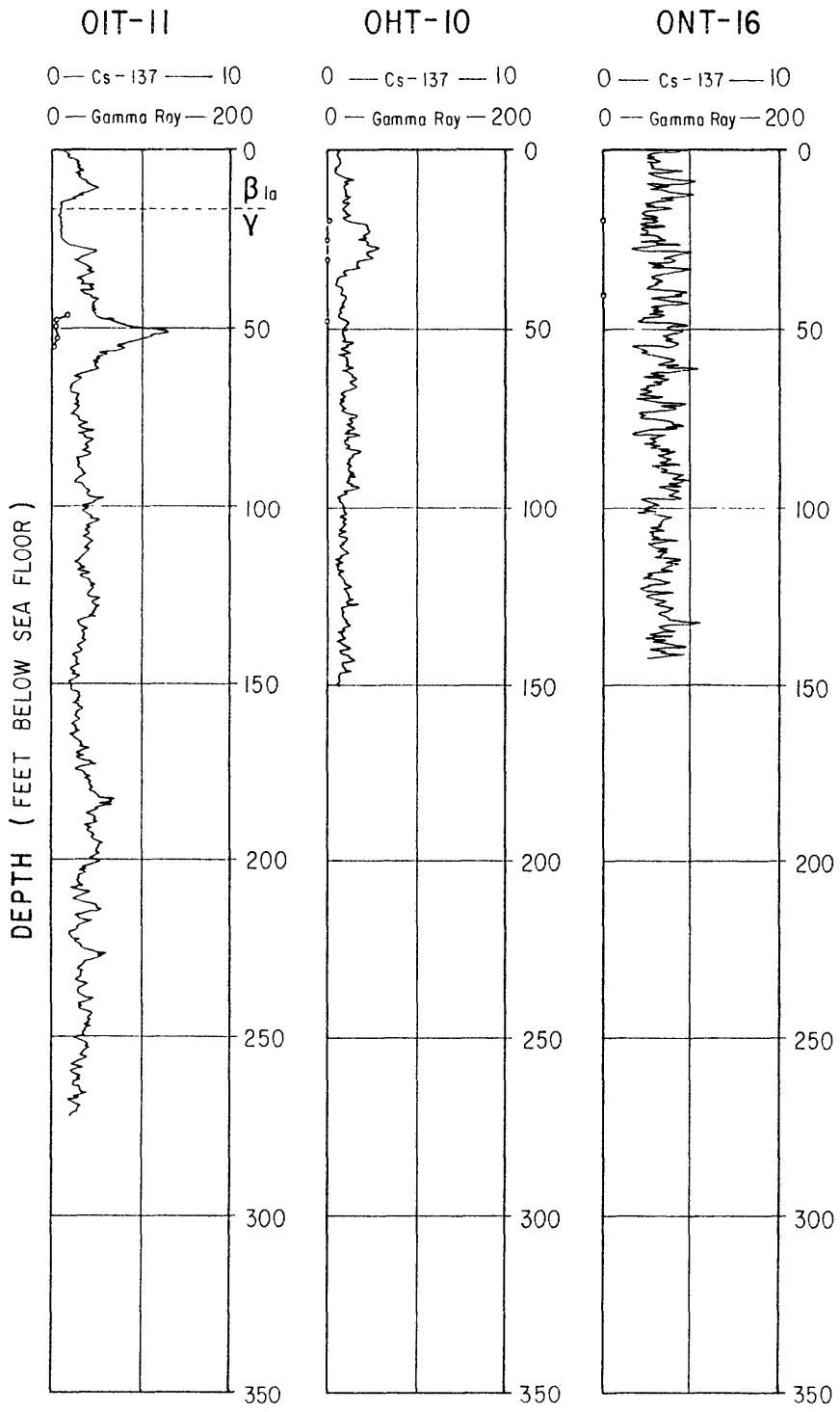

FIGURE 12-4. -- Cs-137 levels of samples and downhole gamma logs from the OAK debris-blanket boreholes versus depth below the sea floor. Crater zones (see Chapter 14) are also indicated.

Figure 12-5 presents the levels of Cs-137 analyzed and the downhole gamma logs for the KOA crater boreholes. In general, the abundances of device-produced radionuclides are significantly lower for KOA than for similar boreholes in OAK. While not as apparent, the radionuclide data for KOA appear to strongly support the definition of the crater zones (Chapter 14 of this report).

ACKNOWLEDGEMENTS

The authors would like to thank the staffs of the McClellan Central Laboratory and the NTS Environmental Health Labortory for their efforts in conducting the radionuclide analyses presented in this study. Specifically, we like to thank, Maj. Fred Jaeger and Capt. Richard Runchey, MCL, and Mr. Frank Markwell, NTS. We greatly appreciate the support and many hours of stimulating discussion provided by Lt. Col. Robert Couch, DNA, Drs. Bruce R.Warlaw and T.W. Henry, USGS, and Mr. Steve Melzer, SAI, throughout this study. Appreciation also is extended to Dr. James Metcalf, Sandia National Laboratory, for technical advice in the interpretation of nuclear-device-produced radionuclides.

REFERENCES

Dolan, P.J., 1959a, Gamma spectra of Uranium-235 fission products at various times after fission: Armed Forces Special Weapons Project Report 524, Washington, D.C.

Dolan, P.J., 1959b, Gamma spectra of Uranium-238 fission products at various times after fission: Defense Atomic Support Agency Report 526, Washington, D.C.

Glasstone, S., and Dolan, P.J., 1977, The Effects of Nuclear Weapons: (third edition) U.S. Department of Defense and U.S. Department of Energy, Washington, DC.

Henry, T.W., Wardlaw, B.R., Skipp, B., Major, R.P., and Tracey, J.I., Jr., 1986, Pacific Enewetak Atoll Crater Exploration (PEACE) Program, Enewetak Atoll, Republic of the Marshall Islands; Part 1: Drilling operations and descriptions of boreholes in vicinity of KOA and OAK craters: U.S. Geological Survey Open-File Report 86-419, 497 p., 32 figs., 29 pls., 13 tbls., 3 appendices.

Ristvet, B.L., Tremba, E.L., Couch, R.F., Fetzer, J.A., Goter, E.R., Walter, D.R, and Wendland, V.P., 1978, Geological and geophysical investigations of the Eniwetok nuclear craters: Air Force Weapons Laboratory Technical Report 77-242, Kirtland Air Force Base, NM.

U.S. Department of Health, Education, and Welfare, 1970, Radiological Health Handbook, Revised Edition, Rockville, MD.

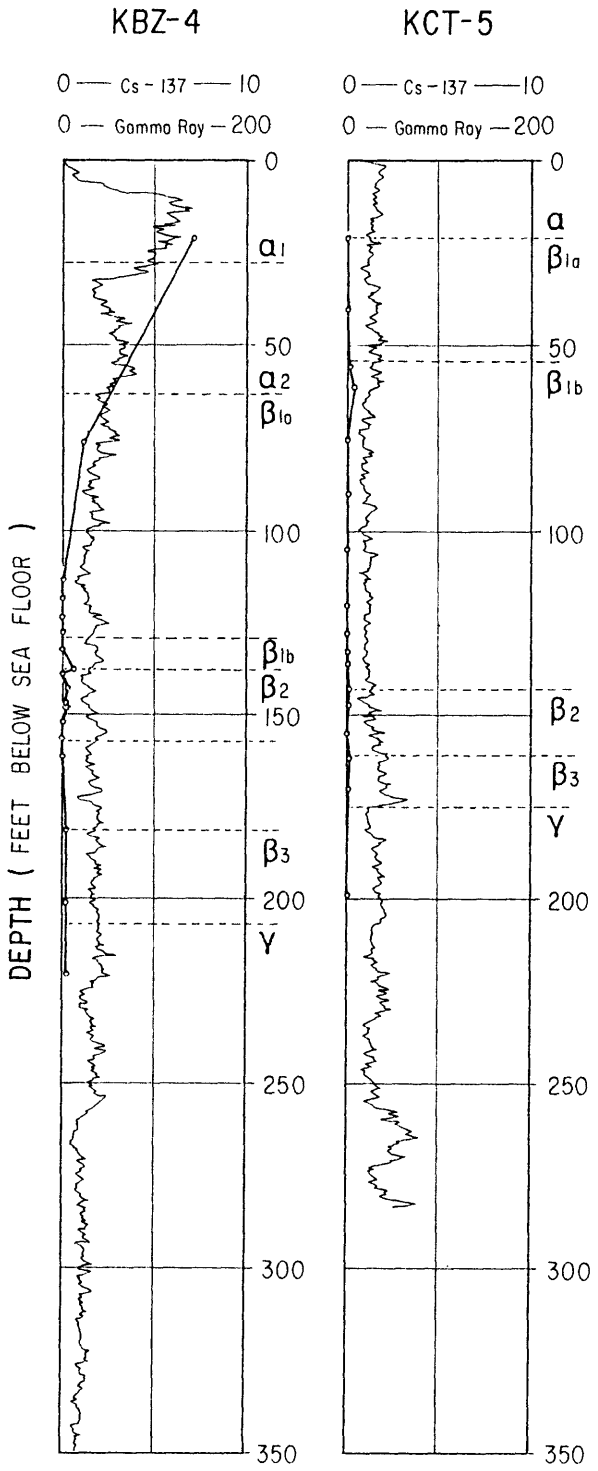

FIGURE 12-5. -- Cs-137 levels of samples and downhole gamma logs from the KOA crater drill holes versus depth below the sea floor. Crater zones (see Chapter 14) are also indicated.

CHAPTER 13:

ADDITIONAL SUBMERSIBLE STUDIES; DETAILED OBSERVATIONS OF THE SEAFLOOR OF OAK, KOA, AND MIKE CRATERS

by

Richard A. Slater[1], David J. Roddy[2],
David W. Folger[3], Robert B. Halley[3], and Eugene A. Shinn[4]

INTRODUCTION

Thermonuclear-explosion testing was conducted at the Pacific Proving Grounds on Enewetak Atoll, Marshall Islands, from 1948 to 1958. Many of these explosion events excavated deeply enough into the atoll islands to form craters that now lay as deep as 60 m underwater. At each site, the cratering processes produced extensive subsurface deformation in the reef strata, and formed complex morphologies on the seafloor, including large craters surrounded by deformed rims and ejecta deposits.

The PEACE Program, a detailed geological and geophysical study, was conducted on Enewetak in 1984 and 1985 by the U.S. Geological Survey for the Defense Nuclear Agency to improve understanding of crater dimensions, structural deformation, cratering processes, and various stages of long-term crater modification. The results of these studies were described in Folger (1986, USGS Bulletin 1678), in two previous USGS Open-File Reports (Henry, Wardlaw, and others, 1986; and Cronin, Brouwers, and others, 1986), and in the Chapters of the current Open-File Report. One important aspect of this work has been the improved definition of different morphological features in the craters and on the surrounding rims. These sea-floor studies were completed using several different techniques, including bathymetric echo-soundings, sidescan sonar, scuba observations, seafloor-material sampling, core drilling, and submersible observations. Integration of these data has substantially improved interpretation of many of the crater-related morphologies and their relation to different crater-forming processes.

This report presents additional data on one of these studies, the submersible observations in OAK crater (8.9 Mt), KOA crater (1.37 Mt), and MIKE crater (10.4 Mt). Detailed sets of observations have been assembled and are given here for each of 42 research dives made in 1984 and 1985. The data

---

[1]Consultant, Oxnard, CA.

[2]Branch of Astrogeology, U.S. Geol. Survey, Flagstaff, AZ.

[3]Branch of Atlantic Marine Geology, U.S. Geol. Survey, Woods Hole, MA.

[4]Branch of Oil and Gas Resources, U.S. Geol. Survey, Miami, FL.

were taken from a review of all video and voice tapes completed during these dives, and they present the major observations at each navigational fix along the dive tracks. Bathymetric maps, showing replotted, accurate dive tracks keyed to the navigational fix locations listed in this report, have been completed by R. A. Slater and are included as Plates 13-1 through 13-4 (pls. 13-1 and 13-4 are located in the pocket at the end of this volume). These data represent the most current sea-floor observations available on the craters of OAK, KOA, MIKE, and surrounding areas and are designed to assist workers in relating the seafloor morphologies to (1) the different features in the craters and on the rims, (2) the processes that formed them, and (3) the large array of other geological and geophysical data collected in the PEACE Program.

SETTING

The submersible research dives described in this report were conducted in the northern part of the Enewetak lagoon in OAK, KOA, and MIKE craters in water 5 to 60 m deep, and in surrounding areas in the lagoon as far as 2 km from the craters. Visibilities from the submersible varied from approximately 1 m to more than 30 m depending upon the debris content in the water. Generally, good visibilities were present along the upper crater walls adjacent to the reef surface where water depths averaged 5 to 10 m. Currents carrying material from the reef plate areas northeast of KOA commonly reduced visibilities in that crater.

METHODS OF STUDY

The techniques and methods of data acquisition for the submersible 1984 and 1985 operations are described by Halley and others (1986) for the 1984 and 1985 field work. In summary, 144 dives were made in July and August of 1984 in the two-man research submersible Delta, operated by MARFAB of Torrence, California. In July of 1985, 57 dives were completed. This report describes the 42 research dives that had video and voice recordings completed in OAK crater (17 dives in 1984, 8 in 1985) and KOA and MIKE craters (17 dives in 1984).

The Egabrag II served as support vessel for the submersible during the 1984 field season, as well as for many of the other marine operations. The Egabrag II served as support vessel for the submersible during part of the 1985 field season, and the drill ship Knut Constructor and a whaler were the support vessels during the remainder of the that field season. Positional tracking of the submersible by both support vessels was accomplished with a Honeywell Hydrostar Navigation System interfaced with a Motorola FALCON IV Miniranger System that gave the location of the support vessel.

A VHS TV/Voice system was used to record the seafloor observations of many of the research dives. The video camera also displayed the data, title, and elapsed time in the field of view. It was common for the observer to voice record the elapsed time, Greenwich Mean Time (GMT), depth, and fix number, along with his seafloor observations. Some dives exceeded two hours in length on the larger crater and rim traverses. Additional information on

the submersible operations, navigation, and tracking, including seafloor material sampling, was discussed by Halley and others (1986).

On the following pages of this report, detailed observations of each of the 42 research dives are given as a function of Fix Number, Greenwich Mean Time (GMT), VHS TV Time, Water Depth, and Observations. The dives in OAK crater are listed first (see table 13-1, p. 6) and are accompanied by Plates 13-1*, 13-2, and 13-3. The dives in KOA and MIKE craters are listed second (see table 13-2, p. 102) and are accompanied by Plate 13-4*. The Fix Numbers and Observations in the following sections are keyed to the Fix Numbers and navigation fix locations on Plates 13-1 through 13-4. In the observations, the abbreviations o/c means on course and c/c means change course. The heading of the submersible is given in degrees of magnetic heading.

REFERENCES

Cronin, T.M., Brouwers, E.M., Bybell, L.M., Edwards, E.E., Gibson, T.G., Margerum, R., and Poore, R.Z., 1986, Pacific Enewetak Atoll Crater Exploration (PEACE) Program, Enewetak Atoll, Republic of the Marshall Islands; Part 2: Paleontology and biostratigraphy, application to OAK and KOA craters: U.S. Geological Survey Open-File Report 86-159, 39 p., 20 figs., 12 tbls., 3 appendices.

Folger, D.W., ed., 1986, Sea-floor observations and subbottom seismic characteristics of OAK and KOA craters, Enewetak Atoll, Marshall Islands: U.S. Geological Survey Bulletin 1678. [Contains eight chapters by various authors.]

Folger, D.W., Hampson, J.C., Robb, J.M., Woellner, R.A., Foster, D.S., and Tavares, L.A., 1986, Bathymetry of OAK and KOA craters; in Folger, D.W., ed., Sea-floor boservations and subbottom seismic characteristics of OAK and KOA craters, Enewetak Atoll, Marshall Islands: U.S. Geological Survey Bulletin 1678.

Halley, R.B., Slater, R.A., Shinn, E.A., Folger, D.W., Hudson, J.H., Kindinger, J.L., and Roddy, D.J., 1986, Observations of OAK and KOA craters from the submersible; 32 p., 13 figs., 1 appendix; in Folger, D.W., ed., Sea-floor observations and subbottom seismic characteristics of OAK and KOA craters, Enewetak Atoll, Marshall Islands: U.S. Geological Survey Bulletin 1678.

Henry, T.W., Wardlaw, B.R., Skipp, B., Major, R.P., and Tracey, J.I., Jr., 1986, Pacific Enewetak Atoll Crater Exploration (PEACE) Program, Enewetak Atoll, Republic of the Marshall Islands; Part 1: Drilling operations and descriptions of boreholes in vicinity of KOA and OAK craters: U.S. Geological Survey Open-File Report 86-419, 497 p., 32 figs., 29 pls., 13 tbls., 3 appendices.

---

* Plates 13-1 and 13-4 are located in pocket at end of this report.

PLATE 13-1 (located in pocket). -- Research submersible dive tracks, fix numbers, and fix locations completed in 1984 in OAK crater. Dive tracks overlayed on OAK bathymetric map from Folger, Hampson, and others (1986). Navigation fix locations shown by symbols on dive tracks, and navigation fix numbers are adjacent to fix symbols. Arrows show direction of submersible during dives, and numbers inside rectangles are dive numbers. Dashed lines show uncertain or generalized track locations. GZ = ground zero for nuclear event.

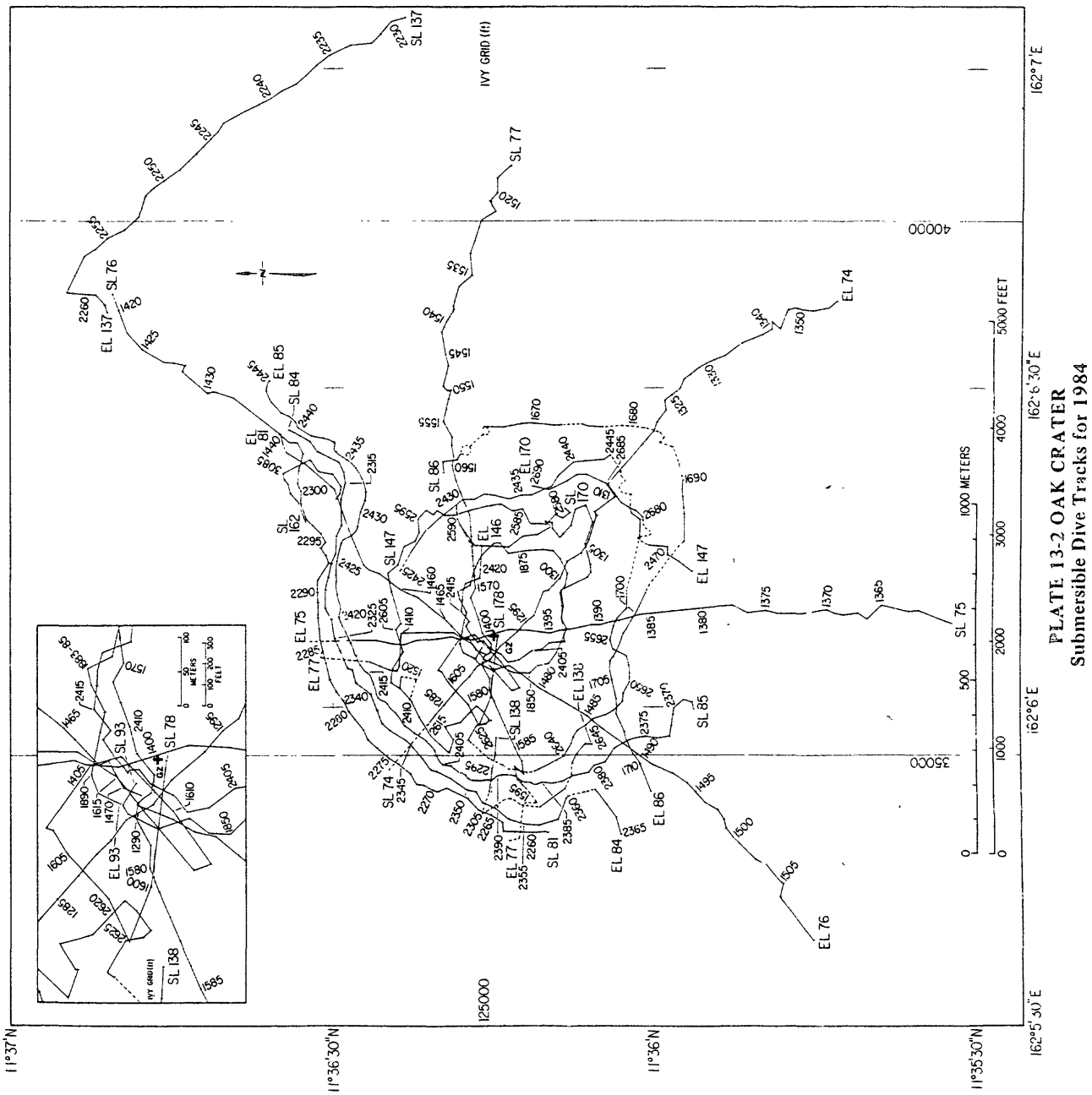

PLATE 13-2. -- Location of 1985 submersible dives in OAK crater. Beginning and ending of track lines are identified as, SL 356 = start line 356; EL 356 = end line 356. Navigational fixes shown by tics on dive tracks, annotated with fix number at 5-fix or greater intervals. Positions of sediment hills (H) are shown in the crater terrace area. GZ = ground zero. From Halley, Slater, and others (1986).

PLATE 13-3. -- Location of 1984 submersible dive tracks in OAK crater. Beginning and ending of track lines are identified as, SL 75 = start line 75; EL 76 = end line 76. Navigational fixes shown by tics and dive tracks, annotated with fix number at 5-fix or greater interval. Tracks dashed where location uncertain. GZ = ground zero. From Halley, Slater, and others (1986).

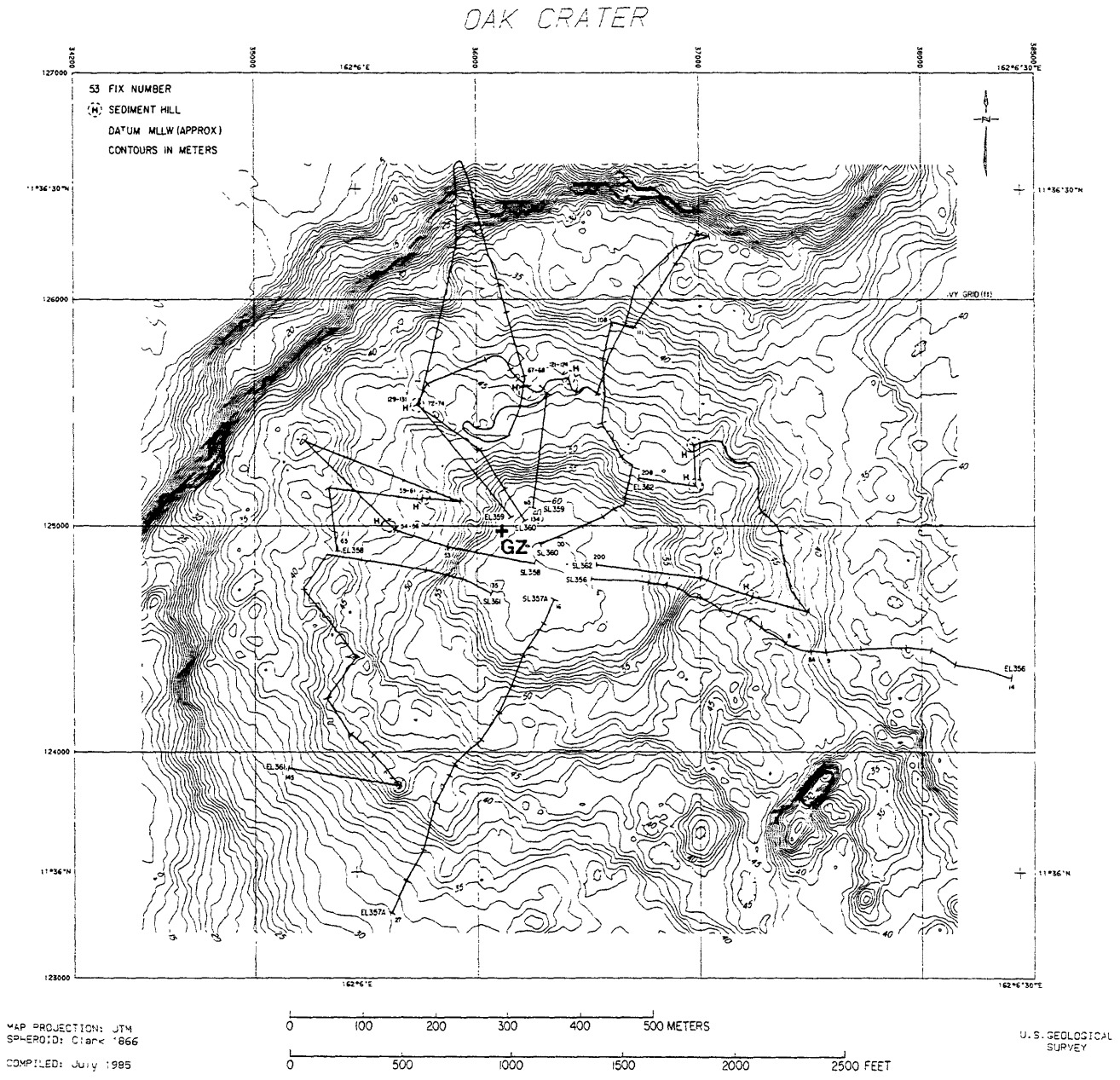

PLATE 13-3—OAK CRATER
Submersible Dive Tracks for 1985

PLATE 13-4 (located in pocket). -- Research submersible dive tracks, fix numbers, and fix locations completed in 1984 for KOA and MIKE craters. Dive tracks overlayed on KOA and MIKE bathymetric map from Folger, Hampson, and others (1986). Navigation fix locations shown by symbols of dive tracks, and navigation fix numbers are adjacent to fix symools. Arrows show direction of submersible during dives, and numbers inside rectangles are dive numbers. Dashed lines show uncertain or generalized track locations. GZ = ground zero for nuclear event.

TABLE 13-1. -- Research observations of OAK crater submersible dives, taken from TV/Voice recordings made during dives in 1984 and 1985. Plates 13-1, 13-2, and 13-3 show Fix Numbers and locations for observations. Dives 136, 137, 162, and 357B not plotted on Plate 13-1. TV/Voice recordings available for all dives except those marked with asterisk (*).

DIVE #	FIX TIMES	FIX #	DATE	OBSERVERS
74	01:35-03:24	1280-1354	7/15/84	SL - SH
75	04:15-05:16	1356-1415	7/15/84	SL - HA
76	21:06-23:00	1416-1514	7/16/84	SL - FO
77	00:19-01:43	1516-1595	7/16/84	SL - SH
78	03:22-05:00	1596-1623	7/16/84	PR - HA
81	01:48-02:50	2258-2306	7/17/84	SL - FO
84	21:46-22:34	2308-2365	7/18/84	SL - HA
85	23:29-00:49	2366-2445	7/18/84	SL - HA
86	02:19-03:39	1650-1711	7/18/84	SL - FO
93	21:38-22:35	1841-1892	7/20/84	SL - KR
136	22:30-23:14	2189-2228	7/30/84	SL - HA
137	00:38-01:46	2229-2292	7/30/84	SL - RO
138	02:39-03:24	2293-2335	7/30/84	SL - RO
146	22:21-00:27	2357-2424	8/01/84	SL - SH
147	01:25-02:24	2425-2478	8/01/84	SL - SH
162	23:24-02:00	3079-3144	8/04/84	SL - SH
170	22:05-00:21	2572-2690	8/06/84	SL - HA
356	10:25-10:54	1-14	7/01/85	SL - HA
357A	14:03-15:06	16-43	7/01/85	SL - HA
357B	15:56-16:04	48-51	7/01/85	SL - HA
358*	09:43-11:18	53-63	7/02/85	SL - HA
359*	13:51-15:24	65-75	7/02/85	SL - HA
360	08:21-10:15	100-134	7/03/85	SL - HA
361*	13:51-15:05	135-145	7/03/85	SL - HE
362*	08:23-09:01	200-208	7/04/85	SL - MA

OBSERVERS

FO - David W. Folger
HA - Robert B. Halley
HE - Thomas W. Henry
KR - Kenneth Kreyenhagen
MA - Wayne E. Martin
PR - Douglas N. Privitt
RI - Byron L. Ristvet
RO - David J. Roddy
SH - Eugene A. Shinn
SL - Richard A. Slater

SUBMERSIBLE PILOTS

Richard A. Slater, Pilot/Geologist
Douglas N. Privitt, Pilot

DIVE #74

OAK Crater
Enewetak (OAK)
Slater and Shinn

Describe NW-SE traverse of OAK crater. Used TV/Voice recordings. Track is perpendicular to baseline. No navigation fixes for A - L locations.

Fix #	GMT	TV Time	Depth(m)	Observations
A	0145	0:26:52	5	Track o/c 130°, coarse sand covered terrace, ripples, then 30°-40° slope.
B		0:27:55	12	Small terrace, coarse sand.
C		0:28:15	14	Same as above.
D		0:28:41	15	Thin algal mat in places.
E		0:29:10	17	Flat terrace; occasional mounds with fecal pellets on top.
F		0:29:45	19	Drop-off at this point to 40° slope.
G		0:30:45	29	Sandy, cobble-covered terrace.
H		0:31:05	30	Same as above.
I		0:31:35	36	Rippled seafloor.
J		0:32:11	39	c/c 130°.
K		0:32:58	42	Seems to be bottom of a valley.
		0:33:40		Going up slightly.

Dive 74 cont.

Fix #	GMT	TV Time	Depth(m)	Observations
L		0:34:00		Sub stopped for navigation; on flat seafloor with Callianassa mounds (15-20cm) loose weed on sandy seafloor; very little current; evidence of storm-related ripples on seafloor at this depth.
1281		0:45:30		o/c 130°.
1282	0205	0:46:52	40	Same as above.
1283	0206	0:47:44		Dropping off to the left, mounds (30cm high, 80-100cm across) overlapping each other.
1284		0:48:24	42	Coarse sand.
1285	0207	0:49:30	42	o/c 130°, seafloor level, lots of mounds as above.
1286	0209	0:51:20	45	Slowly sloping down, seafloor all the same.
1287		0:52:54	46	Abrupt change to no mounds.
1288		0:53:55	48	Very flat sandy seafloor.
		0:54:15	49	Echinoids on seafloor; c/c 135°.
1289		0:55:08	52	Gentle slope.
		0:55:35	55	
1290	0213	0:56:00	58	
1291		0:56:51	60	Flat sandy seafloor covered with echinoids.
		0:57:20		c/c 130°.
1293	0217	0:59:10	60	Sandy seafloor, coarse sand with some fine sand.

Dive 74 cont.

Fix #	GMT	TV Time	Depth(m)	Observations
1294		1:00:00	60	c/c 125°.
1295	0219	1:01:20	60	o/c 125°; flat, featureless, sandy seafloor, occasional helmet shells, small (4cm) urchins again.
1297		1:04:10	59	Same as above.
1298	0223	1:04:50	58	Starting up gradual slope; lots of urchins at base of slope, slope drops off on a diagonal to the left.
1299		1:06:32	53	
1300	0225	1:07:20	52	o/c 125°; occasional mounds and burrows again.
1302		1:09:18	50	Start of steeper slope of 10°-15°.
1303		1:10:42	45	
1304		1:11:38	45	c/c 120°.
1305		1:12:05	45	Small (3cm) button corals or anemones; going up this slope is really a series of terraces.
		1:13:20	42	
1306	0231	1:13:30	42	o/c 120°.
1307		1:14:50		Another rise; coarse sand and pebbles on top.
1308		1:15:08	40	c/c 125°.
		1:16:19	43	Came down again off ridge.
1309		1:16:58	44	Ridge covered with Halimeda, anemones.

Dive 74 cont.

Fix #	GMT	TV Time	Depth(m)	Observations
1310	0236	1:18:30	43	Sitting on different type of topography, a large mound (10m across) covered with organic growth--soft corals, Halimeda, anemones.
1311		1:19:45		Another similar mound or ridge about 2.5m high.
				Moving around off course to look at mound. Large mound about 5m high; 30°-40° slope, covered with Halimeda and other growth (base at 43m, top at 38m); no rock outcrop, but there is rubble on surface--appears like ridges running perpendicular to sub's track than mounds.
1314		1:22:10		Another ridge 1m high, 10m across.
		1:22:36	38	c/c 130°, patches of algal mats.
				NOTE: Course for the last 4 minutes has been erratic.
1315		1:23:55	37	Lots of Callianassa mounds, Halimeda bushes, occasional large mounds or ridges.
1316	0247	1:25:30	34	Another ridge roughly perpendicular to sub's track, covered with coarse sand, pebbles and cobbles plus abundant organic growth including some corals.
1317		1:27:05	35	

Dive 74 cont.

Fix #	GMT	TV Time	Depth(m)	Observations
		1:27:25	37	Seafloor almost completely covered with organic growth (mostly _ Halimeda, algal scum).
1318		1:28:45	38	
1319		1:29:30	40	
1320	0248	1:30:30		c/c 120°.
		1:30:50		c/c 125°; still seeing a series of ridges roughly parallel to sub's track (2-5m high); mainly sand but some rubble and organic growth.
1322		1:32:10	43	c/c 130°; larger ridge parallel to track.
1323		1:33:00		Lots of rock rubble.
1324		1:34:35	43	c/c 135°; seem to be parallel to ridges now; flat seafloor; no mounds or burrows.
1326	0254	1:35:30		c/c 140°.
		1:37:25		Just flat sandy floor now with occasional small mounds.
1329		1:39:15	44	
1330	0258	1:40:30	44	c/c 145°; flat sandy floor.
1332		1:42:30		c/c 135°; coarse sand and pebbles.
1334		1:44:30	46	
1335	0303	1:45:30	49	o/c 135°.
		1:45:55		c/c 130°.

Dive 74 cont.

Fix #	GMT	TV Time	Depth(m)	Observations
		1:47:15	49	Found mound. Lots of rock and organized growth; stopped sub; mound is (hit reset button on TV, 0307-0:00:34) 3m high; 30-40° slope; trying to pick up a rock; rocks turned out to be corals.
1340	0310	0:04:30	44	Still on same mound; looks like a pinnacle reef.
		0:07:50	49	o/c 125°; starting to move again.
		0:09:10		Back on flat sandy seafloor.
1345	0315	0:09:20		Stopped.
		0:10:45	49	Started again; o/c 130°.
		0:12:38	47	Another small hill; lots of coral, Halimeda, etc.
1350	0320	0:14:20		Lots of small mounds with corals, sponges, Halimeda, etc., o/c 130°.
		0:16:20	49	All flat sandy seafloor.
1355	0325	0:19:20		END OF DIVE.

DIVE #75

OAK Crater
Enewetak (OAK) JD 198
Slater and Halley
Describe N-S transect of OAK crater. Used TV/Voice recordings.
No elapsed time on tape for first 16 minutes.

Fix #	GMT	TV Time	Depth(m)	Observations
		0:00-0:02	42	On bottom; slight slope (5-10°); o/c 355°; coral heads (1m); large Halimeda plates in sediment.
1356	0414		42	Slight slope down to right, many coral heads (1m) lots of rubble (dead coral); coral encrusted ledge (37m deep); ledge (1m high); o/c 355°; low mounds (1-2m high).
1360	0418		33	On top of mound; circled mound; very steep sides (30-40°); o/c 355°; top of mound at 37m and bottom at 43m.
1365	0423		45	o/c 355°; seafloor same; soft and flat; lots of biological growth; some burrows.
		Time 04:26:37 = 0:16:00		
1368		0:17:00	45	o/c 355°.
1369		0:18:30		Dead coral heads and rubble.
1370	0429	0:19:30		o/c 355°; fine, silty sand; burrows; algal mat growth; off course a bit.
1371		0:21:30	43	Flat, sandy floor with burrows.
1375	0434	0:24:30	42-43	o/c 355°; flat sandy seafloor.

Dive 75 cont.

Fix #	GMT	TV Time	Depth(m)	Observations
1376		0:25:30	40	
1378		0:27:00	40	Algal growth common; Halimeda and grass-like algae.
		0:27:30		Ridge covered with corals, sponges, algae, etc; top at 37m and flat.
		0:29:30		c/c 350°.
1380	0439	0:29:30		o/c 350°; Callianassa mounds, algal growth, flat seafloor.
1382		0:31:00-0:32:00	35	Over gentle mound of sand or more like 3 or 4 ridges of sand (3-6m undulating seafloor).
1383		0:33:30		Back into Callianassa mound covered seafloor.
		0:34:00	34	Flat seafloor.
		0:35:00		Starting down steep (25°) slope.
1385	0445	0:35:30	39	Flat barren, sandy seafloor.
1386		0:36:30	40	Down another scarp; then flat sandy seafloor; no mounds.
1387		0:37:30	42	Just passed over sandy (2-3m high) soft mound or ridge; no rocks or recent biological growth.
1389		0:39:40	48	Still going down very gentle slope; all sand.
1390	0450	0:40:30		c/c 355°; soft, flat, sandy seafloor.

Dive 75 cont.

Fix #	GMT	TV Time	Depth(m)	Observations
		0:42:00	49	
1392		0:42:30	51	Starting to head down slope.
		0:43:00	54	
1393		0:43:30	57	o/c 355°.
1394		0:44:30	69	c/c 000°; a few mounds (0:45:00).
1395	0455	0:45:30		Flat sandy floor; occasional Callianassa mounds.
1396		0:46:40	60	120m from GZ; o/c 000°.
1398		0:48:30	60	c/c 355°; very fine sand; flat floor.
		0:50:00	60	
1399		0:50:20	60	15m from GZ.
		0:51:00	59	Going up slightly on flat sandy floor.
1400	0501	0:51:30		Just past GZ.
		0:52:00		Starting up steeper slope at diagonal (up to left or west).
		0:53:00	57	More Callianassa mounds.
1402		0:53:40	54	
		0:54:00-0:55:00	51	Stopped for 60 seconds to change tape; o/c 355°; up slope at diagonal (up to left).
		0:56:00	49	Leveling off; lots of Callianassa mounds.

Dive 75 cont.

Fix #	GMT	TV Time	Depth(m)	Observations
1406	0506	0:56:30		c/c 000°; another rise 45m); large Callianassa mounds; terrace wider here than seen on previous dives.
1409		0:59:30	43	Silty sandy seafloor; scattered Callianassa mounds.
1410	0510	1:00:30	41	c/c 005°.
		1:00:50	40	Slight slope.
		1:01:10	38	
		1:02:00		TV tape ends.
1415	0515		30	Upslope with large blocks (less than 1m) of coral rubble.
m			24	Slope 38°; going up fast.
n			9	Larger blocks or plates 50cm x 3-4m, slope levels off.
			3	END OF DIVE.

DIVE #76

OAK Crater
Enewetak (OAK) JD 198
Slater and Folger
Describe NE-SW transect of OAK crater. Used TV/Voice recordings.
Time of fixes probably 30-45 seconds late.

Fix #	GMT	TV Time	Depth(m)	Observations
1418	2119	0:00:00	27	Start of traverse; o/c 221°; slight slope up to sub's right; Callianassa burrows; fairly flat seafloor; algal scum common.
		0:03:10		
1420	2121	0:04:15	24	Going up slope diagonally.
1421	2122	0:05:30		Sandy seafloor covered with algal growth of mainly Halimeda.
		0:05:48	21	Small hummocks up to 1/2m across; sand texture coarsening (from medium to coarse); c/c 210° to parallel depth contour; fairly steep slope now 25° down to left.
1422	2123	0:06:48	18	Slope 32°; algal mats; no Halimeda.
1424	2126	0:09:19	9	Many small slumps (2-3m across) in sand seafloor.
1426	2128	0:11:30		Sandy seafloor, slope 30°; stairstep pattern from creep and/or slumps; algal mat; fine to coarse sand; some organic gravel fragments.
1428	2130	0:13:32	12	c/c 200-210° to stay on contour.

Dive 76 cont.

Fix #	GMT	TV Time	Depth(m)	Observations
1430	2132	0:15:20		Sandy seafloor; occasional blocks of rock on the right; seafloor mottled; fairly flat; rippled.
1432	2134	0:17:00	6	Went right to see blocks, then back to original track.
	2135	0:18:08	15	
		0:18:30		Fine sand with some larger organic fragments.
1434	2136	0:18:50		c/c 180° to stay on contour; more slump and/or creep features.
	2137	0:19:50		Parallel lines on seafloor perpendicular to slope; still following contour, back o/c 210°.
14[illegible]	2138	0:21:50	11	
		0:22:40		On a flat, gravelly terrace.
1438	2140	0:23:20	9	Flat, sandy gravelly seafloor; few burrows or hummocks; seafloor is gray to olive-drab; light gray in burrows.
1439	2141	0:24:38	8	Many blocks of coral and/or reef rock (up to 0.5m in diameter).
1440	2142	0:25:31	8	o/c 210°; flat sandy floor (790m from GZ); some Halimeda again; very fine sand with coarser organic fragments.

Dive 76 cont.

Fix #	GMT	TV Time	Depth(m)	Observations
1443	2145	0:28:30	9	Some shallow (10cm deep-0.5m across) pits and hummocks of biological origin; abundant brown algal bushes (10-15cm high).
1445	2147	0:30:10	9	o/c 210°; Same as above, sloping <10° to left; very fine sand with veneer of coarser material; small algal plants common.
1447	2149	0:32:34	12	
1448	2150	0:33:36		Edge of drop-off.
		0:33:56	18	35° slope; bottom sediments seem the same as above.
1449	2152	0:35:35	24	Same as above.
1450	2153	0:36:00	27	Same as above.
		0:36:30		Flattens out.
	2153	0:36:40	30	c/c 200°; seem to be in a trench; seafloor is hummocky (5-10cm relief); looks like recent biological activity.
1453	2156	0:39:25	29	Same as above.
1454	2157	0:39:53	30	Crossed a mound.
		0:40:25		o/c 200°; sharp little hummocks and ridges (10cm).
1455	2158	0:41:19		Large subtle mounds; depths fluctuate on a scale of 2-3m.
1456	2159	0:42:40	33	Seafloor covered with large hummocks (up to 0.5m); c/c 190°.

Dive 76 cont.

Fix #	GMT	TV Time	Depth(m)	Observations
1458	2201	0:44:25	36	Seafloor very soft; with extensive biological reworking.
1459	2202	0:45:13	39	Seafloor flatter again; small mounds up to 30cm.
1460	2203	0:46:00		
		0:46:30	42	Seafloor drops sharply; about a 3m scarp; then a fairly flat seafloor with small mounds on a gently undulating surface (large low mounds and valleys 2m relief over a distance of 15-20m); visibility not good enough to see these macrofeatures.
1463	2206	0:49:00	46	c/c 190°; seafloor very flat; only occasional 20-30cm mounds or pits.
1465	2208	0:51:10	48	
		0:51:48		Sharp drop-off or scarp.
1466	2209	0:52:15	51	
		0:52:40	54	Another sharp drop-off 20° or more.
1467	2210	0:53:15	58	Flat seafloor; very find sand, many small (a few cm in diameter) pits: occasional 0.25 to 0.5m across mounds (10-15cm high).
		0:54:50	59	Seafloor slightly rising; o/c 190°.
1469	2212	0:55:30	56	
		0:56:00	55	
		0:56:20	53	
		0:56:50	52	On top of large mound.

Dive 76 cont.

Fix #	GMT	TV Time	Depth(m)	Observations
1470	2214	0:57:18	52	On top of large mound dropping off.
1472	2216	0:59:25	56	Circling around to look at mound; looks more like an E-W trending ridge.
1474	2218	1:01:29	54	o/c 190°.
1475	2219	1:02:15	52	o/c 190°; slope (20°) down to left; very fine sand; a few more small mounds (volcano-shaped); o/c 190°.
1477	2221	1:04:20	52	Moving gradually upslope; seafloor the same.
1478	2222	1:05:35	51	Moderately hummocky seafloor (10cm relief).
1480	2224	1:07:15	51	o/c 190°; very fine sand; some coarse organic particles (fine algal mat being munched by urchins over most of crater floor).
1481	2225	1:08:05		Starting upslope; large soft mounds (up to 0.5m) on slope; coarser sediments.
		1:08:44	48	Zone of small button-like corals or anemones about 1cm across.
1482	2226	1:09:20	46	
1483	2227	1:10:40	45	
	2228	1:11:10	45-42	Scarp 30°.
1484		1:12:00	42	
		1:12:35	40	Flat terrace; fine sand; small hummocks; o/c 190°.

Dive 76 cont.

Fix #	GMT	TV Time	Depth(m)	Observations
		1:13:00		Another scarp; looks rocky but possibly covered with rock debris.
1485	2230	1:13:13	39	o/c 190°; rock-covered scarp; Halimeda on rocks, then flat sandy seafloor; small hummocks and pits (this scarp or rim is a series of steps--not a continuous slope); occasional large hummocks (up to 0.5m high).
1487	2232	1:14:55	33	c/c 195°; some algal bushes; abundant small mounds and pits; sediment white to light gray, mottled to a darker gray to tan, lots of Halimeda now.
1488	2233	1:16:10	29	Slope 5°.
1489		1:17:05	28	Slope down to left 10°.
		1:17:50	23	Light colored sand seafloor with 5-10cm relief; lots of algal plants (mainly Halimeda) and mats.
1490	2235	1:18:20	22	Fairly flat sandy seafloor; lots of Halimeda bushes; slope down to the left.
1491	2236	1:19:50	19	Coarse sand to fine gravel; abundant random hummocks (5-10cm).
1493	2238	1:21:00	17	
		1:21:25		c/c 205°.
1494	2239	1:21:55	14	Same as above; seafloor leveling off at 15m.

Dive 76 cont.

Fix #	GMT	TV Time	Depth(m)	Description
1495	2240	1:23:12	14	Same as above; flat, light-colored, very coarse sand in small hummocks; lots of algal plants (10 sq m); intermittent algal mats; occasional 0.5m mounds.
1499	2244	1:27:00	14	
		1:27:40	16	
1500	2245	1:28:15	14	Same as above, with more algal mats.
1502	2247	1:30:15	13	Very caorse sand (Halimeda plates) covered with algal plants; c/c 205°.
1504	2249	1:32:30	13	
		1:33:30	11	
1505	2251	1:34:20	11	Sitting at cement block (1m to a side) with anchor ring and chain.
1508	2254	1:37:00		Sediment is mainly large Halimeda plates; lots of living Halimeda plants.
1510	2256	1:39:10	11	Same as above; light gray mounds on dark gray algal mat surface; many 20-30cm mounds, lots of living Halimeda bushes.
1514	2260	1:43:30	10	o/c 205°. Occasional head corals.
1515	2301	1:44:10	11	END OF DIVE.

DIVE #77

OAK Crater
Enewetak (OAK) JD 199
Slater and Shinn
Describe E-W transect of OAK crater. Used TV/Voice recordings.

Fix #	GMT	TV Time	Depth(m)	Observations
		0:04:30	45	On seafloor; o/c 265°.
1516	0019	1:15:00		o/c 265°.
1517		0:06:30	42	On coral promontory; lots of coral, sponges, algae, etc.
1518		0:08:00	45	o/c 265°; sandy flat seafloor.
1519		0:09:20		c/c 275°; 2m scarp covered with rubble (dead coral).
1520	0024	0:10:20		Series of ridges (about 3m high).
1521		0:11:22	45	Steep slope in NE direction after 10m ridge.
1522		0:12:40		c/c 280°; very fine sand seafloor.
1524		0:17:15		More rubble (dead coral) covers dome; 35-45° slope (30m across, 30m at top, 46m at base); circling around mound.
1530	0034	0:20:20		Still circling almost perfect conical dome; maybe a slight E-W extension.
1531		0:21:20		o/c 275°.
1533		0:23:00	45	Sandy, flat seafloor.
1534		0:24:30	45	c/c 270°.
1535	0039	0:25:20	45	Flat, fine sandy seafloor; no features.

Dive 77 cont.

Fix #	GMT	TV Time	Depth(m)	Observations
1537		0:27:20	43	c/c 260°.
1538		0:28:00	36	On small mound.
1539		0:29:05		Top of mound.
1540		0:30:20		c/c 250°.
1541		0:31:30	42	Base of mound; stopped for 1 minute.
1543		0:33:00		o/c 250°.
1544		0:34:20	42	Fine sandy seafloor; Callianassa mounds common.
1545	0049	0:35:20	42	Sand seafloor; many Callianassa mounds.
1546		0:36:10	42	At base of mound; mound covered with corals, algae, sponges.
		0:37:30	39	On top of mound; mound has slight N-S orientation; mainly conical.
		0:38:30	40	Back at base; flat sandy seafloor with some Callianassa mounds; o/c 250°.
		0:39:20	39	c/c 240°.
1548		0:41:00	36	Small mound.
1549	0055	0:41:30	36	On top of small mound.
1550		0:42:20	39	On flat floor; soft bottom; o/c 250°.
1551		0:43:30	36	Another small mound; flat, flat; lots of algae, corals, etc.

Stop for 1 minute

Dive 77 cont.

Fix #	GMT	TV Time	Depth(m)	Observations
1553		0:45:20		
1554		0:46:30		c/c 240°; soft; Callianassa mounds.
1555	0101	0:47:20	39	o/c 240°; sandy seafloor with occasional Callianassa mounds.
1556		0:48:30		Another small mound.
		0:49:00		On top of mound.
1557		0:49:30	39	Sandy floor.
1558		0:50:30	36	Another mound.
1559		0:51:30		Flat again; lots of coral pinnacles, mounds of varying shapes.
1560	0106	0:52:30		c/c 230°.
1561		0:53:30	40	Flat sandy seafloor with Callianassa mounds.
		0:55:00	42	Starting to drop off.
1563		0:55:30	45	Scarp, then level again.
1564		0:56:20	48	Fine sand, many Callianassa burrows.
		0:57:20	50	Lots of Callianassa mounds.
1565	0112	0:58:20	50	In a little gully.
1566		0:59:10	49	Moved up soft white mound (3m high).
1567		1:00:00	49	Another mound; series of 3 mounds; 30m apart; just sand with Callianassa mounds; o/c 240°.

Dive 77 cont.

Fix #	GMT	TV Time	Depth(m)	Observations
1568		1:01:10	52	Scarp, then flat seafloor with lots of 30cm mounds.
1569		1:02:30	54	
		1:03:00	57	Scarp, then flat seafloor.
1570	0117	1:03:20		o/c 240°.
			58	Flat, sandy seafloor with many Callianassa mounds.
1571		1:04:20	59	
		1:04:40	59	c/c 220°.
1572		1:05:20	59	
1573		1:06:10	60	Flat, sandy seafloor.
1574		1:07:20	59	
		1:07:50	58	Starting up 10° slope.
		1:08:40		c/c 230°; slope 20°.
1575		1:09:40	54	Changing course to find top of mound; didn't see top, just slope.
1576	0124	1:10:20	52	
1577		1:11:40	49	
1578		1:12:40	46	Steady 10° slope.
1580	0128	1:14:20		Fix at top of ridge.
		1:14:40		Dropping back down; lots of big Callianassa burrows.
1581		1:15:50		c/c 225°.
1582		1:16:30	43	Start up steep slope.

Dive 77 cont.

Fix #	GMT	TV Time	Depth(m)	Observations
		1:16:50		Across ridge then down again (crossing perpendicular to ridges; 2-3cm relief).
1585	0133	1:19:20	38	Flat sandy seafloor.
1586		1:20:30	39	Up steep 30° slope.
1587		1:21:30	30	On top of slope, stopped.
1590	0138	1:24:30		Still on top of ridge.
1592		1:26:20		Started; o/c 235°.
1593		1:28:00	30	Going up slope.
1594		1:28:00	23	Up 35° slope.
		1:29:00	17	Seafloor levels off.
1595	0143	1:29:20	15	On top of ridge; near drop-off (stopped until 1:32:20).
		1:32:20		Ridge trending N-S.
X		1:33:00-1:37:00		Ran along ridge; took sample; off scarp; o/c 235°.
Y		1:38:40	23	On flat sandy seafloor.
		1:39:30		Going upslope again, rubble on slope; large 3-4m blocks.
Z		1:41:00	9	On crater rim.
		1:41:40	6	Outward dipping crops with appearnace of upturned flap; explored area.
				END OF DIVE

DIVE #78

OAK CRATER
Enewetak (OAK) JD 199
Halley and Privitt
Describe exploration of GZ Area and Mounds in central OAK crater.
Used TV/Voice Recordings.

Fix #	GMT	TV Time	Depth(m)	Observations
1596	0322		60	On seafloor (used arm to show bottom type); unconsolidated silty sediment.
1599	0325	0:07:24	60	Still at down position.
		0:11:00	60	o/c 270°; flat silty seafloor.
		0:12:30		Up a slight incline.
S		0:12:45	54	
		0:14:00		20° slope.
T		0:14:30		Flattening out; occasional Callianassa mounds.
		0:15:45	48	
U		0:17:10	46	Starting downslope off mound.
		0:17:30		Stopped for fix; sediment sandier here on side of mound than on flat crater floor.
1600	0342	0:23:50	45	
		0:24:30		Started up again; o/c 270°.
1601		0:25:20		Lots of Callianassa mounds; flat seafloor.
1602		0:26:20		c/c 045°.
1603	0345	0:27:00		
		0:28:00	41	Dropping off, down a steep slope.

Dive 78 cont.

Fix #	GMT	TV Time	Depth(m)	Observations
		0:28:50	45	Seafloor flattens out.
1604	0347	0:29:00	45	Flat seafloor; no mounds or burrows.
		0:31:50	45	
		0:32:20		Lots of Callianassa mounds.
1605	0351	0:33:10		
		0:33:30		c/c 135°.
		0:34:10		Edge of mound; sand-covered mound; no rock.
1606		0:35:40	44	On top of mound; 10m across at top, 44m depth on top.
1607	0355	0:37:00		Base of mound.
		0:38:30	45	
		0:39:00		o/c 135°.
V		0:40:30		Slight rise 1m high and 3m long (ridge).
		0:41:30		Flat seafloor; no mounds.
		0:42:00	51	Going down slight slope.
1608	0400	0:42:20	52	Slope to right.
		0:43:30		Heading down slope; o/c 180°.
		0:44:00	59	
1609		0:45:30	60	Back on muddy crater seafloor.
		0:46:30		Flat seafloor.
		0:47:20	60	Slight slope up to right.

Dive 78 cont.

Fix #	GMT	TV Time	Depth(m)	Observations
		0:48:30	57	Flat seafloor.
W		0:49:20	54	Contouring around side of mound.
		0:50:30	54	About 20° slope.
		0:51:30	49	Sub has been wandering around.
		0:53:00		o/c 190°; slope is up to the right.
1610	0411	0:53:20		West of GZ; o/c 160°.
		0:54:30		Flat sandy seafloor; still contouring around hill, slight slope up to right.
		0:56:00	51	o/c 270°.
		0:56:30		Very flat seafloor, no slope.
1611	0415	0:57:20		On flat seafloor.
		0:58:20		c/c 040°.
1612	0417	0:58:50 1:00:00	48	Flat seafloor; no burrows or mounds.
		1:01:20	48	Same as above.
1613	0420	1:02:20	51	o/c 040°; flat sandy seafloor.
		1:04:00	60	After drop-off.
1615		1:05:00	60	o/c 040°; crossing previous track.
		1:07:00		Heading upslope; stopped for 1 minute.
X		1:08:00	57	30° slope of muddy sand.
		1:09:20	52	Still going upslope.

Dive 78 cont.

Fix #	GMT	TV Time	Depth(m)	Observations
Y		1:09:40	49	Seafloor flattening out.
		1:10:20	47	Top of knoll; top about 3m across; sub stopped; gravel and sand at top.
1616	0431	1:13:10	47	Top of mound.
		1:17:00		o/c 000°.
		1:18:00	48	Didn't drop down much; flat bottom.
1617	0437	1:19:00		Flat seafloor; occasional Callianassa mounds.
Z		1:21:00	43	
		1:21:40		c/c 270°.
		1:22:20		A slight rise in seafloor.
1618		1:23:00		Flat sandy seafloor.
1620		1:25:00	45	Starting up slope to right.
1621	0444	1:25:40		Going up slope; getting more gravely; o/c 000°; this mound looks linear.
1622		1:27:00	40	Stopped for sample; rubble (up to 15cm) and gravel; sitting on top of ridge (3m wide at top).
		1:37:40		o/c 000°; probably on crater wall (maybe ridge was a spur running parallel to crater wall). [This was not the crater wall].
		1:39:40		Over another ridge.
ZZ		1:40:50	34	o/c 330°; sandy.

Dive 78 cont.

Fix #	GMT	TV Time	Depth(m)	Observations
1623	0500	1:42:00	30	Starting up steep slope.
		1:42:50		Lots of blocks and rubble on sandy slope; 35 to 40° slope.
		1:43:20	18	Going up slope.
		1:44:00		Terrace of rock (overturned slab?); running along 4m escarpment (on left side).
				END OF DIVE

DIVE #81

OAK Crater
Enewetak (OAK) JD 200
Slater and Folger
Describe OAK crater along 6 to 8m depths along upper rock escarpment. Used TV/Voice recordings. No elapsed times on TV tape.

Fix #	GMT	TV Time	Depth(m)	Observations
2258	0148		6	On edge of drop-off, o/c 000°; rubble and sand, cobbles and boulders, some rubble 45-50cm in diameter.
2260	0150			Moving back up to 6m, sand and rubble.
2262	0152		3	Moving back out to 6m depth.
2263	0153		6	On rock edge, rock rippled and fractured.
2264	0154		6	Moving along rock rim, 3m scarp.
2265	0155		6	Still on rock rim, scarp 4m depth.
	0155:30			Large block broken off plate, fell down slope (saw on previous dive).
2266	0156		9	
2267	0157		11	Rim is deepening toward crater center. Another large block broken off here; sub moving in and out slightly; rim is intermittent with sand chutes in between outcrops.
2268	0158		9	Still moving along rim; plate fractured.
	0159			On sand flat, moving up into shallower water.
	0200		5	Stopped on sand flat.

Dive 81 cont.

Fix #	GMT	TV Time	Depth(m)	Observations
2269	0201		5	Moving over sand flat, down to rim.
2270	0202		6	Still sand, flat, no rock.
2271	0203			Still sand.
2272	0204		6	All sand, flat; sand slope (20°-30°), sub course more NE.
2273	0205		6	o/c 030°, on sand slope.
2274	0206		6	Running along edge of crater sand scarp; another sand scarp going up to left to near the water surface; 20m wide sand terrace in between; shallower scarp is recent sand delta.
2276	0208		6	Scarps run together, now just one sand scarp.
2277	0209		7	o/c 060°.
2278	0210		8	o/c 030°, one large sand slope dipping 30°.
2279	0211		8	Still on sand slope, o/c 045°.
0280	0212		8	Running along sand slope.
2282	0214		7	Same as above.
2283	0215		6	Same as above.
2284	0216		6	Same as above, o/c 060°.
2286	0218		8	o/c 070°, very fine sand, slope.
2288	0220		8	Starting to see occasional 1-2m blocks of rock right after fix 2288.

Dive 81 cont.

Fix #	GMT	TV Time	Depth(m)	Observations
2289	0221			o/c 090°, more rock rubble (all sizes).
2290	0222		8	On 20° slope, rubble covered.
2291	0223		6	Terrace again, running along rim, steep drop off to right; rubble all sizes up to 2m across.
	0224		8	Sub stopped; first outcrop-scarp, more fractures and broken chunks than on southern side.
2292	0236		10	o/c 060°; large slabs of broken rock, rubble, rippled rock again.
2293	0237		10	Moving across flat terrace covered with rock rubble.
2294	0238		11	Big flat plates of rock, fractured; 1-2m escarpment.
2296	0240		3	Up on top of flat rock terrace; still fractured, lots of rubble.
2297	0241		6	At tide gauge buoy; flat sand terrace; lots of rock rubble.
2298	0242		6	Many large rock plates up in 3m of water; mainly sand terrace between rock and drop-off.
2300	0244			Still the same; large angular blocks; turning right to find drop-off.
2301	0245			Crossing rubble-covered sand terrace.

Dive 81 cont.

Fix #	GMT	TV Time	Depth(m)	Observations
2302	0246		8	On large flat sand terrace, gradual slope.
2304	0248		9	On drop-off again, o/c 000°; all sand, 6m wide, sandy terrace, then sand slope down into lagoon.
2306	0250		9	All sand; near drop-off.
				END OF DIVE

DIVE #84

OAK Crater
Enewetak (OAK) JD 200
Slater and Halley
Describe 50' contour along west side of OAK crater.
Used TV/Voice recordings.

Fix #	GMT	TV Time	Depth(m)	Observations
			9	Landed on rubble, heading NE for deeper water; 11m at drop-off, 35° sand slope-covered with dark algae, turning around to start traverse.
2308	2146	0:10:33	15	One-third down slope of 35°; terrace 5m above sub; heading 190°; slope steady.
2310	2148	0:12:30	15	On a small promontory, o/c 210°.
2311		0:13:10		Cross old sub track.
2312	2150	0:14:30	15	o/c 180°; terrace only 2m above sub now.
		0:15:30		Another small promontory, o/c 210°.
		0:16:00		Bench now at 15m.
2313	2152	0:16:30	15	On flat bench.
		0:17:50		o/c 260°; 15m.
2315	2154	0:18:30	15	o/c 250°; steep slope down to left, terrace at 15m on right.
2316		0:19:30	15	o/c 290°, some rubble.
2317	2156	0:20:30	15	Lots of rock debris, rubble 10-15cm (passing tidal buoy).
		0:22:00		Large block above sub.
2319	2158	0:22:30	15	Lots of large blocks above sub 5-6m, sub on slope again.

Dive 84 cont.

Fix #	GMT	TV Time	Depth(m)	Observations
2320		0:23:30		Back into sand, then more rock and rubble.
2321	2200	0:24:20	15	35° slope, rock debris probably rolled down from above.
2322		0:25:30		Promontory, large block (8-10m) just above sub (3m above).
2323	2202	0:26:20	15	Swinging around promontories, o/c 210°; terrace 3-5m above sub.
		0:28:00		Large rock.
2327	2206	0:28:20	15	Large rock outcrop, then sand terrace at 15m (terrace is found at different depths from 9 to 15m).
2328		0:29:30		Large flat rocks, looks like outcrop.
2329	2208	0:30:20	15	Large flat rock outcrop (1m scarp) down to 18m.
2340		0:31:20		Same as above.
2341	2210	0:32:20	17	On flat sand terrace, drop-off 6m to left.
2342		0:33:30		Drop off at 18m, large sand terrace, 15m contour to the right.
2343	2212	0:34:20	18	Rock (outcrop?) again, large sand terrace (15° slope).
2344		0:35:20		All sand.
2345	2214	0:36:20	15	On break of slope, mostly sand, occasional boulders.

Dive 84 cont.

Fix #	GMT	TV Time	Depth(m)	Observations
2346		0:37:20	15	More rock again, rock flat blocks at break, rock slumped down to 18m in places.
2347	2216	0:38:20	17	Flat rock terrace (1m scarp at break in slope).
2348		0:39:20	15	o/c 195°, flat fractured rock outcrop.
2349	2218	0:40:20	15	Rock at 14m with lots of pieces broken off and sliding down slope.
2350		0:41:20		Same as above.
2351	2220	0:42:20	15	Large flat rock outcrop with ripples on surface.
2352		0:43:20	11	Very large outcrop.
		0:44:00		Rock terrace up 6m.
2353	2222	0:44:20	12	Lots of rock rubble on slope, sub on slope well below rock bench with lots of blocks and rubble on slope.
2354		0:45:20	15	Promontory.
2355	2224	0:46:30	15	Break of slope 3m above, sitting on sand terrace; delta of debris just to right coming down to 15m terrace.
2357	2226	0:48:20	15	On sand terrace, crossing promontory.
2359	2228	0:50:20	15	On outer edge of terrace, Callianassa burrows.
2360		0:51:30	17	Flat seafloor, cutting across terrace at an angle, o/c 200°.

Dive 84 cont.

Fix #	GMT	TV Time	Depth(m)	Observations
2361	2230	0:52:20	14	Still on flat sandy bench, *Callianassa* burrows.
2363	2232	0:54:20	9	Same as above.
2365	2234	0:56:20	5	END OF DIVE.

DIVE #85

OAK Crater
Enewetak (OAK) JD 200-201
Halley and Slater
Describe 30m contour along base of OAK crater escarpment.
Used TV/Voice recordings.

Fix #	GMT	TV Time	Depth(m)	Observations
		0:00:00	27	Flat, sandy, lots of Callianassa burrows, heading down very gentle slope to 30m.
2366	23:29	0:04:00	30	o/c 040°, sandy, lots of mounds and burrows, very flat.
2368	23:31	0:06:00	30	Sandy, flat seafloor with many Callianassa mounds.
2369	23:32	0:07:00		About 1m high and 5m long mound, trending in E-W direction, paralleling sub on left.
2370	23:33	0:08:00	30	6-9m wide mound on right 0.5m high, some rubble at base.
2371	22:34	0:09:00	30	Flat sandy seafloor, many Callianassa mounds.
2372	23:35	0:10:00	30	Flat plain, difficult to stay on contour.
2373	23:36	0:10:00		o/c 000°. Only a few degree slope.
2374	23:37	0:12:00	30	Slight increase in slope (5°) up to left, flat to right, all sand, burrows, and Callianassa mounds.
2376	23:39	0:14:00	30	o/c 315°, same as above.
2378	23:41	0:16:00	30	
2379	23:42	0:17:00		Heading 000°, going around delta or promontory of sand, 15° slope on left.

Dive 85 cont.

Fix #	GMT	TV Time	Depth(m)	Observations
2380	23:43	0:18:00	30	o/c 325°, slope on left, flat sandy floor on right.
2381	23:44	0:19:00		Starting to drop off on right.
2382	23:45	0:20:00	30	On a little terrace, another terrace 2m above sub and another terrace 1m below sub, 15-20° slope in between.
		0:20:30		Drops off to right 40°, bottom 3-4m below on right.
2383	23:48	0:21:00		On 40° slope now, o/c 000°, flat seafloor at 34m on seafloor.
2384	23:47	0:22:00	30	On 40° slope, some rubble (cobble size).
2386	23:49	0:24:00	29	On 40° slope, sub moving in and out gradually.
2388	23:51	0:26:00	30	On 40-45° sand slope.
		0:26:30		Going around large promontory, slope drops off to right, can't see flat seafloor.
2389	23:52	0:27:00		Still moving around promontory, 6-9m long ridge, lots of cobbles, a few large blocks (2-3m).
2390	23:53	0:28:00	30	o/c 000°.
2391	23:54	0:29:00		Large blocks and rubble, flat floor just below sub on right.
2392	23:55	0:30:00	30	Large block with rippled-marked surface.

Dive 85 cont.

Fix #	GMT	TV Time	Depth(m)	Observations
2394	23:56:30	0:30:30	27	Oil drum in extensive rock rubble and blocks, stopped sub, good TV of 2 sharks.
2396	23:59	0:33:00	27	Still at oil drum, looks empty.
2397	0:00	0:34:00		Start up again, cliff just above sub, many 3-4m blocks.
2398	0:01	0:35:00	27	Lots of rubble and blocks.
2399	0:02	0:36:00		Stopped again, tape broke.
2400	0:03	0:37:00	30	On 35-40° slope, sand with lots of rubble up to 1m.
2401	0:04	0:38:00		Large block or outcrop(?) on slope.
2402	0:05	0:39:00	30	35° slope of sand and rubble, some 2-3m blocks.
2404	0:06:30	0:40:00	30	Oxygen bottle (or cannon(?), stopped for 1 minute.
		0:41:30		Large block (4-5m) on sand slope.
2405	0:08	0:42:00	29	Starting to swing around, o/c 060°.
2406	0:09	0:43:00	30	o/c 040°, on slope with lots of rubble and blocks.
		0:44:30	30	Going around promontory, flat floor down below (43m?).
2408	0:11	0:45:00	30	Small terrace above and flat floor (3m) below.

Dive 85 cont.

Fix #	GMT	TV Time	Depth(m)	Observations
2409	0:12	0:46:00	30	Very large (4-5m) block.
		0:46:30	30	Terrace on right is more like a ridge running parallel to slope but filled in behind.
2410	0:13	0:47:00	30	On terrace now, drops off at right.
2411	0:14	0:48:00		On flat sandy terrace, some rubble.
2412	0:15	0:49:00	30	Series of promontories, talus piles; sub moving in and out around these, they always have lots of rubble on their surface including occasional blocks, o/c 045°, debris extensions of rubble into crater.
2414	0:17	0:51:00	30	o/c 030°, still weaving in and out, this fix right on a talus pile nose; lots of rubble on promotories; flat seafloor only 1m below sub now; very large blocks way up slope on left.
2416	0:19	0:53:00	30	Lots of large blocks, especially up slope on left; still swinging in and out, sand in valleys, rubble on promontories.
2418	0:21	0:54:30	30	Large promontory at this fix (most promontories are on the northern section of escarpment).
2420	0:23	0:56:30	30	20° slope, mainly sand now, occasional rubble.
2421	0:24	0:57:30		o/c 045°.

Dive 85 cont.

Fix #	GMT	TV Time	Depth(m)	Observations
2422	0025	0:58:30	30	Very large sandy promontory; still weaving in and out 90°; flat seafloor to right and gentle slope up to left, occasional Callianassa mounds.
2423		0:59:30	30	Oil drum.
2424	0:27	1:00:30	30	Very large rock outcrop(?) or block up to left as far as one can see, flat sand floor to right.
2425	0:28	1:01:30	30	Lots of rubble now.
2426	0:29	1:02:30	30	Mainly sand, 15° slope up to left, flat to right.
2428	0:31	1:04:30	30	Mainly sand, 25° slope (more than before); near tide gauge.
2430	0:33	1:06:30	30	Flat sand seafloor, many Callianassa mounds.
		1:07:30	27	Crossing large low ridge of sand pointing into crater.
2431	0:35	1:08:30	29	o/c 009°, crossing horn of sand (double horn).
2433	0:37	1:10:30	30	o/c 010° still on gentle slope, all sand.
2435	0:39	1:12:30		Moving more to the right; good turtle shot at 1:13:30-1:14:00.
2437	0:41	1:14:30	30	All sand, o/c 045°.
2439	0:43	1:16:30	30	15° sand slope to left, flat seafloor to right, many Callianassa burrows and mounds; o/c 020°.

Dive 85 cont.

Fix #	GMT	TV Time	Depth(m)	Observations
2441	0:45	1:18:30	30	Slope is lessening somewhat; o/c 015°.
2443	0:47	1:20:30	30	One 2m block lying on flat sandy seafloor.
2445	0:48:40	1:22:10	30	End of dive; very flat sandy plain.
				END OF DIVE

Much of this dive is plotted too shallow by navigation, and we question the accuracy (R.A. Slater).

DIVE #86

OAK Crater
Enewetak (OAK) JD 201
Folger and Slater
Describe ejecta blanket on lagoon side of OAK crater.
No elapsed time on TV and some TV tape out of focus. Navigation did not give many fixes. Used TV/Voice recordings.

Fix #	GMT	TV Time	Depth(m)	Observations
1649	0218		39	o/c 130°, down position, v. fine sand (very poor visibility); c/c 115°.
1650	0219		36	Very fine sand, burrowed, Callianassa mounds; no slope on seafloor.
1654	0223		34	o/c 115°.
1655	0224		34	On mound 3m high, 9m across; on top are some 25-50cm angular boulders, mainly living coral and Halimeda; several low mounds here with lots of debris(?) on tops. Mounds trending in a N-S direction.
1660	0229			Stopped, then start up again from mounds (2nd mound 30m in diameter 3m high, connected to first mound); large block (2m diameter, very angular) with rubble on top of another small ridge (N-S trend).
1662	0231		37	Very fine sand, burrowed, Callianassa mounds, dropping off down slope.
1664	0234			Going down SE-facing scarp, covered with dead, flat corals.

Dive 86 cont.

Fix #	GMT	TV Time	Depth(m)	Observations
1665	0235		35	On top of mound; base (41m), top (35m) pinnacle reef covered with debris (dead coral?); steep on S-SE side, gentle elsewhere.
1667	0237			Starting again, many small mounds (1m high, 3-4m wide).
	0238		42	Mounds and debris on right side of track, burrowed sandy seafloor on left, o/c 160°.
1669	0241		39	o/c 160°, very fine sand, burrows, many mounds; starting up gentle slope between 1670 and 1671.
1670	0242			o/c 160°, sand seafloor, burrows, many irregular-shaped low mounds; sharp N-S scarp on right.
1671	0245			Side of mound, base 36m, top 34m.
1672	0247		36	o/c 180°, very fine sand, burrows, some small mounds.
1673	0248		34	o/c 180°, flat to the right, steep drop off to the left (east).
1675	0250		34	On horseshoe-shaped mound, steep side to the east (camera off, sub stopped from 0249-0252).
1677			29	c/c 195°, 26m near top of pinnacle, shallower to left, steep drop-off (30°), all sediment.

Dive 86 cont.

Fix #	GMT	TV Time	Depth(m)	Observations
			36	At base of pinnacle, rapid change in sub depth throwing off navigation location.
1680	0250		39	Just past 42m valley or gully, went down 26m into valley, sand floor.
1681	0252		39	c/c 205°, same sandy seafloor with many elongate mounds or ridges.
1683	0259			o/c 205°, mound on the right.
1684	0300		37-39	c/c 255° base of large pyramid-shaped pinnacle reef steep slope (up to 80°) with plate corals; 29m top (1m across at top).
1686	0303		29	Top of pinnacle.
1688	0305		40	o/c 260°, flat sandy seafloor.
1689	0306		40	o/c 260°, going down gentle sand slope.
1690	0308		42	o/c 260°, flat sandy seafloor off to right, no mounds, occasional Callianassa burrows.
1691	0309		42	Same as above, featureless.
1692	0310		45	Very fine sand, Callianassa mounds and burrows.
	0311			c/c 295°, climbing up slope to left.
	0312		40	o/c 295°.

Dive 86 cont.

Fix #	GMT	TV Time	Depth(m)	Observations
	0313		40	Leveling off.
1693	0314		37	o/c 270°, running along channel (to right), debris on left.
1694	0315		37	o/c 290°, ship far away.
1695	0316		37	Very fine sand, Callianassa mounds and burrows, ship too far away for navigation.
1697	0318		35	Very fine sand, Callianassa mounds and burrows.
1698	0320		38	Very fine sand, mounds 9-30m across 9-30m apart, undulating seafloor, ship back overhead.
1699	0321		40	o/c 295°, flat featureless seafloor.
1700	0322		41	o/c 295°, very fine sand, slightly variable topography, a few Callianassa mounds, worm holes.
1702	0324		40	c/c 280°, same as above.
1703	0326		44	c/c 265°, scarp, dropping off, looks like we are going into the crater.
1705	0328			o/c 265°, scarp, drop-off to 47m.
	0331		41	Climbing up scarp.
1706	0332		37	
1707	0333		34	All sand, Callianassa burrows.

Dive 86 cont.

Fix #	GMT	TV Time	Depth(m)	Observations
	0335			TV off.
1710	0337		24	TV on, no change in bottom, flat sand with Callianassa burrows; gradual slope all the way, no terraces, no rock, no rubble.
0340			15	same slope all the way up.
				END OF DIVE

The location of many features are present due to several conditions, including no elapsed time on TV, navigation took odd fixes and gave very few fixes for TV tape, and ship too far away. We consider many locations on map to not be as accurate as on other dives.

DIVE #93

OAK Crater
Enewetak (OAK) JD 201
Slater and Kryenhaven
Describe inner OAK crater at 52m contour depth (counter-clockwise).
Used TV/Voice recordings.

Fix #	GMT	TV Time	Depth(m)	Observations
	0:01			Start of traverse, o/c 310°, 15m from GZ.
1840	2136	0:01:20	57	Silty sand featureless seafloor, burrowed.
		0:03:10	51	On large low mound.
1841	2138	0:03:20	54	On slope of mound.
1842	2134	0:04:40	51	Stopped.
1843	2140	0:05:20	51	Start again, same seafloor, o/c 180°.
1845	2142	0:07:10	51	Silty sand, burrowed seafloor, featureless.
1847	2144	0:09:10	48	Sub weaving up and down between 45m and 51m.
		0:10:10	51	Came down slight slope (off mound?).
1848	2146	0:11:10	54	10-15° slope to the right, o/c 180°, slight slope to left, still featureless, a few burrows and mounds.
1850	2148	0:13:20	53	o/c 120°, same type of seafloor but flat.
1851	2149	0:14:30	54	177m from GZ (215° T).
1852	2150	0:15:20	52	o/c 180°, same type of seafloor, flat.
		0:16:40	52	o/c 100°, flat seafloor, occasional Callianassa mounds and burrows.

Dive 93 cont.

Fix #	GMT	TV Time	Depth(m)	Observations
1853	2152	0:17:20	52	o/c 050°.
		0:18:30	52	Slight slope up to right.
1854	2154	0:19:20	52	o/c 000° (going around mound?).
1855	2155	0:20:20	52	o/c 120°, same seafloor, occasional slope up to right.
1856	2156	0:21:20	54	o/c 030°, 198m (175° T) from GZ.
1857	2157	0:22:30	54	20° slope up to right, same seafloor.
1858	2158	0:23:20	52	o/c 090°, same as above.
1860	2200	0:25:20	51	244m from GZ, slope up to left, in subtle mound area?
1862	2202	0:27:20	52	o/c 080°, slope up to right again.
1863	2203	0:28:20	51	Flat seafloor, occasional Callianassa mounds and burrows.
1864	2204	0:29:20	52	o/c 010°, sloping up to right about 20°, sub stopped as ship seems a long way off, sea urchins grazing algae out of sand along a line; helmet shell picking off stragglers.
1869	2211	0:36:20	51	o/c 030°, start up again, 290m (120° T) from GZ.
1871	2213	0:38:20	52	o/c 330°, slope up to right 215°, sub weaving in and out (around mounds?)

Dive 93 cont.

Fix #	GMT	TV Time	Depth(m)	Observations
1873	2215	0:40:20	52	Ship distant again, sub stop for ? minutes.
1875	2217	0:42:10	52	o/c 000°, sub still weaving in and out, slope up to right.
		0:45:20	220	Flat seafloor (030° T) from GZ.
1877	2221	0:45:40	51	o/c 330°, seafloor flat and featureless, occasional Callianassa mounds and burrows.
1879	2222	0:47:20	52	Going around mound or promontory.
1880	2223	0:48:20	52	o/c 300°, 20° slope up to right.
1881	2224	0:49:10	52	o/c 270°, same type of seafloor.
1882	2225	0:50:20	52	Going around large mound or promontory to right, o/c 320°, slope up to right 15-20°.
1883	2226	0:51:40	51	Log on seafloor.
1886	2229	0:54:10	51	o/c 225°, same type of seafloor.
1888	2231	0:56:10	52	85m (010°) from GZ, o/c 250°, slope 15-20° up to right and down to left.
1890	2233	0:58:10	51	o/c 210°, same type of seafloor, still on slope.
1892	2235	1:00:10		o/c 180°, completed circle, then went 030° up to right.
				END OF DIVE

TV information not very good as there was little to see; seafloor the same all the way around, more large mounds and/or promontories on northern and eastern side.

DIVE #136

OAK Crater
Enewetak (OAK) JD 212
Slater and Halley
Describe control line SW of OAK crater from lagoon to edge of reef.
Used TV/Voice recordings. Dive track #136 not plotted on Plate 13-1.

Fix #	GMT	TV Time	Depth(m)	Observations
		0:00:00	46	Start of dive, many mounds of coral growth.
2188	2229	0:03:30		320-330° will be course; (0:04:00) start traverse.
2189	2230	0:04:30	46	Seafloor silty, muddy sand, some Callianassa burrows and mounds; many 1-2m coral patches, occasional large coral mounds.
2191	2232	0:06:20	43	About 50% sediment and 50% coral cover on mounds.
2192	2233	0:07:20	40	Top (?) of large coral mound.
2193	2234	0:07:20	37	Still moving up slope slowly, lots of coral growth.
2195	2236	0:10:20	30	Algal covered sandy seafloor; o/c 320°.
2196	2237	0:11:20	30	Mainly leafy brown algae (Padina type) and Halimeda.
2197	2238	0:12:20	30	Same as above, scattered coral heads.
2199	2240	0:14:20	27	Sandy, flat, lots of soft algae, algal scum.
2200	2241	0:15:20	24	Same as above.
2201	2242	0:16:20	21	On top of mound with 20° slope on back side.

Dive 136 cont.

Fix #	GMT	TV Time	Depth(m)	Observations
	2243	0:17:20	27	Sandy, flat, lots of soft algae, a few coral.
2202	2244	0:18:20	30	Same as above, Fungia type coral.
2203	2245	0:19:20	30	Starting up steep slope (10-15°) lots of soft algae.
2204	2246	0:20:20	24	Sandy, lots of soft algal plants.
2205	2247	0:21:20	21	Flat area, still same seafloor with algae.
2206	2248	0:22:20	18	o/c 320°, same as above.
2207	2249	0:23:20	20	Flat, lots of soft algal plants.
2209	2251	0:25:20	18	Flat, sandy, no soft algae, occasional small coral heads.
2210	2252	0:26:20	15	Flat, sandy, some soft algae and corals.
2211	2253	0:27:20	14	Same as above.
2212	2254	0:28:20	12	Flat, sandy some soft algae and corals.
2213	2255	0:29:20	12	Same as above, occasional Callianassa mounds and burrows.
2214	2256	0:30:20	14	Brown algae scum, lots of mounds and burrows.
2215	2257	0:31:20	12	Same as above.
2217	2259	0:33:20	12	Same as above.
2218	2300	0:34:16	12	Same sandy, occasional soft algal plants and hard coral.
2219	2301	0:35:20	11	Sand, mounds and burrows (10-20cm high).

Dive 136 cont.

Fix #	GMT	TV Time	Depth(m)	Observations
2220	2303	0:37:20	6	All sand.
2221	2304	0:38:20	6	All sand.
2223	2305	0:39:20	5	All sand, turning around to head back to deeper water.
	2307	0:41:20	6	o/c 90°, all sand.
	2309	0:43:20	9	Sand, algal scum.
2224	2310	0:44:20	12	Paralleling the reef, all sand, mounds and burrows.
2225	2311	0:45:20	12	Sand, soft algal plants.
				END OF DIVE

This area looks a lot different than the crater area; lots of soft algal plants. At about 10m (and below) the slope steepens from 5° to 10° with no rock.

DIVE #137

OAK Crater
Enewetak (OAK) JD 213
Slater and Roddy
Describe control line NE of OAK crater from lagoon to edge of reef.
Used TV/Voice recordings. Dive track #137 not plotted on Plate 13-1.

Fix #	GMT	TV Time	Depth(m)	Observations
2229	0038	0:03:00	47	On bottom, o/c 320°, flat sand seafloor.
2231	0040	0:05:00		Flat sandy seafloor, occasional coral mounds.
2232	0041	0:06:00	46	3-4m high coral mound, then sand.
2233	0042	0:07:00	46	Another 3-4m high mound with corals.
	0043	0:08:00	43	Top of low mound.
2234	0044	0:09:00	43	Flat sandy seafloor, occasional 1m coral mound.
	0045	0:10:00	43	Flat, sandy, no algae or coral.
2235	0046	0:11:00		Flat, sandy, occasional small coral mound.
	0047	0:12:00		Flat, sandy.
2237	0048	0:13:00	46	Flat, sandy.
2239	0050	0:15:00		Flat, sandy, coral covered mound to starboard (3-4m high).
2241	0052	0:17:00	43	o/c 320° flat, sandy, no mounds or burrows.
	0054	0:19:00		Mound to the left (15-18m wide, 5m high).
2243	0055	0:20:00	41	Flat, sandy, more coral heads, small coral mounds.

Dive 137 cont.

Fix #	GMT	TV Time	Depth(m)	Observations
2245	0057	0:22:00	40	Flat, sandy, occasional Callianassa mounds and burrows.
2247	0059	0:24:00	40	o/c 320°, flat, sandy, occasional coral mounds (1-2m high).
2249	0101	0:26:00	40	Same as above, lots of Callianassa mounds and burrows.
2251	0103	0:28:00	37	Same as above, mound on left (15m wide, 5m high).
		0:29:30	34	Same as above, flat, sandy.
2253	0105	0:30:00		Climbing up mound, scattered coral and algal growth.
	0106	0:31:00	34	Flat, sandy, many Callianassa mounds and burrows.
2254	0107	0:32:00	30	Climbing up mound with scattered corals and algae.
2255	0108	0:33:00	29	On top of mound.
2256	0109	0:35:00	27	Large mound on left (30m wide, 10-12m high).
2257	0110	0:37:00	15	Climbing up 30° slope.
2259	0112	0:37:00	15	Climbing up 30° slope, sand covered.
	0113	0:38:00	5	Leveling out, flat, sandy.
2260	0114	0:39:00	3	Turning southwesterly to run along inside of reef.

Dive 137 cont.

Fix #	GMT	TV Time	Depth(m)	Observations
2261	0115	0:40:00	5	All sand, o/c 180°.
2263	0117	0:42:00	6	All sand, o/c 180°, drop off at 8m, stopped.
2264	0119	0:44:15	8	At same position on drop-off, start up again.
2266	0121	0:46:00	9	Running along slope on 9m contour, just below drop off.
2270	0125	0:50:00	9	Same as above (ship seems far away).
2272	0127	0:52:00	9	Same as above, all sand.
2274	0129	0:54:00	9	Same as above, ship still far away.
2276	0131	0:46:00	9	Same as above, running along sand slope just below drop off.
2278	0133	0:58:00	9	Same as above, rare (up to 1m) coral patches.
2280	0135	1:60:00	9	Same as above.
2281	0136	1:01:00	9	Starting to see more rubble, coral, and soft algal.
2284	0139	1:04:00	9	Flat now at 9m, sand, rubble (ship still far away).
2285	0140	1:05:00	9	Sub track turning to west at 9m, gravel.
2288	0142	1:07:00	9	On 9m terrace, o/c 270°, lots of rubble.
2290	0144	1:09:00	9	At tidal buoy.

Dive 137 cont.

Fix #	GMT	TV Time	Depth(m)	Observations
2292	0146	1:11:00	5	On cliffs, fractures in rock.
				END OF DIVE

This dive area differed greatly from other control dive SW of crater. This area looked more like the crater area with a steep slope up to reef, but no rock outcrops. Navigation not accurate after fix 2259 as ship couldn't follow sub into shallow water.

DIVE #138

OAK Crater
Enewetak (OAK) JD 213
Slater and Roddy
Describe features from OAK crater to reef and examine other features of interest. Used TV/Voice recordings.

Fix #	GMT	TV Time	Depth(m)	Observations
2293	0239	1:12:00	40	On bottom, o/c 270°, ±300m from GZ.
2294	0240	1:13:00	37	Flat, sandy seafloor, many Callianassa mounds and burrows.
	0241	1:14:00		Going up 20° slope, ridge.
2295	0242	1:15:00	26	On top of ridge, stopped for awhile, camera off.
2297	0245	1:16:30	26	Large, 1-3m angular blocks, sitting at base of crater slope.
2299	0247	1:18:30	26	Same place, ±460m from GZ. (good shark pictures).
2301	0251	1:22:30	26	Same place, starting up slope.
2302	0253	1:23:30	22	Large blocks on slope (11m at top of cliff 1:25).
2305	0254	1:25:30	10	On top of rock ridge (cliff).
2307	0256	1:27:30	17	Rock rubble on sand slope, o/c 180°.
	0258	1:29:30	23	On flat sand floor, slope to the right, ridge to left.
2308	0300	1:31:30	17	o/c 150°, going up sand slope to top of ridge then south along ridge crest.

Dive 138 cont.

Fix #	GMT	TV Time	Depth(m)	Observations
2310	0302	1:33:30	12	o/c 180° along 6m wide ridge crest.
2311	0303	1:34:30	12	Stopped at south end of ridge crest, then start o/c 140°.
2313	0306	1:37:30	20	Going down 30° slope at angle, mainly sand, some rubble, c/c 100°.
2316	0308	1:39:30	29	o/c 090°, flat sand seafloor, many Callianassa mounds and burrows.
2317	0309	1:40:30	33	Same as above, c/c 080° (camera off).
2319	0311	1:42:30	34	Looking for Ristvet ejecta areas, can not find any, just flat sand with many Callianassa burrows and mounds. Wrong location?
2321	0314	1:45:00	31	Same as above, c/c 270°, camera on and off.
				END OF DIVE

Note: Camera on and off last 10 minutes so can not track sub. Could not find Ristvet's ejecta area. Navigation poor from fix 2301 through 2311.

DIVE #146

OAK Crater
Enewetak (OAK) JD 215
Slater and Shinn
Describe mounds and ridges in OAK crater. Used TV/Voice recordings.

Fix #	GMT	TV Time	Depth(m)	Observations
2356	2230	0:02:30	46	On bottom, mound next to down position; coarse-grained sand covering seafloor.
2357	2231	0:04:00	42	Top of mound, occasional angular blocks.
2358	2233	0:05:30		Still climbing up mound complex, swale in middle, elongated to NE, some rock rubble, Callianassa burrow and mounds common.
2359	2334	0:06:30	38	Top of mound, drops off sharply to south, sediment mound or ridge (not pinnacle reef), sub stopped for awhile, ±300m from GZ.
		0:03:30		o/c 200°, dropping off, several terraces (slump features?).
		0:09:30		Slope up to the right.
M		0:10:30	48	o/c 200°, lots of Callianassa mounds and burrows.
		0:11:30		c/c 180°, starting to rise.
2361	2239	0:12:00		o/c 180°, went over 2m low mound, stopped on south side.
		0:13:00	52	Seems like sediment has filled in around the mounds from the north (or reef side), o/c 180°.

Dive 146 cont.

Fix #	GMT	TV Time	Depth(m)	Observations
2363	2243	0:16:00	50	c/c 160°, coming up to mound, seafloor is sandy, mound is actually a ridge running SE-NW, drop-off on both sides.
2366	2245	0:18:00	45	o/c 160°, on ridge crest, going around ridge.
2367	2246	0:19:00		c/c 175°, seems like a series of ridges (folds in a carpet) trending SE-NW.
2369	2248	0:21:00	43	On barchan-like feature, covered with coarse (maximum 3-4cm) debris; after exploring around it, it looks like a blow-out.
2372	2251	0:24:00		Still on barchan-like feature, coarse material and opening is toward GZ (bearing from GZ is 120°, ±330m).
2374	2253	0:26:00		Still in same area, topography complex and meandering, series of ridges and mounds, o/c 170°.
2376	2255	0:28:00		Base of ridge perpendicular to GZ, steep side away from GZ, sub meandering.
2378	2257	0:30:00		o/c 170°.
2379	2258	0:31:00	43	c/c 280°, sub stopped (330° to GZ, 440m).
2381	2230	0:33:00		o/c 280°, coarse sand, Callianassa mounds and burrows.

Dive 146 cont.

Fix #	GMT	TV Time	Depth(m)	Observations
2382	2302	0:35:00	41	Sub stopped, looking at button corals and burrowing anemones pulling into seafloor. Lots of small debris, coarse sand, sitting on large nose of sediment (about 30m across).
		0:59:00		Start up again, o/c 270°, going down slope.
		1:00:00	48	Series of steps down to crater floor.
2395	2329	1:02:00	48	Callianassa burrows and mounds on flat crater floor.
		1:03:00	51	N-S trending 3m high ridge; o/c 170°.
2396	2331	1:04:00		c/c 270°.
2398	2333	1:06:00	51	o/c 270°, base of large mound, paralleling slope, up slope to subs left of sub (south), runs east-west (might be edge of crater).
2400	2336	1:09:00	52	
2401	2337	1:10:00		Sub swinging around to SW, probably paralleling inner rim of crater, sub meandering in and out of reentrants.
2402	2339	1:12:00		Sub heading westerly on 57m contour.
2403	2340	1:13:00	57	Slope up to left, Callianassa burrows and mounds common, following rim clockwise around GZ.

Dive 146 cont.

Fix #	GMT	TV Time	Depth(m)	Observations
2404	2341	1:14:00		±150m from GZ, heading more northerly.
2407	2344	1:17:00	55	Swinging to NE.
2409	2346	1:19:00	54	Swinging around promontory, heading 000°, flat coarse sand seafloor, slight slope up to left.
2410	2347	1:20:00	57	Some Callianassa mounds and burrows.
2411	2348	1:21:00		Heading NE.
2412	2349	1:22:00	54	Course easterly, sediment coarser than before.
2413	2350	1:23:00	54	Same seafloor.
2415	2352	1:25:00	54	Steep slope up to left, flat seafloor to right.
2417	2354	1:27:00		On log with lion fish.
		1:28:00	52	Heading SE, seafloor sloping down to right.
2418	2356	1:29:00		Have gone nearly around GZ, close to original down position, heading East.
2420	2358	1:31:00	52	Lots of Callianassa mounds and burrows, slope still up to left, finished loop around crater.
2422	0001	1:34:00	51	Lots of Callianassa mounds and burrows.
				END OF DIVE.

Area covered in first part of dive is very interesting. The seafloor is a nearly continuous series of meandering ridges, lopsided mounds, barchan-like features and blow-out like features. Coarse debris might be winnowed material.

DIVE #147

OAK Crater
Enewetak (OAK) JD 215
Slater and Shinn

Describe mound area on lagoon side of OAK crater. Used TV/Voice recordings.

Fix #	GMT	TV Time	Depth(m)	Observations
2424		1:44:00		On the bottom, o/c 160° (actually going closer to 135°).
2425	0125	1:45:30	39	All sand, lots of Callianassa burrows and mounds.
2427	0128		39	Coarse sand in many Halimeda plates.
2428	0130	1:48:00	39	Following along a ridge to the left.
2430	0132	1:50:00	39	c/c 175°, all sand, mounds and burrows, ridge ending.
2431	0133	1:51:00	39	Seafloor sloping down to the right, cutting diagonally across a ridge.
2432	0134	1:52:00	39	Hard to hold 175° as ridges lined up at 135°.
2433	0135	1:53:00	42	All sand slope dipping down to right, lots of Callianassa burrows and mounds.
2434	0136	1:54:00	40	c/c 160°, same seafloor.
2435	0137	1:55:00		All sand.
2436	0138	1:56:00		Slight slope down to right, fairly level seafloor.
2437	0139	1:57:00		Rising up is a mound or ridge, sediment coarsening.
2438	0141	1:59:00	36	On top of large mound, trending SE-NW.

Dive 147 cont.

Fix #	GMT	TV Time	Depth(m)	Observations
2439		2:01:00	37	Sub stopped for 1 minute, then o/c 160°.
2441	0144	2:02:00	39	Flat sandy seafloor, visibility poor in low areas.
2442	0145	2:03:00	42	Starting up mound, north side steep.
2443	0146	2:04:00		Still climbing up mound which is covered with plants and debris.
2444	0147	2:05:00	34	On top of mound, trending SE-NW 150°.
2445	0148	2:06:00	34	On top of mound at other end.
2446	0148:30	2:06:30	34	Continuing o/c 225°, down slope.
2448	0150	2:08:00	39	At bottom of mound, stop sub to look at big burrowing anemone with lots of clown fish.
2452	0154	2:12:00	39	Start up again.
2453	0155	2:13:00		o/c 270°, some rock and debris.
2454	0157	2:15:00	37	Picked up rock sample, o/c 240°.
2456	0158	2:16:00	37	Dropping of scarp, lots of rock and debris.
2457	0200	2:18:00	42	Many mounds in area, undulation topography heading up mound.
2458	0201	2:19:00	29	Going up 45° slope to top of symmetrical mound, slope covered with coral, rocks and plants.

Dive 147 cont.

Fix #	GMT	TV Time	Depth(m)	Observations
2459	0202	2:20:00	29	On top of mound (looks like pinnacle reef).
2461	0204	2:22:00	46	On base of mound, c/c 220°.
2462	0205	2:23:00		Flat, sand floor.
2463	0206	2:24:00	43	Same as above.
2464	0207	2:25:00		Heading up mound again.
2465	0209	2:27:00	33	On top of mound (pinnacle reef).
2466	0210	2:28:00	33	Still on top of mound.
2467	0211	2:29:00	33	Same place, start up on course 215°, c/c 170°, ridge N-S.
2468	0213	2:31:00		Bottom of mound, flat sand floor.
2469	0214	2:32:00	42	Flat sand floor, no relief.
2470	0215	2:33:00		Starting up mound.
2471	0216	2:34:00		Still heading up mound.
2472	0217	2:35:00	34	On top of mound.
2473	0218	2:36:00		o/c 300°.
2474	0219	2:37:00		Flat sandy seafloor, small mound to right.
2475	0221	2:39:00	34	Rock, coral and plants (ship far away). Sub stopped waiting for navigation.
2477	0223	2:41:00	34	Same location, nice rock sitting on seafloor.
2478	0224	2:42:00	34	Same location.
				END OF DIVE

DIVE #162

OAK Crater
Enewetak (OAK)
Slater and Shinn
Describe depressed reef plate ledges on reef side of OAK crater.
Used TV/Voice recordings. Not plotted on Plate 13-1 because navigation was too poor).

Fix #	GMT	TV Time	Depth(m)	Observations
	2320	0:00:00	9	On seafloor.
	2322	0:02:00		Started up across flat sandy seafloor looking for rock, o/c 270°, some large blocks of ejecta on sand.
	2327	0:07:00	6	Next to reef plate exposure, 1m scarp.
	2328	0:08;00		Underway, running along 1m scarp, will take 1 minute fix.
	2329	0:09:00		Stopped for a few minutes.
3081	2337	0:13:00	5	Underway again along intermittent 1m scarp.
3083	2335	0:15:00		Large block to right sitting on sand flat.
3084	2336	0:16:00	6	2m wide boulder sitting on rop of scarp.
	2338	0:18:00		Heading out to deeper water, o/c 135°.
	2339	0:19:00	6	Crossing sand flat.
3086	2340	0:20:00	8	Near edge of drop off, all sand.
	2341	0:21:00	11	Stop to free buoy, sand seafloor at drop-off.
	2343	0:23:00		Start again, o/c 225° on 11m contour.
3089	2345	0:25:00	11	Turning corner.

Dive 162 cont.

Fix #	GMT	TV Time	Depth(m)	Observations
3090	2346	0:26:00	12	
	2348	0:28:00	18	On 18m terrace, navigation lost.
	2349	0:29:00	14	Navigation still off.
3092	2350	0:30:00	12	Stopped.
3094	2352	0:32:00	11	Start again.
3096	2354	0:34:00	12	Lots of ejecta and rubble with plant growth, on sand terrace.
3097	2357	0:37:00	9	Start of a scarp, large block crater side of scarp.
		0:38:00	9	Moving along scarp to right, lots of debris and rubble to left.
3099	2358	0:38:00	9	Next to scarp drop off and chutes of debris coming from above, look like ejecta rays coming up from crater but are probably debris. (Stopped to change TV battery).
		0:02:00	18	On 1m scarp (might not be in place) stopped for fix.
3106	016	0:03:30	18	Another ledge above 18m ledge at about 11m.
		0:06:00	10	On top of flat, fractured rock, ledge just below sub.
		0:07:30		Following 11m scarp, scarp fractured with large and small debris falling off and rolling or sliding down 35-40° sand slope.

Dive 162 cont.

Fix #	GMT	TV Time	Depth(m)	Observations
		0:10:00	9	Still following ledge, rock surface is large and flat but rises gently, up to 6-7m? toward reef.
		0:11:00	9	Rubble now, no rock outcrop.
		0:13:00	8	Sand now, no rock or outcrop.
		0:15:00	12	Large, flat block, 1-2m high, 4-5m wide (slump?)
		0:16:30		Going up and down for awhile.
3120?	0:32?	0:19:00	12	Rock ledge, 1m scarp.
		0:20:00	12	Running along slope, debris tongues common.
		0:21:00	9	Flat slabs of rock (3-4m wide, 20 - 30cm high) lying on sand surface near drop-off.
		0:24:00	12	Mainly sand with some flat rocks slabs as above.
		0:25:00	15	Large slab of rock tilting toward crater, 1m scarp.
		0:27:00	18	Mainly sand with lots of rock debris, filming manta ray doing loops.
		0:30:00	16	1m scarp, not continuous, more like a series of flat blocks 3-4m wide.

Dive 162 cont.

Fix #	GMT	TV Time	Depth(m)	Observations
		0:32:00	18	On 1m scarp, continuous now, flat rock surface above scarp is slanting toward lagoon; lost navigation signals.
		0:35:00		Sub surfaced so navigation could find it.
3124?		0:37:00	18	Sub back on bottom.
		0:39:00	20	Flat rock blocks and debris, going back to up position.
		0:40:00		Sub is back to up position, turning to head SW again.
		0:42:00	20	On flat block and debris, navigation lost sub again.
		0:43:00		Navigation back.
		0:44:00	20	On 1m scarp of rock outcrop, appears to be in place, navigation intermittent.
		0:45:00	17	Flat rock block, but mainly sand, heading along rim in 18m in southerly direction, navigation lost.
		0:46:00	18	All sand seafloor.
		0:47:00	21	Flat rock blocks, not in place, tilting toward lagoon.
		0:49:00	18	Flat rock blocks, not in place, some debris but mainly sand, navigation still lost.

Dive 162 cont.

Fix #	GMT	TV Time	Depth(m)	Observations
		0:50:00	12	Some flat rock blocks, in place?
		0:51:00	17	1m scarp, looks more in place than shallower blocks.
		0:52:00	16	Cruising along 1m scarp which is intermittent (in place?)
		0:53:00	14	Large area of flat rock with 1m scarp.
		0:54:00	12	Back to 11m scarp which sems to be in place.
		0:56:00	11	Running along 1m scarp, fairly continuous.
		0:57:00	11	Near drill site, still following 1m scarp.
		0:58:00	8	Running along 1m scarp, lots of fractures on flat surface, some sand and debris.
		0:59:00	8	Large flat rock area, rippled surface, 1m scarp.
		1:00:00	6	Still on same flat area.
		1:02:00	6	Upturned plate (probably rotated block from slumping).
		1:04:00	8	Sand with loose rock rubble.
		1:05:00	9	Flat sand, some debris.
		1:06:00	9	Heading for deeper water.
		1:09:00	17	Sand slope flattens out at this depth.
		1:10:00		

Dive 162 cont.

Fix #	GMT	TV Time	Depth(m)	Observations
	2:00	1:11:00		Last fix at surface.
				END OF DIVE

New navigator did not give fix numbers, making plotting difficult (R. A. Slater).

DIVE #170

OAK Crater
Enewetak (OAK) JD 215
Slater and Halley
Describe outer edge of inner OAK crater along 40-45m contour.
Used TV/Voice recordings.

Fix #	GMT	TV Time	Depth(m)	Observations
2577?	22:05	0:01:45	43	On bottom, GZ ±400m, all sand, down position, bearing to target 035°.
		0:04:15		Underway, silty-sandy seafloor, occasional Callianassa burrows and mounds.
2578	2208	0:04:45	43	On drop-off; following drop-off, flat to the right and sloping down to the left.
2580	2210	0:06:45	43	Sub zig-zagging around blow-out type feature, heading generally NW.
2581	2211	0:07:45	43	Block of rock and gravel at base and west side of steep slope or ridge running N-S.
2582	2212	0:08:45	43	Small promontory, gravel covered mound, otherwise all sand or sandy silt.
2583	2213	0:09:45	45	Cutting across nose or promontory in NE direction.
2584	2214	0:10:45	45	All sand, on rim or escarpment.
2585	2215	0:11:45	45	Still on escarpment, all sand, another promontory.
2586	2216	0:12:30	45	Still the same.
2587	2217	0:13:30	43	Heading north over promontory or mound right on rim.

Dive 170 cont.

Fix #	GMT	TV Time	Depth(m)	Observations
2588	2218	0:14:30	43	Still running along rim, a 1m block of rock.
2589	2219	0:15:30	43	Ridge, covered with gravel, swinging around to NW.
2590	2220	0:16:30	42	Heading NW along escarment, coarser material on scarp.
2591	2221	0:17:30	40	Along rim, blocks of ejecta (up to fist size) scattered around.
2592	2222	0:18:30		Stopped for 30 seconds, on earlier sample site(?)
2593	2223	0:19:30		Underway again.
2594	2224	0:20:30	37	Series of small ridges or promontories oriented or pointed NW to West.
2595	2225	0:21:30	37	Flat on top of escarpment, slopes downward to left.
2596	2226	0:22:30	37	Drop-off at this point, sub heading back and forth from N to W.
2597	2227	0:23:30		West side of promontory covered with gravel (lots of calcareous algae).
2598	2228	0:24:30	37	Weaving in and out of promontories but staying along escarpment, heading NW.
2599	2229	0:25:30	37	Occasional blocks and cobbles on flat area above escarpment, heading W.

Dive 170 cont.

Fix #	GMT	TV Time	Depth(m)	Observations
2600	2230	0:26:30	37	Large ridge jutting south out into crater.
2601	2231	0:27:30		Same as above, running south along ridge, visibility great now.
2602	2232	0:28:30		Sub stopped for 1 minute.
2603	2233	0:29:30	39	Heading westerly - gravel or coarse debris slopes are facing GZ.
2604	2234	0:30:30	39	Sharp promontory out onto flat crater floor, small promontories are on larger promontories.
2605	2235	0:31:30		Cutting across another N-S trending promontory, 20-30cm debris, mainly all sand with Callianassa burrows and mounds.
2606	2237	0:33:30		Very large southerly pointing promontory, cutting across nose with gravel on top, a few rocks, heading SW.
2608	2239	0:35:30		Still on large promontory, reversing trail to explore mound.
2609	2240	0:36:30	40	On large mound, elongated N-S.
2610	2241	0:37:30		Near top of mound, nearly all sand, some Callianassa burrows and mounds.
2611	2243	0:39:30	42	Mound looks like extension of large ridge running into crater from reef.

Dive 170 cont.

Fix #	GMT	TV Time	Depth(m)	Observations
2613	2245	0:41:30	39	Heading west, back on track, all sand, slope up to right.
2614	2246	0:42:45	40	Sharp steep rise up to right, lots of rock debris, some large, 3-4m blocks (looks like base of reef slope).
2616	2249	0:45:30	39	Heading southeast, on large ridge paralleling reef, (then heading NW to go around ridge).
2617	2250	0:46:30		Over crest of ridge.
2618	2251	0:47:30	36	Still on ridge but back on rim heading SE.
2619	2252	0:48:30		Can see crater floor off to left and below sub.
2620	2253	0:49:30	42	On a NE trending ridge.
2621	2254	0:50:30	43	All sand, some Callianassa burrows and mounds, not much slope.
2622	2255	0:51:30		Down on crater floor but a slight slope up to right, c/c to SW after a one minute stop.
2624	2257	0:53:50		Heading west, mound off to left, all sand.
2626	2259	0:55:30	37	All sand, Callianassa burrows and mounds, c/c to South, flat to right, drops off at left.
2627	2300	0:56:30	37	All sand, slope down to left.
2628	2301	0:57:30	33	Stopped at a 1m angular rock with smaller debris around it.

Dive 170 cont.

Fix #	GMT	TV Time	Depth(m)	Observations
2630	2303	0:59:30	33	Still stopped at rock location.
2631	2304	1:00:30	33	Sampled some of rock, camera off.
2634	2321	1:00:30	33	Started up again, other large rocks in area.
2636	2323	1:02:20	28	Sand with rock debris.
2637	2324	1:03:20		Slope faces east.
2638	2325	1:04:20		In box canyon, heading SE.
2639	2326	1:05:20		All sand, visibility poor.
2640	2327	1:06:20	36	Lots of rock debris on north-trending ridge (?), mainly flat having a hard time keeping on drop-off, heading SE.
2642	2329	1:08:20		Roughly following inner crater wall but not clear.
2643	2330	1:09:20		Same, with occasional Callianassa burrows and mounds.
2644	2331	1:10:10	37	Sub stopped for 1 minute.
2646	2333	1:12:10		Heading SE, debris covered promontory.
2648	2335	1:14:10		All sand, lots of Callianassa burrows and mounds, trying to stay on escarpment but difficult to do so.
2649	2336	1:15:10		Same as above.
2650	2337	1:16:00	39	Heading SE, several mounds in this area.

Dive 170 cont.

Fix #	GMT	TV Time	Depth(m)	Observations
2651	2338	1:17:00	41	Definitely on inner slope again.
2652	2339	1:18:00		Mound to right, lots of solitary corals on sand.
2653	2340	1:19:00		Some rock debris on ridge (barchan shaped), inside small box canyon again.
2654	2341	1:20:00		Still in canyon, all sand, N to NW exposure.
2655	2343:20	1:21:20	42	All sand, slope up to right, heading east.
2656	2343	1:22:00	42	All sand.
2658	2345	1:24:00	42	Blow-outs, barchans or box-canyons common in this area.
2659	2346	1:25:00	42	Rock rubble (up to 15cm) on north facing scarp.
2660	2347	1:25:00	42	Same as above.
2661	2348	1:26:00	42	Large ridge pointing north, rubble on nose.
2662	2349	1:27:00	42	Heading NE around mound or box-canyon again.
2663	2350	1:28:00	42	Flat on right, drops down to left, all sand.
2664	2351	1:29:00	42	Topography more complex, sub weaving in and out, but rim or escarpment is sharp, heading north around ridge.
2665	2352	1:30:00	42	Lots of gravel and debris on north end of ridge.

Dive 170 cont.

Fix #	GMT	TV Time	Depth(m)	Observations
2666	2353	1:31:00	42	Heading east along gravel covered north end of ridge.
2667	2354	1:32:00		Same as above (ship seems far away).
2668	2355	1:33:00		Same as above.
2669	2356	1:34:00	46	Down in crater (?), floor is flatter, Callianassa burrows and mounds.
2670	2357	1:35:00	45	Pinnacle reef covered with rock, sub stopped, some large slabs of rock, 33m on top of pinnacle (ship still far away).
2671	0:00:20	1:38:00	33	Still on pinnacle reef, 2-3m tabular blocks of rock.
2672	0:02:00	1:40:00	45	Still on pinnacle reef, at base.
2675	0:05:30	1:41:30		Heading north to get across sand channel.
2677	0:07:30	1:43:30		Heading NW, all sand in flat channel.
2678	0:08:30	1:44:30	42	Large mound to left, still on sand.
2679	0:09:30	1:45:00		c/c to East, either on mound or rim.
2680	0:11:30	1:47:00		Pinnacle reefs (more cone-shaped with lots of rock and rock debris on sides).
2681	0:12:30	1:47:30		Heading North, large pinnacle to right.

Dive 170 cont.

Fix #	GMT	TV Time	Depth(m)	Observations
2682	0:13:40	1:48:30		Going around large pinnacle reef.
2683	0:14:30	1:49:30		On edge of large mound or reef, heading NE.
2684	0:15:30	1:50:30		Lots of rock debris on slope to right and on top of small (5-10m across) mounds.
2686	0:17:30	1:52:30		Trying to get back to beginning position.
2687	0:18:30	1:53:30		Moving in and out of mounds, slope up to right, all sand.
2688	0:19:30	1:54:30	42	Mainly sand with patches of rock debris.
2689	0:20:30	1:55:30	42	Same as above.
2690	0:21:30	1:56:30	42	Lost sample on surface.
				END OF DIVE

DIVE #356

OAK Crater
Enewetak (OAK)
Slater and Halley
Describe radial SE from center of OAK crater.
Used TV/Voice recordings.

Fix #	GMT	TV Time	Depth(m)	Observations
				Down near center of crater, 60m, o/c 090°, Callianassa mounds and burrows, (about 1 burrow mound/sq m), no fixes.
1	10:25	0:02:30	58	Near base of slope, Callianassa mounds and burrows, 10-20cm relief, fine sediment.
2	10:26	0:03:30		Moving up inner slope (±8°).
3	10:28	0:05:30	53	Edge of terrace on slope, then another steep slope with coarser sediment, still Callianassa mounds and burrows.
4	10:30	0:07:10	47	Top of inner slope, then only a few (±5°) degree slope.
		0:09:00	44	Still moving up gentle slope, sediment the same as before current pushing sub to south, sub heading 090°.
5	10:32	0:09:30	44	Now on flat terrace, actually a series of 15-30m wide terraces with scarps in between.
6	10:34	0:11:45	43	On nose of promontory pointing north, gravel covered.

Dive 356 cont.

Fix #	GMT	TV Time	Depth(m)	Observations
7	10:36	0:13:45	43	Another gravel covered northerly trending promontory, (edge of debris blob?). Sticks of dead coral, live button corals, 30° slope up promontory.
8	10:39	0:17:00	41	Dropped off small scarp, slope up to right.
8		0:18:40	40	Starting up west facing scarp, nose of promontory is to left, several 15-20cm rocks (first seen on this traverse), slope up to right.
9	10:42	0:19:45	37	Slope up to right, on flat terrace.
10	10:44	0:21:45	36	Flat area, relief only a few meters over 30m area, up slope to left.
11	10:46	0:23:30	35	Base of rise, then going up horseshoe shaped feature open to west, top at 34m.
		0:24:30	36	1m deep, 6m wide hole.
12	10:48	0:25:30	34	On top of 20° slope, base at 38m.
13	10:50	0:28:00	33	Top of pinnacle reef(?), living Acropora on top, blocks of rock 32-33m depth on top, 15-20m across pinnacle.
		0:29:00		Dropped back down to 36m off pinnacle, flat sediment floor.
14	10:54	0:31:00	36	Flat sediment floor.

Dive 356 cont.

Fix #	GMT	TV Time	Depth(m)	Observations
				Bouy on taut line, changed for future dives for better accuracy.
				END OF DIVE

DIVE #357A

OAK Crater
Enewetak (OAK)
Slater and Halley
Describe radial SW from center of OAK crater. Used TV/Voice recordings.
Fixes 28-43 are not plotted on Plate 13-1.

Fix #	GMT	TV Time	Depth(m)	Observations
16	1403	0:00:00		On bottom, o/c 180°, 61m, flat.
17	1405	0:02:00	60	o/c 180°, flat seafloor.
18	1407	0:04:00	58	Base of inner slope (about 15°) slope smooth.
19	1409	0:06:00	51	Top of inner slope.
		0:07:30	49	Top of slight rise.
20	1411	0:08:00	49	After this fix sub went down to 50m, then level.
21	1413	0:10:20	49	At base of slope.
22	1415	0:12:30		Hole in seafloor (4m wide, 1m deep) on gentle scarp.
23	1417	0:14:00	43	Near last fix, sediment becoming coarser, heading down slope, then flat (42m).
24	1420	0:17:00	42	Slowly climbing, large rubble covered mound to right, moving up mound about 20° slope.
25	1422	0:19:00	36	Nearing top of large mound or slope.
26	1424	0:21:00	33	Leveling off on broad flat area.
27	1426	0:23:20	32	Level sediment surface, medium grained.
28	1429	0:26:30	31	Slight slope up to right (Buoy ±33m behind sub).

Dive 357A cont.

Fix #	GMT	TV Time	Depth(m)	Observations
29	1432	0:29:00		At base of slope (pinnacle reef).
30	1433	0:30:00	23	At top of pinnacle reef, c/c to 090°.
31	1437	0:34:20	32	Heading down slope.
32	1440	0:37:00	41	Level sandy sediment floor.
33	1442	0:39:00	40	3m high pinnacle reef covered with living coral.
34	1444	0:41:00	35	Top of large pinnacle reef, c/c to 045°. Note: Pinnacle reefs have dipping beds from flat corals while mounds in crater have only loose debris.
35	1447	0:44:30	43	Flat lagoon floor just after ridge, very few mounds and burrows.
36	1430	0:47:00	43	Same as above.
37	1452	0:49:00	42	Same as above, but more gravel, small mound on right (5m wide 1m high with rocks).
38	1454	0:51:00	42	Coarser sediment on slightly undulating surface slope is up to left (blob?); scattered rocks.
39	1457	0:54:00	37	Up on top of blob, coarse sediment.
40	1459	0:56:15	36	Starting down slight slope, rubble and rocks common.

Dive 357A cont.

Fix #	GMT	TV Time	Depth(m)	Observations
41	1501	0:58:00	40	Many circular holes, 10-15m across, 2m deep, still lots of rubble.
42	1503	1:00:00	42	5m scarp onto flat floor, 43m at base.
43	1506	1:03:00	42	Flat sandy floor.
				END OF DIVE

DIVE #357B

OAK Crater
Enewetak (OAK)
Slater and Halley
Finish dive #356 on outer portion of Oak crater.
Used TV/Voice recordings. Not plotted on Plate 13-1.

Fix #	GMT	TV Time	Depth(m)	Observations
48	1556	0:00:30	44	o/c 315°, out on lagoon floor, then heading up slope (15°-25°) algal covered.
49	1600	0:04:15	31	On elongated N-S trending mound, then down back of mound, 36m on flat.
50	1602	0:06:00	37	Callianassa mounds and burrows on broad flat area.
51	1604	0:08:00		END OF DIVE.

DIVE #358

OAK Crater
Enewetak (OAK)
Slater and Halley
Describe mounds west of center of OAK crater.
Used Voice recordings (no TV).

Fix #	GMT	TV Time	Depth(m)	Observations
				Down position (60m) under drill ship, flat seafloor.
53	0943		49	Upper rim of inner slope, one knot current.
54	0950		46	Mound (21m wide at base), rubble on west end top of mound 42m, base at 46m.
55-56	0957-1002			Also on same mound
57	1025		35	Top of large smooth hill, base was at 45m.
58	1042		52	Back at upper rim of inner slope
59	1048		45	Mound on terrace, (10m wide, 2m high), top at 45m.
60-61	1051-1052			Same mound, sample #4 from top of mound.
62	1112		39	Top of ridge/mound, base at 43m, elongate E-W, gentle slope toward the East.
63	1118			Promontory on flat terrace surface.
				END OF DIVE.

DIVE #359

OAK Crater
Enewetak (OAK)
Slater-Halley
Describe mounds north of center of OAK crater.
Used Voice recording (no TV).

Fix #	GMT	TV Time	Depth(m)	Observations
				Start under drill ship (60m).
65	1351			Base of inner slope, (60m), then started up slope bottom half of slope is smooth, hummocky on top half (54m) small terrace on slope, (48m) top of inner slope, heading 000° flat terrace (48m), then (47m), start up slope at (46m).
66	1359			Promontory (46m), change course to 270°, running along slope up to right, down to left (43m), then swinging around promontory reversed coarse (46m) looking for mounds, turning NE.
67	1413			Ridge (44m), taking sediment sample #7, coarser material on NW side of ridge, no current on seafloor.
68	1423			Same location as Fix 67 (44m), still sampling on top of promontory connected to the NW by ridge; heading 000° promontory about 7-12m across; terrace at (39m) (tape off for awhile).

Dive 359 cont.

Fix #	GMT	TV Time	Depth(m)	Observations
70	1441			Barrel site (37m), took rock sample here, then moved NE to crater wall, up wall to (9m) then back down to base of wall.
71	1456			Elongated (E-W) mound (31m) 15m long, bouy right above sub, heading 210°; (42-43m) large flat sand terrace, sub heading 180°.
72	1512			Mound (16m diameter) coarse gravelly on top (42m on top), sample #6, about 3m high (mound seems to be in same location as one found at fix 129 on earlier dive but descriptions of mounds are different).
73	1514			Same location.
74	1515			Same location, 46m at base of mound, started south again, series of scarps with reverse slopes on terraces around (49m), heading down inner slope.
75	1524		60	On crater floor.
				END OF DIVE

DIVE #360

OAK Crater
Enewetak (OAK)
Slater and Halley

Describe radial NE from center of OAK crater. Used TV/Voice recordings.

Fix #	GMT	TV Time	Depth(m)	Observations
100	0821	0:00:00	60	o/c 045°, on flat crater floor, fine sediment with mounds and burrows.
101	0825	0:03:30	60	o/c 045°, stopped for fix, same seafloor.
102	0827	0:05:30	59	o/c 045°, starting up gradual slope, still many Callianassa mounds and burrows.
		0:06:30		Start up inner slope.
103	0829	0:07:30	58	o/c 045°, heading up inner slope.
		0:08:30		c/c 325°.
104	0831	0:09:30	54	o/c 325°, mid-inner slope.
		0:10:30	48	At top of inner slope c/c 315°.
105	0833	0:12:00	48	Running along upper edge of inner slope.
106	0835	0:13:30	48	Along large 4-5m hole, 2m deep, probable drill hole, c/c 000°, start up at 0:17:00, passing several small scarps around 44-45m.
107	0841	0:19:30	41	Sand, smooth surface, o/c 010°, occasional mounds and burrows.
108	0843	0:21:10	39	Sand, many Callianassa mounds.
109	0845	0:23:00	39	Heading West, then East looking for bouy.

Dive 360 cont.

Fix #	GMT	TV Time	Depth(m)	Observations
110	0847	0:25:30	39	On buoy, but no drill hole, buoy must have drifted West.
111	0849	0:27:20	39	Seafloor still the same.
		0:28:20	39	Starting up slope (about 20°) no rubble.
			32-33	On top of scarp (pulled buoy underwater) stopped at (0:30:00) buoy probably 60m behind the sub.
112	0856	0:34:30	33	Starting up again, o/c 000°, heading up gentle slope.
		0:36:00	31	In horseshoe shaped feature, open to South 1 to 1.5m deep.
113	0858	0:36:30	29	Flat sand floor.
		0:37:30	29	Mound on ridge on right.
114	0900	0:38:30	28	Sand covered ridge on right, sub running east in gulley between ridge and wall.
115	0902:30	0:41:00	28	Reversing course.
116	0904	0:42:30	30	o/c 210°, going down gentle slope.
117	0906	0:44:45	32	Slope starting to drop off more, 10° slope, o/c 180° going down a series of steps, as the sub heads for the crater the slope goes up gradually before falling off steeply.
118	0908	0:47:00	40	Smooth sand terrace, o/c 180°.

Dive 360 cont.

Fix #	GMT	TV Time	Depth(m)	Observations
		0:47:30		Next to buoy again, Buoys 45m apart on surface.
		0:50:00	46	Buoys tangles again, sub stopped at base of scarp.
119	0913	0:51:15	46	Still at same spot, start up at 0:52:30, heading West.
120	0915	0:53:45	45	Running along 45m contour, slope is up to right, flat sand floor to left.
121	0917	0:55:45	44	Mound (about 5-7m wide, 1m high) with coarse sediment at top.
122-24	0920-0950	0:55:00-1:27:00		On mound, taking sediment samples.
125	0950	1:29:20	45	o/c 270°, running along NW-SE trending ridge.
126	0953	1:31:20	42	Running along large mound or ridge, heading SW crossed earlier sub track (mounds 5m wide by 34m long).
127	0955	1:33:40	42	Fix on ridge.
128	0958	1:36:25	42	Running along flat terrace.
129	1001	1:39:20	42	On small mound, 1m high, 7m wide, coarse sediment on top, stopped to sample (fix 130 and 131 here too), good pictures of Halley taking samples.
		1:47:00	42	Starting up again, o/c 135°.

Dive 360 cont.

Fix #	GMT	TV Time	Depth(m)	Observations
132	1010	1:48:20	46	Heading down inner slope.
133	1012	1:50:20	58	Still heading down inner slope.
		1:51:00	59	On crater floor, buoy pulled under.
134	1015	1:53:10	61	On crater floor, buoy straight up.
				END OF DIVE.

DIVE #361

OAK Crater
Enewetak (OAK)
Slater-Henry
Describe mounds southwest of center of OAK crater.
Used Voice recording (no TV).

Fix #	GMT	TV Time	Depth(m)	Observations
135	1351		60	Start of dive on flat crater floor.
136	1355		58	Base of inner slope.
137	1359		49	Upper rim of inner slope, then crossed flat smooth terrace.
138	1408		46	Terrace, then large (16m diameter) mound, base at 45m, top at 39m, sample #10 from top of mound.
139	1429		40	Heading South.
140	1434		45	Small 3m wide mound.
141	1439		43	Another small 3m wide mound, these mounds are actually connected to the slope toward the west.
142	1442		42	Top of large mound.
144	1449		46	Sub sitting in large bowl 17-22m across.
145	1505		33	Secondary crater 7m wide, 2m deep.
				END OF DIVE.

DIVE #362

OAK Crater
(0823-0901)
Enewetak (OAK)
Slater-Martin
Describe mounds northeast of center of OAK crater.
Used Voice recordings (no TV).

Fix #	GMT	TV Time	Depth(m)	Observations
200	0823		60	On bottom of crater, flat seafloor.
201	0827		49	Top of inner slope.
202	0833		46	Elongate E-W mound, coarse sediment on top 30m wide, 3m high.
203	0837		40	Change course to north, the sub went up a series of scarps and terraces between fixes 202 and 203, prominent terraces at 40m and 43m.
204	0843		43	On promontory nose, scarp along promontory runs N-S.
205	0847		46	Changed course to more NE.
206	0854		46	Mound near drop-off.
207	0856			Elongate mound, 30m wide, 3m high.
208	0901		49	Top edge of inner slope.
				END OF DIVE.

TABLE 13-2. -- Research observations of KOA and MIKE crater submersible dives, taken from Video/Voice recordings made during dives in 1984. Plate 13-4 (in pocket) shows Fix Numbers and location for observations. Dive 132 not plotted on Plate 13-4. TV/Voice recordings of all dives available.

DIVE #	FIX TIMES	FIX #	DATE	OBSERVERS
87	21:00-21:50	1713-1756	7/19/84	SL-FO
88	22:34-23:04	1757-1780	7/19/84	PR-FO
89	23:47-00:11	1781-1803	7/19/84	PR-HA
90	00:10-01:14	1804-1839	7/19/84	SL-FO
102	22:23-23:44	2450-2520	7/21/84	SL-SH
107	20:59-22:40	2523-2629	7/22/84	SL-HA
108	23:20-23:40	2630-2650	7/22/84	SL-HA
109	01:17-02:46	2651-2738	7/22/84	SL-RO
113	03:04-03:40	2813-2900	7/24/84	SL-RO
121	22:28-23:46	2901-2972	7/26/84	SL-HA
122	01:28-02:53	2973-3051	7/26/84	SL-HA
123	03:46-04:12	3052-3077	7/26/84	SL-HA
129	22:08-22:46	1929-1965	7/28/84	SL-RO
130	23:37-00:40	1966-2017	7/28/84	SL-RO
131	01:38-02:28	2018-2060	7/28/84	SL-RO
132	03:40-03:55	2062-2076	7/28/84	SL-RO
135	01:58-02:42	2148-2186	7/29/84	PR-RO

OBSERVERS

FO - David W. Folger
HA - Robert B. Halley
PR - Douglas N. Privitt
RO - David J. Roddy
SH - Eugene A. Shinn
SL - Richard A. Slater

SUBMERSIBLE PILOTS

Richard A. Slater, Pilot/Geologist
Douglas N. Privitt, Pilot

DIVE #87

KOA and MIKE Craters
Enewetak (KOA)
Slater and Folger
Describe KOA crater baseline traverse from MIKE through KOA GZ.
Used TV/Voice recordings.

Fix #	GMT	TV Time	Depth(m)	Observations
		0:00:00	27	Start of dive in MIKE crater, fine sandy seafloor, mounds and burrows; o/c 060°, light gray sediment.
		0:04:00		Sub stopped.
		0:08:30		Started up again o/c 060°.
1712	2059	0:09:00	27	Hummocky, silty fine sand covered seafloor, mounds and burrows c/c 050°.
1714	2101	0:10:30	27	Same as above, many mounds 5-10cm high, some 30cm high.
1716	2103	0:12:30	27	c/c 045°, Same as above, sediment white to light gray color.
1718	2106	0:15:30	27	o/c 035°, Same as above.
1720	2108	0:17:30	27	Same as above.
1722	2110	0:19:30	27	c/c 040°, Same as above, very hummocky.
1724	2112	0:21:30	27	o/c 040°, Same as above.
1726	2114	0:23:30	27	o/c 040°, Same as above.
1728	2117	0:26:30	27	At base of slope (30-40°), blocks of rock on slope--slope strikes N-S, gravel-sized rubble.
1729	2119	0:28:30	17	On top of slope, flat area 17m on top, covered with coral, rubble and sand (and coral debris).

Dive 87 cont.

Fix #	GMT	TV Time	Depth(m)	Observations
1731	2121	0:30:30	17	Still on top of slope.
1732	2122	0:31:30	17	Top of drop-off, steep slope (45°), o/c 040°, perpendicular to slope.
1733	2123	0:32:30	24	Base of slope, flat, silty fine sand sediment (terrace?).
1735	2125	0:34:30	24	On debris (mainly coral) covered area, numerous living coral, steep dropoff to left.
1737	2127	0:36:30	24	Slope is up to right, down to left, still abundant coral and rubble, Halimeda common.
1739	2129	0:38:30	24	Flat sandy area (terrace?), then dropoff to 27m, hummocky, silty, sandy seafloor.
1741	2131	0:40:30	27	Flat hummocky, silty, sandy seafloor.
1743	2133	0:42:30	30	Flat hummocky (up to 30cm relief) seafloor mounds and burrows.
		0:43:00	33	Same as above.
1744	2136	0:44:45	33	Same as above.
1745	2136	0:45:30	33	Same as above, visibility 0.5m.
1747	2138	0:47:30	33	Same as above.
1749	2140	0:49:30	32	Same as above.
1750	2141	0:50:30	30	Same as above, o/c 040°.
1751	2143	0:52:30	29	Same as above.
1753	2145	0:54:20	26	Same as above.

Dive 87 cont.

Fix #	GMT	TV Time	Depth(m)	Observations
		0:55:00		Start up slope.
1754	2147	0:56:20	23	Flat again (terrace?), hummocky, mounds and burrows.
1755	2148	0:57:20	21	Slight slope, seafloor the same.
		0:58:00	18	Same as above.
1756	2150	0:58:30	17	Cannot obtain more fixes.
		(0:59:30)	15	Slope 15-20°, o/c 040°.
		(1:00:00)	12	Sand and rubble.
		(1:00:30)		Rising up to surface along modern prograding slope.
				END OF DIVE

DIVE #88

KOA Crater
Enewetak (KOA)
Privitt-Folger
Describe KOA crater traverse perpendicular to baseline through GZ.
Used TV/Voice recordings.

Fix #	GMT	TV Time	Depth(m)	Observations
		(1:02:30)	6	On bottom, 20° slope, running up slope then will reverse course, living corals.
		(1:06:00)		Turning around, start of traverse, can't get navigaion fix yet, o/c 140°, heading down 15° slope.
1757	2234	1:07:30	11	Sandy slope (sub stopped until 1:08:30)
		1:09:30	14	1-2m blocks on right.
1758	2237	1:10:30	15	Going up over ridge of coral and rubble.
1759	2239	1:11:45	18	At edge of dropoff, sandslope 45°, o/c 140°.
1761	2241	1:13:30	24	On flat sediment covered seafloor, mounds and burrows up to 30cm high.
1763	2244	1:16:30	26	Same as above, visibility 1-2', c/c 150° at 1:17:30.
1765	2246	1:18:30	27	Same as above, c/c 140° at 1:20:30.
1767	2248	1:20:45		Same as above, c/c 130° at 1:22:00.
1769	2250	1:22:45	33	Same as above, c/c 120° at 1:24:00.
1771	2252	1:24:45	33	Same as above, Callianassa mounds and burrows, 30cm relief on microtopography, sediment color off-white to light tan.

Dive 88 cont.

Fix #	GMT	TV Time	Depth(m)	Observations
1773	2254	1:26:45	30	Same as above, starting up slight slope (10°).
1775	2257	1:30:00	24	Same as above, fine silty sand, 10° slope.
1777	2259	1:31:30	23	Same as above.
1778	2301	1:32:30		Going up small scarp.
1779	2302	1:34:45	14	Flat, sandy, hummocky seafloor (terrace?).
1780	2304	1:36:30	16	Last fix, staying o/c 120°, starting to rise up slope.
		1:38:00	8	Coral, rocks, rubble.
		1:39:00		Modern prograding slope, sand, rubble.
				END OF DIVE.

DIVE #89

KOA Crater
Enewetak (KOA)
Privatt-Halley
Describe KOA crater diagonal transect through GZ.
Used TV/Voice recordings.

Fix #	GMT	TV Time	Depth(m)	Observations
		01:45-01:54		Headed up slope in order to get to starting point for traverse.
		1:54:00	3	Coarse sand and gravel, recent sediment on flat seafloor, zeroed TV camera.
		0:00:00	3	Start traverse, heading down 30° recent sand slope.
		0:01:00	15	Level hummocky seafloor, sandy (sub stopped at 01:30).
1781	2347	0:02:30	15	Start up again, across slightly slope to flat, but hummocky seafloor.
1782	2348	0:03:30	18	Mounds and burrows, about 30cm relief maximum.
1783	2349	0:04:30	23	Heading down slope.
1784	2350	0:05:30	26	Leveling off, Callianassa mounds and burrows, 30cm relief maximum c/c 175°.
1785	2351	0:06:30	27	Flat hummocky seafloor of silty fine carbonate sand, many Callianassa mounds and burrows, 30cm micro-relief.
1786	2352	0:07:30		Same as above, c/c 165°.
1787	2353	0:08:30		Same as above.
		0:10:00	32	Dropping downslope into deeper water.

Dive 89 cont.

Fix #	GMT	TV Time	Depth(m)	Observations
1789	2356	0:11:30	33	Same seafloor as at fix 1785, visibility 1m.
1791	2358	0:13:30	33	Same as above, close to GZ.
		0:15:00		c/c 170°.
1793	0001	0:16:30	33	Same as above.
1795	0003	0:18:30		Same as above.
1797	0005	0:20:30	27	Same as above, c/c 175°.
1800	0008	0:23:30	24	Same as above, visibility 2-3m.
		0:24:00	23	
		0:25:00		Moving along slope and diagonally down to right.
1802	0011	0:26:30		Sandy sediment with algal growth on surface.
		0:27:10	14	No more navigation fixes.
		0:29:00		Coral rubble coarse sand, scattered live coral, gentle (5-10°) slope up to left.
				END OF DIVE

DIVE #90

KOA Crater
Enewetak (KOA)
Slater-Folger
Describe KOA crater diagonal transect through GZ.
Used TV/Voice recordings.

Fix #	GMT	TV Time	Depth(m)	Observations
		0:00:00		Sub on seafloor.
		0:01:00	9	Start traverse, rubble-covered, o/c 100°, scattered living corals, some blocks are boulder size, carbonate sand.
		0:03:00	12	Mainly carbonate sand, hummocky.
1804	0040:30	0:04:30	14	Some coral rubble but mainly carbonate sand.
		0:05:30		Heading down slope, 21m at bottom.
		0:06:30	21	c/c 125°, silty sand, hummocky seafloor Callianassa mounds and burrows.
1805	0043	0:07:10	23	Some living coral and rubble.
1806	0044	0:08:00		Heading up slope, rubble-covered terrace.
1807	0045	0:08:30	20	On top of rubble-covered terrace.
1808		0:09:30	24	Down slight slope (about 10°) to flat floor again.
1809	0047	0:10:30	27	Silty sand, Callianassa mounds and burrows, about 30cm maximum relief.
		0:11:30	30	Same as above.
1810	0049	0:12:30	33	c/c 100°, Same as above.
1811	0050	0:13:30	33	c/c 095°, Same as above.

Dive 90 cont.

Fix #	GMT	TV Time	Depth(m)	Observations
1813	0052	0:15:30	33	o/c 095°, Same as above, close to GZ.
1815	0054	0:17:30	33	Same as above, c/c 090°.
1817	0056	0:19:30	30	Silty sand, Callianassa mounds (30cm high, 75cm in diam) and burrows, sediment light tan in color.
1819	0058	0:21:30	27	Same as above, visibility 10', c/c 085°.
1820	0059	0:22:30		Stopped to pick up lawn chair dropped overboard from EGABRAG.
1821	0100		24	Started up again, lost elapsed time on TV.
1823	0102		23	Same seafloor as seen at fix 1817, heading up 10° slope at diagonal, sloping down to right, elapsed time back on TV.
1825	0104	0:27:30	21	Mounds and burrows more subdued.
1826	0105	0:28:30	18	Starting up steep slope.
1827-28	0106	0:29:30	15	Blocks of rock, living corals on 15m terrace.
1829	0108	0:31:30	12	Sand-covered terrace.
1830	0109	0:32:30	12	Large patch of staghorn coral, found I-beams, waiting for ship to get closer for navigation fix (they didn't get very close), no further navigation fixes.

Dive 90 cont.

Fix #	GMT	TV Time	Depth(m)	Observations
		0:40:00	9	Up steep sand slope, more large angular blocks of rock and thickets of living staghorn coral.
		0:43:30	9	Starting up modern prograding slope.
		0:44:30	3	
		0:45:00		END OF DIVE.

DIVE #102

KOA Crater
Enewetak (KOA)
Slater and Shinn
Describe 6-m contour of KOA crater. Used TV/Voice recordings.

Fix #	GMT	TV Time	Depth(m)	Observations
2450	2223	0:00:00	6	Start of traverse, all sand.
2452	2225	0:02:00	6	All carbonate, rippled sand, o/c 030°.
2454	2227	0:04:00	7	Cement slab? or rock 1m by 1m, slope off to left, all sand.
2456	2229	0:06:00	8	Rippled carbonate sand, seafloor flattens out at 8m, o/c 030°.
2457	2230	0:07:00	6	Flat seafloor.
2458	2231	0:08:00	6	Coral rubble, angular blocks of rock.
2459	2232	0:08:45	6	Angular blocks of beachrock (?), cables running up slope.
2461	2234	0:11:00	6	o/c 030°, scattered living corals, angular blocks of rock, cables running up slope.
2463	2236	0:13:00	6	Rubble, scattered living corals, carbonate sand.
2465	2238	0:14:00	6	Lots of living coral and carbonate sand, some rock.
2467	2240	0:16:00	6	Mainly rock and coral rubble, promontory drops off to left, sub is running along edge of dropoff, o/c 330°.

Dive 102 cont.

Fix #	GMT	TV Time	Depth(m)	Observations
2469	2242	0:18:00	6	Carbonate sand between fix 2467 and 2469, more living coral, rock and I-beams (railroad rails) at 2469, sub stopped, all rails dipping away from GZ.
2474	2249	0:25:00	6	Sub started traverse again, heading 360°.
2475	2250	0:26:00	6	Mainly carbonate sand, scattered living corals, coral rubble in places (stopped for 1 minute).
2477	2252	0:28:00	7	Mainly carbonate sand, rubble (gravel-size).
2479	2254	0:30:00	6	On slope of 20°, down to left (TV camera off for 1 minute).
2482	2256	0:32:00	6	On modern prograding delta slope (30-35°).
2484	2258	0:33:00	6	Off delta, only carbonate sand now.
2486	2300	0:35:00	6	o/c 300°, all carbonate sand, slope down to left.
2488	2302	0:37:00	6	Coral rubble and carbonate sand, on modern delta again, slope 30-35°.
2490	2304	0:39:00	6	o/c 290°, coral rubble on modern delta.
2491	2305	0:40:00	6	o/c 270°, same as above.
2492	2306	0:41:00	6	Same as above.
2494	2308	0:43:00	6	Carbonate sand, slope 10-15°.

Dive 102 cont.

Fix #	GMT	TV Time	Depth(m)	Observations
2496	2310	0:45:00	6	o/c 300°, carbonate sand, sub running along drop off, flat to the right, slope down to left.
2498	2312	0:47:00	7	Rock slabs outcropping, looks like rim rock.
2499	2313	0:49:00	9	Still on outcropping rock, circling around outcrops.
2501	2324	0:54:00	6	Starting on traverse again.
2503	2327	0:57:00	6	On 10-15° sand slope between fixes 2501-2503, then found more rim rock at #2503, outcrops look like upturned flap, sub circling around outcrop in 9m of water.
2504	2328	0:58:30	9	Fix on upturned slab in 9m of water.
2506	2330	1:00:00	6	On flat, carbonate, sand terrace.
2508	2332	1:02:00	6	Occasional rock slab or block with living coral, mainly carbonate sand.
2509	2333	1:03:00	6	Lots of rock, living coral and rubble.
2510	2334	1:04:00	6	Flat sandy seafloor.
2512	2336	1:06:00	6	Large area of rock, living coral.
2514	2338	1:08:00	7	Mainly rubble, coral debris on flat terrace.

Dive 102 cont.

Fix #	GMT	TV Time	Depth(m)	Observations
2516	2340	1:10:00	6	Flat rim rock outcropping amid rubble and living coral, o/c 180°.
2517	2341	1:11:00	6	Seafloor covered with rubble.
2518	2342	1:12:00	6	Flat sand covered terrace, occasional rock and rubble.
2520	2344	1:14:00	6	END OF DIVE.

DIVE #107

KOA Crater
Enewetak (KOA)
Slater and Halley
Describe 12-m contour of KOA crater. Used TV/Voice recordings.

Fix #	GMT	TV Time	Depth(m)	Observations
		0:00:00	12	On the bottom, waiting for navigation.
2523	2059	0:05:00	12	On rubble area near E-W trending ridge.
2524	2101	0:07:00	12	Still on down position, fixing tape recorder.
2525	2102	0:06:30	12	Setting up sub to start traverse.
2527	2104	0:08:30	12	Started traverse, counter clockwise around crater.
2528	2105	0:10:50	12	Sandy seafloor, algal growth (tuffs and mat) on sand.
2529	2105	0:11:20	12	Promontory pointing to GZ with rubble cover, visibility \3 meters.
2531	2107	0:12:50	12	Rock blocks (up to 1m across) on right, living corals on them.
2532	2108	0:13:50	12	Mainly sand, occasional rock.
2533	2109	0:14:30	12	Same as above.
2534	2110	0:15:30	12	Large staghorn coral patch, o/c 090°.

Dive 107 cont.

Fix #	GMT	TV Time	Depth(m)	Observations
2535	2111	0:16:30	12	Promontory nose pointing towards GZ, rock (up to 1m high, 3m across) and staghorn coral patch on nose, sub heading NE to nose (these promontories are similar but much smaller than the promontories seen in OAK).
2537	2113	0:18:30	12	Crossing 6-7m wide rubble patches (ejecta rays?), cobble to small boulder size rubble, all sand between rays, rubble rays seem to be about 1 minute apart.
2539	2115	0:20:30	12	On prominent promontory, rubble, living coral.
2540	2116	0:21:30	12	Rock outcrop, 3m high, lots of living coral.
2541	2117	0:22:30	12	Still on same outcrop, 15-18m wide, flat on top.
2542	2118	0:23:30	12	Same as above, overhanging in places.
2543	2119	0:24:30	12	Same as above, over 30m long, 3-5m high.
2544	2120	0:25:30	12	Sand covered seafloor, some Callianassa mounds and burrows.
2545	2121	0:26:30	12	15° slope to right, flat to left, silty sand covered seafloor.
2547	2123	0:28:30	12	25° slope to right, ejecta block(?) (6m x 1m x 6m).

Dive 107 cont.

Fix #	GMT	TV Time	Depth(m)	Observations
2548	2124	0:29:30	12	Promontory goes into crater, outcrop, living coral.
2549	2125	0:30:30	12	35° slope, still in ejecta block(?) (±1m) area, living coral.
2560	2127	0:32:30	12	Most rock is above 9m contour with blocks rolling down to 12m, steep sandy slope.
2561	2128	0:33:30	12	32-33° sand slope, flat floor just 3m below sub.
2562	2129	0:34:30	12	Sub heading NE, sand slope.
2563	2130	0:35:30	12	Rubble covered promontory.
2564	2131	0:36:30	12	Sub stopped for awhile, TV off.
2568	2137	0:37:15	12	Sand slope with some scattered rubble (up to cobble size).
2569	2138	0:38:15	12	Starting around another promontory.
2570	2139	0:39:15	12	Sand slope, sub heading easterly.
2572	2141	0:41:15	9	Flat sand seafloor, some small mounds and burrows.
2574	2143	0:43:15	12	Large mound, top at 9m, rock slabs at top, living coral.
2575	2144	0:44:15	12	Still circling mound.

Dive 107 cont.

Fix #	GMT	TV Time	Depth(m)	Observations
2576	2145	0:45:15	12	Back on track, area in general is flat with many mounds or hills (6-9m across), difficult to follow contour.
2578	2147	0:47:15	12	Still in same area, rock and coral on top of most mounds.
2580	2149	0:49:15	12	On promontory, covered with rubble, coral, sub swinging about 90° back and forth through hills.
2582	2151	0:51:15	11	Staghorn coral, rubble, 1m blocks.
2583	2152	0:52:15	12	Same as above.
2584	2153	0:53:15	12	Another promontory or nose, rubble and coral.
2585	2154	0:54:15	12	Rubble and living coral patches, sub heading north.
2587	2156	0:56:15	12	All sand for last minute.
2588	2157	0:57:15	12	All sand, 15° slope up to right, flat to right.
2590	2159	0:59:15	12	Same as above.
2592	2201	01:01:15	12	Modern sand coming down steep (40°) sand slope.
2594	2203	01:03:15	12	Steep 40° sand slope.
2596	2205	01:05:15	12	Steep 45° sand slope, recent dark rubbly sediment.

Dive 107 cont.

Fix #	GMT	TV Time	Depth(m)	Observations
2598	2207	01:07:15	12	Same as above, seems to be a problem with navigation, fix # and time jumping ahead while TV tape time remains constant (TV turned on and off?) Switching to navigation time for the rest of this dive.
2604	2213	1:10:00	12	Sub heading 300°, sand slope flattening out, first rock outcrop for sometime.
2605	2214	1:11:00	12	Promontory again, sub turning 90° in and out flat rock slabs, 2m across.
2606	2215	1:11:30	12	
2607	2216	1:12:15	12	End of large promontory, lots of rock, blocks and rubble, many Tridacna shells.
2611	2220	1:15:00	12	Heading out along another large promontory top at 11m, lots of rock.
2612	2220	1:16:00	12	End of promontory, then flat sandy area.
2614	2223	1:18:00	11	Sub stopped on flat sandy, rubble area, took sample.
2616	2227	1:19:00	11	Sub started up again, flat sandy seafloor with rubble covering outer ends, or promontories, no living coral.
2618	2229	1:21:00	12	Rubble (mainly coral) on promontory distal end.

Dive 107 cont.

Fix #	GMT	TV Time	Depth(m)	Observations
2619	2230	1:22:00	12	On sand slope, some rubble occasionally.
2620	2231	1:23:00	11	On another rubble-covered promontory with living coral.
2621	2232	1:24:00	11	Large rock blocks with coral, mounds, promontories and otherwise confusing topography.
2622	2233	1:25:00	12	On promontory distal end.
2624	2235	1:27:00	12	Sub wandering in and out of mounds and promontories scattered rubble (up to 30cm) on sandy seafloor.
2626	2237	1:29:00	12	Same as above.
2627	2238	1:30:00	12	Same as above.
2629	2240	1:31:00	12	Sand slope.
				END OF DIVE

DIVE #108

KOA Crater
Enewetak (KOA)
Slater and Halley

Describe completion of 6-m contour of KOA crater. Used TV/Voice recordings.

Fix #	GMT	TV Time	Depth(m)	Observations
		01:00:00	11	On bottom, all sand.
2630	2320	0:03:30	9	Flat, sandy seafloor, some cobble-sized rubble.
2632	2322	0:05:30	6	o/c 120°, flat sandy seafloor, scattered gravel.
2634	2324	0:07:30	6	Same as above, occasional 1m blocks of rock.
2635	2325	0:08:30	6	On debris ray (?), c/c 060°.
2636	2326	0:09:30	5	Flat sandy seafloor, occasional rubble.
2638	2328	0:11:30	6	c/c 100°, flat sandy seafloor.
2639	2329	0:12:30	6	Gentle slope up a few degrees to the right and down a few degrees to the left.
2640	2330	0:13:30	6	Some rock 1-2m, mainly sand with some cobbles, o/c 030°.
2642	2332	0:15:30	6	Rocky area, living coral, rock flat on top.
2644	2334	0:17:30	6	Swinging around rocky promontory then on sand slope.
2645	2335	0:18:30	6	On 25° sand slope.
2646	2336	0:19:30	6	Still on sand slope.
2647	2337	0:20:30	6	Flattening out, drops off steeply to left.

Dive 108 cont.

Fix #	GMT	TV Time	Depth(m)	Observations
2648	2338	0:21:30	6	On sand slope.
2650	2340	0:23:30	6	Rock on left for approximately 30m, sub on top of rock ledge, scarp just to left.
				END OF DIVE

DIVE #109

KOA Crater
Enewetak (KOA)
Slater and Roddy
Describe 18-m contour of KOA crater. Used TV/Voice recordings.

Fix #	GMT	TV Time	Depth(m)	Observations
	0:00	0:00:00		On seafloor, heading for 18m contour.
2658	0125	0:01:00	15	All sand.
2659	0126	0:03:00	18	Start traverse, o/c 080°, all sand.
2661	0128	0:05:00	18	10° slope up to right, sand, Callianassa mounds and burrows, o/c 090°.
2663	0130	0:07:00	18	Just crossed over large soft subtle mound, all sand.
2665	0132	0:09:00	18	All sand, Callianassa mounds and burrows, 10° slope up to right, o/c 050°.
2667	0134	0:11:00	18	Same as above, sub is gently moving in and out around subtle lobes or mounds.
2669	0136	0:13:00	18	Same as above.
2670	0137	0:14:00	18	First rock rubble seen up to right (±15m).
2671	0138	0:15:00	18	20-25° sand slope up to right.
2672	0139	0:16:00	18	Same as above, some rock rubble, (lost some TV time as TV was accidently turned off).
2678	0145	0:19:00	18	Found railroad tracks, lots of living coral, rails lined up E-W, bent over to the east or northeast.

Dive 109 cont.

Fix #	GMT	TV Time	Depth(m)	Observations
2680	0147	0:21:00	14	Still on rails.
2681	0148	0:22:00	14	East end of rails. Excellent view of bending of rails.
2682	0150	0:24:00	15	Back on traverse, trying to get deeper.
2685	0153	0:27:00	15	Patch of living coral, some rock rubble.
2687	0155	0:29:00	15	Mound or edge of ridge on right, rock rubble and coral on mound.
2688	0156	0:30:00	18	o/c 350°, all sand, some Callianassa mounds and burrows.
2690	0159	0:33:00	18	o/c 340°, sub lost and wandering for last few minutes.
2693	0201	0:35:30	18	All sand, Callianassa mounds and burrows, slope up to right.
2695	0203	0:37:00	18	Same as above
2698	0205	0:40:00	18	Sub circled in last 2 minutes as visibility very bad.
2700	0208	0:42:00	15	Trying to get back on course, all sand.
2702	0210	0:44:00	17	o/c 330°, just went around large nose or lobe, slope up to right 15-20°.
2704	0212	0:46:00	18	Slope up to right 40°, all sand, o/c 270° nearly flat to the left.
2706	0214	0:48:00	18	Steep sand slope, up to right, some dark gray modern sand and debris coming down slope.

Dive 109 cont.

Fix #	GMT	TV Time	Depth(m)	Observations
2708	0216	0:50:00	17	Out on the distal end of a large promontory.
2710	0218	0:52:00	17	Sand slope up to right o/c 270°.
2711	0219	0:53:00	17	Flat sand floor, featureless.
2712	0220	0:54:00	17	Heading more southerly to get into deeper water.
2714	0222	0:56:00	18	Sand slope up to right, going around promontory.
2715	0223	0:57:00	18	o/c 290°, same as above going in and out around promontories.
2716	0224	0:58:00	18	Slope gentler, all sand, Callianassa mounds and burrows.
2717	0225	0:59:00	18	Going over a promontory nose.
2718	0226	1:00:00	18	All sand, sub stopped for 30 seconds, o/c SW.
2720	0228	1:02:00	18	All sand, o/c 240°, all carbonate sand.
2722	0230	1:04:00	18	o/c 210°, same as above, slope up to right.
2724	0232	1:05:00	18	Same as above.
2725	0233	1:07:00	18	All rock rubble, cobbles (5-10cm) then back in sand.
2726	0234	1:08:00	18	Going around promontory nose.
2727	0235	1:09:00	18	Same as above, another promontory nose, rock rubble and blocks at end. Promontories seem to be about 1 minute apart.

Dive 109 cont.

Fix #	GMT	TV Time	Depth(m)	Observations
2729	0237	1:11:00	18	All sand, again on nose of promontory.
2731	0239	1:13:00	18	All sand, sub swinging back and forth from south to west around promontories.
2732	0240	1:14:00	18	Rock rubble and blocks, living coral.
2733	0241	1:15:00	17	Sub stopped for 0.5 minute.
2735	0243	1:17:00	18	All sand, slope up to right.
2737	0245	1:19:00	18	Sub stopped, visibility very poor, aborted dive.
				END OF DIVE

DIVE #113

KOA Crater
Enewetak (KOA)
Slater and Roddy

Describe rails and 24-m contour in KOA crater. Used TV/Voice recordings.

Fix #	GMT	TV Time	Depth(m)	Observations
	0:00	0:00:00		On the seafloor by rails, rails 2m apart, bent toward E-NE (030°).
		0:05:00		Heading back along rails (210°).
2814	0307	0:06:45	24	At deep end of rails, sub running 030°.
2816	0309	0:08:00	24	All sand, some Callianassa mounds and burrows, visibility poor.
2818	0311	0:10:00	27	Same as above, slight slope up to right, o/c 000°.
2820	0313	0:12:00	26	Same as above.
2821	0314	0:13:00	24	Same as above.
2822	0315	0:14:00	24	Fine silty carbonate sand, hummocky seafloor, with 5-15cm relief from Callianassa mounds and burrows.
2824	0317	0:16:00	25	Same as above, visibility only 1-2'.
2825	0318	0:17:00	26	Same as above, o/c 000°.
2826	0319	0:18:00	24	Same as above, no promontories or noses.
2828	0321	0:20:00	24	Slope still up to the right, going around big mound or promontory, rubble.
2830	0322	0:22:00	24	Same as description at fix 2822, o/c 325°.

Dive 113 cont.

Fix #	GMT	TV Time	Depth(m)	Observations
2832	0324	0:23:00	23	Same as above.
2833	0325	0:24:00	23	Heading around promontory, rubble on end.
2835	0327	0:26:00	24	All fine sand, Callianassa mounds and burrows o/c 270°.
2837	0329	0:28:00	24	Same as above, o/c 310°.
2839	0331	0:30:00	24	Fine silty carbonate sand, hummocky seafloor with 5-15cm relief from Callianassa mounds and burrows, o/c 270°, visibility very poor, TV pictures very poor, slight slope up to right.
2841	0333	0:32:00	24	Same as above, going around small promontory just before and after this fix, slope about 20°.
2842	0334	0:33:00	24	End of promontory, rubble.
2843	0335	0:34:00	23	Same seafloor as around fix 2839, o/c 270°.
2844	0336	0:35:00	24	Same as above, slight slope up to right.
2845	0337	0:36:00	24	Same as above, o/c 210°.
2846	0338	0:38:00	24	Same as above.
2847	0340	0:39:00	24	Same as above, o/c 180°.
2848	0341	0:40:00	24	Same as above.

Dive 113 cont.

Fix #	GMT	TV Time	Depth(m)	Observations
				Promontories have slightly steeper slopes and rubble (mainly coral and shells) around their noses (distal ends).
2851	0343	0:42:00	24	Same as above, going around promontory.
2853	0345	0:44:00	24	Same as above, o/c 220°.
2855	0347	0:46:00	24	Seafloor, same as above.
2856	0348	0:47:00	24	Seafloor confusing, sub swinging easterly.
2857	0349	0:48:00	24	At end of large promontory.
2858	0350	0:49:00	24	Swinging around another promontory, rubble on nose, swinging from east to west but basically heading south.
2859	0351	0:50:00	23	Keeping slope up to right but topography is confusing.
2861	0353	0:52:00	24	o/c 180°, fine silty carbonate sand, 5-15cm relief from Callianassa mounds and burrows.
2863	0355	0:54:00	24	Same as above.
2865	0411	0:58:00		Navigation buoy lost several minutes ago, retying it on, last several fixes wrong.
2866	0412	0:58:30	24	Large mound or tongue, o/c 180°.
2867	0413	0:59:30	24	Going around another promontory, some rubble on nose.

Dive 113 cont.

Fix #	GMT	TV Time	Depth(m)	Observations
2869	0415	0:01:30	24	o/c 150°, slope up to right approximately 20-25°.
2870	0416	0:02:30	24	o/c 215°, seafloor the same as around fix 2861.
2872	0418	0:04:30	24	Same as above, heading around promontory, fix on nose, rubble on nose.
2874	0420	0:06:30	24	Same as above, some rock blocks on top of promontory fix on nose.
2875	0421	0:07:30	20	On top of mound, drops off all around, sub stopped.
2876	0422	0:08:30	20	Sub started up, o/c 165°.
2877	0423	0:09:30	17	Seafloor flat.
2878	0424	0:10:30	18	o/c 160°, scarp, then flat, scarp.
2879	0425	0:11:30		
2880	0426	0:12:30	21	Fine silty sand with rubble, slight slope up to right.
2881	0427	0:13:30		Crossed submarine track.00,1050
2882	0428	0:14:30	21	Seafloor the same as around fix 2861.
2884	0430	0:16:30	24	Rubble, living coral, blocks of rock.
2885	0431	0:17:30	24	Rubble, cobbles, boulders, o/c 270°.
2886	0432	0:18:30	24	Large blocks of rocks up to 1m across.
2887	0433	0:19:30	24	Same as above.

Dive 113 cont.

Fix #	GMT	TV Time	Depth(m)	Observations
2888	0435	1:21:30	24	Same area, sub probably crossed over into MIKE crater.
				END OF DIVE.

DIVE #121

KOA Crater
Enewetak (KOA)
Slater and Halley
Describe completion of 18-m contour and do 24-m contour of KOA crater.
Used TV/Voice recordings.
Note: (Fixes 2901-2944 REPEAT DIVE #113)

Fix #	GMT	TV Time	Depth(m)	Observations
		0:03:07	23	On the seafloor, will move up to 18m. contour.
2901	2228	0:17:30	18	Fine silty carbonate sand, hummocky seafloor with 5-15cm relief from Callianassa mounds.
2903	2230	0:09:30	18	Same as above, seafloor quite flat.
2905	2232	0:11:30	18	Same as above, sub stopped on promontory, rubble, TV out of focus.
2907	2234	0:13:30	18	TV still out of order, then TV ok.
2908	2235	0:14:30	17	Slight slope up to right, seafloor the same.
2909	2237	0:16:30	18	Fine silty carbonate sand, hummocky seafloor with 5-15cm relief from Callianassa mounds, seafloor flat.
2911	2239	0:18:30	18	Same as above.
2913	2241	0:21:30	17	Same as above, very good TV pictures.
2914	2242	0:22:00	17	Completed 18m contour, moving downslope to 24-m contour to complete that contour.
2915	2248	0:27:00	24	Start 24-m contour, slight slope up to left o/c 110°.

Dive 121 cont.

Fix #	GMT	TV Time	Depth(m)	Observations
2916	2250	0:29:30	24	Same as above.
2918	2252	0:31:30	24	Same seafloor as around fix 2914, sub stopped for 1 minute.
2920	2254	0:33:30	25	Same as above, visibility very poor.
2922	2256	0:35:30	24	Same as above.
2924	2258	0:37:30	24	Same as above, slight slope up to left.
2926	2300	0:39:30	24	Same as above, o/c 090°.
2928	2302	0:41:40	25	Same as above.
2930	2304	0:43:30	24	Same as above.
2932	2306	0:45:30	23	Fine silty carbonate sand, hummocky seafloor, with 5-15cm relief from Callianassa mounds, seafloor sloping gently up to left.
2934	2308	0:47:30	22	Same as above, sub stopped for 1 minute.
2936	2310	0:49:30	24	Seafloor the same, just went over large nose or mound.
2938	2312	0:51:30	25	Same as above, visibility poor, then clears, then poor again.
2940	2314	0:53:30	24	Same as above, o/c 180°.
2941	2315	0:54:30	24	Heading around a promontory with rubble near nose.
2942	2316	0:55:30	24	Right on promontory nose, swinging back to 180°.

Dive 121 cont.

Fix #	GMT	TV Time	Depth(m)	Observations
2944	2318	0:57:30	23	Fine silty carbonate sand, hummocky seafloor with 5-15cm relief from Callianassa mounds, seafloor slightly up to left, o/c 180°.
2946	2320	0:59:30	23	Same as above, starting around promontory, o/c 270°.
2948	2322	1:01:30	22	Same as above, cutting across nose of promontory.
2950	2324	1:03:30	24	Same as above, crossed over small promontory just before fix, slope steepening to 30°.
2951	2325	1:04:30	24	Same as above, found 9-12cm cable or pipe looped up about 1m above the seafloor, trending N-W, exposed for 3-4m.
2953	2327	1:06:30	24	At same point.
2954	2328	1:07:30	24	Started traverse again.
2955	2329	1:08:10	24	Seafloor the same as fix 2944.
2957	2331	1:10:10	24	Same as above, o/c 270°.
2959	2333	1:12:10	24	Same as above.
2961	2335	1:14:10	23	Same as above.
2962	2336	1:15:10	24	Same as above, slope about 20° up to left.
2964	2338	1:17:10	24	Same as above, o/c 315°.

Dive 121 cont.

Fix #	GMT	TV Time	Depth(m)	Observations
2966	2340	1:19:10	24	Same as above, flattening out, some gravel now, sub swinging in and out.
2968	2342	1:21:10	24	Same as above, more gravel (biologic debris).
2969	2343	1:22:10	23	Same as above, sub weaving in and out from SE to West.
2970	2344	1:23:10	24	Same as above, o/c 135°.
2972	2346	1:25:10	24	Same as above.
				END OF DIVE.

DIVE #122

MIKE Crater
Enewetak (MIKE)
Slater and Halley
Describe 11-m contour of MIKE crater. Used TV/Voice recordings.

Fix #	GMT	TV Time	Depth(m)	Observations
		0:01:50		On the seafloor, using wide-angle lens on TV.
2973	0128	0:02:00	11	o/c 340°, started up at 01:30.
2975	0130	0:04:00	11	Fine silty carbonate sand, flat seafloor.
2977	0132	0:06:00		Same as above, slight slope up to left, c/c 270°.
2978	0133	0:07:00		Scattered rock and living corals, cobble-size rubble, c/c 340°.
2980	0136	0:10:00	3	Scattered rocks, living corals, rubble, sub trying to find MIKE crater, c/c 220°.
2983	0140	0:14:00	3	Scattered rocks, gravel.
2985	0145	0:19:00	4	Gravel of carbonate debris, sand, o/c 220°.
2987	0147	0:21:00	6	Starting down slope to find start of traverse.
2988	0148	0:22:00	11	Start of traverse, all sand.
2990	0150	0:24:00	11	o/c 240°, fine silty carbonate sand, little micro relief, slight slope (5°) up to right, o/c 270°.
2992	0152	0:26:00	11	Same as above, o/c 235°.
2994	0154	0:28:00	11	Same as above, o/c 270°.

Dive 122 cont.

Fix #	GMT	TV Time	Depth(m)	Observations
2996	0156	0:30:00	11	Same as above, swinging around promontory, gravel.
2998	0158	0:32:00	11	Another promontory covered with rock rubble and gravel.
2999	0159	0:33:00	11	Modern sand delta from reef, some rubble.
3001	0201	0:35:00	11	Same as above, stopped to pick up Helmet shell.
3005	0205	0:38:00	10	Same as above, more cobble and boulder-size debris.
3007	0207	0:40:00	11	Silty fine carbonate sand, little micro relief, slight slope up to right.
3009	0209	0:42:00	11	Same as above, except some Callianassa mounds, o/c 195°.
3011	0211	0:44:00	11	Same as above, slope a little steeper.
3013	0213	0:46:00	11	Same as above, seafloor flatter again, o/c 180°.
3014	0214	0:47:00	11	Crossing nose of promontory, rubble on nose.
3015	0215	0:48:00	11	Silty fine carbonate sand, slight slope up to right.
3019	0219	0:52:00	11	o/c 180°, same as above.

Dive 122 cont.

Fix #	GMT	TV Time	Depth(m)	Observations
3021	0221	0:54:00	11	Silty fine carbonate sand, slight slope up to right, seems to be a buried terrace at this depth, occasional Callianassa mounds.
3023	0223	0:56:00	11	Same as above.
3025	0225	0:58:00	11	Same as above.
3027	0227	1:00:00	10	Same as above, but much steeper slope with large flat blocks (several meters across) of rocks on top of slope (on a promontory nose).
3028	0228	1:01:00	10	Silty fine carbonate sand, slight slope up to right.
3031	0231	1:04:00	11	Rubble and blocks of rock, rubble is mainly skeletal.
3032	0232	1:05:00	11	Large (several meters across) blocks of rock and rubble.
3034	0234	1:07:00	11	Fine carbonate sand slope with occasional rock, o/c 165°.
3036	0236	1:09:00	11	Crossing a rock-covered promontory nose.
3038	0238	1:11:00	11	Silty fine carbonate sand, slight slope up to right, occasional Callianassa mounds, o/c 120°.
3040	0240	1:13:00	11	Same as above.
3041	0241	1:14:00	11	Crossing promontory, rubble strewn.

Dive 122 cont.

Fix #	GMT	TV Time	Depth(m)	Observations
3042	0242	1:15:00	11	Still gravelly, rubble-covered promontory, rock blocks.
3044	0244	1:17:00	11	Same as above.
3046	0246	1:19:00	10	Same as above, some rock blocks 2-3m across.
3048	0248	1:21:00	10	Same as above, living corals on rocks, looks like a back-reef area.
3050	0250	1:23:00	11	Same as above, swinging to south.
3051	0253	1:26:00	11	END OF DIVE.

DIVE #123

MIKE Crater
Enewetak (MIKE)
Slater and Halley
Describe 11-m contour of MIKE crater. Used TV/Voice recordings.

Fix #	GMT	TV Time	Depth(m)	Observations
3052		0:01:00	9	On the seafloor, rubble-covered flat sand seafloor, picked up sample.
3053	0349	0:02:30		Start heading down gentle slope (5°) to 11m.
		0:03:30		Pipe draped on seafloor, sub stopped.
3055	0351	0:04:00		5cm diameter pipe, heading 210°.
3057	0353	0:06:00	11	o/c 000°, Silty fine carbonate sand, flat seafloor.
3058	0354	0:07:00	11	Flat, fractured blocks of rock, living coral on top.
3059	0355	0:08:00	11	Fine carbonate sand, flat seafloor o/c 030-060°.
3061	0357	0:10:00	11	Same as above, some rubble.
3063	0359	0:12:00	11	Same as above, occasional patches of rubble.
3065	0401	0:14:00	11	o/c 030°, crossed wire or cable perpendicular to sub track.
3066	0402	0:15:00	11	o/c 000°, rubble-covered area, hummocky area, low mounds 1-2m across.
3068	0404	0:16:00	11	Fine sand, gentle (5°) slope up to right, o/c 045°.

Dive 123 cont.

Fix #	GMT	TV Time	Depth(m)	Observations
3069	0405	0:17:00	11	All white rippled sand seafloor.
3070	0406	0:19:00	11	o/c 010°, white rippled sand.
3072	0408	0:21:00	11	White carbonate sand, a few living corals.
3074	0409:30	0:22:30	11	On flattened twisted aluminum(?) pipe sticking out of seafloor about 2m, moves easily when pushed by sub.
3076	0411	0:24:00	11	Leaving pipe, o/c 060°.
3077	0412	0:25:00	11	Crossed over into KOA.
				END OF DIVE

DIVE #129

MIKE Crater
Enewetak (MIKE)
Slater and Roddy
Describe N-S diagonal across MIKE crater through GZ.
Used TV/Voice recordings.

Fix #	GMT	TV Time	Depth(m)	Observations
		0:00:00	6	On seafloor, rubble, rock blocks up to 1/2m, o/c 210°.
1928	2207	0:02:00	6	Start traverse.
1929		0:03:00	9	On 10° slope, all carbonate sand.
1930	2209	0:04:00	11	Terrace, o/c 200°, featureless seafloor.
1931	2210	0:05:00	15	On 10° slope, all carbonate sand.
1932	2211	0:06:00	18	o/c 190°, same as above.
1933	2212	0:07:00	21	o/c 190°, sub stopped for 2 minutes, trying to focus TV.
1936	2215	0:10:00	26	Same as above.
1937	2216	0:11:00	26	Same as above.
1938	2217	0:12:00	27	Same as above.
1939	2218	0:13:00	27	Fine silty carbonate sand, hummocky seafloor from Callianassa burrows and mounds, visibility very poor.
1940	2219	0:14:00	27	Same as above, o/c 190°.
1942	2222	0:17:00	27	Same as above, "Land of the Big Worms". Wow.
1944	2224	0:19:00	27	Same as above.
1946	2226	0:21:00	27	Same as above.
1948	2228	0:23:00	27	Same as above, near GZ.

Dive 129 cont.

Fix #	GMT	TV Time	Depth(m)	Observations
1949	2229	0:24:00	27	Same as above, passed GZ, about 21m away.
1950	2230	0:25:00	27	Same as above.
1952	2232	0:27:00	27	Same as above.
1954	2234	0:29:00	27	Same as above, (sub speed avg. 1.1 knot).
1956	2236	0:31:00	27	Same as above.
1958	2238	0:33:00	27	Same as above.
1959	2239	0:34:00	26	Starting up slope, sediment the same.
1960	2240	0:35:00	22	Same as above, c/c 185°.
1961	2241	0:36:00	19	Some rubble and blocks.
1962	2242	0:37:00	17	More rubble and sand, flat area (terrace?).
1963	2243	0:38:00	15	Callianassa mounds of carbonate sand, some rubble.
1964	2244	0:39:00	15	c/c 190°, same as above.
1965	2245	0:40:00	12	All carbonate sand, Callianassa mounds;
		0:41:00	11	rock area, rubble, living coral.
				END OF DIVE.

DIVE #130

MIKE Crater
Enewek (MIKE)
Slater and Roddy
Describe 9-m contour and SW diagonal across MIKE crater from GZ.
Used TV/Voice recordings.

Fix #	GMT	TV Time	Depth(m)	Observations
		0:49:00	27	On seafloor near GZ.
1966	2337	0:50:00	27	Silty fine carbonate sand, hummocky seafloor from 15-20cm high Callianassa mounds, visibility poor.
1967	2341	0:54:30	27	o/c 235°, same as above.
1969	2343	0:56:30	27	c/c 225°, same as above.
1971	2345	0:58:30	27	Same as above.
1973	2347	1:00:30	26	o/c 200°, same as above.
1975	2349	1:02:30	24	Slope starting to rise, c/c 220°, seafloor same as above.
1977	2351	1:04:30	20	Same as above.
1978	2352	1:05:30	18	Gentle slope, featureless plain except for Callianassa mounds.
1979	2353	1:06:30	15	Same as above.
		1:07:00	12	Same as above.
1980	2354	1:07:30	11	Terrace, but seafloor the same.
1981	2355	1:08:30	9	o/c 200°, all sand with small mounds.
1982	2356	1:09:30	9	All rubble, cobbles and boulders, end of transect.
1983	2357	1:10:30	9	o/c 180°, start of 9m contour transect.

Dive 130 cont.

Fix #	GMT	TV Time	Depth(m)	Observations
1984	2358	1:11:30	6	All rubble, sand, rocks, living coral o/c 180°.
1986	0000	1:12:30	3	c/c 160°.
1987	0001	1:14:30	3	Sub stopped to look at fire hose on seafloor.
1990	0004	1:17:30	3	Starting up from fire hose site.
		1:19:30	3	Too shallow for navigation, rock outcrops, fractures, blocks several meters across, extensive area of outcrop over several minutes of travel.
1992	0010	1:24:00	9	Still in rocky area, lots of living coral.
1994	0012	1:25:30	8	Rubble and sand on promontory o/c 060°.
1995	0013	1:26:30	8	Same as above.
1996	0014	1:27:30	7	Same as above, some large rock outcrops with living coral.
1998	0016	1:29:30	6	Rubble, rock outcrops 5-10 m long, living coral, sub swinging from S to E.
2000	0018	1:31:30	8	Sand, rock outcrops, living coral.
2002	0020	1:33:30	9	Mainly all carbonate sand, some rubble o/c 210°.
2004	0022	1:35:30	9	Same as above, o/c 225°, ship far away.

Dive 130 cont.

Fix #	GMT	TV Time	Depth(m)	Observations
2006	0024	1:37:30	8	Same as above, (sub had stopped for a few minutes).
2008	0026	1:39:30	8	I-beam laying on seafloor, otherwise the same, o/c 220°.
2009	0028	1:41:30	7	All sand, Callianassa mounds, thin rubble again, ship having trouble with navigation, sub too shallow.
		1:48:30	7	Lost contact with ship over past 5 minutes, seafloor has been all sand or rubble.
2015	0038	1:51:30	12	All white carbonate sand.
2017	0040	1:53:30	15	END OF DIVE.

DIVE #131

MIKE Crater
Enewetak (MIKE)
Slater and Roddy
Describe NW-SE diagonal across MIKE crater through GZ.
Used TV/Voice recordings.

Fix #	GMT	TV Time	Depth(m)	Observations
		1:54:00	6	On seafloor, mainly rubble, moved into shallow water to start traverse.
		1:57:00	6	o/c 100°, start traverse.
2018	0137	1:57:30	6	Carbonate sand with rubble (mainly shell detritus) in patches.
2020	0139	1:59:30	14	Slope dropping off, then 17m terrace, c/c 115°.
2021	0140	2:00:30	18	Heading down slope, then leveling off, all sand.
2022	0141	2:01:00	18	o/c 115°, silty fine carbonate sand, Callianassa mounds.
2023	0142	2:02:00	21	Same as above, visibility poor now.
2024	0143	2:03:00	24	Same as above.
2026	0145	2:05:00	26	o/c 110°, silty fine carbonate sand, no micro relief.
2027	0146	2:06:00	27	Same as above, again the "Land of the Big Worms". Wow^2.
2028	0147	2:07:00	27	c/c 115°, Same as above, occasional Callianassa mounds.
2030	0149	2:09:00	27	Same as above, c/c 110°.
2032	0151	2:11:00	27	Same as above.
2034	0153	2:13:00	27	Same as above.

Dive 131 cont.

Fix #	GMT	TV Time	Depth(m)	Observations
2035	0154	2:14:00	27	Same as above, ±3m from GZ.
2036	0156	2:16:00	27	Same as above.
2038	0158	2:18:00	27	Same as above (Sub speed about 1.5 knots).
2040	0200	2:20:00	27	Same as above.
2042	0202	2:22:00	27	Same as above.
2043	0203	2:23:00	27	Same as above.
2045	0205	2:25:00	27	Same as above.
2047	0207	2:27:00	27	Same as above.
2048	0208	2:28:00	26	Same as above, (except starting up gentle slope).
		2:28:30	24	Same as above, heading up gentle slope (10°).
		2:29:30	23	Same as above.
2050	0210	2:30:00	21	Same as above.
2051	0211	2:31:00	18	Same as above.
2052	0212	2:32:00	17	Sand, Callianassa mounds, occasional living corals.
2053	0213	2:33:00	15	Same as above.
2054	0214	2:34:00	12	Same as above, but occasional rock blocks.
2056	0216	2:36:00	9	Same as above, on 8-10cm pipe running along seafloor.
2059	0220	2:40:00	9	Same as above.
2060	0227	2:47:00	6	Moved along 3m rock ledge between fixes 2059 and 2060.
				END OF DIVE.

DIVE #132

Engebi Island Area
Enewetak (ENGEBI)
Slater and Roddy
Describe area off Engebi Island. Used TV/Voice recordings.
Not plotted on Plate 13-4.

Fix #	GMT	TV Time	Depth(m)	Observations
		2:53:40	24	o/c 045°, heading toward Engebi.
2062	0340		24	o/c 045°, silty fine carbonate sand with occasional small patch reefs (2m high).
2064	0343	2:59:30	24	o/c 045°, sandy seafloor.
2066	0345	3:01:30	18	On top of larger patch reef.
2067	0345	3:02:15		Still on large patch reef.
2069	0347	3:03:30	21	Back on sandy seafloor, Callianassa burrows common.
2071	0349	3:05:30	20	Lots of man-made debris (pipes, cable, trailer, barrels, boat) o/c 045°.
2072	0351	3:07:30	18	Same as above.
2074	0353	3:09:30	18	Same as above, large trailer with tires.
2075	0354	3:10:30		Large coral patch reef, last fix; sub continued on into shallow water, coral patch reefs, carbonate sand and man-made WWII debris.
				END OF DIVE.

DIVE #135

Enewetak
Privitt-Roddy
Describe saddle area between KOA and MIKE craters.
Used TV/Voice recordings.

Fix #	GMT Time	TV Time	Depth(m)	Description
		0:00:00	8	On the seafloor.
2148	0157	0:01:30	8	Start of traverse, o/c 318°, mainly sand.
2150	0159	0:03:00	9	o/c 320°, rubble of skeletal debris on sand.
2152	0201	0:05:00	11	o/c 320°, mainly carbonate sand featureless seafloor.
2154	0203	0:07:00	20	Same as above.
2156	0205	0:09:00	21	Same as above.
2157	0206	0:10:00	24	Same as above.
2158	0207	0:11:00	24	c/c 315°, Same as above, bottom sloping down.
2159	0208	0:12:00	27	Fine silty carbonate sand, Callianassa mounds common.
2160	0209	0:13:00	26	Starting up steep slope (15°).
2162	0211	0:15:00	18	Sitting on top of saddle, rubble, TV out of focus.
2163	0212	0:16:00	15	Sitting on top of mound, delay by navigation.
2166-67	0219			Fixes on top of mound, left o/c 315°, not much of a drop-off in this direction until near next fix.
2170	0223	0:27:00	27	Fine silty carbonate sand, some Callianassa mounds.

Dive 135 cont.

Fix #	GMT Time	TV Time	Depth(m)	Description
2172	0225	0:29:00	28	Same as above.
2174	0228	0:32:00	26	Starting up slope, very poor visibility.
2176	0230	0:34:00	21	Same as above, o/c 315°.
2178	0233	0:37:00	18	Still all carbonate sand with Callianassa mounds.
2180	0235	0:39:00	18	Same as above.
2182	0237	0:41:00	15	Same as above.
		0:42:30	12	Occasional rock blocks; with living coral.
2184	0240	0:44:00	10	Same as above, mainly sand.
2186	0242	0:46:00	3	Modern sand slope.
				END OF DIVE.

CHAPTER 14:

GEOLOGIC INTERPRETATION OF OAK AND KOA CRATERS

by

Bruce R. Wardlaw[1] and Thomas W. Henry[2]

U.S. Geological Survey

INTRODUCTION

A consistent geologic interpretation of OAK and KOA craters is emerging from the analyses of the broad array of geologic, geophysical, and radiation-chemistry data assembled during the PEACE Program.

OAK and KOA craters were formed over a quarter of a century ago (1958) from two high-yield, near-surface, thermonuclear bursts. OAK crater resulted from a 8.9 megaton weapon exploded from a LCU anchored in about 14 ft of water in Enewetak lagoon, and KOA from a 1.4 megaton device situated in a water tank on an island 7 ft above the H&N datum. Both shots removed large volumes of carbonate rock and sediment. The OAK event removed a large portion of cemented reef plate on its northern side and a larger volume of water and finer-grained lagoon sediments on its other sides. KOA excavated much of the low-lying island on which it was staged and also appreciable volumes of water and lagoon sediments. The ground zeros of both craters today are water-filled; the ground zero of OAK is in 198.7 ft of water, and KOA is in 109.1 ft of water.

The physiographic features of OAK and KOA are readily seen in the side-scan sonar mosaics produced during the Marine Phase of the PEACE Program (see Folger, Robb, and others, 1986). A number of the surficial features in OAK and KOA craters are similar to those found in land-based, high-explosive, low-yield nuclear, and terrestrial impact craters, generally formed in saturated silicate terrains.

Most of the material excavated by the OAK and KOA devices undoubtedly was removed in a matter of seconds by the dynamics of the thermonuclear explosions. However, OAK and KOA craters, as they are observed today, are quite different from the initial craters. The excavational craters were profoundly modified by a set of longer term processes (hours to months) induced by the detonations themselves and by a second set of natural geologic processes acting over much longer periods of time (months to decades). The major factors that modified the excavational craters were shock-induced liquefaction and consolidation, subsequent piping of liquefied materials from depth toward and/or to the surface, consequent subsidence of the region

---

[1] Branch of Paleontology and Stratigraphy, Washington, DC.
[2] Office of Regional Geology, Reston, VA.

adjacent to and beneath the excavational craters, and major and repeated failures of the sidewalls of the initial and subsequent crater. Because these craters were formed in water-saturated environments, some of these processes were more pronounced than they would have been had the devices been detonated in an air-saturated medium. This chapter deals with the effects of sidewall collapse and failure, subsidence, and piping.

Traditional crater terminology does not always adequately apply to the Enewetak craters studied, although the authors and other PEACE Program workers have attempted to minimize the introduction of new terminology.

OAK and KOA craters can be characterized in the subsurface by paleontologic and geologic crater zones that, in turn, can be related to event history. In the following sections, the geologic and paleontologic crater zones are developed and discussed for OAK and KOA craters and for the OAK debris blanket. An analysis of the mixing of the megascopic materials and review of the paleontologic mixing is included as Appendix 14-1. A comprehensive geologic model is developed for both craters, stressing the role of sedimentary package (SP) 3 in the formation of these craters. Initial structural interpretations for MIKE crater are presented from the analysis of the multichannel-seismic lines. The role of piping and injection and loss of crater material into the lagoon are presented also.

CRATER ZONES

The geologic crater is defined by the zone of sonic degradation (ZSD), in which sonic velocities are depressed below expected velocities. Normal or (more correctly) expected sonic velocities are determined from the sonic signature of reference boreholes. On the multichannel-seismic cross sections, the ZSD appears as a "fuzzy" area in which seismic reflectors are not coherent and occur surrounded by an area where coherent reflectors are present but downturned. The ZSD represents units of rock and sediment that are fractured or shattered, mixed, and otherwise distrubed significantly enough to retard the sonic velocities relative to what they were before the nuclear events occurred. All geologic crater zones lie within the ZSD.

The paleontologic zones are developed in Cronin, Brouwers, and others (1986) and in Chapter 11 of this report and are reviewed in Appendix 14-1 of this Chapter. These zones are for the crater (in descending depth): mixed, transition, and unmixed. For the debris blanket, the zones are (in descending depth): mixed, transitional, disturbed, and unmixed. In dividing the mixed zone for both craters, subzones 1 and 2 identified in Appendix 14-1 for KOA crater are combined. The general relationship of paleontologic zones to geologic zones is shown in Table 14-1.

The geologic crater zones are shown in Figure 14-1. The geologic zones encountered at ground zero are as follows:

1. **Alpha 1.** (α_1). -- Mud. Late-stage, fine-grained sedimentation in the central crater area with abundant brown, piped material in OAK.

TABLE 14-1. -- Relationship of paleontologic and geologic zones in the crater and debris blanket.

[PALEONTOLOGIC ZONES]	[GEOLOGIC ZONES]
CRATER GROUND ZERO:	
MIXED 1--Very mixed with mostly upper biostratigraphic zones and piped material	ALPHA 1 (α_1) Mud ALPHA 2 (α_2) Graded sand (distal) and slumps (proximal)
2--Mixed material from most sed. packages 1 and 2 and piped material that decreases in mixing and abundance downward	BETA 1a (β_{1a}) Late-stage collapse rubble
3--Mixed material from mostly lower biostratigraphic zones of crater and sparse piped material	BETA 1b (β_{1b}) Early-stage collapse rubble
TRANSITION	BETA 2 (β_2) Transition sand
UNMIXED	BETA 3 (β_3) Rubble floatstone GAMMA (γ) Fractured, displaced DELTA (δ) Fractured, relatively undisplaced EPSILON (ε) Relatively unfractured, in place
DEBRIS BLANKET:	
MIXED DEBRIS	ALPHA (α) Graded sand BETA (β) Rubble
TRANSITION	
DISTURBED ZONE	DISTURBED ZONE
UNMIXED	GAMMA (γ) Fractured, relatively undisplaced EPSILON (ε) Relatively unfractured, in place

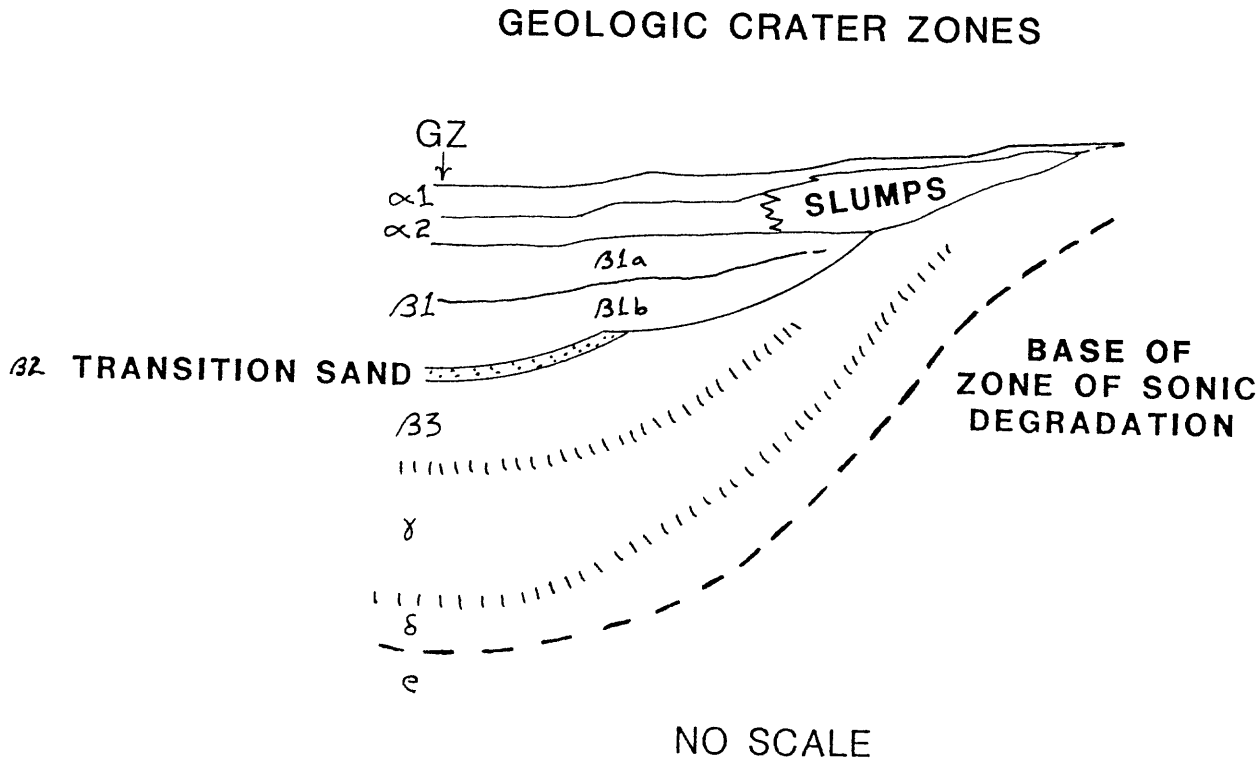

FIGURE 14-1. -- Idealized geologic crater.

2. **Alpha 2.** (α_2). -- Graded sand (distal) and slumps (proximal). Late-stage slope failures and sand turbidite flows containing abundant brown, piped material. (Proximal means near material-source, distal means far from material-source).

3. **Beta 1a.** (β_{1a}) -- Late-stage collapse rubble. This zone involves proximal rubble and distal sand (as in OPZ-18) with granules of rubblized material. The zone contains abundant brown piped material near the top and is transitional from the rubble below and slumps above.

Both alpha 2 and beta 1a show high gamma-ray activity (see fig. 14-20).

4. **Beta 1b.** (β_{1b}) -- Early-stage collapse rubble. Thick rubble bed overlain by sands with sparse brown piped material within the zone.

Both zones beta 1a and beta 1b are less distinct in the central part of the crater supposedly because of mixing primarily due to late-stage piping.

5. **Beta 2.** (β_2) -- Transition sand. Pulverized sand within the transition paleontologic zone. It has limited lateral extent (see figs. 14-4 and 14-5).

6. **Beta 3.** (β_3) -- Rubble floatstone and increasingly less displaced and fractured rock and sediment (**gamma**, γ, and **delta**, δ) that make up the base of the zone of sonic degradation (ZSD).

7. **Epsilon.** (ε) -- In-place, relatively unfractured stratigraphic section.

The geologic zones as encountered in the debris blanket are as follows:

1. **Alpha, undifferentiated.** (α) -- Graded sand. This zone is only found in boreholes OHT-10 and OJT-12 and may be related to a large slump and turbidite flow that breached the debris blanket and flowed into the lagoon (as seen on the OAK enhanced sidescan-sonar image).

2. **Beta, undifferentiated.** (β) -- Rubble. Debris with no brown piped material.

3. **Disturbed zone.** This zone represents slightly altered stratigraphy (see Appendix 14-1).

4. **Delta and Epsilon.** (δ and ε) -- Relatively unaffected stratigraphy.

The depths to various crater zones for the transition and ground-zero boreholes for both OAK and KOA craters are given in Table 14-2.

CRATER FEATURES

Late-Stage Subsidence. -- A comparison of preshot, early postshot, and recent bathymetry (fig. 14-2) indicates that KOA crater is characterized by

TABLE 14-2. -- Depths (bsl) to tops of the crater zones in selected OAK and KOA boreholes. Boreholes selected on completeness of geologic sampling. ZSD = Zone of Sonic Degradation, M1 = Mixed Zone 1, M2 = Mixed Zone 2, M3 = Mixed Zone 3, TZ = Transiton Zone, UM = Unmixed Zone.

OAK GEOLOGIC CRATER ZONES

ZONE	OBZ-4	OPZ-18	OCT-5	OKT-13	OFT-8	OIT-11	OET-7	OHT-10
Alpha 1	198.7	201.9	163.7	164.7	130.8	155.0	-	-
Alpha 2	229.2	-	164.6	165.3	131.1		106.9	137.3
Beta 1a	271.7	246.5	174.1	177.0	139.4	155.1		145.2
Beta 1b	309.1	337.2	244.1	190.8	152.9			
Beta 2	394.9	377.0	-	-	-	-	-	-
Beta 3	415.1	412.3						[190.8]
Gamma	564.2	522.4	346.3	227.3	204.1	171.7	119.5	286.8
ZSD	1138.7	-	863.7	831.7	-	-	-	-

[ ] denotes disturbed zone

OAK PALEONTOLOGIC ZONES

M1	198.7	201.9	163.7	164.7	130.8	155.0	106.9	137.3
M2	~271.7	~246.5	~174.1	~177.0	~139.4	↓	↓	↓
M3	~309.1	~337.2	~244.1	~190.8	~152.9	↓	↓	↓
TZ	378.7	375.9	323.7	220.7	195.8	↓	↓	191.3
UM	418.7	419.9	333.7	244.7	204.8	171.7	119.5 286.8	[213.3]

KOA GEOLOGIC CRATER ZONES

	KBZ-4	KCT-5	KFT-8	KDT-6
Alpha 1	109.1	-	-	-
Alpha 2	137.3	98.9	77.8	56.2
Beta 1a	167.7	120.0	96.5	79.9
Beta 1b	238.5	~153.1	106.0	
Beta 2	247.2	242.5	-	-
Beta 3	266.2	259.9	-	
Gamma	316.2	274.3	153.8	~110.1
ZSD	1101.1	-	-	-

KOA PALEONTOLOGIC ZONES

M1	109.1	98.9	77.8	56.2
M2	162.9	~120.0	96.5	↓
M3	233.1	~148.9	-	↓
TZ	246.6	239.0	106.3	99.8
UM	251.1	254.1	177.1	114.7

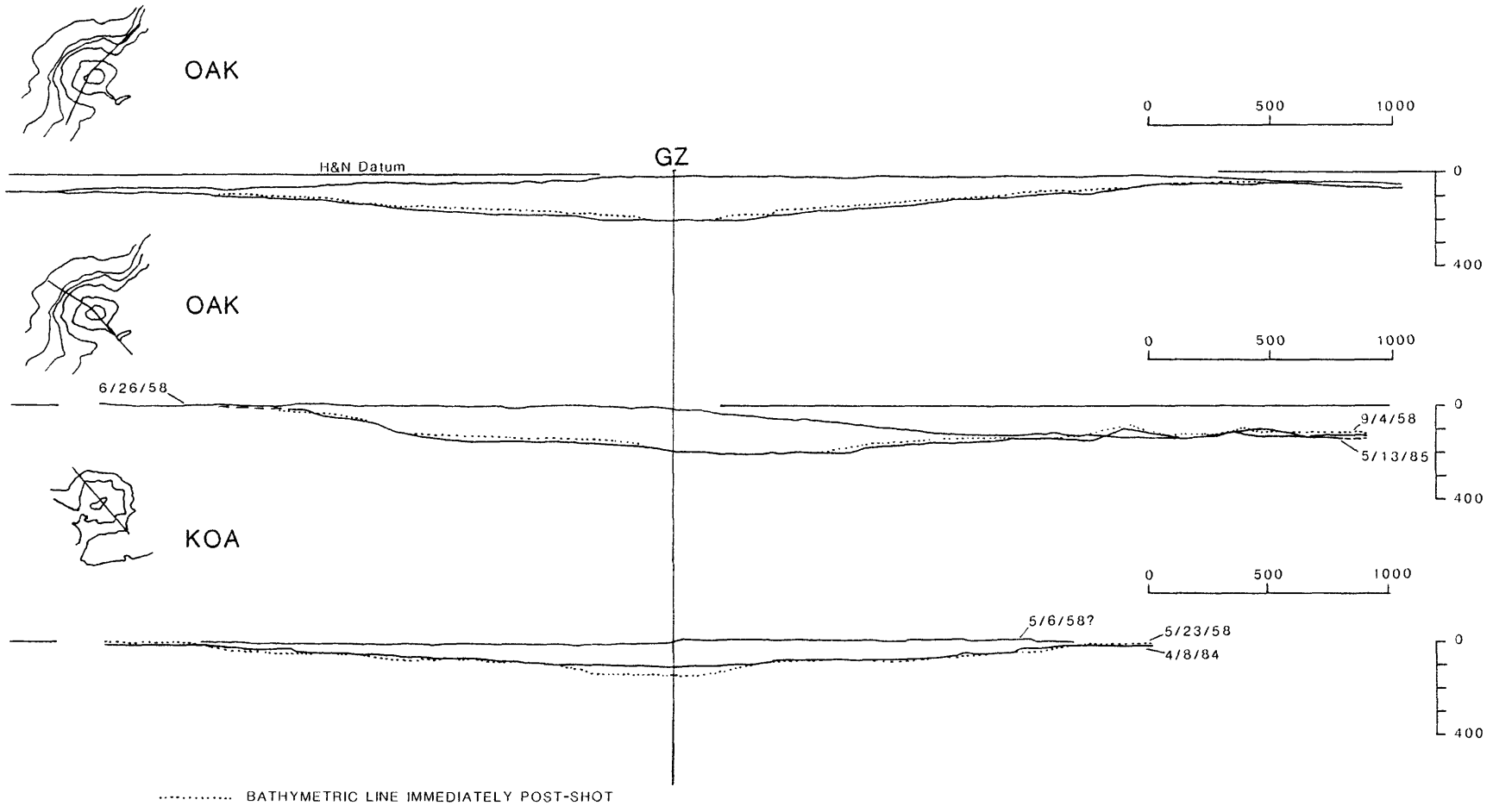

FIGURE 14-2. -- Bathymetric lines for OAK and KOA craters that are pre-shot (solid), immediately post-shot (dotted), and recent (solid), showing late (post-shot) subsidence and sedimentation.

sedimentation exceeding subsidence, and OAK crater by subsidence exceeding sedimentation.

Crater Material in the Lagoon. -- Muddy sediments in the northwestern portion of the lagoon appear to be partly derived from crater material. Observations leading to this conclusion include:

(1). Normal lagoon sediments and sedimentary package (SP) 1 (Holocene) sediments generally contain less than 10 weight percent low-magnesium (low-Mg) calcite (Chapter 4). The mud facies in the northwestern portion of the lagoon is anomalously high in low-Mg calcite (fig. 14-3). Low-Mg calcite is common in SP 2 and dominant in SP 3. The high low-Mg calcite values in surface sediments probably are due to crater excavation of older, diagenetically altered calcite-rich strata and subsequent sedimentation of these materials in the lagoon.

(2). Naturally produced carbonate muds normally contain only a very small fraction of clay-sized material. However, in the northern part of the atoll, the mud facies has a significant percentage of clay-size carbonate. This common clay-size fraction appears anomalous, probably indicating crater-derived material.

(3). The only radioactive sediments noted in the field were those from the mud facies (Chapter 10) near MIKE and KOA crater sites. These samples (38 and 39) showed measurable activity, probably from cesium-137. McMurtry and others (1985) demonstrated that, for barge-based events of Hardtack off Runit (YVONNE) Island, radionuclides are concentrated in clay-size carbonate sediment believed to be "blast-pulverized". Thus, it appears that a substantial part of the mud in the northwestern portion of the lagoon was derived from pulverization and crater excavation. There is no way to assess the amount of this crater-derived material or during which cratering event it was produced.

Piping. -- Brown-stained, organic-rich sediments from sedimentary interval II (SP 4, 5, and 6) have been piped to the surface in substantial quantities. Several sand mounds (Chapter 13 of this report or sediment hills of Halley, Slater, and others, 1986) or sand volcanoes, covered with moderate-brown, coarse detritus are common on the terraces of OAK crater. No sand volcanoes were observed in the KOA area, but most surficial features have been obscured by slumping (Folger, Robb, and others, 1986).

Several thin sand dikes of brown-stained sediments, confirmed by paleontologic analysis to be from SP 4, 5, and 6, were drilled and were inclined at a high angle to the borehole under the central crater region and terraces of OAK. Dikes were observed in boreholes OPZ-18 at 667.8 - 668.5 ft, OKT-13 at 615.0 - 615.2 ft, OTG-23 at 472.3 - 473.2 ft, and OFT-8 at 291.1 - 291.9 ft (all depths below H&N datum, bsl). No dikes were penetrated by the KOA boreholes.

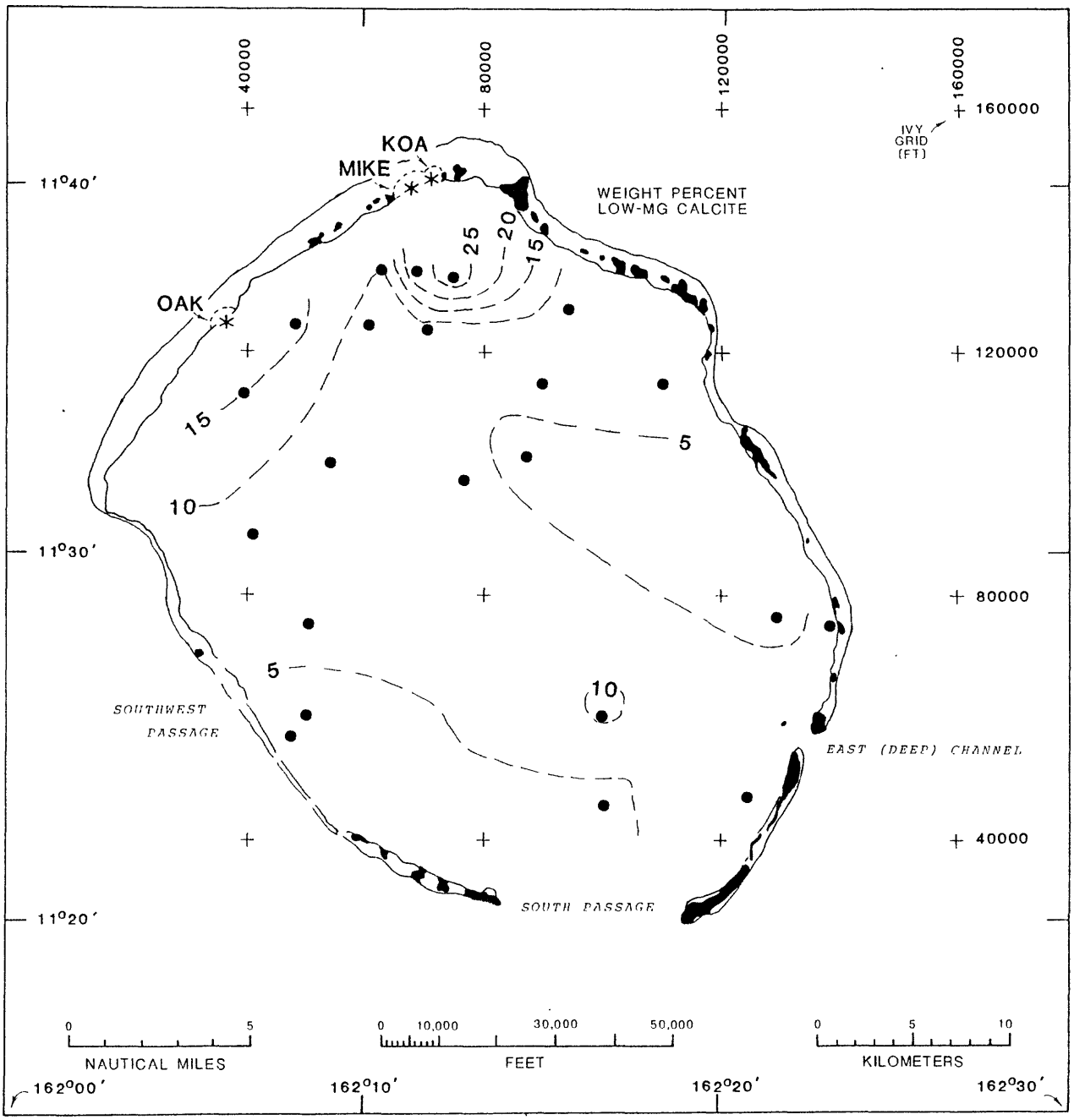

FIGURE 14-3. -- Distribution of low-magnesium calcite in lagoon samples (by weight percent).

In OAK crater, large fragments (up to cobble size), sand, and microfossils commonly were piped. In KOA crater, only sand-sized material including microfossils was piped.

In the subsurface of KOA crater, piped material is found in crater zone alpha 2 (graded sands) in boreholes KDT-6, KFT-8, and KCT-5 (see Appendix 14-1). No piped materal was identified in crater zone alpha 1 (mud) within the central region of the crater. In borehole KBZ-4, piped material is found in alpha 2 (graded sands) and beta 1a (late-stage collapse rubble). The abundance of piped material in beta 1a decreases downward through the zone. Microfossils are segregated and appear to have been sorted during piping.

In the subsurface of OAK crater, piped material is found more extensively in crater zones than in KOA. Piped material is common in crater zones alpha 1 (mud) in the central crater region and alpha 2 (graded sands) under the terraces and central crater. Boreholes OHT-10 and OJT-12 contain piped material within alpha 2 (graded sands) overlying the debris blanket. In the central crater region and terraces, piped material is common within the upper part of beta 1a (late-stage collapse rubble). In borehole OIT-11 piped material is within the upper part of a debris/rubble unit assigned to the undifferentiated beta zone. In boreholes OBZ-4 and OPZ-18, piped material occurs throughout the beta 1a zone, generally decreasing downward, and occurs sparsely in beta 1b.

In KOA crater, piped material appears to have been vented in a zone confined near the center evidenced by the hydrodynamic sorting within KBZ-4 that resulted from the piping. Piped material is only found within graded sands outside of KBZ-4. Therefore, piping in this crater seems to have been relatively short-lived, primarily post-collapse rubble, pre-mud deposition.

Piping was much more extensive and long-lived in OAK crater. It appears to have initiated during late-stage collapse-rubble deposition and continued through graded-sand and mud deposition. Sand volcanoes still remain on the seafloor on the terraces, testifying to the late-stage activity. Piped material in the early stage collapse rubble in OPZ-18 and OBZ-4 may, like in KBZ-4, represent vented material. The piped material in graded sands over the debris blanket, outside the general distribution of probable piping, may indicate a sand-turbidite flow toward the lagoon. The possible breach and flow deposit exhibited on the lagoon floor on the enhanced seafloor image of OAK crater (Folger, Robb, and others, 1986) is possibly the distal extension of this flow. This "event" clearly was concurrent with piping, but probably was after the formation of the collapse rubble (i.e., probably occurred during late-stage slumping).

Injection. -- Holocene sediment appears at an anomalous depth in borehole OPZ-18 within the transition sand (390.6 - 400.6 ft bsl) and in a thin dike(?) below the transition sand (434.5 - 435.2 ft bsl). Both of these features contain yellowish-gray and light-greenish-gray, muddy Halimeda sands found only in the Holocene lagoon sediments. The unit within the transition sand contains moderate-red Homotrema, also diagnostic of the Holocene. The lower unit contains pale-red Homotrema (not as diagnostic) but is both rich in aragonite (Chapter 4) and organic material (Chapter 5), confirming its probable Holocene origin. These units were not examined paleontologically.

The unit within the transition sand is at an angle to the borehole axis and may imply injection. The lower unit appears like a dike, may have a mixed zone with underlying rubble, and also suggests injection.

Seismic Interpretation. -- The multichannel-seismic profiles (Grow, Lee, and others, 1986) provide an excellent framework for three-dimensional interpretation. The long streamer used during the Marine Phase tends to enhance flat features and suppress slopes. Unfortunately, seismic lines, at least in the OAK area, were not adjusted, and the same reflector at an intersection of profiles can be up to 10 to 15 m (30 to 40 ft) different in depth. The borehole geology confirmed by biostratigraphic analyses, x-ray mineralogy, organic analyses, gamma-ray logs, and other downhole geophysical data provides an accurate but limited picture. Seismic-profile interpretation and borehole geology must be integrated. The interpretation of the seismic profiles presented by Grow, Lee, and others (1986) is not completely consistent with the borehole geology. Subtle step-ups of seismic horizons are discernable in the seismic profiles. If these step-ups are noted and are interpreted as stratigraphic step-ups, then the seismic lines and geology match well. Within the geologic crater, seismic reflectors represent both crater zones and some stratigraphic horizons. With the current geologic crater model, geologic and crater horizons can be differentiated reasonably. Wardlaw has reinterpreted the roughly perpendicular lines through OAK and KOA ground zeros (figs. 14-4 and 14-5, respectively). In the reinterpretations, not only are the seismic reflectors correlated with the physical stratigraphic framework, they are also consistent with the current geologic crater model as well. As noted in Chapter 1 of this report, Grow, Lee, and others (1986) used preliminary field notations and interpretations to compare seismic stratigraphy to borehole geology. A comparison of the current stratigraphic notation and that used in Grow, Lee, and others (1986) is shown in Figure 14-6.

Structural Surfaces. -- Two important surfaces, the top of the Pleistocene (disconformity 1, biostratigraphic zone AA/BB boundary) and the probable top of the Pliocene (disconformity 5, biostratigraphic zone GG/HH boundary) were selected for detailed analysis from selected multichannel-seismic survey lines (see figs. 14-7 and 14-8). The interpretations that follow (figs. 14-9 through 14-16) are by Wardlaw.

For the OAK area, where many seismic-survey lines were run, data points were compiled for each borehole and every seismic line intersection (fig. 14-7). For the KOA area, because of logistic reasons related to safe manuverability of the Egabrag II which ran the USGS seismic lines, there are far fewer intersecting lines, and the interpretations are more speculative. Every fifth fix point on a seismic line was compiled along with each borehole and intersection (fig. 14-8).

The probable preshot surfaces are shown for OAK, KOA, and MIKE (figs. 14-10, -12, -14, and -16). The post-shot surfaces are also given (figs. 14-9, -11, -13, and -15). From these two sets of figures, the probable disruption or displacement for these craters can be reasonably inferred.

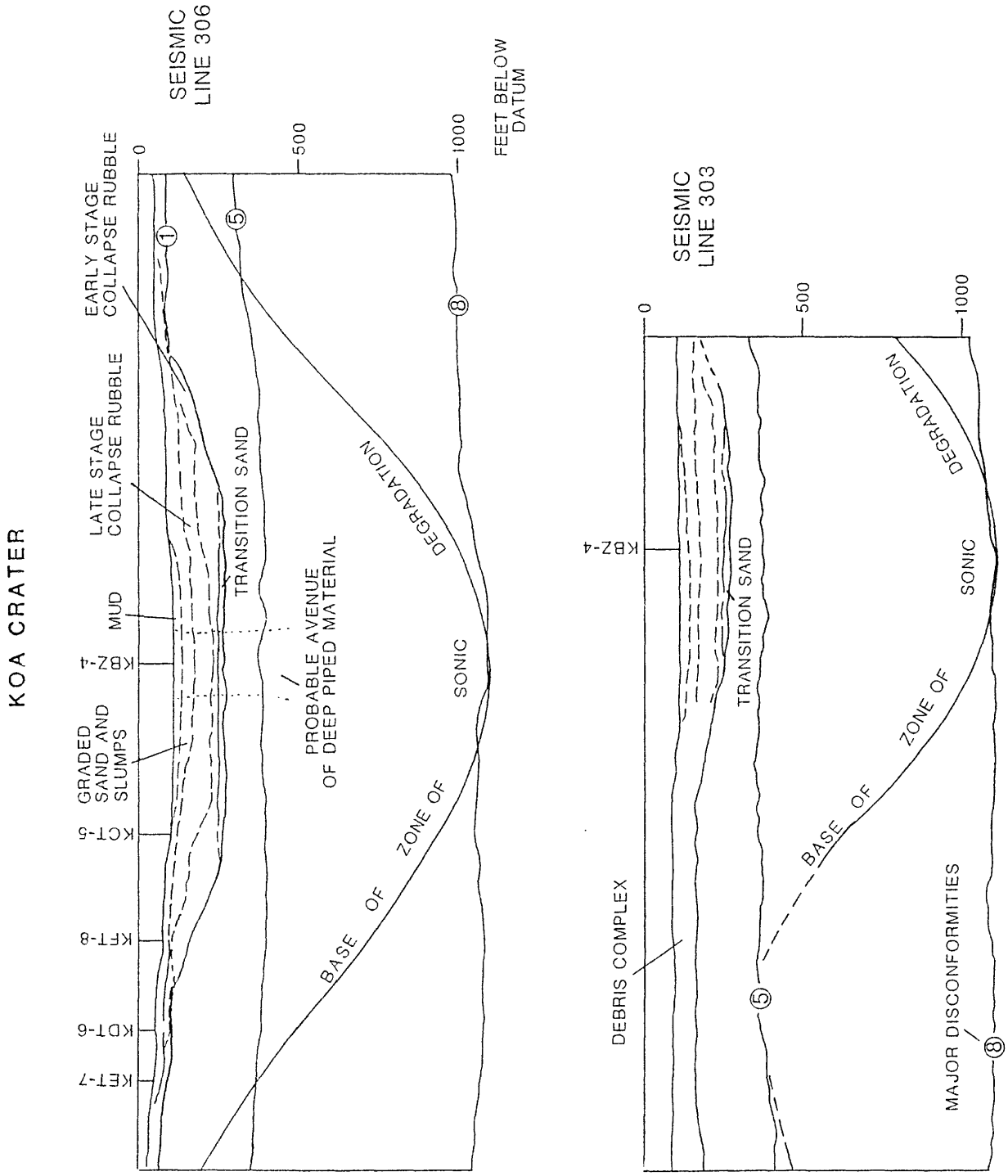

FIGURE 14-4. -- Geologic interpretation of multichannel seismic lines 303 and 306 run during Marine Phase of PEACE Program in proximity of KOA crater. Location of lines shown in Grow, Lee, and others (1986, fig. 11).

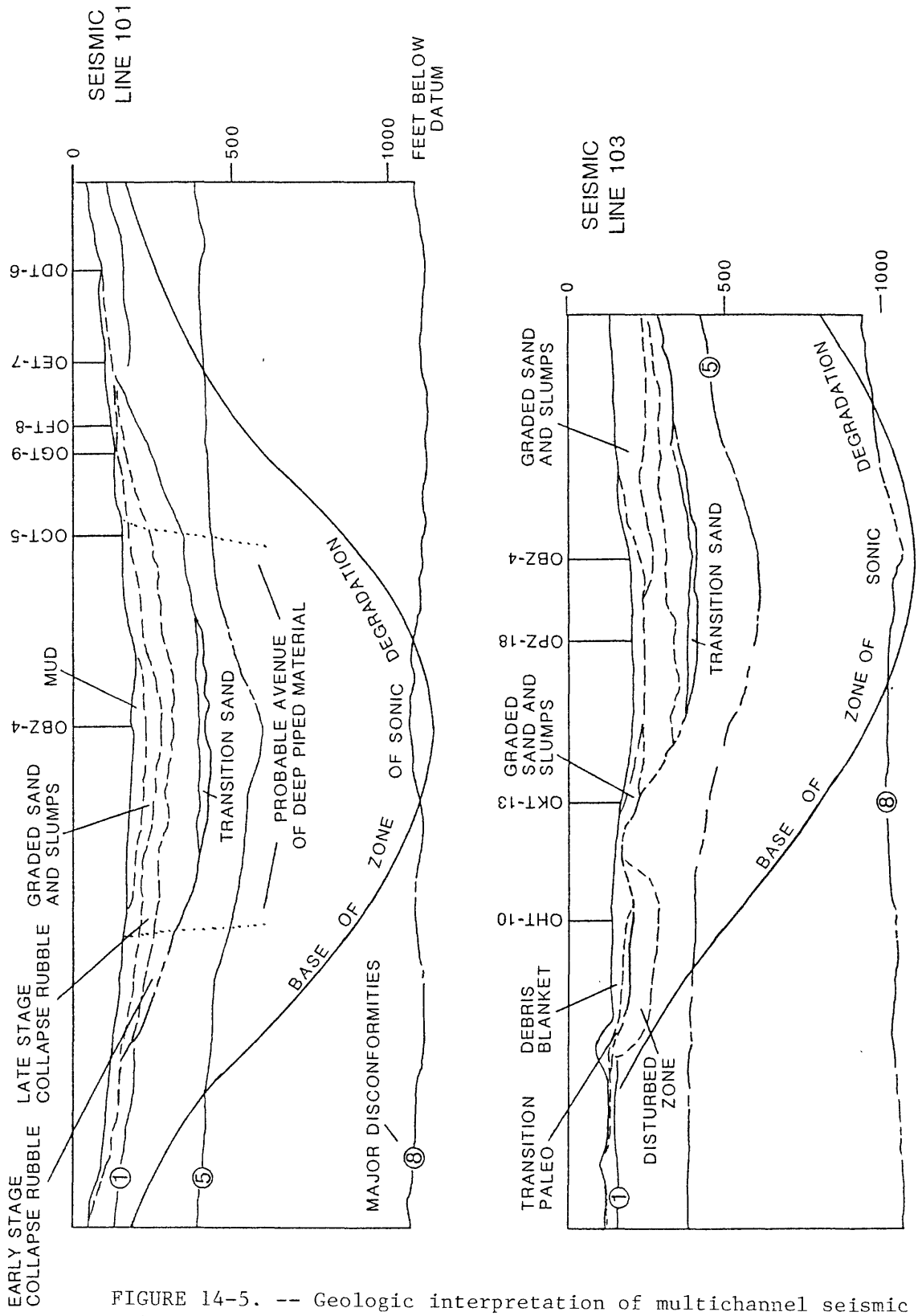

FIGURE 14-5. -- Geologic interpretation of multichannel seismic lines 101 and 103 run during Marine Phase of PEACE Program in proximity of OAK crater. Location of lines shown in Grow, Lee, and others (1986, fig. 3).

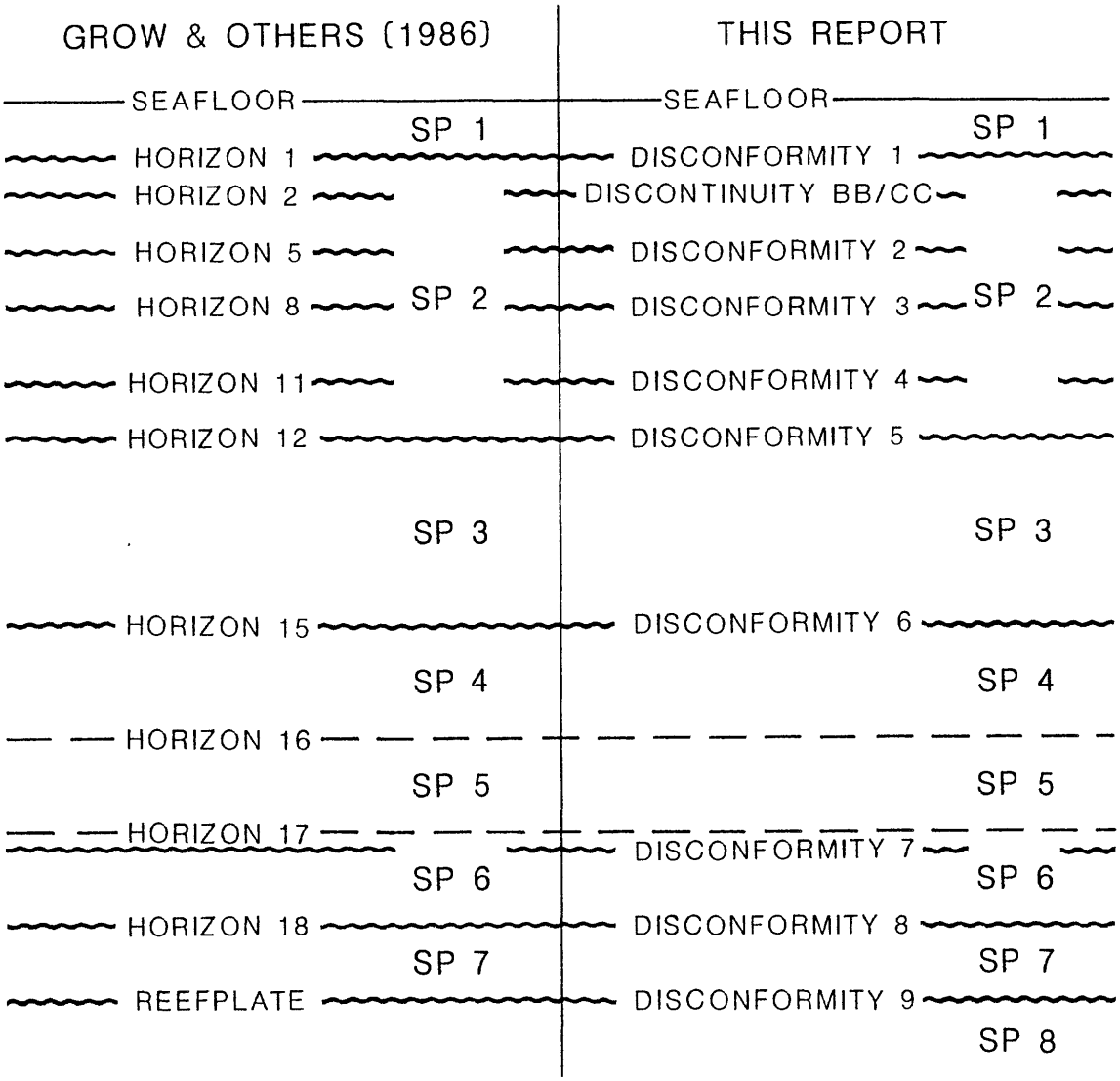

FIGURE 14-6. -- Comparison of stratigraphic horizons used in Grow, Lee, and others (1986) and stratigraphic framework of this report (see Chapter 2). Abbreviation SP = Sedimentary Package.

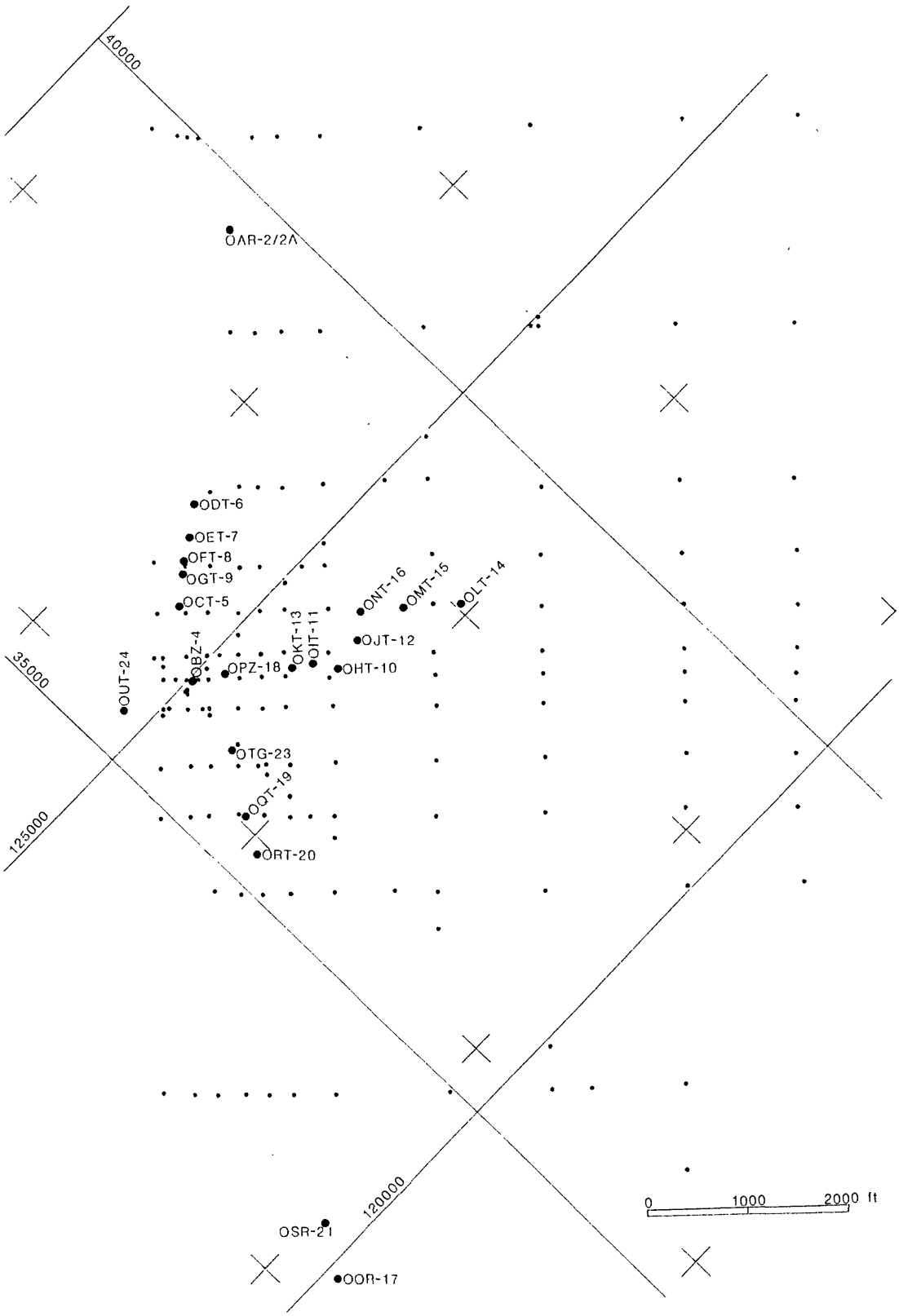

FIGURE 14-7. -- Base map for OAK crater area showing compilation points for structural surfaces. Boreholes shown by larger dots. Borehole OBZ-4 is at ground zero. North is to upper left of figure.

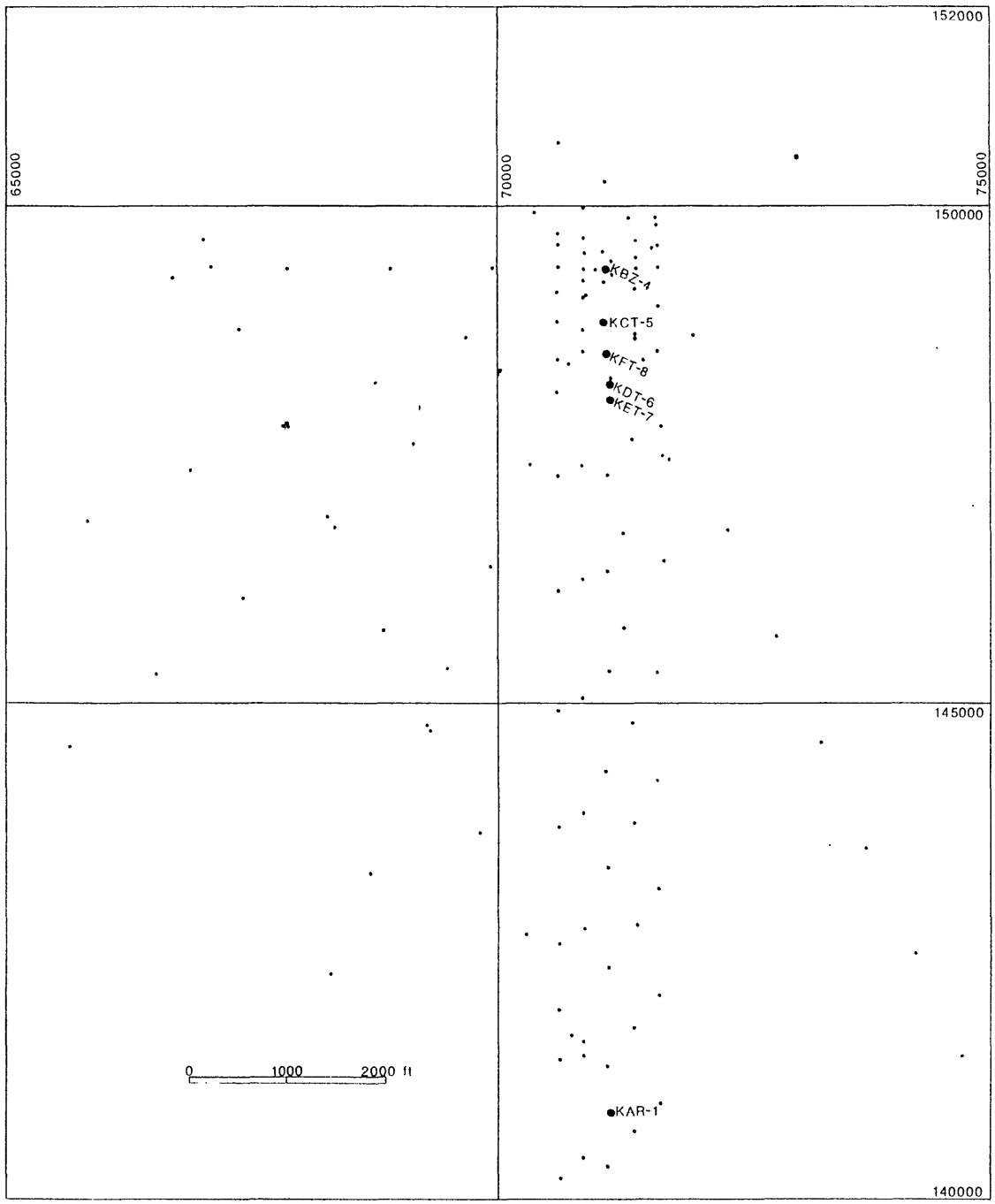

FIGURE 14-8. -- Base map for KOA crater area showing compilation points for structural surfaces. Boreholes are shown by larger dots. KBZ-4 is located at KOA ground zero.

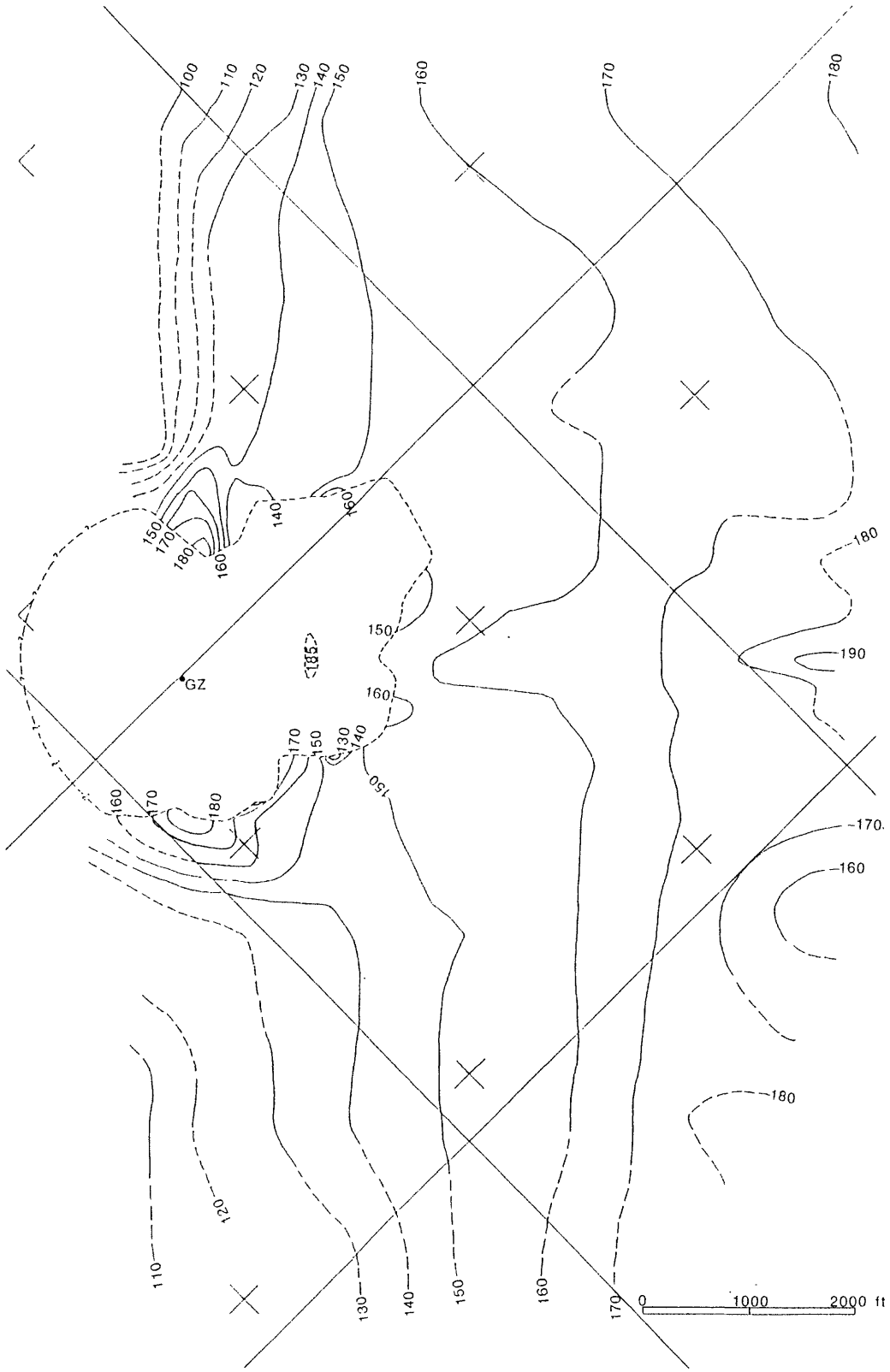

FIGURE 14-9. -- Map of OAK crater area showing present-day (post-shot) location of Pleistocene surface. Contours in ft below H&N datum. North is to upper left.

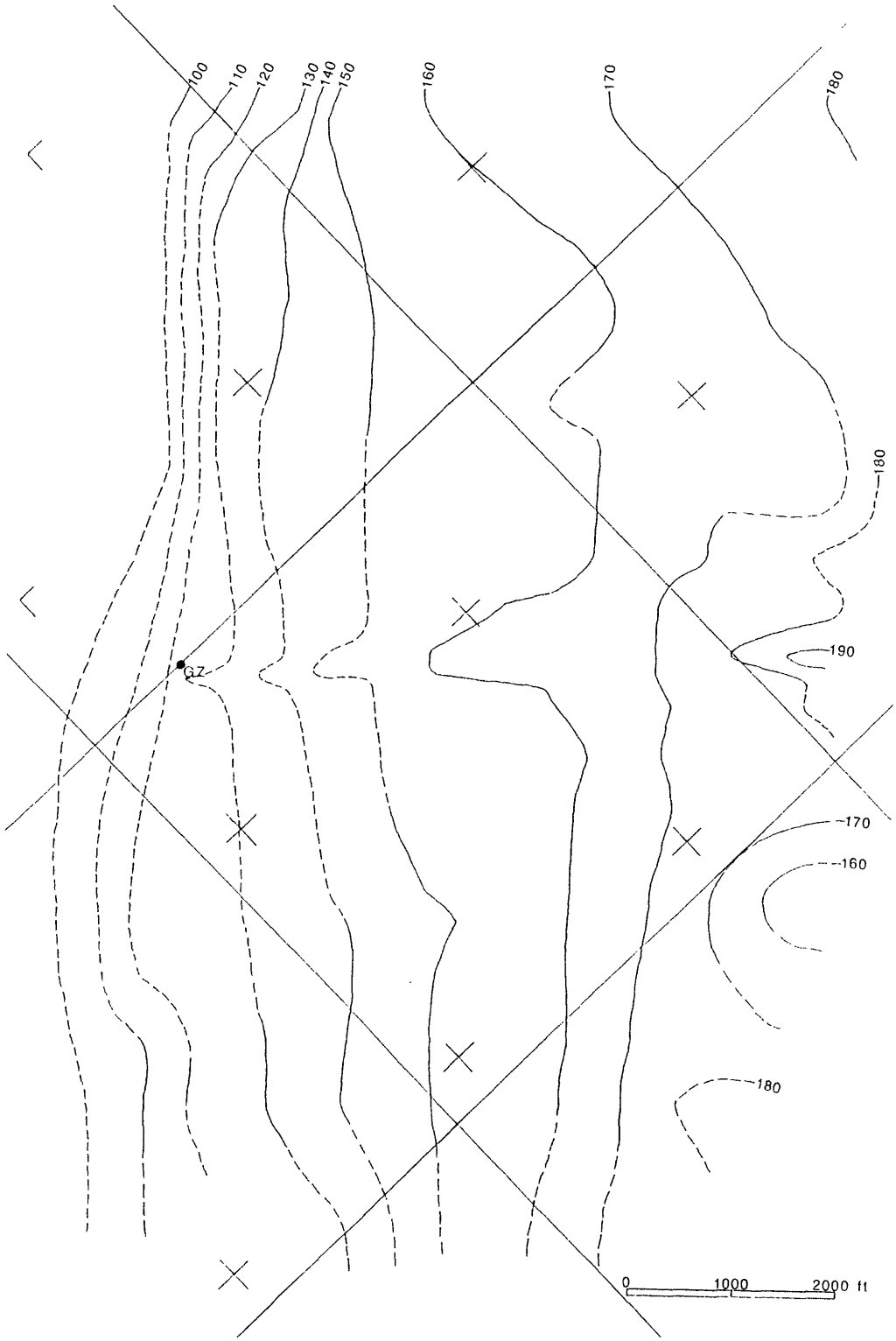

FIGURE 14-10. -- Map of OAK crater area showing probable pre-shot Pleistocene surface. Contours in ft below the H&N datum. North is to upper left of figure.

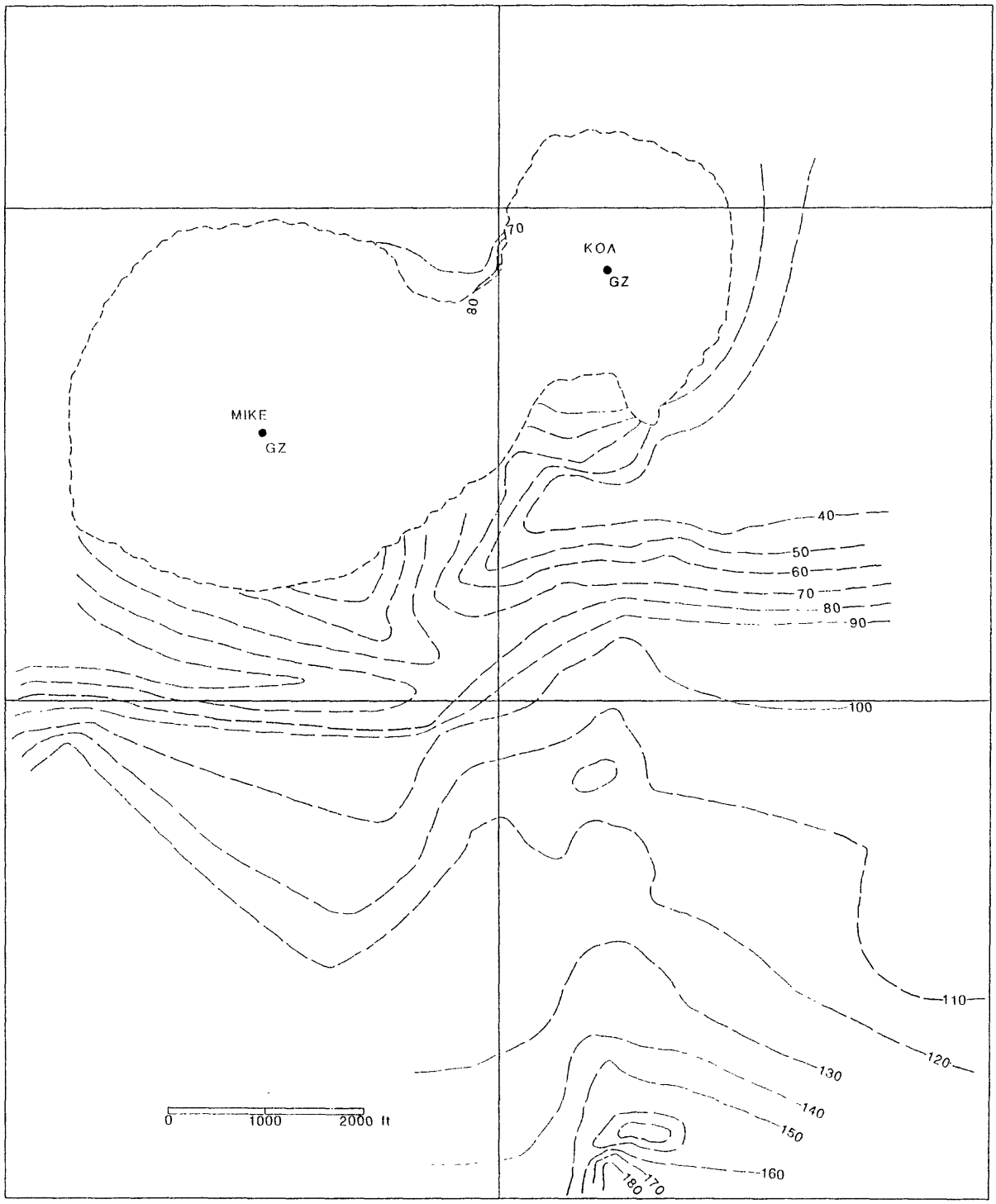

FIGURE 14-11. -- Map of KOA crater area showing present-day (post-shot) location of Pleistocene surface. Contours in ft below H&N datum.

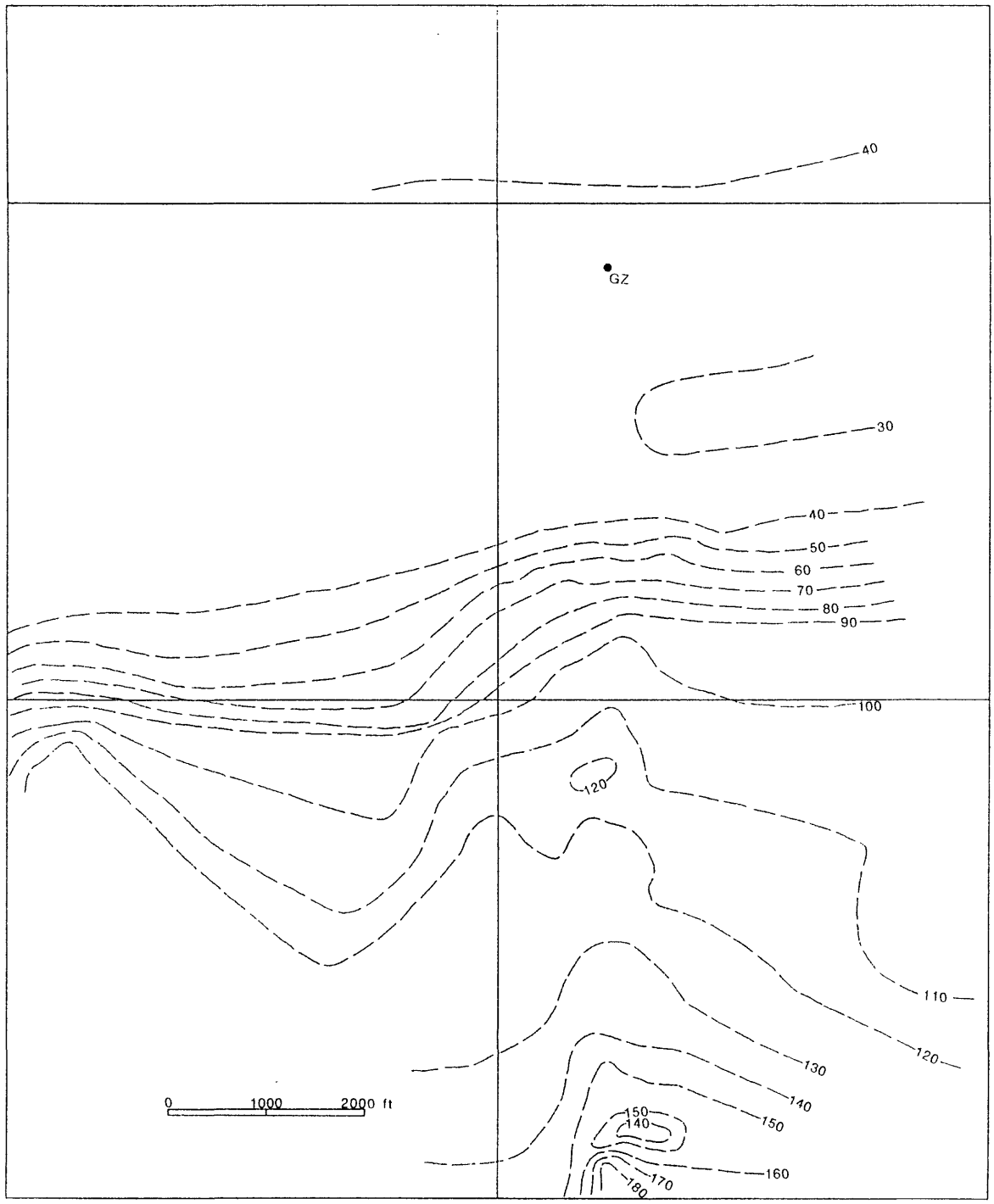

FIGURE 14-12. -- Map of KOA crater area showing probable pre-shot Pleistocene surface. Contours in ft below the H&N datum.

FIGURE 14-13. -- Post-shot Pliocene surface, OAK crater. Contours in ft below H&N datum. North is to upper left of figure.

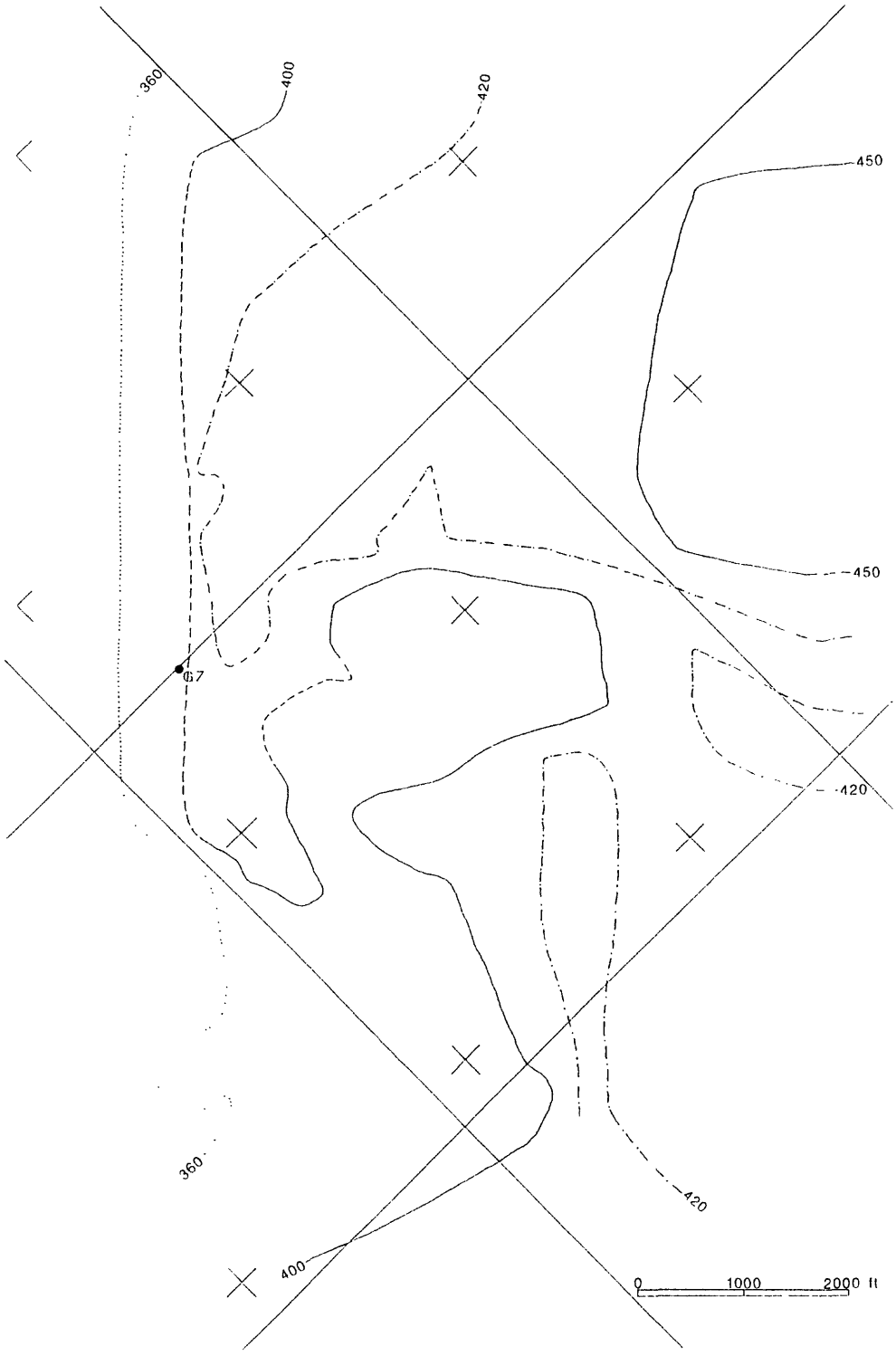

FIGURE 14-14. -- Probable pre-shot Pliocene surface, OAK crater. Contours in ft below H&N datum. North is to upper left of figure.

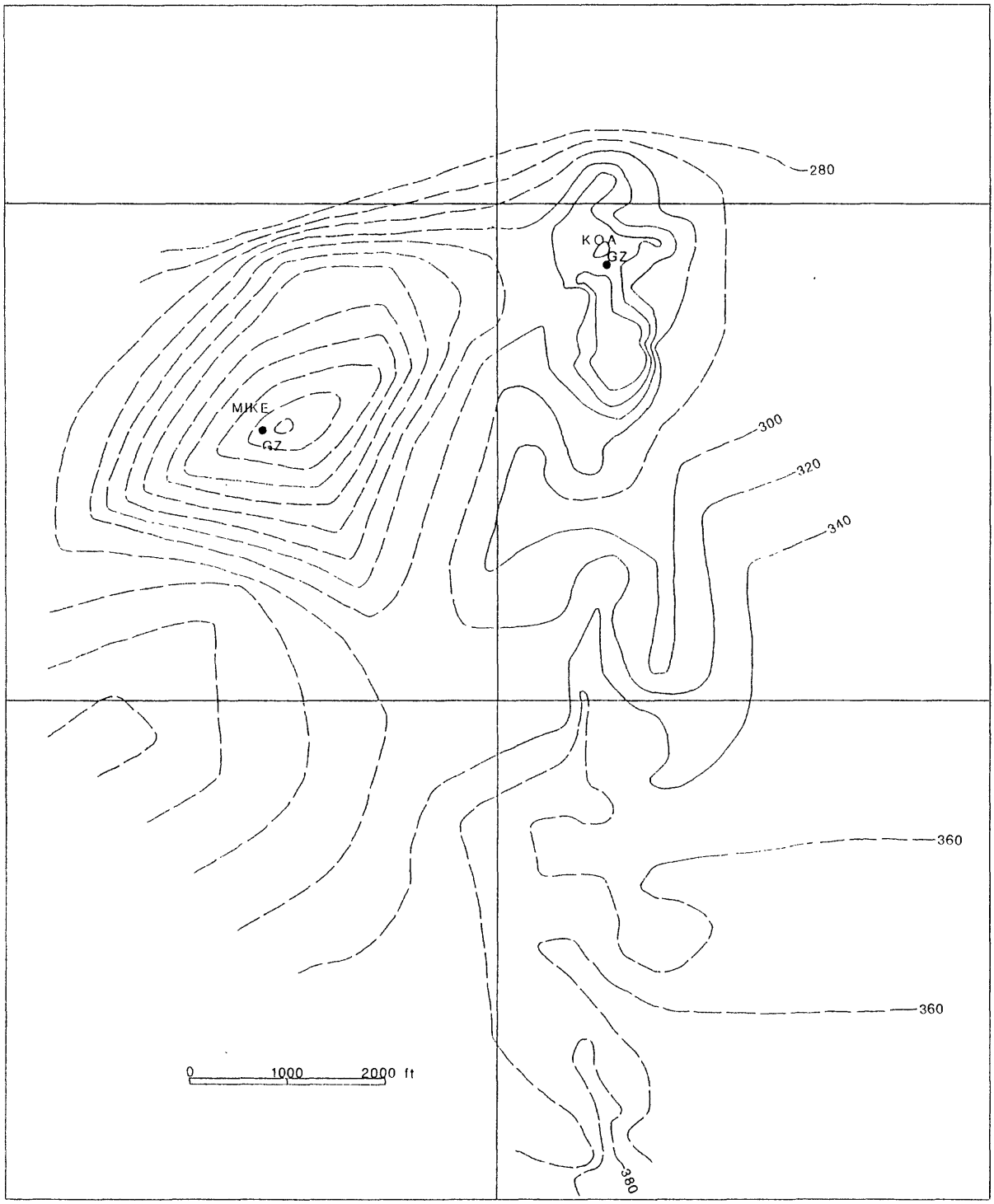

FIGURE 14-15. -- Post Pliocene surface KOA and MIKE craters area. Contours in ft below the H&N datum.

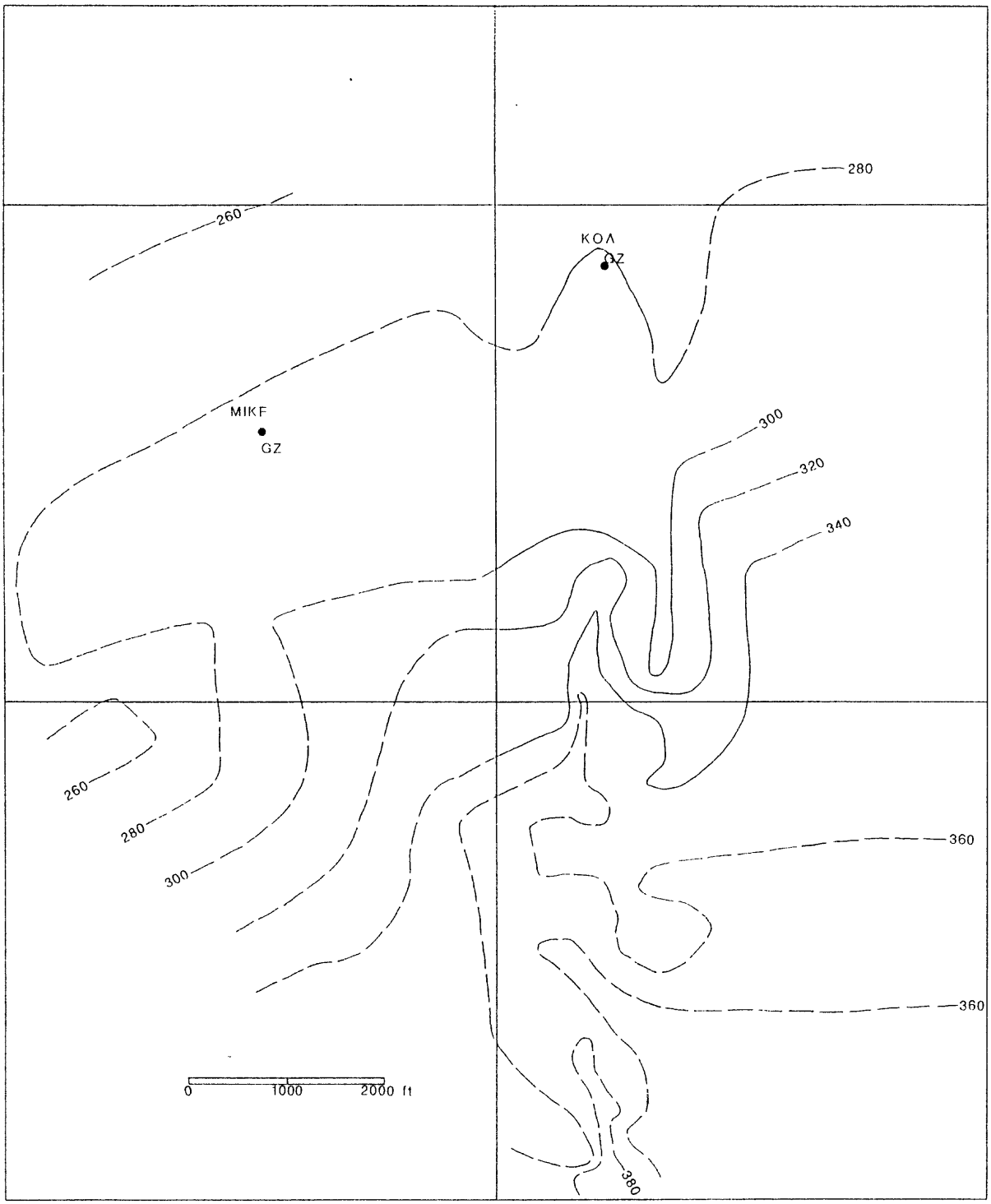

FIGURE 14-16. -- Probable pre-shot Pliocene surface, KOA and MIKE craters area. Contours in ft below H&N datum.

Sedimentary Package 3. -- Sedimentary package 3 generally represents the most competent unit in the upper 1,000 ft of the section. It shows some variation across the lagoon and these differences should be assessed.

In carbonates, pervasive recrystallization to low-Mg calcite commonly is accompanied by dissolution and cementation and is a general indicator of limestone formation. The x-ray mineralogy data (fig. 14-17, data from Chapter 4) clearly show the pervasive recrystallization by loss of aragonite and concomitant increase in low-Mg calcite in SP 3 and the alteration zone at the top of SP 4. The actual sample recovery curves for the three reference holes also are shown in this figure.

The few excursions to moderate aragonite content within the upper part of SP 3 may represent infilling of voids and caverns by overlying material. Both OAR-2/2A and KAR-1 show aragonite excursions lower in the package. The natural processes involved in the recrystallization of a substantial part of the section indicate that the top of SP 3 (disconformity 5) is a major exposure surface.

The stratigraphic sections of boreholes OOR-17 and KAR-1 are very much alike. Both contain exposure surfaces within SP 3. Both show more cementation and recrystallization in the lower part of SP 2. Both show more prevasive recrystallization within the alteration zone at the top of SP 4. OAR-2/2A does not show these features. The seismic reference survey data (Chapter 9; fig. 14-18, this chapter) indicate that KAR-1 and OOR-17 are very similar and that OAR-2/2A is considerably different. In an upublished report to DNA, Blouin and Timian (1986) confirm the sonic differences between KAR-1 and OAR-2/2A by ultrasonic analysis. Sedimentary package 3 in OAR 2/2A clearly shows some slower velocities and therefore probably contains some intervals of less cementation. Chapter 9 discusses the probability that the rugosity of the boreholes through sedimentary package 3 generally yielded low sonic velocities as determined by the downhole sonic tool (Chapter 7), so, the sonic is not a good comparison log for this interval. Figure 14-19 shows that x-ray mineralogy defines the interval of SP 3 and alteration zone of SP 4 well. The low-Mg calcite "trough" representing these units can be followed into the crater along the southwest transect of OAK crater.

Significant differences in SP 3 still exist for cratering considerations. OOR-17 is an excellent reference hole for OAK ground zero, occupying a similar ecologic position and composed of a similar depositional facies. KAR-1 is lagoonward of KOA ground zero and may not be as adequate a reference for that crater. The little that is seen of the lower part of SP 2 and upper part of SP 3 in EXPOE boreholes on depositional strike with KOA (i.e., boreholes XSA-2, XBK-1, and XEN-3) suggest that KAR-1 may be an adequate reference hole.

The thickness of SP 3 and the alteration zone at the top of SP 4 is markedly different between crater areas. This interval is 185.6 ft thick at OAR-2/2A, 181.5 ft thick at OOR-17, and 246.1 ft thick at KAR-1. Also, the elevations of the top of SP 3 differs. In the OAK area, the top of SP 3 is about 400 ft below the H&N datum (this includes preshot OAK ground zero). In contrast, at preshot KOA ground zero, it was probably about 280 ft below the

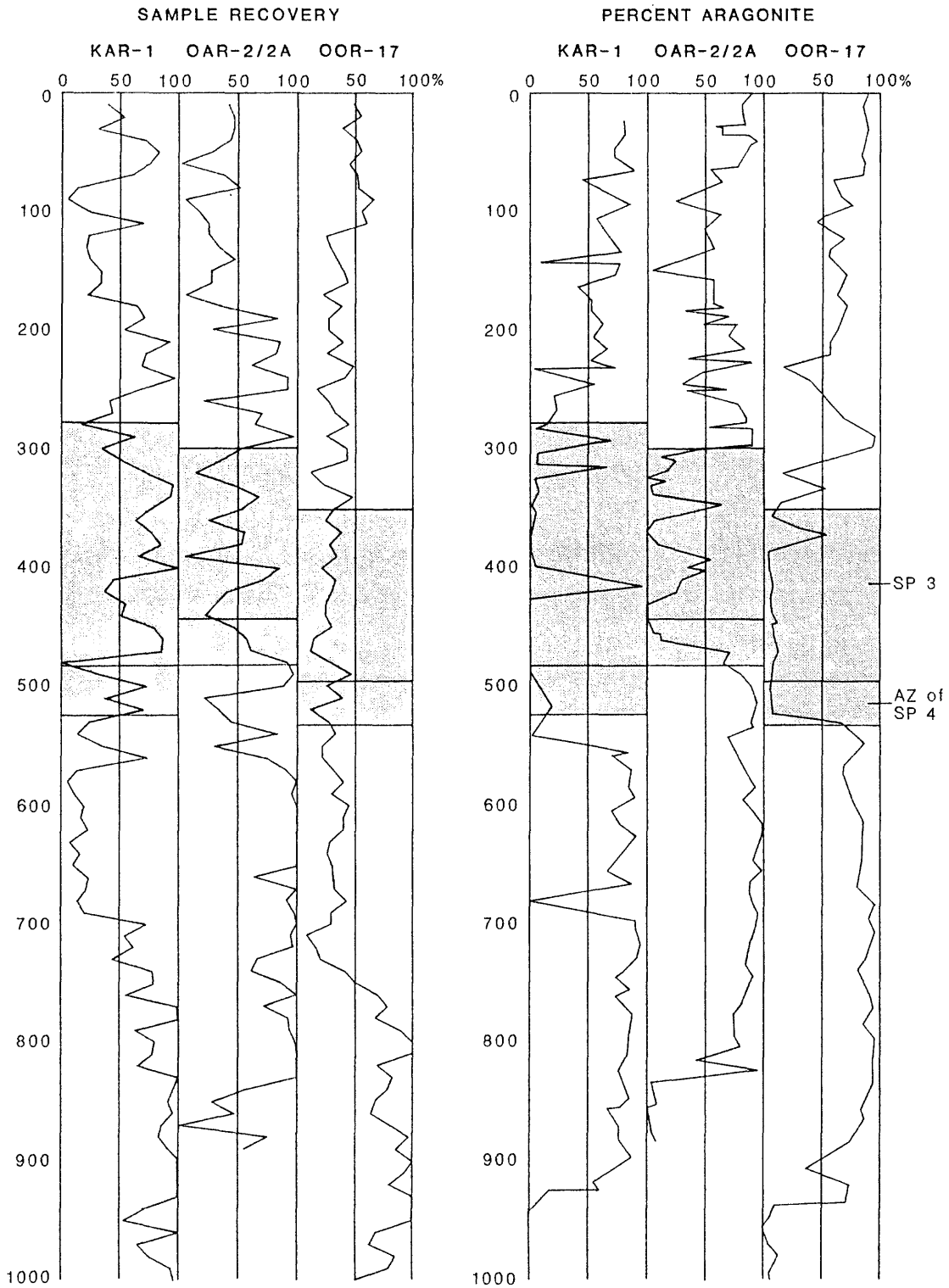

FIGURE 14-17. -- Percent sample recovery and weight percent aragonite in upper 1,000 ft (below H&N datum) of PEACE Program reference holes.

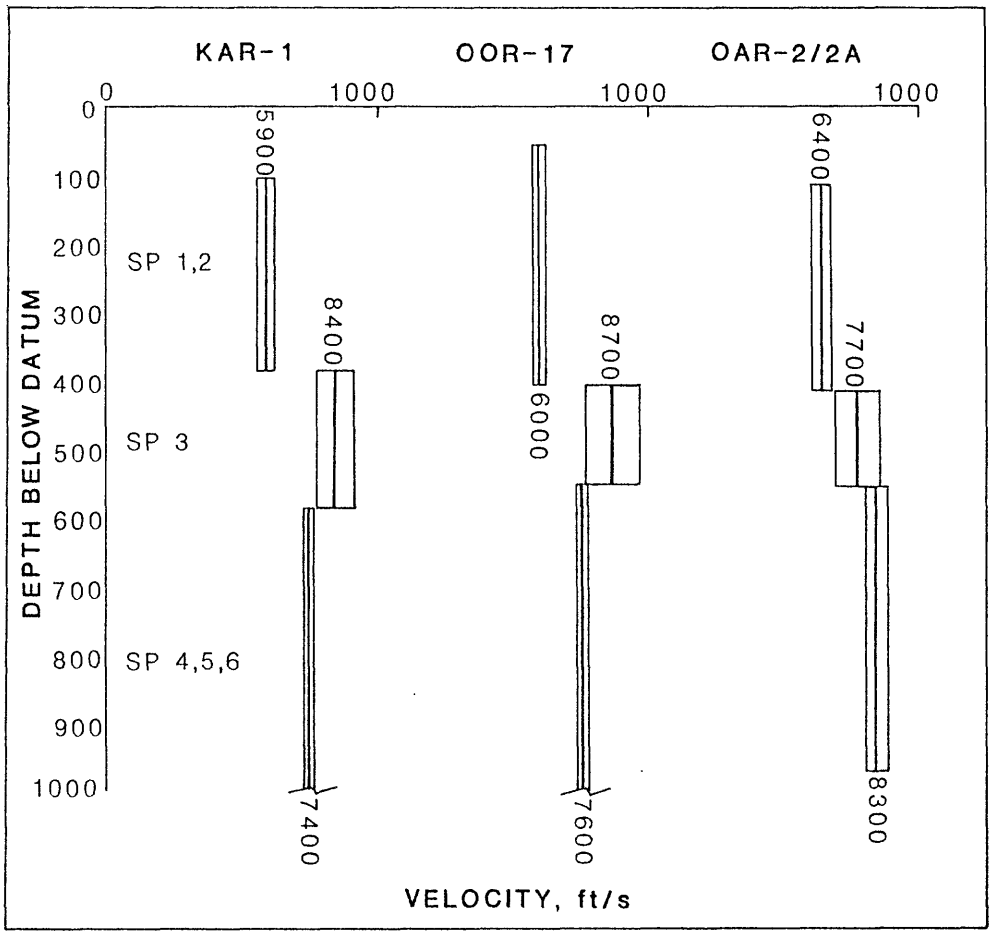

FIGURE 14-18. -- Seismic reference survey velocities in PEACE Program reference holes (see Chapter 9).

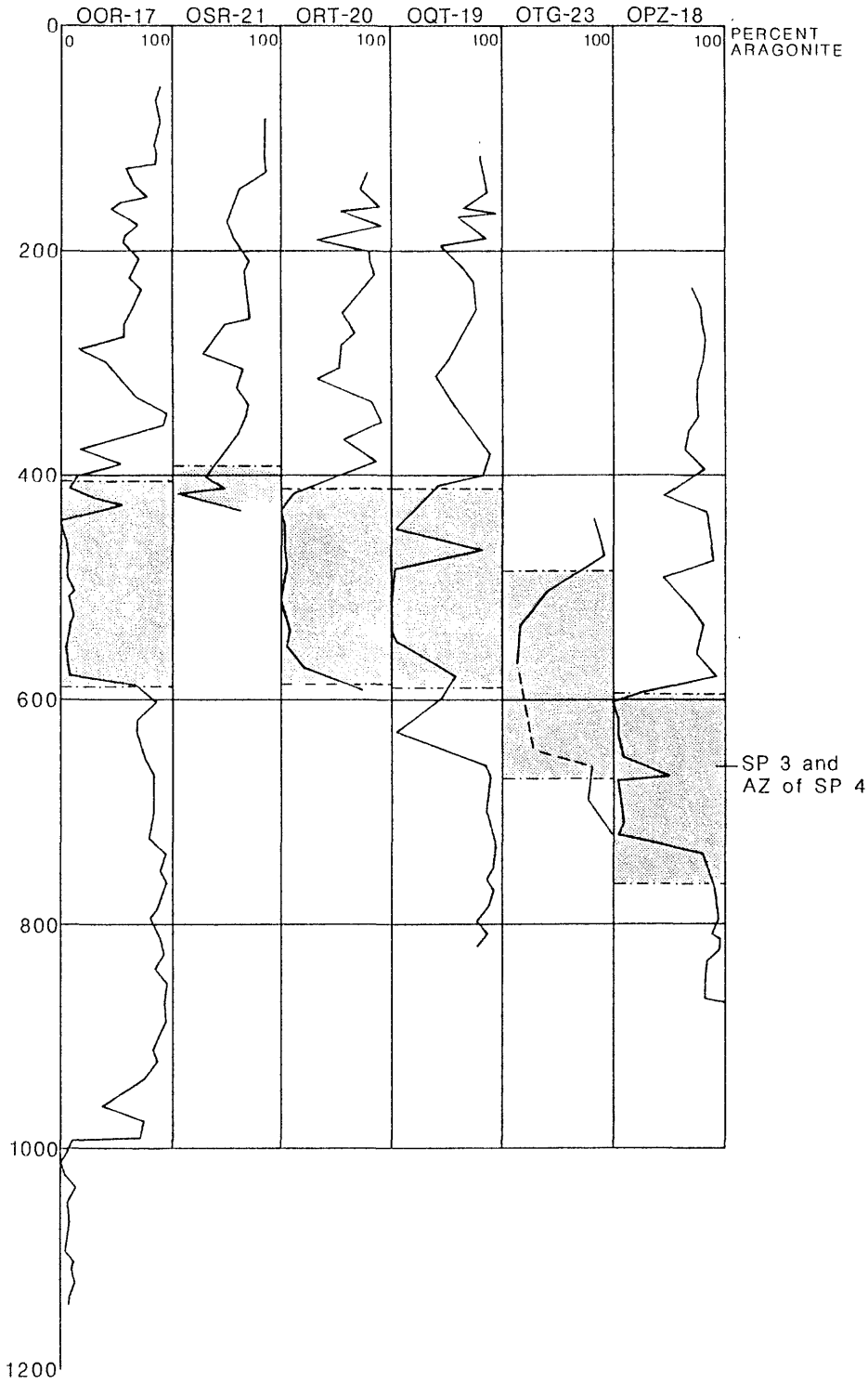

FIGURE 14-19. -- Weight percent aragonite in boreholes from southwest transect of OAK crater (OOR-17 to OPZ-18). Shaded area is sedimentary package 3 and alteration zone of upper part of SP 4.

datum, considerably shallower than OAK. The differences in thickness and elevation of SP 3 may be major factors in the differences between the two craters.

Gamma Logs. -- In Enewetak boreholes, elevated gamma activity appears to reflect: (1) the presence of device-produced radionuclides, (2) the presence of brown-stained, organic-rich Miocene/Pliocene sediments, and (3) various other factors. In the crater area, a gamma peak occurs within muddy sediments overlying a discontinuity (OIT-11, fig. 14-20). It appears that other peaks also can be related to thick zones of "tea-brown" (organically stained) micrite cement. Brown-stained, organic-rich Miocene/Pliocene sediments occur stratigraphically in sedimentary interval II (particularly SP 5) and in piped material from those strata.

Chapter 12 of this report convincingly shows Cs-137 levels coincide directly to the gamma activity in the alpha, beta-1, and beta-2 crater zones for boreholes OPZ-18, OBZ-4, OCT-5, OKT-13, and KBZ-4. Furthermore, the radionuclide analysis demonstrates that the gamma activity of the brown-stained, organic-rich sediments is caused largely by naturally occurring isotopes of thorium and uranium. These radionuclides were not observed within the alpha, beta 1, and beta 2 crater zones.

Naturally occurring thorium and uranium isotopes were detected in borehole OIT-11 probably accounting for the "other" peak in gamma activity (fig. 14-20). Similarly, in borehole OHT-10, a small peak in the gamma activity probably reflects naturally-occurring thorium and uranium.

Figures 14-20 and 14-21 compare the gamma log, paleontologic and geologic crater zones, and general lithology for KOA and OAK crater areas. Only boreholes on complete transects with full geologic sampling and open-hole gamma logs were utilized for this detailed comparison. Essentially, the gamma logs confirm the general trends in radionuclide abundance reported in Chapter 12. The beta 2/beta 3 boundary (where present) and the beta 1/gamma boundary (where present) appear to represent the demarcation between occurrence and nonoccurrence of device-produced radionuclides. Naturally occurring radionuclides appear to reflect the presence of piped material in the beta 3 crater zone. Device-produced radionuclides are most abundant within the bottom of alpha 2 (graded sands) and top of beta 1b (late-stage collapse rubble) in OBZ-4 and OPZ-18, respectively. In KBZ-4, they are most abundant at the base of alpha 1 and at the top of alpha 2. In KCT-5, there is only a trace of radionuclides (device-produced and natural). In borehole OCT-5, device-produced radionuclides are most abundant within the lower part of the beta 1a crater zone. In OKT-13, device-produced radionuclides show two peaks, one within beta 1a, and the other, larger one, near the base of beta 1b.

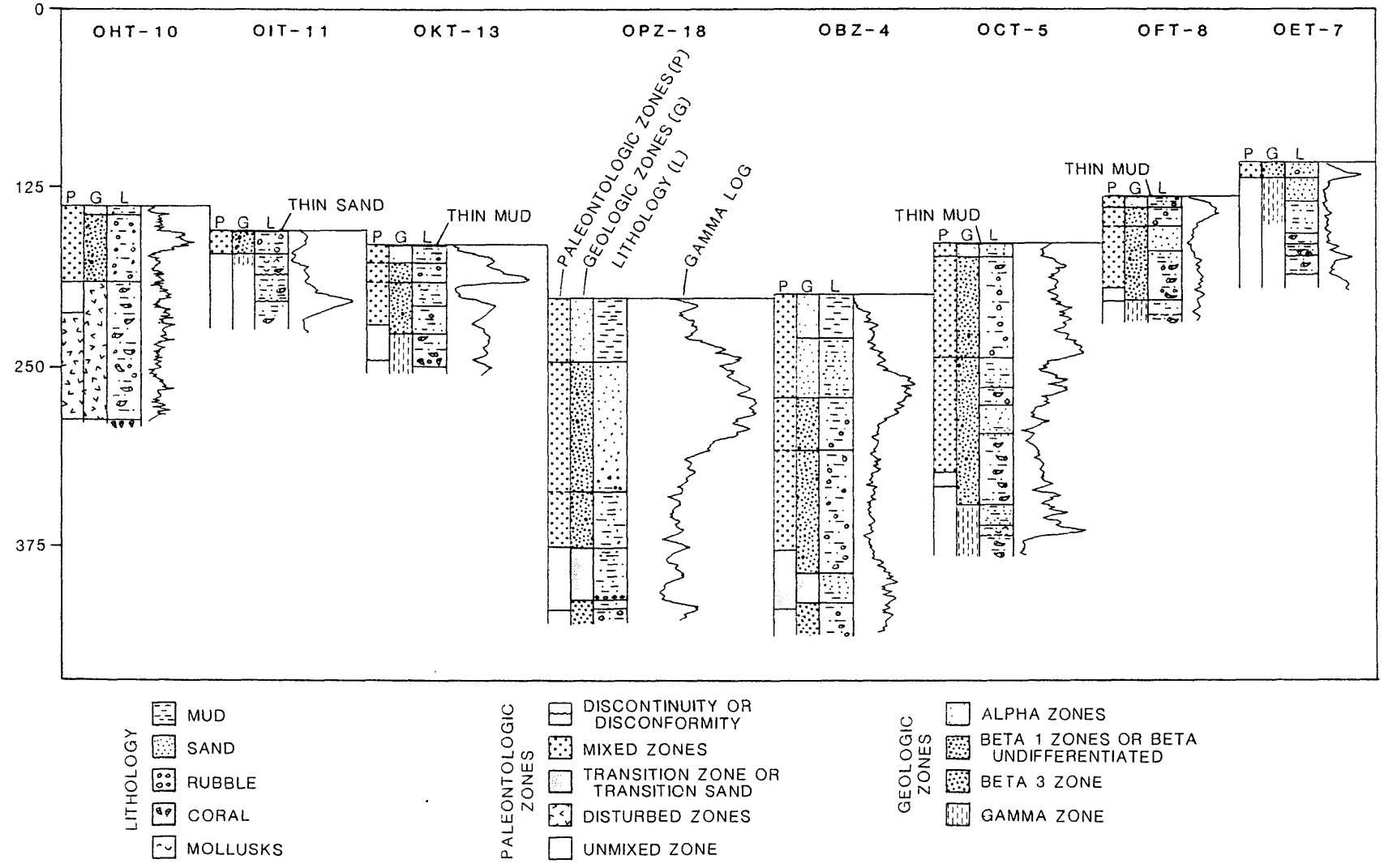

FIGURE 14-20. -- Borehole lithology (L), geologic and paleontologic crater zones (G and P, respectively), and gamma-ray logs for selected boreholes, OAK crater.

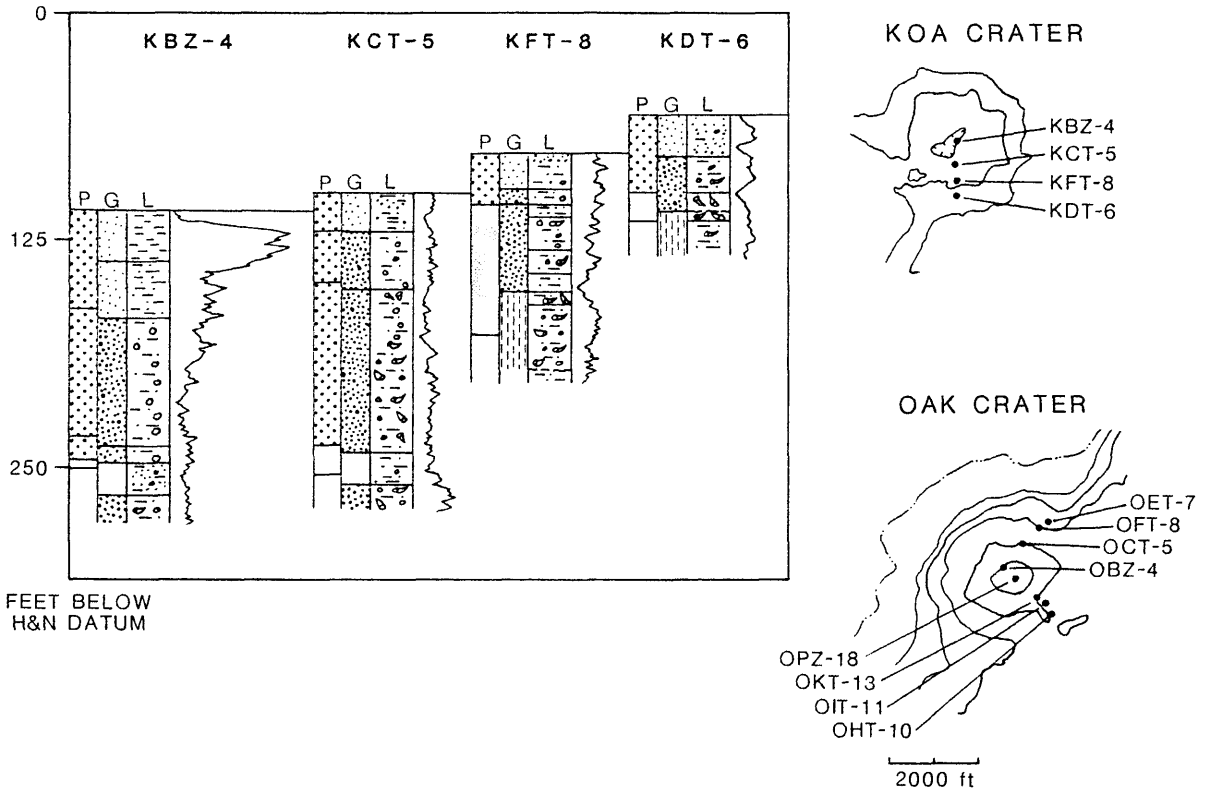

FIGURE 14-21. -- Borehole lithology (L), geologic and paleontologic crater zones (G and P, respectively), and gamma-ray logs for selected boreholes, KOA crater.

COMPARISON OF OAK AND KOA CRATERS

The following comparisons and contrasts between OAK and KOA craters are warranted by the analyses conducted.

(1). The significant cemented and altered zone (rock; SP 3 and the alteration zone at the top of SP 4) was probably 246 ft thick with the top at 280 ft bsl at KOA ground zero and 183 ft thick with the top at 400 ft bsl at OAK ground zero.

(2). Sedimentary package 3 is depressed approximately 193 ft at OAK ground zero and approximately 89 ft at KOA ground zero.

(3). The base of the zone of sonic degradation is similar in both craters -- 1,139 ft bsl for OAK ground zero and 1,101 ft bsl for KOA ground zero.

(4). The transition sand (beta 2) is more extensive in KOA than OAK, with an average diameter of approximately 918 ft at KOA and 816 ft at OAK. The transition sand is more strongly elongate oval at KOA than at OAK.

(5). A debris blanket is extensive on the lagoon side of OAK; only two possible debris mounds of limited distribution exist on the MIKE-side of KOA.

(6). The late-stage collapse rubble (beta 1a) is similar in both craters. The rubble becomes thicker and muddier in the direction of the lagoon at OAK (i.e., toward its distal margin) and in the direction of MIKE crater in KOA. For all intent and purpose, MIKE served as a "lagoon", similar to the lagoon off OAK, but not as extensive, for the KOA event.

(7). The early stage collapse rubble (beta 1b) is similar in both craters, although it is thicker in OAK. The beta 1b zone thins toward the lagoon at OAK and thins toward MIKE crater at KOA.

(8). Mud (alpha 1) occupies the central region of both craters.

(9). The graded sands (alpha 2) are similar in both craters. The zone is common throughout the KOA crater, but absent near the bathymetric center (OPZ-18) of OAK crater.

(10). Deep piped material is common only in alpha 2 in KOA and appears to have been vented in a limited area at the central crater (KBZ-4 contrast figs. 14-4 and 14-5). Deep piped material is common to alpha 1, alpha 2, and beta 1a in OAK and appears to have been vented in an extensive area of the central crater and terraces.

(11). KOA crater is characterized by late-time sedimentation exceeding subsidence. OAK crater, in contrast, is characterized by late-time subsidence exceeding sedimentation.

(12). Device-produced radionuclides appear to be mostly limited to the beta 2 zone and above in the craters. Radionuclides were only detectable in KBZ-4 for the KOA crater. In OAK crater, peak abundance of device-produced radionuclides progressively moves down in the crater zones away from GZ within what must have been the original crater radius. For example, the peak abundance is in alpha 2 at OBZ-4, top of beta 1a at OPZ-18, bottom of beta 1a at OCT-5, bottom of beta 1b at OKT-13.

RELATIVE TIMING OF DEPOSITIONAL EVENTS

For OAK crater, from oldest to youngest, the sequence of depositional events are:

(1). Formation of transition sand.

(2). Collapse of excavational-crater wall/rim to destroy lateral extent of transition sand and to form early-stage collapse rubble.

(3). Penecontemporaneous formation of debris blanket by probable partial failure and movement of the excavational-crater wall/rim lagoonward.

(4). Infilling of remaining crater bowl by wash- and/or fall-back and crater-margin collapse to form late-stage collapse rubble, initiation of subsidence and concomitant piping.

(5). Margin slumping and graded-sand (turbidite flow) deposition. One slump and resulting turbidite flow was large enough to have flowed across the crater, "breach" the debris blanket, and have flowed into the lagoon. Subsidence and piping continued.

(6). Late-time infilling of central part of the crater with mud, continued subsidence and piping. Mud deposition has continued to present. Local slumping and sand deposition has continued along the reef margin.

For KOA crater, the events (from oldest to youngest) are:

(1). As in OAK.

(2). As in OAK.

(3). Penecontemporaneous formation of debris mounds by partial MIKE-ward collapse and movement of crater wall/rim.

(4). Infilling of remaining crater bowl by wash- and/or fall-back and crater-margin collapse to form late-stage collapse rubble, initiation of subsidence.

(5). Margin slumping and graded-sand (turbidite-flow) deposition and piping in the central part of the crater.

(6). Late-time infilling of central part of the crater with mud, continued by localized slumping and sand deposition around most of crater (except near MIKE). Subsidence has lessened markedly.

ACKNOWLEDGMENTS

The authors would like to thank Lt. Col. Robert F. Couch, Jr., L. Stephen Melzer, Byron L. Ristvet, and Edward L. Tremba for their many stimulating discussions on the drill ship and back at the office that set the direction of this report. The authors also thank Wayne E. Martin and Robert G. Stamm whose invaluable assistance and support made this report possible.

REFERENCES

Cronin, T.M., Brouwers, E.M., Bybell, L.M., Edwards, E.E., Gibson, T.G., Margerum, R., and Poore, R.Z., 1986, Pacific Enewetak Atoll Crater Exploration (PEACE) Program, Enewetak Atoll, Republic of the Marshall Islands; Part 2: Paleontology and biostratigraphy, application to OAK and KOA craters: U.S. Geological Survey Open-File Report 86-159, 39 p., 20 figs., 12 tbls., 3 appendices.

Folger, D.W., Robb, J.M., Hampson, J.C., Davis, P.A., Bridges, P.M., and Roddy, D.J., 1986, Sidescan-sonar survey of OAK and KOA craters; 18 p., 6 figs.; in Folger, D.W., ed., Sea-floor observations and subbottom seismic characteristics of OAK and KOA craters, Enewetak Atoll, Marshall Islands: U.S. Geological Survey Bulletin 1678.

Grow, J.A., Lee, M.W., Miller, J.J. Agena, W.F., Hampson, J.C., Foster, D.S., and Woellner, R.A., 1986, Multichannel seismic-reflection survey of KOA and OAK craters; 46 p., 39 figs.; in Folger, D.W., ed., Sea-floor observations and subbottom seismic characteristics of OAK and KOA craters, Enewetak Atoll, Marshall Islands: U.S. Geological Survey Bulletin 1678.

Halley, R.B., Slater, R.A., Shinn, E.A., Folger, D.W., Hudson, J.H., Kindinger, J.L., and Roddy, D.J., 1986, Observations of OAK and KOA craters from the submersible; 32 p., 13 figs., 1 appendix; in Folger, D.W., ed., Sea-floor observations and subbottom seismic characteristics of OAK and KOA craters, Enewetak Atoll, Marshall Islands: U.S. Geological Survey Bulletin 1678.

McMurtry, G.M., Schneider, R.C., Colin, P.K., Buddemeier, R.W., and Suchanek, R.H., 1985, Redistribution of fallout radionuclides in Enewetak Atoll lagoon sediments by calianassid bioturbation: Nature, v. 313, no. 6004, p. 674-677, 3 figs., 1 tbl.

APPENDIX 14-1:

MIXING REVIEW

Mixing within the crater is indicated by the presence of lithoclasts from several different stratigraphic levels, macrofaunas, and microfaunas. Mixed lithoclasts cannot be differentiated easily, but strontium-isotopic studies should help resolve some of the problems. Mixing within KOA and OAK craters is summarized in Table 14-3.

Megafossil Mixing

Mixed megafossil material generally consists of sand- to gravel-sized corals and molluscs from sedimentary interval II (i.e., SP 4, 5, and 6), the organic interval, that is uniquely brown colored. Mixing in KOA is not as obvious as in OAK, but KOA does have sparse occurrences of megascopic materials indicating deep mixing.

Two pebble-sized brown coral fragments were found at 78.7-79.0 ft in borehole KBZ-4. A few broken granule- to pebble-sized coral clasts were found at 16.4 ft in KFT-8. Common brown skeletal fragments were found from 3.2-10.4 ft with a brown coral cobble at 9.0 ft in KDT-6.

In contrast to KOA, the evidence for mixing in OAK is clear. In OBZ-4, brown medium sand-sized skeletal elements occur at 15.3 ft. From 69.6-73.0 ft brown coral clasts first occur. Scattered granule- to small pebble-sized pieces of brown coral occur from 83.7-104.1 ft. Brown clasts become sparse and were not observed from 163.3-176.2 ft. The lowest occurrence of brown coral clasts within the crater is 186.8 ft. The lowest megascopic evidence of Holocene material (moderate-red Homotrema) is 152.1 ft.

The material from the upper part of OPZ-18 is very fine grained, and mixed brown material is more difficult to identify. It appears that scattered lignite(?) flakes from 0.0-44.6 ft may represent mixing from the organic interval. From 44.6-135.3 ft brown sand grains are scattered throughout, a granule-sized piece of charcoal occurs at 64.9 ft, and brown foraminifers occur at 52.5 ft. From 135.3-160.0 ft, a few brown coral fragments occur. Material is sparse below this, but two brown coral clasts occur at 160.4 and 163.7 ft. A moderate-yellowish brown coral of questionable origin is reported from 226.8 ft. The lowest demonstrable occurrence of a Holocene component (i.e., moderate-red Homotrema) is at 198.7 ft. Possible moderate-red

TABLE 14-3. Paleontologic crater zones and relation to the transition sand in OAK and KOA crater boreholes.

KOA CRATER:

	KBZ-4	KCT-5	KFT-8	KDT-6
Mixed Zone	0-137.5	0-140.1	0-28.5	0-43.6
Transition Zone	137.5-142	140.1-155.2	28.5-99.3	43.6-58.5
Transition Sands	138.1-157.1	143.6-161.0	---	---

OAK CRATER:

	OBZ-4	OPZ-18	OCT-5	OKT-13
Mixed Zone	0-180	0-174	0-160	0-56
Transition Zone	180-220	174-211	160-170	56-80
Transition Sands	196.2-216.4	175.1-210.4	---	---

	OFT-8	ODT-6
Mixed Zone	0-12.9	1.8-4.4
Transition Zone	65-74	---
Transition Sands	---	---

Debris Blanket:	OHT-10	OJT-12	ONT-16	OMT-15	OLT-14
Mixed Zone	0-54	0-20.9	0-12.9	0-8.9	0-7.5
Transition Zone	54-76	20.9-67	12.9-14.7	8.9-15.5	---
Disturbed Zone	76-149.5	67-94.2	14.7-41.6	15.5-28.5	

Homotrema is reported deeper from 232.6-233.3 ft from a unit that appears like a thin dike (possibly injection?). Micropaleontology does not support AA faunas at either of these levels, but the paleontology has not been adequately studied to be definitive.

In OCT-5 scattered sand-sized to granule-sized, brown skeletal grains and a possible piece of charcoal occur from 2.7-10.2 ft. From 11.2-28.2 ft brown coral clasts are common.

In OKT-13 brown coral clasts are scattered in the graded unit from 1.9-11.1 ft. Scattered brown coral sticks occur from 12.3-26.1 ft.

In OGT-9 scattered brown corals occur at 3.9 ft, a few fragments of brown corals are found from 3.9-6.2 ft, and sparse brown corals occur from 7.4-9.1 ft.

No brown skeletal grains, corals, or mollusks have been observed in ODT-6, OET-7, OFT-8, OLT-14, OMT-15, ONT-16, OQT-19, ORT-20, and OUT-24. No samples were taken in the upper part of OTG-23, so mixing in this interval cannot be determined by macroscopic means.

OIT-11 appears to be located just outside of the crater margin. One granule-sized fragment of a pale-yellowish-brown coral (Seriatopora), possibly indicating mixing from the organic interval, occurs in a rubble unit, 0.1-3.9 ft.

From boreholes within the debris blanket, only OHT-10 and OJT-12 contained brown mixed material. Common small pebble- and granule-sized brown corals occur from 0.0-7.9 ft in OHT-10. In OJT-12, brown corals and molluscs are common from 0.0-3.6 ft and sparse from 6.3-11.2 ft. Mixed brown material occurs in both boreholes in graded beds at the top of the sequence.

Microfossil Mixing

Microfaunas recovered can be divided into mixed, transitional and unmixed zones. The "in-situ" zone previously used (Cronin, Brouwers, and others, 1986) is now referred to as the unmixed zone (see Chapter 11). The term in situ carries a connotation not intended by the authors. Such unmixed intervals may be (and commonly are) displaced spatially from their original position as a consequence of primary or secondary effects of the nuclear blast. Thus, in this sense, these intervals are not in situ. Thus, the term "in situ" is abandoned. The transition zone corresponds well to the geologic crater zone of transition sand (where preserved) which is thought to be the base of the crater.

KOA Crater. -- In KBZ-4, four subzones of the mixed zone can be identified: (1). 0.0-28.8 ft--mixed faunas dominated by material from AA-BB-CC with some DD, EE, FF material. (2). 28.8-53.8 ft--mixed faunas from zones AA-EE with "piped" material from zones FF-MM. There is a differentiation among the faunal elements; the ostracodes appear to be equally divided from zones FF-HH and KK-MM and all the foraminifers appear to be from KK-MM. (3). 53.8-124.0 ft--mixed faunas from zones AA-EE with less mixing, apparently

downward, and with piped material. The faunal elements are markedly differentiated in the piped material; the ostracodes appear to be from zones FF-II and the foraminifers from zones KK-LL. (4). 124.0-137.5 ft--Mixed faunas from zones BB-EE with much less mixing and most elements are from zones CC-DD. The transition zone is from 137.5-142.0 ft. The lowest Holocene (AA) is from around 100 ft. The lowest material from depth (organic interval) within the crater is 93.2 ft.

KCT-5 is similar to KBZ-4 in that material from zones AA-EE is mixed in the upper 50 ft or so and becomes less mixed downward. Material from the organic interval is sparse, unlike KBZ-4, found only at 15 ft, in the lower part of a graded bed.

KDT-6 exhibits faunas from zones AA-EE from 0.0-30.0 ft. 30.0-58.5 ft has faunas that are probably disrupted but not clearly mixed. Common brown skeletal fragments occur from 3.2-10.4 ft with a brown coral cobble at 9.0 ft, all within a poorly graded bed.

OAK Crater. -- It appears that the style of mixing in OBZ-4 is similar to KBZ-4 in that it may be divisible into zones that generally decrease in mixed material and in the range in depths that that material represents downward. An obvious difference is that microfossils from the organic interval occur in the uppermost portion of OBZ-4. This perhaps represents prolonged piping and/or less significant slumping from the crater margin compared to KOA. Material within the upper part of the mixed zone is largely from zones AA-FF and in the lower part is represented largely by material from EE-GG and FF-GG. The lowest occurrence of a brown coral clast within the crater is 186.8 ft. The lowest occurrence of ostracodes from depth is 182.4 ft. The lowest occurrence of Holocene material (moderate-red Homotrema) is 152.1 ft. This succession of occurrences is similar to, though deeper than, those in KBZ-4. The common mixed material includes zone FF which is not common in KBZ-4. Material from intermediate depths (JJ-HH) may be mixed to depths a little lower possibly occurring in samples at 190 and 213 ft. Another obvious difference from KBZ-4 is the fact that the material mixed in OBZ-4 includes larger clasts so that it could be observe in the core.

OPZ-18 appears to be similar to OBZ-4 but has not been adequately studied for detailed analysis. The odd pale yellowish brown coral report from 226.8 ft could represent material from intermediate depths (JJ) similar to material in OBZ-4 but slightly deeper.

In OCT-5 microfaunal evidence for mixed material from depth is abundant from 0.2-17.8 ft, within a graded bed (to 10.2 ft) and in a rubble unit beneath it. Material from 57.6 ft appears to represent zone GG and would suggest mixing from intermediate depths in the middle of the mixed zone. The mixed zone is largely represented by material for zones AA-FF presumably distributed in a style similar to the style of mixing in OBZ-4.

OKT-13 shows less clear mixing and to much shallower depths (similar to KFT-8). It has mixed brown material in a graded bed at the top of the sequence and in the underlying rubble unit similar to OCT-5.

In OFT-8 no megafossil evidence was found but the mixed zone included probable AA-FF microfossil material.

In OGT-9 mixed brown corals occur scattered through graded beds at the top of the sequence. The borehole was shallow and presumed to be similar to OFT-8.

OIT-11 has a single brown coral at the top of the sequence in a debris/rubble "blanket" unit. The unmixed zone occurs at 16.7 ft. The upper 16.7 ft was not studied paleontologically so cannot be further characterized.

Mixing in the OAK Crater Debris Blanket. -- The style of mixing in boreholes from the debris blanket is subtly different from that in boreholes within the geologically defined crater. Material from depth (brown corals) is restricted to graded beds at the top of the sequence in OHT-10 and OJT-12. This is similar to OGT-9. No brown material was found in OMT-15 or ONT-16 and no graded beds were observed. The mixed zone appears to consist of microfaunas from AA-FF and possible GG in all boreholes. The transition zone is different in the debris blanket than within the crater. It consists of generally unmixed faunas with sparse mixed elements from various zones that appear to show a change to deeper zones downward. Also, a new zone is delimited. This is the disturbed zone. Faunas are unmixed. The geology is generally unmixed and not greatly disturbed but no disconformities, discontinuities, or normal stratigraphic markers are observed.

OLT-14 exhibits a thin debris blanket that appears to consist of mixed AA-BB faunas. The mixing continues downward into the uppermost part of what appears to be in place geology of SP 1.